LA-14112-PR
Progress Report
Approved for public release,
distribution is unlimited

Physics Division Activity Report

2003

Los Alamos
NATIONAL LABORATORY

Managing Editor: Grace Hollen

Science Writers-Editors: Josef Bachmeier, Todd Heinrichs, and Grace Hollen

Design Direction: Jean Butterworth

Composition: Jean Butterworth

Illustration and Design: Kemp Beebe, Jean Butterworth, AnnMarie Cutler, Anita Flores, Vicente Garcia, Gloria Sharp, Ward Zaelke

Technical Review: Joysree Aubrey, Cris Barnes, Carter Munson, Martin Cooper, Doug Fulton, Pamela French, Mikkel Johnson, Geoffrey Mills, Andrea Palounek, Brent Park, Albert Petschek, Robert Scarlett, Susan Seestrom, Jeffrey Schinkel, Jack Shlachter, David Scudder, Charles Wood

Physics Division managers and the editors would like to acknowledge the valuable contributions of all subject-matter experts throughout the Division and from other Laboratory organizations who provided technical information and guidance.

CD Integration Design and Production: Jean Butterworth

Printing Coordination: IM-4 Imaging Services

The four most recently published reports in this unclassified series are LA-13048-PR, LA-13355-PR, LA-13606-PR, and LA-13870-PR.

Los Alamos National Laboratory, an affirmative action/equal opportunity employer, is operated by the University of California for the United States Department of Energy under contract W-7405-ENG-36.

This report was prepared as an account of work sponsored by an agency of the United States Government. Neither The Regents of the University of California, the United States Government nor any agency thereof, nor any of their employees, makes any warranty, express or implied, or assumes any legal liability or responsibility for the accuracy, completeness, or usefulness of any information, apparatus, product, or process disclosed, or represents that its use would not infringe privately owned rights. Reference herein to any specific commercial product, process, or service by trade name, trademark, manufacturer, or otherwise, does not necessarily constitute or imply its endorsement, recommendation, or favoring by The Regents of the University of California, the United States Government, or any agency thereof. The views and opinions of authors expressed herein do not necessarily state or reflect those of The Regents of the University of California, the United States Government, or any agency thereof. Los Alamos National Laboratory strongly supports academic freedom and a researcher's right to publish; as an institution, however, the Laboratory does not endorse the viewpoint of a publication or guarantee its technical correctness.

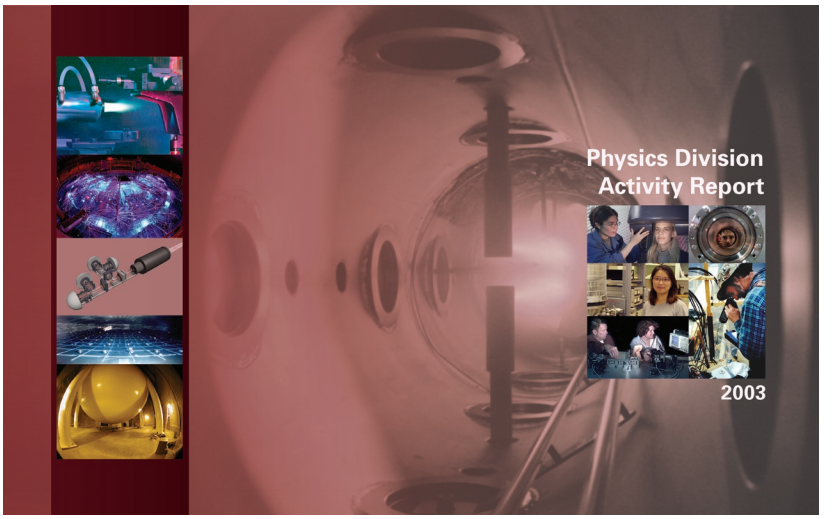

About the cover: The background image on the cover shows the end view of the magnetic reconnection scaling experiment. The plasma stream in this photo is several centimeters in radius and travels several meters down the cylindrical vacuum chamber to an external anode plate. The images on the front cover (from top left to right): (1) Michelle Espy (P-21) adjusts the magnetoencephalography (MEG) helmet on a test subject. MEG provides images of neural currents in the brain that can be used to diagnose epilepsy, stroke, and mental illness and to study brain function. (2) Chris Grabowski, a P-24 collaborator from the Air Force Research Laboratory in Albuquerque, New Mexico, peers through the small quartz tube used in the fusion-energy research machine called FRX-L, which aimed at achieving the first physics demonstration of magnetized target fusion. (3) Chen-Yu Liu (P-23) discusses her research to characterize the performance of cryogenic solids (solid deuterium) as superthermal ultra-cold neutron sources. Liu was recently awarded the 19th Louis Rosen Prize for her outstanding Ph.D. thesis, "A Superthermal Ultra-Cold Neutron Source." (4) Leonard Tabaka (P-22) examines a Faraday fiber prior to conducting an experimental shot carried out in Sarov, Russia. Scientists from Los Alamos National Laboratory (LANL) and from the All-Russian Scientific Research Institute of Experimental Physics recently performed a series of experiments aimed at determining the dynamic yield strength of copper. These "Russian High Strain Rate" experiments are important to refine and validate computational models of dynamic material strength under high-strain and strain-rate conditions. (5) David Clark (P-22) and Dale Tupa (P-25) align an interferometer—the heart of a diagnostic known as VISAR (velocity interferometer system for any reflector), which measures the surface velocity of test objects during dynamic experiments at LANL's Proton Radiography (pRad) facility.

The small images on the back cover (from top to bottom): (1) Researchers at LANL have invented and applied R&D award-winning technology, known as the atmospheric-pressure plasma jet (shown here), to the decontamination of radiological, chemical, and biological agents from surfaces. (2) When used to produce a near Planckian x-ray source, the Z pulsed power accelerator at Sandia National Laboratories (SNL) can drive targets up to 5 mm in diameter to temperatures above 200 eV, allowing researchers from P-22, P-24, X-1, X-2, and SNL to study the physics of radiation transport in regimes of interest to X Division. (3) The image shown here is an original rendering of a receiver that is part of the free-space quantum-key distribution system developed by members of P-21. Polarized photons are received by the telescope and randomly read by one of four detectors. Those readings form the basis for a cryptographic key whose secrecy is guaranteed by the laws of quantum physics. (4) This image shows an inside view of the Milagro Observatory—a new type of astronomical telescope that "sees" the universe at very high energies. Located at LANL's Fenton Hill site, Milagro allows researchers to continuously monitor the entire overhead sky in the TeV-energy regime. (5) The spherical tank shown here contains the MiniBoone detector located at the Fermi National Accelerator Laboratory in Illinois. MiniBoone is the first phase of the larger Booster Neutrino Experiment (BooNE) that will definitively test the Liquid Scintillator Neutrino Detector (LSND) evidence for neutrino oscillations and will precisely measure the oscillation parameters. The LSND took data at LANL from 1993-1998 to obtain evidence that neutrinos oscillate from the muon neutrino form into the electron neutrino form.

LA-14112-PR
Progress Report

Issued: February 2004

Physics Division Activity Report

January 1–December 31, 2003

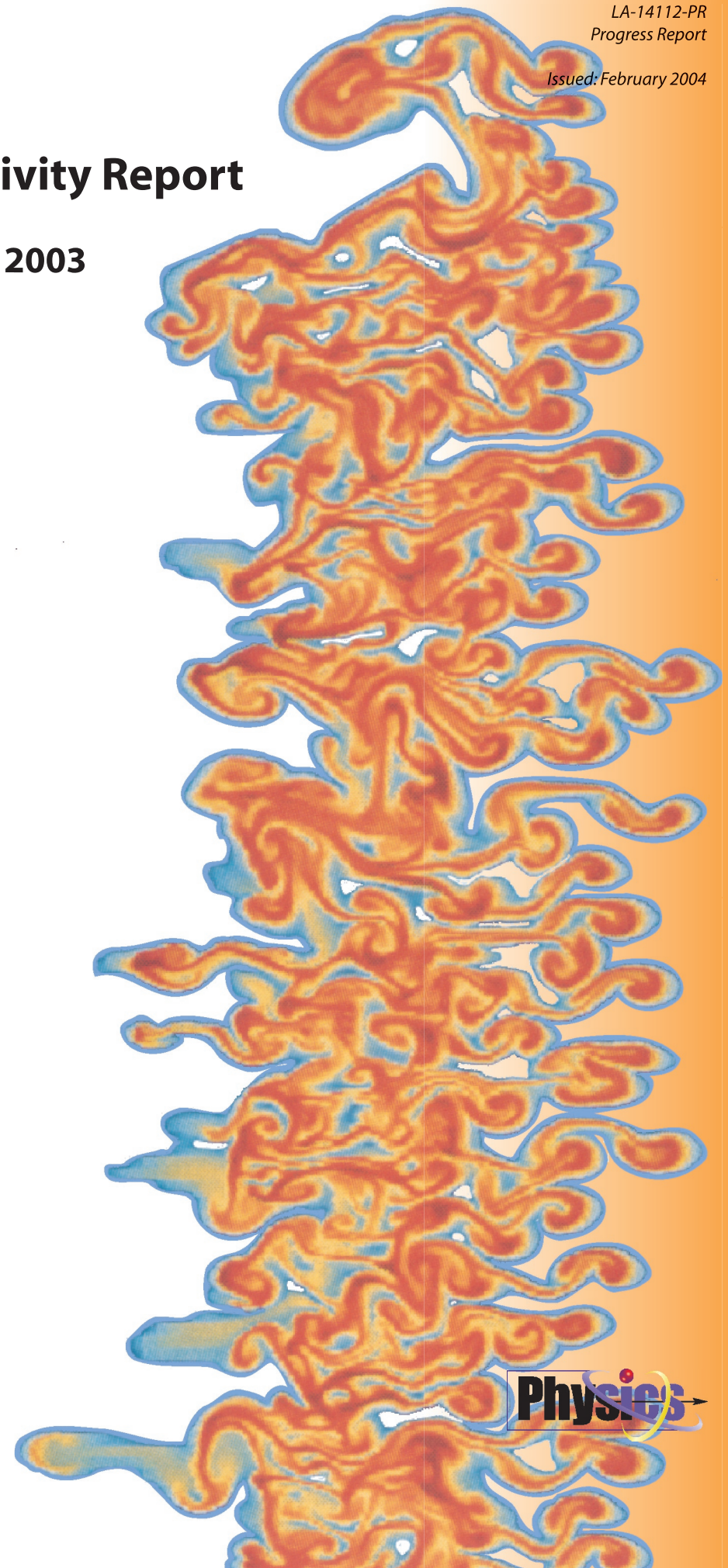

1943 - 2003
Los Alamos
NATIONAL LABORATORY
Ideas That Change the World

Physics

Physics Division Activity Report

January 1–December 31, 2003

Abstract

This issue of the Physics Division Activity Report describes our activities and achievements in applied and basic science during the calendar year 2003. The report covers the activities of the five Physics Division groups, which represent the main areas in which we serve Los Alamos National Laboratory and the nation: Biological and Quantum Physics, Hydrodynamics and X-ray Physics, Neutron Science and Technology, Plasma Physics, and Subatomic Physics. This report includes a message from the Physics Division Leader, Susan Seestrom; general information about the mission and organization of the Division; our staffing and funding data for the fiscal year; descriptions of the activities of each of our groups; highlights of major research efforts throughout the Division; descriptions of the individual projects that we support; and a list of our publications and conference presentations.

Contents

Group Descriptions 1

Material Studies

Research Highlights 23

Project Descriptions 43

Plasma Physics

Research Highlights 55

Project Descriptions 79

Instrumentation

Research Highlights 89

Project Descriptions 109

Nuclear Physics and Astrophysics

Research Highlights 125

Project Descriptions 153

Biophysics

Research Highlights 167

Project Descriptions 179

Atomic Physics

Research Highlights 185

Facilities

Research Highlights 201

Project Descriptions 213

Appendices

Appendix A: Acronyms 219

Appendix B: Publications 222

Division Leader's Introduction

The year 2003 began in great turmoil at Los Alamos National Laboratory (LANL). Our Director and Principal Deputy Director vacated their positions in the midst of public allegations of fraudulent procurement activity on the part of Laboratory employees and alleged attempts by the management to cover up and retaliate against those who were conducting internal investigations. Admiral George "Pete" Nanos was appointed acting Laboratory Director on January 2, 2003, and then appointed permanently in May 2003 by the University of California (UC) Regents. Even though the allegations of procurement fraud proved to be unfounded, the scrutiny applied to LANL in all areas of potential business, safety, or security problems continued throughout the year. We have responded to numerous immediate requirements for data, procedures, and new documents to demonstrate accountability for property, classified media, training, work authorization, foreign visitors, etc. We have some of the very best business and safety staff in our division; they have been indefatigable and tenacious in ensuring our scientists deal with sensible procedures and requirements. Also this year, we completed the very first Facilities Strategic Plan for the Physics (P) Division. We believe this is key to solving the serious problems of poor-quality laboratory space and insufficient office space. It has earned us the possibility of occupancy in a new stockpile stewardship building that will be proposed for congressional-line-item funding in 2004.

Of course, the uncertainty that surrounds the Department of Energy (DOE) contract with the UC affects employees at both a personal and professional level. It is the reputation of the UC that enables us to continue to attract and retain the very best scientists to LANL, and we are concerned that a departure of UC from the management of our science could significantly hinder our ability to perform world-class science and develop state-of-the-art technology. I am extremely proud that in spite of these uncertainties and distractions that our staff continues to be honored with important awards and fellowships; for example, the Laboratory received eight American Physical Society fellowships in 2003—more than any other organization, including UC or other DOE national laboratories.

The broad field of physics continues to be very healthy at LANL. A recent statistical study of publications and citations shows that nearly half of all LANL publications are in the physics field, as are half of the citations. The number of citations for our physics publications places LANL as the eleventh ranked physics department in the country and first among the DOE national laboratories [see E. Ben-Naim, "Los Alamos National Laboratory Publications 1993-2003: A Statistical Study," Los Alamos National Laboratory report LA-UR-03-9087 (2003)].

Despite the distraction of our workforce to attend to the business, safety, and security requirements for conducting the business of science at the Laboratory, P Division scientists continued to produce high-quality scientific work. I am also proud that our Division communications team published the 2003 Activity Report (which describes work performed throughout the Division) so quickly after the new year. This report, like the Physics Division as a whole, is largely organized by physics disciplines, and we continue to lead experiments in areas of importance both for national security and basic science. Under the rubric of materials studies, one of the major strategic goals for the laboratory, P Division researchers continued their tradition of capturing complex, dynamic data in harsh environments on plutonium in subcritical tests. Other research highlights examine the behavior of materials under extreme loading produced by magnetic compression and laser-driven shock waves. Diagnostic development remains a hallmark of the Division, and we have made significant progress in the implementation of both temperature and velocity probes.

Plasma physics remains a core capability of the Division with applications to nuclear-weapons performance, energy production, and astrophysics. Our researchers are involved in sophisticated imaging experiments to study the evolution of turbulent systems and the spatial emission of neutrons from a hot, compressed capsule. Plasma experiments studying radiation flow are described in a research highlight that discusses work performed at the Z facility at Sandia National

Laboratories, and our leadership in magnetized target fusion is highlighted in an article on the LANL FRX-L facility.

Our own in-house laser facility, the Trident laser, provides a diverse set of pulse-shape, energy, and wavelength options in a heavily diagnosed environment, available to both local and outside users, and Trident occupies an important place in P Division's portfolio.

Technology advances have been made in the use of both muons and electrons as radiographic probes. These unique techniques are showcased in a variety of separate research highlights that describe the methods and applications using charged particles for imaging and interrogating objects. Our detector work is at the forefront of the field as exemplified in an article about our gated x-ray framing cameras, and we are applying our nuclear-physics techniques to homeland security issues in the development of the Very Large Area Neutron Detector (VLAND) concept.

Among the most exciting results in the recent past are those obtained through our experiments at the Sudbury Neutrino Observatory, located deep underground in an active nickel mine in Ontario, Canada, where we witnessed new physics in the unambiguous observation of solar-neutrino flavor transformation. We anticipate significant results from a variety of other nuclear-physics experiments over the coming years. Progress towards measurement of the neutron electric dipole moment, neutrino oscillations in accelerator experiments, and parity-violating gamma asymmetry in the NPDGamma experiment are each described separately in highlight articles. Our work on the Pioneering High-Energy Nuclear Interaction Experiment (PHENIX) continues with the Silicon Vertex Tracker project, which will enable the study of charm and beauty quark signals at the Relativistic Heavy Ion Collider. Astrophysical data are being collected at two facilities described in this report, namely the High Resolution Fly's Eye (HiRes) in Utah and our own Milagro Teravolt Gamma Ray Observatory at Fenton Hill.

Susan J. Seestrom, Physics Division Leader

In the Biophysics arena, our scientists have been engaged in neural-circuit modeling as we have extended our understanding of information processing in the vertebrate retina. For several years, we have been improving and applying the most sensitive magnetic sensors yet known, superconducting quantum interference devices (SQUIDs), to the non-invasive study of the electrical activity in the brain. We are now coupling this type of data with that obtained from other tools in work described in a research highlight on the integration of brain information from multiple diagnostic probes.

Three research highlights are categorized as atomic physics because they deal with the uniquely quantum behavior of matter at the atomic scale. The work involves fundamental tests of the random nature of quantum mechanics and application of this randomness to the practical problem of encryption and key distribution. We are also exploring the exciting regime of Bose-Einstein condensates in which large clouds of atoms are governed by quantum mechanics.

I believe these research highlights speak for themselves about the quality of research in P Division. Overall, 2003 was a very eventful year at LANL, yet we remain optimistic that the Laboratory will continue to prove that UC management is sound and accountable so that our research can continue at the high level expected by our leadership, our scientists, and the nation.

Mission and Goals

The mission of Physics (P) Division is to further our understanding of the physical world, to generate new or improved technology in experimental physics, and to establish a physics foundation for current and future Los Alamos National Laboratory (LANL) programs.

The goals of P Division are to

- provide the fundamental physics understanding supporting LANL programs;
- investigate the basic properties of nuclear interactions, high-energy-density and hydrodynamic systems, and biological systems with a view toward identifying technologies applicable to new LANL directions;
- identify and pursue new areas of physics research, especially those to which the unique capabilities of LANL may be applied;
- explore interdisciplinary areas of scientific endeavor to which physical principles and the methods of experimental physics can make an important contribution; and
- maintain strength in those disciplines that support LANL's mission.

P Division pursues its goals by

- establishing and maintaining a scientific environment that promotes creativity, innovation, and technical excellence;
- undertaking research at the forefront of physics with emphasis on long-term goals, high risks, and multidisciplinary approaches;
- fostering dialogue within the Division and the scientific community to realize the synergistic benefits of our diverse research interests;
- encouraging the professional development of each member within the Division; and
- conducting all of its activities in a manner that maintains a safe and healthful workplace and protects the public and the natural environment.

S. J. Seestrom
Division Leader

J. S. Shlachter
Deputy Division Leader

A. P. T. Palounek**
Deputy Division Leader

P. R. French
Chief of Staff

Program Development

G. H. Canavan
Scientific Advisor
LANL Senior Fellow

D. M. Coates
Industrial Partnership Coordinator

Program Execution

T. J. Bowles
Nuclear Physics Program

A. Hauer
Secondary Experiments PE Mgr*

J. S. Shlachter
Boost Physics PE Mgr

A. P. T. Palounek
Advanced Radiography PE Mgr

R. E. Reinovsky
Pulse Power Hydro Program Mgr

G. A. Wurden**
Fusion Energy Project Mgr

Division Support

Executive Staff and Administration
S. S. Strottman
J. P. Tapia
D. J. Colombe
S. A. Quintana

ES&H, Security, Operations
S. J. Greene

Business Team Leader
R. James

HR Generalist
P. D. Beck

Communications
G. Y. Hollen

P-21: Biological and Quantum Physics
C. C. Wood, *Group Leader*
W. R. Scarlett, *Deputy GL*
S. M. Glick, *Deputy GL*

P-22: Hydrodynamics and X-Ray Physics
D. W. Scudder, *Group Leader*
J. B. Aubrey, *Deputy GL*

P-23: Neutron Science and Technology
R. D. Fulton, *Group Leader*
J. E. Schinkel, *Deputy GL*
B. K. Park, *Deputy GL*

P-24: Plasma Physics
C. W. Barnes, *Group Leader*
C. Munson, *Deputy GL*
M. Ray, *Administrative Deputy GL*

P-25: Subatomic Physics
M. D. Cooper, *Group Leader*
M. B. Johnson, *Deputy GL***
G. B. Mills, *Deputy GL***

*PE = Program Element
**Acting

Financial Data

Cost and Budget History

	FY00	FY01	FY02	FY03
Direct Operating Costs	48.5	49.4	55.8	61.8
Direct Capital	15.7	3.9	6.1	5.5
LDRD	5.0	7.4	8.1	8.3
Indirect (G&A, Overhead)	17.9	19.7	20.8	17.0
Total Costs	87.1	80.4	90.8	92.6
Total Budget	93.2	90.4	101.0	100.7
Remaining	6.1	10.0	10.2	8.1
FTEs	267	283	295	322

FY 2003 Direct Costs by Funding Source

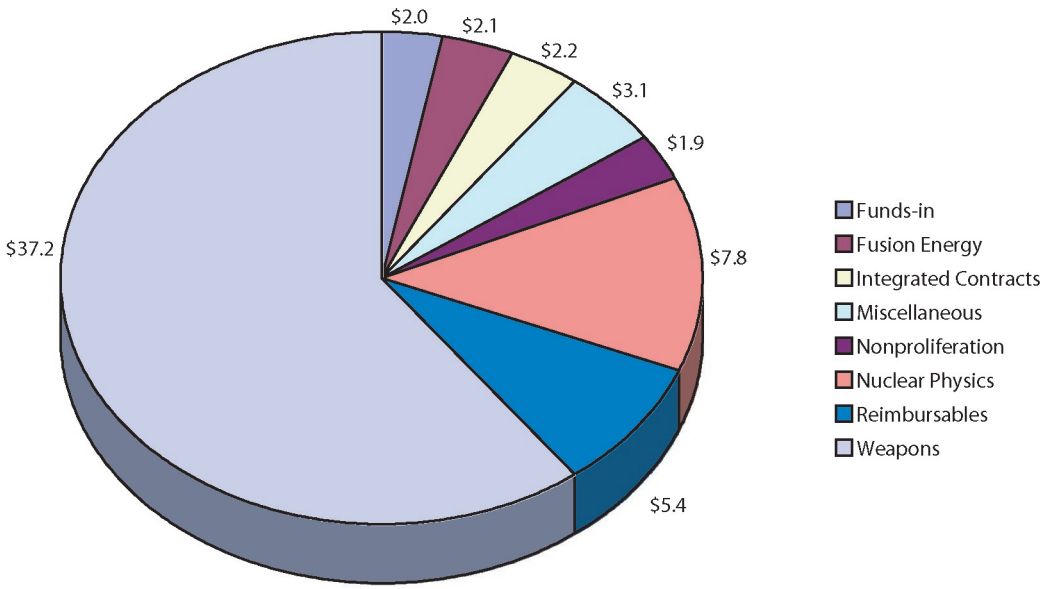

P-21: Biological and Quantum Physics

Charles Wood,
Group Leader
Robert Scarlett,
Stephen Glick,
Deputy Group Leaders

The Biophysics Group (P-21) was founded in 1988 with the goal of applying the scientific and technical resources of P Division to the biosciences. In October 2002, P-21 broadened its scope to become the Biological and Quantum Physics Group with the addition of the Quantum Information Team from P-23. This organizational change was initiated by P Division leadership for two reasons. First, P-21 has longstanding experience in supporting entrepreneurial projects for non-DOE (Department of Energy) government agencies such as the National Institutes of Health (NIH), the Department of Defense (DOD), and the intelligence community, many of which are key sponsors for work in quantum information. Second, the Quantum Team and the Biophysics Group share common interests in the *Physics of Information* at all levels, from quantum information processing, computing, and cryptography to biological information processing by the nervous system. This common focus on the basic science and applications of information processing has already led to numerous constructive interactions between the biological and quantum components of P-21.

Biological Physics

P-21's historical mission has been to contribute to an understanding of biological phenomena by means of the scientific, technical, and conceptual resources of physics; to use biological systems to elucidate general physical principles underlying complex phenomena; and to apply, where appropriate, our scientific and technical capabilities to core LANL programs. Just as the 20th century is regarded as the century of the physical sciences, the 21st century will likely become the century of the biological sciences. P-21 and biophysics as a discipline are well positioned to contribute to this biological *revolution in progress* through our emphasis on understanding biological systems using the scientific, technical, and conceptual resources of physics. Recent advances in biophysical measurement and in molecular biology are beginning to allow detailed physical understanding of biological phenomena that were previously understood only in qualitative terms. P-21 is well placed by virtue of its capabilities and research interests to contribute significantly to this important trend in the biosciences. In addition to the goal of achieving a physical understanding of biological phenomena, the biophysical research in P-21 shares a number of other common characteristics. Specifically, we investigate the relationships between structure, dynamics, and function of biological phenomena over a wide range of scales (e.g., from biomolecules to the whole human brain). We also make extensive use of detection, imaging, and reconstruction techniques [(e.g., x-ray crystallography, single-molecule electrophoresis, high-speed photon-counting optical imaging, magnetic resonance imaging (MRI), and magnetic-field measurements using technologies based on superconducting quantum interference devices (SQUIDs)]. Moreover, we attempt to achieve a detailed interplay between high-resolution physical measurements and large-scale computational modeling and analysis of complex systems, and we develop new facilities in support of our scientific and technical goals, including the following:

- a dedicated x-ray beam line for protein crystallography at the National Synchrotron Light Source (NSLS) at Brookhaven National Laboratory

Group Description

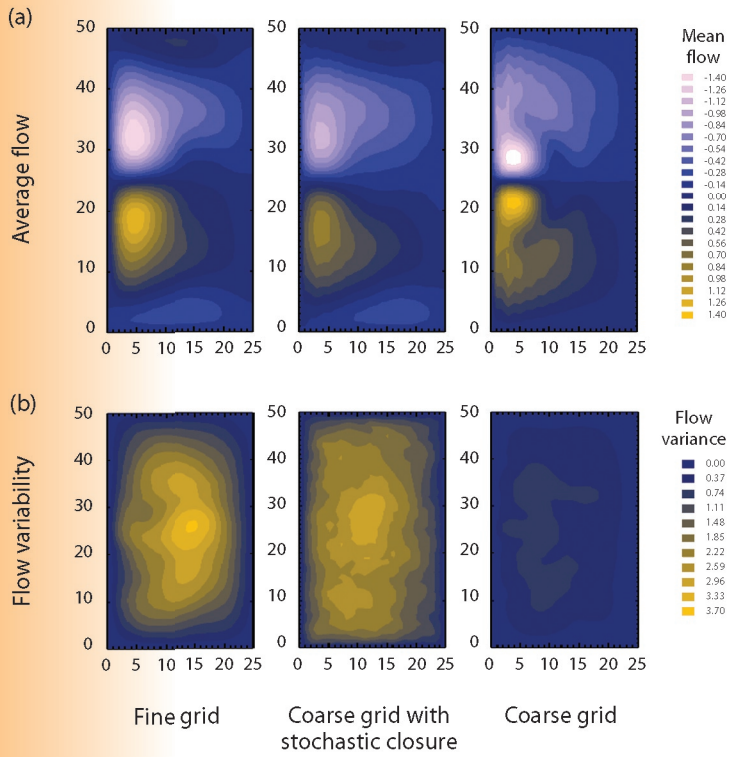

Figure 1. P-21 has developed a new probabilistic approach to the problem of "closure" in large-scale numerical models that require spatial grids. Based on ideas originally developed in the context of P-21's work on brain imaging, this "stochastic closure" approach uses probabilistic methods to make substantial improvements in a model's ability to estimate both average quantities (a) and measures of variability (b) compared to conventional closure approaches. This work is supported by a LANL LDRD-DR project (David M. Schmidt, P-21, Principal Investigator) that involves applications of stochastic closure in biomedical imaging, ocean modeling, flow in porous media, and weapons hydrodynamics.

(BNL)—which we are in the process of handing over to our consortium partners, the Canadian National Research Council, Roche Pharmaceuticals, and BNL Biology;

- a multi-modality imaging facility that includes a large-bore MRI capability, a whole-head magnetoencephalography (MEG) system, whole-head electroencephalography (EEG) arrays, and optical imaging and tomography;
- a high-speed, time-domain measurements and electronics laboratory and fabrication facility; and
- a growing SQUID applications laboratory.

We depend heavily on the tight connection and daily interplay between biologists and physical scientists within the group, the Division, and the Laboratory, and we apply the knowledge, techniques, and capabilities developed in our biological studies to problems of national security and those of specific interest to LANL when our ongoing efforts can offer unique solutions and significant mutual benefit. For example, P-21 has developed a new approach to the problem of "closure" in large-scale numerical models based on partial differential equations (Figure 1). This work is the focus of a Laboratory-Directed Research and Development-Director's Reserve (LDRD-DR) funded project involving members of the ocean-, flow-, and weapons-modeling communities.

Quantum Information Science

A key discovery of twentieth century science was the realization that information is physical. The representation of "bits" of information by classical physical quantities, such as the voltage levels in a microprocessor, is familiar to everyone and is the basis of the "information explosion" of the latter half of the twentieth century. More recently, the field of quantum information science has made great progress in understanding information in terms of the laws of quantum mechanics. For example, a unit of quantum information, known as a "qubit," can be represented by single-photon polarization states. Remarkable new capabilities in the world of information security have been predicted that make use of quantum-mechanical superpositions of information, a concept that has no counterpart in conventional information science. For example, quantum cryptography allows two parties to communicate securely even in the presence of hostile monitoring by a third party (as described below). P-21's Quantum Information Team has experimental projects under way in quantum cryptography, in quantum computation, in quantum optics with trapped strontium ions, and atom interferometry with Bose-Einstein condensates.

Quantum cryptography. One of the main goals of cryptography is for two parties ("Alice" and "Bob") to render their (binary) communications unintelligible to a third party ("Eve"). This can be accomplished if Alice and Bob both possess a secret random-bit sequence, known as a cryptographic key. For example, in "one-time-pad" encryption, Alice adds the key to the original message, known as plaintext, and communicates the sum (ciphertext) to Bob. He is able to recover the plaintext by subtracting his key from the ciphertext, but Eve, who is assumed to have monitored the transmitted ciphertext, is unable to discern the underlying plaintext through the randomization introduced

with Alice's key. So, although key material conveys no useful information in itself, it is a very valuable commodity, and methods for Alice and Bob to generate key material securely are correspondingly important. Using quantum key distribution (QKD), Alice and Bob can create shared cryptographic key material whose security is ensured by the laws of quantum mechanics.

QKD offers many security and ease-of-use advantages over existing key-distribution methods. Traditional key distribution using trusted couriers requires cumbersome security procedures for preparing, transporting, and handling the key before any communications can take place and may even be impractical (e.g., re-keying a satellite). In contrast, quantum keys do not exist before the QKD transmissions are made, and a key can be generated at message-transmission time. Public-key cryptography also avoids many of the difficulties of key distribution by courier but provides only the conditional security of intractable mathematical problems, such as integer factorization. Accurate assessment of an adversary's computing power over the useful lifetime of encrypted information, which may be measured in years or even decades, is notoriously difficult—unanticipated advances in fields such as quantum computation could render public key methods not just insecure in the future but also retroactively vulnerable. QKD could be used for real-time key generation in cryptographic applications where this long-term risk is unacceptable. Recent progress in QKD is described in a research highlight in this report.

P-21's Quantum Information Team leads the world in many aspects of quantum cryptography. We have demonstrated all aspects of quantum key exchange over 48 km of fiber at LANL and are leading a demonstration of these capabilities over an existing fiber network for the U.S. government. Free-space quantum cryptography was invented by our team, and we have now fully demonstrated the practicality of this approach for a variety of applications over a 10-km range (Figure 2).

Quantum computation. With two or more qubits, it becomes possible to consider quantum logical-"gate" operations in which a controlled interaction between qubits produces a (coherent) change in the state of one qubit that is contingent upon the state of another. These gate operations are the building blocks of a quantum computer, which in principle is a very much more powerful device than any classical computer because the superposition

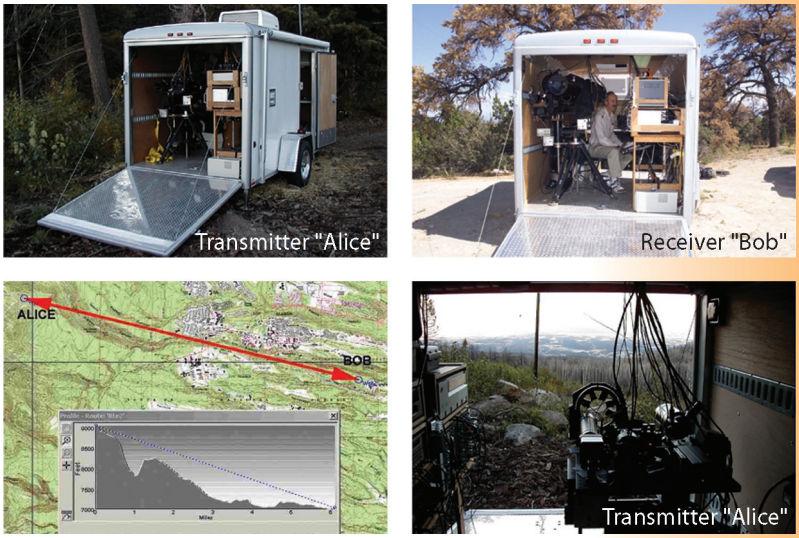

Figure 2. P-21 and collaborators have developed techniques for free-space QKD for which they received a 2001 R&D 100 Award. Shown here are the portable transmitter ("Alice") and receiver ("Bob") used in a free-space QKD experiment over 10 km between Pajarito Mountain and LANL Technical Area 53 (map at bottom left).

principle allows an extraordinarily large number of computations to be performed simultaneously. In 1994, it was shown that this "quantum parallelism" could be used to efficiently find the prime factors of composite integers. Integer factorization and related problems that are computationally intractable with conventional computers are the basis for the security of modern public-key cryptosystems. However, a quantum computer running at desktop-PC speeds could break the keys of these cryptosystems in only seconds (as opposed to the months or years required with conventional computers). This single result has turned quantum computation from a strictly academic exercise into a subject whose practical feasibility must be urgently determined. The architecture of a quantum computer is conceptually very similar to a conventional computer—multiqubit, or "multibit," registers are used to input data. The contents of the registers undergo logical-gate operations to effect the desired computation under the control of an algorithm, and a result must be read out as the contents of a register.

Many areas of the fundamental science underpinning quantum computation have not yet been thoroughly studied. The P-21 Quantum Information Team is actively engaged in several of these areas. For example, we are using trapped ions to measure the randomness of atomic transitions, which constitute a key test of the predictions of quantum mechanics. Other studies involve ultra-cold atoms collapsed into a Bose-Einstein condensate. These experiments, more fully described in other parts of this report, contribute to the worldwide goal of a complete understanding of this forefront of physical science.

P-22: Hydrodynamics and X-ray Physics

David Scudder, Group Leader
Joysree Aubrey, Deputy Group Leader

The activities of the Hydrodynamics and X-ray Physics Group (P-22) help to support LANL's mission of ensuring the safety and reliability of the nation's nuclear stockpile. Group members are also involved in research that addresses fundamental issues related to hydrodynamic phenomena at extreme pressures, high energy-density plasmas, and fusion physics. Other endeavors have led to innovations with commercial potential.

The tremendous challenge of certifying the stockpile in the absence of testing requires that we marshal all the capabilities and resources at our disposal. As the materials in nuclear weapons age, they are removed further and further from the states under which they were tested. Defects in devices and engineering modifications have introduced uncertainties in performance and reliability. To address these issues, we must have a fundamental understanding of the physical processes involved in the performances of nuclear weapons and the limits of models developed and benchmarked during the testing era. P-22 contributes to this challenge in a number of ways through the re-analysis and re-evaluation of archival NTS data in support of stockpile stewardship activities and validation of weapons design codes, diagnostic development and training to enhance the test readiness posture of the nation, and the execution of above-ground experiments with the aim of understanding and resolving weapons physics issues. The group has the resources to assemble multi-disciplinary teams to address these challenges. Our involvement with various experimental programs has required efforts in diverse areas such as optics, hydrodynamics, plasma physics, radiation transport, pulsed-power science, weapons physics, x-ray spectroscopy and imaging, microwaves, electro-magnetics, and nuclear and atomic physics. A number of the projects described below are featured in more detail in this report.

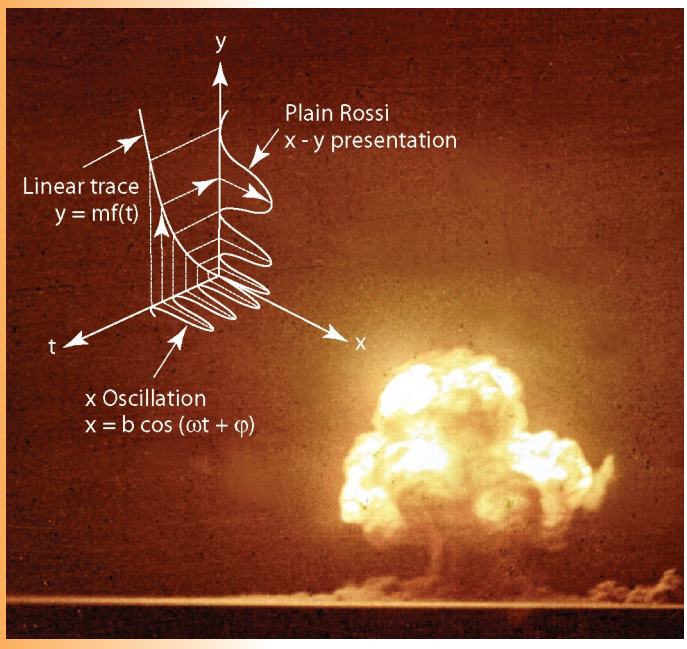

Figure 1. Archival photo of the Trinity event (July 16, 1945). The inset is a schematic representation of the Rossi technique.

NTS data and weapons physics. The first alpha (neutron multiplication rate) measurement was performed by Bruno Rossi on the Trinity event (Figure 1). This diagnostic became a standard tool for assessing the nuclear and thermonuclear performances of devices fielded at the Nevada Test Site (NTS) and elsewhere.

Neutrons in a supercritical assembly increase exponentially according to the formula $N(t) = N_0 e^{\alpha t}$. If α is not a constant, then the equation is modified to $N(t) = N_0 e^{S \alpha(t)\, dt}$. The time-dependent neutron population is proportional to the resulting leakage gamma radiation from the surface of the device. The exponentially increasing gamma flux is converted to an electrical current by a series of detectors that span the dynamic range of the signal. The electrical signal

in turn is recorded on oscilloscopes driven by oscillators at appropriate frequencies. The Rossi technique consists of the superposition of the exponentially increasing signal on a sinusoidal trace (inset in Figure 1). The time-dependent behavior of the gamma radiation can be extracted by using the known frequency of the sine wave. P-22 is the custodian of archival data from the NTS and is in the process of developing modern methods of analysis and applying them to nuclear events. In collaboration with our colleagues from D-1, ESA-WR, and T-13, we are developing rigorous methods of error analysis for the data in order to deliver higher-fidelity information to the nuclear weapons design and code development community. The re-analysis effort has given us new insights into the physics of individual devices and weapons systems.

High-energy density hydrodynamics (HEDH). Members of the group have done pioneering work in developing and applying pulsed-power facilities to explore hydrodynamic phenomena at extreme pressures and convergent geometries. Under the HEDH program, experiments were conducted to address issues related to LANL's main mission of supporting the nuclear stockpile in the absence of testing. The 4.6-MJ Pegasus II and the 23-MJ Atlas facilities were used to study dynamic material properties under extreme conditions. Experiments included studies of convergent material flow in asymmetric geometries. The data were used to validate models in modern weapons design codes. Other experiments looked at the growth of preformed perturbations during implosions, strength at high strain rates, frictional forces between materials with differential velocities, and spall in materials driven by 50-kbar convergent shocks. The future of the LANL pulsed-power program is full of challenges and exciting new opportunities. The Atlas facility has been moved to the NTS and will be re-commissioned during the spring of 2004. In addition to conducting experiments on the pulsed-power facilities at LANL, P-22 group members have had a long collaboration with scientists at the All-Russian Scientific Research Institute of Experimental Physics at Arzamas-16 (VNIIEF). The Russians have developed large-scale explosive pulsed-power facilities capable of generating fields of thousands of tesla. Joint experiments have explored instability growth in convergent geometries, magnetized target fusion, the design and development of a megajoule x-ray source, and the properties of materials in high fields and at cryogenic temperatures.

In collaboration with DX and X Divisions, we are actively involved in stockpile-related hydrodynamic experiments on the PHERMEX (Pulsed High-Energy Radiographic Machine Emitting X-rays) facility. We have fielded and analyzed high-fidelity, four-frame radiographs for a series of shots. In addition, we have contributed to the effort to bring the second axis of the Dual Axis Radiographic Hydrotest (DARHT) facility on-line. This work included experiments to explore beam-target interactions, development of a pulse coil for DARHT, and the fielding of an electron spectrometer and analysis of the resulting data. The beam-target interaction studies are being conducted in collaboration with DX-6 using DARHT-I as part of a "risk-mitigation" effort for DARHT-II operation. We have also collaborated with DX Division on the scientific and engineering activities related to the Dynamic Experiment (DynEx) program. A series of experiments to measure containment vessel oscillations using microwave interferometry was performed. The objective of these experiments was to determine the radial wall displacement of a 6-ft-diam containment vessel during detonations of different amounts of high explosives. The resulting data were used with other diagnostic data to validate models of vessel behavior.

P-22 plays a very active part in the LANL proton radiography (pRad) program by providing VISAR (velocity interferometer system for any reflector) measurements for dynamic experiments. These experiments include studies of spall and evolution of surface features. The ability to record the details of velocity structure during an experiment is very important for understanding the physics of dynamic processes. The combination of multiple radiographic images and spatially distributed VISAR data from the same experiment provides theorists with high-quality data for benchmarking materials models. Detailed continuous velocity measurements between images contribute to the overall understanding of dynamic processes.

In support of the Dynamic Materials Campaign, we have conducted research in collaboration with DX-2 and P-23 on the production of ejecta from the surfaces of shocked materials and subsequent transport of the particles into gas. These experiments were performed on tin targets at the LANL gas gun facilities. Detailed information about the densities and velocities of particle clouds generated from shocked surfaces

Group Description

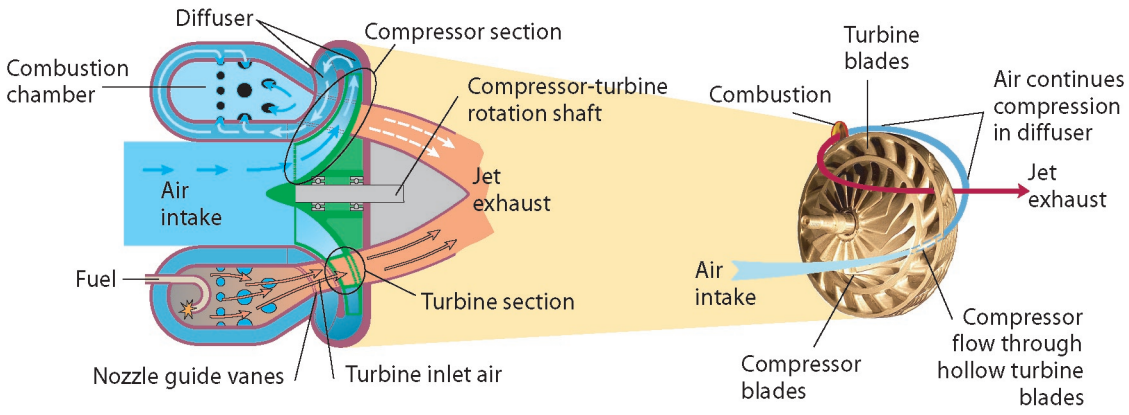

Figure 2. Composite drawing of the ASRT schematic and photo, showing how the ASRT operates. Air from the compressor section of the ASRT is channeled through the outer hollow turbine blades on the same rotor. The air, on its way to the combustion chamber, cools the turbine section allowing the engine to operate at higher temperatures. The fuel efficiency is increased in this case.

is necessary for the development of models of the phenomenon. Another series of experiments is being conducted (in partnership with DX-2) to investigate the behavior of shocked materials off the principal Hugoniot curve. The resulting data provide information about the target material equation of state (EOS) under pressure and temperature conditions that are not easily accessible by other means. In collaboration with P-23, DX-2, and MST-7, P-22 staff used optical pyrometry to measure the temperature of shocked materials to elicit information about solid-solid and solid-liquid phase transitions. Such information has been very valuable in testing EOS models of materials

Strongly coupled plasmas and radiation hydrodynamics. The understanding of the properties of strongly coupled plasmas and the interaction of these plasmas with radiation is important for fusion and weapons physics applications. We are involved in various research projects in these areas using both local facilities and those elsewhere, such as the Z machine at Sandia National Laboratories (SNL) and the Omega laser at the University of Rochester. We are conducting investigations of fundamental processes that are relevant to fusion and strongly coupled, multi-material plasmas. The work is being done locally under an LDRD project and involves two experiments aimed at measuring the ion-ion diffusion coefficient and the temperature equilibration rate between ions and electrons in a dense plasma. We have also studied the propagation of radiation in materials using the x-ray source generated by SNL's Z machine, which generates currents of 20 MA and a peak electrical power of about 40 TW. This source has been used to study the physics of radiation-matter interactions.

New initiatives. Members of P-22 are developing methods of encoding information to deliver digital television images using the existing analog NTSC (National Television System Committee) format. The data for high-definition TV (HDTV) can be viewed by analog TV receivers. No hardware modifications are required for the old monitors or the new high-definition sets. The information for the digital images (quantized coefficients in the transform space) is transmitted by modulating the carrier in a novel way. A second innovation developed by a group member, the Advanced, Single-Rotor Turbine (ASRT) (Figure 2), was recently nominated for an R&D 100 Award. The compressor and turbine are combined into a single piece, increasing reliability while reducing engine complexity and size, as well as fabrication and maintenance cost. Envisioned applications for this technology include portable power units and residential distributed power supplies, as well as small jet engines and turbo-shaft engines for turboprop aircraft, helicopters, and tanks. Centrifugal turbines could also be implemented in turbo-chargers for piston engines and turbo-pumps for liquid-fueled rockets, refrigeration, and applications in the chemical-processing industry.

P-23: Neutron Science and Technology

Doug Fulton, Group Leader
Jeffrey Schinkel, Brent Park, Deputy Group Leaders

The Neutron Science and Technology Group (P-23) executes a wide range of projects spanning weapons physics and nuclear physics through fundamental and applied research. The core capabilities of the group are in the application of state-of-the-art techniques in particle and light detection and in the recording of transient events. Our efforts in weapons physics contribute to the national security mission of LANL through the stockpile stewardship program by participating in the design and fielding of subcritical experiments (SCEs), small-scale dynamic experiments, and the reanalysis and archiving of data from past nuclear weapons tests. Our fundamental research contributes to science in support of LANL programs through studies on nuclear and weak-interaction physics and on state-of-the-art measurements of astrophysical phenomena such as solar neutrinos and ultra-high-energy gamma rays. Applied research includes the application of imaging and neutron technologies to problems relevant to national defense, homeland security, and industry. A number of the projects and programs described below are featured in this report.

Weapons physics. Members of P-23, working in collaboration with P-22 and various groups in DX, ESA, X, NMT, and MST Divisions, designed and executed the Stallion series (Vito, Mario, Rocco, and Armando) of SCEs. The purpose of Vito was to examine ejecta formation in a particular region of a weapon, and it successfully demonstrated the LANL "racklet" technique that facilitates rapid and cost-effective turnaround between SCEs (Figure 1). The racklet method was subsequently employed for Mario and Rocco. The purpose of Mario and Rocco (and soon Armando) was to compare the properties of cast versus wrought plutonium.

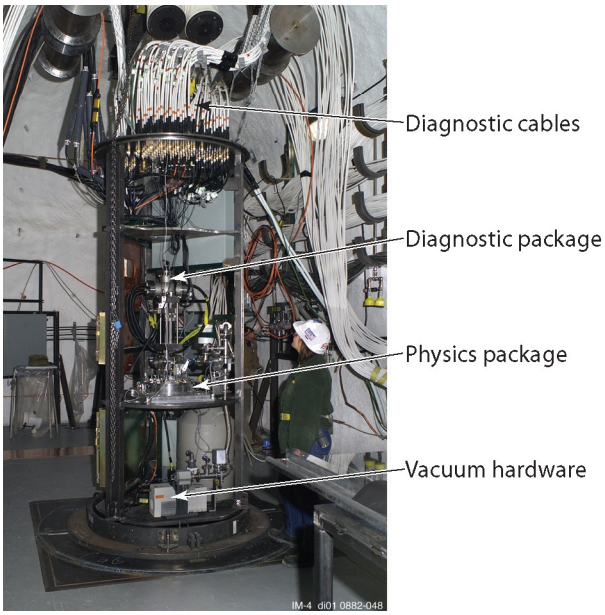

Figure 1. The racklet assembly before it was lowered into the confinement hole was successfully demonstrated on the Vito SCE.

The specific properties investigated in SCEs include ejecta formation, spall features, and surface temperature. Holography, used to measure ejecta-particle-size distributions, provides information about ejecta-particle transport in a gas environment. Another method, soft x-ray imaging, was developed to measure ejecta-density distributions from shock-loaded metals, and pRad was used for the first time to study material failure in depleted uranium and other materials. Surface temperature is measured with a high-speed, time-resolved, multi-wavelength near-infrared surface pyrometer. All these methods provide data that contribute to our understanding of the strength, failure properties, and EOS of materials important to the weapons program. Another EOS constraint can be obtained from volume temperatures. Neutron resonance spectroscopy (NRS) determines volume temperatures by using Doppler-broadened neutron resonances to measure internal temperatures in dynamically

loaded samples. Although still a nascent technique, our researchers plan on using NRS to measure the temperatures attained in shocked metals, at frictional interfaces, and in the "dead zones" of detonated chemical explosives.

P-23 also supports pRad and other facilities and capabilities such as DARHT by developing and fielding imaging systems and advanced detector systems. Historically, P-23 has been the locus for advanced imaging technologies developed to meet the demands of the weapons program. Our imaging expertise is currently being applied to inertial-confinement-fusion (ICF) experiments via neutron pinhole imaging. This simple yet powerful technique allows us to capture neutron images of capsules used in ICF experiments and thus contributes to improvements in capsule design. However, the application to ICF requires pinhole dimensions that push the limits for fabrication and fielding. In 2003, new milestones in pinhole fabrication were met, resulting in the highest resolution images recorded to date, as well as the first "double-aperture" image. We continue to investigate different technologies that will provide needed infrared cameras and pixilated detector technology for pRad, hydrodynamic experiments, and SCEs.

We also continue to preserve, analyze, and document the NTS and Pacific Ocean weapons test data to gain an understanding of how nuclear weapons systems perform. P-23 analyzes imaging data from the pinhole neutron experiments (PINEX) and neutron-emission measurements from neutron experiments (NUEX) and threshold experiments (THREX). The physicists and engineers who performed the original measurements are correlating and reanalyzing the data from different events, using new methodologies and improved analytical techniques. Our aim is to develop better physics models and provide certified NTS data that will allow validation of the Advanced Strategic Computing Initiative (ASCI)—an important goal of the stockpile stewardship program.

Nuclear physics and astrophysics. The neutrino research effort in P-23 has focused on our continuing role in the Sudbury Neutrino Observatory (SNO) in Ontario, Canada (Figure 2). SNO is searching for three interactions of solar neutrinos: the charged-current, the neutral-current, and the elastic-scattering interactions. Recent results indicated a total neutrino-flux measurement in good agreement with predictions of the Standard Solar Model (SSM). The detection of muon and/or tau neutrinos through neutral current interactions in SNO supports flavor transformation that accounts for the electron neutrino deficit. A second avenue of research into neutrinos is the Majorana experiment that aims to characterize the nature of the neutrino, its mass spectrum, and the absolute mass scale.

A broad and ambitious set of neutron-research projects involves colleagues in P-25 and a host of collaborating universities and institutions. Two of these projects—the NPDGamma ($n + p \rightarrow d + \gamma$) and ultra-cold neutron (UCN) experiments—will soon be commissioned. The NPDGamma experiment will help researchers better understand the nature of weak interactions between strongly interacting hadrons by measuring the parity-violating directional gamma-ray asymmetry to an accuracy of 5×10^{-9}, i.e., to within approximately 10% of its predicted value. This project has involved the design, construction, and commissioning of a pulsed, cold-neutron beam line along flight path 12 (FP12) at the Lujan Neutron Scattering Center (Lujan Center) at the Los Alamos Neutron Science Center (LANSCE). FP12 will also be used, upon completion of the NPDGamma experiment, to measure the electric dipole moment (EDM) of the neutron. The goal of the EDM project is to achieve over two orders of magnitude improvement to the limit of the EDM by using UCNs (produced and stored in a bath of superfluid ^{4}He) and SQUIDs to monitor ^{3}He precession. FP12 may also be used to measure pulsed-cold neutron beta decay as a test of the Standard Model of electroweak interactions. This experiment incorporates an existing ^{3}He spin-filter neutron polarizer and a new large-area spectrometer that are expected to reduce systematic errors to less than 0.1%. Data acquisition for these projects, as for weapons physics (above), has typically driven improvements in detector capability—a hallmark of P-23. We are also collaborators on the Q_{weak} experiment, which will be conducted at the Thomas Jefferson National Accelerator Facility. This experiment will measure the weak charge of the proton in a test of the Standard Model. To do so will require the use of current-mode detection and low-noise, front-end electronics—two areas of our expertise.

P-23 is conducting an equally ambitious program of astrophysics research through its Milagro Observatory located in the Jemez Mountains above

Los Alamos, New Mexico, and by its participation in the High Resolution Fly's Eye (HiRes) experiment located in Utah. Milagro is the first detector of its kind—a large, water Cerenkov extensive-air-shower (EAS) detector—that can monitor the entire overhead sky in the TeV-energy regime. Since its inception, Milagro has successfully detected the Crab Nebula with flux measurements that agree with values obtained using air Cerenkov telescopes. Building on this work, Milagro subsequently was used to produce a TeV gamma-ray map for the entire northern hemisphere. The HiRes experiment looks for cosmic rays of energy greater than 10^{20} eV. HiRes detects the EASs that result from an ultra-high-energy cosmic ray (UHECR) entering the atmosphere using two independent sites (12.6 km apart) to stereoscopically view the fluorescence caused by an event. A third experiment is the Wide-Angle Cerenkov Telescope (WACT) that employs an array of six atmospheric Cerenkov telescopes. WACT measures the lateral distribution of Cerenkov light created by EASs, allowing inference of the nuclear species of the primary cosmic ray. We have also re-examined archival data collected by the Burst and Transient Source Experiment (BATSE) and Energetic Gamma Ray Experiment Telescope (EGRET) satellites to discover a new high-energy component in one of the 24 gamma-ray burst emissions.

Finally, we have recently developed two experimental plans to search for a time variation of the fine-structure constant, alpha. The first plan involves comparison of three atomic optical frequency standards based on ion traps. The second plan involves a dysprosium-atomic-beam apparatus that will enable radio-frequency (rf) spectroscopy rather than optical-frequency metrology.

Our mission has been to solve challenging experimental-physics problems relevant to our national security—aiming to reduce the threat of war by helping to ensure the reliability of our nuclear-weapons stockpile and by limiting the proliferation of weapons of mass destruction. We anticipate many exciting developments in the coming years, including experiments to measure the time variation of the fine-structure constant, new studies into the nonlinear interaction of ultra-short laser pulses with structured fibers, a series of new SCEs at the NTS to be conducted in collaboration with the United Kingdom, and a proposed experiment (Majorana) to measure the fundamental character of the neutrino via double beta decay.

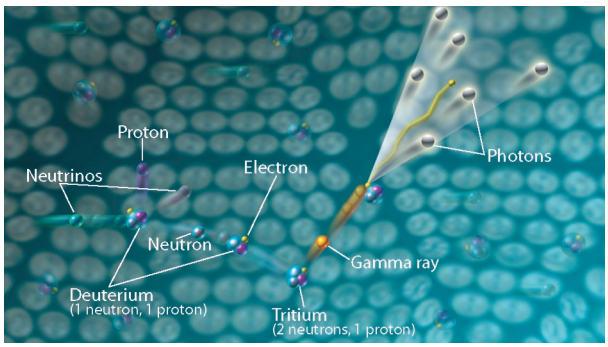

Figure 2. Rendering of the physics inside the SNO, showing one of three neutrino reactions detected by SNO. A neutrino entering the detector interacts with a deuterium nucleus. The reaction produces a proton, neutrino, and neutron. The neutron is captured by another deuterium nucleus, producing a tritium atom in the process. The tritium atom decays and in that process releases a gamma ray, which then collides with an electron. Cerenkov light is emitted and detected by photomultiplier tubes (shown in the background in this image) that line the inside of the SNO vessel.

P-24: Plasma Physics

Cris Barnes, Group Leader
Carter Munson, Deputy Group Leader
Mike Ray, Administrative Deputy Group Leader

The Plasma Physics Group (P-24) has the mission "to nurture and use LANL's core discipline of experimental plasma science in basic and applied research to benefit LANL and the nation." The group applies an extensive knowledge of plasma physics, atomic physics, laser-matter interaction physics, dynamic material properties, laser and pulsed-power technology, and plasma diagnostic engineering and technology—all to study matter in the plasma state. P-24 addresses problems of national significance in inertial and magnetic fusion, laboratory plasma astrophysics, nuclear weapons stewardship, conventional defense, environmental management, and plasma-based advanced manufacturing (see http://www-p24.lanl.gov).

- The High-Energy-Density Physics and Fusion team conducts target-physics experimental campaigns at our own Trident laser, as well as the Omega laser at the Laboratory for Laser Energetics (LLE) (University of Rochester) and the Z pulsed-power facility at SNL. They study physics issues relevant to achieving inertial fusion and relevant to weapons physics and basic high-energy density physics, in particular, in the areas of laser-plasma instabilities, beryllium materials characterization, and the other properties of dynamic materials, fusion-burn diagnosis and capsule implosions, hydrodynamics and mix, and radiation flow and radiation hydrodynamics. The team is developing a variety of diagnostics and experiments for the National Ignition Facility (NIF).
- The Trident team performs experiments relevant to ICF, weapons physics, and basic high-energy-density physics while operating the Trident laser facility (a three-beam, 500-J green laser, now with 20-J sub-picosecond capability) (Figure 1). They also work on advances in laser and optical science.
- The Magnetic Fusion team conducts experiments emphasizing innovative confinement concepts and diagnostics development. The primary focus is a field-reversed-configuration experiment aimed at investigating magnetized target fusion. Other projects include collaborations at the Massachusetts Institute of Technology, Princeton University, and the University of Washington. There is a growing focus on plasma science and laboratory plasma astrophysics, including a reconnection-scaling experiment and a new flowing-magnetized-plasma experiment.
- The Applied Plasma Technologies team applies energetic non-equilibrium plasmas to environmentally conscious and industrially efficient processes, with emphasis on basic physics, commercial applications, weapons-stockpile surety, and homeland defense. The work includes studies on non-thermal atmospheric pressure plasmas and new applications such as plasma combustion and plasma aerodynamics.
- The Diagnostic, Engineering, and Operations team provides engineering and technical support for many of the projects in the group. In addition to supporting experiments and diagnostics used at Omega, Trident, and soon NIF, the team designs, engineers, builds, and maintains diagnostic systems such

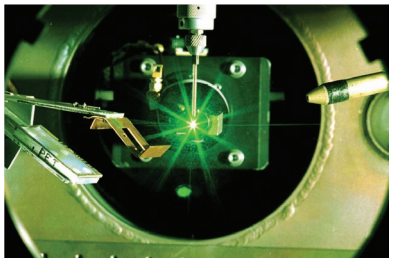

Figure 1. View inside the Trident laser laboratory target chamber. Targets may be illuminated with up to several hundred joules of energy in pulses ranging from picoseconds to microseconds in length.

as x-ray framing cameras, neutron imagers, gas Cerenkov burn-history diagnostics, streaked optical pyrometers, and target positioners. The team also operates a world-class research machine shop and provides photographic laboratory and digitization support.

- Finally, the Administrative team provides secretarial, operational, safety and security, computational and network, and general management support for the group.

In FY 2003, the group employed 81.5 full-time equivalent people on an $18 million budget. The group typically has over 100 people working during the summer months, including a student population of 25 during last summer. To attract and educate these students, challenge and inspire our staff, and provide connections to visiting scientists, we created a more formal Plasma Physics Summer School (http://wsx.lanl.gov/RSX/summer-school/Summer_school_homeage.htm) with twenty-one lectures and seminars. The group maintains a vital post-doctoral researcher program with nine postdocs at present, including a Reines Fellow and a Director's Funded postdoc. The postdoc program has contributed to a demographic staff profile that is nearly flat with age. Twenty percent of the postdocs and staff are foreign nationals as the group maintains a commitment to hiring the best scientific talent to meet its mission. The group recognizes that its future scientific work will involve ever more complicated measurements on complicated experiments. We thus have a significant and growing component of engineering staff in the group and are actively recruiting and hiring a larger proportion of technicians for the group, mostly at the entry level to be trained over the next decade by our outstanding corps of senior technicians.

P-24 is located at TA-35 in primarily six buildings covering a little over 53,000 sq ft. This area includes experimental laboratories for the Trident laser, the FRX-L magnetized-target-fusion experiment (Figure 2), the flowing-magnetized-plasma experiment, the reconnection studies experiment, the Applied Plasma Technologies Laboratory, several laboratories for diagnostic development and checkout (i.e., x-ray sources, materials diagnostics, two laser laboratories, and an optical-diagnostic checkout facility), the machine shop and photo laboratories, and smaller laboratories associated with many of the technicians. Because P-24 is located near the Materials Science Division Target Fabrication Facility and major collaborators for our high-energy-density physics and fusion work and has plenty of parking, the group is well situated for its laboratory infrastructure.

P-24 has strategic objectives in high-energy-density physics, with specific plans to grow LANL's involvement in NIF and in the science campaigns aimed at studying primaries (Campaign 1, or "Boost") and secondaries (Campaign 4). Strategic objectives also include high-intensity short-pulse (sub-picosecond) laser-matter interactions, the properties of materials under dynamic conditions, innovative fusion confinement concepts such as magnetized target fusion, development of laboratory plasma astrophysics, and new applications of non-thermal plasmas. All of these are exciting fields of physics with strong growth potential that can contribute to achieving our vision "to be recognized as a world-leading organization for plasma physics and fusion science and technology, a home of trusted expertise, a place of choice for people to work and visit, and a partner of choice for sponsors and collaborators."

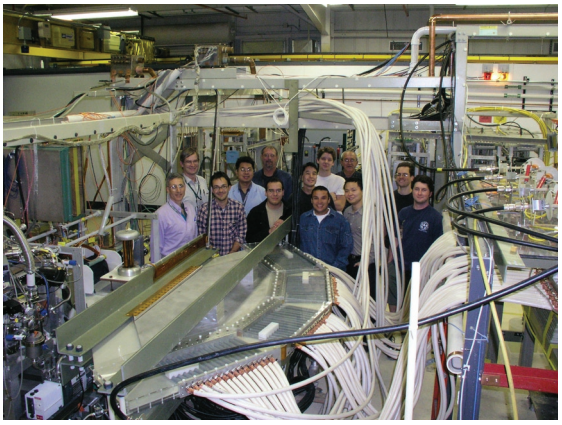

Figure 2. Members of the FRX-L magnetized-target-fusion experimental team, standing behind the collector plate between the main capacitor bank (right) and the field-reversed theta pinch (left).

P-25: Subatomic Physics

Martin Cooper, Group Leader
Mikkel Johnson, Geoffrey Mills, Acting Deputy Group Leaders

The Subatomic Physics Group (P-25) was created in 1994 as part of a reorganization of P Division initiated by former P Division Leader Peter Barnes. The scientific staff of P-25 was formed from P-2 (Medium-Energy Physics) and the research groups MP-4 and MP-10 of the Medium-Energy Physics (MP) Division. The common thread uniting these groups was leadership in investigations of issues of subatomic physics that could be addressed in experiments at a number of accelerator facilities, including the Los Alamos Meson Physics Facility (LAMPF), currently known as the Los Alamos Neutron Science Center; the Fermi National Accelerator Laboratory (FNAL); the European Organization for Nuclear Research (CERN); and the Superconducting Super Collider (SSC). Because of the diverse physics being conducted in MP-4, MP-10, and P-2 and tight funding at the time, it was clear that the group would have to undergo a consolidation of its research priorities. John McClelland (now Deputy Director for Experimental Physics in the Weapons Physics Directorate at LANL) was the first group leader of P-25, and under his direction the research priorities were narrowed and about half of the group redefined its area of focus.

A number of the programs and projects described below are featured in this report. As noted, P-25 staff members often participate in large-scale collaborations that involve physicists from universities and institutions from around the world, and the group contributes to or leads experiments at a variety of facilities. The intellectual atmosphere in the group is enhanced by local workshops and students who come to participate in the research and by a small theory group that brings in numerous theory visitors involved in research areas of interest to the group.

New themes in P-25 became studies of fundamental issues of the Standard Model (the primary focus) and the search for a basis for stronger collaborations between fundamental physics and the weapons community. The group's current experimental activities emerged during the mid 1990s. Neutrino physics, with an emphasis on searches for neutrino oscillations, now focuses on the MiniBooNE experiment at FNAL (Figure 1). This experiment is the first phase of the larger Booster Neutrino Experiment (BooNE) that will definitively test results from the Liquid Scintillator Neutrino Detector (LSND) (which took data from 1993-1998 at LAMPF) to confirm neutrino oscillations and will precisely measure the oscillation parameters. This experiment will also test CP (charge conjugation/parity transformation) and CPT (the combined operation of charge conjugation, parity inversion, and time reversal) violation in the lepton sector and will explore new methods of detecting "double beta decay" of nuclei to further understand the nature of the neutrino. In addition to neutrino studies, P-25 is involved in the relativistic-heavy-ion investigations currently under way at the Relativistic Heavy

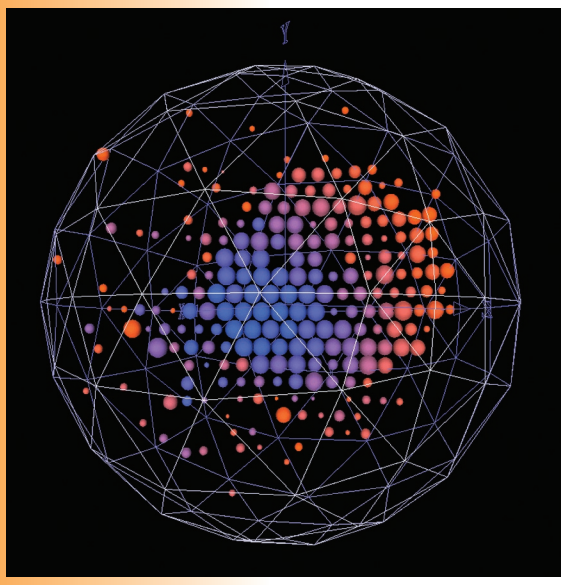

Figure 1. The colors in this typical MiniBooNE neutrino event relate to elapsed time—the blue represents early photomultiplier-tube (PMT) hits and the orange represents later PMT hits. In this particular data event, there were fewer than six veto hits and over 200 tank hits.

Ion Collider (RHIC) at BNL. The goal of these investigations is to create and to study the exotic properties of a primordial quark-gluon plasma in a laboratory. This activity was an outgrowth of the successful relativistic-heavy-ion program at CERN, which was under way in P Division at the time P-25 was formed, and the joint research program in P and MP Divisions to study Drell-Yan and charmonium physics at FNAL.

Another theme in P-25 involves neutron physics at LANSCE, which is aimed at studying symmetry violation and searching for physics beyond the Standard Model. Members of P-25 are currently searching for the EDM of the neutron, which was an outgrowth of early work in fundamental symmetries. Proton radiography—a technology that images dynamic variations of macroscopic objects over small time intervals with millimeter spatial resolution—is a new activity that was inspired by P-25's familiarity with accelerator physics and its understanding of advanced detectors for imaging and handling high data rates (Figure 2). (Application of the same underlying principles is also contributing new ideas for homeland defense.) P-25's pRad program has three goals: (1) to demonstrate that high-energy pRad is a suitable technology for meeting the goals established for the advanced radiography program, (2) to advance the technology of charged-particle radiography, and (3) to apply 800-MeV pRad to the needs of the science-based stockpile stewardship program. Members of the pRad team recently commissioned a new radiography system that images dynamic events with an order of magnitude higher spatial resolution and another system that significantly improves the sensitivity to thin objects. A prototype electron-radiography system, designed by P-25 and constructed at the Idaho Accelerator Center (IAC), was used to continue investigations in the use of electrons as direct probes for static and dynamic radiography of thin systems. Other projects and activities are listed below:

- The development of a silicon vertex detector upgrade for the PHENIX (Pioneering High-Energy Nuclear Interaction Experiment) detector at RHIC enhances the capability for studying the gluon distributions in colliding nuclei and the early evolution of the formation of the quark-gluon plasma by directly detecting heavy quark decays.
- The first measurement of the Drell-Yan cross section in p-p collisions over a broad kinematic range has been made, and the most extensive study of p-d collisions uncovered a pion cloud-like feature of the nucleon.
- In an investigation of spin physics at the RHIC, members of P-25 successfully measured J/Ψ production with the newly installed south muon detector from the first polarized p-p collisions at RHIC.
- P-25 is collaborating with P-23 to provide better sources of UCNs—neutrons that can be trapped by ordinary materials and then used for a variety of experiments probing fundamental quantities with high precision.
- In the first test of an experiment aimed at improving the limit on the EDM of the neutron, the properties of dilute mixtures of ^{3}He in superfluid ^{4}He and a measurement of the diffusion coefficient for ^{3}He were made—this work led to a Laboratory Distinguished Performance Award for the UCN team.
- The HiRes experiment at the Dugway Proving Grounds in Utah is measuring UHECRs ($> 10^{18}$ eV) with detectors sensitive to the air fluorescence of showers caused by cosmic rays entering the atmosphere—HiRes will ultimately help researchers understand the types of mechanisms that can produce such energies.
- Recent theoretical activity in P-25 has focused on parity violation in chaotic nuclei, deep inelastic scattering and Drell-Yan reactions as a means to explore quark propagation in nuclei, quantum chromodynamics (QCD) at finite temperatures, and phase transitions in the early universe.
- P-25 is making numerous contributions to homeland defense based on novel applications

Figure 2. Members of P-25 performing calibration tasks before a pRad shot.

of nuclear physics techniques, including muon radiography and Compton-gamma-ray imaging—both of which are high-sensitivity detection techniques that could aid in the surveillance for contraband special nuclear material—and VLAND (Very Large Area Neutron Detector), which applies neutrino detector technology to the identification of special nuclear materials.

- P-25 group members continue to be active in education and outreach activities, both as participants in programs sponsored by LANL, whereby high school, undergraduate, and graduate students work on projects within the group, and as individual citizens who volunteer their time for various activities (visit http://users.hubwest.com/hubert/mrscience/science1.html for information for an example of this activity).

The cutting-edge science described here not only advances fundamental knowledge and spawns creative ideas for new technology, but it also is a key ingredient of LANL's ability to attract and retain the high-caliber talent it needs to fulfill its mission of national security.

Physics Division Interactions with Industry and Technology Transfer

D.M. Coates
(Physics Division Office)

Commensurate with the fact that the DOE has made technology transfer a priority for its national laboratories, P Division is aggressively pursuing partnerships with industry to transfer Division-invented technologies into the private sector. Additionally, P Division's efforts are complementary to a recent request by Laboratory Director Pete Nanos that we leverage industrial partnerships to make critical performance improvements for executing Divisional business plans. It is gratifying that the range of technologies that P Division is grooming for transfer to industry is quite broad. Described below are some of these technologies.

Technology Highlights

Muon radiography for detection of clandestine nuclear material. Muons, elementary particles that shower down on the earth, hold promise as a sensitive means of detecting nuclear materials being smuggled into the country. These charged subatomic particles are produced when cosmic rays strike air molecules in the upper atmosphere. A team of LANL scientists has developed a way to use muons to detect terrorist attempts to smuggle uranium or plutonium into the country. The technique, known as muon radiography (Figure 1), also detects lead and tungsten, which could be used to shield the gamma rays emitted by nuclear materials. Muon radiography tracks the scattering angles of the particles as they pass through material. High-*Z* materials produce much more muon scattering than do lower-*Z* materials. Particle detectors above and below a vehicle or container record each muon's path before and after the muon passes through the cargo. A change in the muon's trajectory means that the muon has been scattered by the cargo. Using the path information and muon-scattering theory, a computer program then constructs a three-dimensional image of the cargo's dense, high-Z objects. We are in the process of transferring information to a number of companies interested in commercializing the technology. In addition to outside companies, the Department of Homeland Security is highly interested in the technology for national security reasons. A patent on the technology is being drafted by the DOE.

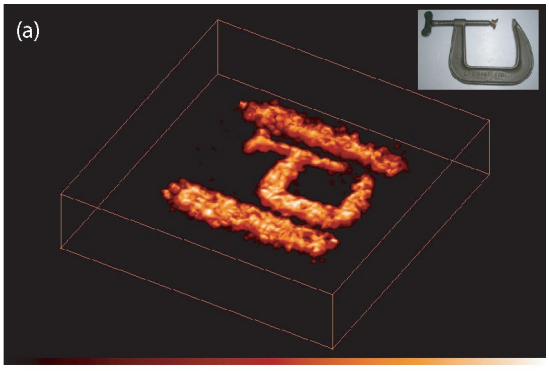

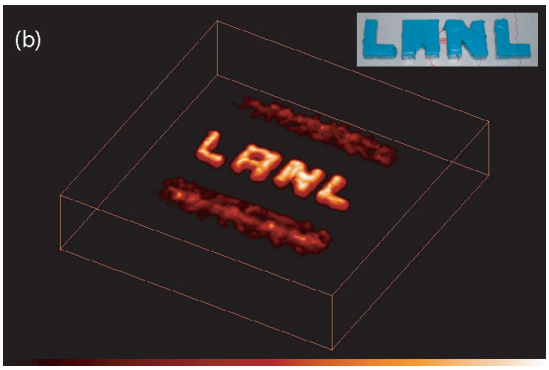

Figure 1. Experimentally produced cosmic-ray muon radiographs of (a) a steel c-clamp and (b) the acronym "LANL" constructed from 1-in.-lead stock. The bar-like features visible on either side of the images result from steel beams used to support a plastic object platform. This work was carried out at LANSCE.

Advanced combustion technologies using atmospheric plasmas. Fuels are broken down (cracked) into smaller molecular fragments, boosted into reactive excited states, or made into "free-radicals," before combustion with a highly efficient plasma technology. This technology allows for very "lean-burn" modes of combustion to be used for reduction of NO_x—a highly desirable feature of the technology. "Proof of principle" has been demonstrated in experiments using propane as the fuel in a specially made plasma chamber/burner

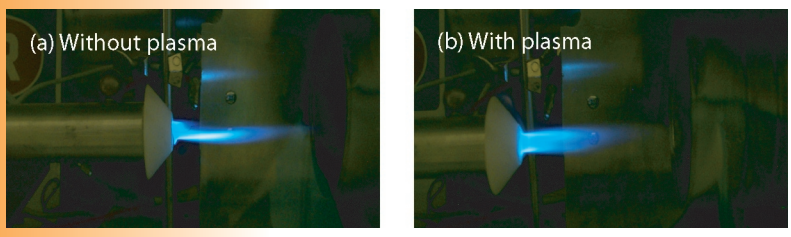

Figure 2. Illustration of the coaxial dielectric-barrier, non-thermal plasma reactor used in the combustion enhancement studies. Figure 2(a) shows the propane air flame without plasma, and Figure 2(b) shows the more robust flame with plasma.

device (Figure 2). The technology has been advertised and information exchange is in progress at this time. Interested companies include two major auto manufacturers and a company that is exploring the concept for forming a new company around the technology. A number of patents have been filed on the technology and other uses, such as ozone generation for water treatment and the destruction of hazardous air pollutants, are being considered as another manifestation of the technology.

High-efficiency compact turbine engine. A unique turbine engine configuration that offers many potential improvements, including fuel efficiency, more compactness, and lower manufacturing costs, has been invented. The Advanced, Single-Rotor Turbine (ASRT) engine achieves these improvements through use of a new flow-path strategy that results in superior cooling of the critical turbine section. The ASRT channels intake air from the compressor through the hollow turbine blades on its way to the combustion chamber (Figure 3). This design cools the critical turbine section of the engine and allows the engine to operate at higher temperatures, thus using its fuel much more efficiently. Alternatively, it allows the engine to operate at current temperatures but be constructed from cheaper, lower-temperature alloys. The one-piece compressor/turbine reduces engine complexity and weight. We are working with DOE to explore the design and commercialize the engine. Two turbine companies are in negotiation with us for a CRADA (Cooperative Research and Development Agreement) to develop the concept. Although the ASRT engine can have impact in aircraft auxiliary power units, in distributed power strategies in the home and small business, and as an aircraft thrust/propulsion unit, its first application may be for the U.S. Army as a battlefield power-generation unit. The patent portfolio for the engine is growing beyond the first issued application with filings on turbo-machinery applications and improved combustor designs.

INFICOMM—Power-efficent wireless technologies for cell phones, telemetry, and rf identification. The growth of wireless may ultimately be limited by the dependence of cell phones on battery power. While battery technologies have advanced over the past decade to allow for much smaller telephones, typical "talk" times are currently limited to around

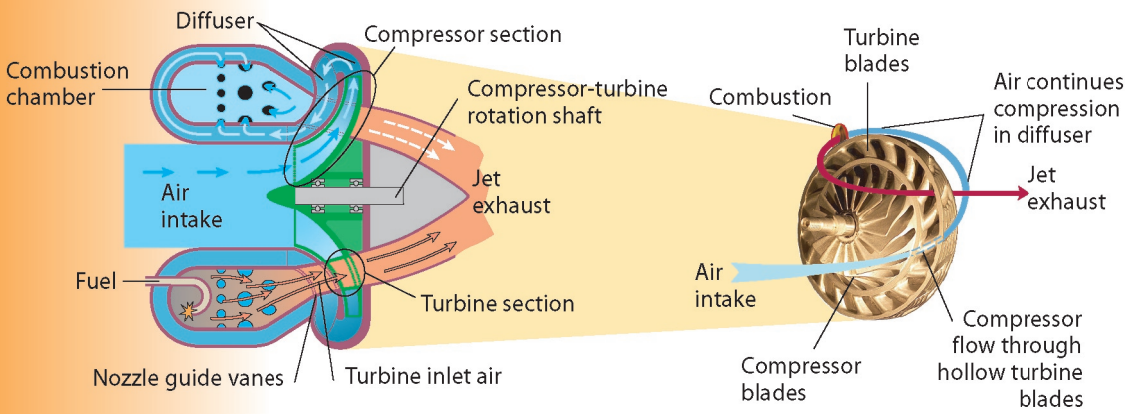

Figure 3. Composite drawing of the ASRT schematic and photo, showing how the ASRT operates. Air from the compressor section of the ASRT is channeled through the outer hollow turbine blades on the same rotor. The air, on its way to the combustion chamber, cools the turbine section allowing the engine to operate at higher temperatures. The fuel efficiency is increased in this case.

2 to 4 hours and "standby" times are from 20 to 40 hours. For many cell-phone users, the battery is insufficient for voice services and expanded wireless capabilities. Researchers at LANL have developed a wireless communications technology, known as INFICOMM, that provides expanded wireless voice and data applications via essentially unlimited battery life, eliminates potential health risks of rf energy, minimizes impact of battery disposal on the environment, and lowers cell-phone costs. This unique technology uses "modulated-reflection" technology (i.e., the reflection of rf energy provided by a tower's transmissions reflected off of the cell phone's antenna to carry the return half of the communication). This strategy thus reduces or eliminates the cell phone's need for battery power consumption for its transmissions back to a tower. The technology has broad applications in many areas, including cell phones, telemetry, and rf identification systems. We are working with Chevron-Texaco on a CRADA to explore the technology for sending sensor telemetry from down-hole to above ground. The patent portfolio has been growing and should include four patents with the originally issued patent.

KEYPATH—Using atmospheric turbulence to generate and exchange cryptographic keys. A new cryptographic-key-transmission technology for laser-through-air modes, known as KEYPATH, has recently been declassified and is being advertised to the communications industry. The technology uses a unique strategy for creating distinct key codes that cannot be intercepted by any known means and should be invaluable for sending the codes to satellites. We have recently opened dialog with companies on the technology, and initial responses to this new technology have been enthusiastic. A patent application on the technology is in draft. Members of P-22 are taking measurements over paths of varying lengths to demonstrate the effectiveness of the system.

Magnetocarcinotheropy. A magnetic-based method of detection and treatment of cancer has been invented and has been discussed with a wide range of companies. A patent has been issued on the technology. Although most companies are enthusiastic about the technology, delays in actually demonstrating "proof of principle" of the technology have caused companies to feel that the risk of jumping in as a partner is too high at this early stage of exploration. Hence, we will likely have to move the technology further before we lower the risk level to the point that companies will fund efforts around the technology.

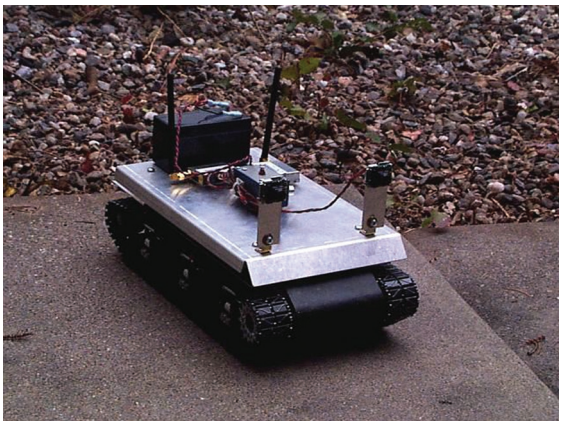

Figure 4. Prototype robot guided by a new vision system invented by researchers at LANL.

Robotic vision using biological theoretical principles. Researchers at LANL have invented an exciting vision system derived from biological vision processes. The system, resulting from LANL expertise in electrical engineering, parallel processing, and computational neuroscience, demonstrated a novel approach to traditional problems in computer vision such as the "aperture" problem and motion disruptions that occur during a robot's steering operations. The vision system guided a prototype robot (Figure 4) around an unknown obstacle course in a fully autonomous configuration, in many ways surpassing the state of the art in conventional computer-vision techniques. The current system was implemented on a Linux cluster with future plans to move to a fully custom analog or digital hardware system. We are currently engaging the robotics industry to use our method in commercial products.

Electromagnetic geophysical research. Researchers at LANL are pursuing four distinct, yet electro-magnetically related, geophysical applications in cooperation with an industrial partner, Stolar Research Corporation. The first is a portable instrument that has been devised for detecting both dielectric and conductive buried landmines. The principle involved requires the interference between an incident electromagnetic wave, its ground-reflected component, and the scattered wave from the landmine. The sensor is a patch antenna whose impedance changes in the presence of the scattered wave. The second application is a

ground-penetrating radar for coal mining. Coal-mine operations generally occur in stratified layers where avoiding cutting into rock layers beyond the coal-rock surface is important. A sensor placed in the cutting drum could measure the thickness of coal layers by detecting standing waves produced by a near discontinuity in the dielectric constant and conductivity of the two layers. A third geophysical application involves the development of magnetic-induction methods to locate and determine the depth of the subsurface line source of a magnetic field. The origin of the field may be self-generated or -induced by a surface transmitter. The latter requires the generation of a low-frequency electromagnetic wave that scatters off the structure (such as a tunnel), part of which returns to the surface. The weak-scattered wave is generally in the background noise but may be detected by measuring the field gradient (i.e., the spatial rate of change), thereby greatly increasing the signal-to-noise ratio. Both detection and depth result from the sensor output. The fourth geophysical application involves tunnel communications. Radio communications in tunnels generally are very inefficient because of factors such as mode interference, waveguide cutoff, and wall attenuation. Success has been achieved by using low-frequency surface waves coupled into parallel tunnel conductors by means of a transmitter driving a magnetic dipole antenna. The surface waves consist of inhomogeneous transverse electromagnetic waves that are guided by any conductor parallel to the tunnel walls. Reception is achieved by a similar small-loop magnetic dipole feeding a radio receiver. The primary application of this method of tunnel communications is for mine safety with special emphasis on communication during fires.

Conclusion

The range of technologies that P Division is pursuing with industry is indeed broad and spans diverse arenas, including the prevention of nuclear-weapons entry into the U.S., new communications methodologies, energy/propulsion systems, and advanced cancer detection and treatment technologies. We believe that P Division is leading the way in meeting the LANL objective of creating and transferring important and commercially exciting technologies to the industrial sector. Such technologies will aid in giving the U.S. economy the leading-edge technical advantage it needs to remain in world leadership.

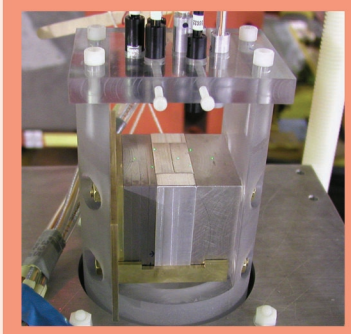

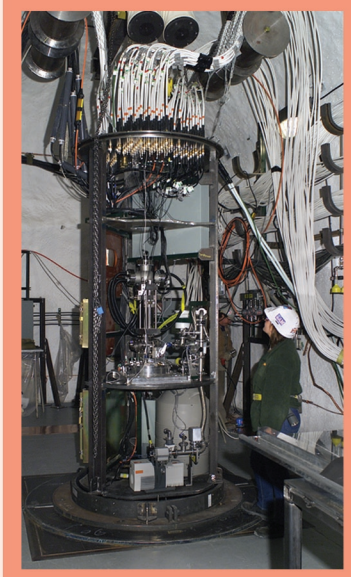

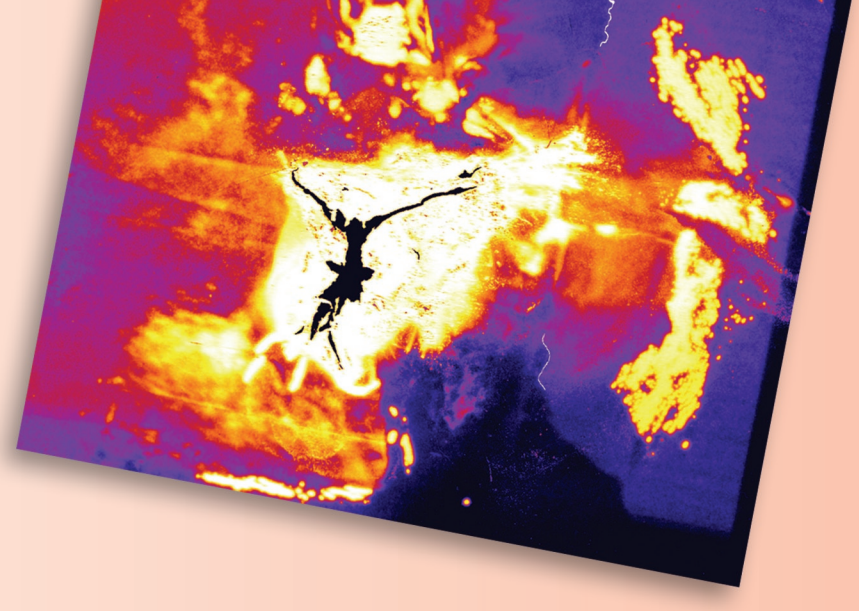

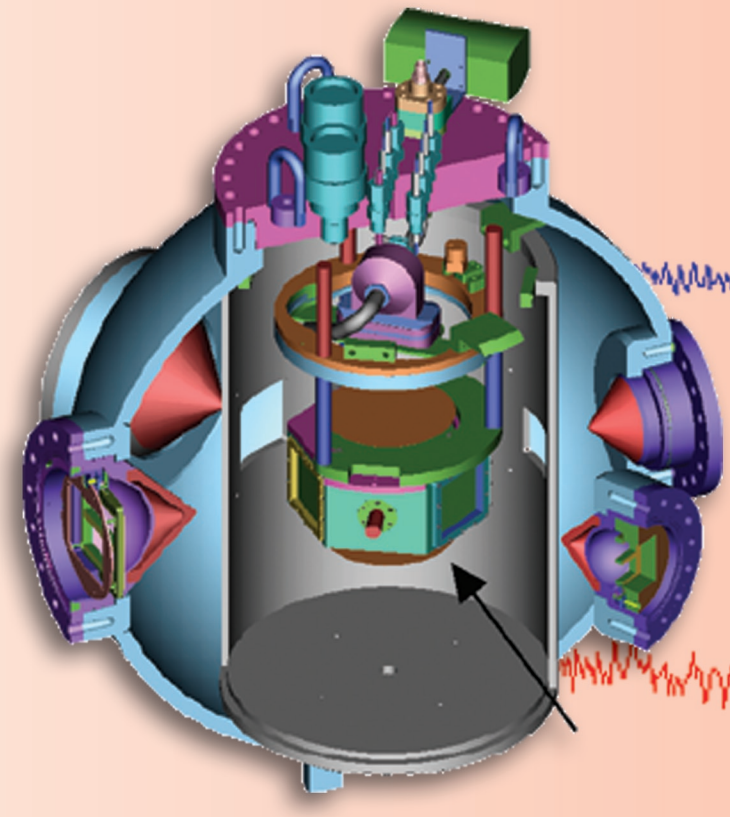

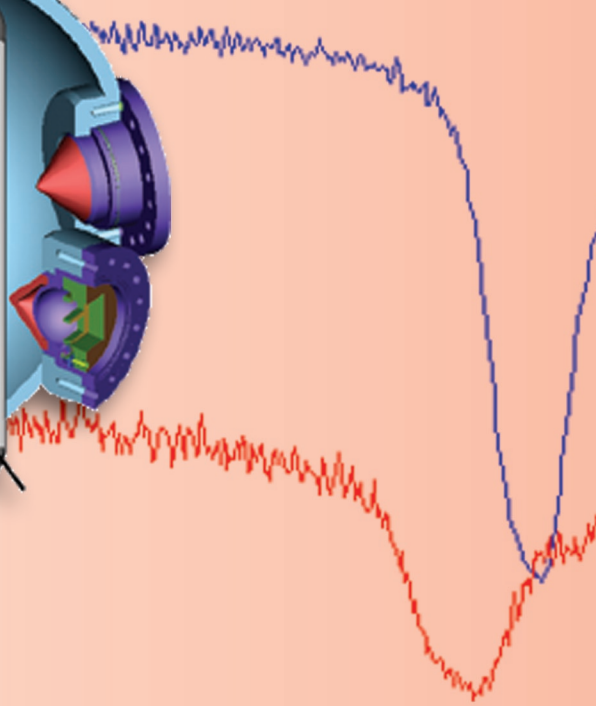

Material Studies

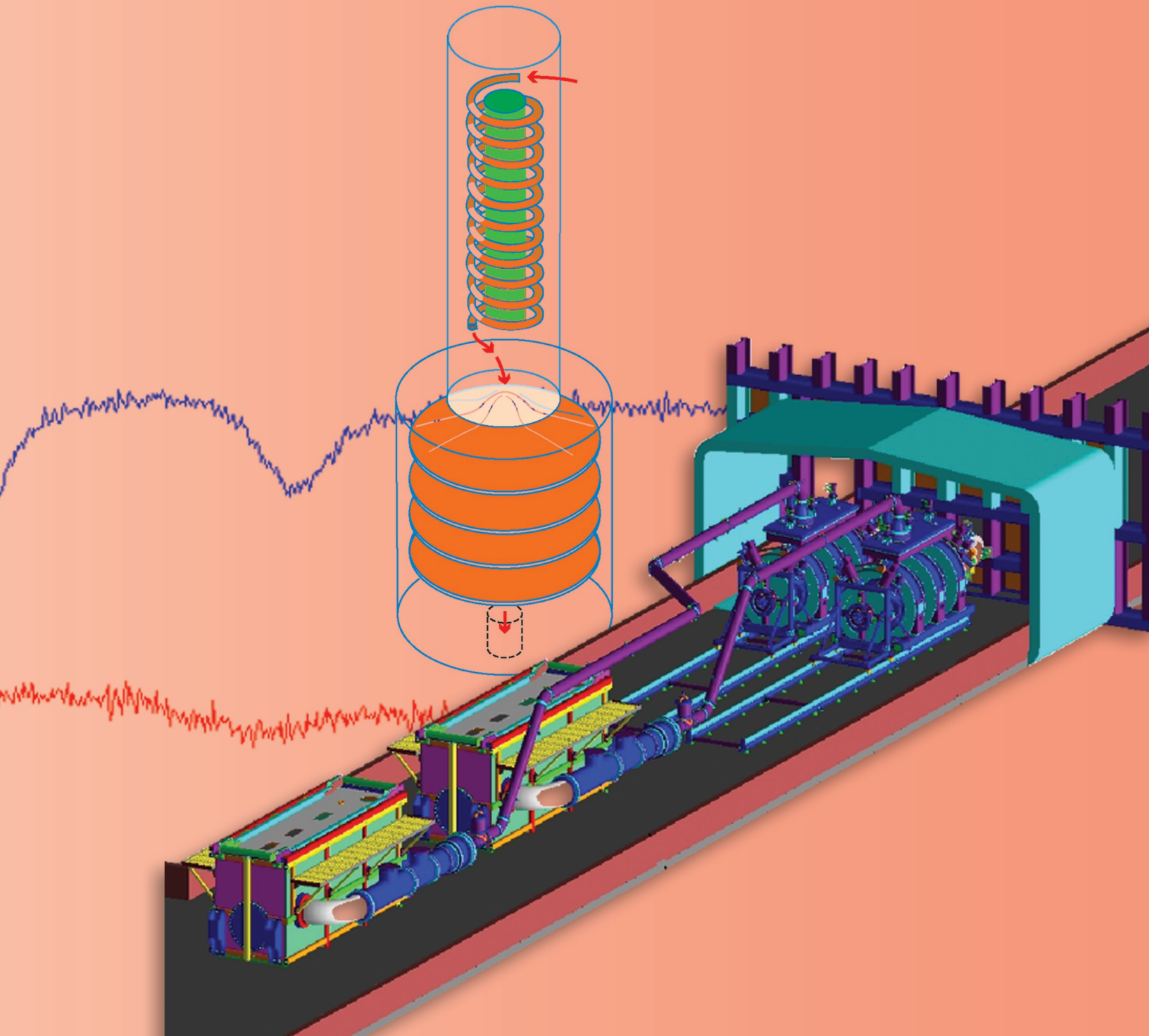

Material Studies Contents

Research Highlights

Dynamic Material Studies in Subcritical Experiments: Rocco, Mario, Vito, and Armando 23
High-Strain-Rate Experiments to Determine the Dynamic Yield Strength of Copper 27
Basic Material Properties Using Laser-Driven Shocks 31
pRad VISAR: An Interferometer-Based Optical Diagnostic for Proton Radiography 35
Temperature of Shocked Materials 39

Project Descriptions

Ejecta Density Measurements Using Soft X-ray Radiography 43
Cross Validation of Ejecta-Areal-Density Measurement Techniques 43
Surface-Temperature Measurements Under Shock Compression 44
Fundamental Properties of Beryllium for ICF Applications 44
High-Speed Pyrometry Measurement of Shocked Tin and Lead 45
Subcritical Experiment Diagnostics 45
SNM Midcourse Detection 46
Sputtering from Fission Fragments 46
Laser-Driven Flyer Plates Generate Shock Waves in Weapons Materials 47
In-Line Holography for Ejecta Particle Size Measurements 47
Equation of State of Beryllium 48
Quantitative Ejecta and Timing Diagnostic Studies 49
Friction Studies at pRad 50
Measurements of the Dynamic Properties of Beryllium Benefit the ICF and Weapons Program 50
Failure-Mechanism Studies of Depleted Uranium Using Proton Radiography 51

Dynamic Material Studies in Subcritical Experiments: Rocco, Mario, Vito, and Armando

R.D. Fulton, M.D. Wilke, N.S.P. King (P-23), representing the Subcritical Experimental teams from Los Alamos National Laboratory, the Atomic Weapons Establishment, Bechtel Nevada, and Sandia National Laboratories

Members of P-22 and P-23 in collaboration with DX, ESA, MST, and X Divisions and with international and national organizations designed and executed a series of SCEs, known as the Stallion series (Vito, Mario, Rocco, and Armando). Mario and Rocco were executed to evaluate the properties (principally strength) of cast and wrought plutonium samples driven by high explosives. Vito was conducted primarily to look at ejecta in a particular region of a weapon. The cast and wrought samples used in our experiments were representative of the materials produced via the different manufacturing processes employed at Rocky Flats and LANL. The specific properties investigated in this series included ejecta production, spall features, and surface temperatures. "Ejecta" is small particulate matter that is "ejected" from the surface of a solid when a strong shock wave interacts with the surface. "Spall" is a general term used for bulk-material failure at the surface of a solid created by a strong shock interacting with the surface. Both ejecta and spall formation depend upon, for example, material strength, grain size, impurities, and other material properties and upon the strength and temporal profile of the shock pressure. An important constraint upon the final state of a shock-driven metal is the surface temperature—which will help further our understanding of the behavior of shocked material.

Vito—Demonstrating a New Technique for the Rapid Turnaround of Subcritical Experiments

Vito, the first SCE in the Stallion series, was fired successfully on February 14, 2002, in the U1a complex at NTS.[1] The experiment—a very successful collaborative effort with LANL, Bechtel Nevada, and the Atomic Weapons Establishment (AWE)(United Kingdom)—achieved a number of important milestones, including the re-establishment of a long-standing LANL-AWE collaboration in performing experiments at the NTS. These historical experiments had been closely aligned with joint theoretical and experimental weapons physics objectives, which are now more focused on maintaining a nuclear-weapons capability without nuclear testing. The second milestone achieved by Vito was a highly successful demonstration of the LANL "racklet" technique (Figure 1). This technique permits the rapid and cost-effective turnaround between SCE experiments with a reuse of diagnostic "clean-room" areas downhole.

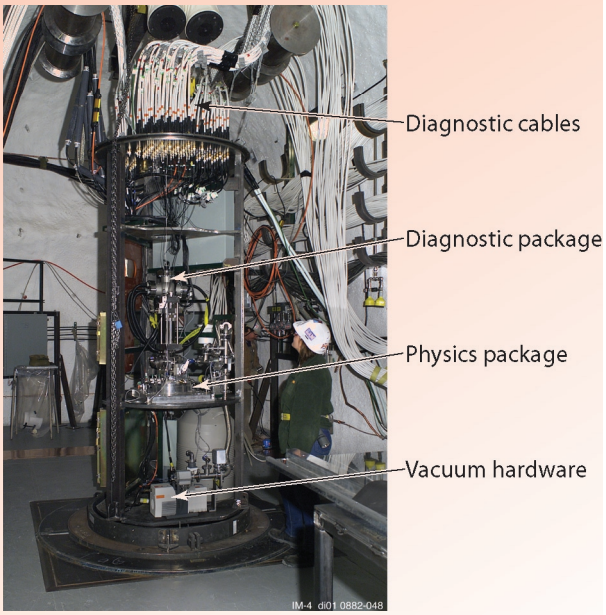

Figure 1. The Vito racklet assembly before it was lowered into the confinement hole.

We obtained a unique data set of high-quality measurements by combining LANL-AWE experimental techniques. Piezoelectric probes[2]

and Asay foils coupled with a laser and streak camera system to record Fabry-Perot and VISAR signatures[3] led to results that enhanced our understanding of the generation of ejecta particles and the distribution of spatially dependent surface velocities. AWE and LANL each provided specialized diagnostics for characterizing the detonation properties of the physics package. Both the physics and the diagnostic packages were shipped separately to the NTS from the AWE and were assembled and installed in the U1a complex. A small team of engineers and diagnostic specialists from AWE were the primary leads for the physics package and the diagnostics measurements. (Improvements to the timing and firing system resulted in an optimized system for future SCEs.) LANL provided electronic readouts for streak cameras that resulted in excellent signal-to-noise ratios in the AWE Fabry-Perot-based velocity measurements. LANL specialists also fielded a VISAR system for data comparison.

In the newly tested racklet technique, both fiber optic and electrical cables enter the experimental chamber from the lid and are routed to the timing and firing system, the energy-release package, the physics package, and the diagnostic package. The diagnostic cables are routed through a secondary containment bulkhead to recording and clean rooms that house digital oscilloscopes, streak cameras, and lasers. We procured special auger equipment to drill a 5-ft-diam, 35-ft-deep confinement hole into the drift invert (tunnel floor). In preparation for the Vito event, the racklet assembly was lowered into a canister that had already been placed into the augered hole to protect the experiment from the surrounding material that would fully confine the experiment. After the Vito event, the cables were cut and moved to a neighboring hole for reuse in another experiment.

Figure 2. Schematic of the diagnostics used on the Mario and Rocco SCEs.

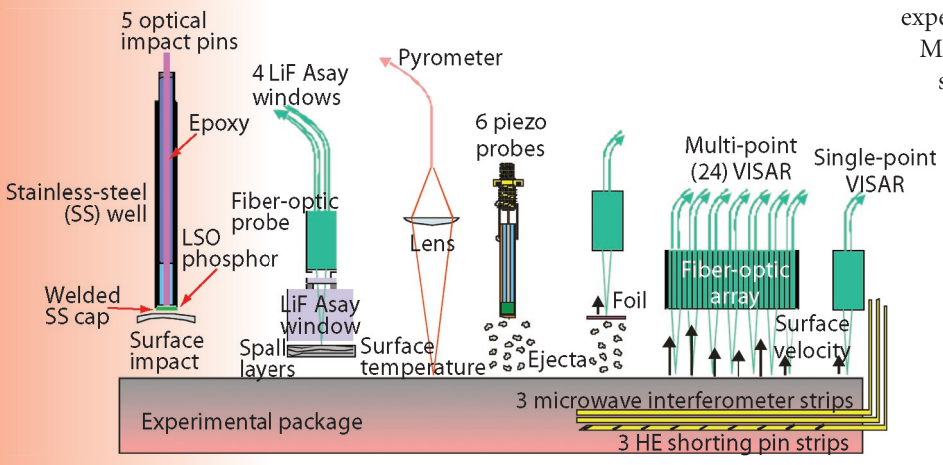

The Vito event demonstrated the success of the racklet technique for SCEs. Through repeated subsequent SCEs, the overall efficiency of the technique was improved, and it now provides a LANL-demonstrated rapid-turnaround capability for the U1a complex. The success of the Vito event resulted in the design of a more complex follow-on collaborative experiment with AWE at the NTS U1a complex.

Mario and Rocco—Addressing the Generation and Dynamic Development of Spall

Mario and Rocco followed the Vito experiment in a collaboration that involved personnel from LANL, SNL, and Bechtel Nevada. The P Division experiments provided important data related to spall, ejecta, and the surface temperature of shocked plutonium in a weapons-relevant geometry. The Rocco and Mario diagnostics and package designs were identical, but Rocco provided data on the physical property of cast plutonium at conditions approaching those found in nuclear weapons to complement the data on wrought plutonium obtained from the Mario experiment.

Like Vito, Mario and Rocco used the racklet technique (described above) for deployment and execution of the physics experiments. But unlike Vito, two "confirmatory" experiments were executed as "dry runs" for Mario and Rocco in 6-ft-diam confinement vessels in the "G" drift region of the U1a complex. Normally conducted at LANL before being executed at the NTS, these confirmatory experiments were conducted at the NTS to better match component delivery schedules, to save time in setting up the diagnostic recording systems, and to eliminate the need to build recording cable plants at both LANL and the NTS. The confirmatory experiments and diagnostics were identical to Mario and Rocco except for the confinement spheres and the use of specially designed surrogate alloys instead of plutonium. Because these surrogate alloys exhibited some of the properties of plutonium, the confirmatory experiments were not only important as dry runs for Mario and Rocco, but they also provided useful data to help interpret the data from Mario and Rocco. The combination of the confirmatory experiments and the actual events were executed with rapidity reminiscent of the heyday of underground nuclear testing.

The Mario and Rocco experiments addressed material-physics issues (in particular, the generation and dynamic development of spall) that were used in computer simulation codes to model the nuclear-explosion process. The high-quality data obtained from Mario and Rocco were important both for their significance to the SCE program and for execution of the upcoming Armando SCE (described below), which will image identical experimental packages via x-ray radiography to measure the spatial distribution of the spall layers. Rocco used the same diagnostic suite as Mario to make a direct comparison between the behavior of wrought and cast plutonium under shock conditions.

The diagnostics used in the Mario and Rocco shots (Figure 2) included line VISAR, point VISAR Asay foil (which measures ejecta mass), Asay windows, piezoelectric probes, optical pins, and infrared pyrometry. Electrical pins and flat Mylar microwave-interferometry strips inside the high explosive measured its performance. P Division and SNL developed the Asay-window diagnostic for the Mario and Rocco experiments. Information on the state and thickness of the spalled layers below the target surface can be inferred by allowing these layers to collide in a "domino fashion" into an LiF window and by observing the change in velocity of the metal-LiF interface. A number of small high-explosive-driven experiments were conducted in firing chambers at DX and at the LANL pRad facility to validate individual diagnostic techniques, particularly the Asay window technique, with modeling support from X Division.

Armando—Verifying Surface Behavior Observed on Mario and Rocco

Armando—the last of the SCEs in the Stallion series to be executed in April 2004—will use a reduced set of the diagnostics deployed on Rocco and Mario, including point VISAR, surface velocity diagnostics, and optical pyrometers, to verify the behavior of the target surface observed in the Rocco and Mario shots. The primary diagnostic for Armando will be x-ray radiography along two equivalent axes separated by 60°. Physics packages identical to those used in the Rocco and Mario shots will be combined in a hexagonal (HEX) package (six sides) vertically separated with the free surfaces facing one another. This geometry will allow us to obtain equivalent x-ray radiographs of the two materials at the same time in their dynamic evolution. The third axis of the HEX package will be used for VISAR and pyrometry access.

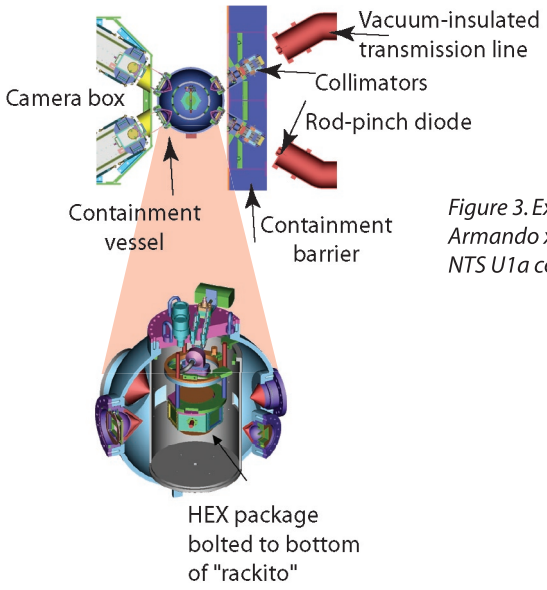

Figure 3. Experimental layout of the Armando x-ray radiographic system at the NTS U1a complex.

The experimental package will be in a 3-ft-diam (inside diameter) confinement vessel. This vessel and a camera box that houses an x-ray-to-light-converting scintillator and camera system will be placed within a "zero room" created by a large bulkhead. (The term "zero room" is derived from "ground zero"—the location on the surface beneath which a nuclear event was detonated in the days of underground testing. The SCE is contained within the zero room.) Thin radiographic windows in the bulkhead and confinement vessel allow x-rays to pass through the package and the confinement vessel with minimal attenuation (Figure 3). By fielding the experiment within a confinement vessel, the zero room can be reused for multiple experiments.

The Cygnus x-ray sources (Figure 4) will extend down a drift external to the zero room. These sources will be composed of a Marx bank system, which will be contained in a large oil-filled tank that will pulse-charge an adjacent pulse-forming line (PFL). The output of the PFL will be a short (60 ns), large-amplitude (1 MV) electrical pulse that will propagate down an 8-in.-diam, water-filled, coaxial transmission line. This electrical pulse will be coupled into inductive voltage adder cells that will add the voltage in parallel to produce a 2.25-MV low-impedance drive pulse for the rod-pinch diode. This last stage of voltage addition will be accomplished in a high vacuum suitable for diode operation.

The radiography that will be used on the Armando SCE represents a significant leap in performance. It

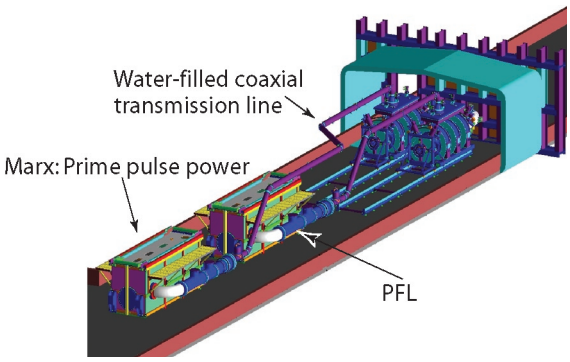

Figure 4. Layout of Cygnus x-ray sources in the U1a.05 drift (tunnel) at the U1a complex.

has been the result of a multi-year, multi-laboratory effort involving LANL, SNL, AWE, Bechtel Nevada, the Naval Research Laboratory (NRL), the Titan Corporation Pulse Sciences Division, and the Mission Research Corporation. Many innovations have combined to lead to this leap in performance, but perhaps the most important has been the effective realization of the rod-pinch diode originally developed at NRL. The rod-pinch has a similar geometry to standard x-ray diodes that have been used in industrial flash x-ray sources for several decades. However, NRL discovered that, when operated at low impedance (large currents at ~ 40 kA), the diode would transition from classic space-charge-limited flow into magnetically limited flow, whereby the electrons would be transported to the end of the central anode rod and then "pinch," thus producing a very bright, small diameter x-ray source. The Cygnus x-ray source was designed to provide a low-impedance source of voltage to effectively drive the diode into the magnetically limited regime. Measurements have demonstrated a 1-mm-diam x-ray spot that produces 4 rad at 1 m in a reproducible manner.

The detector system is equally innovative. It combines technologies developed for DARHT and pRad to create a very high-resolution imaging system. The detector converts the x-rays transmitted through the experimental package into visible light in a tiled, cerium-doped LSO (lutetium oxyorthosilicate) scintillator, which makes the high efficiency and high resolution of the detector system possible. The light produced is transported by a lens system to an LN_2-cooled charge-coupled-device (CCD) chip that captures and records the image. To preserve maximum image resolution, the combined CCD camera system is not gated; all time resolution therefore derives from the flash nature of the illuminating x-ray pulse. The scintillator-camera combination must, however, be maintained in a light-tight configuration throughout the high-explosive detonation and long enough thereafter (~ 30 s) for the information to be read out of the CCD camera system to a remote data-logging computer.

Conclusion

To date, the Stallion SCE series has provided high-quality information of critical importance to the LANL design effort while simultaneously helping to reinvigorate the mutually beneficial collaboration with AWE on weapons-physics experiments. Execution of the final experiment in the series—Armando—will provide high-quality radiographic data previously unobtainable and will result in a facility that is ideally suited to further investigate the dynamic properties of plutonium under shock loading.

References

1. N.S.P. King, "The Vito/Etna subcritical U1A experiment," *Weapons Insider* **9(1),** 1–2 (2002).
2. C.S. Speight, L. Harper, and V.S. Smeeton, "Piezoelectric probe for the detection of shock-induced spray and spall," *Review of Scientific Instruments* **60(12),** 3802–3808 (1989).
3. J. Asay and M. Shahinpoor (Eds.), *High-pressure shock compression of solids* (Springer-Verlag, New York, 1993).

Acknowledgment

These types of experiments could not have been performed without the efforts of a large number of colleagues from DX, P, ESA, MST, and X Divisions at LANL and from SNL, Bechtel Nevada, and the AWE. This work was sponsored by DOE Defense Programs.

For more information, contact Robert Fulton at 505-667-2652, fulton_robert_d@lanl.gov.

High-Strain-Rate Experiments to Determine the Dynamic Yield Strength of Copper

R.T. Olson, D.T. Westley, B.G. Anderson, L.J. Tabaka, J.S. Ladish, J.L. Stokes (P-22), W.L. Atchison (X-1), G. Rodriguez, Q. McCulloch (MST-10). J.H. Goforth, H. Oona (DX-2), R.E. Reinovsky (P-DO), representing colleagues from the All-Russian Scientific Research Institute of Experimental Physics, Sarov, Russia

A series of experiments, known as the Russian High Strain Rate (RHSR) experiments, has been designed and partially completed to determine the dynamic yield strength of copper. The data obtained from this experimental series are used to validate theoretical and computational models of material behavior at high strains (100%–150%) and strain rates (~ 10^6/s).[1] To achieve these high strains and strain rates, a two-stage explosively driven pulsed-power generator is used to produce high currents that magnetically implode a cylindrical aluminum liner onto a copper sample. The sample, also cylindrical, incorporates machined sinusoidal perturbations of two different wavelengths on its outer surface. Theoretical models predict that the growth rate of these perturbations is wavelength dependent and directly related to the dynamic yield strength of the copper.

The RHSR experiments are important to refine and validate computational models of dynamic material strength under high-strain and strain-rate conditions. Validation of such models is an essential element of the ASCI-code-development effort that will support nuclear-weapons certification in the future. Additionally, these experiments have the added benefit of fulfilling a goal of the National Nuclear Security Administration (NNSA) to significantly increase collaboration between Russian and U.S. weapons laboratories on fundamental science issues.

Experimental Design

Because the Atlas pulsed-power capacitor bank is presently being relocated from LANL to the NTS, the high currents needed to perform this type of experiment are currently not easily attainable in the U.S.[2] However, the VNIIEF scientific research institute in Sarov, Russia, has developed an explosively driven pulsed-power generator that can supply the required 35-MA current.[3] The VNIIEF device consists of two parts: a helical explosive magnetic generator (HEMG) and a multi-element disk explosive magnetic generator (DEMG) (Figure 1). Both devices use rapid magnetic flux compression to generate a very high, short pulse of electrical current. The basic concept behind these devices is that a small "seed" current creates magnetic flux through a volume within the generator. Igniting high explosives rapidly collapses this volume, and because the flux is initially preserved, a portion of the work done by the high explosive is converted to electrical current. In the case of the RHSR device, the HEMG delivers 6.5 MA as the "seed" current for the DEMG that in turn delivers ~ 35 MA through a liner inside the physics package.

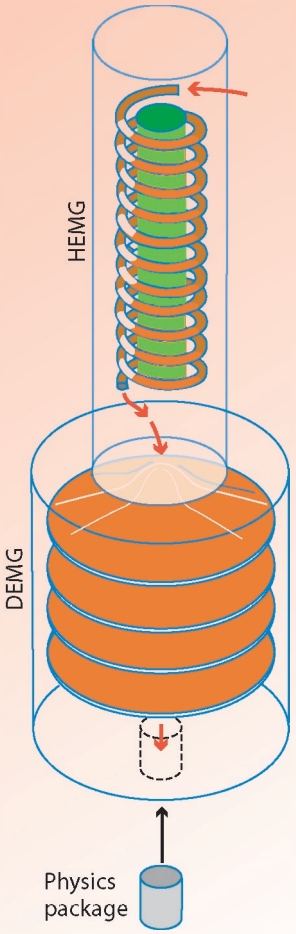

Figure 1. The combination of the HEMG and DEMG deliver a peak current of ~ 35 MA through the liner in the physics package.

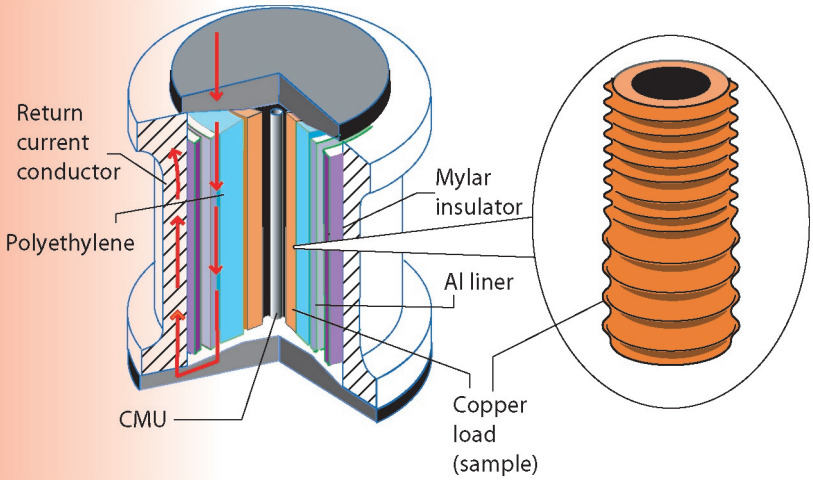

Figure 2. The cylindrically symmetric physics package contains a copper sample that is imploded by the aluminum liner.

The liner is an aluminum cylinder with a 4-mm-thick wall and an inner diameter of 96 mm. The current flowing through it causes the liner to magnetically implode and push on polyethylene that fills the entire space between the liner and a 52.6-mm-diam copper sample (Figure 2). The copper sample has 2.0- and 4.0-mm-wavelength sinusoidal perturbations machined on its exterior surface with initial amplitudes of 1.0 mm. The volume inside the cylindrical copper sample is evacuated and contains a stainless-steel central measuring unit (CMU).

During the implosion, the polyethylene shocklessly transfers the pressure from the liner to the copper cylinder causing it to radially compress to a peak pressure of 160 kbar at a strain rate of ~ 9 x 10^5/s. Under these conditions, the copper-polyethylene interface is Rayleigh-Taylor unstable, and the perturbations will grow as a function of time during the implosion.[4,5] The design of the RHSR experiments assumes that the dynamic yield strength of polyethylene is small enough that it can be neglected, and as a result, its hydrodynamic properties closely approximate those of a fluid. This assumption is important because it allows the dynamic yield strength of the copper to be determined directly from the growth rate of the perturbation amplitude.

Experimental Diagnostics and Data

A Faraday rotation diagnostic is used to measure current delivered from the DEMG to the load as a function of time.[6] The diagnostic consists of a single-mode quartz fiber that encircles the entire electrical current path to the liner. An 830-nm laser diode injects linearly polarized light into the fiber, and current flowing through the load creates a magnetic field that causes the polarization of the light in the fiber to rotate. The light rotation angle is subsequently detected using an optical polarization analyzer once it exits the fiber. The time-dependent current through the load is then calculated using the Verdet constant (2.65 +/- 0.03 rad/MA) of the fiber that relates the light-polarization rotation angle to the enclosed current. Because this measurement technique is only sensitive to current that passes through the area defined by the fiber loop, an accurate measure of the current through the liner can be obtained.

A B-dot is an inductive probe that consists of a center-wound wire loop inserted into current-carrying regions of the load, HEMG, and DEMG. Current flowing in the region of the B-dots generates a time-varying magnetic field that induces a small current in each B-dot loop. This B-dot signal is proportional to the time derivative of the current flowing in the experimental device. Because the B-dot is extremely sensitive to changes in current, it provides critical timing information about the performance of the device, including the start of current flow, peak current time, and copper impact on the CMU.

Thus far, two of the three planned experiments have been performed: RHSR-0 and RHSR-1. The peak current, as measured with the Faraday rotation diagnostic, was 34.9 MA for RHSR-0 and 34.6 MA for RHSR-1 (Figure 3). The B-dot data obtained from the RHSR-0 experiment shows that peak current occurred at 27.1 μs after the high-explosive detonator in the DEMG was initiated.

A VISAR is an interferometer used to measure the velocity of a reflective surface as a function of time.[7,8] The VISAR uses a 532-nm laser coupled to a glass fiber that transports the light to the inside surface of the copper load via the CMU. Light reflected from the copper surface is recollected and transmitted down a separate glass fiber to an interferometer. Upon entering the interferometer, the reflected light is split into two optical paths with different optical lengths and subsequently recombined to interfere with one another. Motion of the copper sample produces a Doppler shift in the recollected light and, as a result, an interference fringe shift that is recorded as a function of time. The velocity of the reflective copper surface is proportional to this fringe shift and was measured to be 3.1 mm/μs at impact with the CMU in both

RHSR-0 and RHSR-1. Additionally, the VISAR data indicated the impacts occurred 32.5 μs after the DEMG detonators were initiated (Figure 4). These data provide information about both the load hydrodynamics as a function of time and the time when the load reaches a radius of 10 mm during the implosion.

Low-energy x-ray radiographs were obtained to measure the perturbation growth of the load at three distinct times during the hydrodynamic explosion. Two different x-ray source designs were used in the experiments: one was designed and built by LANL, and the VNIIEF team provided the other. The LANL x-ray source consists of an x-ray head coupled to a 900-kV Marx bank via ~ 20 m of coaxial cable.[9] The x-ray head contains a 1.5-mm-diameter tungsten anode, which generates a 20-ns-long x-ray pulse. The x-ray spectrum of this pulse is comprised primarily of K_α-line and Bremsstrahlung radiation with an endpoint energy of ~ 350 kV.

Transverse x-ray radiographs of the dynamically evolving copper perturbations are acquired by locating the x-ray heads and films on opposite sides of the load. A steel enclosure protects the film from shrapnel generated by the ~ 175-lb high-explosive charge in the DEMG and the aluminum-return-current conductor. The film is recovered after the experiment to be developed and digitized for later analysis.

The flash x-ray sources were fired to record images from ~ 1.5 μs before impact to ~ 1.5 μs after impact of the copper sample upon the CMU. These radiographic times were chosen to provide images both during the shockless perturbation growth phase of the implosion and to observe the effect of the reflected shock generated upon impact with the CMU. Only the single radiograph produced with the VNIIEF x-ray source was successfully recovered from RHSR-0. Damage to the LANL films by the high explosive and shrapnel prohibited any additional successful data retrieval. Improvements in the film protection systems enabled the successful recovery of all three radiographs from the RHSR-1 experiment, although each piece of film sustained moderate to severe shrapnel damage.

The radiographs from both experiments showed shockless-perturbation-amplitude growth of $A/A_0 \sim 2–3$ before CMU impact. The amplitude then rapidly dropped to $A/A_0 \sim 0.7$ once the reflected shock exited the copper sample (Figure 5). Given the assumption that the polyethylene moves and flows like a fluid under these dynamic conditions, the perturbation amplitude exhibited significantly less growth than the $A/A_0 \sim 8–12$ predicted by the theoretical models. There are two possible explanations for this result: (1) the strength model used in the computations does not adequately describe the dynamic strength properties of copper, or (2) the assumption that the polyethylene was a dynamically strengthless material is invalid.

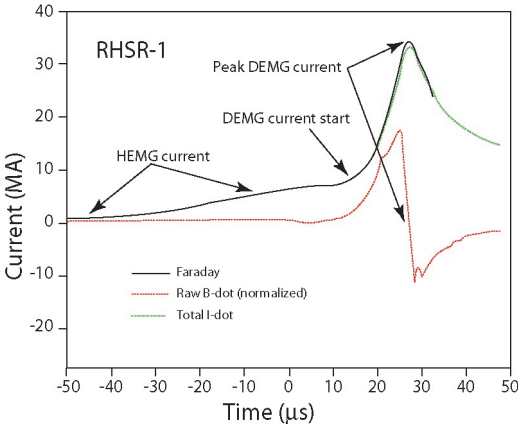

Figure 3. B-dots, proportional to the time derivative of current flowing in the DEMG, indicate peak current occurred at 27.1 μs after detonator initiation. The Faraday rotation diagnostic recorded a peak current of ~ 35 MA.

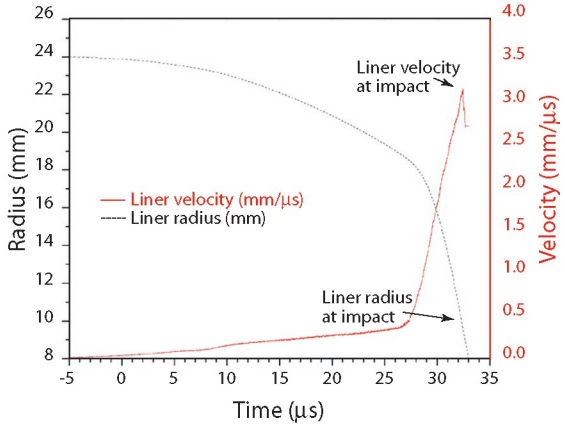

Figure 4. VISAR data indicates the inner surface of the copper is moving 3.1 mm/μs at impact with the CMU.

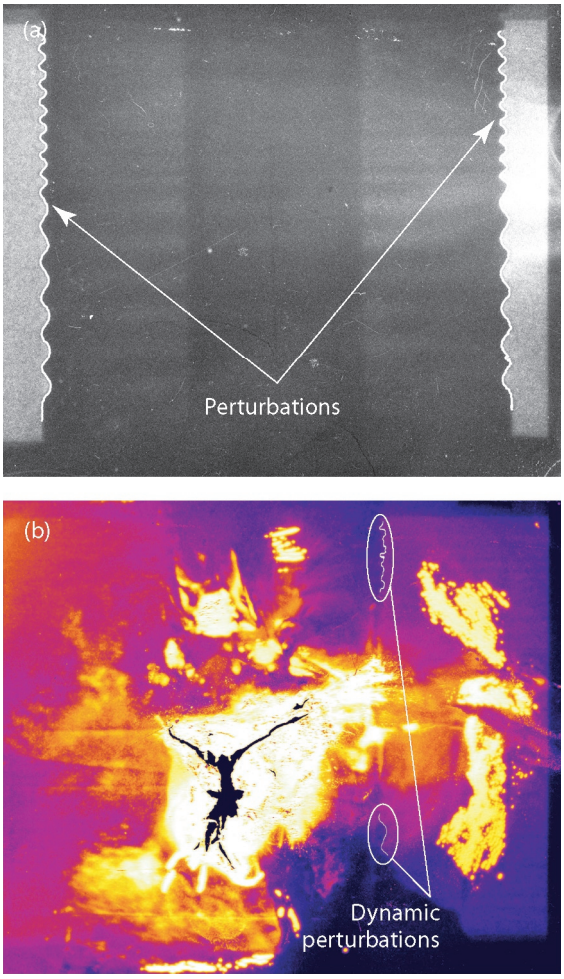

Figure 5. The static (a) and dynamic (b) x-ray radiographs acquired by LANL show the RHSR-1 perturbation edges with the dynamic image quality significantly affected by shrapnel damage. The dynamic radiograph was acquired 1.0 µs after impact of the copper on the CMU.

Conclusion

RHSR-2 is currently being designed using a liquid material (such as butane, water, or ethylene glycol) to eliminate the ambiguity introduced by the polyethylene. However, given this change in materials, a redesign of the load is necessary to maintain the same shockless condition in the fluid that was present using polyethylene in the RHSR-0 and RHSR-1 experiments. The RHSR-2 experiment with its redesigned load is currently scheduled for February 2004.

References

1. D.J. Steinberg, S.G. Cochran, and M.W. Guinan, "A constitutive model for metals applicable at high-strain rate," *Journal of Applied Physics* **51**, 1498 (1980).
2. R.E. Reinovsky *et al.*, in *Proceedings of the 2003 IEEE International Pulsed Power Conference* (Dallas, TX), in publication (2003).
3. V.K. Chernyshev *et al.*, in *Proceedings of the 1997 IEEE International Pulsed Power Conference* (Baltimore, MD), pp. 1441–1447 (1997).
4. D.H. Sharp, "An overview of Rayleigh-Taylor instability," *Physica D* **12**, 3 (1984).
5. M.G. Sheppard *et al.*, in *Proceedings of the 1997 IEEE International Pulsed Power Conference* (Baltimore, MD), pp. 1399–1403 (1997).
6. J.L. Stokes *et al.*, in *Proceedings of the 2001 IEEE International Pulsed Power Conference* (Las Vegas, NV), pp. 365–367 (2001).
7. L.M. Barker and R.E. Hollenbach, "Laser interferometer for measuring high velocities of any reflecting surface," *Journal of Applied Physics* **43**, 4669 (1972).
8. W.F. Hemsing, "Velocity sensing interferometer (VISAR) modification," *Review of Scientific Instruments* **50**, 73 (1979).
9. B.G. Anderson *et al.*, in *Proceedings of the Ninth International Conference on Megagauss Magnetic Field Generation and Related Topics*, (Moscow, Russia) in publication (2003).

Acknowledgment

The authors would like to acknowledge the efforts of the numerous individuals both at LANL and VNIIEF who provided the essential logistical support necessary to conduct these experiments. Without these people acting as interpreters, manufacturing parts, arranging travel, and shipping equipment through customs, the RHSR experimental series would not have happened. This work is supported by the NNSA via the Office of Defense Programs.

For more information, contact Russell Olson, 505-667-6667, rtolson@lanl.gov.

Basic Material Properties Using Laser-Driven Shocks

D.C. Swift, A. Hauer, D. Paisley, J. Niemczura, T. Tierney, R. Johnson (P-24), J. Wark, A. Loveridge, A. Allen (University of Oxford), B. Remington, D. Kalantar (LLNL), D. Thoma, J. Cooley, R. Hackenberg (MST-6), K. McClellan (MST-8), A. Koskelo, S. Greenfield (C-ADI), P. Peralta, E. Loomis (Arizona State University)

Shock waves can be induced in samples by illumination with an intense laser; pressure is generated as the target absorbs energy, and atoms are ablated from the surface to form a plasma plume. Our team is investigating the response of materials to dynamic loading using the Trident laser with *in situ* optical and x-ray diagnostics complemented by post-shot microstructural analysis.

Accurate models of the response of materials to dynamic loading are important for simulations of the performance and safety of weapons and for the design of the fuel capsule in ICF. These models are devised and calibrated using experiments in which samples are subjected to high pressures, usually from shock waves induced by the detonation of high explosives or the impact of flyers.[1] New classes of models are being developed that use more detailed underlying physics, such as dislocation dynamics, rather than *ad hoc* empirical relations to describe the response. Laser-driven materials experiments offer promising possibilities to contribute to model development, including convenient new diagnostics such as transient x-ray diffraction (TXD) to measure the response of materials at the microstructural level.

Laser-Induced Shock Experiments

Shock waves—whether induced by laser ablation or more traditional methods—can be regarded as a region of high pressure that moves through a body of material. By measuring the response as material is subjected to dynamic loading and unloading, we can understand its behavior in terms of a pressure-volume-temperature relation (often called the EOS), phase diagram, phase-change kinetics (including chemical reactions), plasticity, and fracture. The simplest measurement is the speed of the shock wave, from its transit time through the sample. The velocity imparted to the material by the shock is inferred from the velocity history at the surface of the sample; features in the velocity history also provide information about plasticity and phase changes.[1] We have developed and applied other diagnostics on laser experiments. TXD—applied to single crystals and polycrystalline ensembles—provides detailed information on the shock response of material at the level of the atomic lattice, including plasticity and phase changes.[2,3] Ellipsometry measures the polarization-dependent reflectivity of a surface and can be a sensitive test for phase transitions. We have recorded surface velocity and displacement in one and two spatial dimensions—with time resolution as well—to investigate the effect of a material's microstructure on shock propagation.[4,5]

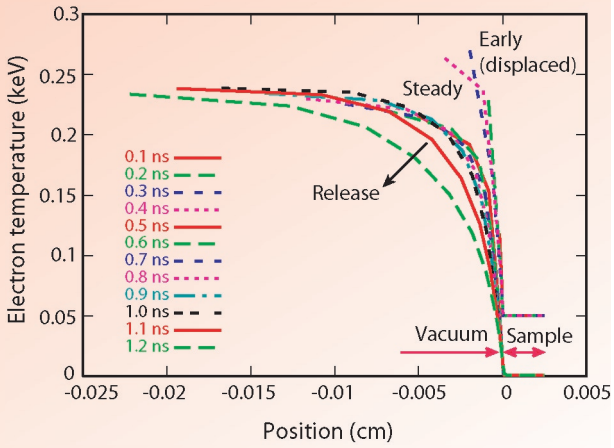

Figure 1. Profiles of electron temperature at different times during the interaction of a 1-ns-long laser pulse and 1 PW/m² with a 25-μm-thick iron target.

Laser-induced shock experiments have some disadvantages compared with traditional shock techniques. Principally, it is more difficult to ensure that the shock has a constant pressure. (Conversely, it can be easier to induce other loading histories such as multiple shocks, decaying shocks, and isentropic ramp waves.) However, using a laser to induce the initial shock wave can make it easier to apply new diagnostics, because synchronization is generally more straightforward than with shocks launched by explosives or a flyer impact. Also, compared with other techniques, it is often easier to recover shocked samples from laser experiments.[6]

Several interesting discoveries have emerged from laser-induced shock experiments on nanosecond time scales at Trident. Shocks along the ⟨100⟩ crystal directions in silicon show no evidence of plastic flow.[2] The stress at which plastic flow occurs on these time scales has been investigated for single crystals and polycrystalline foils of materials, including beryllium, iron, tantalum, nickel-titanium, nickel aluminide, and ruthenium aluminide. The results have contributed to the development of time-dependent plasticity models and of simulations with explicit treatment of the motion of dislocations.[4,7,8,9] In the rest of this article, we will review recent advances in dynamic loading by laser ablation and in TXD.

Dynamic Loading Induced by Laser Ablation

Shocks and other loading histories can be induced in samples of material by surface ablation resulting from the absorption of laser energy. At the start of the laser pulse, energy is deposited in the skin depth at the surface of the sample. Material at the surface ablates in the form of a plasma; subsequent laser energy is deposited in this plasma. Reaction and the plasma itself apply pressure to the remaining material in the sample, until the laser pulse ends and the plasma cloud dissipates (Figure 1).

A laser pulse of constant irradiance does not induce a constant pressure in the sample. We see a pressure spike in the first ~ 100 ps while the ablation plasma is established, followed by a period in which the plasma profile close to the sample is roughly constant and acts as a rocket. If a constant pressure shock is desired—necessary for accurate measurements of the EOS—then we must adjust the irradiance history of the laser pulse. At Trident, optical zone plate arrays are used to distribute the laser energy uniformly over a spot on the sample. For dynamic-materials work, we have mainly used a zone plate giving a 4-mm spot. At this scale, Trident can deliver irradiances up to ~ 10 PW/m^2, inducing pressures of up to several tens of gigapascals. For laser-pulse durations around 1 ns, the sample thickness is 10 to 500 μm, so the drive is safely one-dimensional over most of the area of the spot.

In nanosecond mode, the Trident laser pulse consists of 13 sequential elements, each 180 ps long, whose amplitude can be controlled independently. As well as being able to set the irradiance history to produce a constant pressure, we have also generated decaying shocks (analogous to the von Neumann spike or Taylor wave induced by detonation waves in chemical explosives) and isentropic compression waves (starting with a low irradiance and increasing

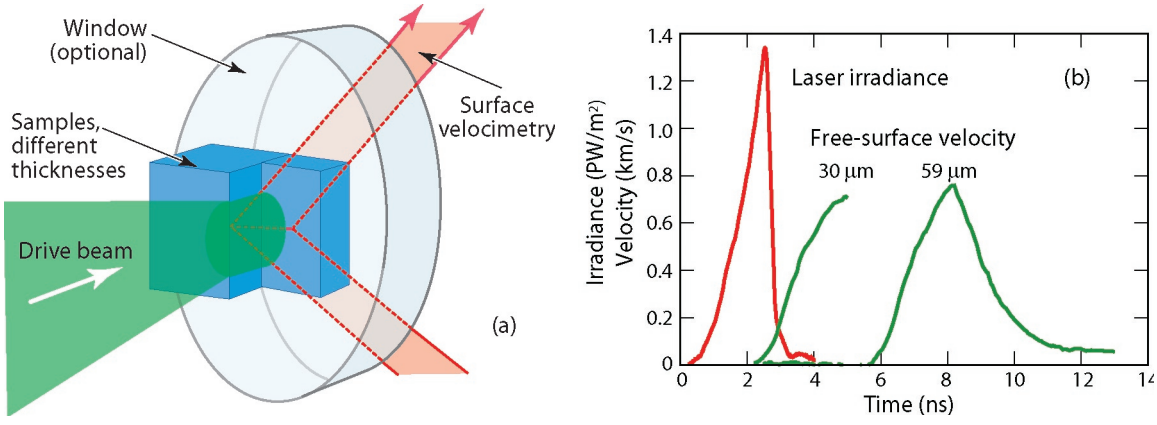

Figure 2. Schematic of side-by-side targets of different thickness used for laser-induced isentropic compression experiments (LICE) (a) and example results from Trident shot 15018 (silicon crystals) showing ramped laser pulse and smooth acceleration history at the surface of each sample (b).

gently to drive a smooth ramp wave through the sample). Isentropic compression experiments (ICE) driven by pulsed electrical power on microsecond time scales have been used to measure the EOS in beryllium and lead; we have used the laser-driven equivalent (with the unfortunate acronym of LICE) to generate ramp waves on nanosecond time scales in aluminum, silicon, iron, and tantalum (Figure 2).

Transient X-ray Diffraction

In TXD, a source of x-rays is used to infer the state of the crystal lattice by diffraction during the passage of a shock wave. We have used a laser-generated plasma as the x-ray source by focusing a beam delivering ~ 200 J in ~ 1 ns to a spot ~ 100 μm in diameter on a foil around 10 μm thick. For titanium and manganese foils, the resulting plasma emits predominantly helium-like line radiation (i.e., from atoms stripped of all but one electron) whose wavelengths are 2.61 and 2.006 Å, respectively—useful for experiments on a variety of materials. We have recorded the diffracted x-rays with two-dimensional time-integrating detectors (x-ray film and image plates) and one-dimensional time-resolving detectors (x-ray streak cameras). The coverage in terms of solid angle is typically quite small, so usually a particular small set of diffraction lines is followed as a function of drive pressure, rather than uniquely identifying a complete diffraction pattern from each experiment.

Previously, experiments have been performed on shocks in single-crystal samples, demonstrating the onset of plasticity and solid-solid phase transformations.[2,10] We have now performed some initial TXD experiments on dynamic melting in single crystals of gallium, which we use as a convenient melt prototype because its low melting temperature (29.8°C) makes it easier to distinguish the effects of melt from plasticity and phase transitions (Figure 3). Our ultimate application is beryllium for ICF capsules, where, in addition to plasticity and a possible solid-solid phase change, melt is expected to occur at ~ 150 GPa, requiring TXD to be performed over a wide range of diffraction angles.

We have also demonstrated time-resolved diffraction from rolled polycrystalline foils of beryllium, using a collimator so that only a small region of the sample was illuminated (Figure 4). For single crystals, the position on the sample surface at which diffraction occurs moves as the lattice is compressed. Polycrystal TXD allows a greater variety of samples to be used and also makes it easier to perform experiments at higher pressure, where the single-crystal diffraction point would move too far across the surface of the sample.

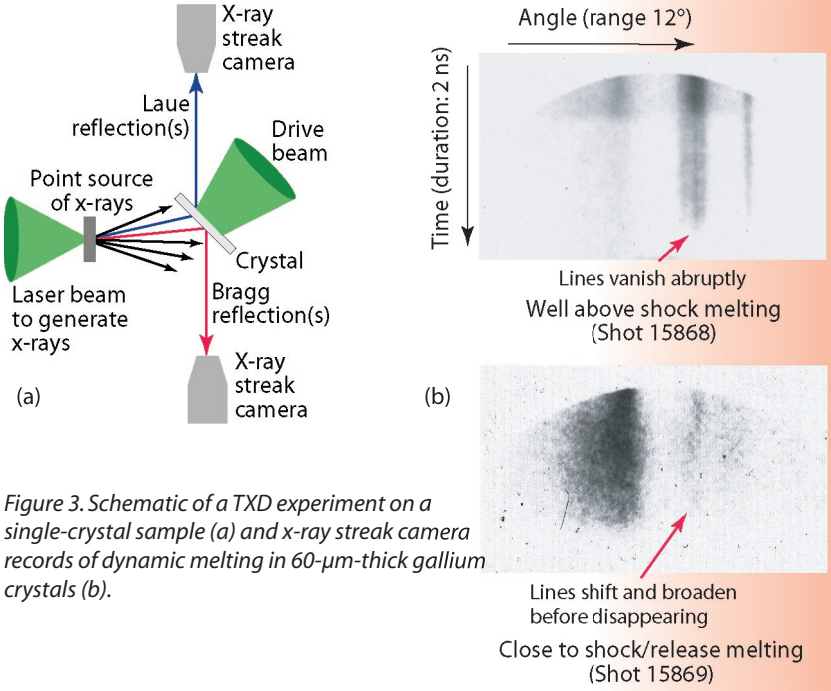

Figure 3. Schematic of a TXD experiment on a single-crystal sample (a) and x-ray streak camera records of dynamic melting in 60-μm-thick gallium crystals (b).

Conclusion

Dynamic loading by laser ablation has provided valuable insights into the detailed response—plasticity and phase changes—of materials on nanosecond time scales and pressures to tens of gigapascals. This regime is important in the development of improved material models for weapons and ICF applications. The use of lasers has made it easier to develop new diagnostic techniques, providing subnanosecond temporal resolution and greater ease in synchronizing the measurement with the drive. We expect to develop these techniques further and apply them to a wider range of materials, working more closely with the development of advanced, physically based models.

References

1. A.V. Bushman, G.I. Kanel, A.L. Ni *et al.*, *Intense Dynamic Loading of Condensed Matter* (Taylor and Francis, London, 1993).
2. A. Loveridge-Smith, A. Allen, J. Belak *et al.*, "Anomalous elastic response of silicon to uniaxial shock compression on nanosecond time scales," *Physical Review Letters* **86**(11), 2349–2352 (2001).

3. M.A. Meyers, F. Gregori, B. K. Kad *et al.*, "Plastic deformation in laser-induced shock compression of monocrystalline copper," in *Shock Compression of Compressed Matter–2001*, M.D. Furnish, N.N. Thadhani, and Y. Horie, Eds. (American Institute of Physics, New York, 2002), AIP Conference Proceedings 620, pp. 619–622.
4. D.C. Swift, D.L. Paisley, G.A. Kyrala *et al.*, "Simultaneous VISAR and TXD measurements on shocks in beryllium crystals," in *Shock Compression of Compressed Matter–2001*, M.D. Furnish, N.N. Thadhani, and Y. Horie, Eds. (American Institute of Physics, New York, 2002), AIP Conference Proceedings 620, pp. 1192–1195.
5. S.R. Greenfield, D.L. Paisley, and A.C. Koskelo, "Transient interferometric studies of shocked bicrystals," in *Proceedings of the APS Topical Conference on Shock Compression of Condensed Matter*, held in Portland, Oregon, July 21–25, 2003 (to appear).
6. P. Peralta, E. Loomis, K.J. McClellan *et al.*, "Characterization of laser-driven shocked NiAl monocrystals and bicrystals," in *Proceedings of the APS Topical Conference on Shock Compression of Condensed Matter*, held in Portland, Oregon, July 21–25, 2003 (to appear).
7. R.E. Hackenberg, D.C. Swift, J.C. Cooley *et al.*, "Phase changes in Ni-Ti under shock loading," in *Proceedings of the International Workshop on New Models and Hydrocodes for Shock Wave Processes in Condensed Matter*, Edinburgh, Scotland, May 19–24, 2002 (to appear).
8. K.J. McClellan, D.C. Swift, D.L. Paisley *et al.*, "Dynamic properties of nickel-aluminum alloy," in *Proceedings of the APS Topical Conference on Shock Compression of Condensed Matter*, held in Portland, Oregon, July 21–25, 2003 (to appear).
9. D.C. Swift, D.L. Paisley, A. Forsman *et al.*, "Dynamic flow stress and polymorphism in shocks induced by laser irradiation," in *Proceedings of the 5th Symposium on High Dynamic Pressures*, held in St. Malo, France, June 23–27, 2003 (to appear).
10. D.C. Swift, G.J. Ackland, A. Hauer *et al.*, "First-principles equations of state for simulations of shock waves in silicon," *Physical Review B* **64**, 214107 (2001).

Acknowledgment

Our team would like to recognize the contribution of the staff of the Trident laser facility in performing these experiments. We would also like to recognize the ICF and Science and Technology Base Program Offices for supporting this work.

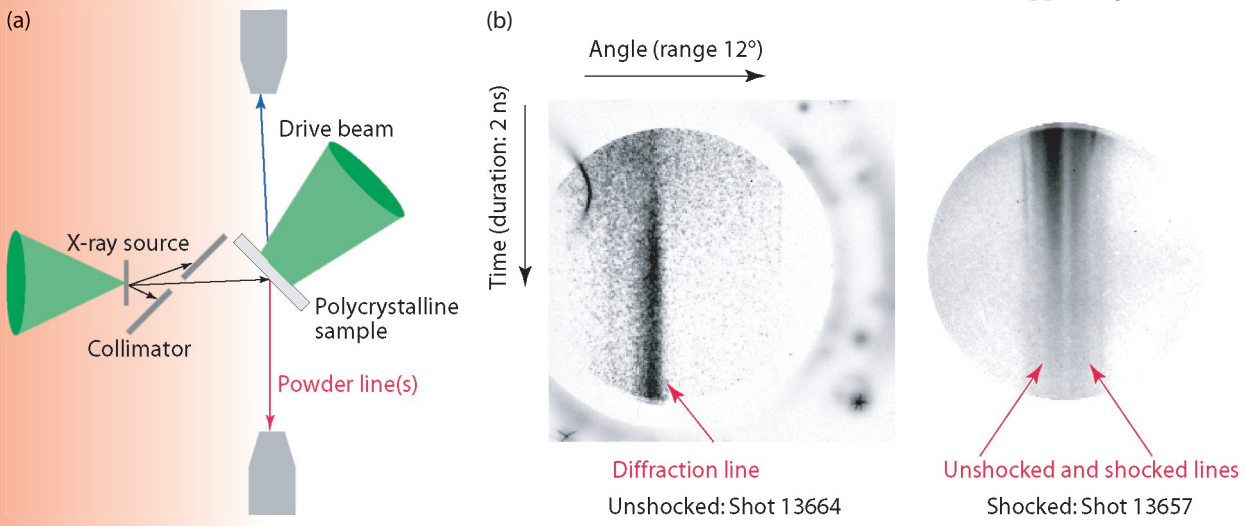

Figure 4. Schematic of a TDX experiment on a polycrystalline sample and x-ray streak-camera data demonstrating powder lines for 125-μm-thick beryllium foils (a). The shock in Shot 13657 was ~ 20 GPa. The width of the diffraction lines was dominated by the aperture in the collimator (b).

For more information, contact Damian Swift at 505-667-1279, dswift@lanl.gov.

pRad VISAR: An Interferometer-Based Optical Diagnostic for Proton Radiography

D. Tupa (P-25), D.A. Clark, O.F. Garcia, B.J. Hollander, D.B. Holtkamp (P-22)

One method to determine the velocity of a moving surface is to measure the Doppler-shifted frequency of light reflected off that surface. A sensitive measurement of frequency can be made with an interferometer. One specific interferometer configuration for such a measurement was developed at SNL and LANL and is called VISAR, for velocity interferometer system for any reflector.[1,2] We have developed and implemented a VISAR capable of measuring up to seven points simultaneously for the LANL pRad facility. In this article, we briefly describe how our VISAR works and how it is used to supplement proton radiographs.

How VISAR Works

A VISAR is diagrammed in Figure 1. After reflecting off the surface in question, light enters the interferometer from the fiber-optic input on the left-hand side (LHS) and is incident on a 50/50 beamsplitter. Half the light is reflected off the beamsplitter, the LHS mirror, and is incident on the beamsplitter again. The other half of the light traverses the right-hand side (RHS) of the interferometer. For imaging, the RHS is optically equivalent to the LHS despite having an optically flat element, an etalon, in the beam path. The etalon induces a frequency-dependent phase shift between the light traversing either side of the interferometer. After the light is recombined at the beamsplitter, the relative phase shift is measured by keeping count of the Michelson-type fringes through the fiber-coupled output of the device; the fringes are manifested as modulations in the light intensity. The light frequency can be deduced from this relative phase shift. A single fiber-coupled output would suffice for a measurement, but the eighth-waveplate, output polarizing beamsplitters, and additional outputs allow for greater precision throughout the measurement range and calibration against light-intensity variations and unwanted scattered light.[2]

In addition to allowing for measurements with reflected light from diffuse surfaces, having each side of the interferometer optically equivalent allows measurements of velocity of different points at the same time. Rather than a single optical fiber for input, a bundle of seven fibers is used (Figure 2).

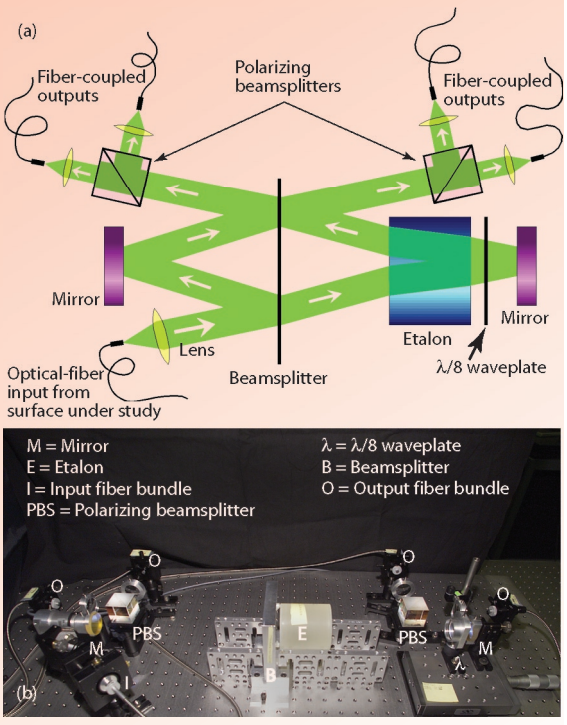

Figure 1. (a) Schematic diagram and (b) photo of the pRad VISAR. Details are given in the text.

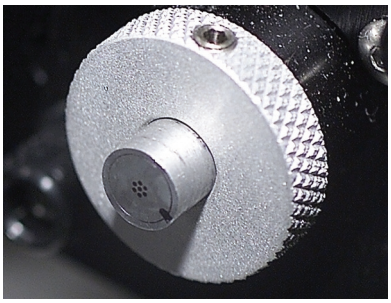

Figure 2. Photo of the input fiber bundle on which the ends of the seven individual fibers can be seen. The diameter of the hole for each fiber is 370 μm.

Each fiber in the bundle carries light reflected from a different test point on the experiment. The input bundle is carefully imaged onto four identical fiber bundles at the four output arms of the interferometer. The four output intensities of each of the seven test points can then be recorded simultaneously on a streak camera.

The streak camera records data with a 1,000- × 1,000-pixel CCD with 15 ns/pixel, typically. The noise on the velocity measurement is usually below 40 m/s. The breakout time, the time of a sudden change in surface velocity caused by shock, can usually be determined with an instrumental precision of ± 30 ns. In parallel with the streak camera, the light intensities from at least one point can also be recorded with photomultipliers and a digitizing oscilloscope. Typical sample time for the scope is 2 ns.

Integrating VISAR with pRad

The pRad dome (located in Area C at LANSCE) environment presents challenges for setting up a VISAR system. Hazards such as radiation and high explosives are integral to the facility, so the VISAR light source, optics, and data-acquisition equipment must be located outside the pRad dome. Conversely, the VISAR must be operated in such a way that workers are not endangered by its high-power laser.

A schematic overview of how the VISAR equipment is integrated into the pRad area is shown in Figure 3. A separate, interlocked room houses the VISAR equipment and controls. The light for the VISAR comes from a laser producing 10 W at 532 nm. After passing through an attenuator and a fast switch, the laser beam enters a seven-way switchyard, where it can be divided into seven beamlets of arbitrary intensity. Each of the seven beamlets is coupled into a fiber-optic cable that carries the light 100 m to the pRad dome. A vacuum feed-through connects this supply fiber to the VISAR probe. The VISAR probe is a compact optical device placed in the vacuum chamber with the test object. The probe (Figure 4)

- directs the collimated laser light to the surface of the test object,
- gathers the light that is reflected back, and
- couples it back into a second fiber of the vacuum feed-through.

The output of the probe is returned to the VISAR room, where it is directed into one of the seven interferometer input fibers.

Experimental Results

VISAR surface-velocity measurements and proton radiographs complement each other well. Proton radiographs reveal three-dimensional views of the total volume of an object during a dynamic event but do so at discrete intervals of 3 μs, typically, and the images are integrated over 50 ns. VISAR can only reveal the velocity of the exterior surface of the object but provides a relatively continuous record with measurements every 2–15 ns.

Experiments to study high-explosive-induced damage and spall[3,4] in selected metals demonstrate how VISAR data can enhance observations of dynamic experiments. These experiments study the behavior of metals when the free surface reflects a Taylor wave generated by high explosives. Figure 5 is a diagram of such experiments performed in conjunction with pRad operations.

Some results of these experiments, showing the velocity of the metal surface as measured by the VISAR, are shown in Figure 6. The terminal velocity, velocity pullback, shock breakout, and ringing period of the surface can be seen in the VISAR data. This information yields independent measurements of parameters such as the spall strength of the material and thickness of the first spall/damage layer.

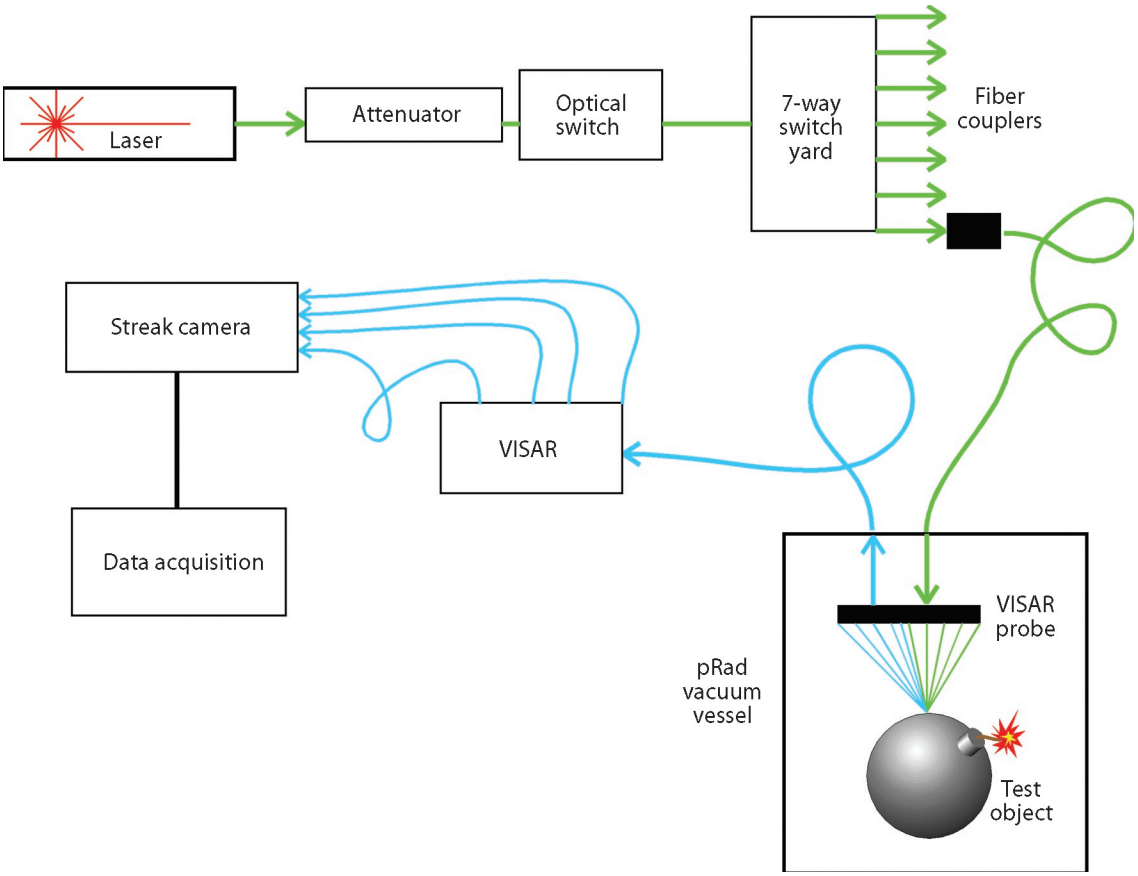

Figure 3. Schematic of the VISAR measurement apparatus, as used for pRad.

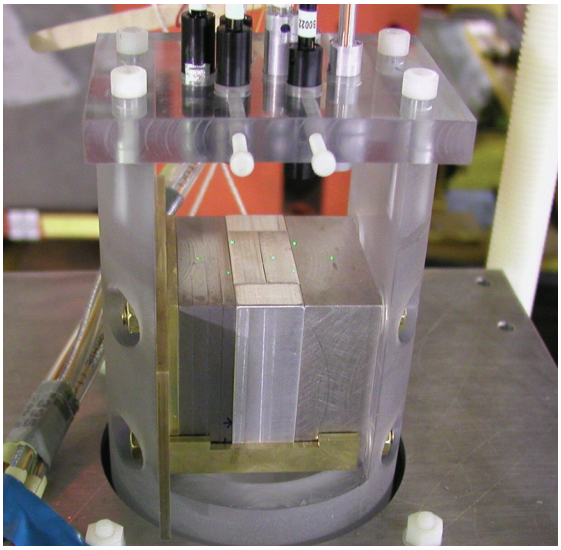

Figure 4. Seven VISAR probes aligned onto a pRad experiment. The black and metallic cylinders held by the upper Lucite block are the probes. Seven points of green light on the surface of the test object are from the alignment laser light coming through the probes; scattered light from each spot is gathered by the respective probe to be analyzed by the VISAR interferometer.

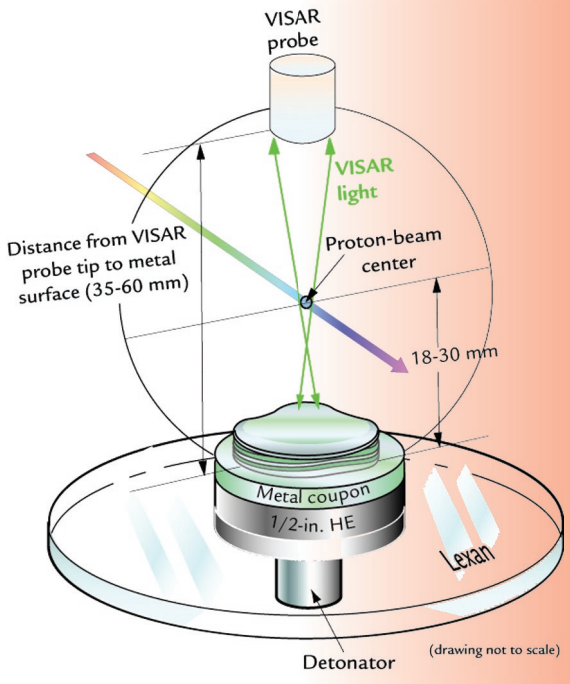

Figure 5. Diagram of high-explosive spall/damage experiment. The composition and thickness of the metal cylinder, or coupon, varies for different experiments.

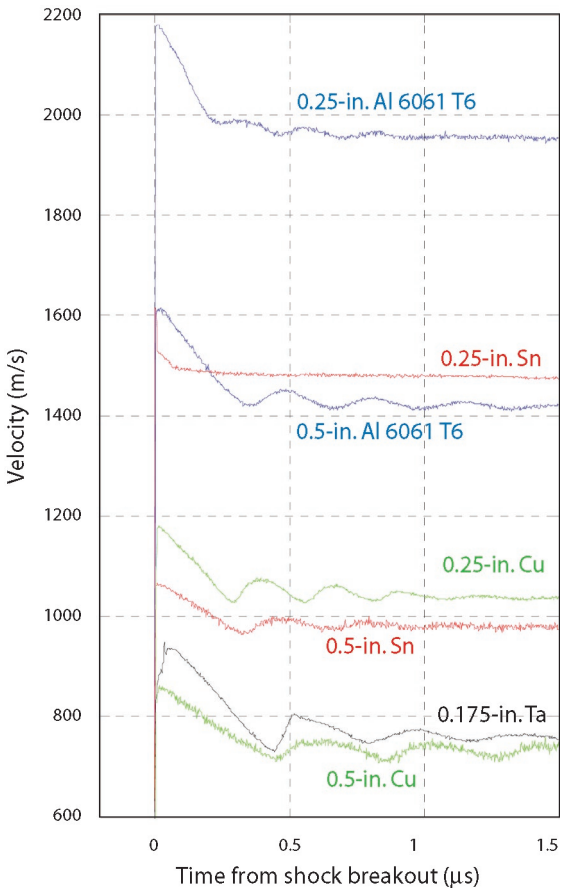

Figure 6. VISAR measurements of surface velocity from several pRad experiments. Results are shown for differing thicknesses of 6061-T6 aluminum (blue), tin (red), copper (green), and tantalum (black). Zero time is adjusted for breakout at the same time for each experiment. The entire time scale of the graph is < 3 µs, the typical spacing between pRad images.

Conclusion

A VISAR system has been installed in pRad to measure the surface velocity of test objects during dynamic experiments. The system has been upgraded to allow measurements of up to seven points on the surface simultaneously. The system has been used for over a dozen experiments in the last year at pRad. The pRad VISAR is ready to be available upon request to users at pRad to supplement the information learned in their experiments.

References

1. L.M. Barker and R.E. Hollenbach, "Laser interferometer for measuring high velocities of any reflecting surface," *Journal of Applied Physics* **43**(11), 4669–4675 (1972).
2. W.F. Hemsing, "Velocity sensing interferometer (VISAR) modification," *Review of Scientific Instruments* **50**(1), 73–78 (1979).
3. D.B. Holtkamp D.A. Clark, I.A. Garcia *et al.*, "Development of a non-radiographic spall and damage diagnostic," in *Proceedings of the 2003 Conference of Shock Compression of Condensed Matter*, M.D. Furnish, Ed. (to appear in April 2004).
4. D.B. Holtkamp, "High explosive-induced damage and spall in selected materials studied with proton radiography," in *Proceedings of the 2003 Conference of Shock Compression of Condensed Matter*, M.D. Furnish, Ed. (to appear in April 2004).

Acknowledgment

The experimental program at pRad is operated by the Proton Radiography Collaboration, which staged and executed all the shots performed with pRad VISAR, including those summarized in Figure 6. For VISAR operations, Karen A. Esquibel (P-22) provided technical assistance, Paul Nedrow (P-23) installed and operated the streak camera, and Anthony J. Zukaitis (Bechtel-Nevada) assisted with data analysis. Funding for this work came from the Advanced Radiography Program Element (Campaign 3) of the Weapons Development Program.

For further information, contact Dale Tupa at 505-665-1820, tupa@lanl.gov.

Temperature of Shocked Materials

V.W. Yuan, J.D. Bowman, G.L. Morgan (P-23), D.J. Funk, D.G. Thompson (DX-2), R.A. Pelak, L.M. Hull (DX-3), C.E. Ragan (X-5), J.E. Hammerberg (X-7), M.S. Shaw (T-14)

Neutron resonance spectroscopy (NRS) uses the Doppler broadening of neutron resonances to determine the temperature in samples undergoing dynamic loading. This technique has emerged as a unique method for making temperature measurements in the field of shockwave and high-explosive physics—as such, it can be applied to Science-Based Stockpile Stewardship and the Weapons Program. NRS can determine temperatures on very short time scales (1 μs or less) and has been used to determine the internal volume temperature in shocked molybdenum and in explosively driven metal jets. In 2003, the NRS team began the first experiments to measure the temperature behind the burn front of detonating high explosives; measurements of this burn temperature have never before been made *in situ*. For many materials of interest, dynamic temperature measurements appear possible at many attainable conditions on the EOS surface.

Why Neutrons?

NRS experiments use low-energy neutrons because these minimally perturbing probes possess advantages over other available temperature diagnostics. First, optical opacity or ancillary light emissions do not limit the technique because photons are not detected. Second, the technique uses small amounts of resonant tags, or dopants, that can be localized in the samples being studied. For a given experiment, the type of dopant and quantity (about 1 at. %) is selected so that it causes minimal perturbations to the dynamically loaded sample. The localization of the doped region allows us to make temperature measurements in a steady shock region internal to the sample rather than at a free surface or visible interface where rarefactions can alter the state being characterized.

What is a Neutron Resonance?

When a beam of neutrons passes through a sample of atomic weight A, those neutrons possessing certain resonant energies (usually in the epithermal region below a few hundred eV) can be captured by sample nuclei to form an excited state in the "compound nucleus" of atomic weight A+1. The capture interaction removes neutrons from the beam passing through the sample. A detector placed downstream of the sample measures the neutron flux as a function of the time when the neutrons arrive; there are dips (Figure 1) in the observed spectra at the energies at which the compound nuclei were formed. The depths of the resonances and their energies are unique to the materials traversed by the neutrons. NRS experiments can take advantage of this uniqueness to localize temperature measurements in space by inserting a dopant that resides only in the region of interest. The shapes of these resonances depend on both intrinsic resonance properties and on the Doppler broadening produced by the motion of atoms in the target sample. By measuring the amount of broadening produced, NRS determines the temperature of the sample.

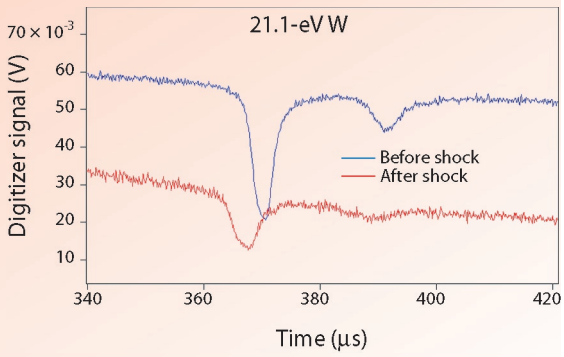

Figure 1. Resonances at 21 eV and 18 eV in the transmitted neutron flux through an isotopically enriched ^{182}W sample before and after the material is shocked. The two curves show the comparative broadening of the resonances, as well as the shifts in resonance positions.

LANSCE Accelerator Provides an Intense Source of Neutrons

Obtaining the necessary statistics for accurate NRS temperature measurements requires a copious source of epithermal neutrons in a single pulse. The linear accelerator at LANSCE produces 800-MeV protons that are loaded into the Proton Storage Ring where they are accumulated and then released as a short, intensified beam pulse. (Each pulse contains about 30 trillion protons.) The intense proton pulse is directed at a uranium spallation target and produces many high-energy neutrons upon striking the target. These high-energy neutrons then bounce around in a polyethylene moderator where they slow down to epithermal energies and emerge into the NRS secondary beam line. With this special setup, NRS achieves neutron brightness levels an order of magnitude higher than is presently available at the main LANSCE production target.

A fast temperature "snapshot" is required to study dynamically loaded systems. For instance, to measure the temperature after the passage of a shockwave, the measurement must be recorded after the sample is fully shocked but before any rarefactions return from the front, rear, or side surfaces. The time window for measuring the unreleased temperature in a shocked metal is about 1 μs (Figure 2). The time resolution of the NRS measurement is determined by the spread in transit times of resonant neutrons traversing the sample. In the Blue Room at LANSCE, the sample can be placed at a short distance (within 1 m) from the moderator, and fast time resolutions of several hundred nanoseconds are achievable.

Figure 2. Rendering of an NRS experiment to measure temperature in a shocked metal. (a) An explosively launched aluminum flyer initiates the shock in a molybdenum target, which contains a region doped with ^{182}W. Neutrons probe the doped region after the passage of the shock wave but before the return of rarefactions. Figure 2(b) is a view inside the target chamber used in the NRS experiment at LANSCE.

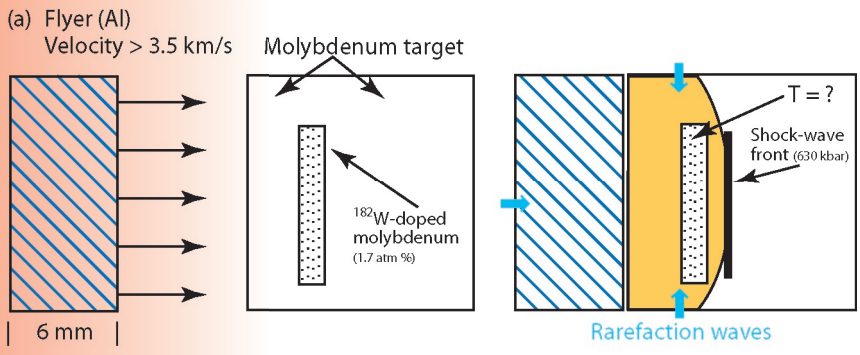

(b)

Temperature Behind the Passage of a Shock Wave in Molybdenum

The NRS experimental effort with highest priority is the measurement of the temperature behind a strong shock in a metal. This type of measurement provides a means for testing various EOS models. NRS is currently the only technique capable of measuring the internal temperature without significantly altering the shocked state. The NRS team has performed temperature measurements in molybdenum within 1 μs of the passage of a shock wave through the sample. Within the constraints imposed by the high-explosive load limit in the containment vessel, the sample size, geometry, and location of the doped region in the metal were selected to maximize the time between passage of the shock and the appearance of rarefaction waves at the doped region. A preliminary analysis of the NRS data indicates that two shots provided temperatures of 785 ± 59 K and 908 ± 35 K for particle velocities of 0.90 and 0.96 km/s, respectively. Figure 3 shows that both measured temperatures are higher than those presently predicted by the best SESAME EOS[1] for molybdenum (SESAME 2984).

For safety reasons, the dynamic shots are fired at an angle to the neutron beam so as to prevent penetration of the containment vessel windows by shrapnel. Because of this tilt angle, the beam does not arrive simultaneously at all parts of the doped layer. The nonsimultaneity of arrival can alter the perceived temperature; we are currently modeling the effect that the tilt of the sample has on the derived temperature. So far, the effect of the tilt is too small to account for the difference between our experimental results and theory. The NRS team is currently working on design changes for future experiments that would reduce the hydrodynamic effects introduced by the sample tilt. A review of the NRS program by the Campaign 2 management encouraged EOS studies in metals as a high priority. In the latter part of the LANSCE 2003–2004 run cycle, we plan to perform additional experiments on molybdenum and/or other metals.

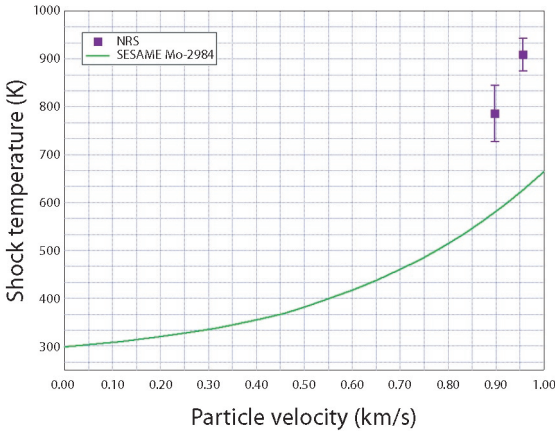

Figure 3. Shock temperature values extracted from NRS data are compared to theoretical values calculated using SESAME 2984 EOS. Temperatures are higher than the predicted values.

Measurement of the Temperature Behind the Burn Front of Detonating High Explosives

In a second experimental thrust, we measured the temperature behind the burn front of a high explosive detonated by a 6-mm-thick aluminum flyer plate. (The setup was similar to the one used in the shocked-metal experiment described above.) Through the use of a flyer plate, we can support the pressure behind the detonation front at a value just below the Chapman-Jouguet (CJ) point for the explosive (Figure 4). An NRS determination of the temperature inside detonation products of high explosives would fill a major gap in the characterization of its EOS. The largest uncertainty in theoretical modeling comes from the chemical equilibrium composition. Calculations by Sam Shaw (T-14) indicate that a shift from the combination of CO_2 and carbon in the products to CO can reduce the released energy by around 25%. Shaw calculates the corresponding shift in temperature to be around 1,000 K. This very strong correlation of the temperature with the composition is what makes the NRS measurements so useful. Several thermodynamic methods using potential energies exist for treating the EOS of high-explosive products, and these can be calibrated against experimental data. Additional calculations confirm that the WO_3 dopant has negligible effect on the high-explosive temperature. The fine-tuning of Shaw's model against NRS temperature measurements would greatly narrow the allowed parameter space and provide insight into the EOS of the high explosive.

The initial dynamic high-explosive EOS experiment performed by the NRS team did not result in a valid temperature measurement because of unanticipated dopant-clumping in the sample. Clumping can result in non-uniform thickness that distorts the extracted temperature; if the clumps are large enough, the temperature will not equilibrate within a clump. A subsequent NRS dynamic experiment used a new method of high-explosive formulation that was designed to reduce the clumping of the dopant in the high-explosive samples. Analysis indicates that the new formulation significantly reduced the clumping within the sample but did not completely eliminate it. The NRS measurement also indicated a particle velocity nearly one-half that predicted, but unfortunately the independent VISAR velocity measurement was lost because the VISAR optical fiber was damaged prematurely by the explosive. For future experiments, we will use a formulation of doped high explosive that incorporates nanoparticle tungsten-oxide dopant to further reduce non-uniformity and clumping. However, further shots may not take place until other higher-priority experiments are completed.

Measurement of the Temperature at a Sliding Interface at High Pressures and Velocities

Another challenge that the NRS team plans to address is determining the properties of a shocked metallic interface. One such interface of great interest exists between two materials possessing significantly different shock speeds. If a shock is initiated in both at the same time (Figure 5), the shock on one side of the interface will outrun the shock on the other side, causing the two materials to slide relative to each other at high velocity while experiencing a large normal force caused by the high-pressure shock. To date, there are no experimental data on the temperature rise at a compressed, sliding interface at high pressures and velocities. A constitutive model of the tangential

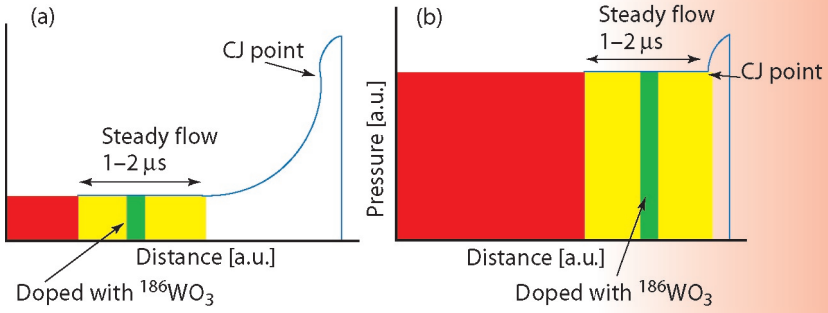

Figure 4. (a) This rendering depicts an unsupported detonation. (b) This rendering depicts how an aluminum flyer plate in the NRS experiment supports the pressure behind a detonation front at a value just below the CJ point for the explosive.

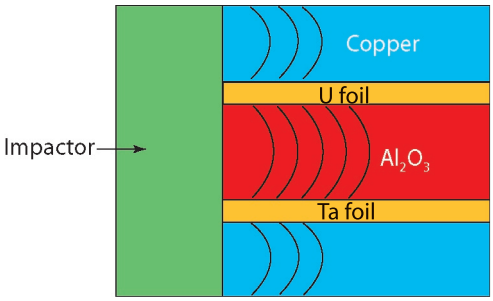

Figure 5. Schematic showing shock in sapphire (Al_2O_3) outrunning the shock in the adjoining copper. The neutron beam is passed through the sandwich, and resonances in Ta and U foils located at the Al_2O_3/Cu interfaces provide temperature data.

force as a function of pressure, temperature, sliding velocity, and the state of interfacial deformation at short times (t < 50 μs) was constructed.[2-4] However, there has been little in the way of experimental data to guide models that are important to the code development efforts of X Division. Measurements of the interfacial temperature will provide bounds on the parameters in the models and their uncertainties.

Our first NRS friction experiment will measure the temperature under dynamic conditions. The sample will consist of a sandwich comprised of an Al_2O_3 slab between slabs of copper (each slab being 2 cm thick). In addition, thin foils (50 to 100 μm thick) will be placed at the interfaces—a tantalum foil at one interface and a uranium foil at the other. An explosively launched aluminum flyer plate traveling parallel to the interfacial planes will impact the sandwich at about 2.5 km/s. Because shock in the Al_2O_3 travels much faster than the shock in the copper, a steady sliding state of about 1 cm in length should be achieved for a little over 1 μs. The shock pressure should be about 200 kbar, and relative interfacial velocities between the Al_2O_3 and foils should be about 0.5 km/s. The neutron beam will pass through the target while the temperature is elevated from the frictional heating. The temperature rise in the foils should be between 100 and 1,000 K, depending on the magnitude of the frictional force; by measuring the temperature, we should gain knowledge of the frictional force. There are resonance lines in tantalum and uranium at 39 eV and 37 eV, respectively, and they are separated enough in energy for temperature measurements to be possible at the two interfaces in the same experiment.

References

1. B.I. Bennett, J.D. Johnson, G.I. Kerley, and G.T. Rood, Los Alamos Scientific Laboratory report LASL-7130 (unpublished); Los Alamos Scientific Laboratory brochure LASL-79-62 (unpublished); Equation-of-State and Opacity Group, Los Alamos National Laboratory brochure LALP-83-4 (unpublished); S.P. Lyon and J.D. Johnson (Eds.), "SESAME, the Los Alamos National Laboratory equation of state database," Los Alamos National Laboratory report LA-UR-92-3407 (1992).
2. J.E. Hammerberg *et al.*, "Nonlinear dynamics and the problem of slip at material interfaces," *Physica D* **123**, 330–340 (1998).
3. J. Röder *et al.*, "Multichain Frenkel-Kontorova model for interfacial slip," *Physical Review B* **57**, 2759–2766 (1998).
4. J. Röder *et al.*, "Dry friction: modeling and energy flow," *Physica D* **142**, 306–316 (2000).

Acknowledgment

We would like to acknowledge those individuals without whose efforts and help this work could not have been performed. Ron Rabie, now retired, has been an integral member of the collaboration and a driving force. We are indebted to the DX firing crews who helped setup and fire our explosive shots, in particular, Howard Stacy, Pat Quintana, Don Murk, Robert Lopez, Steve Dennison, Fidel Martinez, Joe Bainbridge, and Vern Lawrence. The work of Bruce Takala, the Blue-Room Experimental Area Manager and LANSCE-3 technicians Greg Chaparro and Lloyd Hunt are essential to the setting up of our apparatus in the Blue Room, as is Gil Peralta from P-23. We have had valuable discussions with Carl Greeff of T-1, and he has provided calculations of predicted temperatures relevant to the shocked metal experiment. Finally, the LANSCE-6 operations crew provided invaluable assistance in tuning and delivering the sole-use proton beam that is absolutely necessary for carrying out these experiments. The NRS work has been funded by Campaign 2 of the DOE Defense Programs. Excursions into the studies of metal jets have received funding from a DOE/DoD memorandum of understanding.

For more information, contact Vincent Yuan at 505-667-3939, vyuan@lanl.gov.

Ejecta Density Measurements Using Soft X-ray Radiography

D.S. Sorenson, N.S.P. King, K. Kwiatkowski, I. Campbell (P-23), R.T. Olson (P-22), J.L. Romero (University of California, Davis)

Soft x-ray imaging has been developed and used for measuring ejecta density distributions from shock-loaded metals. Ejecta are metal particles (solid or liquid) that are emitted from a shock-loaded surface. Over the years, we have developed an electronic imaging system capable of recording up to four images. In particular, we have focused on three main areas: multiframe camera systems, image-relay systems, and scintillators. Our system is currently capable of measuring ejecta densities down to 0.5 mg/cm^2 over a 50-mm^2 field of view using lutetium oxyorthosilicate/yttrium oxyorthosilicate scintillators (200–300 μm thick). The x-ray sources typically give 15 mrad at 1 m with a spot size of 1.5 mm. We can obtain typical interframe times of hundreds of nanoseconds to many microseconds. Images formed on the scintillator are relayed through coherent bundles and connecting-fiber-optic reducers over a distance of about 3 m.

We are also developing various models of our experiments using Monte Carlo methods. These models enable us to accurately calculate plutonium transmission versus areal densities, which we use to calibrate our data. Figure 1 shows an example of data and a simulation for a range of metal foils. We expect to continue improving the soft x-ray imaging system and the simulation models to allow us to more accurately determine ejecta density distributions.

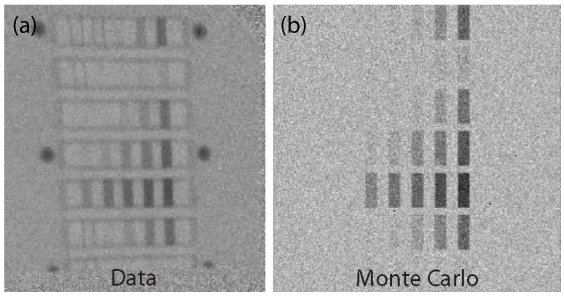

Figure 1. Comparison between data (a) and a Monte Carlo prediction (b).

Cross Validation of Ejecta-Areal-Density Measurement Techniques

R.T. Olson (P-22), W.T. Buttler (P-23), W.W. Anderson (DX-2)

Ejecta-diagnostic-development experiments are being performed as a collaborative effort between P and DX Divisions. These experiments use piezoelectric pins, Asay foils, and x-ray radiography to simultaneously measure the ejecta areal density generated by a planar shock from the surface of a tin gas-gun target. Each measurement technique measures a different physical quantity that can be related to the ejecta areal density. The piezoelectric pins generate current as ejecta imparts a time-varying force to a lead-zirconate-titanate (PZT) ceramic material. The Asay foil velocity is recorded as ejecta inelastically collides with and transfers momentum to a thin foil. X-ray flux through the ejecta cloud is attenuated according to the type of ejecta material and its density. The data acquired by each diagnostic technique are then independently analyzed and compared to cross-validate the precision and accuracy of each technique. Experiments performed thus far indicated that the Asay foil and x-ray radiographic techniques provide areal-density measurements that agree to within ~ 15% of one another. The PZT pins have recorded areal densities that range from identical to a factor of three higher than the other techniques. Currently, additional experiments are being conducted to understand the reason behind this discrepancy.

Surface-Temperature Measurements Under Shock Compression

A.W. Obst, K. Boboridis, J.R. Payton, A. Seifter, W.S. Vogan (P-23)

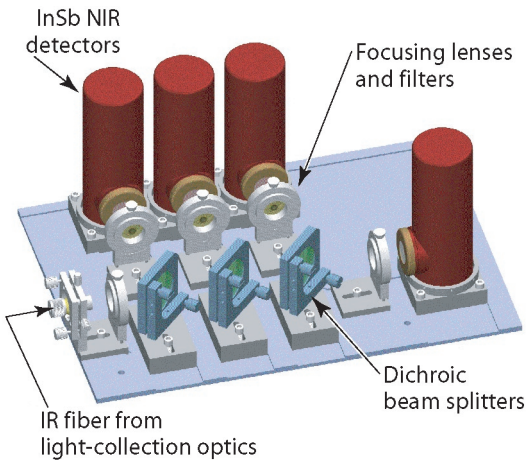

Figure 2. Rendering of an NIR pyrometer developed by members of P-23. Light incident from the left is wavelength split at each of the three dichroic beamsplitters. The four InSb NIR detectors then collect the light.

The accurate measurement of the temperature of shock-compressed materials is of great interest in high-pressure physics. Shock-physics experiments serve as a primary diagnostic in constraining the EOS of materials and in determining the state of ejecta and spallation from these surfaces. Shock techniques at LANL include the use of laser ablation at the Trident laser facility, gas guns at Ancho Canyon, and high-explosive Forrest flyers at TA-40, Chamber 8. We use high-speed, time-resolved, multi-wavelength near-infrared (NIR) surface pyrometry to measure shock temperatures from 400 K to 1,500 K. The detector unit of an NIR pyrometer developed by P-23 is shown in Figure 2. This instrument was calibrated at the National Institute of Standards and Technology (NIST) in Gaithersburg, MD.

Inferring the thermodynamic or true surface temperature from blackbody radiance-temperature measurements requires a knowledge of both the static and dynamic emittance, or equivalently emissivity, of materials under shock compression—both as a function of wavelength and temperature. Toward this end, we are developing a number of surface-study diagnostics, including high-speed laser NIR polarimetry; integrating-sphere reflectometry; and, for absolute calibration purposes, a pulse-heating system. The first two surface diagnostics have been built and are operational, whereas the pulse-heating system is under construction. A further EOS constraint is provided by comparing surface and volume temperatures, where the latter is obtained from NRS. The NRS high-explosive Forrest flyer experiments were done at LANSCE, whereas the comparative surface high-explosive Forrest flyer measurements are being done at TA-40, Chamber 8.

Fundamental Properties of Beryllium for ICF Applications

J.A. Cobble, D. Swift, T. Tierney (P-24), A. Nobile, B. Day (MST-7), D. Tubbs, N. Hoffman (X-1)

P-24 is actively engaged in a set of qualification experiments for beryllium as an ablator material for radiation-driven ICF. For a successful fuel implosion, among other requirements, the drive must be extremely uniform. This is where questions concerning beryllium arise. Although its strength and conductivity exceed that of alternate ablator materials, its structure is anisotropic. During that time in the implosion before the beryllium melts, this anisotropy is believed to drive hydrodynamic instabilities which can, in principle, destroy the target before ignition occurs. Understanding the anisotropy is complicated by the grain structure of the beryllium. For larger grains, this problem is aggravated, while for small enough grains, the inhomogeneities are expected to "average out." We must know the behaviors of these options for specifying a successful target design that we can fabricate for a reasonable cost.

We have begun experiments at the Omega laser at the University of Rochester to investigate the microstructure of beryllium and its role in Rayleigh-Taylor hydrodynamic instabilities. During the summer of 2003, we drove machined sinusoidal perturbations in planar beryllium samples with x-ray radiation from laser-driven hohlraums. The goal was twofold: to develop diagnostic techniques with the aim of observing the growth rate of instabilities caused by the beryllium microstructure and to develop a radiation-drive environment similar to that expected in the first few nanoseconds of requisite laser drive at NIF now under construction at Lawrence Livermore National Laboratory (LLNL). The initial Omega experiments provided data that encourage us to continue the research. P-24 is closely allied with theoretical physicists in X-1 who model the experiments for comparison with the Omega results.

High-Speed Pyrometry Measurement of Shocked Tin and Lead

D. Partouche-Sebban, R.R. Bartsch, D.B. Holtkamp, P. Rodriguez, J.B. Stone, L.J. Tabaka, D.T. Westley (P-22), F.G. Abeyta, W.W. Anderson, M.E. Byers, F.J. Cherne, D. Dennis, J.S. Esparza, C.M. Fowler, R.S. Hixson, P.A. Rigg, D.L. Shampine (DX-2)

P and DX Divisions have recently undertaken a study of the Hugoniot and melt curves of tin and lead in the pressure-temperature diagram up to about 60 GPa in pressure. In most shock experiments, the sample temperature needs to be measured in less than a microsecond. Currently, high-speed optical pyrometry seems to be the best way to perform this measurement. This is still a challenge for any metal because a strong optical background is generally present in such experiments and needs to be totally eliminated. Moreover, when studying metals, pyrometry accuracy is mainly limited by the fact that the emissivity of the shock-loaded sample is not known accurately. As a result, we carefully select the pyrometer wavelengths in order to minimize the effect of emissivity uncertainty on these experiments.

The preliminary results on tin are promising and supplement previous data to confirm that the Hugoniot curve of tin is somewhat higher than expected. Reflectivity diagnostics are also fielded to obtain data on the sample surface emissivity during the experiment in order to both improve the accuracy on temperature and perhaps to detect phase transitions.

The experimental program on lead will begin in early 2004. In particular, several kinds of transparent windows (LiF, PMMA, and sapphire) will be used to cover a large part of the melt curve in the vicinity of where it coincides with the Hugoniot curve.

Subcritical Experiment Diagnostics

D.A. Clark, C.M. Frankle, D.B. Holtkamp, P. Rodriguez, J.R. Smith, L.J. Tabaka, D.T. Westley (P-22), with significant collaboration from other LANL groups, Sandia National Laboratories, Bechtel Nevada, and the Atomic Weapons Establishment

In the summer of 2002, the SCEs, Mario and Rocco, and two confirmatory shots were fired in the U1a complex at NTS. An earlier confirmatory shot was fired at LANL in December 2001. On those shots, P-22 fielded three diagnostics. A series of optical pins were used to record the arrival time of the expanding metal surface at preset distances. Free-surface optical pyrometry was used to measure the surface temperature of the plutonium at shock breakout. Four Asay windows (a VISAR diagnostic viewing the plutonium surface through a lithium-fluoride window) were used to diagnose the spall behavior of the plutonium.

The Armando SCE and its confirmatory shot are scheduled for April 2004. Both will be fired in the U1a complex. P-22 has played a significant role in the development and fielding of the Cygnus flash x-ray machines, which will be the primary diagnostic for the Armando shot. P-22 will also field free-surface optical pyrometry as a secondary diagnostic.

The Krakatau and Unicorn SCEs and their confirmatory shots are scheduled for FY 2005. Krakatau will be fired in the U1a complex, and Unicorn will be fired in a hole at U6c (which is in the Yucca Flats area of the NTS). The current plan for Krakatau calls for P-22 to field optical pins, free-surface pyrometry, multipoint VISAR, and possibly Asay windows. On Unicorn, P-22 will field a *reaction-history-like* gamma-ray-flux diagnostic, using field-test neutron generators to interrogate the package.

SNM Midcourse Detection

G.H. Nickel (P-22), R.E. Mischke, D.M. Lee (P-25)

In April 2003, LANL was asked by the Missile Defense Agency (MDA) to examine the feasibility of using the nuclear characteristics of special nuclear material (SNM) as a discrimination signature for a missile attack. The threat was presumed to consist of a single launch with many decoys—unlike the previous Strategic Defense Initiative work that considered hundreds of launch vehicles.

While the goal of this study was to determine the possible signature signals—not to develop an engineering design, the practicality of any proposed solution was important. Our team made comparisons to previous studies, actual deployed space systems, existing detectors, and reasonable extensions of current radiation-source technology. After considering a variety of sensors, our team determined that natural radiation or emissions created by cosmic rays would not be practical, except at distances of a few meters. The use of nondirectional active methods, such as neutron sources, would require extremely short ranges as well. Our team concluded that a highly directional active system such as an advanced neutral-particle accelerator, together with an array of detectors, could be feasible.

Our study was prepared and presented to the MDA "Blue Team" by members of P-DO, P-22, and P-24. The engineering design of such a system, although difficult, could be the subject of another study.

Sputtering from Fission Fragments

A. Klein, G.L. Morgan (P-23), D.G. Madland (T-16)

We are currently designing and constructing an experiment to measure the yield of neutral particles and clusters of particles that are sputtered from californium, uranium, and plutonium by internal fission. Although low-energy, heavy-ion-induced sputtering has been extensively studied for charged secondary ions, the neutral yield has so far only attracted scant interest because of the experimental difficulties of detecting neutral particles. In addition, conventional theoretical models, like the binary collision model (BCM) and molecular-dynamics (MD) calculations, will either breakdown at fission-fragment energies (BCM) or are currently impossible because of limited computer resources (MD).

Our setup will consist of an open source; a catcher foil, which will collect the sputtered material; and a silicon photodiode. All of the elements under study are decaying by alpha (α) decay. The silicon photodiode will measure the α activity of the sputtered material on the foil, thus allowing us to precisely determine the amount of material that has been desorbed from the target material. In a later stage of the experiment, we plan to measure the cluster size and energy distribution of the neutrals as well.

Laser-Driven Flyer Plates Generate Shock Waves in Weapons Materials

D.L. Paisley, D.C. Swift, T.E. Tierney, S. Luo, R.P. Johnson, C. Munson (P-24)

Laser-driven flyer plates can be used to impart shock waves into condensed-matter targets to study the results of dynamic shock-loading and release, similar to what happens in weapons systems. These plates can also be used in basic research to study the dynamics of materials (Figure 3). Using a laser to launch a one-dimensional flyer plate instead of using it to directly shock a material decouples the laser parameters from the flyer plate as it impacts a target material. A properly launched flyer plate resembles the projectile of a gas gun used to impact a target material, but it is usually smaller in size (8-mm in diameter). The smaller size of the laser-launched flyer plate without the normal sabot used in gas guns makes target recovery after an experiment much easier, especially with SNM, and mitigates most of the collateral damage to the target material. Laser-launched flyer plates can complement more traditional experimental methods and be used to perform unique experiments that may be difficult to do by other methods. The Trident laser at LANL can be configured with a long pulse length [2-μs full-width at half maximum (FWHM)] and greater than 500 J.

A 100–500 J, 2-μs FWHM temporal profile with a uniform spatial-profile laser beam is transmitted through a transparent substrate to an ablative layer sandwiched between the substrate and the flyer plate. As the laser energy is deposited in the ablative layer, the resulting "trapped" plasma expands and accelerates the flyer plate away from the substrate. Depending on aerial mass and energy, plate velocities of 0.1–5 km/s can be achieved. Currently, we are using 0.5- to1.5-mm thick flyer plates accelerated to 0.1–0.5 km/s to study the constitutive properties of weapons-related materials, and, in particular, the dynamic tensile strength (spall) as it relates to material composition and morphology. Flyer plates are launched into targets, and data are collected using multi-point VISAR and line interferometry as the primary diagnostics to measure shock and/or free-surface velocities. We anticipate Trident experiments to contribute an understanding to age-related changes in SNM that might affect the nation's enduring stockpile.

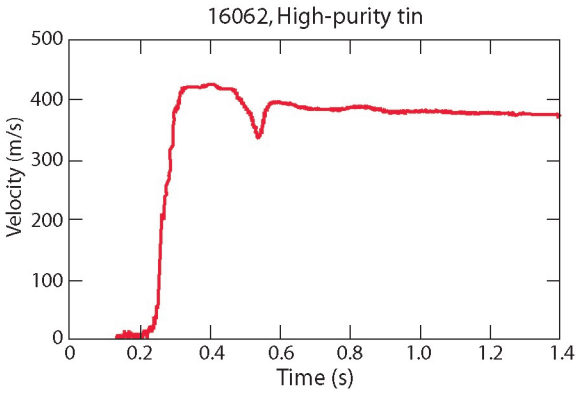

Figure 3. A laser-launched aluminum flyer plate is launched into a tin target, and the free surface of the tin is recorded by VISAR. The free-surface velocity profile obtained with VISAR allows us to determine the dynamic spall strength of the tin.

In-Line Holography for Ejecta Particle Size Measurements

D.S. Sorenson, D.R. Dillon, I.H. Campbell, W.T. Buttler, S.K. Lamoreaux (P-23), D. Tupa (P-25), R.P. Johnson (P-24), R.W. Minich (Lawrence Livermore National Laboratory), J.L. Romero (University of California, Davis), T.W. Tunnell, R. Fredrickson (Bechtel Nevada)

Holography has been used at NTS in the Cimarron and Thoroughbred shots at the U1a complex and at the Pegasus facility at LANL to measure ejecta-particle-size distributions. Ejecta are metal particles (solid or liquid) that are emitted from a shock-loaded surface. These measurements, in turn, allow us to calculate how the ejecta particles are transported in a gas environment.

The shape of the particle-size distribution reveals information about the fragmentation process. We are working toward a better understanding of how the particle-size distribution depends on the material properties of the shocked metal and an understanding of the shock-wave conditions. One of our goals is to develop a fragmentation model that we can apply to a variety of metals and pressure conditions. To advance this model, we have planned a series of experiments at the two-stage gas gun at LANL to measure particle-size distributions for shock-loaded tin for a range of pressures well below and above melt. We plan to extend these measurements using the TA-55 plutonium gas gun and Joint Actinide Shock Physics Experimental Research facility at NTS. As a part of this effort, we have built a frequency-doubled Nd:YAG high-power (0.6 GW) laser capable of providing a 120-mJ, 200-ps-wide laser pulse. The laser can be fired externally in single-shot mode. In addition, we are making improvements to the analysis programs used to reconstruct the particles. We have completed evaluating the laser and are in the final stages of designing the two-stage holography ejecta experiments.

Equation of State of Beryllium

D.C. Swift, R.P. Johnson, G.A. Kyrala, D.L. Paisley, T.E. Tierney (P-24), A. Hauer (P-DO), D.J. Thoma, J.C. Cooley (MST-6), M.D. Knudson (Sandia National Laboratories)

We used the flyer and ICE capabilities of the Z machine at SNL to investigate the EOS of beryllium to ~ 200 GPa on the STP (standard temperature and pressure) isentrope and around the principal shock Hugoniot—the locus of thermodynamic states that can be reached from a given initial state by the passage of shocks of different strength. This work was performed in support of the beryllium capsule design effort for ICF; our ultimate goal is to measure the onset of shock melting and hence to help control the seeding of ablative Rayleigh-Taylor instabilities.

In the flyer experiments, we impacted copper flyers traveling between ~ 7.5 and 9 km/s into samples of beryllium ~ 500 μm thick. The samples were backed by lithium-fluoride windows. We obtained laser Doppler velocimetry records at the beryllium/lithium-fluoride interface. In each experiment, the target assembly covered only half of the area of the flyer. We measured (also by Doppler velocimetry) the acceleration history of the flyer to characterize its state at the moment of impact.

Though superficially the shots seem quite simple, we had to include several corrections to explain features in the velocity history: the presence of a residual aluminum liner on the back of the copper flyers (we also performed control experiments with aluminum samples), residual drive pressure at the moment of impact, and the impedance mismatch between the beryllium sample and the lithium-fluoride window. The velocity histories exhibited additional features that may indicate shock or release melting. The peak interface velocity observed in each experiment—a measure of the EOS—was in good agreement with simulations using the published EOS for beryllium. Hugoniot points deduced from each experiment also matched the published Hugoniot EOS to within their uncertainty. Elastic precursor waves were expected to run ahead of the lower-pressure shock waves, but the velocity records did not have adequate time resolution to distinguish the precursors and, hence, to measure their amplitude, which would have helped verify models of plasticity in the 10- to 100-ns regime.

The ICE shot used beryllium samples ~ 250 and 500 μm thick to study the evolution of smooth compression waves as they propagated through the beryllium. Again, we obtained velocity histories by laser Doppler velocimetry. Between zero (i.e., the aluminum liner only) and 250 μm, the compression wave remained smooth and its evolution could be explained using the published EOS. Between 250 and 500 μm, the compression wave in the experiment apparently developed into a shock. This behavior was not reproduced in simulations using the same EOS—although the thicker experiments were subjected to a similar pressure history. The most likely explanation at present is that there were gaps in the assembly of the thicker samples, which would have led to the formation of shock waves.

The experiments on beryllium have demonstrated that published EOS from the SESAME and Steinberg compendia seem to be valid up to 200 GPa from the STP isentrope to the principal Hugoniot. We have elucidated some of the effects which need to be accounted for when interpreting detailed material response from flyer-impact experiments at Z. There may be some evidence for shock melting under conditions relevant to the ICF capsule.

Quantitative Ejecta and Timing Diagnostic Studies

W.T. Buttler (P-23), I.H. Campbell, D.R. Dillon, N.S.P. King, G.L. Morgan, J.R. Payton, D.S. Sorenson, M.D. Wilke (P-23), R.T. Olson, D.T. Westley, D.M. Oro (P-22), C.L. Morris (P-25), W.V. Anderson, F.G. Abeyta, M.E. Byers, R.S. Hixson, P.A. Rigg, D.L. Shampine (DX-2)

At LANL, we are quantitatively investigating the *Dynasen* piezoelectric pins as a useful, inexpensive alternative to the cumbersome Asay foils that require expensive, complex interferometric systems. We are considering two different *Dynasen* technologies: PZT and lithium niobate ($LiNbO_3$). To support this investigation, we have performed three series of gas-gun experiments in collaboration with DX-2 and P-22 to verify the static pin calibrations in regimes where material are known to be ejected from the vacuum-surface interface (ejecta). In the first series of experiments, configurations were such that the pressure profile was one-dimensional in nature. In addition, our experiments were performed with a supported shock, or a square pressure profile. The function of the grooves was to generate enough ejecta to be observed and characterized by an x-ray diagnostic fielded on each set of shots. In addition, most of the experiments included an Asay foil. The motivation of the different diagnostics was to independently compare areal densities as observed between the different technologies. Another set of experiments was performed on a different gas gun, using polished tin targets, a supported shock profile, x-ray diagnostics, piezoelectric pins, and Asay foils. A final set of experiments was performed with high explosives (unsupported shock, or *Taylor* wave) at NTS.

The probes themselves are thought to respond to viscous forces, such that the recorded voltage signal, $V(t)$, varies as the time derivative of the force: $F(t) = A\rho(t)u^2(t)$, where $\rho(t)$ is the ejecta volume density, $u(t)$ is the ejecta velocity, and A is the *normal* area of the piezoelectric material. The dynamic force is recovered from the measured piezoelectric-probe voltage, $V(t)$, by dividing by the termination resistance and probe sensitivity S ($S = 400$ pC-N^{-1} for the PZT and $S = 24$ pC-N^{-1} for the $LiNbO_3$), and then integrating the resulting corrected signal from the jump-off time to the time of arrival of the hard, free surface at the stationary probe. The probe is positioned at a well-defined distance behind the target. This result is then divided by the probe area A and the velocity of the ejected material, $u(t)$, and integrated again to recover the areal density of the material as a function of time. This result is then directly compared with the Asay foil results to determine whether the static sensitivity is accurate or whether there is a fixed, dynamic sensitivity that will accurately recover a quantitative representation of the observed Asay foil result; it is generally accepted that the Asay foil is a quantitative measurement.

The general conclusion of these experiments is that both technologies work well in a regime where the total areal density is at or below ~ 10–15 mg-cm^{-2}. As an upper limit on an appropriate regime, some experiments performed at LLNL were in good agreement at ~ 20 mg/cm^{-2}. The advantage of piezoelectric probes as compared to Asay-foil technology or x-ray diagnostics is the passive nature of the diagnostic and its low profile. Because of its profile, many tens of probes can be positioned to observe areal densities in tight, complex geometries. Lastly, the velocities, determined from the arrival of the free surface at the locations of the piezoelectric probes, have agreed to within 1–2% of velocities measured by other diagnostics, such as interferometry technology and x-ray diagnostics.

Friction Studies at pRad

G.A. Kyrala (P-24), J.E. Hammerberg (X-7), C.E. Ragan, III (X-5), K. Rainey (DX-3), D.A. Clark, B.J. Hollander, O.F. Garcia, K.A. Esquibel (P-22), C. Morris, D. Tupa, F.E. Merrill (P-25)

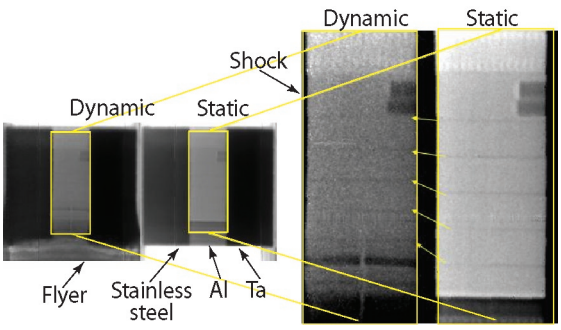

Figure 4. Diagram of the tantalum/aluminum/stainless-steel target with embedded tungsten wires.

This study is part of an LDRD-DR funded project, the "Physics Issues in Proton Radiography." This project's goal is to determine if pRad is a useful tool in friction studies. A secondary goal is to obtain data from a real target at slightly higher impact/shock velocities than those used on Atlas and Pegasus. Molecular-dynamic simulations show that the frictional force increases with sliding speed and then decreases to a very low value at the higher velocities. Frictional forces have been measured extensively at low velocities and low pressures (where the sliding speed is slower than the sound speed), but little has been done at higher velocities and higher pressures. The aim of our work is to establish the validity of the calculations in this intermediate regime using the imaging of implanted witness wires as a measure of the bending forces. Successful measurements using x-rays have been made on Pegasus but with limited spatial resolution. With the advent of well-developed tools for making measurements at the microscopic and mesoscopic scales, where a position resolution of < 15 μm over a 2-cm^2 field of view was demonstrated, we decided to take advantage of such a high-resolution tool for friction studies at the LANSCE pRad facility in Area C.

A friction experiment was fielded on October 16, 2003. This experiment used a flat-plate geometry, consisting of three 6-cm × 6-cm × 2-cm flat plates in the order (from right to left) of tantalum, aluminum (6061-T6), and stainless steel (21-6-9) (Figure 4). The target was impacted by a 15-mm-thick aluminum flyer plate at a nominal velocity of 2.2 mm/μs, driven by a Forrest flyer driver. In the midplane of the aluminum plate, a series of five 400-μm-diam wires were placed perpendicular to the tantalum/aluminum and stainless-steel/aluminum interfaces. The initial vertical wires are distorted near the interface during shock-loading as the aluminum shock outraces the tantalum and stainless-steel shocks. This loading results in a differential velocity along the interface, $0 < v < 1.1$ mm/μs, depending on the magnitude of the frictional force. Under these conditions, a steady state in pressure and relative velocity exists for a period of approximately 4 μs after shock arrival, after which release waves lead to significant unloading. During this time, the interface pressure is approximately $P = 200$ kbar with a relative velocity determined by the frictional force. Along with the radiographic measurement of wire configuration with time, a 7-point VISAR at the exit surface was employed to measure free-surface velocity at interfacial and noninterfacial sites as a check on the computational analysis and radiographic analysis of the wires. Initial results indicate a weaker frictional force than that measured in the Pegasus experiment, which was at slightly lower pressures and at one-half the flyer-impact velocity. This result (i.e., smaller or minimal bending at the pRad resolution) is consistent with a model that predicts a frictional force decreasing as a fractional power of the velocity [approximately as $v^{(-3/4)}$]. More extensive analysis of the data provided by this successful experiment is in progress.

Measurements of the Dynamic Properties of Beryllium Benefit the ICF and Weapons Program

D.C. Swift, D.L. Paisley, G.A. Kyrala, T.E. Tierney, S. Luo (P-24)

Scientists at SNL and LANL are supporting the weapons program and, at the same time, exploring new designs of fuel capsules for ICF by conducting experiments to study the EOS of beryllium and its properties (e.g., grain size, grain orientation, metal alloys, and solid-solid phase change). LANL's Trident laser and SNL's Z machine have allowed us to measure the EOS and flow stress in beryllium and to investigate solid-solid phase change and melt using flyer plates and ICEs. In collaboration with SNL, we have designed and conducted experiments on the Z machine using a multi-point VISAR as the primary

diagnostic. On Trident, we used VISAR, line interferometry, and transient x-ray diffraction as our primary diagnostics.

On Trident, we shocked 12- to 125-μm-thick beryllium foil samples and crystals by directly irradiating them with 30–200 J of laser energy for 1.0 and 2.5 ns, producing shock pressures up to 50 GPa (Figure 5). The primary feature that we were interested in was the elastic precursors that occurred at 0.7 km/s for the crystals and 0.5 km/s for the foils. On the Z machine, flyer plates were launched at beryllium targets to record shock on impact and/or particle velocity through the targets. Furthermore, we used the Z machine to study the effects of quasi-isentropic compression waves (at an estimated pressure of 195 GPa) in beryllium. These data will help define an ICF capsule design and provide weapon designers with additional information on beryllium. We will conduct further experiments on Trident, on the Z machine, and later at NIF to more fully understand how beryllium can be used in ICF capsules and provide data to weapons designers for code validation.

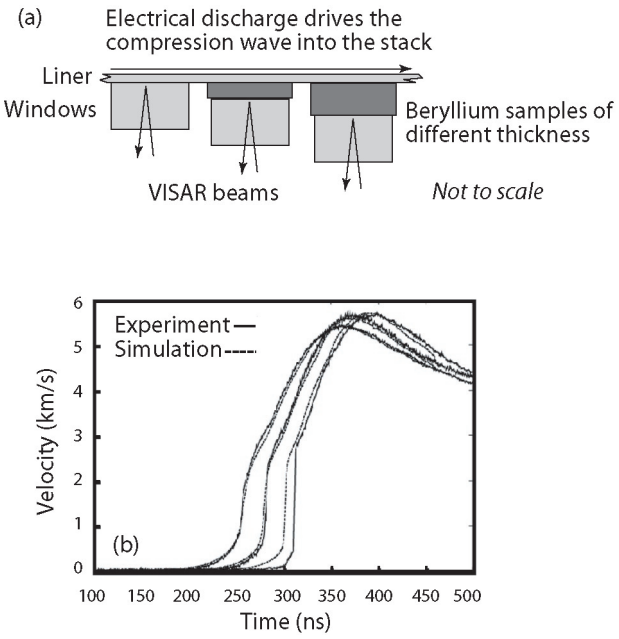

Figure 5. (a) A schematic of the quasi-ICE and (b) the comparison of an experimental result with simulation.

Development of well-validated material-failure-modeling capabilities requires both theoretical and experimental efforts. Because failure mechanisms depend strongly on material characteristics, it is difficult to predict the failure behavior of a material based on measurements made on other materials. Advances are needed to describe the complete physical processes and provide numerical-model implementation and testing. Model validation requires experiments that study phenomenology and material characterization, as well as more highly integrated validation experiments.

The pRad program at LANSCE delivers a multipulse capability that can produce a radiographic time sequence of dynamic systems. With the new capability to perform dynamic experiments that contain depleted uranium (DU), the pRad team was able to record a time sequence of the failure process in DU. We performed a series of experiments using 40-mm- and 80-mm-diam hemispherical shells of DU filled with high explosives. The explosive-loading accelerated a hemisphere into a biaxial stretching motion that led to material failure. We designed the experiments to study the failure process as a function of strain rate, initial shell thickness, and detonation configuration. The shot series included two 40-mm and two 80-mm DU hemispheres. A 40-mm steel hemisphere was also used to test new procedures and verify timing. All shots returned data that are currently being analyzed.

Figure 6 displays 4 of the 17 time-sequence transmission radiographs of the first 40-mm DU experiment. The evolution of the failure process towards a state where the material has fractured into cornflake-like pieces is clearly evident. Further analysis should yield estimates of DU density across the image, including fracture regions.

Failure-Mechanism Studies of Depleted Uranium Using Proton Radiography

K.B. Morley (P-23), for the Proton Radiography collaboration; L. Hull, P. Rightley, K. Prestridge (DX-3)

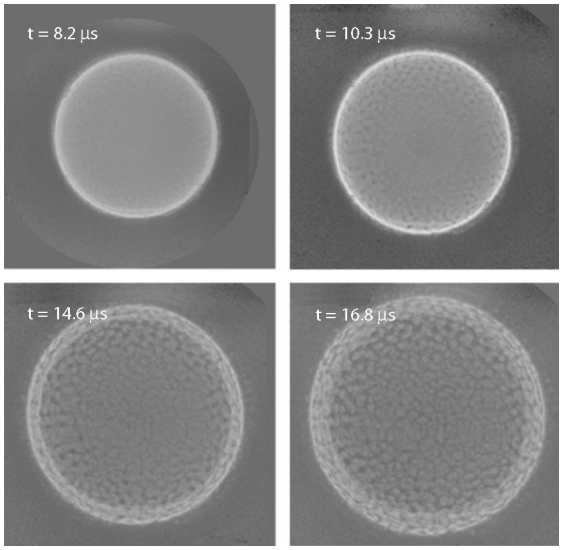

Figure 6. Transmission radiographs of the first 40-mm DU experiment; times are relative to the load ring.

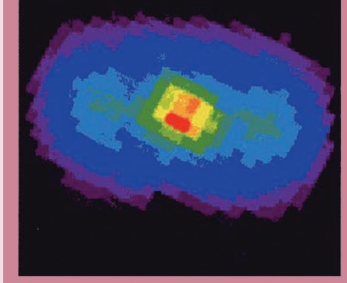

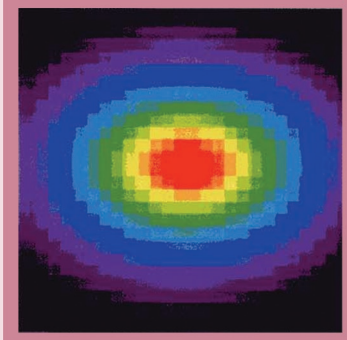

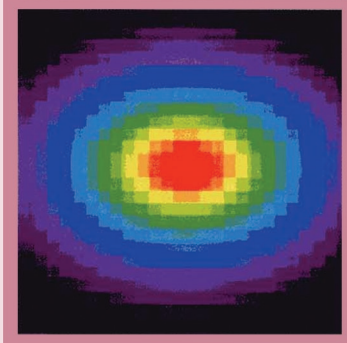

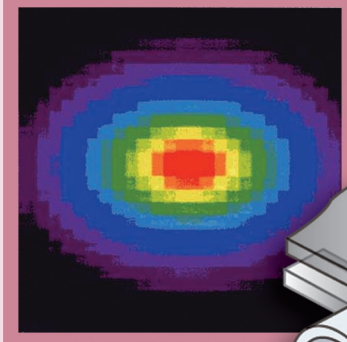

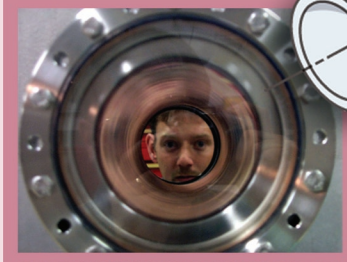

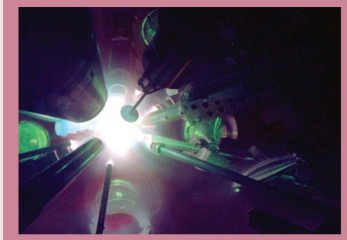

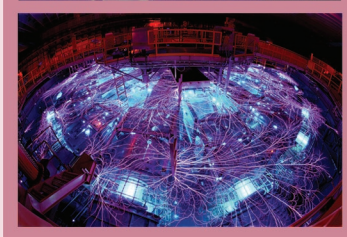

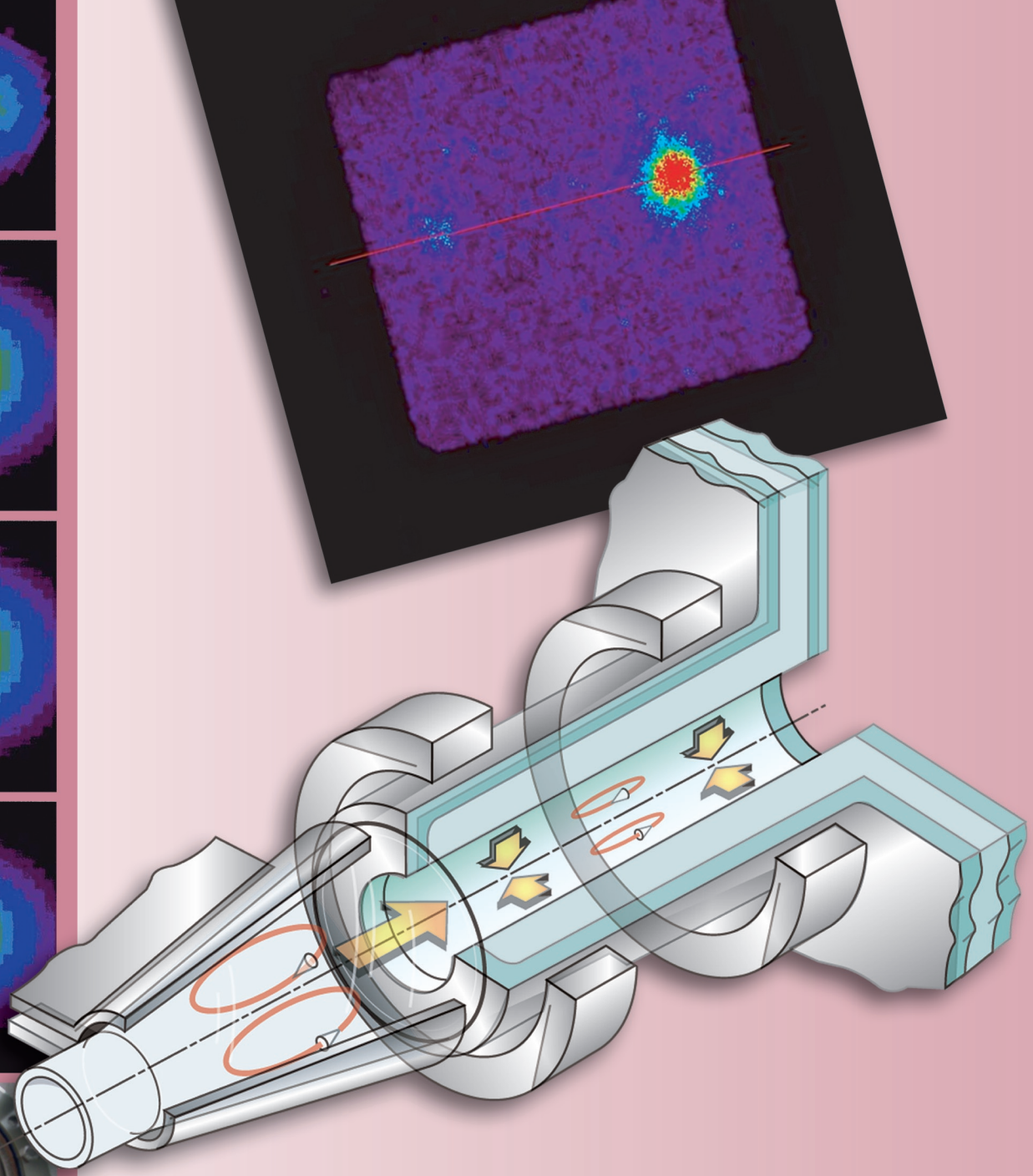

$$\delta_{ph} = (\lambda \Sigma \tan\theta \Sigma 1n2 + D_{clr})\left(1 + \frac{1}{M}\right)$$

$$p\frac{d}{dt}\left(\frac{p_i}{p}(u_i - u)\right) + \Sigma_j \frac{p_i p_j}{p} v_{ij}(u_i - u_j) = -p_i(u_i - u)\Sigma \nabla u -$$

Plasma Physics

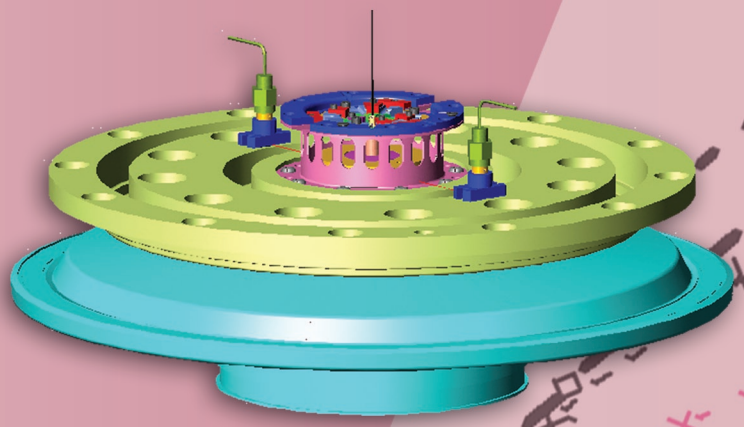

$$\nabla \Sigma P_i + \frac{p_i}{p} \nabla \Sigma P$$

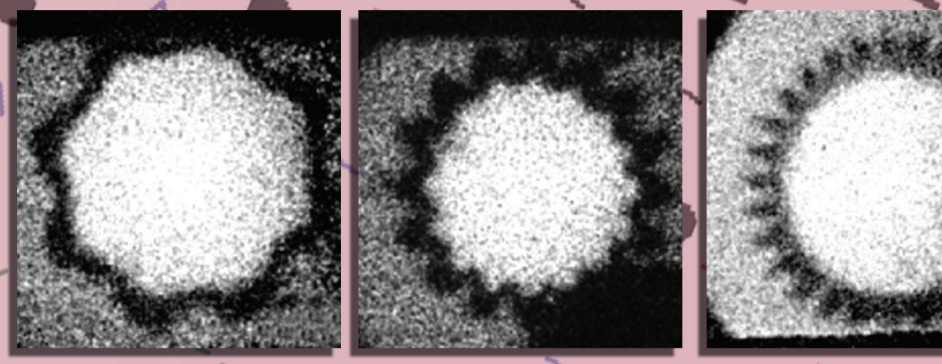

Plasma Physics Contents

Research Highlights

Understanding the Richtmyer-Meshkov Instability in the High-Energy-Density Regime 55

Neutron Pinhole Imaging for Inertial-Confinement-Fusion Experiments 59

"Magnetic Reconnection" Studies Conducted at Los Alamos National Laboratory 63

Radiological, Chemical, and Biological Decontamination Using Atmospheric-Pressure Plasmas 67

Experimental Physics Using the Z Accelerator at Sandia National Laboratories 71

FRX-L: A Plasma Injector for Magnetized Target Fusion 75

Project Descriptions

Neutron Generation Using Inertial Electrostatic Confinement 79

National Fusion Collaborations 79

Combustion Enhancement of Propane by Silent Discharge Plasma 80

Neutron-Imaging Studies of Asymmetrically Driven Targets on the Omega Laser 80

Developing a Fundamental Understanding of Laser-Plasma Interactions 81

Experimental Investigation of Fundamental Processes Relevant to Fusion-Burning, Strongly Coupled, Multi-Material Plasmas 82

Applied-Science Internship Program 82

X-ray Diffusion Through a Thin Gold Wall 84

Radiation-Hydrodynamic Experiments on the Z Accelerator 85

Quick-Reaction Capability 85

Understanding the Richtmyer-Meshkov Instability in the High-Energy-Density Regime

S.H. Batha, M.M. Balkey, C.W. Barnes, J.R. Fincke, N.E. Lanier (P-24), N.D. Delamater, R.M. Hueckstaedt, G.R. Magelssen, J.M. Scott (X-2), R.D. Day (MST-7), A.M. Dunne, C.J. Horsfield, K.W. Parker, S.D. Rothman (Atomic Weapons Establishment)

Fusion, the process that produces thermonuclear reactions in the sun, may someday be a solution to the world's energy problem as a virtually inexhaustible, relatively clean, and cost-effective energy source. For several decades, researchers worldwide have been investigating several approaches to initiate and control thermonuclear reactions. These methods involve the creation of a hot, dense plasma (an electrically conducting fluid composed of freely moving ions and electrons) heated to millions of degrees and held together long enough to produce useful energy through fusion reactions. One method (ICF)[1] implodes a pearl-size spherical capsule (a common geometry used in ICF experiments) that contains fusion fuel: deuterium (D) and tritium (T). Laser energy (or x-rays generated by the lasers) is deposited on the outside of the capsule, which ablates and drives shocks in towards the DT fuel. The fuel is ignited and burns for less than a billionth of a second. Ideally, the inertia of the highly dense plasma should hold it together long enough to produce fusion conditions. But achieving sustained thermonuclear fusion under laboratory conditions is difficult and has therefore become a "Grand Challenge" problem for the U.S. science community.

As shocks pass through material interfaces, they create Richtmyer-Meshkov Instabilities (RMI)[2,3] that "mix" the different materials. In *high-energy-density* ICF experiments using the Omega laser[4] at the LLE (University of Rochester), researchers are performing a series of implosion experiments to gain a better understanding of RMI. If not mitigated, the RMI creates "mixing" that introduces impurities into the fusion fuel. Impurities can dilute and cool the fusion fuel and quench the thermonuclear reaction. Although the typical ignition capsule used in ICF experiments is spherical, measuring the extent of mix at target interfaces in a sphere is difficult, if not impossible. For our RMI experiments, we used a cylindrical target that allows us to measure and observe mix axially along the interfaces while they are converging.

Understanding "Mix" in Fusion Reactions

The target assemblies used in our experiments were composed of materials with different densities (Figure 1). In each assembly, a small epoxy cylinder (outer target layer) was filled with polystyrene foam (inner target layer); an aluminum marker band with corrugations (perturbations) in its outer surface was inserted between the epoxy cylinder and the foam (Figure 1). The areas subject to RMI in these experiments involved two regions on the target assembly: (1) the interface between the epoxy cylinder and the marker band and (2) the interface between the marker band and the foam.

Fifty of the 60 Omega lasers illuminate the target assemblies with 18 kJ of energy. This energy heats them to extreme temperatures causing approximately one-half of the epoxy cylinder to vaporize and expand outward (away from the cylinder), while the other half is pushed inward (implodes) by a strong shock wave—a pressure force that travels faster than the speed of sound in the

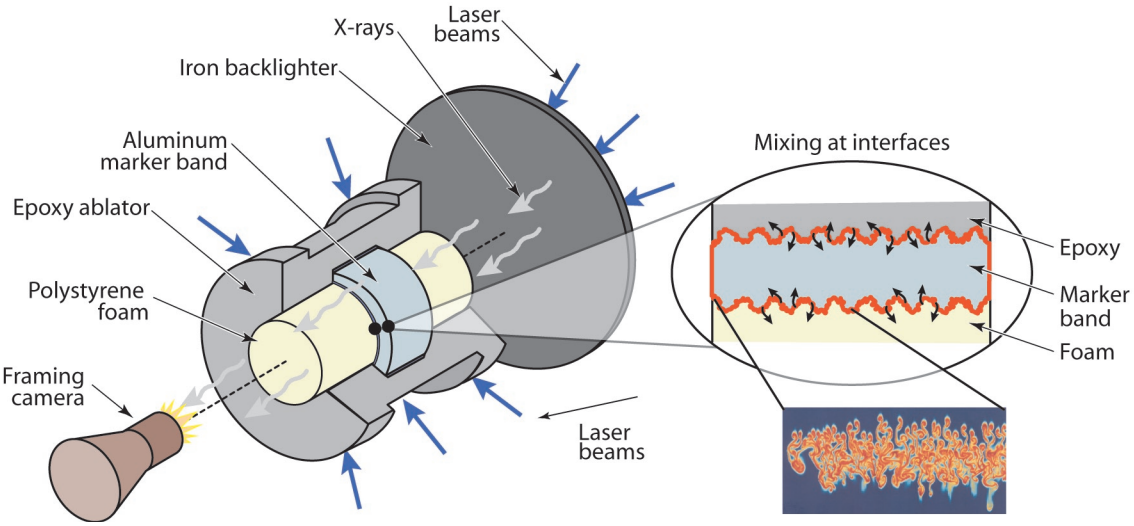

Figure 1. Rendering of a typical target used in the RMI experiment. These targets are about 2.25 mm long and 1 mm in diameter. A rough surface is machined into the outside of the aluminum marker band. The inset shows mixing at the interfaces. The target below (oriented in the same position as the rendering of the target) and an image of "mix" obtained from an advanced simulation are shown.

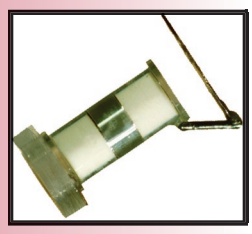

material. The passage of the shock wave through the target assembly heats the target materials and causes them to become plasmas. As a result, the interfaces along both sides of the marker band are accelerated, and the materials mix over time. The danger of RMI is that if the mixing becomes severe enough in an ignition capsule, fusion reactions end, and thermonuclear ignition—the ultimate goal of all ICF experiments—fails. To measure the amount of mixing, 5 additional laser beams from Omega strike an iron foil at one end of the cylinder after a small time delay. X-rays are emitted, travel lengthwise through the cylinder, and are collected by a framing camera that records 16 images through a pinhole. Each image spans approximately 60 ps, and the 16 images are distributed over 1 ns.[5]

Richtmyer-Meshkov Instability

The Richtmyer-Meshkov instability is a hydrodynamic instability driven by the passage of a strong shock past an interface between two fluids. Any perturbation present at the interface will grow proportionately with time. Most previous research into RMI has been done with intentionally seeded, simple perturbations in a flat geometry. Our recent high-energy-density RMI experiments[6,7] had several distinct features over these other RMI experiments. We imploded a cylindrical target to capture the same effects of a *convergent* geometry as those in an ICF capsule implosion. The target material in our RMI experiment was *compressible*—that is, the density increased when the shock passed through it. In addition, the materials that comprised the composite target in our experiments were *miscible* and could therefore mix freely into one another.

Moreover, we were interested in studying the effects of shock waves in the *strong-shock* regime where Mach (supersonic) numbers are greater than 10. With such strong shocks, the RMI grows in proportion to the Mach number. Finally, the Reynolds number was about 1 million, which placed the fluid flow well into the turbulent fluid regime. (In fluid mechanics, the Reynolds number is the ratio of inertial to viscous forces. A high Reynolds number means that the flow can become turbulent because the viscosity of the fluid does not damp the effects of any local disturbance.) Currently, no accepted theoretical or computational model exists for explaining such complex environments. Experimental data in such regimes are needed if controlled thermonuclear fusion energy is eventually to become a reality.

The critical measurement and signature of the RMI in this experiment is the expansion of the interfaces of the radiographically opaque marker band into both the foam and epoxy. A typical datum is displayed in Figure 2a in which the transmissive inner foam, the opaque marker band, and the translucent epoxy outer layer are visible. Data in these experiments were azimuthally averaged to make quantitative comparisons with advanced computer simulations. The width of the marker layer is defined as the difference between the inner and outer 50% transmission points (Figure 2b), and systematic parallax effects are removed. By analyzing each of the 16 images obtained in one experiment and then repeating the experiment with different measurement timing, we can record an entire implosion history (Figure 3).

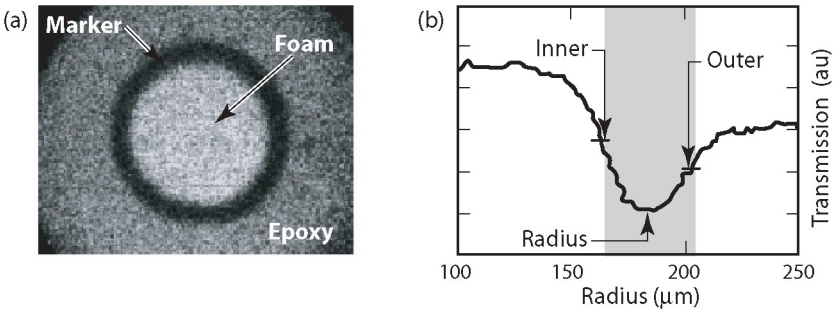

Figure 2. A radiographic image of a smooth aluminum marker (a). The average radial profile (b) is obtained from an azimuthal average of the transmission.

The computer modeling used in the RMI experiments excellently reproduced the marker widths and the position of the marker bands with initially very smooth marker surfaces. Both the experiment and the code show a steady increase in the marker width as the cylinder implodes, reaching a maximum width when the cylinder has reached minimum volume. As the cylinder "bounces" or expands, the marker width decreases.

The key scientific question that we are trying to answer is how do surface imperfections—that is, the initial conditions—affect the evolution of the RMI? We addressed this question by machining surface features (like the thread of a screw) along the length of the outer surface of the aluminum marker band. Surface perturbations like these produce a much wider marker band than do initially smooth bands (Figure 2). Randomly rough surfaces are not seen to mix any more than initially smooth surfaces.

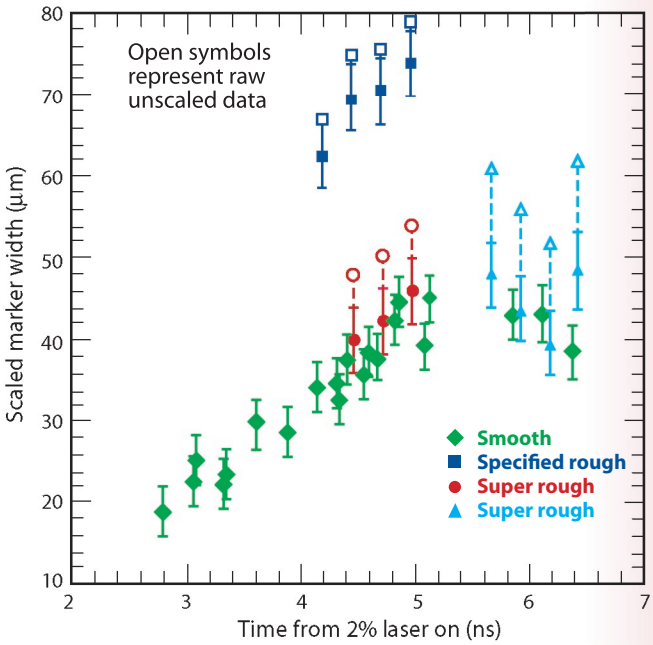

Figure 3. The measured marker-width evolution shows that the marker increases in width until about 5 ns when the cylinder reaches maximum compression. The data points at even larger marker widths are for targets that had the marker surface prepared in a particular manner (i.e., screw thread) to enhance mixing.

A conceptually much simpler outer surface is an azimuthally varying sinusoidal surface, like a tube with corrugations running the length of the tube.[8] This direct analog to numerous planar experiments is readily simulated with several different advanced computational codes and is potentially tractable theoretically. Such targets have been manufactured and experimentally tested. Figure 4 shows the experimental data from three experiments where the number of oscillations was 8, 16, or 28. The initial peak-to-valley size of the perturbation (6 μm) was the same for each experiment. Based on measurements and modeling of planar experiments, we expected that the size of the perturbations in our experiments would be directly dependent on the number of initial perturbations. In other words, we expected the growth in the 28-perturbation target to be 3.5 times larger than the 8-perturbation target at the same time. However, as shown in the data of Figure 4, this did not happen. In fact, the perturbations in all three cases (the 8, 16, or 28 perturbation targets) have approximately the same amplitude. Simulations using complex codes actually predicted the same trend. We are still determining the physical reason for these results in ongoing work.

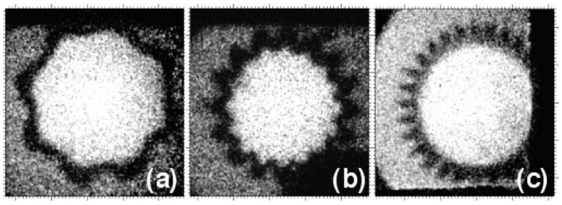

Figure 4. Axial radiographs of single-mode sinusoidally perturbed targets with mode numbers of 8 (a), 16 (b), and 28 (c).

Conclusion

The fundamental physical explanation for these results—that some types of surfaces grow whereas others do not when a strong shock is applied—is not known. Our experiments found that the type of perturbation at the interface affected the subsequent level of instability growth. Computer simulations were able to reproduce some of the results (Figure 4) but not others (Figure 3). We are pursuing experimental and computational lines of inquiry to understand the physics and modeling of these simplified experiments. Computational modeling is using features of the advanced codes, such as modern mix models and three-dimensional simulations, to address these issues. Experimentally, we implemented improvements to the framing-camera diagnostic to improve its spatial resolution. These improvements seem to have increased the quantitative accuracy of these experiments. We are also pursuing focused experiments on the effect of perturbation wavelength. Besides full-surface perturbations, the effects of material defects, like those seen at the joint of a beryllium capsule during implosion, are being investigated. Finally, we are measuring the effect of a second shock on the marker layer. Future experiments in convergent, compressible fluid instabilities in the presence of strong shocks are being planned for the NIF.[9] These cylinders will be imploded by soft x-ray radiation, which will allow faster implosion velocities, the use of larger cylinders, and better relative resolution of the mixing zone.

References

1. J.D. Lindl, *Inertial confinement fusion: The quest for ignition and energy gain using indirect drive* (Springer, New York, 1998).
2. R.D. Richtmyer, "Taylor instability in shock acceleration of compressible fluids," *Communications on Pure and Applied Mathematics* **13**, 297 (1960).
3. E. Meshkov, "Instability of the interface of two gases accelerated by a shock wave," *Soviet Fluid Dynamics* **4**, 101 (1969).
4. T.R. Boehly, D.L. Brown, R.S. Craxton, R.L. Keck, J.P. Knauer, J.H. Kelly, T.J. Kessler, S.A. Kumpan, S.J. Loucks, S.A. Letzring, F.J. Marshall, R.L. McCrory, S.F.B. Morse, W. Seka, J.M. Soures, and C.P. Verdon, "Initial performance results of the Omega laser system," *Optics Communications* **133**, 495 (1997).
5. J.D. Kilkenny, "High-speed proximity focused x-ray cameras," *Laser and Particle Beams* **9**, 49 (1991).
6. C.W. Barnes, S.H. Batha, A.M. Dunne, G. R. Magelssen, S.D. Rothman, R.D. Day, N.E. Elliott, D.A. Haynes, R.L. Holmes, J.M. Scott, D.L. Tubbs, D.L. Youngs, T.R. Boehly, and P. Jaanimagi, "Observation of mix in a compressible plasma in a convergent cylindrical geometry," *Physics of Plasmas* **9**, 4431 (2002).
7. N.E. Lanier, C.W. Barnes, S.H. Batha, R.D. Day, G.R. Magelssen, J.M. Scott, A.M. Dunne, K.W. Parker, and S.D. Rothman, "Multi-mode seeded Richtmyer-Meshkov mixing in a convergent, compressible, miscible plasma system," *Physics of Plasmas* **10**, 1816 (2003).
8. M.M. Balkey, R.D. Day, S.H. Batha, N.E. Elliott, T. Pierce, D.L. Sandoval, K.P. Garrard, and A. Sohn, "Production and metrology of cylindrical inertial confinement fusion targets with sinusoidal perturbations," Los Alamos National Laboratory report LA-UR-03-3682 (2003); to be published in *Fusion Science and Technology* (2003).
9. E.M. Campbell and W.J. Hogan, "The national ignition facility—applications for inertial fusion energy and high-energy-density science," *Plasma Physics and Controlled Fusion* **41** (12B, B39) (1999).

Acknowledgment

The RMI experiments are a collaborative effort between LANL and the AWE and are sponsored by the DOE NNSA.

For more information, contact Steven Batha at 505-665-5898, sbatha@lanl.gov.

Neutron Pinhole Imaging for Inertial-Confinement-Fusion Experiments

G.P. Grim, G.L. Morgan, M.D. Wilke (P-23), P.L. Gobby (MST-7), C.R. Christensen (P-24), D.C. Wilson (X-2)

The technique of imaging via pinhole is simple and yet remarkably powerful. Because of its simplicity, its basic optical principles have been considered for nearly three thousand years. As early as the fifth century B.C., Chinese philosophers used the pinhole to demonstrate the linearity of light propagation. Over the course of the next two millennia, notables, such as Aristotle, Leonardo da Vinci, and Johannes Kepler, among others, conducted studies with pinholes to advance knowledge in the field of astronomy. These studies included the imaging of solar eclipses and the determination of the correct day of the vernal equinox.

The first use of the pinhole technique to image neutrons from the fusion of deuterium and tritium occurred in April 1957 on the Boltzman shot during the early stages of nuclear weapons development in the U.S. Because of the penetrating nature of neutrons, the pinhole apparatus was modified, but the technique was fundamentally the same as for imaging light. In a typical neutron-pinhole experiment[1-4] (Figure 1), neutrons from a source that is to be imaged impinge upon a pinhole assembly and are either transported without scattering to the detector, or they interact within the assembly and are not recorded. In the experiments presented here, the neutrons are detected when they interact in a 3-cm-diam by 5-cm-long bundle of 0.5-mm-diam scintillating fibers. The scintillation light from the neutron interactions within the bundled fibers is totally internally reflected along the fibers and coupled into a series of coherent fiber-optical-transport elements. After the light passes through these elements, it is captured by a CCD camera and recorded in digital form on a computer for later analysis.

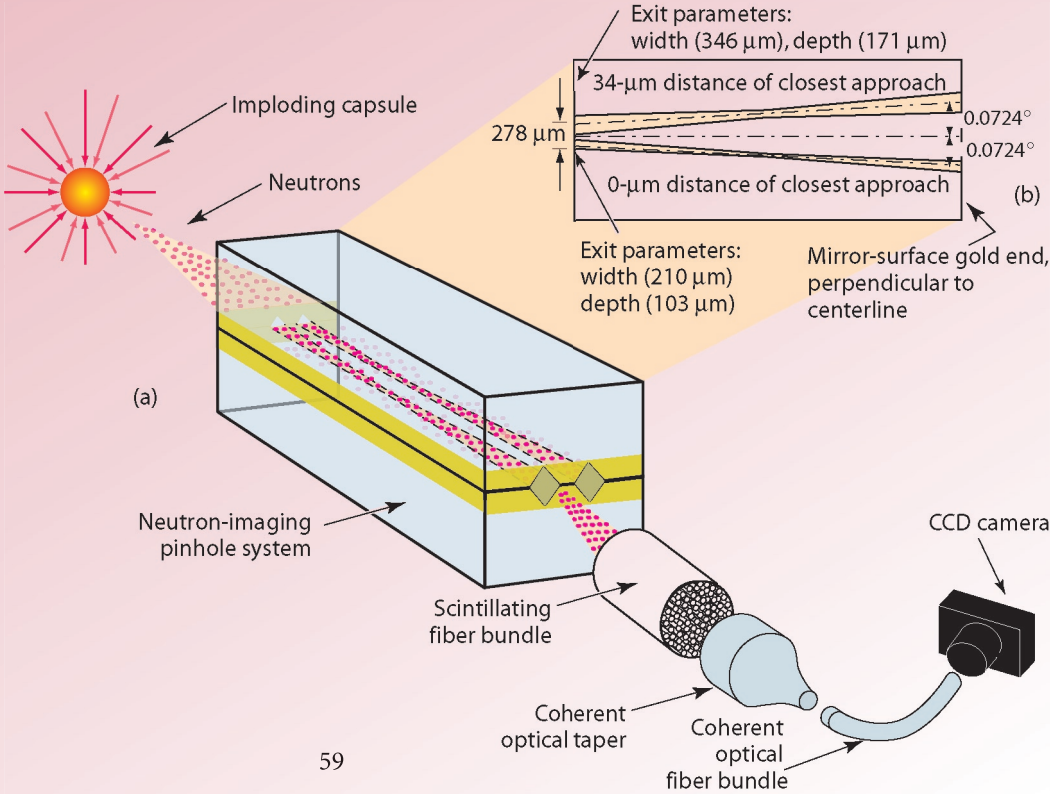

Figure 1. Typical pinhole neutron experiment. Figure 1(a) is a rendering of a typical implosion shot, and Figure 1(b) is the schematic of the pinhole apparatus used in the experiments on the Omega laser.

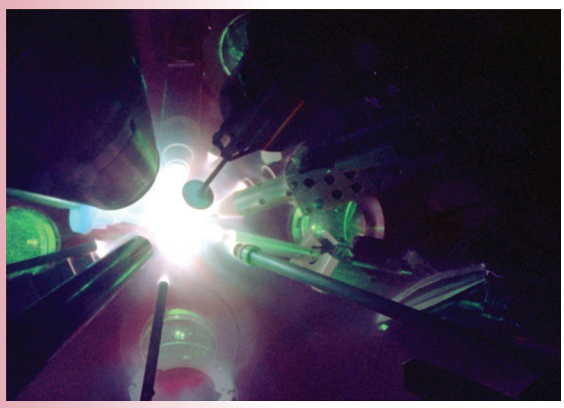

Figure 2. Inside the target chamber of the Omega laser. The bright spot at the center of the chamber is the light produced from imploding a DT capsule on shot 31184. The elements protruding from the wall include various x-ray and neutron diagnostics and the neutron pinhole used for the experiments described herein.

During the days of weapons testing, typical pinholes were about 1 m in length and weighed roughly 70 kg. The diameters of the pinholes were typically 0.25 mm, and the fields of view were typically 5 cm. Capturing neutron images of capsules used in ICF experiments requires a pinhole that is roughly 20 cm in length with a diameter approaching 20 μm and a field of view of about 500 μm. These dimensions push the limits of pinhole fabrication and fielding. The resulting images, however, provide powerful tools for the study of ICF capsule design. During 2003, new milestones in fabricating neutron-pinhole assemblies were met; as a result, the highest-resolution images recorded to date have been achieved along with recording the first "double-aperture" image using the Omega laser at LLE (University of Rochester). Data collected from these experiments were used to understand models of the dynamics of DT fuel and capsule-shell "mix." Understanding mix is critical not only for the design of ICF capsules and the environment necessary to achieve ignition at NIF but also for insight into the dynamics and performance of nuclear weapons.

Figure 3. Shot 31184 taken on April 1, 2003, with the Omega laser. Figure 3(a) is the color-coded intensity distribution of neutrons from the source as seen by both the high- and low-resolution pinholes. The red portion represents the high-fluence region, whereas the blue represents the low-fluence region. Figure 3(b) is the intensity profile of the red line drawn through the Figure 3(a).

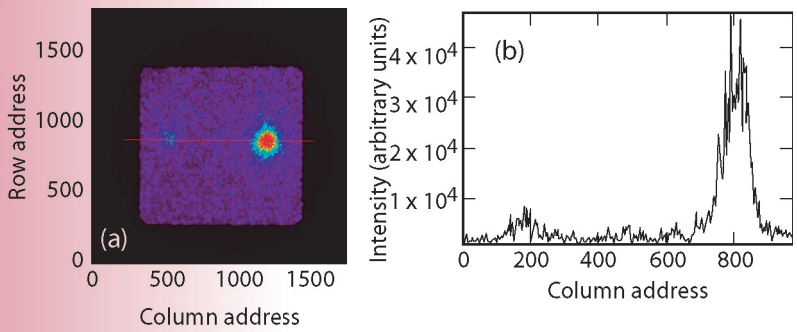

Pinhole Design and Fabrication

In a light-imaging pinhole system, the ideal pinhole is a perfectly opaque, infinitesimally thin, infinite plane that is pierced by an aperture, assumed circular for practical purposes. The source plane resolution of the pinhole image is determined by the aperture diameter and image magnification, whereas the field of view is infinite in extent. With penetrating radiation, the plane must be replaced with a plate of finite thickness to provide suitable opacity. As a consequence, the aperture becomes a three-dimensional profile through the plate. Thus, the field of view is no longer infinite but is determined by the geometry of the aperture profile. Along with this, the previous use of the two-dimensional aperture diameter to define the source plane resolution is modified to that of an "effective diameter." For the work done here, the effective diameter is defined as the radial distance from the pinhole axis at which paraxial neutrons have a probability of one-half of interacting. For a pinhole profile constructed from a double conic profile (i.e., intersecting left- and right-handed, right circular cones), a simple approximation to the source plane resolution is given by:

where λ is the mean-free path of the radiation in the material, θ is the opening angle of the cone sections,

$$\delta_{ph} = (\lambda \cdot \tan\theta \cdot 1n2 + D_{clr})\left(1 + \frac{1}{M}\right), \quad (1)$$

D_{clr} is the clear diameter of the pinhole, and M is the magnification of the system (i.e., the ratio of the image distance to object distance). For typical ICF experiments, M is large, O(100), and therefore the last factor may be ignored, and thus the source plane resolution is equal to the effective diameter.

In the experiments discussed here, a pinhole system capable of imaging 100-μm-diam objects with a spatial resolution approaching 15 μm was used. Figure 1b shows a schematic of the pinhole assembly designed with these specifications. The assembly was fabricated by precision machining two groves into two halves of a pair of matched tungsten plates, each plated with approximately 500 μm of gold. The mean-free path of 14-MeV neutrons in gold is approximately 3 cm. The tungsten provides rigidity, whereas the gold can be machined with diamond tools. The gold on each plate was first flattened with a large-radius (125 μm) tool. After the plate was locked in a horizontal position, grooves were machined into it using a 5-μm-radius, 90° diamond tool. The precision lathe used for this work has three orthogonal axes, each controlled to an accuracy of 0.025 μm. This accuracy allowed the two grooves in each plate to be precision cut into the gold. The plates were then aligned and mated together to create two pinholes within the assembly, 20 cm long. The two pinholes were designed to image an object in both apertures at a distance of 21 cm from the center of the assembly. For 14-MeV neutrons, the effective diameters of the two pinholes were roughly 22 and 52 μm with corresponding fields of view of about 400 and 600 μm, respectively.

Figure 2 shows how the pinhole assembly was deployed. The image shows the inside of the target chamber at the Omega laser. Various diagnostics, including the neutron-pinhole assembly, can be seen protruding from the chamber wall. The face of the pinhole assembly is placed 11 cm from

the center of the chamber and points toward the capsule position with an accuracy of 250 μrad. The bright spot in the center is the light produced from the implosion on shot 31184. The scintillator is placed 1,300 cm from the chamber center along the axis of the pinhole assembly. Figure 3 shows the relative intensity of neutrons interacting in the scintillator for this shot. The image is a magnified representation of the 14-MeV neutron source produced by the imploded DT capsule, blurred by the finite resolution of the pinhole imaging technique. The capsule was filled with 5 atm of equal (atomic) quantities of deuterium and tritium and imploded with approximately 23 kJ of energy from 60 beams. The total yield from the shot was 4×10^{13} neutrons. Figure 3(a) is the color-coded x-y intensity distribution showing the relative fluence of 14-MeV neutrons. The red area represents the region of higher-fluence regions, whereas the blue represents the lower-fluence regions. Figure 3(b) is the intensity profile of the red line shown in Figure 3(a). The line profile shows a clear indication of neutrons from both pinholes. The intensity from the small pinhole is less—that is, relative to the larger pinhole intensity—by the ratio of the effective pinhole areas, but the improved resolution of the small pinhole may be used in a complementary fashion to provide added information in the reconstruction of the image.

Asymmetric Direct Drive and Mix Physics

Using data such as those shown in Figure 3, it is possible to study phenomena important to the design of ICF capsules, in particular, the dynamics of fuel and capsule-shell mix. Historically, implosion simulations over-predict fusion-neutron yields from ICF capsules. The discrepancy is thought to occur by enhanced radiation and dilution of the fuel concentration at the fuel-shell interface due to mixing of these elements. During FY 2002 and 2003, these dynamics were studied by comparing neutron and x-ray images of ICF implosions with those predicted by a multi-fluid interpenetration model developed by Scannapieco and Cheng.[5] The model developed by Scannepieco and Cheng is attractive because it derives a set of multi-fluid moment equations from first principles while introducing only one free parameter. Further, this free parameter can be related to the collisional frequency of the system, which moves the approximations used to constrain the system from the governing equation level to the characteristic quantity for binary collisions.[5] During the experimental campaign, data from both symmetric and asymmetric implosions were collected and compared with the model. Applying the interpenetration model to an ICF capsule results in an equation of motion given by

$$p\frac{d}{dt}\left(\frac{p_i}{p}(u_i - u)\right) + \Sigma_j \frac{p_i p_j}{p}\nu_{ij}(u_i - u_j) = -p_i(u_i - u)\cdot\nabla u - \nabla\cdot P_i + \frac{p_i}{p}\nabla\cdot P, \quad (2)$$

where the collisional-drag frequency, ν_{ij}, is given by

the following formula:

$$\nu_{ij} \equiv \frac{C_s}{\Lambda + \alpha\int|u_i - u_j|dt}. \quad (3)$$

The parameter α is the experimentally determined quantity referred to above and represents the ratio of the mixing length to the thickness of the mix layer. The term Λ is the collision mean-free path.[6,7] The work in Reference 4 suggests that different modes of mixing are characterized by different values of α. These different modes include planar mixing or various types of jet mixing in stagnant surroundings. Figures 4 and 5 show the comparison between neutron images of prolate- and oblate-capsule shots along with simulated images where the parameter α is varied. As can be seen from these images, as α is increased (which corresponds to increasing the amount of mix), the size of the burn region decreases (which more closely models the experimental results). Figures 6 and 7 summarize the dependence of neutron yield on asymmetry. The interpenetration model predictions of this dependence as α is varied are overlaid on these two figures. The results of these comparisons (and of others that are not shown here) indicate a value of α = 0.07 +/– 0.01, which models the data well for capsules filled with DT at pressures of 2.5, 5, and 10 atm.

Conclusion

A number of conclusions have been drawn from these experiments. First, the results indicate that neutron production from DT fusion appears to be insensitive to the level of asymmetry being induced. Further, the interpenetration model of Scannapieco and Cheng[1] appear to predict this insensitivity with a single value of the parameter α at a number of different fuel pressures. Finally, it appears that a single mix parameter can be used to model symmetric and asymmetric implosions. These results provide solid constraints that hydrodynamic and "mix" modelers can use to advance the capability of codes applied to the design of ICF capsules and other relevant physics experiments.

The goal of the ICF research community is to achieve "ignition" of an ICF capsule at some point in the future. To achieve this goal, a tremendous effort must be expended to understand many of the impediments—not the least of which is the physics of capsule implosion, which, in turn, depends on

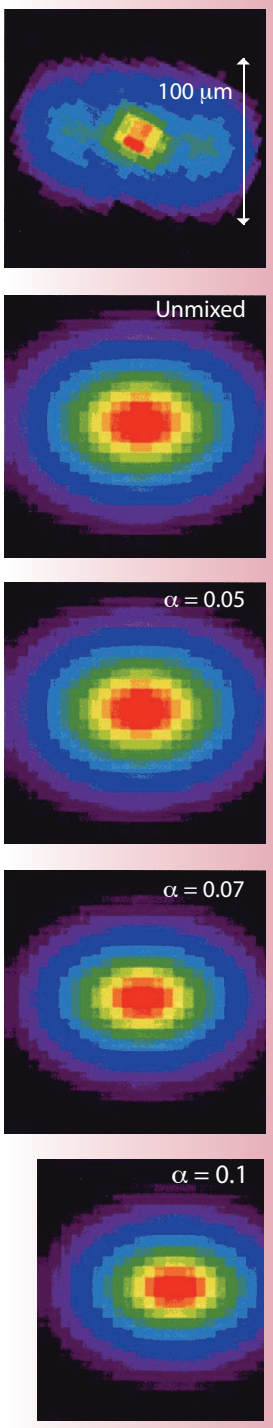

Figure 4. Comparison of shot 26665, a prolate implosion, and simulations using the model from Reference 1. By increasing the amount of mix (i.e. increasing α), the data are more closely modeled.

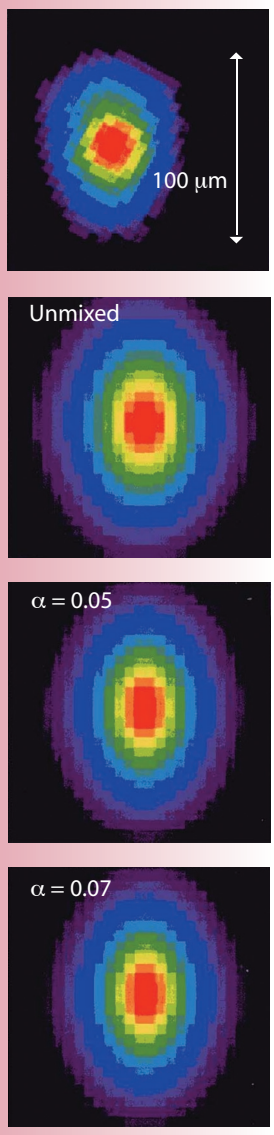

Figure 5. Comparison of shot 26666, an oblate implosion, and simulations using the model from Reference 1. As in Figure 4, the increasing amount of mix better models the size of the nuclear burn region.

the dynamics of mix. Neutron-imaging-diagnostics development and deployment in ICF experiments have played, and will continue to play, a critical role in understanding mix and other phenomena in ICF target design as the march towards ignition progresses.

References

1. D. Ress *et al.*, "Neutron imaging of inertial confinement fusion targets at Nova," *Review of Scientific Instruments* **59**, 1694 (1988).
2. J.-P. Garconnet *et al.*, "Neutron penumbral imaging of inertial confinement fusion targets," *Laser and Particle Beams* **12**, 563 (1994).
3. G.L. Morgan *et al.*, "Development of a neutron imaging diagnostic for inertial confinement fusion experiments," *Review of Scientific Instruments* **72**, 865 (2001).
4. C.R. Christensen *et al.*, "First Results of pinhole neutron imaging for inertial confinement fusion," *Review of Scientific Instruments* **74**, 2690 (2003).
5. A.J. Scannapieco and B. Cheng, "A multifluid interpenetration mix model," *Physics Letters A* **299**, 49 (2002).
6. S.I. Braginkskii, *Reviews of Plasma Physics* **1** (1965).
7. L. Spitzer, *Physics of Fully Ionized Gases* (Intersciences Publishers, New York, 1962).
8. B.E. Launder and D.B. Spalding, *Mathematical Models of Turbulence* (Academic Press, London, 1972).

Acknowledgment

To accomplish the work discussed herein required a significant effort on the part of individuals not listed above. In particular, we owe a debt of gratitude to the MST-7 team that fabricated the pinhole assembly, particularly Jacob Bartos and Felix Garcia, along with the target fabrication teams at both LANL and General Atomic. We would also like to thank Peter Ebey of ESA-TSE for ensuring there were DT targets available and Nick King of P-23 for the development of our camera and scintillating system. Finally, the data would not exist without the staff at the LLE, whose skillful operation of the Omega laser made this possible. In particular, we would like to thank William (Jack) Armstrong of LLE for his technical support and effort. This work was supported by DOE Contract No. W-7405-ENG-36.

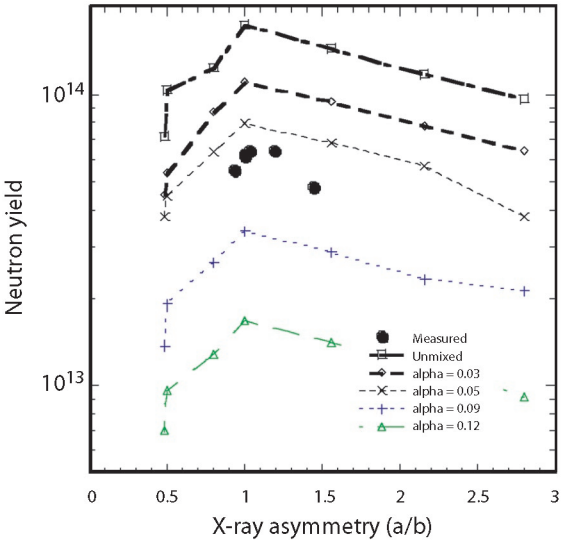

Figure 6. Comparison between data and simulation (as the amount of mix is varied) of neutron yield as a function of the asymmetry at capsule fills of 5 atm. The vertical axis is the yield in total neutrons, whereas the horizontal axis is the degree of asymmetry as measured from x-ray images. In the case of the model predictions, the x-ray images are simulated as well.

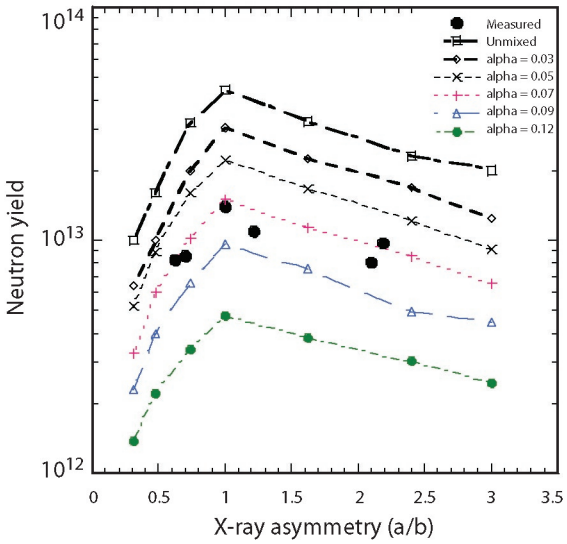

Figure 7. Same as Figure 6 but for 2.5-atm capsule fills.

For more information, contact Gary Grim at 505-667-8985, gpgrim@lanl.gov.

"Magnetic Reconnection" Studies Conducted at Los Alamos National Laboratory

T.P. Intrator, I.G. Furno, S.C. Hsu, E.W. Hemsing (P-24), G.M. Lapenta, P. Ricci (T-15)

Most of the known universe (about 99%) is composed of plasma, which is an ionized gas. Although ions and electrons are not joined as atoms and molecules, each can flow in fluid patterns. This state not only contains eddies, flow fields, waves, and shocks but also electric and magnetic fields. Some of the most interesting questions regarding the structure and dynamics of our universe involve this coexistence of flows and fields. A structure that generates magnetic fields from conductive-fluid flow is called a *dynamo*, and the annihilation of a magnetic field is called *magnetic reconnection*. When reconnection occurs, the magnetic-field energy is transferred to the plasma. Our research is focused on *magnetic reconnection* and is part of a larger P Division effort to establish a plasma-astrophysics presence in the world scientific community. Our research connects to LANL missions, including the physics of plasma devices for magnetic-fusion research, space "weather," satellite communications, and ASCI computing.

During five decades of study, researchers have largely regarded magnetic reconnection as a "black-box" process that begins with the dissipation of magnetic-field energy and ends in plasma-particle acceleration and/or thermal heating. Indeed, the slow build up of magnetic energy followed by an explosion that converts it into particle energy is almost always present in any magnetized plasma.[1,2,3] These dynamic explosions release energy anisotropically, whereby slow flows occurring in one direction can elicit large accelerations in another. In nature, these fast time scales can be orders of magnitude quicker than expected resistive diffusion times.

A detailed understanding of the magnetic-reconnection process has only recently started to emerge. Understanding this process could help researchers improve the control and confinement of magnetic-fusion plasmas and understand the stability and magnetic structure of magnetic-fusion-confinement devices. Moreover, long-standing solar-physics questions involving the origins of coronal heating, coronal mass ejections, and other coronal-magnetic activity might finally be solved. Accurate predictions of geomagnetic disturbances could be made, and the effect of solar wind interactions with the earth's magnetosphere on spacecraft environments could

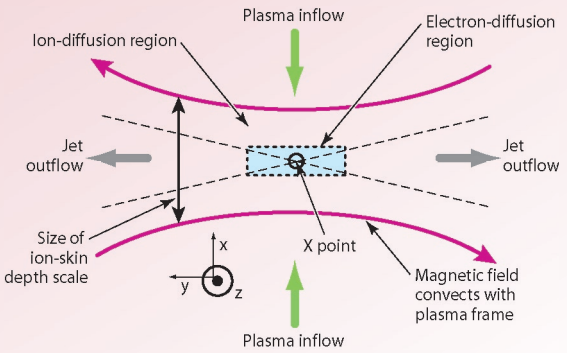

Figure 1. Schematic showing the reconnection plane, including slow plasma inflow velocity in the vertical direction. Anti-parallel magnetic fields convect inwards through a region of ion-skin-depth dimension. On the smaller electron-skin-depth scale (dashed box), a diffusion region containing electron microphysics determines the reconnection process. These two spatial scales have never been observed together in the laboratory. Note the similarity between this figure and Figures 3 and 4. The X point would occur if the size of the reconnection region were vanishingly small.

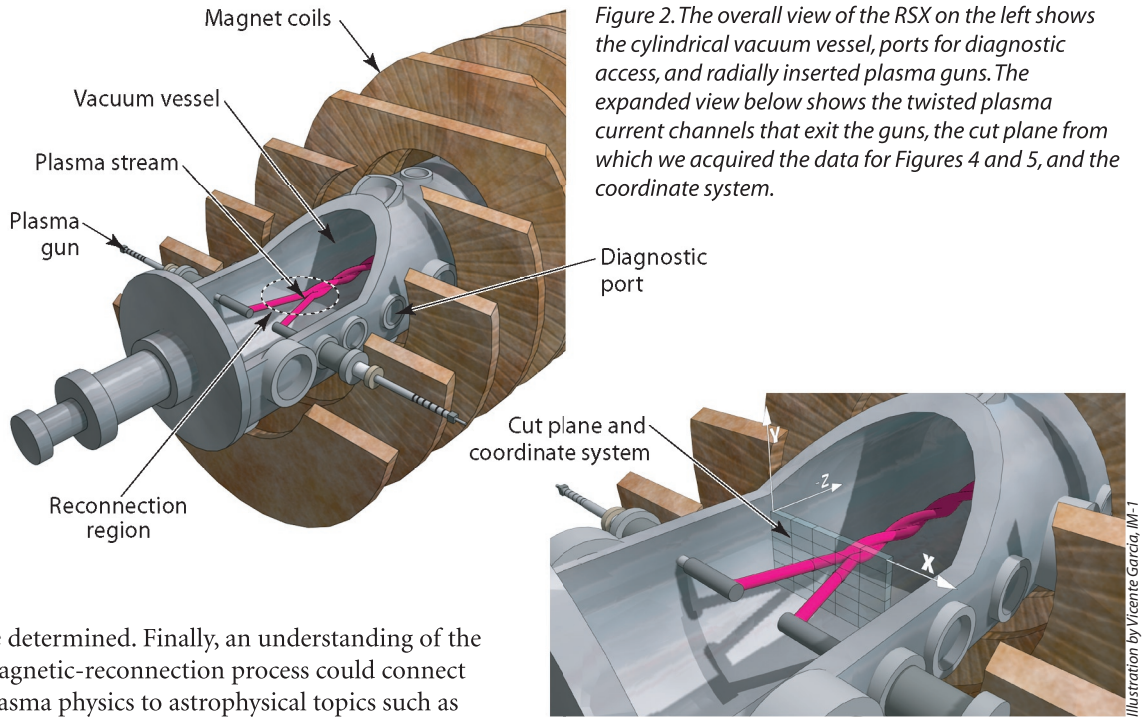

Figure 2. The overall view of the RSX on the left shows the cylindrical vacuum vessel, ports for diagnostic access, and radially inserted plasma guns. The expanded view below shows the twisted plasma current channels that exit the guns, the cut plane from which we acquired the data for Figures 4 and 5, and the coordinate system.

be determined. Finally, an understanding of the magnetic-reconnection process could connect plasma physics to astrophysical topics such as accretion disks; jet, star, and galaxy formation; and cosmic-ray acceleration—topics that had traditionally been studied only from the perspective of hydrodynamics, general relativity, and atomic physics.

Frozen-Flux Concept and Reconnection

Plasmas can be very good electrical conductors. Electric and magnetic fields cannot penetrate or *diffuse* into perfect conductors because induced eddy currents cancel out these fields. Conversely, fields that are "stuck" inside conductors take a long time to *diffuse* out (i.e., the magnetic flux is *frozen* into the moving plasma). Current flows much more easily along a field than across it, so magnetic field lines can be imagined as conducting wires that move with the plasma. During this process, oppositely directed field lines can be convected toward each other by fluid flow (e.g., the inflow region in Figure 1). Between the oppositely directed fields, there is a magnetically neutral line (*current sheet*) across which there is a reversal of the magnetic field. Diffusion occurs in that region, and the *frozen-in* condition of ideal magnetohydrodynamics (MHD) is broken. The magnetic fields can diffuse through the plasma, allowing the annihilation of oppositely directed magnetic field lines and forcing the lines going in one direction to connect to the ones going in the opposite direction. These "reconnected" field lines act as rubber bands under tension and pull away horizontally from the diffusion region. Consequently, plasmas are flung as if by a slingshot, which could explain many impulsive phenomena.

Microphysics of Fast Reconnection

At present, a major debate exists regarding the microphysics that influence a fast reconnection rate. This topic has been considered theoretically from two distinct perspectives beyond the scope of resistive MHD. "Anomalous" micro-instability-induced resistivity [which in the collisionless limit can be orders of magnitude larger than the classical (Spitzer) resistivity] can be invoked to explain enhanced dissipation rates inside the reconnection layer. On the other hand, neglected terms of the two-fluid generalized Ohm's law (i.e., the electron momentum equation) can become important on spatial scales smaller than the ion-skin depth c/ω_{pi}, where c is the speed of light, and $\omega_{pi}(\omega_{pe})$ is the ion (electron) plasma frequency.[4] A key experimentally testable feature of the two-fluid reconnection theory is the expected development of a reconnection layer with a two-scale spatial structure. This feature arises because ion and electron motion decouple in between ion and electron c/ω_{pe} skin-depth length scales. With its scalability in collisionality and magnetic fields, the Reconnection Scaling

Experiment (RSX), which is currently under way at LANL, should allow us to address this question and/or observe signatures of the electron layer. We can independently scale plasma density (and thus the collision frequency), and we can scale the axial magnetic field to change the ion gyro radius.

We are exploring magnetic reconnection in the RSX. Two parallel current plasma channels are produced using plasma guns. Most other experiments are toroidal, but this one has a simpler linear geometry. The RSX cylindrical vacuum chamber has many ports for easy placement of diagnostics and plasma guns (Figure 2). The overall view shows a cutaway schematic of two current channels created by two plasma guns, which are inserted radially into the vacuum chamber. A set of external coils generates the axial guide field B_Z. The expanded view shows the helical twisting and merging of these current channels. The coordinate-system axes are indicated for a cut plane through this interaction region. Typically in RSX, we generate hydrogen plasmas with a large Lundquist number ($S > 100$), current densities of $J < 1$ MA/m^2, and electron densities and temperatures in the range of $n_e \sim 1$ to 30 x 10^{13} cm^{-3} and $T_e \sim 10$ to 20 eV, respectively. One major advantage of the plasma-gun technology is that no complicated startup scheme or evolution to equilibrium is required. It also allows a high degree of flexibility in scaling the source characteristics independently of the different parameters important in the reconnection process.[4,5] Because the plasma guns create the plasma, both the collisionality (density) and the magnetic-field component, normal to the reconnection layer (current density), can be controlled independently of the plasma-formation process.

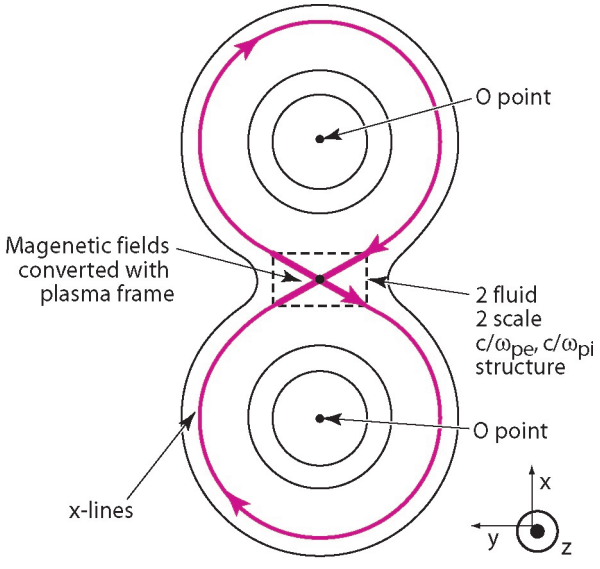

Figure 3. The O points locate the center of each current channel; an X point is located in the diffusion region, which is indicated by dashed lines. The x-y plane corresponds to Figures 1, 3, and 4.

Data from RSX

We completed measurements of the magnetic structure in a two-dimensional cut plane (Figures 2 and 3). Figure 3 shows the magnetic topology and diffusion region from the cut plane in Figure 2. Magnetic probes inserted into the plasma gave us a time history at each point, and we explored the full plane over many repetitive shots. An example of vector data (B_x, B_y) in the x-y plane for a time late in the evolution of the reconnection layer is shown in Figure 4. The diffusion region is indicated by the dashed circle, where a jump in B_x is apparent on a vertical cut at x = 0.280 m. These data were taken using a large-guide magnetic field of $B_{0z} = 400$ Gauss. This magnetic field was large enough to magnetize the ions even in the diffusion region where the B_x field vanishes and to maintain a very small beta [$\beta = nT/(B^2/2\mu_0) << 1$, which is the ratio of particle pressure to magnetic pressure]. A sketch of the B_x time history for this vertical cut is shown in Figure 5. Four selected times show how the jump in magnetic field increases with time. Interestingly, the scale size of this diffusion layer is approximately 0.5 cm. This scale size is far smaller than the ion-skin depth (≈ 7 cm) and not too

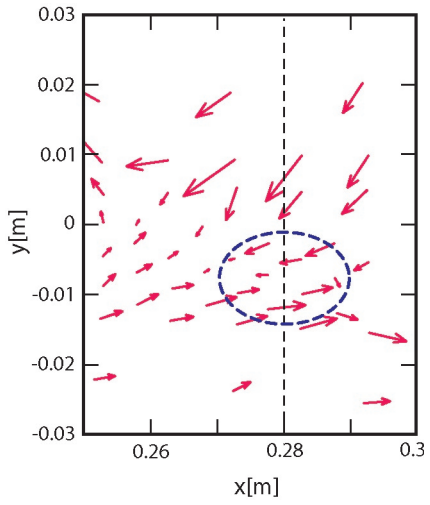

Figure 4. Vector data (B_x, B_y) in the x-y plane. Note the reversal in B_x across the neutral sheet region (dashed circle).

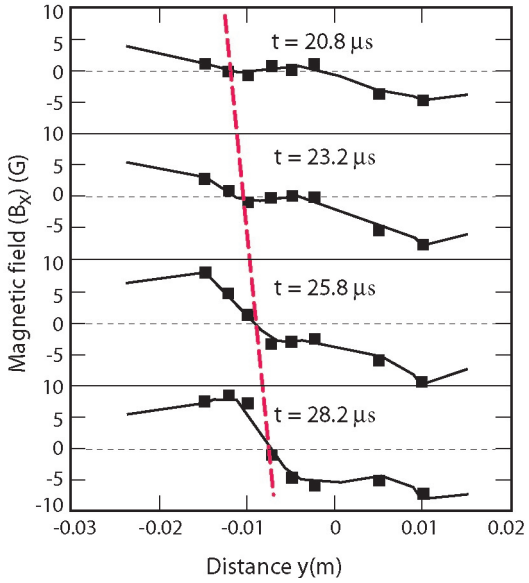

Figure 5. Magnetic field B_x on a vertical cut at y = 0.28 m. Note how the jump in B_x becomes steep as time progresses for each time indicated on each panel of the figure.

different from the electron-skin depth (≈ 0.2 cm) and the ion gyro radius (0.8 cm). In the near future, we will scan the effects of the externally applied guide field. However, this is at least one example where the size of the diffusion region is quite different from the ion-skin depth predicted by the usual reconnection theories.

Conclusion

Most of the known universe is plasma, and reconnection is ubiquitous in much of it. Magnetic reconnection is thought to convert magnetic-field energy into particle, beam, and thermal energy. The debate concerning the microphysics of reconnection includes predictions that the scale length for the neutral current sheet is the ion-skin depth. Nevertheless, we show here one counter example, using data from RSX at large-guide magnetic field. We intend to investigate the scaling of these results.

References

1. D. Biskamp, "Collisional and collisionless magnetic reconnection," *Physics of Plasmas* **4,** 1964 (1997).
2. J.F. Drake, "Magnetic explosions in space," *Nature* **410**, 525 (2001).
3. J. Glanz, "Unlocking secrets of magnetic fields' power," *New York Times*, October 24, 2000.
4. M. Shay, J. Drake, R. Denton, and D. Biskamp, "Structure of the dissipation region during collisionless magnetic reconnection," *Journal of Geophysical Research* **103**, 9165 (1998).
5. I.G. Furno, T.P. Intrator, E. Torbert *et al.*, "Reconnection scaling experiment: A new device for three-dimensional magnetic reconnection studies," *Review of Scientific Instruments* **74**, 2324 (2003).

Acknowledgment

The RSX is a collaborative effort between P Division and T Division at LANL and is sponsored by LANL LDRD funding.

For more information, contact Thomas Intrator at 505-665-2927, intrator@lanl.gov.

Radiological, Chemical, and Biological Decontamination Using Atmospheric-Pressure Plasmas

L.A. Rosocha, J. Park (P-24), J.R. FitzPatrick (C-AAC), H.W. Herrmann (on entrepreneurial leave to APJeT, Inc.)

Researchers at LANL have applied a technology known as the atmospheric-pressure plasma jet (APPJ) to the decontamination of radiological, chemical, and biological agents from surfaces. [This unique technology (Figure 1) was invented at LANL in 1995[1] and won an R&D 100 Award in 1999.] An APPJ[2,3] produces a gas stream of highly reactive chemical species identical to those currently used by the semiconductor industry to clean silicon wafers. The APPJ reactor, however, creates non-thermal plasmas that can clean surfaces in "open air" instead of in vacuum. [The electrons, ions, and neutral-gas species that make up non-thermal plasmas are not in thermal equilibrium. The electrons are energetic ("hot"), whereas ions and neutral gases are near ambient temperature ("cool")]. The open-air concept eliminates the cost, time, and effort previously required to plasma-process work pieces in special vacuum chambers and, as a result, opens up a host of new plasma-processing applications. Although the effluent of the APPJ (Figure 1b) may appear somewhat like the flame of a Bunsen burner, its temperature can be maintained cooler than that of a hair dryer's exhaust. Chemically reactive species of oxygen generated by an APPJ device essentially "burn" many organic materials, such as oil and grease, from surfaces at these relatively low temperatures.

APPJ technology is used in a number of industrial and military applications. In materials processing, for example, applications range from etching silicon wafers to modifying surfaces to increase their wettability or absorption. Applications involving chemical and decontamination processing include the destruction of chemical and biological warfare (CBW) agents and the removal of radionuclides from surfaces and equipment. The development of this unique technology spans the regimes of bench-top studies to prototype demonstrations.

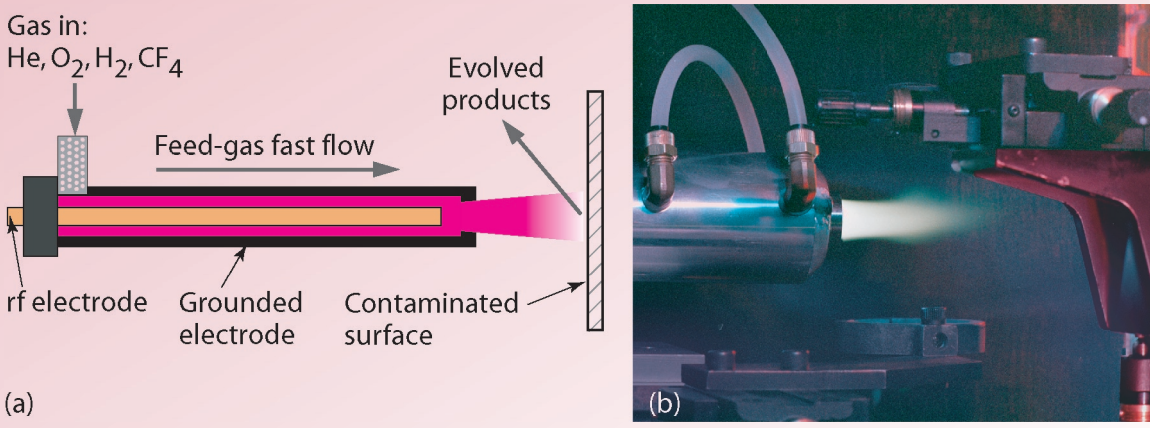

Figure 1. (a) Schematic of an rf-driven APPJ. (b) Photo of the APPJ device in operation.

Atmospheric-Pressure Plasma Jet

The APPJ produces a non-thermal, glow-discharge plasma operating at atmospheric pressure. The discharge uses a feed gas consisting primarily of an inert carrier gas, such as helium, and a small amount of an additive (e.g., O_2) that is activated. The feed gas flows between an outer, grounded, cylindrical electrode and an inner, coaxial electrode powered at an rf of 13.56 MHz (Figure 1a). The electric field produced between the electrodes causes the gas to breakdown into a "plasma state," or an ionized gas capable of conducting electricity. While passing through the plasma, the feed gas becomes excited, dissociated, or ionized by interacting with energetic electrons. Once the gas exits the discharge volume, ions and electrons are rapidly lost via a process known as recombination. Metastable species and radicals are left behind. Oxygen-containing plasmas, for example, produce reactive oxygen species, such as metastable oxygen (O_2^*), atomic oxygen (O), and oxygen ions (O_2^+). These reactive species tend to live relatively longer than electrons and ions and readily oxidize, or combust, many organic compounds on surfaces, including oil and grease.

Plasma feed gases can easily be tuned to produce tailor-made chemistry. For instance, hydrogen can be added in place of O_2 to produce a reducing environment of atomic hydrogen. CO_2 can be used in place of O_2 to minimize the amount of generally unwanted ozone (O_3), which tends to form downstream of an oxygen discharge. Reactive species can be directed onto a contaminated surface at high velocity where they can selectively neutralize organic materials without damaging the underlying surface. The temperature of this gas discharge typically ranges from 50°C to 300°C, which allows for plasma processing of sensitive materials and equipment at low temperatures and accelerated processing of more robust surfaces at higher temperatures.

"Polishing" Actinide-Contaminated DynEx Vessel Surfaces

Members of P-24, in collaboration with the Actinide Analytical Chemistry Group of the Chemistry Division at LANL, are conducting an Environmental Management Science Program (EMSP) to demonstrate general-purpose decontamination of superficial actinide contamination. The EMSP provides the science base for the APPJ application.

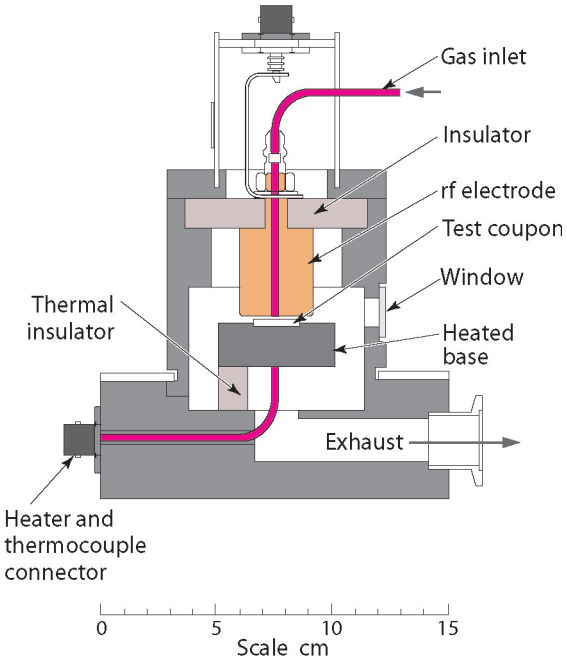

Figure 2. Schematic of the APPJ device used for actinide- and surrogate-actinide-etching studies.

In addition to this general decontamination project, we are investigating APPJ technology as a means to fully satisfy the special needs of the DynEx program in a cost-effective manner. DynEx studies are a required capability for the nuclear weapons program in general and for stockpile stewardship and weapons and weapons-component certification. These studies also provide data essential for the analysis and understanding of weapons-performance issues.

The current technology used for surface decontamination of residual waste from plutonium-processing operations (gloveboxes, tools, pipes, etc.) involves an acid-wash process that generates many liters of mixed-hazardous waste per unit. Moreover, this process requires nearly 8 hours of manual labor and results in considerable personnel radiation exposure. APPJ-plasma processing provides a convenient and waste-free method for decontaminating surfaces and recovering residual quantities of actinides (e.g., plutonium, uranium) that form volatile fluorides. In this method, a plasma generates a reactive chemical "intermediate" (e.g., fluorine atoms) from an inert feed gas (CF_4 or NF_3). This intermediate reacts with an actinide-contaminated surface to form a volatile gaseous product that is then pumped off the surface, leaving

it clean and decontaminated. The off-gas from this procedure is sent through a filtration system that traps and recovers any residual product. Known as "Atmospheric Pressure Decontamination (APD) DynEx Vessel Polishing," the goal of this DOE Defense Programs project is to determine whether the APPJ technology can decontaminate plutonium and uranium from metal surfaces, like actinide-contaminated DynEx vessels, in a *dry, safe* manner.

In APD-etching studies, 1/8-in.-thick, 1-in.-diam stainless steel coupons (disks) were impregnated with small amounts of plutonium and uranium and then exposed to an APPJ effluent. The APPJ device (similar to the one shown in Figure 2) contains a coupon holder and a stage for heating the coupons. The APPJ and associated enclosure are placed inside a glovebox at the Chemistry and Metallurgical Research Facility at LANL. The APPJ was operated at 700 W. About 90% of the uranium was removed in 10 minutes, whereas about 50% of the plutonium was removed in the same amount of time. The plutonium-doped coupons were further exposed at 10-minute intervals (Figure 3). We have also used *surrogate* actinide materials, such as tantalum and tungsten, in etching studies to safely test and evaluate the APPJ technique without the handling hazards and safeguards associated with actinide materials. In these studies, small quantities of NF_3, CF_4/O_2, or SF_6 were added to the primary helium feed gas to produce chemically active atomic fluorine. Using the APPJ method, removal of the actinide surrogate, tantalum, was demonstrated at > 10 μm per minute.

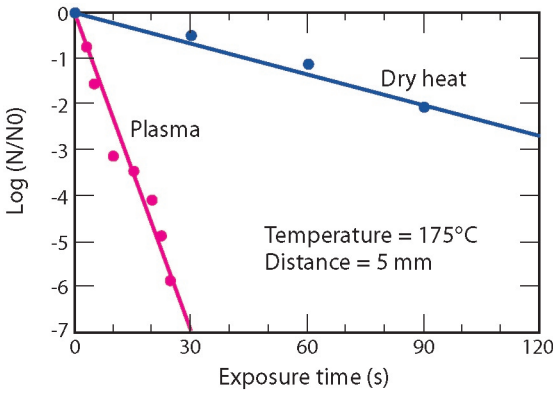

Figure 4. Destruction of the Anthrax surrogate BG using the APPJ method as compared to the dry-heat treatment.

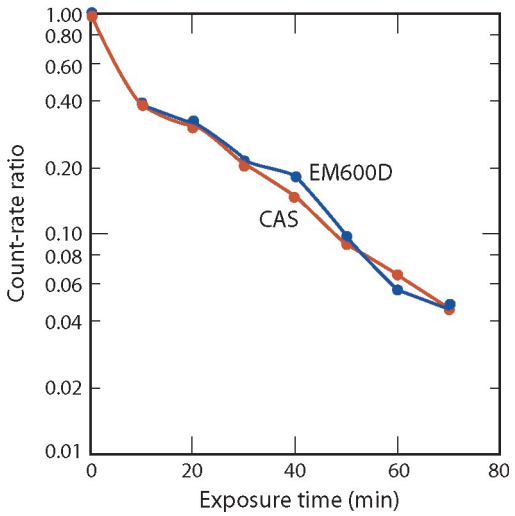

Figure 3. Removal data for plasma processing of plutonium-doped disks (ratio of counts at a given exposure time to counts with no exposure, i.e., initial activity).[4] CAS is an acronym for Canberra Alpha Spectrometer, and EM600D is the Eberline radiation monitor.

Chemical and Biological Weapons Decontamination

Events that happened in the U.S. after September 11, 2001, confirmed that chemical and/or biological agents could be used to inflict terror on civilians and to damage the infrastructure of our nation. Technology is therefore needed not only to detect these horrific weapons but also to reclaim and restore normal activities by decontaminating the areas targeted by CBWs. The P-24 CBW program at LANL is focused on the development of an all-dry, decontamination APPJ process suitable for use on sensitive equipment, such as computers, industrial machinery, and communications centers. As such, the "downstream" APPJ system developed for this program is portable, inexpensive, spot-specific for treatment, and amenable for use with objects of any size. It was used in tests to destroy biological- and chemical-warfare-agent surrogates, as well as actual chemical-warfare agents.[5] Active species produced inside the APPJ are rapidly blown out of the source and impinge a target surface 2 to 10 mm downstream. Most often, a He/O_2 feed gas is used, which produces a mix of atomic oxygen, metastable molecular oxygen, and small amounts of ozone. Figure 4 shows the results for decontamination of Bacillius globigii (BG), a surrogate for Anthrax spores, for both plasma and dry-heat treatments.

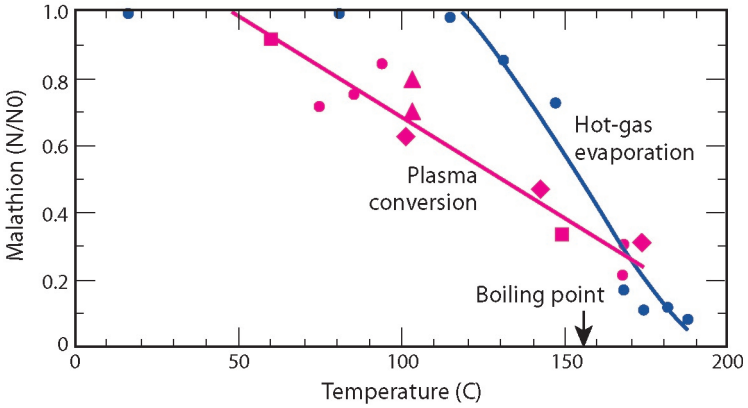

Figure 5. Destruction of the chemical-warfare surrogate, Malathion, using the APPJ method as compared to the dry-heat treatment. (Note: the plasma case has multiple symbols, representing more than one experiment.)

(The dry-heat treatment blows hot air, or some other gas, onto the biological agent.) Results indicate a seven-log kill (i.e., a factor of 10 million removal or decrease of the contaminate) of BG spores in 30 s with an APPJ effluent temperature of 175°C—which is ten times faster than dry heat at the same temperature! The APPJ also decontaminated surrogates for sulfur mustard and VX nerve agent and for actual VX. Figure 5 shows the results for the decontamination of Malathion (a pesticide surrogate for the chemical-warfare agent VX) for the plasma and dry-heat treatments.

Conclusion

In the near future, we will carry out parametric studies to determine the effect of gas mixture, coupon temperature, power, and gas-flow rates in an attempt to optimize the removal of plutonium and uranium from metal surfaces. If those studies indicate sufficient efficacy for the process, we will conduct scale-up studies to aid in the design of systems for decontaminating actual vessels or larger quantities of contaminated metals.

References

1. G.S. Selwyn, "Atmospheric pressure plasma jet," U.S. Patent 5-961-772, January 23, 1997.
2. A. Schütze, J.Y. Jeong, S.E. Babayan, J. Park, G.S. Selwyn, and R.F. Hicks, "The atmospheric-pressure plasma jet: A review and comparison to other plasma sources," *IEEE Transactions on Plasma Science* **26**, 1685 (1998).
3. J. Park, I. Henins, H.W. Herrmann, G.S. Selwyn, J.Y. Jeong, R.F. Hicks, D. Shim, and C.S. Chang, "An atmospheric-pressure plasma source," *Applied Physics Letter* **76**, 288 (2000).
4. L.A. Rosocha and J.R. FitzPatrick, "Recent results on actinide decontamination with an atmospheric-pressure plasma jet," Los Alamos National Laboratory report LA-UR-03-6689.
5. H.W. Herrmann, I. Henins, J. Park, and G.S. Selwyn, "Decontamination of chemical and biological warfare agents using an atmospheric-pressure plasma jet," *Physics of Plasmas* **6(5)**, 2284 (1999).

Acknowledgment

This work is a collaborative effort involving researchers from the P Division and the C Division and was sponsored by the DOE Environmental Management Science Program and Defense Programs.

For more information, contact Louis Rosocha at 505-667-8493, rosocha@lanl.gov.

Experimental Physics Using the Z Accelerator at Sandia National Laboratories

R.G. Watt, G. Idzorek (P-22), R.E. Chrien, D. Peterson (X-2)

The natural world is constantly attempting to reach an equilibrium state most simply thought of as a state in which quantities such as temperature or density are uniform throughout a volume. When quantities such as temperature vary from one point to the next in the volume, these differences can act to produce a force that tries to restore that quantity to a uniform state. These restoring forces can lead to familiar processes such as water being ejected from the end of a hose because of the pressure difference between the inside and the outside of the hose (a pressure gradient). The flow of heat down a bar of metal that has been heated on one end by a torch is another process (thermal diffusion) created by the difference in temperature from point to point along the bar (a thermal gradient). Forces resulting from gradients are less familiar than forces such as gravity, but they can be the driving engine in processes from the very small (mixing of two different liquors in a mixed drink or the rate of chemical reactions in a retort—both driven by concentration gradients) to the extremely large (mass ejection, astrophysical jet creation, and shock formation—all driven by energy density gradients in supernova explosions). While forces that result from gradients play a role in daily life, they can also play a dominant role in less mundane fields such as astrophysics and the physics involved in nuclear weapons.

Radiation Transport

The concept of a radiation temperature (T_{rad}) and of the transport of radiation through stellar systems arises from a logical extension of the familiar concepts discussed above (e.g., heat emission from a thermally warm object). These concepts extend from infrared radiation from a hot metal bar at a few 100 K all the way to x-rays emitted from an extremely hot object (e.g., a blackbody radiator) with an equivalent temperature in the million-degree range. Understanding radiation transport is important because it plays a prominent role in the evolution of stars and in the functioning of a nuclear weapon. Like thermal temperature gradients that cause the diffusion of heat down a metal bar, T_{rad} gradients cause the transport of radiation through systems. For example, radiation from a star is transported from the high T_{rad} region deep within the star where it was created out into the cold surrounding interstellar region. On its way out, the radiation moves through regions where various radiation-transport models may be valid—all driven by T_{rad} gradients. Transport processes in a star are the subjects of intense study using astrophysical simulations.

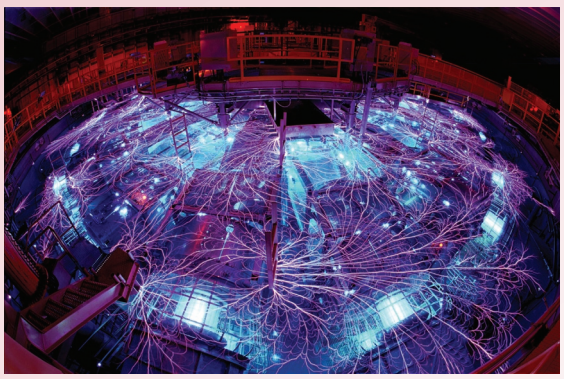

Figure 1. Bird's eye view of the Z accelerator as it fires.

The Z pulsed-power accelerator at SNL generates an environment in which large T_{rad} gradients exist at temperatures of about 2 x 10^6 K (220 eV). This extreme environment allows us to study the underlying physics behind radiation transport. Because of the importance of radiation transport, experimental data are needed to ensure that we have the correct physics understanding, models, and simulation tools. Data from experiments on Z can lead to new models or confirm existing models and thus validate LANL's physics and engineering simulations. Experimental tools like the Z accelerator are needed to produce radiation-transport data and other types of data, including material properties of metals (e.g., beryllium and uranium) of interest to the laboratory.

The Z Accelerator

The Z accelerator reuses the energy-storage system originally built for the ICF PBFAII project at SNL in the early 1980s. The Z accelerator is a high-energy capacitor bank comprised of 36 parallel modules arranged in a circular array. The 36 current pulses are coupled towards the center of the array through a series of pulse-forming networks (PFNs). These PFNs are used to compress the many microsecond current pulses into 100-ns current pulses. After penetrating the wall of a vacuum vessel, the 36 individual current pulses are combined into a single current pulse. This single pulse is then transported into the center of the chamber where it is converted into some form of energy used for an experimental physics study.

The capacitor banks, PFNs, vacuum vessel, and ancillary equipment reside in a several-story building designed for the task. Service utilities in the building provide vacuum, high-pressure air, normal air-conditioning service, and high-voltage service for charging the capacitor bank. Also, a high-capacity crane and a multitude of shielded enclosures (one belonging to P-22) service diagnostic instruments in the electrically hostile environment. The main control room is a shielded enclosure that protects the computer control system when Z fires.

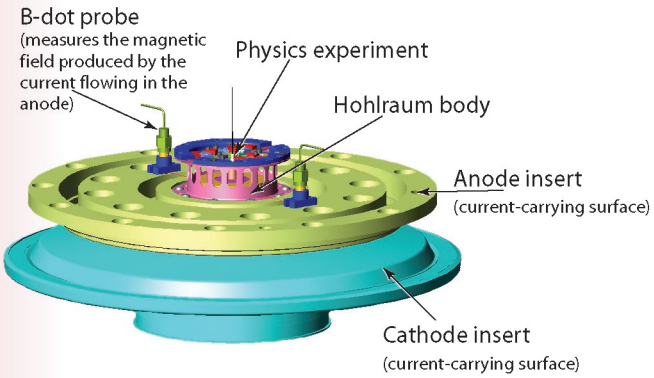

Figure 2. An anode and cathode insert with attached dynamic hohlraum body.

The high-power Z Beamlet Laser (ZBL) was recently constructed as a new capability in an adjacent building to the Z accelerator. (Parts from LLNL's beamlet laser system—the prototype for each arm of the NIF—were refurbished for the construction of ZBL.) The light from ZBL is transported into the Z target chamber through an optical transport system that spans the space between buildings. The ZBL light pulse produces x-rays from a metal foil in the Z vacuum vessel. The x-rays are produced next to a physics experiment at the center of the target chamber. They are typically used as an x-ray backlighter to illuminate the physics experiment and to take a dynamic image of its evolution in a manner similar in concept to DARHT and PHERMEX at LANL.

Figure 1 shows a bird's eye view of the Z accelerator as it is firing. (From the image, one can see why all electronics are generally located in shielded enclosures!) The lightning bolts in the image are above the PFNs. The PFNs reside in low-conductivity water where pulse duration compression from 10 μs to 100 ns takes place for subsequent injection into the target chamber. The discharges (lightning bolts) are due to energy leaking out of the high-voltage switches in series with the PFNs into the surrounding environment. From the water section, the pulse-forming lines feed through an insulating water-vacuum interface and onto a radial magnetically insulated transmission line (MITL), which then feeds the center of the machine where the physics experiment is conducted. Because of the total amount of energy involved (~ 14 MJ at 90 kV) in each discharge, the very center of the MITL has an interchangeable ~ 12-in.-diam insert that holds the physics experiment and the final disposable sections of the anode and cathode current conductors. This insert (Figure 2) is destroyed on each shot. The MITL must be removed and physically cleaned after each shot, which limits the facility to a single shot each day. In an x-ray production mode, Z is the most powerful x-ray source in the world (~ 250 TW in a 3–5 ns pulse) and provides an unmatched tool

for radiation driven experiments conducted by LANL and others. X-ray production, x-ray driven experiments, and other experimental uses of Z will be discussed below.

Radiation-Driven Experiments

For production of x-ray radiation, the electrical current flowing in the system is run through a set of very small diameter wires inside a confining structure, known as a hohlraum, which is used to contain any x-ray radiation that is produced from the experiment. The wires collapse toward the center of the vacuum vessel under the magnetic forces acting on them. The 12-in.-diam sacrificial insert (in the configuration shown in Figure 2) is comprised of a final anode and cathode section with a slotted dynamic hohlraum body mounted on top of the anode. Current delivered by the MITL travels radially inward on the cathode and up through a set of 360 tungsten wires, each ~ 10 μm in diameter, located inside the hohlraum body. The current then returns along the top and down the side of the hohlraum body and finally to the capacitor-bank modules via the anode and the MITL. In this configuration, magnetic forces drive the wires radially inward at high velocity until they stagnate near the axis. Their kinetic energy is converted into thermal energy, which radiates away in the form of x-rays that are absorbed and re-radiated inside the hohlraum body. The resultant x-ray flux is used to drive physics experiments either around the periphery of the hohlraum or on the top of it.

Copious amounts of thermal x-rays are produced when an array of wires collapses either onto themselves (as in a vacuum hohlraum, Figure 3) or onto a low-density foam located on the axis of hohlraum (as in a dynamic hohlraum). The vacuum hohlraum can generate an environment with an equivalent blackbody temperature of 145 eV inside a solid-wall hohlraum. The wall of the hohlraum can then be populated with multiple physics packages for studies of radiation flow inside closed geometries and flow through free-standing low-density foams and for studies of aperture closure driven by radiation and shocks that impinge on the gold hohlraum wall.

Alternatively, the dynamic hohlraum produces radiation from a wire array as it impacts upon a low-density foam located in the center of the array, subsequently thermalizing the kinetic energy in the wires and radiating the energy vertically. This radiation can be directed out of the top and bottom of the pinch to a physics experiment above or below the wire array, rather than around the periphery of the hohlraum body as in the case of a vacuum hohlraum. This process produces a much higher-radiation temperature (220 eV) to drive a single package located above the hohlraum for similar studies. A recent radiation-transport experiment that investigated radiation loss through the thin gold wall of a physics package located above the pinch using the ZBL system for backlit imaging is discussed in this report ("X-ray Diffusion through a Thin Gold Wall," page 84) P Division and SNL use vacuum hohlraums to study both weapons-physics issues and astrophysical jet formation and dynamic hohlraums to study both weapons-physics issues and indirect-drive ICF.

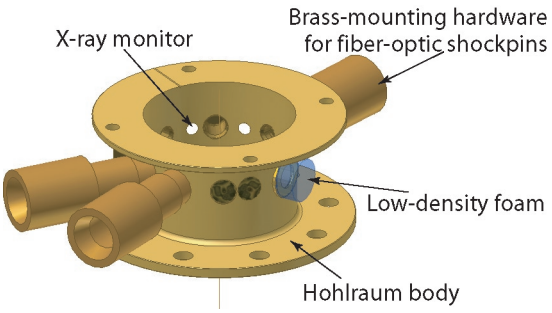

Figure 3. A typical experiment using a vacuum hohlraum with its outside wall populated by a number of experiments. This vacuum hohlraum shows four physics experiments located around the periphery of the hohlraum body. Three experiments are serviced by fiber-optic shock pins that are contained within massive radial structures (the brass-mounting hardware shown in the figure). There are also several apertures covered with foils and a low-density foam physics experiment to be radiographed by the ZBL system. The radiograph of the foam is taken as a radiation-driven shock passes radially through it.

Materials Experiments

For dynamic materials studies, the current is transmitted through the sample and then returned to the capacitor bank through a low-impedance circuit. The conductor wall is the material sample under study. The magnetic field generated between the central rod and the conductive sample can create a pressure in the sample (which is mounted on the return conductor wall) of up to 3.25 Mbar (in copper). This pressure can be used in shockless ICEs. When used in a flyer-plate mode for subsequent impact on material samples in past experiments, the Z accelerator has produced up to 28-km/s velocities in the flyer plate. In either event, the subsequent response of the material under study is used to accurately determine the equation of state of a material to ensure the integrity of simulations. P Division and DX Division use this configuration with the shock physics group at SNL to study many materials.

Several experiments conducted using the Z accelerator are discussed in detail in the project descriptions in this activity report.

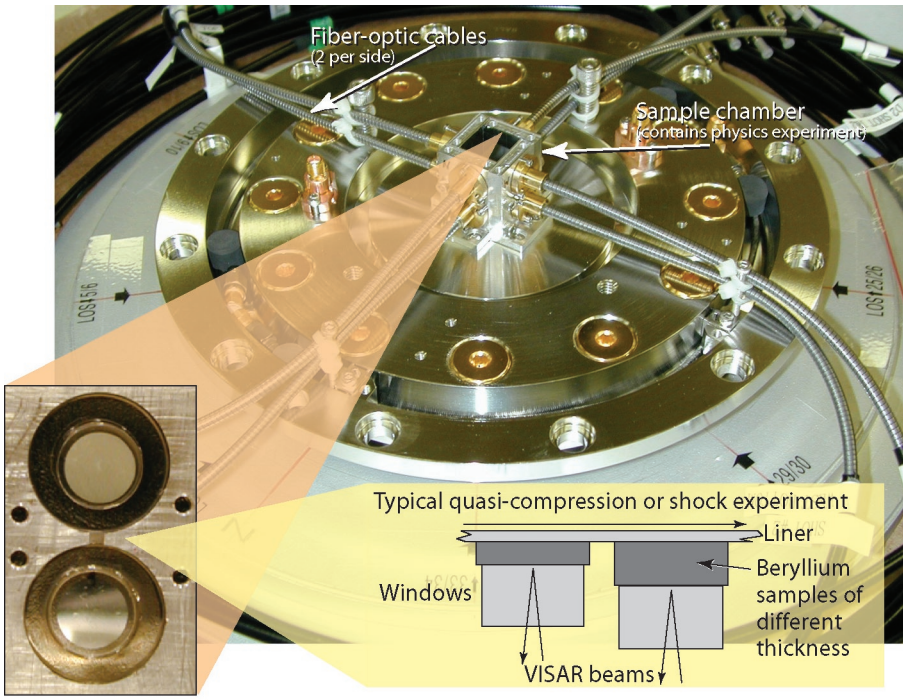

Figure 4. Four sample panels are arranged in a square pattern with each of the four panels having two samples under test. In the pictured experiment, beryllium samples are in intimate contact with the aluminum current-carrying conductor. The beryllium samples are subjected to quasi-isentropic compression. The particle velocity of the beryllium/window interface is recorded using VISAR. By conducting experiments with varying thicknesses of beryllium, we can determine a complete understanding of the isentrope of beryllium.

Acknowledgment

The researchers would like to acknowledge the MST-7 target-fabrication team for preparation of all physics experimental packages used in the Z experiments. We also wish to acknowledge the SNL Z Wire Array Laboratory and the Z Accelerator Load Assembly designers for the design and assembly of all radiation-producing wire-array systems. Finally, these types of experiments could not be performed without the input from a large number of colleagues in DX, P, and X Divisions at LANL during the planning of Z experiments. This work was sponsored by the Office of Secondaries and Inertial Fusion in DOE Defense Programs.

For more information, contact Robert Watt at 505-665-2310, watt_r@lanl.gov.

FRX-L: A Plasma Injector for Magnetized Target Fusion

G.A. Wurden, T.P. Intrator, J.M. Taccetti, S. Zhang, S.C. Hsu, Z. Wang, W. Waganaar, D.W. Begay (P-24), M.G. Tuszewski (NIS-2), C. Grabowski, J. Degnan, E. Ruden, B. Martinez (Air Force Research Laboratory)

Since the early 1950s, LANL has conducted research into ways to achieve controlled thermonuclear fusion to eventually create a new energy source[1] for the benefit of mankind. In the last decade, LANL has largely focused on collaborating with other experimenters around the world to build and diagnose the most advanced (and usually quite large) experimental fusion machines. In the background, several scientists and very small teams at LANL have been developing a new fusion concept that could lead to a faster, better, and cheaper approach to fusion energy.[2] This concept, generically called "magnetized target fusion" (MTF), lies somewhere in-between the more established approaches of magnetic fusion energy (MFE), which uses large magnetic bottles to confine hot plasma for long periods of time, and inertial fusion energy (IFE), which uses lasers or ion beams to implode tiny fuel capsules in a few nanoseconds.

A Different Approach to Generating Fusion Energy

MTF offers the possibility of achieving useful thermonuclear fusion conditions with a radically different approach—combining features of both MFE and IFE. MTF has the potential of operating at higher fuel density and of being more compact than MFE while at the same time alleviating the huge power requirements needed for IFE. As such, MTF will enable the use of slower (and therefore cheaper) pulsed power that has (literally) been around for decades. This innovative method basically begins with the production of an initial "warm" plasma embedded in a magnetic field (Figure 1). This plasma is then injected into an adjacent region where it is compressed to thermonuclear conditions using pulsed-power technology developed by the DOE Defense Programs to study materials under very high-pressure conditions. Defense Programs technology essentially "moves metal fast"—that is, a solid metal "liner" is imploded at extreme speeds. The region into which the MTF plasma is injected is surrounded by a thin aluminum cylindrical liner, which is then crushed in about 20 μs. The compression rapidly increases the magnetic field and the density and temperature of the plasma by a factor of 30 to 100, establishing thermonuclear conditions. As a result, the plasma should easily fuse and therefore release significant amounts of energy.

The ultimate goal of this research is to develop a fully operational pulsed-power fusion machine. The effort will combine 30 years of work at LANL to develop a class of plasmas called "compact tori," including one type, in particular, called the "field-reversed configuration" (FRC),[3] with 20 years of pulsed-power-technology development. To address this goal, we began an effort about four years ago to combine the required initial plasma and the liner implosion technology into a scientific effort that will hopefully lead to the first MTF physics demonstration.

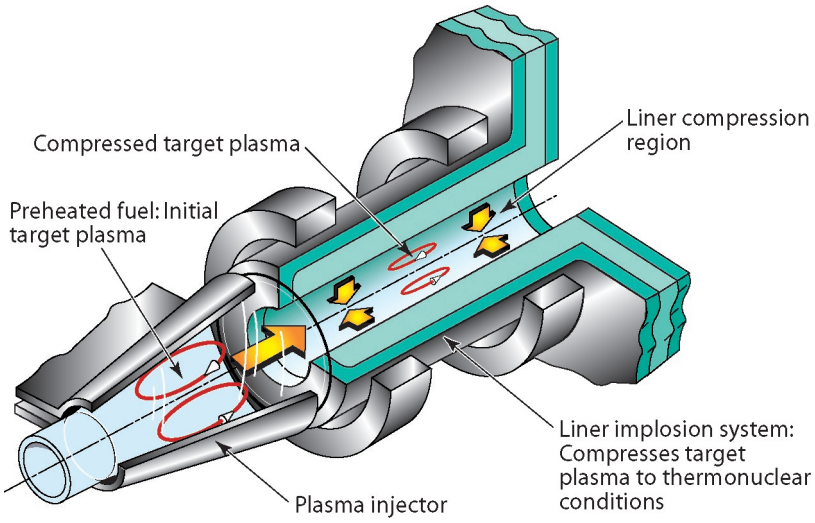

Figure 1. Rendering of MTF elements, including the initial target plasma, which is then injected into a liner compression region where the plasma can be compressed to thermonuclear conditions.

Efforts Toward a Field-Reversed Configuration Machine

The research program at LANL involves efforts (1) to demonstrate a suitable plasma injector, called the "FRX-L,"[4] where FRX refers to "field-reversed experiment," and the "L" refers to "liner," (2) to develop the "can crusher" at the Air Force Research Laboratory (AFRL) in Albuquerque, NM, and mate it to the plasma injector, and (3) to predict and model the plasma implosions using sophisticated computer codes with data from fast-plasma diagnostic tools. Other scientists at the University of Nevada, Reno; General Atomics; and LLNL are also conducting research into elements of MTF.

FRX-L is designed to produce compact, high-density, field-reversed plasma configurations with parameters compatible with what is needed to serve as a MTF target (deuterium) plasma that has a density of ~ 1×10^{17} cm^{-3} and a temperature of ~ 200 eV at magnetic fields of ~ 3 to 5 T and a lifetime of ~ 20 μs. The FRX-L uses four high-voltage capacitor banks (up to 100 kV, storing up to 1 MJ of energy, see Figure 2) to drive a 1.5-MA current in one-turn magnetic-field coils that surround a 10-cm-diam quartz tube (Figure 3) where the target plasma is formed. We use a suite of sophisticated plasma diagnostics to ensure that the target plasma has the correct density, temperature, lifetime, and purity needed for use in MTF. Multi-chord laser interferometry measures the plasma density; high-power laser scattering (Thomson scattering) is used to measure the plasma temperature and density; a variety of plasma spectroscopy measurements are taken to determine the plasma purity; sets of external magnetic probes measure the plasma shape and pressure; bolometers measure the power radiated from the plasma; and fast imaging cameras view the plasma symmetry and wall interactions.

The entire FRX-L experiment is controlled from a shielded screen room, and data from approximately 100 channels of measurements are acquired on high-speed digitizers before being transferred to a database for display after each shot. During a day of operations, 20 to 30 shots (each lasting about 100 μs) can be fired under computer control. A blast door/wall separates the researchers from the high-voltage and high-energy conditions in the experiment. Red and yellow warning lights indicate the status of the experiment; meanwhile, experienced researchers often plug their ears when they hear the building announcement "Main bank is charging"!

Presently, plasma parameters at a density of ~ 2 to 4 × 10^{16} cm^{-3}, temperatures of 100 to 250 eV, magnetic fields of 2.5 T, and lifetimes of 10 to 15 μs are within a factor of 2 to 3 of our desired endpoints for the starting target plasma. In the coming year, while also improving the pulsed power and plasma performance, we will begin translating these plasmas into a test-liner chamber to confirm the plasma cleanliness and lifetime and our ability to trap the plasma in the close-fitting aluminum liner.

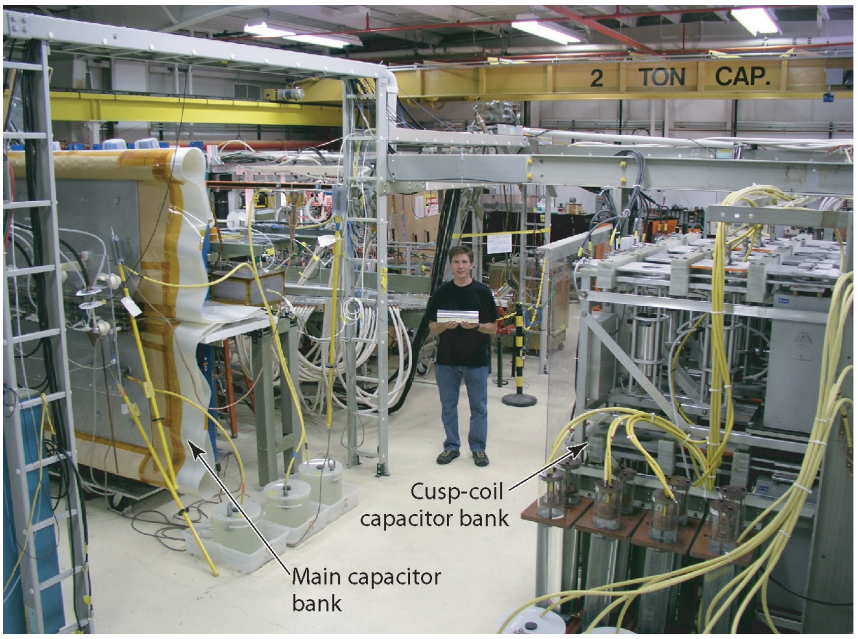

Figure 2. The FRX-L experimental bay, showing the pulsed-power electrical systems that supply energy to the plasma injector. Martin Taccetti (P-24) holds a full-scale aluminum liner in his hands. The main capacitor bank (to the left), delivers 1.5 MA of current to the theta pinch coils. Another bank (on the right) provides energy to the cusp coils.

Figure 3. The initial FRC target plasma is formed inside a small (10-cm-diam) quartz tube. One of our AFRL collaborators, Chris Grabowski, provides the scale for the target plasma by looking through the tube.

Conclusion

Recently we have submitted a proposed extension of the MTF project to DOE, which will authorize the goal of combining our plasma injector with the AFRL "Shiva Star" (Figure 4) liner-implosion system. With partners from the University of New Mexico, the University of Wisconsin, the University of Washington, and the AFRL, we plan to demonstrate fusion-relevant plasma conditions within this decade. The fusion plasma that we hope to produce (at a rate of about 1 shot per week in the laboratory) would be a clean deuterium plasma that will be confined by an enormous magnetic field of 500 T for about 1 μs and will reach a temperature of 5 to 8 keV and a density of ~ 1×10^{19} cm^{-3}! Success could lead to the first demonstration of break-even plasma conditions using magnetized targets in the Atlas liner-implosion facility at the NTS in later follow-on experiments.

References

1. See http://fusionenergy.lanl.gov/
2. R.E. Siemon, I.R. Lindemuth, and K.F. Schoenberg, "Why MTF is a low cost path to fusion," *Comments Plasma Physics Controlled Fusion* **18**(6), 363–386 (1999).
3. M. Tuszewski, "Field reversed configurations," *Nuclear Fusion* **28**(11), 2033–2092 (1988).
4. J.M. Taccetti, T.P. Intrator, G.A. Wurden, S.Y. Zhang *et al.,* "FRX-L: A field-reversed configuration plasma injector for magnetized target fusion," *Review of Scientific Instruments* **74**(10), 4314 (2003).

Acknowledgment

This work is supported by the DOE Office of Science, Fusion Energy Sciences Innovative Confinement Concepts Program, with experimental collaborators from the AFRL and with theory collaborators from LANL, General Atomics, and LLNL.

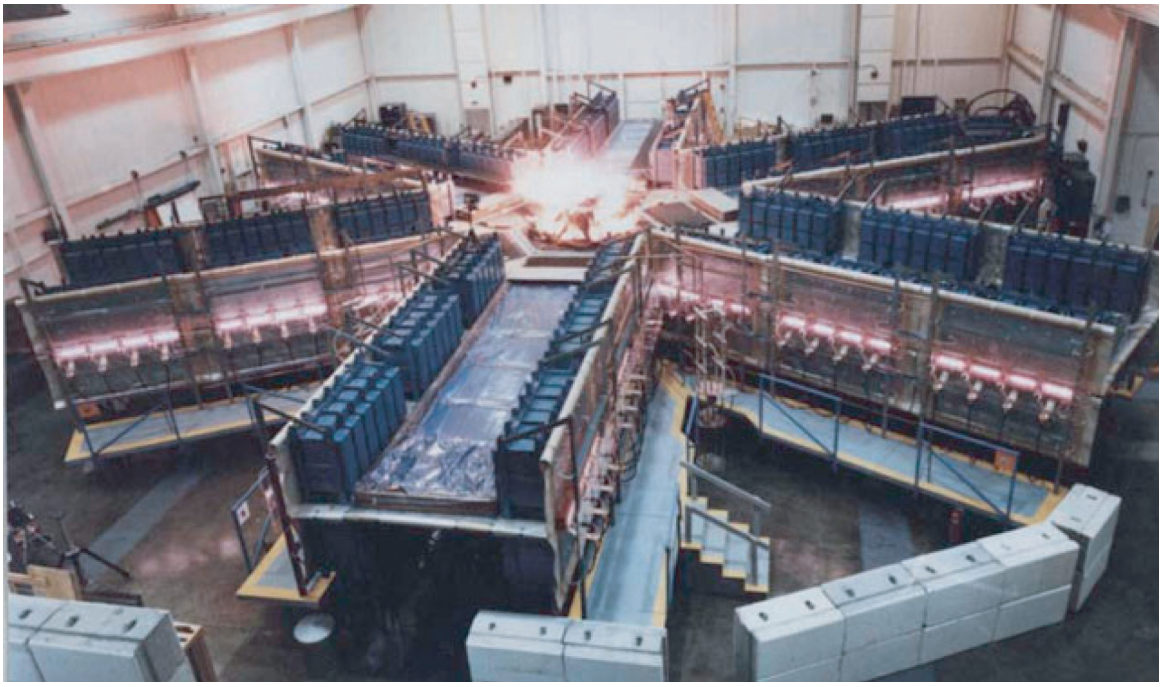

Figure 4. The AFRL pulsed-power machine "Shiva Star," which is about the size of two basketball courts, will be the site for the first combined LANL plasma injector and AFRL Shiva Star liner-implosion experiments earmarked for the 2006–2007 timeframe.

For more information, contact Glen Wurden at 505-667-5633, wurden@lanl.gov.

Neutron Generation Using Inertial Electrostatic Confinement

J. Park (P-24), R.A. Nebel (T-15)

We are developing a compact and portable neutron source based on the inertial-electrostatic-confinement (IEC) plasma device, located at TA-35, Building 27 at LANL. The system consists of highly transparent concentric grids (two or three grids) in a vacuum chamber (Figure 1). Plasmas containing deuterium and tritium ions are produced either by electron injection or by an inductively coupled antenna. Once a plasma is produced, a high-negative-voltage pulse is applied to the inner grid (- 100 kV for 1-ms duration) to accelerate the ions to the center of the vacuum chamber where they collide with each other and the background gases. The ion energy can achieve the full potential of the accelerating grid and thus reach very high energy (50–100 kV) where the fusion cross section becomes large and copious neutrons are produced.

Currently, the device is operated with two grids and uses only deuterium fuel. In the next phase of the project, we will use a mixture of deuterium and tritium to enhance the time-averaged neutron-production rate to > 1 x 10^{10} neutrons/s. The grid system has been recently upgraded with a tungsten-rhenium alloy that allows high-temperature operation; also a pulsed-discharge operation has been implemented to increase peak plasma performance. The goal of this project (in coordination with NIS-6) is to develop a compact, durable (> 5,000-hour lifetime) neutron source for an active nuclear assay of highly enriched uranium for homeland security and other applications. The project also includes a proof-of-principle test of a radical, yet promising, nuclear-fusion concept—the periodically oscillating plasma sphere (POPS)—for fusion-power production. We recently demonstrated the stability of the virtual cathode, which is a prerequisite for POPS, both experimentally and theoretically.

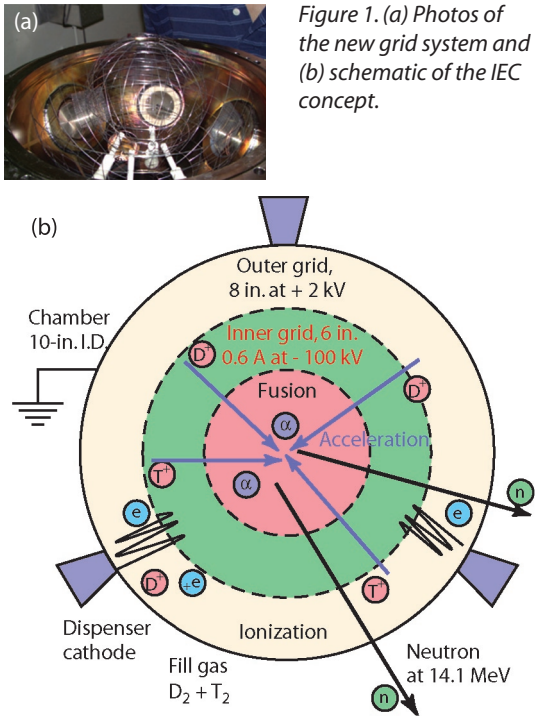

Figure 1. (a) Photos of the new grid system and (b) schematic of the IEC concept.

National Fusion Collaborations

G.A. Wurden, R.J. Maqueda, I. Furno (P-24)

We have off-site fusion collaborations at the University of Washington, Massachusetts Institute of Technology (MIT), and Princeton University. At the University of Washington, we focus on researching the physics of rotating magnetic-field current drive in an FRC plasma. In particular, we have been prototyping multichannel bolometers to measure the radiated power from the FRC plasma.

At MIT, we operate an infrared video-camera system, with a specialized zinc-selenide periscope system that allows us to get a view of the Alcator C-Mod tokamak divertor. Of particular interest is the flow of power onto different parts of the divertor during high-performance plasma operation.

At Princeton University's Princeton Plasma Physics Laboratory, we have been engaged in a study of turbulence in the edge of the National Spherical Torus Experiment spherical tokamak plasma. We operate two intensified, fast, video-camera systems, at rates up to 40,000 frames/s, and use them to view the edge of the plasma when a small gas puff is injected to "light up" the pre-existing plasma turbulence. This technique is called "gas-puff imaging" and allows us to see interesting differences in plasma transport of "blobs" between so-called "low-mode" and "high-mode" confinement regimes, which can then be compared to plasma models using computer simulations.

Combustion Enhancement of Propane by Silent Discharge Plasma

L.A. Rosocha, S.M. Stange (P-24), D. Platts (P-22), D.M. Coates (P-DO)

It is well known that the application of an external electric field to a flame can affect its propagation speed, stability, and combustion chemistry. External electrodes, arc discharges, and plasma jets have been employed to allow combustible-gas mixtures to operate outside their flammability limits by gas heating, injection of free radicals, and field-promoted flame stabilization. Other investigators have carried out experiments with silent electrical discharges applied to propagating flames. These have demonstrated that the flame-propagation velocity is actually decreased (combustion retarded) when a silent discharge is applied directly to the flame region, but that the flame-propagation velocity is increased (combustion promoted) when a silent discharge is applied to the unburned gas mixture upstream of a flame. Two other recent works have considered the possibility of combustion enhancement in aircraft gas-turbine engine combustor mixers by using a plasma-generating fuel nozzle that employs an electric-arc or microwave plasma generator to produce dissociated fuel or ionized fuel and pulsed corona-enhanced detonation of fuel-air mixtures in jet engines. In contrast to these prior works, we have employed a silent discharge plasma (SDP) reactor to break up large fuel molecules into smaller molecules and create free radicals or other active species in a gas stream before the fuel is mixed with an oxidizer and combusted.

Figure 2. A schematic of our SDP reactor "activating" the propane before combustion.

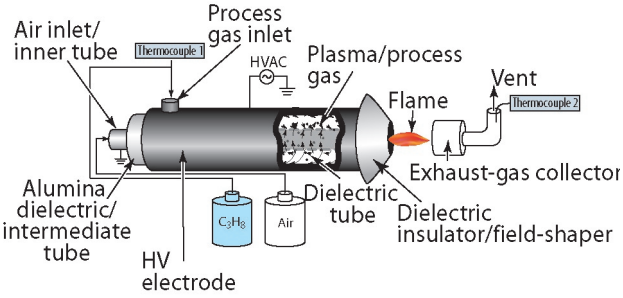

In our work, a cylindrical SDP reactor (Figure 2) was used to "activate" propane before mixing it with air and igniting the combustible gas mixture. With the plasma, the physical appearance of the flame changes, and substantial changes in mass-spectrometer fragmentation peaks are observed (e.g., propane fragments decrease and water and carbon dioxide increase). This indicates that the combustion process is enhanced with the application of the plasma. So far, we have acquired data on the plasma power, specific energy, and degree of combustion enhancement of propane as determined from our experiments with a coaxial SDP reactor. In the future, we would like to conduct experiments with more practical fuels (e.g., gasoline, diesel fuel, and jet fuel).

Neutron-Imaging Studies of Asymmetrically Driven Targets on the Omega Laser

C.R. Christensen (P-24), D.C. Wilson (X-2)

An experimental campaign, known as Asymmetric Direct Drive Spheres (ADDS), involved a series of studies designed to explore the relationship between asymmetry and the mix of capsule-shell material into the DT fuel during ICF implosions. To understand this relationship, we varied the energies of each of the 60 beams on the Omega laser at the University of Rochester to produce symmetric, prolate, or oblate implosions at DT fill pressures of 10, 5, or 2.5 atm.

During the experimental runs, we obtained simultaneous neutron (Figure 3) and x-ray images, and, together with neutron yield and ion temperature, compared them to predictions of ICF mix models. The agreement between our experiments and the ICF mix models is good for all three fill pressures. We expect that the data from the ADDS experimental campaign will be very useful in validating predictions of turbulent-mix models, which often involve quantities that are difficult to determine experimentally. By contrast, the yield proportion of the symmetric/prolate/oblate implosions leads to a testable criterion that depends only on simple geometric factors.

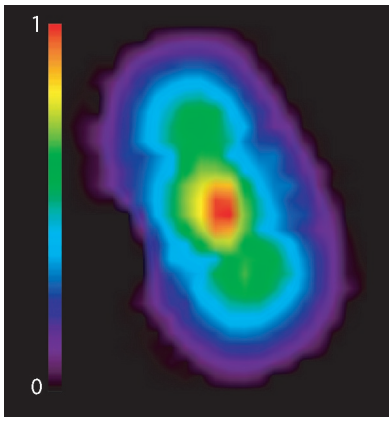

Figure 3. Reconstructed neutron image of a prolate implosion using 13% drive asymmetry.

Developing a Fundamental Understanding of Laser-Plasma Interactions

D.S. Montgomery, J.L. Kline, J.A. Cobble, J.C. Fernández (P-24), H.A. Rose, D.F. DuBois (T-13), B. Bezzerides, E.S. Dodd, D. Barnes, L. Yin, J. Kindel (X-1), H.X. Vu (University of California, San Diego)

Laser-plasma instabilities (LPIs) can severely limit the amount of laser power coupled into targets used to study high-energy-density (HED) physics and must be properly controlled in order to achieve fusion ignition for ICF experiments, such as those planned on NIF. Such instabilities occur when intense laser light scatters off of waves in the plasma, causing the amplitudes of the scattered light and plasma wave to grow exponentially at the expense of the incident laser power.

In realistic laser beams, such as those planned for NIF, the laser-beam intensity profile in the focal region consists of an ensemble of thousands of intense regions, called hot spots. Growth of instabilities occurs mainly in these intense hot spots, and an instability in one hot spot can seed instabilities in other hot spots. LPIs, in this case, can be highly complicated, where various instabilities can compete with one another and can also modify the local laser and plasma conditions, thus changing the conditions for instability growth. In NIF-scale targets, where the laser propagates through several millimeters of plasma, these detailed processes cannot be modeled from first principles because the laser-plasma system must be resolved at scales less than the wavelength of light. The system size is thousands of wavelengths long, and the required computing resources are beyond the reach of planned computers.

Our research focuses on understanding LPIs at the most fundamental level, within a single laser hot spot. This is realized in experiments using a nearly diffraction-limited laser beam at the Trident laser facility to drive instabilities in a preformed plasma. State-of-the-art physics models can simulate the volume of a single hot spot so that we can make direct comparison between numerical simulations and experiments. Additionally, the laser and plasma conditions in these experiments are extremely uniform—such that detailed structures associated with these processes can be resolved, allowing us to discriminate between various processes. One of the successes in 2003 was the observation of a transition from a wave-wave nonlinearity to a wave-particle nonlinearity for large-amplitude electron plasma waves (EPWs). These waves participate in stimulated Raman scattering (SRS), an instability important to laser fusion, and their nonlinear behavior largely determines how much laser power is lost to this unstable process. Using Thomson scattering, we detected the large-amplitude EPW driven by SRS. In a regime where the EPW wavelength was much larger than the Debye screening length, the SRS EPW drove a cascade of multiple EPWs via the Langmuir-decay-instability process, which was also detected by Thomson scattering. In a regime where the EPW wavelength was of the order of the Debye length, we detected a single frequency-broadened EPW. The amount of frequency broadening was consistent with a simple model for electrons trapped in the potential troughs of the EPW. Thus, the EPW nonlinearity transitions from a wave-wave nonlinearity to a wave-particle nonlinearity as the EPW wavelength approaches the Debye length. These observations are in qualitative agreement with numerical simulations and will allow us to better refine our models.

Experimental Investigation of Fundamental Processes Relevant to Fusion-Burning, Strongly Coupled, Multi-Material Plasmas

J.F. Benage, F.J. Wysocki, R.R. Newton (P-22), D. Montgomery (P-24), J.P. Roberts, G. Rodriguez, S.A. Clarke, A. Taylor (MST-10), M.S. Murillo, J.O. Daligault (T-15)

The goal of this project is to make a detailed experimental investigation of fundamental physical processes that occur in a fusion-burning, strongly coupled, multi-material plasma. When plasmas are rapidly heated to reach the conditions necessary for fusion to occur as in an ICF implosion capsule, the plasma conditions will relax to an equilibrium state. Because fusion reaction rates are very sensitive to temperature at low ion temperatures, a small error in the temperature can produce a much larger error in the fusion reaction rate. Thus, the relaxation toward equilibrium and the distribution of energy among plasma constituents could be significantly affected when and if the appropriate conditions for fusion are reached. In addition, because all laboratory fusion schemes require the containment of the plasma by some material other than the fusing particles, contaminant ions are always present in the plasma. These ions become highly ionized and can affect the plasma density and average charge Z. These contaminating ions also interact strongly with the other plasma species. When the interaction energy between the species becomes comparable to the thermal energy, the plasma is called strongly coupled. Unfortunately, such strongly coupled plasmas violate the assumptions made for theories used in modeling the plasma undergoing fusion. Thus, to improve our ability to predict and understand such fusion burning plasmas, we must have better models that are validated by experiment. Toward that end, we are conducting two experiments.

In our first experiment, an intense laser incident on a high-density gas jet creates hot plasma. Using Thomson scattering and absorption spectroscopy, we obtain time-resolved measurements of the electron and ion temperatures to determine the temperature equilibration rate between the electrons and ions in the strongly coupled plasma. In our second experiment, a very short-pulse laser produces a CH plasma and a gold plasma side by side. We obtain the rate of diffusion of light ions through heavy ions in the strongly coupled plasma by measuring the diffusion of the H ions through the gold plasma for various gold-plasma thicknesses. The results of these experiments will provide data to validate theoretical models that have been recently developed to describe these processes. When validated, such models can be incorporated into codes used to model, design, and predict the behavior of fusion-burning plasmas.

Applied-Science Internship Program

T. Intrator (P-24)

Fiscal year 2003 was the second year of existence for the Applied-Science Internship Program (ASIP) in P-24 and P-25 (http://education.lanl.gov/newEPO/CS/ASIP.html). ASIP is an undergraduate experimental training program that targets applied science and engineering skills—physics and engineering of lasers, pulsed power, accelerators, ICF, high-energy density physics, and weapons aspects of dynamic experimentation and diagnostics and underground experimentation. The goals of this program are to recruit students to LANL and rapidly train them to be contributors to the stockpile stewardship program, to develop and hire highly qualified students into LANL's critical-skills pipeline, and to provide a reliable source of exciting jobs and feedback on curriculum development for local institutions so that they can attract higher-quality students.

ASIP adds an essential component to our student pipeline by providing two avenues for recruitment to supply LANL's future workforce. First, continued support of students throughout their academic career increases

the likelihood that they will choose a career at LANL. Second, ASIP expands the process by networking with academia. The program focuses on near-term hires and on undergraduate- and graduate-level students. The large, continuing, year-round student population of ASIP has created a culture that is luring more high-quality students to LANL. ASIP is continually bombarded with excellent resumes elicited by word-of-mouth recommendations from alumni. Program leaders have found jobs for many students that they cannot hire themselves because of funding and space limitations. In P-24, 60% of the students return, stay for long-term internships, or do both. ASIP has reached the point at which expansion will be required to admit more new students. P Division is committed to hiring new staff members from the program. The Division will commit staff members to develop the curriculum; will provide staff support for curriculum development of associates, bachelors, masters, and doctoral degrees; and will recruit students to fill the program. ASIP is a joint venture among P Division, MST Division, and several institutions, including the New Mexico Institute of Mining and Technology, Socorro; MIT; and Northern New Mexico Community College (NNMCC).

In FY 2003, the ASIP program included 26 students and retained a record number of these students—11 out of 13 returned from the previous year's program in P-24 alone (Figure 4). The schools represented included MIT, Stanford University, Princeton University, NNMCC, Purdue University, the University of Michigan, Clarkson University, and the University of Pennsylvania. Eight students had fellowships from outside LANL. One student received a prize at the LANL student symposium for the best engineering poster presentation. Two are doing doctoral theses at LANL, and one is being groomed to become a technician next year. One student is the lead author on a paper that will soon appear in *Review of Scientific Instruments 2003* and another co-authored a paper that has already been published. Three are going to graduate school—two to the University of Wisconsin and one to the University of Nevada, Reno. Two are staying at LANL beyond the summer, and a large number of the FY 2003 students are expected to return in FY 2004. A 2003 Plasma Physics Summer School Seminar Series, which typically attracted more than 30 students per class, was coordinated with the Physical Sciences and the Dynamics Summer School (http://wsx.lanl.gov/RSX/summer-school/Summer_school_homepage.htm). The seminar series included talks on radiation hydrodynamics from an X Division staff member and talks about plasma physics, astrophysics, and experimental issues from P-24 staff members. ASIP organized a LANL-wide workshop on plasma astrophysics that drew more than 70 people. The program received an MIT UPOP (Under-graduate Practice Opportunity Program) Internship Excellence Award that carried with it a $2,000 stipend per MIT UPOP student who interned at P-24.

Figure 4. Students from the ASIP pose for a group photo at a summer 2003 "get together" at mentor Glen Wurden's home.

X-ray Diffusion Through a Thin Gold Wall

R.G. Watt, G. Idzorek (P-22), R. Chrien (X-2)

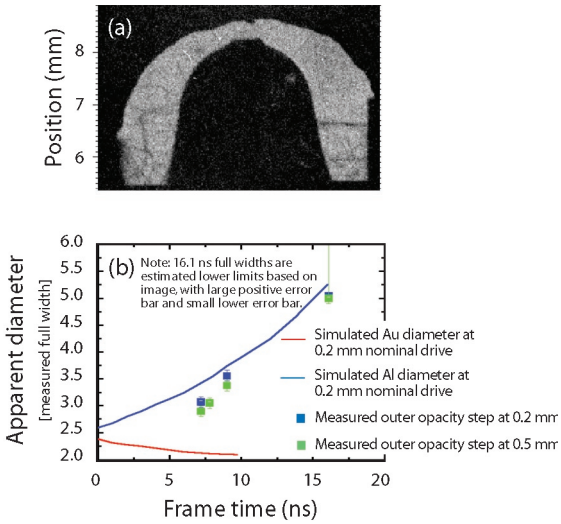

Figure 5. (a) A backlit radiograph of the expanding cylinder about 9 ns after peak radiation drive. (b) A time history of the radiographic measurements compared to threoretical predictions.

The transport of x-rays into or through the thin gold wall of a hohlraum is an energy-loss mechanism in indirectly driven ICF hohlraums. When using a thin-wall hohlraum (TWH) in ICF (which allows us to both reduce the material load on large optics and image the laser-wall interaction region through the wall), the loss mechanism may become significant. Assessing this loss requires obtaining correct simulation results, which in turn, requires having the correct physical models for radiation flow through the wall in the simulation code. Experimental data are needed to confirm that we used the correct models. In the absence of accurate experimental data, simulations might lead us to erroneous conclusions about the efficacy of TWHs for use in experiments at large laser facilities and ultimately on NIF.

Experimental data are being obtained using the Z accelerator at SNL to address this deficiency. A dynamic hohlraum is used to produce x-rays from a radiating volume with a 200-eV-equivalent radiation temperature to drive a TWH. The TWH is comprised of a thin gold layer (1 μm, somewhat thinner than the typical 2- to 3-μm gold layer in a normal TWH) supported on the outside by a 25-μm aluminum layer. The long duration of the drive and the limited thickness of the gold layer allow the radiation wave to break through the gold layer, after which the inward motion of the gold lowers the density below solid and allows diffusive radiation flow through of order 10 radiation mean-free paths in the gold before reaching the outer aluminum. Escaping radiation consequently heats the aluminum layer that surrounds the gold. The motion of the aluminum is used to study the diffusion of radiation through the gold in an integrated experiment in which the diffusion approximation should be valid in the gold. The primary diagnostic is an x-ray-backlit image of the expansion of the closed cylinder as a function of time. Comparison of the predicted and observed position of the outer surface of the aluminum wall provides a good measure of the model used in the calculations.

The expanding closed cylinder is driven by a 200-eV radiation source of 3- to 5-ns duration driven by a dynamic hohlraum with a 4-mm radiation exit hole (REH). The drive radiation from the pinch is transported upward 1.7 mm above the REH by a low-density, foam-filled gold cone to get it to the location of the physics package. Once inside the closed cylinder, the radiation escapes through the gold wall and heats the aluminum, which subsequently expands. The expanded aluminum is thick enough to significantly block 6.7-keV x-rays emitted from an iron back-lighter foil, which is illuminated by ~ 700 J of green laser light incident in about 0.6 ns over a 100-μm-diam focal spot. The image captured on x-ray film on the opposite side of the target from the back-lighter foil is captured inside a tungsten body camera on a series of films after being filtered through an iron filter pack to remove most of the radiation at energies less than 6 keV. The system resolution in this point-projection configuration is about 65 μm.

By comparing the outer aluminum wall's base diameter, the general shape of the aluminum-vacuum interface, and, ultimately, the transmission level of the back-lighter x-rays through the various regions of the hohlraum, we can assess how well the simulations match the measured data and thus attempt to verify the radiation-flow model and the opacity numbers used in the simulation. Figure 5(a) shows a backlit radiograph of the expanding cylinder at approximately 9 ns after peak radiation drive. The figure shows that the originally vertical sides below the hemispherical closed top have now expanded out conically. From a series of such images, we can compare the time history of the diameter at 200 μm above the bottom of the straight section, for instance,

with the predictions. This comparison is also shown in Figure 5(b). This work has shown both close general agreement with the generic behavior of the cylinder (suggesting the radiation diffusion process through the gold wall is being modeled adequately) and some differences that suggest somewhat different 6.7-keV x-ray transmission through the aluminum than anticipated. Continuing work on this experiment should further illuminate both the agreement and the discrepancies.

Radiation-Hydrodynamic Experiments on the Z Accelerator

P.A. Keiter, G.A. Kyrala (P-24), G. Idzorek, R.G. Watt (P-22), R.R. Peterson (X-1), P.J. Adams, R.E. Chrien, D.L. Peterson, B.P Wood, M.M. Wood-Schultz (X-2)

We performed radiation-hydrodynamic experiments using the Z accelerator at SNL. In these experiments, a radiation and shock front is launched in a cylindrical piece of low-density aerogel foam. The pre-shocked target was a 3-mm-long, 7-mm-diam cylinder of 23-mg/cc-density SiO_2 aerogel foam. Initially, these fronts co-propagate—but as the hohlraum temperature increases, the radiation front becomes supersonic and propagates faster than the shock front. The purpose of these experiments is to accurately characterize a relatively simple experimental configuration and to compare the results of the experiments with predictions from different codes. In the simulations, many parameters are varied, including foam density, radiation drive, opacity, and aperture size. Simulations with the RAGE code shows that the breakout of the radiation front is most sensitive to changes in the density of the foam and the radiation drive. X-ray radiography is used to determine the density of the targets and to determine how uniform the density of each target is. The uniformity of the target is important because if large non-uniformities are present, then the radiation front will propagate differently at different spatial locations.

The radiation drive is measured with both x-ray diodes and silicon diodes. These diodes are well calibrated so that the raw signal obtained by the diodes can be converted to a temperature. Silicon diodes also observe the front face of the foam target so that the break-out time of the radiation front can be measured. We have measured the shock shape and position with x-ray radiography. Figure 6 shows a typical radiograph from the experiment. A 6.7-keV iron backlighter is used to produce the diagnostic x-rays. These x-rays pass through the target and are absorbed according to the opacity of the material.

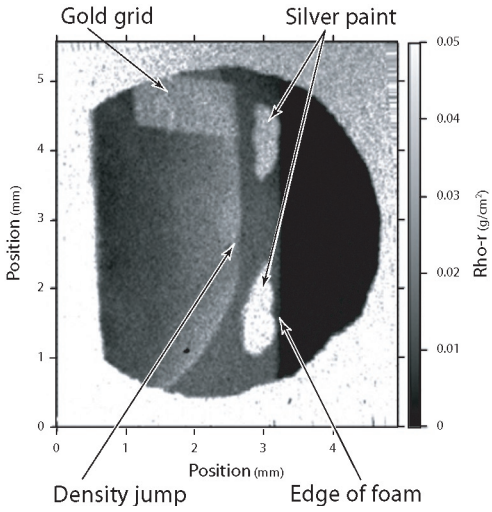

Figure 6. An x-ray radiograph of a 3-mm-long, 23-mg/cc-density foam target. The radiograph was taken 9.7 ns after the peak of the pinch radiation using a 6.7-keV iron backlighter. The opaque rectangle is a gold grid, whereas the two opaque ovals are from silver paint placed on the front surface of the foam; we believe the silver paint diffused into the foam.

Quick-Reaction Capability

C.M. Frankle (P-22)

The quick-reaction-capability project, operated by NIS Division's International Technology program office, provides funding for LANL personnel with particular expertise to assist the Joint Staff. When a specific request for assistance from a combatant commander is made to the Operations Directorate of the Joint Staff, the Joint Staff may request that a person with specific, applicable expertise from LANL be assigned to their office in the Pentagon for several months. The Joint Staff finds that having a technical expert onsite to help address a specific national-security issue is quite useful. Such problems are usually of immediate importance to the DoD and by their nature are generally highly classified. Christen Frankle (P-22) participated in such a rotation during the middle of 2003.

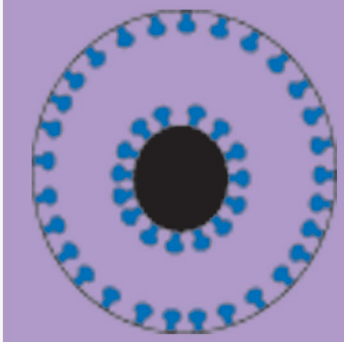

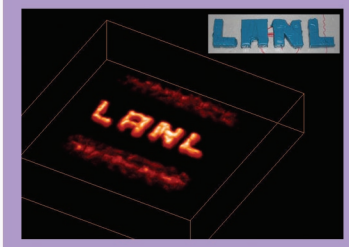

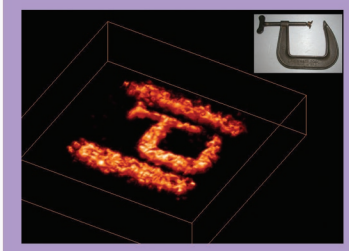

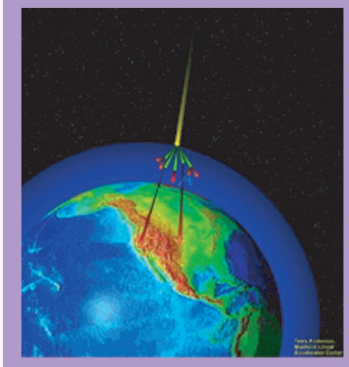

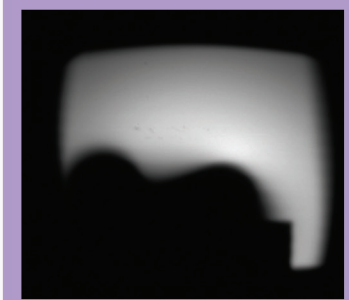

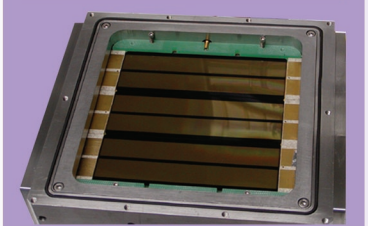

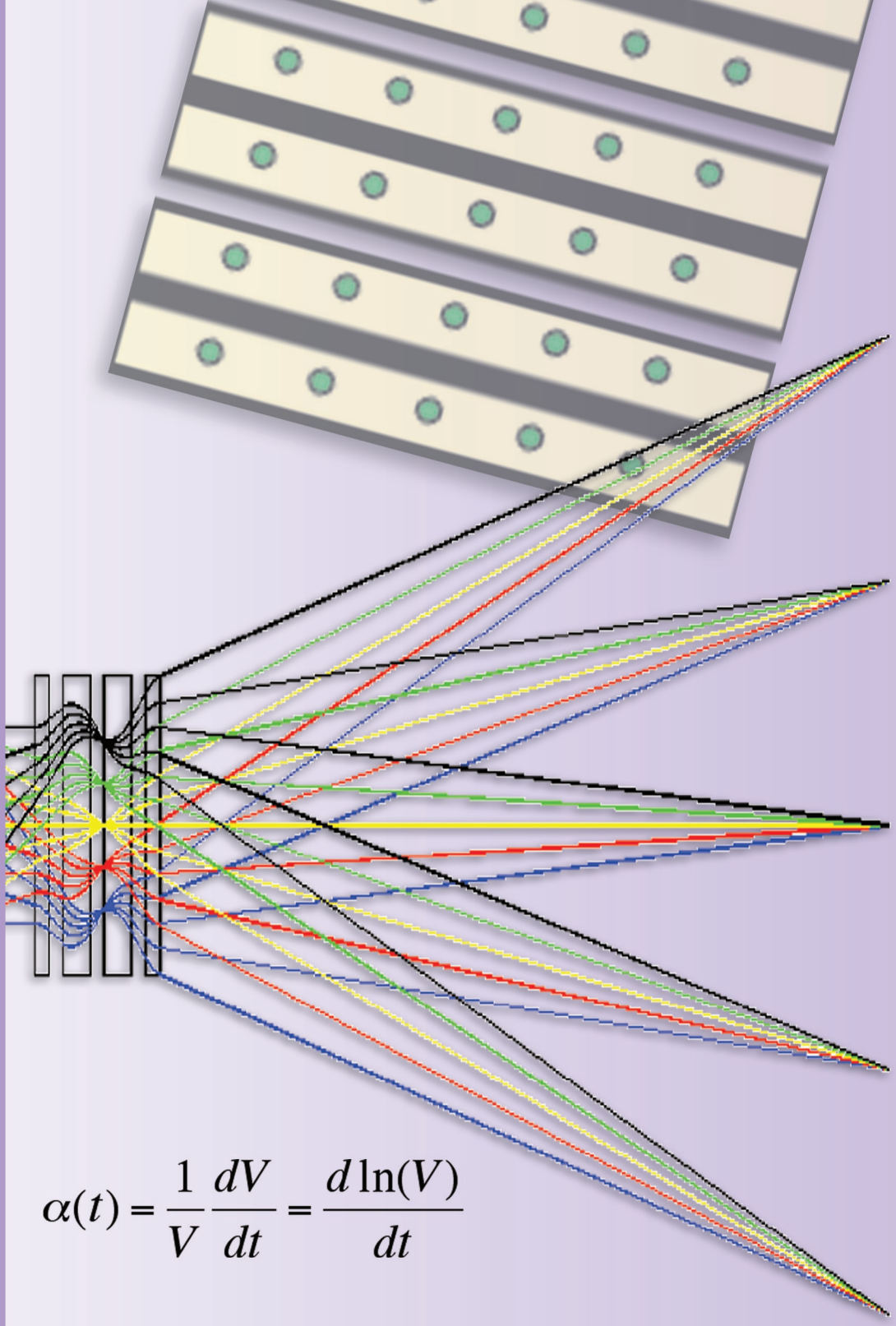

$$\alpha(t) = \frac{1}{V}\frac{dV}{dt} = \frac{d\ln(V)}{dt}$$

$$\sigma_\theta \cong \frac{15}{p}\sqrt{\frac{L}{L_{rad}}}$$

$$\frac{dV}{dt} = \alpha(t)V$$

Instrumentation

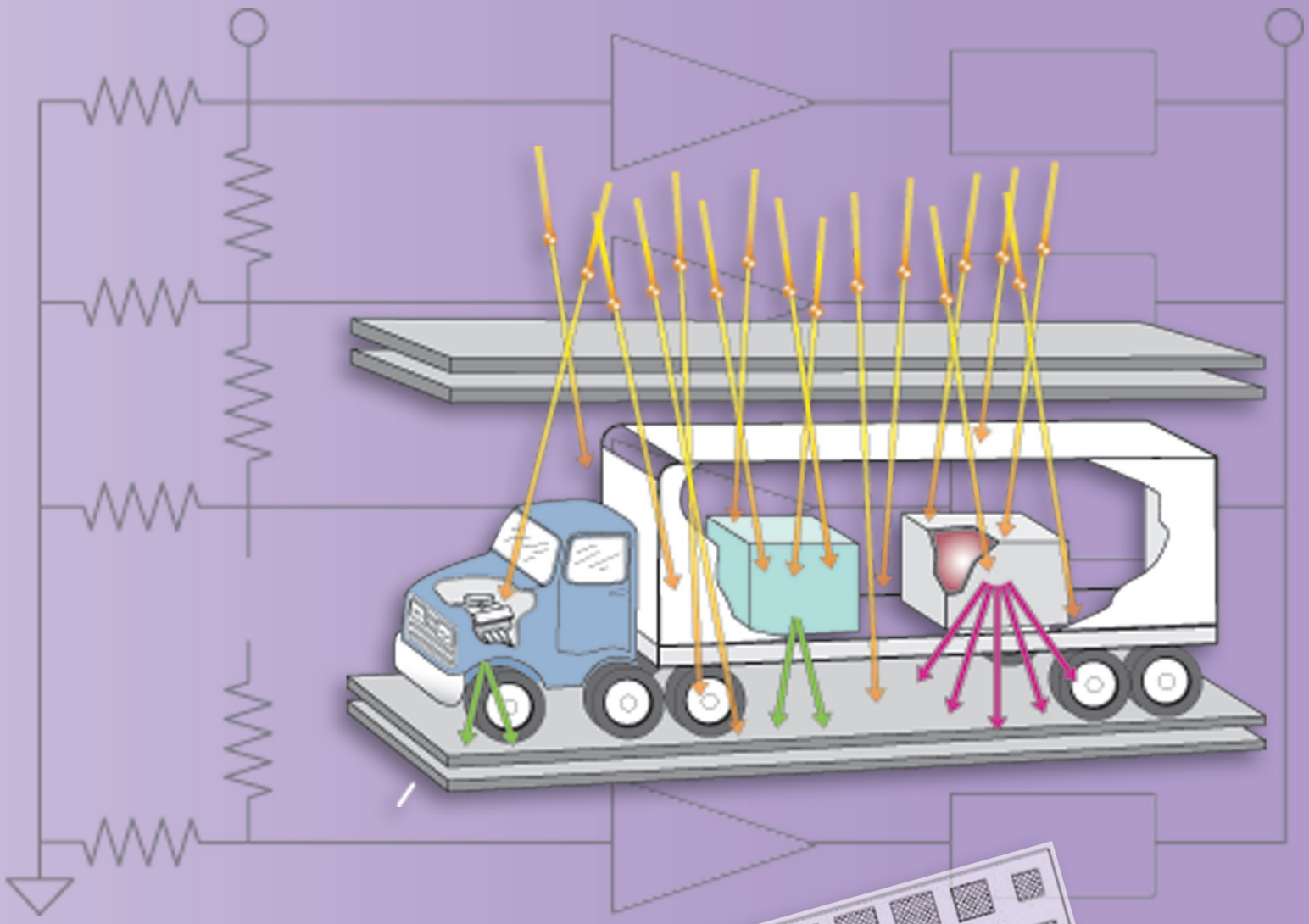

$$V(t) = V_0 e^{\int_{t_0}^{t} \alpha(\tau) d\tau}$$

$$\frac{dn}{dt} = \alpha(t) n$$

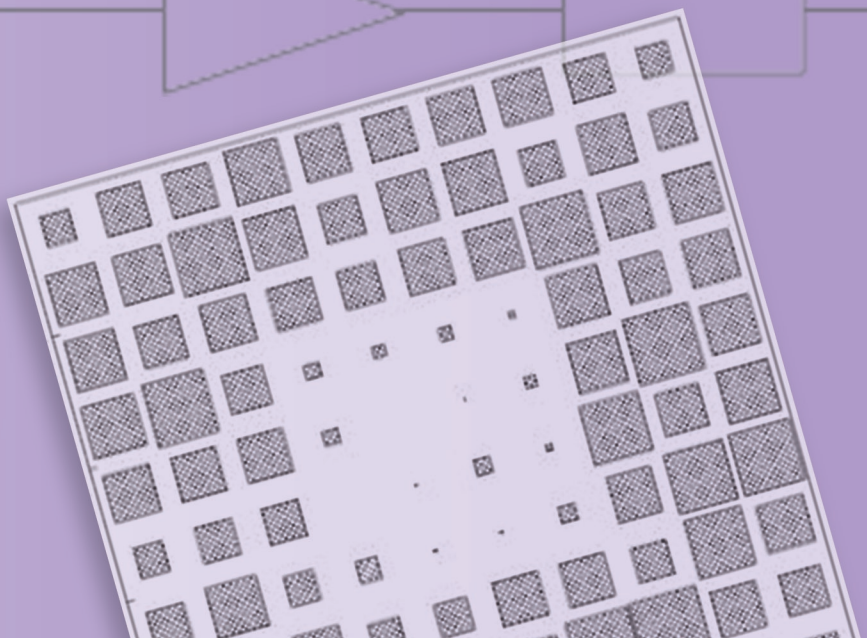

Instrumentation Contents

Research Highlights

Electron Radiography 89

The Digital-Alpha Recording System 93

Applications of Antineutrino Detector Technology to Counterterrorism 97

A Large-Format Gated X-ray Framing Camera 101

Cosmic-Ray Muon Radiography for Homeland Defense 105

Project Descriptions

Physics Measurements for DARHT-II Optimization and Risk Mitigation 109

Enhanced Test Readiness—Sub-Nanosecond Time Domain Electronics Enhanced Test Readiness Program 109

DynEx Confinement Vessel, Shipping Structure, and Cover-Installation Fixture 110

HPGe-Based Handheld Radioisotope Identification Instrument 110

W88 Pit Certification Red Team 111

Compton Gamma-Ray Imaging for High-Sensitivity Detection of Nuclear Materials 111

High-Definition Television 112

Laser-Based High-Resolution, High-Energy X-ray Imaging of High-Energy-Density Targets Using a Backlit Pinhole 112

The PHELIX "Transformer" for Proton Radiography Hydrodynamics 113

Low-Energy X-ray Radiography of Hydrotest Case Dynamics 113

Cygnus Radiographic X-ray Source 114

Advanced Plasma Diagnostic Concepts for National Magnetic Fusion Energy Research 114

40-mm, Gunpowder Breech Launcher for Proton Radiography Experiments 115

VISAR at pRad 115

Thermonuclear Burn Physics Using High-Energy Fusion Gamma Rays 116

KEYPATH: Using Atmospheric Turbulence to Generate and Exchange a Cryptographic Key 116

Interferometer Displacement Measurements of DynEx Vessel Oscillations 117

Advanced Detectors for Proton Radiography—Raising the Bar in Ultra-Fast Imaging 118

Reaction-History Reanalysis 119

Reaction-History Test Readiness 120

Support of Experiments at the Alternating Gradient Synchrotron 120

Generation of Energetic Ion Beams Using an Ultra-Short-Pulse, High-Intensity Laser 121

Electron Radiography

F.E. Merrill, C. Morris, A. Saunders (P-25), K.B. Morley (P-23)

An electron-radiography system, employing the charged-particle radiography technique, was built and commissioned in 2003 to demonstrate the capabilities of low-energy electrons to radiograph thin, static systems. The charged-particle radiography technique was developed with the 800-MeV protons at LANSCE[1] and 24-GeV protons at the Alternating Gradient Synchrotron (AGS) at BNL.[2] At these facilities, protons have been used to radiograph over 150 dynamic events and countless static objects.

At the front end of the electron radiography system, a "matched" electron beam is injected into the object to be radiographed. As the electrons pass through the object, they interact with the nuclei and electrons of the object, scattering the electrons away from their initial trajectory. After leaving the object, the electrons enter a magnetic lens quadrupole system that focuses the electrons back to an image, removing blur introduced by scattering within the object. A collimator, located at the center of the magnetic lens, is used to remove electrons that have been scattered to large angles within the object. The collimator removes fewer electrons passing through thin sections of the object than it does electrons passing through thick sections of the object. Therefore, the electron transmission at each position in the image provides a measure of the integrated density, or areal density, through the object. A schematic of the electron trajectories through the imaging system is shown in Figure 1. Electrons enter from the left, interact with a thin aluminum foil called a diffuser and are prepared for injection to the object as they pass through two matching quadrupoles. With no object in place, as shown in Figure 1(a), the electrons pass through the center of the collimator, and all electrons will arrive at the image location. In Figure 1(b), a scatterer has been placed at the object location. As the electrons pass through the object, they are scattered away from the injected trajectory. The collimator intercepts electrons that are scattered to large angles. Those electrons that pass through the collimator are refocused to an image at the image location. The measured electron transmission at each point at the image location can then be used to calculate an area density map of the object.

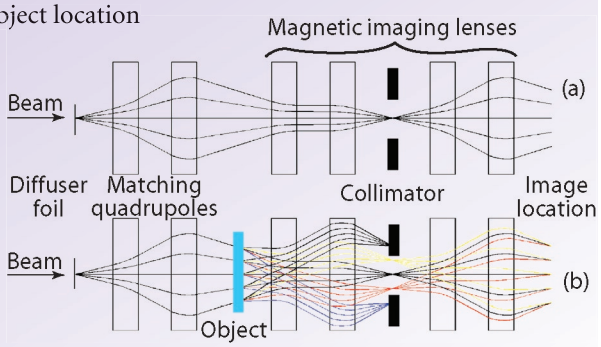

Figure 1. Electron trajectories through the electron radiography imaging system. In Figure 1(a), electrons travel along their "ideal" trajectories because there is no scattering within an object. In Figure 1(b), electrons are scattered away from their ideal trajectory as they pass through the object. The electrons that are scattered to large angles are removed at the collimator location. Those electrons that pass through the collimator are reformed to an image at the image location.

Theory

The magnetic imaging lens is setup in a symmetric Russian quadruplet configuration with alternating quadrupole gradients and is designed to provide a one-to-one map of the electron positions at the object location to positions at the image location. This mapping is described in Equation 1 in TRANSPORT notation:

$$x_i = R_{11}x_0 + R_{12}x_0', \qquad (1)$$

where x_0 and x_0' are position and angle at the object location, x_i is the electron position at the image location, and R is the first order TRANSPORT matrix. By choosing the

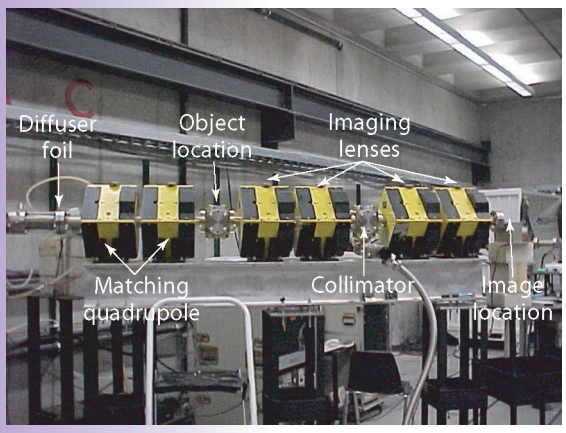

Figure 2. The prototype electron-radiography system. The electrons from the accelerator enter from the left and are prepared for injection into the object by the diffuser foil and the first two matching quadrupoles. They then pass through the first half of the imaging lenses, a collimator, and the second half of the imaging lenses where they exit the vacuum jacket and form an image at the image location.

quadrupole spacings and gradients so that $R_{11} = -1$ and $R_{12} = 0$, we achieve the one-to-one mapping of electron position while also removing blur from scattering within the object.

As the electrons pass through the object, they also lose energy through interactions with electrons in the object materials. The resulting energy spread of electrons exiting the object makes second-order corrections important in the design of the radiography system. In addition to the first-order mapping (described above), Equation 2 shows the second-order mapping of electron position from the object location to image location:

$$x_i = -x_0 + T_{116}x_0\delta + T_{126}x_0'\delta. \quad (2)$$

In Equation 2, $T_{116} = \partial x_i/\partial x_0\partial\delta$ and $T_{126} = \partial x_i/\partial x'_0\partial\delta$ are elements of the second-order TRANSPORT tensor, and $\delta = \Delta p/p$ is the fractional momentum deviation away from the central momentum. When optimizing the resolution in the design of the electron-radiography system, δ is determined by the thickness and composition of the object, and T_{116} and T_{126} are parameters of the lens system and cannot be adjusted without disturbing the first-order focus. Therefore, we must choose the position-angle correlation of the electrons entering the object, also called the matching condition, to be $x'_o/x_o = -T_{116}/T_{126}$ to minimize the effect of second-order chromatic aberations. With this matching condition, the remaining second-order contribution results from scattering in the object, which moves the electrons away from this ideal position-angle correlation. As the electrons pass through the object, they are scattered away from the matched trajectories by an angle, θ. The resulting position mapping from object to image is shown in Equation 3. As shown by this equation, T_{126} becomes the parameter that determines the ultimate position resolution of the electron-radiography system:

$$x_i = -x_0 + T_{126}\theta\delta. \quad (3)$$

An additional requirement of the electron-radiography system is that the scattering angle within the object, θ, is mapped to the radial position at the collimator location. This angle-to-position mapping will allow the precise removal of electrons that are scattered by the object to angles larger than the collimator cut angle, θ_c. Equation 4 shows the mapping of position and angle at the object location to position at the collimator location, x_c. Here M is the TRANSPORT matrix from the object location to the center of the imaging lens at the collimator location:

$$x_c = M_{11}x_i + M_{12}x_i'. \quad (4)$$

If we prepare the position angle correlation at the object location $x'_0/x_0 = -M_{11}/M_{12}$, Equation 4 becomes $x'_c = M_{12}\theta$, which is a simple mapping of scattering suffered in the object to position at the collimator location independent of position at the object location. Mottershead and Zumbro[3] have shown that this correlation requirement is equivalent to the correlation needed to cancel the second-order chromatic effects as discussed above. The fortunate coincidence that the same position-angle correlation of the beam both corrects the chromatic effects and maps scattering angle to position at the collimator location has become known as the "Mottershead miracle" and is a characteristic of the symmetric Russian quadruplet lens system.

Because the requirements of a charged-particle radiography system are simple and the Russian quadruplet configuration meets these requirements in an elegant and compact way, a radiography system can be quickly and efficiently designed and constructed. To demonstrate the capabilities of electron radiography, a prototype system was designed, constructed, and tested using off-the-shelf components.

Prototype System

Because of the development of low-energy electron accelerators by the medical industry for cancer-treatment therapy, the technology required to generate high currents of 20-MeV electrons is commercially available. The IAC in Pocatello, Idaho, has salvaged two of these accelerators from medical facilities and operates them for scientific use. The prototype of the electron-radiography system was therefore designed to use 20-MeV electrons from a Varian Clinac S-band accelerator, which operates at

2.9 GHz and provides a 3.25-mA average current for a pulse length ranging from 200 ns to 2 μs. In this configuration, the Varian Clinac S-band accelerator can deliver up to 4 x 10^{10} electrons per pulse through the electron-radiography system.

The magnetic lens for the prototype electron-radiography system was designed to use an existing set of quadrupole magnets that were salvaged by the IAC from Boeing's Free-Electron Laser program. The lens system consisted of six quadrupole magnets. The first two magnets in combination with a diffuser foil setup the injection match to the object location. The remaining four magnets form the imaging lens with a collimator at the center of the radiography system and the image location at the exit of the vacuum system after the last quadrupole. A picture of the radiography system installed at the IAC is shown in Figure 2.

Results from the Prototype System

The first radiographs that were collected with the prototype system were of a 1/16-in.-thick piece of aluminum with "LANL" machined through the plate. Figure 3 shows the results from the first series of radiographs with the prototype system along with a measure of the resolution from this radiograph. The "step" transition along an edge in the radiograph was used to determine the Gaussian line spread function, which was best fit with a Gaussian distribution having a root-mean-square width of 350 μm as expected from the analysis of chromatic blur for this lens system as discussed above.

Because of their small mass, low-energy electrons are easily scattered. To demonstrate this sensitivity, a gold-marker pen manufactured by the Pilot pen company was used to write "eRad" on a piece of paper. The resulting radiograph of this paper is shown in Figure 4. The ink from this pen is 17% copper and the handwriting resulted in a layer of copper on the paper less than 0.001 in. thick. The ink was clearly imaged with ~ 20% contrast. The radiograph also shows the ~ 5% fluctuations caused by areal-density variations within the paper. Also shown in Figure 4 is a radiograph of the magnetic field from a flat dipole magnet similar to those commonly used to make refrigerator magnets. The electrons are scattered as they pass through the magnetic field of the dipole magnet, similar to multiple scattering within an object. These scattered electrons were then removed by the collimator and re-formed into an image mapping out the integrated magnetic-field strength of the dipole magnet.

An aluminum step wedge was also radiographed with a 10-mrad collimator (Figure 5) to demonstrate the capability of electron radiography to measure areal-density variations of thin systems. The three-step aluminum step wedge was constructed out of 0.0015-in.-thick aluminum foil, resulting in area densities of 10 mg/cm^2, 20 mg/cm^2, and 30 mg/cm^2. A plot of the measured transmission across the step wedge (datapoints, blue) is also shown in Figure 5 along with a theoretical calculation of the expected transmission (solid line, red) based on the known areal density and collimator cut angle.

Further Development

Encouraged by the success of the prototype electron-radiography system, a new effort, recently initiated, will improve spatial resolution and increase the penetration capabilities to extend this radiographic technique to thicker systems. The prototype electron-radiography system was designed to

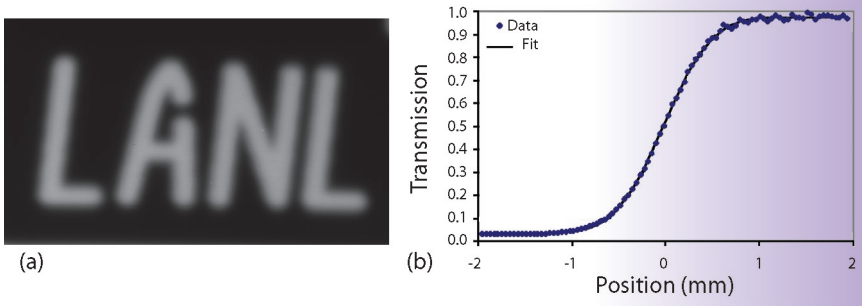

Figure 3. Results of the first radiographs collected with the prototype electron-radiography system. This is a radiograph of a 1/16-in.-thick piece of aluminum with "LANL" machined through the plate. The data points in Figure 3(b) show the measured transition in electron transmission across a sharp edge in the radiograph. The line is a fit to the data points assuming a Gaussian line spread function with a root-mean-square width of 350 μm.

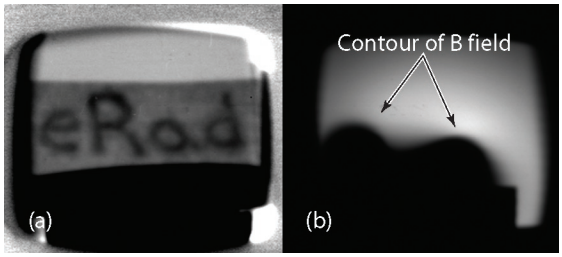

Figure 4. Figure 4(a) is a radiograph of "eRad" written on a piece of paper with a golden marker Pilot pen. This ink is 17% copper, and the writing resulted in a layer of copper less than 0.001 in. thick. The radiograph shows ~ 20% contrast in the writing and 5% variations in the areal density of the paper itself. Figure 4(b) is a radiograph of a dipole magnet similar to those used to make refrigerator magnets. The radiograph shows contours of integrated field strength across the surface of the magnet.

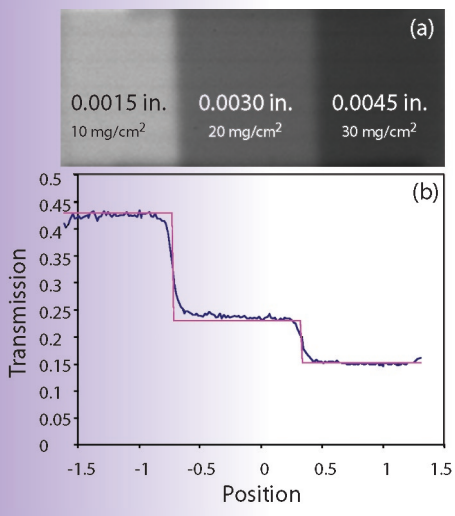

Figure 5. A 20-MeV electron radiograph of an aluminum step wedge with 0.002-, 0.004- and 0.006-in.-thick aluminum steps.

use existing quadrupole electromagnets available at the IAC. To significantly improve the resolution of the radiography system, the quadrupole gradient strength must be increased and the magnets shortened, as demonstrated by Mottershead *et al.*[4] with 800-MeV protons. Higher gradient and shorter quadrupoles are easily achieved through the use of permanent magnet quadrupoles. These magnets can be configured in a x5 magnifier geometry to improve the resolution of a 20-MeV electron-radiography system by a factor of five over the prototype system. The principles behind the magnifying electron-radiography system are identical to the identity lens system, but they introduce a magnification factor into the beam optics. Using these concepts, an electron-radiography system with commercially available permanent magnet quadrupoles has been designed and is being constructed.

Higher-energy electrons must be used to increase the penetration capabilities of electron radiography. The prototype system was designed for 20-MeV electrons because this energy is easily achieved with readily available electron sources. A program is under way to build a 40-MeV electron-radiography system that will also be constructed from readily available and existing accelerator structures and technology. In the future, a pulsed photocathode injector could be coupled to this 40-MeV accelerator to collect multiple radiographs of dynamic events within thin systems.

Conclusion

A prototype electron-radiography system has been constructed and commissioned at the IAC. This prototype system successfully demonstrated the capabilities of low-energy electrons to image thin, static objects. The experimental measurements of spatial resolution and density reconstruction agree well with models and theoretical predictions. With the proof-of-principle work complete, the concepts of charged-particle radiography are now being used to extend the capabilities of electron radiography to radiograph thicker systems with improved resolution.

References

1. N.S.P King *et al.*, "An 800-MeV proton radiography facility for dynamic experiments," *Nuclear Instruments and Methods in Physics Research A* **424**, 84-91 (1999).
2. G.E. Hogan *et al.*, "Proton radiography," in *Proceedings of the 1999 Particle Accelerator Conference*, A. Luccio and W. MacKay, Eds. (IEEE, Piscataway, NJ, 1999), Vol. 1, pp. 579–584.
3. C.T. Mottershead and J.D. Zumbro, "Magnetic optics for proton radiography," in *Proceedings of the 1997 Particle Accelerator Conference,* M. Comyn, M.K. Craddock, M. Reiser, and J. Thomson, Eds. (IEEE, Piscataway, NJ, 1997), Vol. 2, pp. 1397–1400.
4. C.T. Mottershead, D. Barlow, B. Blind *et al.*, "Design and operation of a proton microscope for radiography at 800 MeV," in *Proceedings of the 2003 Particle Accelerator Conference* (to be published by IEEE).

Acknowledgment

We would like to thank Tom Mottershead for his valuable insight and guidance in designing the prototype and magnifier lens systems. We would also like to thank Frank Harmon, the IAC director, for his support of these efforts and the support we received from the IAC staff: Brett King for his attention to detail while constructing the prototype system and Kevin Folkman for his untiring operation of the electron accelerator during our experimental campaigns. This work was funded by the LANL LDRD program.

For more information, contact Frank Merrill at 505-665-6416, fmerrill@lanl.gov.

The Digital-Alpha Recording System

J.D. Moses, S.K. Wilson (P-21)

The digital-alpha waveform recorder, simply called "digital alpha," is a specialized recording system (Figure 1) that has been customized to record optimally the exponentially increasing reaction history signal from a nuclear explosion. This technique uses a resistive voltage divider network to trigger a series of discriminators at pre-calibrated voltage levels. These discriminators provide the stop signal to time interval meters (TIMs)—which are precise digital clocks that share a common start signal in the digital alpha system. The output of the system is a set of voltage-time pairs that describe the input signal. Compared to other recording techniques, this system is easy to calibrate and use, and the data are recorded in a form that is easy to analyze. It has proved to be exceptionally stable when stored for over ten years and therefore may be easily maintained in a state of readiness in case of need.

Historically, the signal from a detector was recorded piecemeal by several Rossi oscilloscopes whose output is a Lissajous-like trace. One axis is driven by a stable time-reference oscillator; the other axis is driven by the signal from the alpha detector. The trace is recorded on film. Many Rossi oscilloscopes are needed to obtain a complete measurement, and a highly trained support staff is needed to operate and maintain them. The analysis of the data is time consuming and difficult—a great deal of effort is required to read the film and piece together the data. Nevertheless, this recording technique has been used on most nuclear tests and is the standard against which other systems must be judged. Much of the expertise in the use of Rossi oscilloscopes has been lost—or soon will be. Transient digitizers could, in principle, provide a modern replacement of these oscilloscopes. However, there are unresolved problems with digitizers because of their limited dynamic range and the lack of experience in using them to record reaction histories of nuclear events. Digital alpha is an automated, precisely calibrated system that is robust, is relatively easy to use, and produces data in a form that is easy to analyze and interpret.

The digital-alpha recording technique originated in the 1970s and was modernized in the late 1980s by the LANL high-speed electronics team and the electronics support group at EG&G (which is now Bechtel Nevada). Digital alpha was deployed on four nuclear tests—the results agreed to within about a percent with legacy systems. Although there is far less experience in operating this recording system than there is with oscilloscope-based techniques, digital alpha is intrinsically far simpler and will therefore more likely return data successfully with inexperienced operators than would a scope-based technique. Digital alpha should therefore be considered as a complement to, or replacement for, the usual reaction-history recording techniques. The system has been customized for reaction-history measurements by optimizing voltage-divider steps for the expected form of the signal. The system could be adapted to other fast-transient signals by customizing it in a similar manner—or by using it as is.

Figure 1. Archival photo of the "digital alpha" system used in experiments at the NTS.

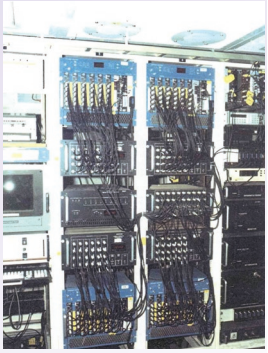

The Signal

The reaction-history signals are related to the rate of production of neutrons in a nuclear device, as follows:

$$\frac{dn}{dt} = \alpha(t)n, \tag{1}$$

where n(t) is the density of free neutrons in the device, and α(t) is a multiplication rate, which depends on environmental variables such as the density of fissionable materials and therefore on time. We assume that our detector generates a current proportional to n(t) and that this current into a coaxial cable gives us the recorded voltage signal. It obeys the same equation as n(t), whereby

$$\frac{dV}{dt} = \alpha(t)V. \tag{2}$$

An operationally useful form of Equation 2 is

$$\alpha(t) = \frac{1}{V}\frac{dV}{dt} = \frac{d\ln(V)}{dt}. \tag{3}$$

Alpha is the time derivative of the natural logarithm of the signal. The measurement of α(t) is the reaction-history measurement. As long as α is positive, ln(V) (and therefore V) increase monotonically with time. The voltage signal of interest is easily determined by integrating Equation 3, as follows:

$$V(t) = V_0 e^{\int_{t_0}^{t} \alpha(\tau)d\tau}. \tag{4}$$

The signal from a given alpha detector typically has a dynamic range of about four orders of magnitude; it emerges from the noise at about 0.5 V and ends when the cable breaks down at around 4 to 5 kV. The bandwidth of a cable is typically about 50 MHz, but the usable bandwidth can be stretched to about 300 MHz by equalizing networks that extend the flat part of the cable-response curve at the expense of signal amplitude. It takes a number of detectors, each with its own recording system, to cover the entire range of the reaction.

Digital-Alpha System Overview

As seen in Equation 3, a direct measurement of the logarithm of the voltage versus time is optimum for a measurement of alpha and has the additional advantage of extending the dynamic range of the system by logarithmic compression of the signal. It is hard to build logarithmic amplifiers of high precision, but it is straightforward to build voltage-divider networks with logarithmic increments and to calibrate these dividers precisely. This ladder network is customized for recording reaction histories.

The ladder in the network (Figure 2) is designed so that for each step the change in ln(V) is constant: $ln(V_{n+1}) - ln(V_n) = ln(V_{n+1})/V_n) = r$, *or* $V_{n+1}/V_n = e^{-r}$. For the present network, r = 0.4. The voltage signal from each step of the ladder is fed into its own voltage discriminator, which generates a sharp timing pulse when its input threshold is reached. The TIMs have previously been given a common start signal and are stopped individually by the trigger pulse from their associated discriminator. Because the discriminator voltage threshold is calibrated, the stop times provide a time-versus-voltage measurement of the reaction-history curve. The TIMs can only be stopped once, so that the present system can only record the monotonically varying part of the signal (i.e., it works only as long as alpha does not change sign). The present TIMs have a time resolution of 50 ps, which is the time resolution of the system. The times are saved in nonvolatile memory so that the data can be read promptly—or later if that is more convenient. Both the timing circuits and the voltage divider network can be precisely calibrated using reference pulses; specialized calibration hardware has been built for this purpose. Alpha is simply expressed in terms of the data—it is the slope of the measured ln(V)-versus-time curve. The error analysis is straightforward, and the result is a well-characterized and well-calibrated reaction-history measurement.

Digital Alpha System Status

The present digital-alpha system was built during the last few years of underground nuclear testing and was under active development right up to the cessation of testing. It was then stored in pieces at Bechtel Nevada until about early 2002 when it was reassembled. Figure 3 compares a calibration of the ladder-discriminator network carried out in 1990 to a calibration of the same network carried out in 2003. The data are the ratios of voltages at adjacent positions in the ladder versus position in the ladder—both measured in powers of **e**. The ladder was built with 1% resistors. The large fluctuations around the design value reflect precision of the resistors. The repeatability of measurements of the ratio is about 0.2%, which is about the variation observed when the measurement is repeated after more than ten years. The system shows no apparent degredation in performance from storage over long periods.

Conclusion

The digital-alpha system is well suited to be held in readiness for a resumption of underground nuclear testing over time scales of decades. It is stable, robust, and relatively easy to use. It provides data in a form that is easy to analyze and characterize; it can therefore be used and understood even after the present generation of experienced test personnel is unavailable. The system is also well suited for the measurement of other fast-transient signals, either by customizing the ladder network to match the expected form of those signals or by using the system as is to take advantage of its logarithmic-compression capability. Applications of this system to experiments other than nuclear testing should be explored further.

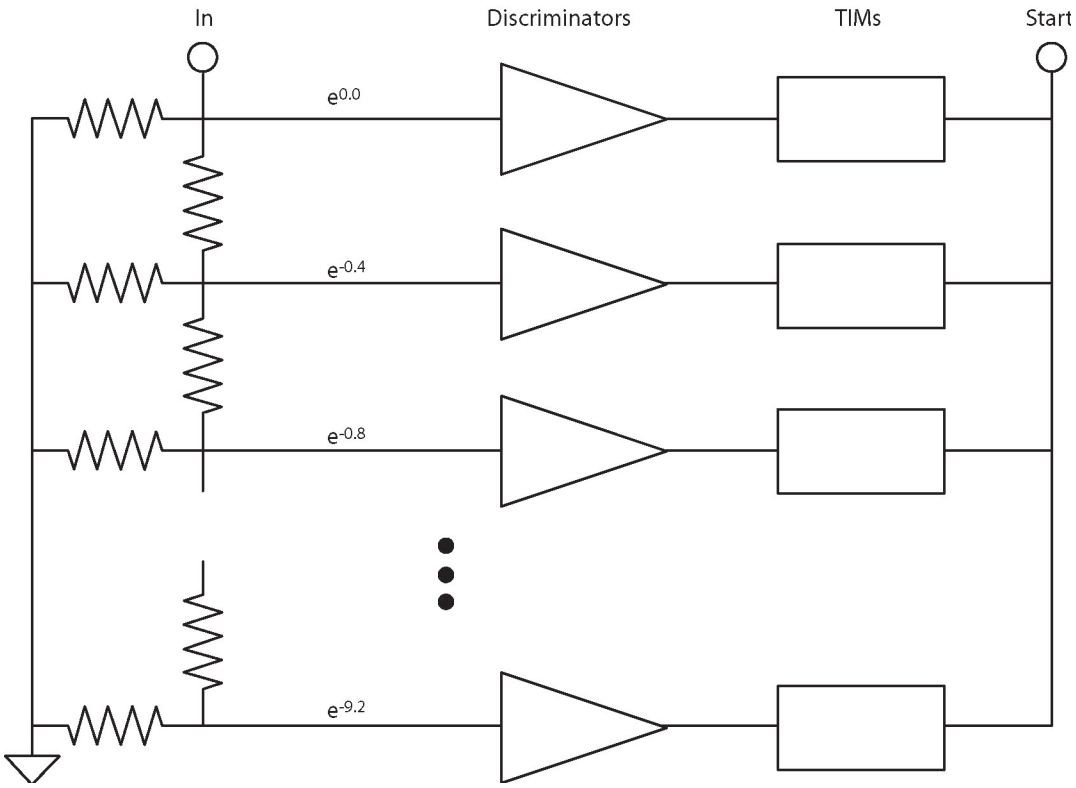

Figure 2. Schematic of the ladder-discriminator-TIM network. The TIMs are started with a common signal. They are individually stopped by the discriminators, which are triggered by the signals from the ladder. The attenuation factor at points in the network is indicated by numbers of the form e^{-x}.

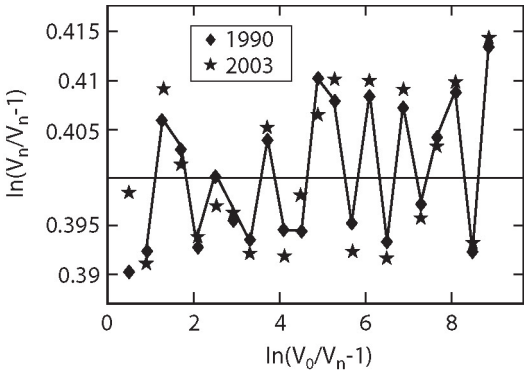

Figure 3. Calibration of the ladder-discriminator network in 1990 and 2003. The points represent the ratio of ln(V) values at adjacent steps along the ladder network. The position along the network is given by the natural logarithm of the attenuation factor. The network was stable over the time that it was stored.

Acknowledgment

The digital-alpha system was stored for twelve years at Bechtel Nevada; some of it was scattered over the NTS. Mike Carlisle (Bechtel Nevada) found all of the pieces of the system, including the system documentation and listings of the data-acquisition and control code. The system could not have been resurrected without his enthusiastic participation. Lyle Jensen and Kathy Breeding (Bechtel Nevada) made essential technical and archeological contributions. They represent much of the remaining expertise on the system hardware and software, respectively, and were invaluable participants in the early phases of this work. Eric Raby (P-21) showed remarkable skill and persistance in rewriting the ancient MSDOS and Windows data-acquisition and -control software to run under a modern operating system. P-21 consultant, Harvey Packard, was able to read the old computer backup tapes containing the design files for the calibration equipment so that these custom designs are not lost. This work was funded under the DOE Enhanced Test Readiness Program.

For more information, contact Samuel K. Wilson at 505-667-7823, kwilson@lanl.gov.

Applications of Antineutrino Detector Technology to Counterterrorism

J.M. Moss, M.D. Cooper, G.T. Garvey, W.C. Louis, G.B. Mills, S.P. McKenney, R.E. Mischke, R.C. Schirato, R.G. Van de Water, N.L. Walbridge, D.H. White (P-25)

The threat of highly organized and well-financed international terrorism requires the development of more sensitive, more versatile, and less expensive methods of detecting the presence of illicit radiological materials. The basic physics community has pioneered very large volume (kiloton) liquid-scintillator detector technology in recent years with the development of detectors for antineutrino physics.[1,2] Smaller-scale versions of "neutrino" detectors offer significant advantages over conventional detector technology for both stand-alone radiation monitoring and for use in active interrogation systems. The concept as applied to counterterrorism problems is called VLAND (Very Large Area Neutron Detector; the same acronym is used whether the application is for neutron or gamma-ray detection).[3]

Advantages of Neutrino-Detector Technology

Current radiation monitors deployed at ports of entry and sensitive facilities such as military bases, reactors, and accelerators employ mature technology, typically plastic scintillators, ^{3}He proportional counters, or ^{6}Li-loaded glass for neutrons, and plastic scintillators and NaI(Tl) scintillators for gamma rays. Scaling this technology to large areas, required for increased detection sensitivity, is exceedingly expensive and cumbersome.

Some of VLAND's advantages as a replacement for the older technology are listed below.

- It can be readily fabricated with large areas, 10 to 100 m^2 or more. This is an enormous advantage in detecting weak signals in passive applications. VLAND is inexpensive compared to competing detector technologies of comparable size and efficiency.
- Because it can be scaled to large sizes, VLAND is a logical component of future active-interrogation and neutron-radiography systems.
- VLAND is highly efficient for both fission neutrons (~ 30%) and MeV-range gamma rays (~ 70% full-energy peak). For detecting fission neutrons, VLAND employs a distinctive signal—a fast-neutron moderation pulse followed by the delayed capture of the 2.22-MeV gamma ray from the $n + p \rightarrow {}^{2}H + \gamma$ reaction. The spatial distribution of this coincidence is also a strong discriminant against background events.
- Cosmic-ray muons are readily detected and identified as such by VLAND. Thus, variations in neutron backgrounds that follow variations in the cosmic-ray flux can be anticipated and valid-event selection can be correspondingly adjusted.
- VLAND is robust; simple to maintain; and may be easily calibrated, monitored, and operated remotely. Neutrino detectors using this technology have operated with virtually no component failure for five-plus years.

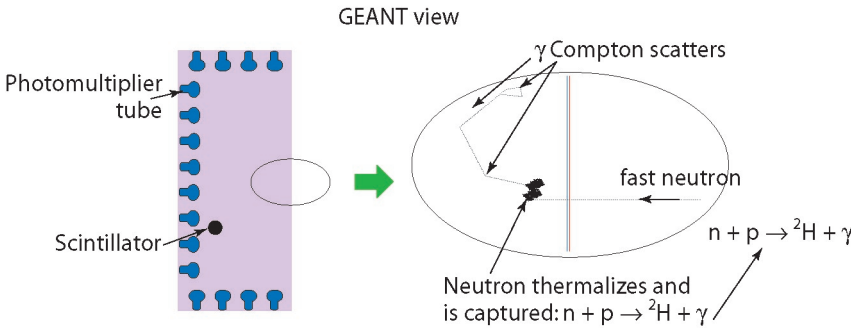

Figure 1. Schematic of VLAND. The enlargement at the right shows a simulated event using the CERN program, GEANT.[4] A neutron quickly moderates (thermalizes), followed by capture, which produces a 2.22-MeV gamma ray. The gamma-ray energy is absorbed by multiple Compton scattering.

Neutrino-Detector Technology Applications

The basic unit thickness of VLAND is about a meter, set by the ~ 30-cm mean-free path of 2.22-MeV photons in a liquid scintillator. Given this condition, any number of configurations of VLAND are conceivable—depending on the specific application. Four possible applications are described below.

As a fast-neutron portal monitor. Figure 1 illustrates the concept for fast-neutron detection. The detector is a meter thick (horizontal dimension) with no photomultipliers on the sensitive (right) face. The detector's height and width may extend several meters. Fast neutrons enter and are moderated within 10 cm of the sensitive face, as is illustrated in the simulation detail at the right of Figure 1. The moderation signal (from recoiling protons) is detected for 25% to 75% of the fission neutron spectrum, depending on the number of photomultipliers and on the light-production efficiency of the scintillator.

Use of a several-square-meter fast-neutron detector would permit more stringent limits be placed on the amount of plutonium passing undetected through transportation portals than is possible with commonly used ^{3}He proportional tubes. We could easily achieve gains in sensitivity by factors of 10 to 100. The fast-neutron signal is not subject to the large variation in background and innocent-radiation rates that plague gamma-ray-portal monitors.

As a gamma-ray detector. When used as a very large area gamma-ray detector, VLAND does not require the one-side-open geometry of Figure 1. Figure 2 shows a configuration that possesses directional sensitivity; such a detector could be mounted on a truck or a boat for large area search operations.

In order to be competitive with NaI(Tl) crystals, configurations that favor good energy resolution would be desirable. Because energy resolution is usually dominated by photon statistics, important factors in its optimization are large photomultiplier coverage and the use of an efficient scintillator. The KAMLAND collaboration[2] has already demonstrated an energy resolution of 7.5%/√E—about a factor of two inferior to that of 4 × 4 × 16 in^3 NaI(Tl) crystals commonly employed in search applications. However, VLAND technology has a distinct advantage over NaI(Tl) because of its much more favorable peak-to-Compton-edge ratio. Within its fiducial volume, simulations show that VLAND would have a 70% photopeak efficiency. This would lead to spectral simplicity that facilitates separation of signal from background and from anthropogenic radiation sources.

As an element of an active interrogation system. In active interrogation, engineered sources of neutrons or high-energy photons are used to stimulate fission in SNM. Characteristic signatures of fission—delayed neutrons or gamma rays—are then recorded by a surrounding detection volume. Active interrogation is a known technology in the arena of nuclear safeguards; here long interrogation times are acceptable and comparatively small volumes need to be examined.

Currently no active interrogation system, even in the prototype stage, is applicable to the search for SNM in large transportation containers (truck trailers, shipping containers, etc.). Scaling the technology from the current ~1-m^3 object size to that of transportation containers requires at least two major advances—more intense radiation sources and large area neutron detectors, such as VLAND (whether the interrogating source is photons or neutrons). Because delayed neutrons

are less energetic than those from fission, some optimization of the detection technology would be required. It may turn out, for example, that a modified VLAND using gadolinium-loaded scintillator would function better in this environment. Thermal-neutron capture on gadolinium yields readily identifiable ~ 8-MeV de-excitation gamma rays.

As an element of a fast-neutron radiography system. Conventional radiography using high-energy photons (nuclear gamma rays or bremsstrahlung from electron accelerators) is being increasingly deployed at critical transportation choke points to search for dense, heavy objects—objects that could be clandestine nuclear devices or components thereof. Muon radiography,[5] still in the research and development stage, promises sensitivity in this area as well.

Serious concerns remain about the ability of current radiographic methods (which were developed for conventional, not counternuclear, smuggling applications) to pick out small but significant quantities of SNM in transport containers in the presence of background clutter from legitimate cargo. A promising complement to current methods could be the radiographic application of fast neutrons.

Plutonium devices and kilogram-size quantities of plutonium are prolific sources of fast neutrons from spontaneous fission—readily detected by even unsophisticated portal monitors. However, when surrounded by a half meter of water or hydrogen-containing plastic, plutonium becomes nearly invisible to passive neutron detection. Highly enriched uranium (HEU, containing > 20% ^{235}U) presents a more complex challenge because it emits very few neutrons and primarily very low-energy gamma rays that are readily shielded by 1 cm of lead. However, the threat of active interrogation using neutrons and/or high-energy photons might well convince a would-be smuggler to protect his HEU with neutron shielding as well.

In contrast to photons, fast neutrons pass relatively freely through lead or iron, but are strongly attenuated in hydrogen-containing materials like water and polyethylene. This complementarity suggests the use of fast neutrons to search for the presence of neutron shielding in transportation vehicles. Figure 3 shows a simulated radiograph in which a shielded quantity of SNM in a 2- × 2-m^2 section of a shipping container is illuminated by a uniformly distributed source of 14-MeV neutrons.

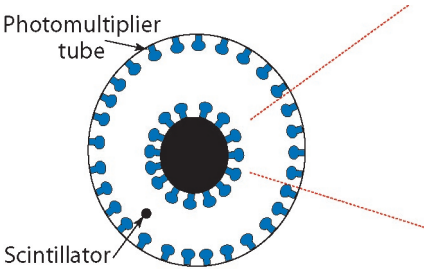

Figure 2. A possible configuration of a liquid scintillator tank for large area gamma-ray search application. The dashed lines indicate the approximate direction of sensitivity.

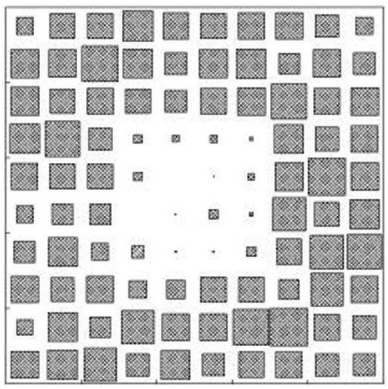

Figure 3. Simulated radiograph of a shipping container holding a shielded quantity of SNM surrounded by 50 cm of polyethylene. The white square in the center shows the outline of the neutron shielding. The contents of the container were simulated by a uniform mass of iron 10 cm thick (representing a container fully loaded to its 20-ton capacity).

Using fast neutrons to search for neutron shielding is fundamentally simpler than photon radiography for two reasons. First, moderation and containment of fission neutrons requires at least 50 cm of water equivalent, usually surrounded by a thin layer of thermal neutron absorber such as cadmium. Thus, the projected size of a shielded object is large—at least 1 m^2—leading to a modest number of pixels required to characterize the area of a shipping container. Second, unlike photons, 14-MeV neutrons have a substantial probability of passing through thick objects, like fully loaded shipping containers, unscattered. Thus, rather than scanning the object with a well-collimated beam in order to minimize in-scattering from adjacent pixels, a large area beam may be used. In Figure 3, 2.5 × 10^5 incident neutrons were used, which is a small fraction of the intensity available in one second from a commercial neutron generator.

A possible implementation of fast-neutron radiography could be as the second station following photon or muon radiography. A potentially threatening, but not completely convincing, dense object from the first radiograph would be examined at a second station with neutron radiography. The spatial overlap of the dense object in the photon radiograph with a region that contains substantial neutron shielding, likely to be a

rare circumstance in normal cargo, would signal the need for more detailed inspection of the container. Because of the simplicity of the neutron source and detector, fast-neutron radiography could be implemented for a fraction (perhaps 10%) of the cost of current photon-radiography stations.

References

1. C. Athanassopoulos, L.B. Auerbach, D. Bauer *et al.*, "The liquid scintillator neutrino detector and LAMPF neutrino source," *Nuclear Instruments and Methods A: Accelerators, Spectrometers, Detectors and Associated Equipment* **388**, 149–172 (1997).
2. K. Eguchi, S. Enomoto, K. Furuno *et al.*, "First results from KamLAND: Evidence for reactor antineutrino disappearance," *Physical Review Letters* **90**, 021802(6) (2003).
3. J.M. Moss *et al.*, "Very large-area neutron detector (VLAND)," Los Alamos National Laboratory report LA-UR-03-1363.
4. R. Brun *et al.*, "GEANT3 (CERN 1987)," DD/EE/84-1 (revised).
5. K.N. Borozdin, G.E. Hogan, C. Morris *et al.*, "Radiographic imaging with cosmic ray muons," *Nature* **422**, 277 (2003).

Acknowledgment

DOE/NA-22 funding supported part of this work.

For further information, contact Joel Moss at 505-667-1029, jmm@lanl.gov.

A Large-Format Gated X-ray Framing Camera

J.A. Oertel, T. Archuleta, M. Bakeman, P. Sanchez, G. Sandoval, L. Schrank, P. Walsh (P-24), N. Pederson (VI Control Systems)

Gated x-ray imaging cameras have been a principal time-resolved x-ray instrument for the national Inertial Confinement Fusion/Radiation Physics (ICF/RP) program for over a decade.[1] Typically, these instruments use micrometer-size pinhole arrays to focus x-rays onto an image plane with the maximum usable image size limited by the height of the microchannel-plate (MCP) electrical microstrip. Most of the instruments currently in use have microstrips on 40-mm channel plates; with 4 or 2 separate strips to provide more time coverage, the image fields are only 6 mm tall with a few up to 15 mm tall.[2] A 6-mm-tall strip used with x12 magnification only allows a 0.5-mm-tall object to be imaged. This configuration causes the image to completely fill the strip and does not allow for any instrument misalignments. What most experimenters regularly do to compensate for the small image field is to focus onto that field with a lower-magnification pinhole configuration. This technique works fine until the experimenter requires higher spatial resolution or would simply like to image larger objects while maintaining resolution. We have designed, built, and fielded a gated x-ray framing camera that uses the equivalent of more than four normal-sized channel plates to provide a larger image plane—the Large Format Camera (LFC). While the LFC does have increased parallax compared to smaller-format systems, this camera (Figure 1) enables researchers to fully image objects from 1 mm to 6 mm tall (x12 to x2 magnification) with high spatial resolution, allows space on the imaging strip for slight misalignments, and provides greater temporal coverage.

Additionally, most gated instruments are constructed around standard 40-mm MCPs with 4 microstrips that can be gated independently. When acquired in a "heel-to-toe" configuration, this type of instrument gives researchers

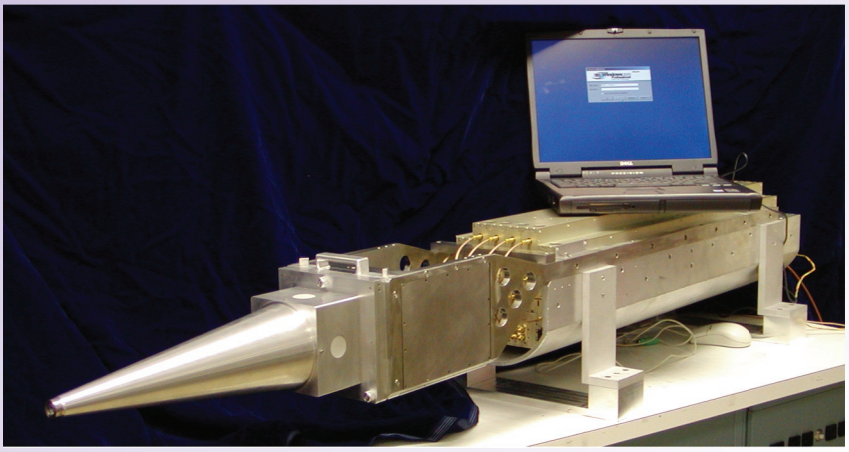

Figure 1. A photograph of LANL large-format x-ray imaging camera with its laptop-computer control system.

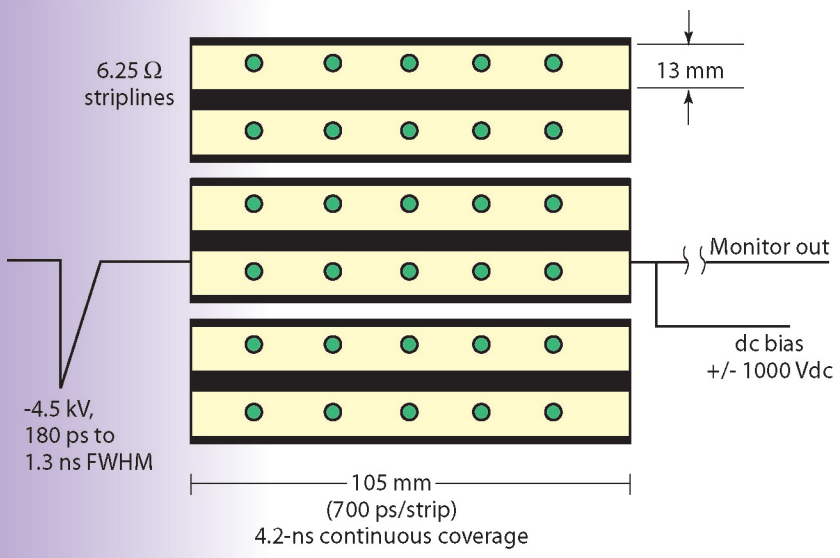

Figure 2. A front view of the gating process using three 105-mm × 35-mm MCPs.

a continuous data record up to 1 ns long. The temporal record is bounded both by the physical length of the microstrip and the propagation velocity of the electrical gating pulse. Researchers have worked around this instrumentation limitation by adding delay time between the individual microstrips and accepting the lost temporal information between the strip times.

For some experiments with a slower hydrodynamic evolution, the large interstrip timing technique is adequate and the missing data contains no useful information. But for fast-moving, long-duration (> 1 ns) plasma events, longer continuous-record lengths can be critical.[3] The small-format design limitations in present instrumentation and the need to prototype technology for NIF instruments motivated the LANL ICF/RP program to fund the LFC.

The LFC design specifications are to provide

(1) a 13-mm-tall microstrip on the MCP, which provides a large field of view with equal or improved spatial resolution;

(2) six 105-mm-long microstrips, which enables a 4.2-ns continuous temporal record;

(3) compatibility with any ten-inch instrument manipulator (TIM) or diagnostic insertion manipulator (DIM) (i.e., the TIM and DIM are standard mechanisms used to insert instruments into ICF target chambers); and

(4) a prototype for the future gated x-ray detector for NIF.

Detailed Instrument Description and Specifications

As with conventional x-ray framing cameras, researchers can accomplish LFC imaging in many different ways. The standard pinhole imaging configuration for an LFC is also the simplest and least expensive.[1,4] Pinhole imaging uses small pinholes (typically 5 to 15 μm in diameter) made of materials with a high atomic number, high-Z materials, such as tantalum or tungsten. Other methods of imaging include the use of a Fresnel zone plate, a grazing incident mirror, and crystal imaging.[5,6,7]

Gating of the image is accomplished by launching a short-duration, high-voltage electrical pulse across a microstrip transmission line on an MCP. A photoelectron signal produced at the front surface of the MCP photocathode is then exclusively amplified during the transit time of the voltage

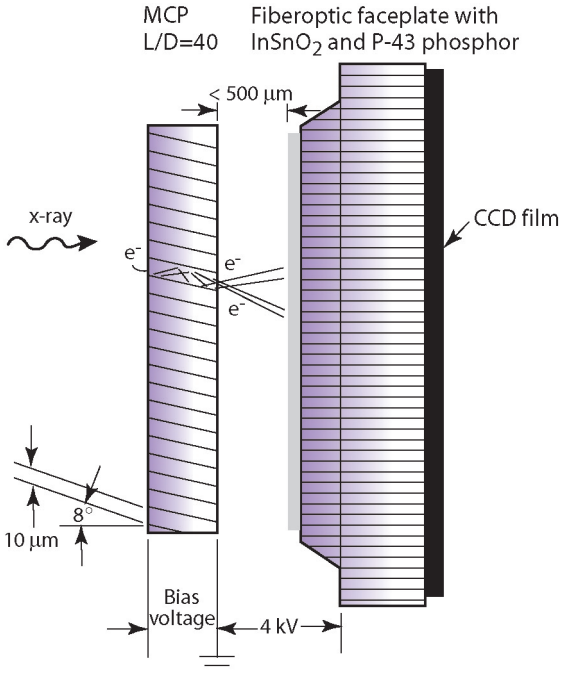

Figure 3. A side view of the MCP and phosphor screen.

pulse across a given point on the microstrip (Figures 2 and 3). By varying the width of the electrical gate pulse, the corresponding optical gate or shutter time can be varied proportionately.[8] This gives researchers increased flexibility in balancing appropriate shutter times and exposures with a plasma-physics experiment.

Amplification or gain of the signal in the MCP scales strongly with the applied pulsed voltage to a large power ($G \sim V^9$).[2] The impedance, Z, of the microstrip on the MCP decreases with increasing height by the following equation:

$$\frac{w}{h} = \frac{2}{\pi}\left[(d-1) - \ln(2d-1)\right] + \frac{\varepsilon - 1}{\pi\varepsilon} \times \left[\ln(d-1) + 0.293 - \frac{0.517}{\varepsilon}\right],$$

where

$$d = \frac{59.95\pi^2}{Z\sqrt{\varepsilon}},$$

and where w is the height of the strip, h is the dielectric thickness, and ε is the effective dielectric constant.[9] The six 13-mm-tall (6.25 ohms), 105-mm-long microstrips require a custom impedance-matching circuit to drive the microstrip from a 50-ohm characteristic impedance. To date, the LFC incorporates a direct-impedance mismatch on the input side of the MCP. Although this is not the most voltage-efficient system, it was recognized as a high-fidelity alternative for propagation frequencies of interest. The output side of the MCP has been carefully designed to provide a path for MCP bias and to minimize reflections that could potentially double expose the image. Much of the impedance-matching network-development work tested (and eventually implemented) on this camera is directly applicable to NIF gated x-ray instruments.

The MCPs[10] and six tapers require a special housing or module in which to be enclosed (Figure 4). This module is designed to mechanically capture the MCPs to an exacting tolerance (±0.001 in.) with respect to each other and the fiberoptic faceplate. To accomplish this, a nonconductive, high-tensile-strength web supports both sides of the MCPs. This web is then retained in a stainless-steel structure that also serves as the ground plane and supports the vacuum electrical feedthroughs. The 112.5-mm[2] fiber-optic faceplate[11] is a composite of thousands of 6-µm-diam fiber optics compressed together in a coherent array. The fiber array is coated on one side with an indium tin oxide[12,13] conductive layer and then overcoated with a green P-43 phosphor to match the CCD sensitivity. As the amplified electrons stream out the back of the MCP array, they collide with the P-43 phosphor emitting visible photons to be collected with a CCD camera[14] or Kodak 2210 film.

The Kentech electronics designed to run this module are also very specialized.[15] The electronics unit provides computer control of the 6 MCP gate pulses and positive and negative direct current (dc) voltages to operate MCP and phosphor bias. Each of the 6 gate pulses can be biased independently, and a trigger-delay circuit enables timing control of each microstrip. Additionally, the high-voltage pulsers, used to gate the MCPs, can be pulse-width adjusted from 200 ps to 1300 ps. To determine the pulser voltage (V_{pulser}) required to drive a 6.25-ohm strip (R_{mcp}), the following equation is used:

$$V_{mcp} = V_{pulser}\Gamma_t = V_{pulser}\left[1 - \frac{R_{pulser} - R_{mcp}}{R_{pulser} + R_{mcp}}\right],$$

where Γ_t is the voltage transmission coefficient.[9]

The Kentech unit controls and monitors all electrical functions via an RS232 connection to a laptop-control computer. This Kentech unit will be very similar to the NIF gated x-ray detector system, and the software for that system is being prototyped on the LFC.

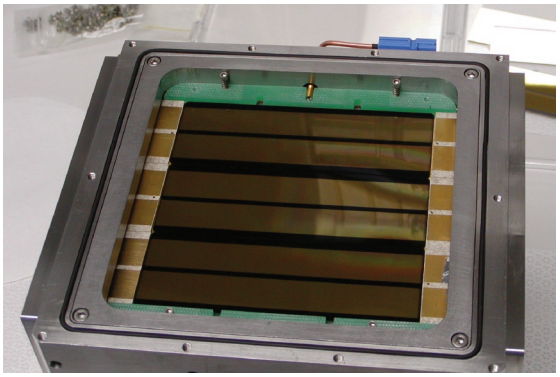

Figure 4. The LFC MCP module containing three 105-mm × 35-mm MCPs.

Conclusion

The LFC is a new LANL x-ray imaging instrument designed to image large NIF-scale ICF/RP objects with a long, continuous temporal history, while maintaining equivalent spatial resolution relative to previous and current small-format instruments. The LFC camera has a 105-mm^2 active area with six 13-mm-tall striplines and a P-43 phosphor overcoat; it is then interfaced to a CCD camera. The electrical gate is variable from 200 ps to 1300 ps and is capable of continuous temporal records of 4.2 ns. This camera is also used to test and evaluate new technologies that will be applied to future NIF x-ray imagers.

References

1. J.D. Kilkenny, "High speed proximity focused x-ray cameras," *Laser and Particle Beams* **9**(1), 49 (1991).
2. O.L. Landen, P.M. Bell, J.A. Oertel *et al.*, "Gain uniformity, linearity, saturation, and depletion in gated microchannel-plate x-ray framing cameras," in *Ultrahigh- and High-Speed Photography, Photonics, and Videography '93*, P.W. Roehrenbeck, Ed. (SPIE, Bellingham, Washington, 1993), Vol. 2002, p. 2.
3. C.W. Barnes, D.L. Tubbs, J.B. Beck *et al.*, "Experimental configuration of direct drive cylindrical implosions on the OMEGA laser," *Review of Scientific Instruments* **70**(1), 471 (January 1999).
4. A.J. Toepfer, L.P. Mix, and H.J. Trussell, "Pinhole imaging techniques for hard x-rays," (SPIE, Bellingham, Washington, 1977), Vol. 106, p. 47.
5. A.V. Baez, "Fresnel zone plate for optical formation using extreme ultraviolet and soft x radiation," *Journal of the Optical Society of America* **51**, 405 (1961).
6. F.J. Marshall, M.M. Allan, J.P. Knauer *et al.*, "A high resolution x-ray microscope for laser driven planar-foil experiments," *Physics of Plasmas* **5**(4), 1118 (1998).
7. F.J. Marshall and J.A. Oertel, "A framed monochromatic x-ray microscope for ICF," *Review of Scientific Instruments* **68**(1), 735 (1997).
8. J.P. Holder, D.R. Hargrove, T.S. Perry *et al.*, "Nanosecond gating of microstripline microchannel plate framing cameras: Characterization and simulation," in *Proceedings of the Ultrahigh- and High-Speed Photography, Photonics, and Videography '03 (Conference 5210),* San Diego, California, August 7–8, 2003.
9. L.A. Trinogga, G. Kaizhou, and I.C. Hunter, *Practical Microstrip Design*, First edition (Ellis Horwood Publishers, Chichester, UK, 1991), p. 30 and p. 110.
10. BURLE Electro-Optics, Inc., Sturbridge Business Park, P.O. Box 1159, Sturbridge, MA, 01566.
11. INCOM, Inc., 294 Southbridge Road, Charlton, MA, 01057-5238.
12. Deposition Research Laboratory, Inc., 530 Little Hills Blvd., St. Charles, MO, 63301.
13. Lexel Imaging Systems, 1501 Newtown Pike, Lexington, KY, 40511.
14. Retriever Technology, 228 S. Saint Frances Dr., Building D, Suite 1, Santa Fe, NM, 87501.
15. Kentech Instruments, Ltd., Unit 9, Hall Farm Workshops, South Moreton, Didcot, Oxfordshire, OX119AG, UK.

Acknowledgment

Our team would like to recognize the ICF/RP Program Office for supporting this work. We also wish to thank the Trident Laboratory laser crew and the Diagnostic Engineering and Operations Team, with special recognition of Cris Barnes and Scott Evans.

For more information, contact John Oertel at 505-665-3246, oertel@lanl.gov.

Cosmic-Ray Muon Radiography for Homeland Defense

L.J. Schultz, J.J. Gomez, G.E. Hogan, C. Morris, A. Saunders, R.C. Schirato (P-25), K.N. Borozdin (NIS-2), W.C. Priedhorsky (NIS-DO)

The threat of the detonation of a nuclear device in a major U.S. city has prompted research aimed at providing more robust border surveillance for contraband SNM. Existing radiographic methods are not only inefficient for the detection of shielded SNM but also involve radiation hazards. Members of P-25 in collaboration with NIS Division have invented a new method that could detect small quantities of shielded SNM in a short time using the natural process of multiple scattering of cosmic-ray muons as a radiographic probe (Figure 1). A chief advantage of this new method is that no artificial radiation dose is applied to the object being examined. We are currently examining how well the method works for complex homeland defense scenarios.

Cosmic-Ray Muons and Multiple Coulomb Scattering

The earth's atmosphere is continuously bombarded by primary cosmic rays, which are energetic stable particles, mostly protons (Figure 2). Interactions between these protons and atmospheric nuclei produce a shower of secondary cosmic rays, including many short-lived pions. These pions decay quickly to muons, which interact with matter primarily through the Coulomb force and have no nuclear interaction. The Coulomb force, which involves the attraction or repulsion of particles or objects because of their electric charge, removes energy from muons more slowly than nuclear interactions would. Therefore, muons can travel a great distance through the atmosphere. Some muons decay to electrons. There are other particles generated in the cascade, but the remnant of the secondary cosmic-ray cascade at the earth's surface is 90% comprised of muons.

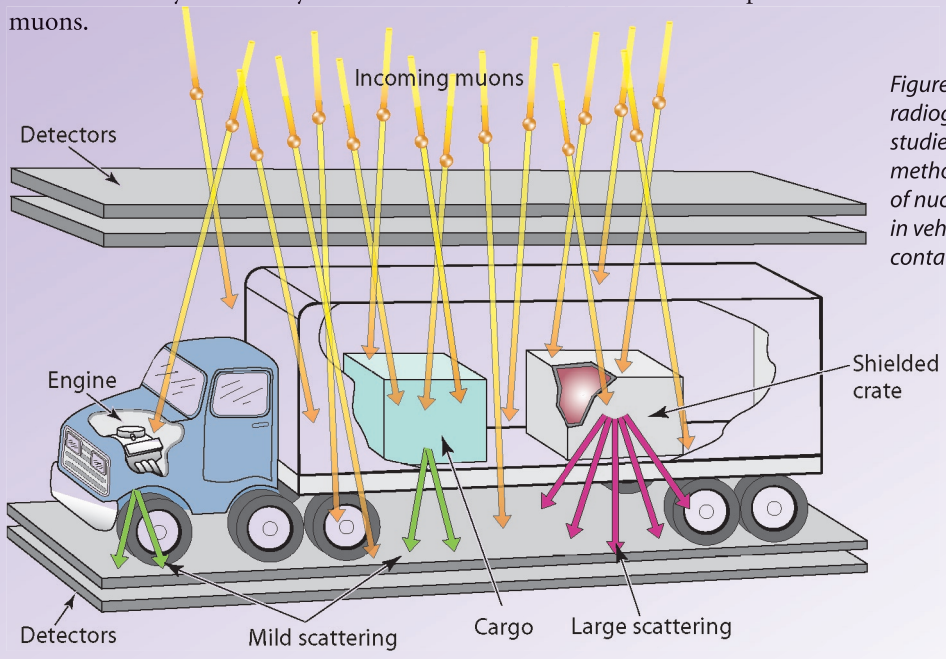

Figure 1. Cosmic-ray muon radiography is being studied as a potential method for the detection of nuclear contraband in vehicles and shipping containers.

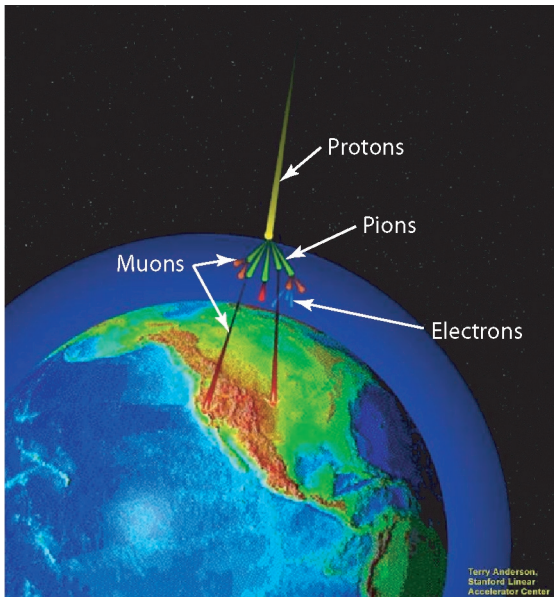

Figure 2. Illustration of the atmospheric cosmic-ray particle cascade.

Consequently, the earth's surface is showered constantly by muons in the form of penetrating, weakly interacting charged radiation. Because about 10,000 muons per minute pass through each square meter of area (arriving from angles spanning the upper hemisphere), this shower of free particles was naturally considered as a radiographic probe. The mean momentum of muons at sea level is about 3–4 GeV/c, which allows them to penetrate through meters of rock. Because the momenta spectrum of the muons is continuous and the average range is long, differential attenuation can be used to radiograph large objects. In the late 1960s, Luis Alvarez placed muon counters below the Second Pyramid of Giza and used differential attenuation to search for hidden chambers within the structure.[1] Researchers continue to perform this type of radiography on large manmade and geographic structures.

Calculating Uncertainty

One can calculate the uncertainty in this sort of radiography. The number of transmitted particles is $N = N_0 \exp(-L/\lambda)$, where λ is the mean-free path, N_0 is the number of incident particles, and L is the depth of the material. The uncertainty in measuring L by counting transmitted particles is $\Delta L = \lambda/\sqrt{N}$. A 1,000-cm^3 volume of uranium would receive an incident flux of 100 muons in one minute. Because the mean-free path of cosmic-ray muons in uranium is on the order of 1 m, the thickness of a 10-cm cube of uranium could be determined to a precision of about its thickness.

Differential attenuation has proven useful for examining very large structures, but we make use of a different interaction between charged particles and matter to enable radiography of much smaller objects. A charged particle (such as a proton, electron, or muon) passing through material is deflected by many small-angle Coulomb scatterings off the nuclei of the atoms that make up the material. The particle will traverse the material in a stochastic path because of these multiple scatterings, and it will emerge at an angle scattered from the original track. The average scattering angle is distributed approximately Gaussian, and the mean-square scattering angle is strongly dependent on the material's Z number (i.e., atomic number, the elements in the periodic system are arranged in order of increasing number of protons in the nucleus) (Figure 3). There is a fairly clear distinction between the scattering from muon passage through common low-, medium-, and high-Z materials.

The width of the scattering distribution of muons is related to the scattering material as

$$\sigma_\theta \cong \frac{15}{p}\sqrt{\frac{L}{L_{rad}}},$$

where p is the particle momentum and L_{rad} is the radiation length. If the muon scattering angle in an object can be measured and if its momentum is known, then the material depth can be measured to a precision of $\Delta L/L = 1/\sqrt{N}$, where N (the number of transmitted muons) is very nearly equal to the number incident. Thus each transmitted muon provides information about the thickness of the object with a precision that is smaller than the thickness of the object. For the 10-cm^3 cube of uranium, for example, the uncertainty is 10% in one minute of exposure rather than the 100% that could be obtained with differential attenuation radiography. This analysis demonstrates the enormous advantage of multiple-scattering muon radiography for this application.

Cosmic-Ray Muon Radiography—Experimental and Simulated Results

To make use of the information carried by scattered muons to probe an object, we tracked individual muons into and out of a target volume wherein objects to be radiographed are placed. (This work was carried out on Line B at LANSCE.) The scattering angle of each muon is measured, and we use tomographic methods to reconstruct

the structure and composition of the objects. To demonstrate proof of principle, we constructed a small experimental apparatus built with a set of four position-sensitive drift chambers. Two groups of detectors, each measuring particle position in two orthogonal coordinates, were placed above an object volume; two other groups of detectors were placed below. The position resolution of these detectors was measured to be about 400-μm FWHM. Each radiograph of two small test objects shown in Figure 4 was made using the information carried by about 100,000 scattered muons. Several hours were required to produce the remarkable detail in these images using our small, relatively inefficient prototype. In a contraband detection scenario, only one or two minutes might be available for inspection. Fortunately, detection of shielded 5- to 10-cm-diam SNM objects requires many fewer muons. Moreover, the cosmic-ray muon momentum spread increases the uncertainty of the scattering signal in the experiment; however, we did not measure the muon momentum.

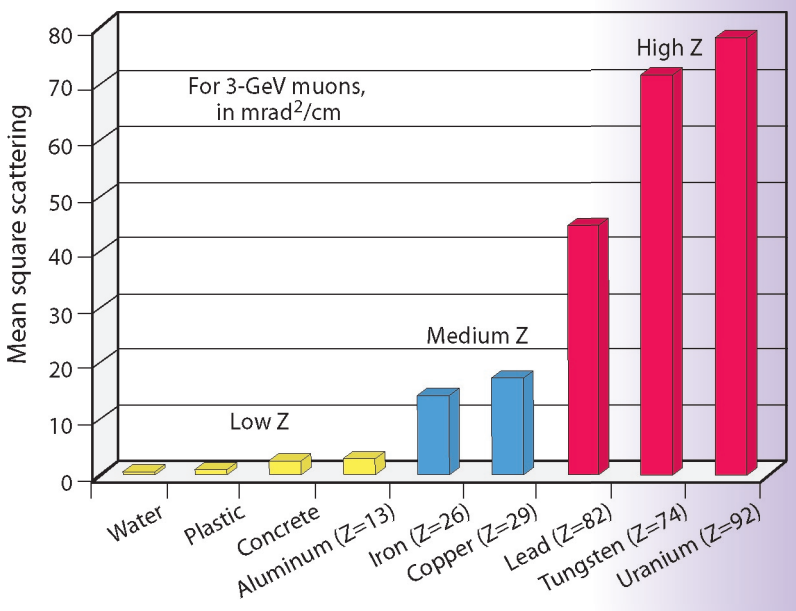

Figure 3. The scattering of muons passing through material varies strongly with the Z number of the material.

We have proposed a method of estimating muon momentum in an effort to further reduce exposure time. In this method, muon scattering is measured through plates of material of known depth and composition positioned below the object volume. To test this method, we developed a simulation code that generates cosmic-ray muons with the appropriate distribution of energies and angles, propagates them through a test volume, and generates the positions at which they would be detected in four detector planes. The muon spectrum, angular distribution, and rate were appropriate for sea level. A detector position resolution of 400-μm FWHM was simulated, and the simulation was validated against the experimental results. Momentum measurement to about 50% precision was assumed.

Figure 4. Experimentally produced cosmic-ray muon radiographs of (a) a steel c-clamp and (b) the acronym "LANL" constructed from 1-in.-lead stock. The bar-like features visible on either side of the images result from steel beams used to support a plastic object platform.

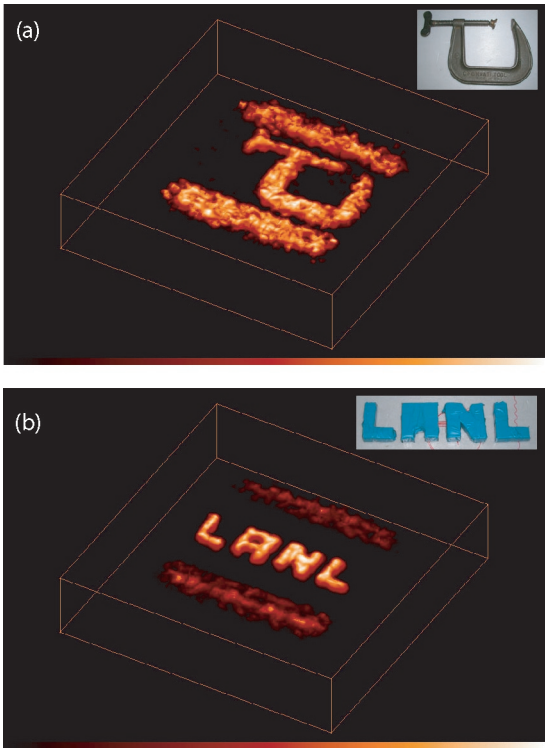

We have examined numerous simulated scenarios wherein SNM contraband is placed within shipping containers that are hidden within various background cargos. Figure 5 presents the results of one of these simulations using a reconstruction method optimized for detecting high-Z material in medium-Z surroundings. A steel-walled cargo container containing 12 tons of distributed iron parts was simulated. One small lead-shielded container carrying a small amount of plutonium was placed within the cargo. The contraband is clearly visible in the one-minute simulated radiograph.

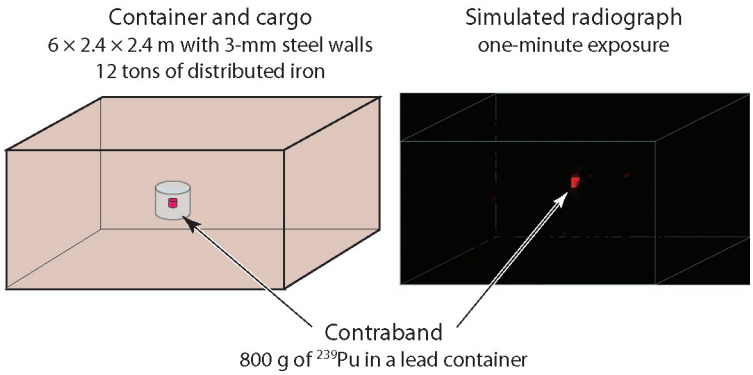

Figure 5. Simulation of a steel-cargo container with SNM contraband buried within iron (left) and a one-minute cosmic-ray muon radiograph (right).

Conclusion

We have developed and experimentally demonstrated a unique radiography method using the multiple-scattering process of cosmic-ray muons. This method, which is particularly sensitive to high-Z dense materials, may prove useful in detecting smuggled cargoes of SNM in incoming vehicles and commercial traffic at U.S. borders in short times with no additional radiation dose to vehicle occupants or border guards. Our current efforts are devoted to confirming our small-scale experimental and full-scale simulated results with a full-scale experimental demonstration; to developing low-cost, field-deployable detectors; and to optimizing our information-processing methods.

References

1. L.W. Alvarez *et al.*, "Search for hidden chambers in the pyramids," *Science* **167**, 832-839 (1970).

Acknowledgment

The researchers acknowledge LANSCE at LANL for providing legacy equipment used in the muon-radiography experiments. We also acknowledge the diligent work of the P-25 technician team. Finally, we acknowledge our collaborators in NIS Division and Gary Blanpied from the University of South Carolina. This work was sponsored by the Office of Nonproliferation Research and Engineering of the DOE NNSA.

For more information, contact Larry Schultz, 505-667-9431, schultz@lanl.gov.

Physics Measurements for DARHT-II Optimization and Risk Mitigation

R.T. Olson (P-22), D.M. Oró (P-22), H.A. Davis (DX-6), D.C. Moir (DX-6)

Electron beam measurements are being performed in support of DARHT-II accelerator operation. These experiments fall into two separate categories: (1) investigating beam-target interaction and (2) measuring time-dependent electron beam energy.

The beam-target interaction studies are performed using the DARHT-I accelerator where a 60-ns-long, 19.8-MeV, 1.7-kA electron pulse is passed through a thin foil. The electron beam has been found to thermally desorb neutral gas species from the foil/target surface that are then subsequently ionized by beam electrons. These ions are trapped in the beam potential thereby generating a time-dependent positive charge density within the electron beam. Interaction between the beam electrons and these ions causes the beam focal point to change as a function of time and results in an effective increase in radiographic spot size. Techniques are currently being investigated to minimize the neutral/ion generation from the radiographic target because DARHT-II will generate four electron pulses ranging up to ~ 400 ns in duration.

The DARHT-II electron beam energy is being measured as part of the accelerator-commissioning activities using a magnetic-sector-electron spectrometer. The technique uses a streak camera to measure the time-dependent beam deflection due to the magnetic field of the spectrometer. The electron energy is then calculated as a function of time using both the magnetic-field strength and electron-deflection distance. This information is used to both diagnose the accelerator performance and define the DARHT-II radiation spectrum.

Enhanced Test Readiness—Sub-Nanosecond Time Domain Electronics Enhanced Test Readiness Program

J.M. Galbraith, S.K. Wilson, E.Y. Raby, J.D. Moses (P-21)

The three-year Enhanced Test Readiness (ETR) program, sponsored by the NNSA, will shorten the time between the authorization of an underground nuclear test and its execution from the current three years to eighteen months. The ETR program covers a broad range of activities related to underground testing; however, P-21, in collaboration with P-22, is involved in the reaction-history component of the program. A critical component involves passing on knowledge from experienced scientists and diagnostics engineers, who are mostly now retired, to a new group of scientists and engineers too young to have participated in the last underground test in 1992. We are now calibrating and testing equipment that has not been operated since the end of underground nuclear tests. For example, the "digital alpha" reaction-history diagnostic (Figure 1) has been partially resurrected—its hardware is being tested, and its software is being upgraded to modern programming languages and computer platforms.

New methods of recording reaction history are being considered. These methods are often driven by the fact that we have lost the capability to support equipment historically used in routine procedures. The old Rossi oscilloscopes, for example, are available, but we cannot manufacture new ones. Fast transient recorders like the Tektronix SCD-5000 are no longer available. New products from commercial vendors, primarily developed for the communications industry, are designed under a vastly different set of requirements than those that we have for reaction history. Specialized cables and interconnect, which were developed during the active underground testing program, are no longer manufactured. Our challenge is to apply new technology and techniques and to integrate them with traditional experience and resurrected equipment in such a way that weapons designers will not notice the difference in test data between a future underground test and one performed twelve years ago.

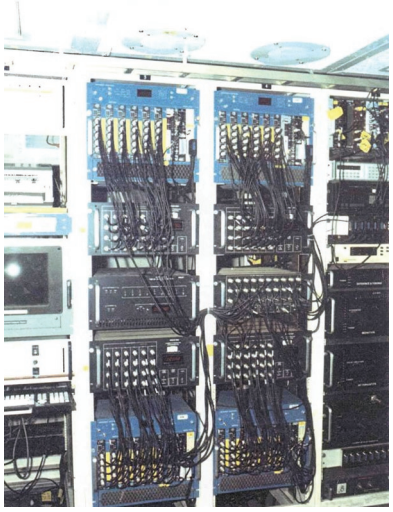

Figure 1. Archival photo of the "digital alpha channel" used in experiments at NTS.

DynEx Confinement Vessel, Shipping Structure, and Cover-Installation Fixture

E.O. Ballard (P-22), C. Romero (DX-5), D.H. Bultman (ARES Corporation)

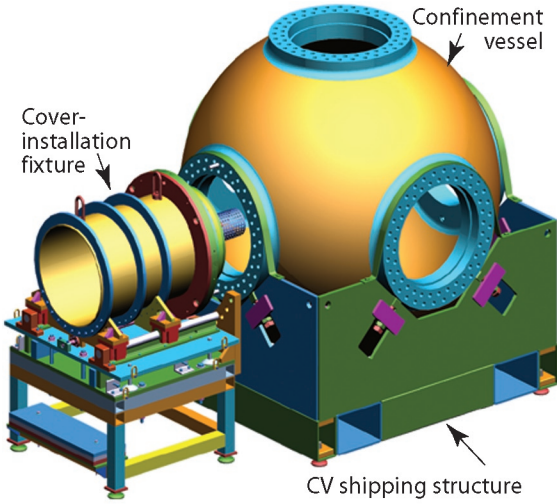

Figure 2. DynEx confinement vessel, shipping structure, and cover-installation fixture.

The DynEx confinement vessel (Figure 2) will be used to contain the energy, debris, and combustion gases from detonation of a high-explosive experiment. The vessel will enable real-time radiographic imaging of the detonation by providing radiographic "windows" integral to flange covers on the nozzle openings. Through these windows, x-rays can enter and exit the vessel boundaries and project onto x-ray scintillator panels outside the vessel, thereby producing visible images. These images are recorded using CCD cameras. The capability for x-ray imaging through the vessel in this manner will be provided along two perpendicular, co-planar axes, which pass through the center of the spherical confinement vessel. Radiographic hardware will be mounted inside the confinement vessel, along with the experiment package, to collimate the x-rays onto the experiment and to support and align the experiment relative to the x-ray sources. Other components mounted in the vessel will mitigate the effect of fragments impacting the vessel wall.

During operation, the confinement vessel will be positioned and supported inside a larger safety vessel, which will serve as a secondary pressure boundary to contain the high-explosive detonation in case of a confinement vessel breach. Flexible piping will connect the two vessels with an in-line, remotely operated valve to permit vacuum pump-down of the confinement vessel before an experiment and followed by ventilation with filtration after the experiment.

Ancillary hardware includes the shipping structure and cover-installation fixture. The shipping structure is also used for hydrostatic testing of the vessel and storage at LANL. The cover-installation fixture enables handling of the heavy radiographic covers during the process of the experiment buildup and alignment.

HPGe-Based Handheld Radioisotope Identification Instrument

C.M. Frankle (P-22), K.B. Butterfield, W.S. Murray, B.A. Sapp, S.A. Salazar (N-2), J.A. Becker, J. Collins, C.P. Cork, L. Fabris, N.W. Madden (Lawrence Livermore National Laboratory)

LANL has a long and successful history of fielding handheld radioisotope identification instruments. Such instruments use gamma-ray spectroscopy to identify isotopes of interest. Early instruments were based on sodium iodide [NaI(Tl)]. NaI(Tl) has good efficiency and can be made quite rugged. However, it suffers from relatively poor energy resolution (dE/E ~ 7%–9%). This makes the identification of isotopes that emit gamma rays of similar energy very difficult—particularly in an automated manner in a handheld instrument intended for an unsophisticated user. A potential improvement is through the use of cadmium zinc telluride (CZT), which has better energy resolution (dE/E ~ 1%–2%). The difficulty with CZT is that detector-grade crystals can only be fabricated in rather small sizes (~1–2 cm^3), which means a very low efficiency. The gold standard for isotope identification is the use of high-purity germanium (HPGe) with an energy resolution of dE/E ~ 0.1%–0.2%. However, HPGe requires cooling to near liquid-nitrogen temperatures (77 K) in order to achieve that resolution, and HPGe detectors also tend to be quite fragile. Liquid nitrogen and its support systems are clearly not compatible with a handheld instrument.

Approximately five years ago, our collaborators at LLNL were successful in attaching a modest-size HPGe crystal to a fairly low-power (~ 10 W) mechanical cooler. We then provided them with a basic design for a detector head that would have an efficiency similar to our existing NaI(Tl)-based instruments and would be suitable for use in a handheld instrument. The result of the collaboration of the HPGe-detector-fabrication expertise of

LLNL with LANL instrument-design expertise is an instrument named GN-5. The GN-5 contains a mechanically cooled HPGe detector (using a mere 3-W average power at room temperature), a bismuth germanate (BGO) Compton suppression shield, and two neutron detectors. This capability is packaged in a rugged, rain-tight case with the simple, push-button operation characteristic of all the GN-series instruments. Deployment of the first units to U.S. government customers is slated for early 2004.

W88 Pit Certification Red Team

B.J. Warthen (P-22), representing the Interdivisional Red Team

P-22 has a representative on the Interdivisional Red Team (team members include representatives from X, T, MST, C, D, DX, and P Divisions), which is tasked with providing peer review to the W88 Core team. We have been collecting information and reviewing how experimental results have been and can be used in the certification process. An important part of this work is to try to determine the value that future experiments may provide to the certification process and help select the most promising experiments.

Compton Gamma-Ray Imaging for High-Sensitivity Detection of Nuclear Materials

J.P. Sullivan (P-25), G.J. Arnone (N-2), D.K. Hayes (N-2), A.S. Hoover (ISR-2), R.M. Kippen (ISR-2), M.W. Rawool-Sullivan (N-2)

Members of P-25, N-2, and ISR-2 are working on a concept that will significantly improve the sensitivity of detectors used for remote sensing of radioactive materials using advanced Compton gamma-ray imaging. This type of imaging can localize gamma rays from radioactive nuclear materials and therefore allow us to distinguish them from background and identify their unique isotopic composition. The technique is important for homeland defense, astrophysics, and medical imaging. Compton scattering is the scattering of a gamma ray from an electron. By accurately measuring the angle and energy of the scattered gamma and the electron it scattered from, the direction of the incoming gamma ray can be calculated with a simple formula. If only the energy of the electron (not its angle) is measured (which frequently happens), the direction of the incoming gamma ray is not determined exactly, but the direction of the cones of light from the Compton scattering can be calculated from the same formulas. In either case, an image is built up from either the vectors (if the electron angle is measured) or the light cones (if not) from many gamma rays. The location of the source or sources can be determined from this image.

In the last year, we developed a prototype detector system, which was designed so that gamma rays could Compton scatter in one of three layers of 300-µm-thick Si-pixel detectors (Figure 3). The scattered gamma rays are then absorbed by one of 42 CsI detectors where they are detected. Each of the three planes of Si-pixel detectors has a sensitive area of 48 x 60 mm, which is divided into 320 pixels, each 3 x 3 mm. We also purchased and tested readout electronics (based on commercially available application-specific integrated circuits) for each pixel (960 total). The electronic noise from both the Si-pixel detectors and the readout system was measured and found to be about 2.6 keV (root mean square). Each of the 42 CsI detectors is approximately 12 x 14 x 10 mm and is attached to a photodiode used in fiber networks followed by a preamplifier. The individual crystals were tested and found to have a typical resolution of approximately 47 keV (root mean square), which we are attempting to improve. The next steps will be to integrate the Si- and CsI-detector readout systems and then to produce and compare images of real sources to our extensive Monte Carlo simulations of the system. Our longer-term goal is to build a real device that will be much larger than the prototype system; we hope to replace the CsI detectors with a higher-resolution detector in this larger device.

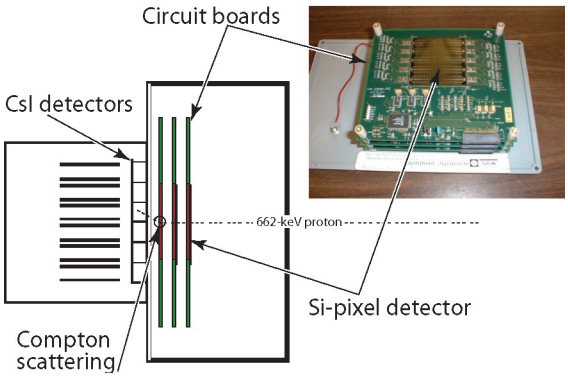

Figure 3. This cross section of the detector system shows the CsI detectors as small rectangles marked by an arrow. A 662-keV photon enters the system from the right, Compton scatters in the third Si-pixel detector, and is absorbed in one of the 42 CsI detectors. The electron (not seen in the figure) resulting from the Compton-scattering event remains in the Si-pixel detector where it was produced. The inset is a photo of the Si-pixel detectors.

High-Definition Television

G.H. Nickel, E. Stauffer, F.J. Wysocki (P-22)

Members of P-22 are developing methods of encoding information to deliver digital TV images using the "NTSC" (National Television System Committee) signal format used by existing analog television sets—the image data for HDTV can also be viewed by analog TV receivers. No hardware modifications are required for the old monitors or the new high-definition sets.

In the scheme described here, the information for the digital images (quantized coefficients in the transform space) is transmitted by modulating the carrier in a novel way. The coefficients are computed for 8 × 8 pixel blocks, as in the current standard, and partitioned into subsets according to the spatial resolution. Our scheme selects low-order coefficients in accordance with the relative bandwidths for the luminance and chrominance components of the video signal to generate the compatible image for the NTSC format. Because these coefficients must appear as an image in the coefficients of analog receivers, they cannot be entropy coded. Instead, they are transformed directly from their digital form back to the image space and transmitted as a "digitally mastered composite video" waveform using amplitude modulation. This transformation is designed to create an image in analog receivers and provide for the recovery of the original discrete data by inversion, without introducing extra sensitivity to signal noise. The remaining "high-order" digital information can be partitioned again, if desired, and transmitted in such a way that it is invisible on analog receivers but recoverable by digital sampling. This information is compressed using entropy coding and offers a compression advantage.

Our research team assembled a demonstration prototype using these principles and commercial off-the-shelf hardware. We used computers with added signal processors and analog-to-digital converters to create the required waveforms and act as HDTV decoders. With further development, it will be possible to apply existing results from information theory and digital-modulation techniques to avoid duplication of television-channel programming (required under the current official transition plan) during the national transition to high-definition content.

Laser-Based High-Resolution, High-Energy X-ray Imaging of High-Energy-Density Targets Using a Backlit Pinhole

J. Workman, J. Fincke, G. Kyrala (P-24), T. Pierce (MST-7)

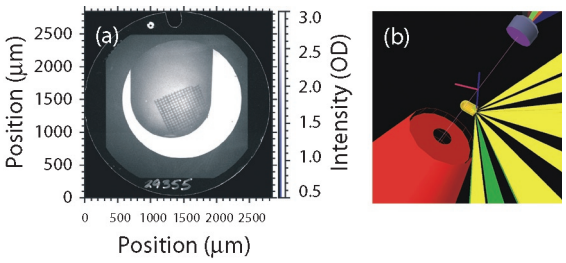

Figure 4. (a) A static x-ray radiograph at 9 keV of a hohlraum on the Omega laser. A 62-µm (20-µm bar width) period grid was used for spatial calibration. (b) Configuration showing diagnostic nose tip, hohlraum, and backlighter substrate.

In P-24, we have demonstrated a new x-ray backlighting technique at 9 keV that produces uniform, large-area, monochromatic, high-resolution images of targets used for laser-driven above-ground experiments (AGEX) and HED physics experiments. X-ray imaging at moderate energy in laser-driven HED physics experiments is an essential, well-established tool for observing dynamic phenomena such as shock trajectories, interface motion, and instability growth. However, the standard technique using an area back lighter, the size of the object to be radiographed, requires an inordinate amount of laser energy to produce a monochromatic x-ray source above 7 keV. Figure 4(a) shows the raw image of a thin-walled gold hohlraum used for radiation-driven experiments recorded on x-ray film using the backlit-pinhole technique. Figure 4(b) shows the hohlraum in the center with 12 laser beams "driving" it. The top right corner of Figure 4(b) shows the backlighter substrate, whereas the red object is the opening of the diagnostic camera. Signal-level improvements over the standard-area backlighting technique have been increased by greater than a factor of 65. This is an important diagnostic development that was driven by requirements for higher-energy x-ray backlighting in current experiments on the Z accelerator at SNL, the Omega laser at the University of Rochester, and future experiments on NIF.

The PHELIX "Transformer" for Proton Radiography Hydrodynamics

W.B. Hinckley, J.E. Martinez, M.C. Thompson (P-22), F. Venneri (LANSCE-3), P.J. Turchi (Phillips Laboratory, U.S. Air Force)

The Precision High Energy Liner Implosion Experiment (PHELIX) is an LDRD concept venture that uses the advantage of the turns-ratio of a common transformer design to produce high currents—for use in magnetically driven, hydrodynamic liner experiments. The advantage of this approach (to isolate the experimental fixture from a driver capacitor bank) lends itself to the possibility of application to the pRad "photographic" capabilities at LANSCE. The pRad facility has proven its capability to produce multiframe (20 frames/ ~ 30 μs) radiographic data of dynamic experiments. The confines of the pRad beam-line area require the use of a compact system—in contrast to a facility like Pegasus II or Atlas where users bring compact x-ray sources to the machine to record experimental data. Here, users bring the hydro-driver/experiment assembly (PHELIX) to the diagnostic, data-gathering device (pRad).

A toridal design, PHELIX uses a multiturn primary winding that is fed electrical energy from a compact capacitor bank (via an array of coaxial cables, similar to Atlas' maintenance-unit design) and a single-turn secondary that feeds the transformed current into a central experiment/liner assembly. The toridal layout is such that the driven liner becomes part of the secondary—minimizing resistive and inductive losses typical of the power-flow channel in similar hydrodynamic/magnetic drivers. The inductive and resistive portion of the circuit is shifted to a higher-impedance side of the network, reducing the loss. This combination of mechanical and electrical design can facilitate either radial or axial pRad of the experiment core by simply rotating the transformer in the beam line. The capacitor bank uses capacitors and rail-type spark gaps developed for Atlas in a compact, oil-filled unit that can roll (on tracks) in and out of the beam line for maintenance and loading experimental apparatus. A prototype transformer was constructed and tested in spring 2003 with promising results. A test and development facility is now being assembled at TA-35 to push the design to a "first-article" test with a target-test-shot date of December 2003 for proof of principle. An attempt at a test liner compression should follow in early 2004.

Low-Energy X-ray Radiography of Hydrotest Case Dynamics

R.T. Olson, D.M. Oró, D.T. Westley, A.M. Montoya, B.G. Anderson (P-22)

Several hydrotests were recently performed at the PHERMEX radiographic facility to examine radiation case dynamics under high-explosive loading. A low-energy, multi-frame x-ray system was also fielded to provide a second line of sight perpendicular to the PHERMEX beam axis. This x-ray system consists of four x-ray heads (each driven by a 900-kV Marx bank) that share a nearly identical line of sight. The x-ray radiographs were recorded on a CCD coupled to an electronic framing camera that images an LSO (cerium-doped lutetium oxyorthosilicate) scintillator via a 6-m-long optical path. The four x-ray heads were timed to provide images before, between, and after the two PHERMEX radiographs. All the equipment, with the exception of the camera and Marx banks, was destroyed during the experiments because of its proximity to the high-explosive charge.

Cygnus Radiographic X-ray Source

J.R. Smith, R.L. Carlson (P-22), R.D. Fulton (P-23), E.A. Rose (DX-3), R. J. Commisso, G. Cooperstein (Naval Research Laboratory), V. Carboni, D.L. Johnson, I. Smith (Titan Pulse Sciences Division), D. Droemer, D.J. Henderson (Bechtel Nevada), J.E. Maenchen (Sandia National Laboratories)

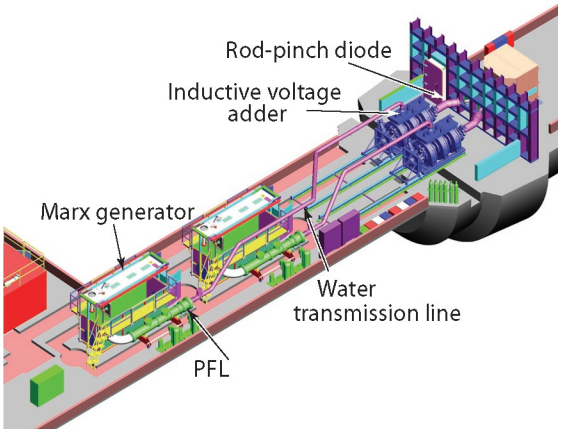

Figure 5. Two Cygnus x-ray sources located downhole at the NTS U1a complex.

Cygnus is a radiographic x-ray source developed for support of the SCE program at NTS. Its architecture, which is scalable, contains the most complex and largest hardware components ever deployed as a diagnostic for underground installation at NTS. Major features of the Cygnus source are a dramatically reduced spot size (as compared to existing alternatives), layout flexibility, and reliability. Cygnus incorporates proven pulsed-power technology (Marx generator, PFL, water transmission line, and inductive voltage adder subcomponents) to drive a high-voltage vacuum diode. In the case of Cygnus, a relatively new approach, the rod pinch diode, is employed to achieve a small source diameter. Cygnus has met the following design specifications: 2.25-MeV endpoint energy, 1.2-mm source diameter, and 4-rads dose at a distance of 1 m. Its reliability has been demonstrated at LANL in a test series that incorporated more than 300 shots. A notable requirement for operation downhole at NTS is a remote, computer-based control and monitoring system, which has also been developed and fielded.

The first application of the Cygnus radiographic source is the Armando SCE, scheduled in 2004, which will be fielded to study the dynamic properties of plutonium. Two Cygnus sources have been manufactured, integrated, and successfully tested as the prime diagnostic for this experiment (Figure 5). They will be configured to give two radiographic images with different views and at different times. The test object will be contained in a vessel thereby permitting reuse of the facility. The new and improved features offered by the Cygnus radiographic source greatly enhance the diagnostic capability for the SCE program at NTS.

Advanced Plasma Diagnostic Concepts for National Magnetic Fusion Energy Research

G.A. Wurden, Z. Wang, J. Park (P-24)

We have been working on a new plasma diagnostic to measure the internal magnetic fields in today's generation of research plasmas. We propose to develop a hypervelocity dust beam (micron-sized dust traveling at ~ 10 km/s) to inject a source of neutrals deep into the National Spherical Torus Experiment spherical tokamak plasma at Princeton University. By taking snapshots of the dust beam (from a tangential view) using high-resolution cameras, we can observe the small "comet-like" tails of the ablating dust particle. Their orientation will give us the direction of the local magnetic field inside of the plasma. This type of information would be of great help in many alternate plasma configurations where the internal magnetic fields (when the plasma is present) are quite different than the original vacuum magnetic fields (when the plasma is absent).

For tomorrow's high-performance fusion tokamak machine—the International Thermonuclear Experimental Reactor, we have been working on restarting a project originally developed at LANL about 15 years ago. That project had as its goal the development of an extremely bright, pulsed, intense diagnostic neutral beam. This atomic beam of hydrogen (or helium), operating at a voltage of ~ 100 keV/AMU, at a current of 10 kA in 1-μs pulses, and at a 10- to 30-Hz repetition rate, will provide a source of neutrals for spectroscopy purposes. Without this source, there are no neutrals normally present deep inside the core of the fusing tokamak plasma. With this source, profiles of plasma-ion temperature, helium-ash buildup, and the plasma-current profile can all be obtained by analyzing light emitted from the neutral atoms in the beam.

40-mm, Gunpowder Breech Launcher for Proton Radiography Experiments

E.O. Ballard (P-22), P.A. Rigg, D.L. Shampine (DX-2)

A 40-mm bore, powder-breech launcher was designed, fabricated, assembled, and tested for use at the LANSCE pRad facility (Figure 6). The 40-mm launcher is an experimental device to be used for determining EOS and metallurgical properties of materials under extreme dynamic-loading conditions in real time. The launcher system consists of a 40-mm smooth-bore launch tube (barrel), a propellant breech, and an enclosed target-chamber and catch-tank assembly. The launch tube/breech assembly measures approximately 11.5 ft in length and rests on bronze bushings at two contact points. The muzzle end of the launch tube is located inside the target chamber, and the entrance point to the chamber is sealed using an O-ring slip seal. Launch-tube recoil is limited to 4 in. of travel by using two industrial shock absorbers, which retain the muzzle of the launch tube inside the target chamber after the shot. Because the only contact between the launch tube and target chamber is through the slip seal, the momentum transferred to the target chamber caused by recoil of the launch tube is negligible. The entire assembly is attached to a platform on rails set perpendicular to the proton beam line in such a way that the target chamber can be aligned and mounted to the beam line. The target chamber and catch-tank contain the projectile and combustion gases from the propellant. The beam-tube volume is also used for containing propellant gases.

The target assembly is located at the muzzle end of the launch tube inside the target chamber and consists of the material of interest for the experiment and various diagnostic electrical pins and optical probes. The projectile consists of a main body comprised of various materials in mass less than or equal to aluminum. Projectile materials include, but are not limited to, Lexan® (polycarbonate), aluminum, or magnesium and weigh from 100 to 500 g. A thin impactor (typically metal but ranging from plastics to single-crystal sapphire) is glued to the front of the projectile for direct impact with the target material. At least one O-ring is included at the rear part of the projectile to serve as a vacuum seal. A thin phenolic shear disk is placed on the back of the projectile to hold it in place until the launcher is fired. The projectile assembly is accelerated down the launch tube using up to 300 g of a Class 1.3 smokeless gunpowder at a velocity to 2 km/s. The projectile (or, more specifically, the impactor) then impacts the target, at which point the experimental measurements take place. A series of seven hanging catch-plates located in the catch-tank then stops the projectile and target shrapnel produced by the impact.

A variety of diagnostic tools can be employed, including pin circuits to examine wave-propagation times, laser interferometry and spectroscopy, CCD cameras, temperature probes, and oscilloscopes.

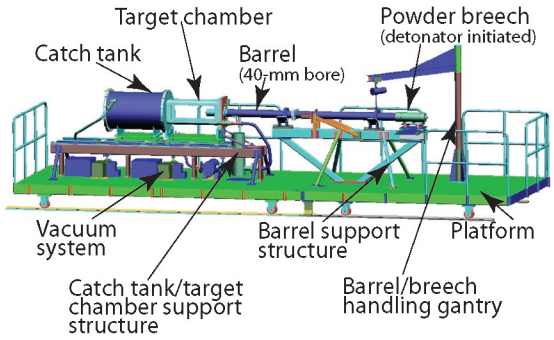

Figure 6. The 44-mm gunpowder breech launcher for pRad experiments.

VISAR at pRad

D.A. Clark, O.F. Garcia, B.J. Hollander (P-22), D. Tupa, (P-25)

VISAR is an important diagnostic that can provide detailed surface-velocity information for pRad experiments in Area C at LANSCE. P-22 has constructed a VISAR system for pRad and provides support to field experiments that use VISAR. In addition, we provide support for general pRad beam operations. Experimental support includes design and installation of VISAR equipment, data acquisition, fiber-optic and coaxial cable plant, safety documentation, experiment documentation, data analysis, and mechanical-technician help.

Thermonuclear Burn Physics Using High-Energy Fusion Gamma Rays

J.M. Mack, D. Esquibel, S.C. Evans, R.S. King, D.K. Lash, J.A. Oertel (P-24), S.E. Caldwell, C.S. Young (P-22), R.R. Berggren (ISR-2), J.R. Faulkner, Jr. (DX-3), R.L. Griffith, R.A. Lerche (Lawrence Livermore National Laboratory)

As fusion ignition conditions are approached using NIF, independent, high-bandwidth, gamma-ray fusion-burn measurements become essential complements to neutron-based diagnostic methods. Time resolution, ~ 20 ps (10–30 GHz), energy discrimination, and significant stand-off distance may be needed for credible burn-history measurements. The idea of using high-energy fusion gamma rays for burn-history evaluation was conceived and pursued as part of the downhole test program at NTS more than two decades ago. With potent fusion sources now available on the Omega laser at the University of Rochester and with upcoming availability at NIF, this possibility exists once again and is being vigorously pursued by a multi-institution collaboration led by P Division, including the key original NTS personnel.

The 16.75-MeV gamma rays that accompany DT fusion provide a high-bandwidth alternative to 14-MeV fusion neutrons for DT burn-history measurements. Fusion of deuterium with tritium produces an excited ^{5}He nucleus, which then has several possible de-excitation modes. The most common mode emits a 14-MeV neutron and a 3.5-MeV alpha particle. Much less frequent gamma-ray modes emit gamma rays at 16.75 MeV to the ground state and possibly at ~ 12 MeV to a broad level near 4 MeV. Recent values for the DT branching ratio (16.75-MeV gamma rays per 14-MeV neutron) vary from 5×10^{-5} to 1×10^{-4}. Because of this unfavorable branching ratio, high-yield DT implosions ($> 10^{12}$ neutrons) are required to provide high-energy gamma-ray output of sufficient strength for a credible measurement.

A thresholding detector, based on the Cerenkov effect, resulting from Compton and pair-production electron interactions in gaseous carbon dioxide, offers a means of separating the high-energy fusion gamma rays from other background sources (Figure 7). When coupled to appropriate streak-camera recorders, a gas-Cerenkov-detector (GCD) system response to 20 GHz is feasible. Initially, as a proof of principle, a GCD system employing a 1-GHz photodiode detector was successfully fielded at the Omega laser facility. A comparable system was also operated with a streak camera replacing the photodiode detector, thus allowing similar measurements to be made at higher bandwidth (~ 15 GHz). High-energy fusion gamma-ray measurements have been made on a number of DT capsule implosions, which have had neutron outputs ranging from 1×10^{12} to 8×10^{13} neutrons. For the first time, using ICF implosions, high-energy fusion gamma-ray signals were unambiguously observed with both instruments at Omega. These results have established the feasibility and utility of high-bandwidth GCD-based, high-energy DT fusion-burn gamma-ray measurements for acquiring burn histories using laser-driven implosions. This new diagnostic method is now approved as a future diagnostic package for NIF.

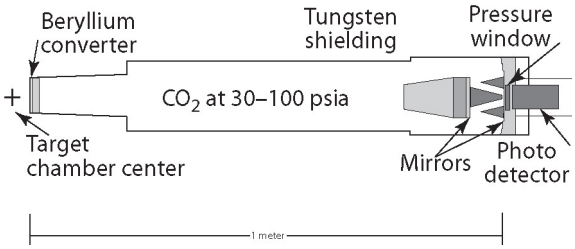

Figure 7. GCD system as configured for insertion into the evacuated Omega laser target chamber. Sixty converging laser beams implode the DT targets placed at the target-chamber center.

KEYPATH: Using Atmospheric Turbulence to Generate and Exchange a Cryptographic Key

G.H. Nickel (P-22), S. Xie (University of Texas, Dallas)

When a laser beam is transmitted through turbulent air, the eddies create time-dependent temperature differences, which in turn cause density variations. If the beam diameter is not too large (several centimeters), the perturbations caused by these variations are simply "tilts" of plane of constant phase and can be shown to be truly random with a correlation time of a few milliseconds. Such "tilts" are easily measured by determining the change in position of the resulting spot in the focal plane of an optical system. Perhaps surprisingly, when two beams are propagated along the same path in opposite directions, measurements at each end of the path demonstrate a high

correlation. Therefore, observations of these "tilts" can be used to generate random sequences, which are the same for both observers. Because this random sequence depends on the particular air column between the observers, it is also secure from measurement by a third observer unless the exact path is traversed. Thus, the sequences are random, correlated, and secure; these are the conditions for the exchange of a cryptographic key. The security of this scheme is due to the impossibility of modeling turbulence exactly.

A demonstration of the effectiveness of this system, called KEYPATH, is under development. Shumao Xie, a graduate student at the University of Texas at Dallas, and George Nickel, a staff member in P-22, have been taking measurements over paths of varying lengths and demonstrating the correlation. To date, paths of 100 m have yielded over 90% correlation in the resulting bit streams, and greater path lengths are being considered. The only fundamental limitation to the length comes from the condition that the turbulence should not change during the time for the light to transit the path. The characteristic correlation time has been measured to be 10 ms, meaning that 100 independent bits of key can be generated each second—and that paths of many kilometers are possible.

Shumao Xie will continue this work as his Ph.D. thesis at the University of Texas, and George Nickel is working with ISR Division to extend the concept to an analogous situation involving transmission of radio signals in the earth's magnetosphere. The work has been approved for patent application.

Interferometer Displacement Measurements of DynEx Vessel Oscillations

D.T. Westley, R.T. Olson, J.K. Studebaker, D.A. Clark, B.G. Anderson, A.M. Montoya, B.N. Vigil, J.C. Armijo (P-22)

The objective of these experiments was to determine the radial-wall displacement of a DynEx containment vessel (Figure 8) during detonation of different high-explosive loading conditions. The data from these experiments and the strain-gauge measurements of the containment vessel's outer surface verify models of vessel behavior. Two types of experiments, mitigated and unmitigated are performed, both of which were conducted at atmospheric pressure. The mitigated experiments use glass balls in the vessel to lessen the shock effects created by the high-explosive pressure wave, whereas the unmitigated experiments simply consisted of a spherical high-explosive charge hanging in an empty vessel. All experiments were configured with spherical PBX-9501, which was centrally detonated with one ER-453 detonator. The high-explosive charges were held in place with a specially designed sling, centering the charge in the vessel to within ± 1 mm.

Microwave interferometers are used to measure displacement of the vessel walls as a function of time. The system uses a pair of microwave interferometers—one with a 24-GHz fundamental frequency and one with a 94-GHz fundamental frequency. A feed horn is used to both emit and collect a signal that is reflected off the surface of the vessel. The reflected signal is amplified, split, and interfered in quadrature with the reference leg of the interferometer. Two detectors record the intensity variation of the interfered signals as a function of time. The phase change and the known wavelength of the system are used to determine the displacement of the outer surface of the vessel. The unmitigated-experiment data indicate initial vessel-wall expansion, as well as vessel motion approaching that of a simple harmonic oscillator with a defined, repeatable period. The mitigated-experiment data indicate that the vessel wall initially expanded on one side and contracted on the other. The oscillations indicate a difference in time between the initial motion and the amplitude of motion as directly proportional to the high-explosive loading.

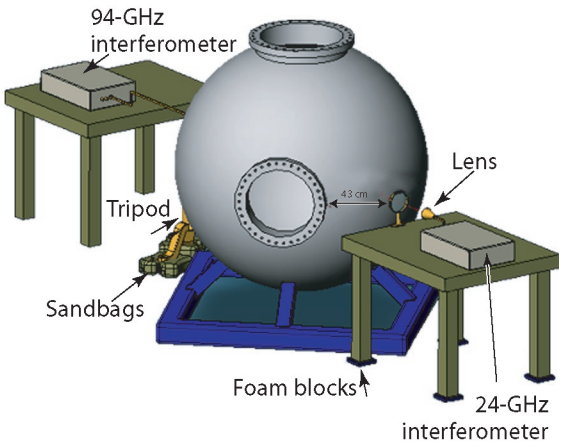

Figure 8. Diagnostic layout of 6-ft-diam DynEx containment vessel and microwave interferometer systems.

Advanced Detectors for Proton Radiography—Raising the Bar in Ultra-Fast Imaging

K. Kwiatkowski, N.S.P. King (P-23), C. Morris (P-25), M. Wilke (P-23), S. Kleinfelder (UC-Irvine), J. Lyke (Air Force Research Laboratory), V. Douance, P.O. Pettersson (Rockwell Scientific), R. Wojnarowski (General Electric-Global Research)

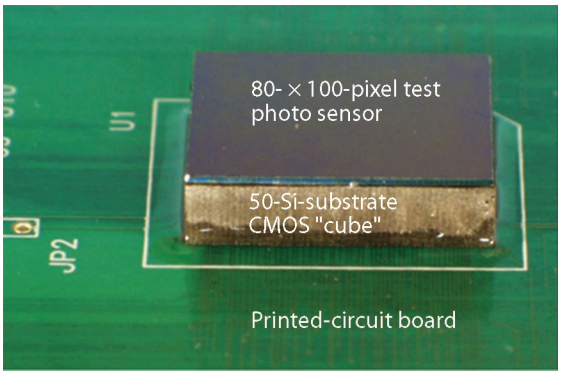

Figure 9. Imaging cube assembly—50 double-density chips stacked on edge with an 80- x 100-pixel test photo sensor that is bump-bonded to the top of the cube.

The invention of pRad has opened new opportunities in flash radiography. The combination of pRad's multiple-frame (~ 50), high-penetrating-power, high-speed, and high-resolution capabilities has made this unique technique a powerful tool in quantitative studies of fast transient phenomena evolving on sub-microsecond timescales. However, pRad has also imposed great demands on the optical imagers used in the experiments. We are developing new detectors to replace the current "seven-shooter" gated CCD camera system. The interim solution is based on a back-illuminated hybrid CMOS (complementary metal oxide semiconductor) imager. This 2-mega-pixel camera, which is being built at Rockwell Scientific, operates in a burst mode. It can acquire three frames spaced 300 ns apart and provides about a 100% fill factor, high quantum efficiency, and a large dynamic range of 11 bits. In parallel, we are developing enabling technologies (sensors, CMOS electronics, and interconnect technology) for an instrument that can fully meet the challenges of high-resolution, multiple-frame pRad. The construction of a mega-pixel, 64-frame, fast-imaging system is complicated by the tremendous requirements on the data-recording bandwidth and by equally severe demands on the instantaneous power that has to be delivered to the front-end electronics and to the sensor during the acquisition time. One approach to reconcile the opposing demands for smaller, denser pixels and greater functionality is to stack the signal-processing electronic chips, like a deck of playing cards, into a three-dimensional cube structure, which can be placed directly below a photo-sensor array. This approach can increase the available pixel silicon area by a factor of 20 to 100. The proof-of-concept cube was recently fabricated in a collaborative effort with General Electric-Global Research Center using test/continuity silicon chips (Figure 9).

Concurrently with the development of the interconnect technology, we have made strides in the design and fabrication of custom CMOS electronics that can deliver the required electrical performance for the 64-frame imager and can be laid out in < 50-μm-wide "channels." We designed and tested an integrated-circuit prototype, as a 12 × 12 CMOS focal plane array, that acquires images at a rate of 4 mega-frames per second with over a 79-dB, or 13-bit, dynamic range. The 200- × 200-μm^2 pixels were equipped with a small photodiode, a charge-integrating amplifier, a direct-integration source follower, 64 frames of *in situ* storage via an array of sample and hold capacitors, and output multiplexing circuitry. The chip can perform either correlated double sampling (recording 32 frames at 4 mega-frames per second) or single sampling (64 frames at 7 mega-frames per second). Additionally, we designed and tested a solid state CMOS "streak camera." This camera performed up to a 400-MHz (2.5-ns) electrical test and over 100 MHz using optical stimulation with more than 10 bits of dynamic range. The prototype contained a one-dimensional array of 150 photodiodes, each with 150 frames of storage. Using three-dimensional packaging techniques, the streak-camera concept can be leveraged to create an ultra-fast camera system capable of capturing images at tens of tera-pixels per second. For example, a common-interchange-format (352 × 288 pixels) imager with a storage capacity for 1,024 frames is feasible. When it is run at 200 MHz, it will acquire over 100 megabytes of image data in 5 μs at the effective speed of over 20 terabytes per second (i.e., 20×10^{12} bytes per second).

Reaction-History Reanalysis

B.J. Warthen (P-22), representing the Reaction-History Reanalysis Team

The reaction-history measurement is a high dynamic-range measurement of gamma rays and was usually made during each underground nuclear event at NTS. On each event, the reaction-history measurement involved several detectors—each requiring several data-recording channels to cover the detectors' dynamic range. Most often, a data-recording channel consisted of a Rossi oscilloscope that produced a vertical deflection proportional to the gamma-ray flux and a horizontal deflection proportional to a sinusoidal time-base. The trace of each Rossi oscilloscope was recorded on film. An example of a very clean Rossi trace film (simulated) is shown in Figure 10.

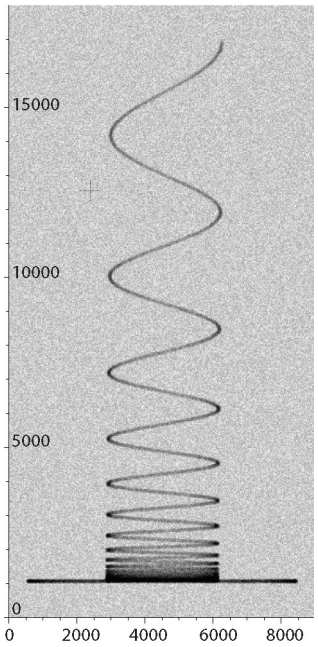

Figure 10. Simulated film of a Rossi trace.

After an NTS event, the films were hand-digitized to produce (x,y) data points that represent the traces; the data points were used to calculate the flux as a function of time, and the flux functions from each of the channels of a detector were combined together to produce a composite flux curve for the detector. The alpha curve was produced by calculating the logarithmic derivative of the flux curve and then applying an adaptive Gaussian filter to the result. The alpha curve (or just alpha, α) is important because it allows for the comparison of the data to a theoretical calculation of the underlying nuclear activity without a detailed knowledge of the absolute calibration of the detection system or the absorbing and scattering effects of the intervening material between the gamma-ray source and the detectors.

After the reaction-history data analysis was completed for an event, a shot report was written to summarize the results of the analysis by recording various α values and showing graphs of the composite flux and α curves. Uncertainty analysis consisted of estimating (by eye) the spread of the composite α curve due to the combination of filtered α curves from each detector. Toward the end of NTS nuclear testing, rather than comparing calculations to discrete values of the α curve, more detailed comparisons were being made to try to match calculations to electronic versions of the entire α curve. When testing ended, the record of the reaction-history measurement for a given event consisted of the event film, which recorded the Rossi traces during the event; logbooks containing experimental setup and calibration information; and a shot report. If the event occurred close to the end of testing, there were also electronic files that contained the flux and α curves.

Today, there is increased interest in comparing calculations with the most relevant data the nuclear weapons community has: the NTS reaction-history archive. The P-22 Analysis and Archiving Team has two important goals that support several projects, including NTS data archiving, nuclear and nonnuclear data validation, and weapon system certification. The first goal is to train new personnel to understand the experimental aspects of the reaction-history measurement and the analysis of the resulting data and to become familiar with the reaction-history data archive. These new personnel will reanalyze the reaction-history data and interact with the designers, modelers, and computer scientists in the future to help interpret the NTS reaction-history data. The second goal is to preserve the collection of reaction-history data and produce reanalysis and uncertainty estimation in a format that can be used for comparison with calculations.

The P-22 team is currently made up of full-time team members and retirees (who have had direct experience designing and fielding reaction-history measurements at the NTS and analyzing the resulting data) and is also supported by Bechtel Nevada. The team is working together to improve the analysis process, to use the new analysis techniques to reanalyze reaction-history data, to develop uncertainty-estimation techniques, and to act as a resource to the weapons community to answer questions about reaction-history measurement and data analysis.

The team is tasked with scanning event films and logbooks to produce an electronic archive of all the reaction-history raw data and with developing and/or improving software that provides computer-aided center-of-trace measurements of event-film images along with an estimation of the uncertainty of the measurement. The team is also tasked with developing techniques and software to provide an estimation of the uncertainty in α due to film digitization and trace location, flux and alpha calculation, and curve composition and then with applying the new analysis techniques to a prioritized event list.

Reaction-History Test Readiness

B.J. Warthen (P-22), representing the Reaction-History Test Readiness Effort

Since the end of underground nuclear testing at NTS in 1993, the national laboratories involved in performing underground nuclear tests (UGTs) (these include LANL, LLNL, and SNL, and Bechtel Nevada) have been maintaining a 24- to 36-month test-readiness posture. This means that if we are requested to do a UGT, the national laboratories are capable of preparing the necessary experimental diagnostics and logistics for the test within 36 months. This posture is maintained by involving technical personnel in ongoing nonnuclear experiments that produce data and results of interest to the nuclear-weapons community.

When nuclear testing ceased, it was assumed that if a UGT were to be requested in the future, there would be enough experienced personnel remaining (either currently employed at the national laboratories or recently retired and willing to return) and enough existing equipment available that 36 months would provide enough time to get ready. Recently, NNSA has requested that the national laboratories transition to an 18-month test-readiness posture. This change, combined with the realization that the above assumption might not still be valid a full decade after the end of testing, has resulted in a test-readiness program being funded at the national laboratories.

P-22 will work with LLNL, Bechtel Nevada, and SNL to reconstitute the capability to perform a reaction-history measurement on a UGT. P-22's involvement in the test-readiness effort includes the following activities:

- participate in the LANL annual event-design exercise;
- design the reaction-history line of sight and work with DX-5 to incorporate the line of sight into the rack design;
- work with X-5 to calculate detector sensitivities;
- work with Bechtel Nevada to determine the status of existing reaction-history-detection, signal-transmission, and recording systems;
- work with P-21, LLNL, and Bechtel Nevada to identify and test data-recording equipment to replace Rossi oscilloscopes; and
- work with P-21, LLNL, and Bechtel Nevada to develop high-bandwidth-detection, signal-transmission, and recording systems for reaction-history measurements.

Support of Experiments at the Alternating Gradient Synchrotron

D.A. Clark, O.F. Garcia, B.J. Hollander (P-22)

P-22 supports pRad experiments at the BNL AGS. Experiment 963 (E963) was carried out in June 2003. P-22 provided support in the months ahead of the scheduled experiment time to design and install fiber-optic and coaxial cable plants for data-acquisition and control systems. P-22 staff played a major role in design, implementation, and operation of the nuclear-scattering portion of E963, as well as general operations and data acquisition for the entire experiment. After the experiment was completed, P-22 contributed several weeks of effort to reconfigure cable systems in preparation for the next series of experiments at AGS.

Generation of Energetic Ion Beams Using an Ultra-Short-Pulse, High-Intensity Laser

J.C. Fernández, J.A. Cobble, B.M. Hegelich, R.P. Johnson, S.A. Letzring, T. Shimada (P-24), J.F. Benage, F.J. Wysocki (P-22), J. Kindel, M.J. Schmitt, D. Winske (X-1), V.A. Thomas (X-4), L.A. Collins (T-4), D.O. Gericke (T-15), J. Kress (T-12), T.E. Cowan, H. Ruhl, Y. Sentoku (University of Nevada, Reno)

Our work is based on recent progress worldwide in applying short-pulse (subpicosecond) intense (~ 10^{19} W/cm^2) lasers to produce high-current, charge-neutralized ion beams with high conversion efficiency (~ 5% of the laser energy) over a range of light ion species (most commonly protons) with energies in the MeV/nucleon range. Our ultimate goal is to advance our understanding in two areas at the frontiers of plasma physics: (1) relativistic laser-matter interactions, applied towards producing, optimizing, and controlling intense, laser-driven, MeV/nucleon ion beams (including heavy ions); and (2) interactions of beams and dense plasmas in regimes of interest for weapons physics (especially boost in primaries) and for fast-ignition fusion.

We rely on the capability at the LANL Trident laser of collocated long pulses (for laser-plasma formation) and high-intensity short pulses (for relativistic laser-matter interactions). Presently, Trident has the most energetic short-pulse laser in the U.S. The study of the relativistic laser-matter interactions responsible for directed-ion acceleration represents an emerging field of great scientific vitality. Our plasma-physics understanding is presently insufficient to explain fully the underlying processes in such interactions. The process of controlling and optimizing the laser-driven ion acceleration (as part of our upcoming research funded by the LDRD program), will build on recent successes by our team of LANL and external collaborators. Our results can be summarized by three main points.

(1) In the regime of interest to us, energetic ions are created and accelerated mostly by a transient MV/μm electrical sheath at the rear surface of the target—not at the front surface that is irradiated by the laser.

(2) The ion beam has a finite divergence, presumably controlled by the physical and geometric characteristic of the sheath, which could be controlled by proper tailoring of the laser-intensity profile or the target geometry.

(3) These ion beams have a very low transverse temperature. Indeed, a Trident-produced proton beam holds the record for low transverse beam emittance, 0.0025 π mm-mrad for 8-MeV protons.

Figure 11 illustrates how this measurement was done, along with a record of the proton beam on a radiochromic film. These results are consistent with the so-called Target-Normal Surface Acceleration model for laser-driven ion acceleration. With untreated metallic targets, most of accelerated ions are protons coming from adsorbed surface contaminants such as water. *In situ* heating of metallic targets to > 1,000°C in the vacuum chamber (using electrical currents just before the laser shot) successfully eliminates the hydrogen contaminants and thus results in efficient acceleration of heavier ions. However, joule heating is incapable of removing metallic oxides at the surface of the target, so most of the energy goes into accelerating O^{6+} rather than ions from the metallic substrate. Other techniques aimed at removing all surface contaminants are being tested.

The interaction of heavy ions having about MeV/nucleon energies with a background low-Z plasma is relevant in the context of weapons-primary operation. Important fundamental physics aspects in such interactions are neither completely elucidated nor experimentally validated. Many physics uncertainties in primaries are shared with other important areas of current scientific research, such as the properties of planetary interiors (e.g., Jupiter), the grand challenge of achieving fusion ignition in the laboratory, and the properties of dense plasmas. Given the general nature and relevance of the underlying physics, generic experimental configurations can be abstracted to study the issues important in all of these areas. Rather than reproducing the specific conditions in a primary or in a fast-ignition capsule, our aim is to devise a generic experimental configuration to make measurements over a wide range of parameters that are useful for validating emerging theoretical models.

Figure 11. (a) Schematic of the experiment on Trident and (b) record of the proton beam on a radiochromic film.

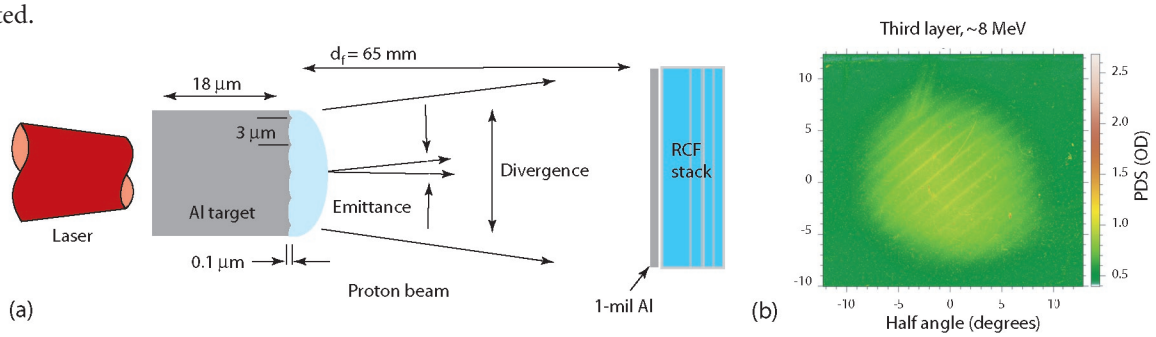

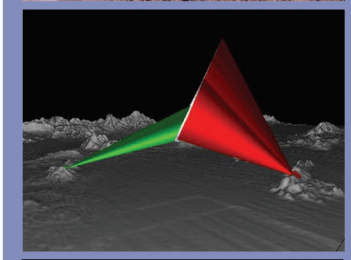

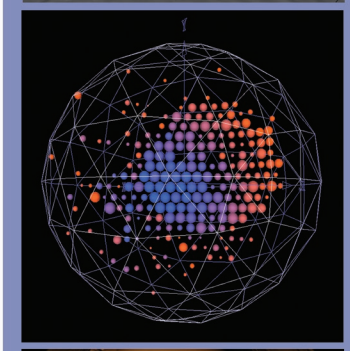

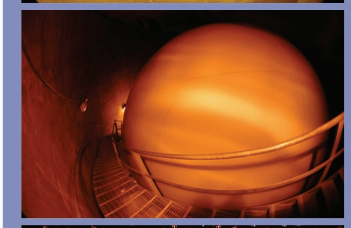

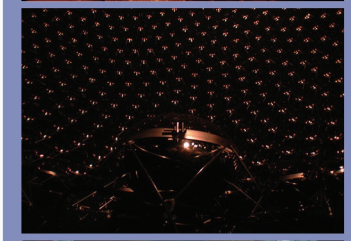

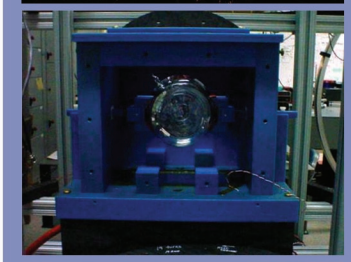

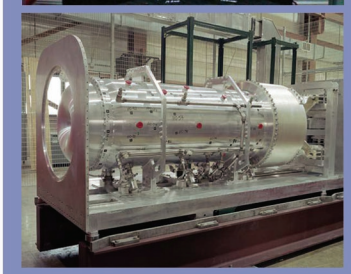

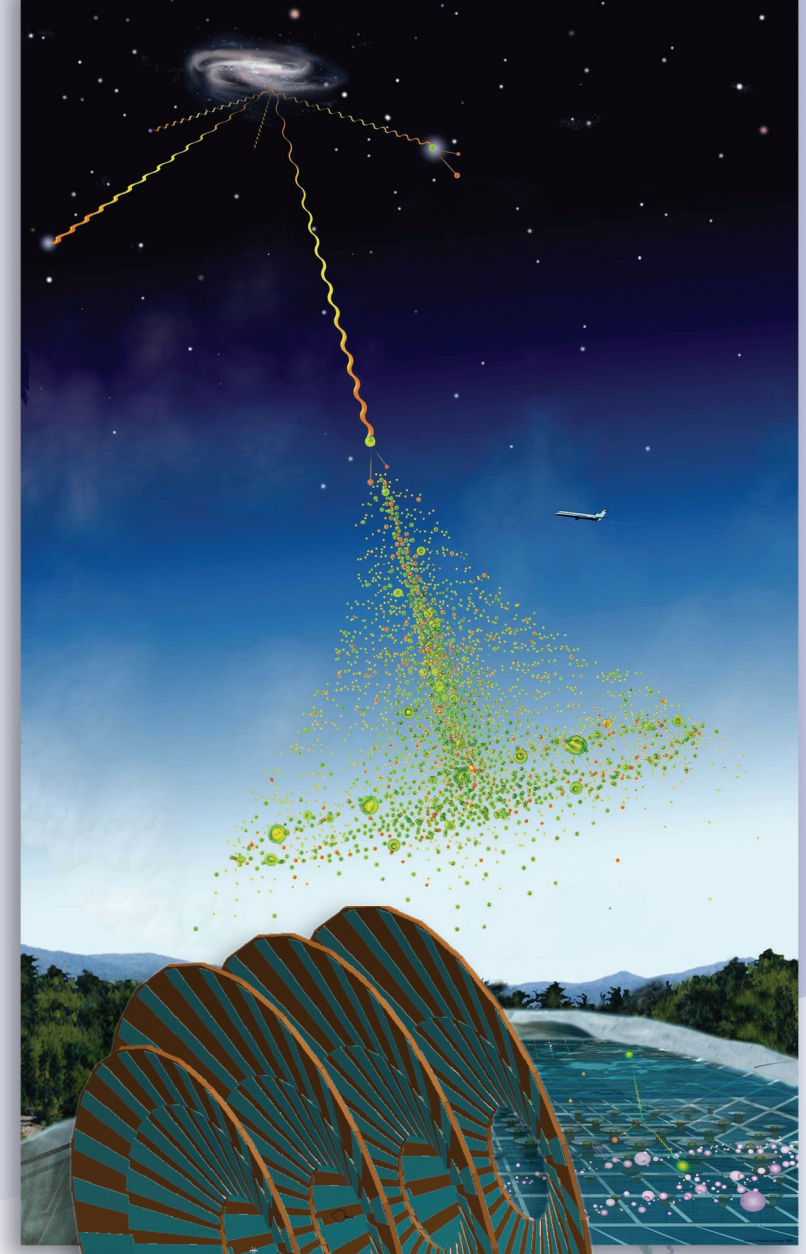

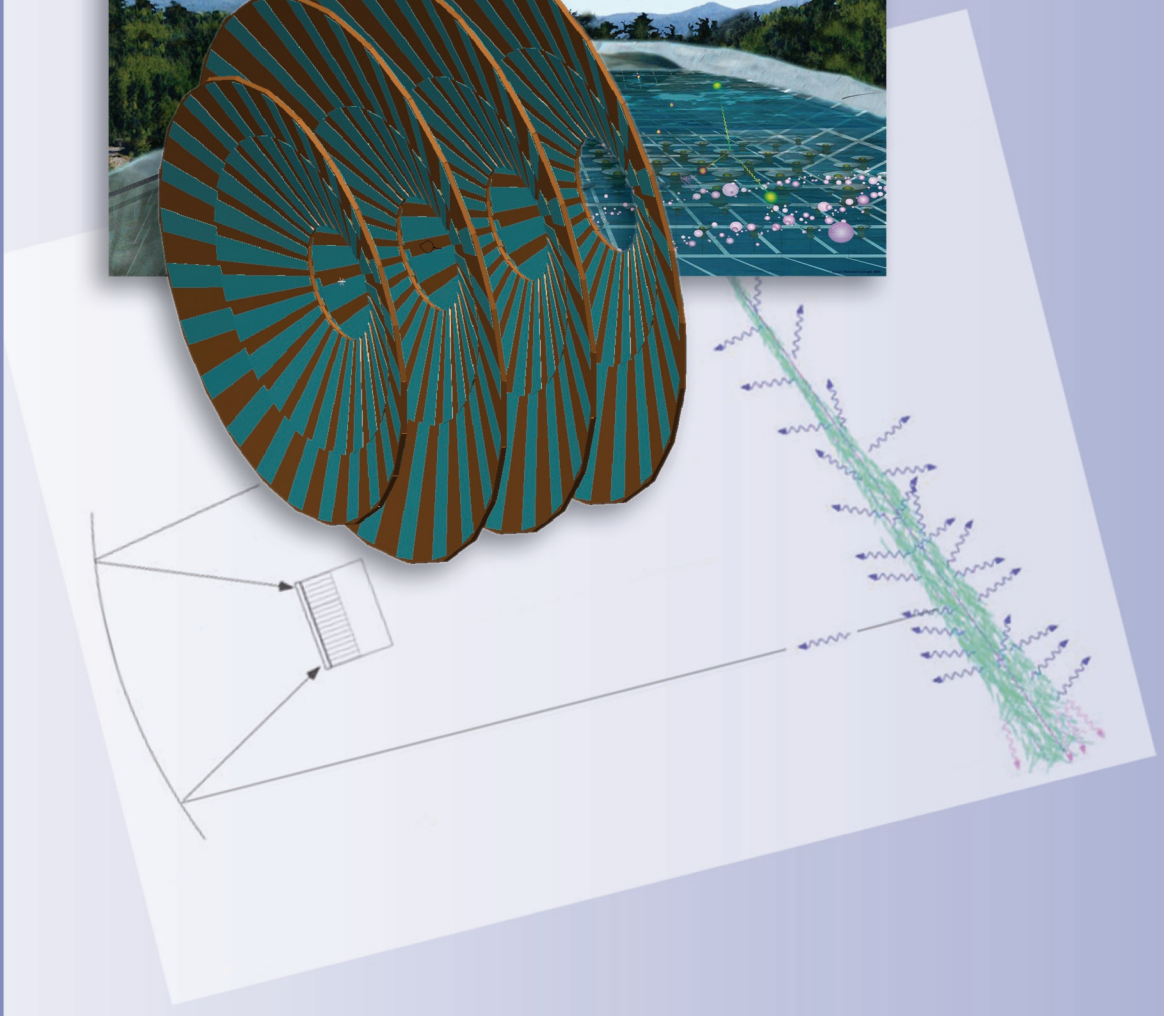

Nuclear Physics and Astrophysics

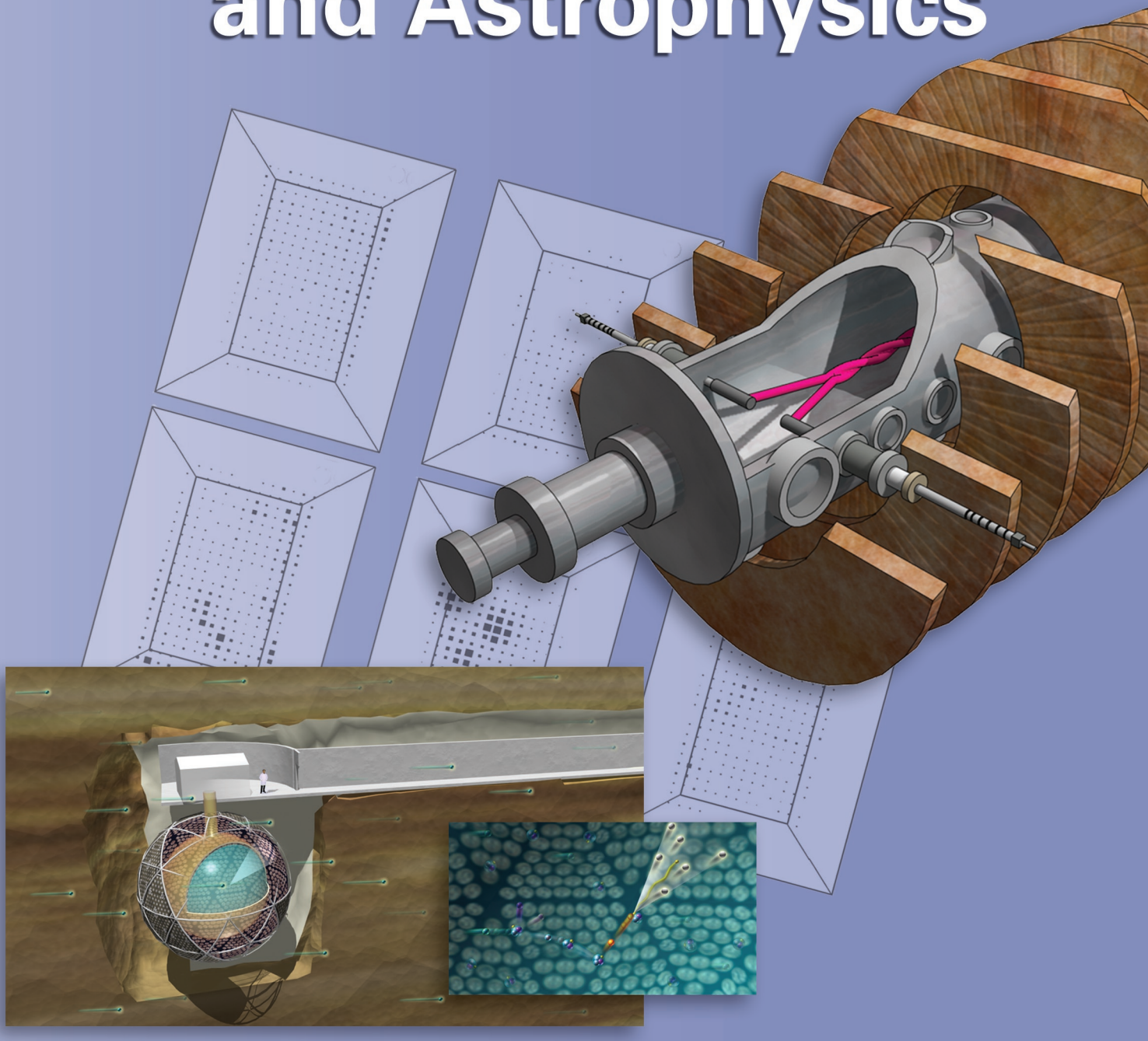

Nuclear Physics and Astrophysics Contents

Research Highlights

The Sudbury Neutrino Observatory—Taking Physics Beyond the Standard Model 125

Accelerator Neutrino Experiments on the LSND and MiniBooNE 129

The Electric Dipole Moment of the Neutron 133

The NPDGamma Experiment 137

Extreme Astrophysics—The High-Resolution Fly's Eye Experiment 141

Teravolt Astrophysics—The Milagro Gamma-Ray Observatory 145

The PHENIX Silicon Vertex Tracker Project 149

Project Descriptions

Theoretical Research on Strong, Electromagnetic, and Weak Interactions 153

Radio-Frequency Emission from a Pulsed Reactor 153

Solid Oxygen as an Ultra-Cold Neutron Source 154

Education and Outreach 154

Alpha-Dot Experiment 155

Plasma Astrophysics on the Flowing Magnetized Plasma Experiment 156

Search for a Permanent Electric Dipole Moment of the Electron Using a Paramagnetic Crystal 156

High-Energy Nuclear Physics 157

The Majorana Experiment 158

Wide-Angle Cerenkov Telescope 158

Q_{weak}: A Precision Measurement of the Proton's Weak Charge 159

Pulsed-Cold Neutron Beta Decay 160

The PHENIX Program at RHIC 161

Neutron-Beta-Decay-Asymmetry Measurement Using the New Ultra-Cold Neutron Source at LANL 162

Gamma-Ray Burst Science 163

Spin Physics at RHIC 163

The Sudbury Neutrino Observatory—Taking Physics Beyond the Standard Model

A. Hime, M.G. Boulay, T.J. Bowles, M.R. Dragowsky, S.R. Elliott, A.S. Hamer, J.C. Heise (P-23), M.M. Fowler, G.G. Miller, J.B. Wilhelmy (C-INC), J.M. Wouters (IM-8), R. Van de Water (P-25)

In the 1930s, in an attempt to preserve the conservation of energy in nuclear beta decay, Wolfgang Pauli invented a new particle—the neutrino. This elusive particle has no electric charge and interacts so weakly that it was almost impossible to detect. More than 20 years later, the neutrino was finally observed by a research team from LANL in an experiment at the Hanford reactor. Two years later, a definitive experiment at the Savannah River reactor clearly demonstrated the existence of the neutrino. Subsequent measurements at various facilities indicated that neutrinos come in at least three different types, or "flavors"—electron, muon, and tau. Determining whether neutrinos have mass is an issue of great importance to particle physics, astrophysics, and cosmology. The search for evidence of neutrino mass and the study of neutrino interactions with nuclei has evoked continuous experimental efforts by scientists from LANL for over 50 years. Accelerator-driven neutrino experiments like those performed on the LSND at LANSCE and now the BooNE (which is currently taking data at FNAL in Illinois to definitively test the LSND findings) provide evidence that could indicate that neutrinos do, in fact, oscillate from one type to another and therefore have mass (see *Accelerator Neutrino Experiments on the LSND and MiniBooNE*, p. 131, in this report). We are performing non-accelerator-based experiments using SNO—a terrestrial detector located 6,800 ft underground in an active nickel mine in Ontario, Canada—to understand why solar neutrino fluxes measured in terrestrial detectors fall significantly short of standard solar model predictions.[1] Both accelerator- and non-accelerator-driven neutrino experiments provide important tests that may challenge the Standard Model of electro-weak interactions while searching for neutrino oscillations.

Resolving the Solar-Neutrino Puzzle

While continuing to probe the neutrino at accelerators, LANL scientists initiated a program of non-accelerator physics that provided alternative means to probe the properties of the neutrino. A high-precision measurement of the spectrum of the electrons emitted in the beta decay of tritium provided a means to search for a very small neutrino mass. This experiment provided a limit on the mass of the electron-type neutrino, which was sufficient to rule out electron-type neutrinos as being the dominant mass in the universe. To dramatically improve sensitivity, scientists shifted the focus of non-accelerator efforts to measurements of solar neutrinos produced 93 million miles away—deep in the nuclear furnace of the sun. LANL played the lead role in a solar-neutrino experiment, known as the Soviet-American Gallium Experiment (SAGE), at the Baksan Neutrino Observatory in the Caucusus mountains of southern Russia.[2] SAGE uses

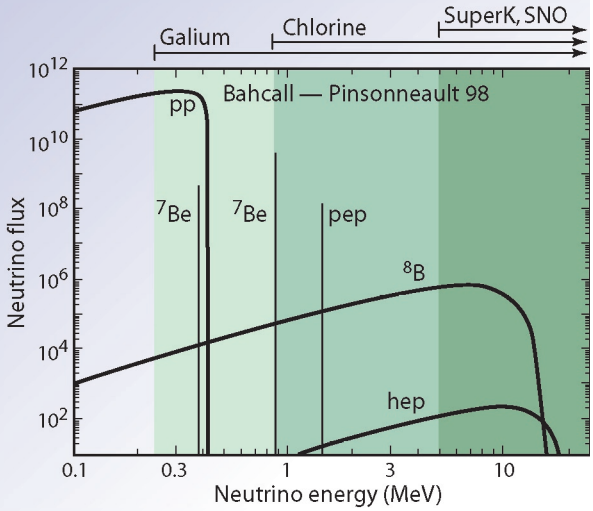

Figure 1. The solar-neutrino energy spectrum as computed by Bahcall and Pinsonneault.[3] Terrestrial-solar-neutrino experiments have measured neutrinos from the sun across the entire energy spectrum. The low-energy radiochemical experiments determine an integral flux of solar neutrinos above their respective thresholds. The water Cerenkov detectors, SuperKamiokande (SuperK) and SNO, measure the ^{8}B flux of solar neutrinos directly.

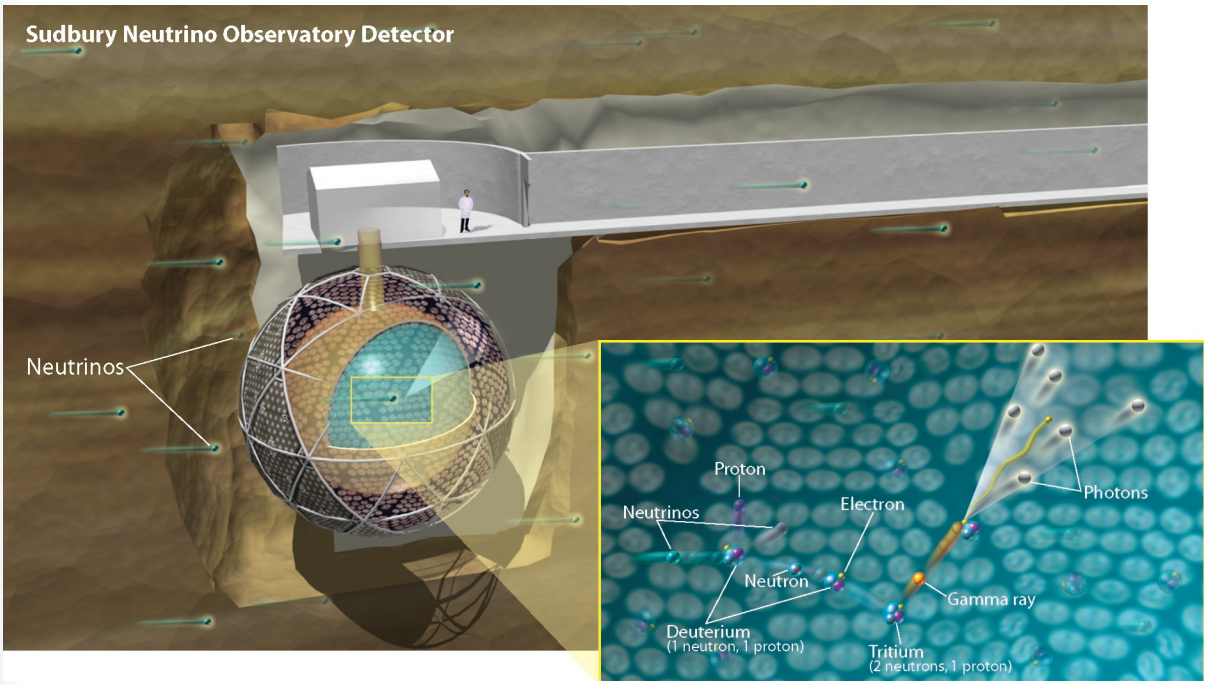

Figure 2. Three-dimensional rendering of SNO. In one of three neutrino reactions (in the inset) detected by SNO, a neutrino entering the detector interacts with a deuterium nucleus. The reaction produces a proton, neutrino, and neutron. The neutron is captured by another deuterium nucleus, producing a tritium atom in the process. The tritium atom decays and in that process releases a gamma ray, which then collides with an electron. Cerenkov light is emitted and detected by PMTs that line inside of the SNO vessel.

50 tons of metallic gallium in which the neutrinos that drive the primary energy-producing fusion reaction in the sun whereby two protons (p-p) fuse to form deuterium can transform the ^{71}Ga nuclei into ^{71}Ge. The individual atoms of germanium that are formed are chemically extracted and counted when they decay back to ^{71}Ga. This measurement provided the first determination of the total flux of neutrinos from the sun and produced a very significant finding—the reduction in flux that had been observed in high-energy neutrinos also extends down to low-energy neutrinos. Measurements of the visible solar luminosity determine uniquely how many of the low-energy p-p neutrinos are produced in the sun. The SAGE results are very hard to understand unless neutrinos oscillate and provide a critical ingredient in resolving the puzzle of the missing solar neutrinos.

For more than three decades, solar-neutrino experiments have been performed in parallel with detailed SSM predictions of the solar-neutrino flux and energy spectrum.[3] With data spanning essentially the entire solar-neutrino spectrum (Figure 1), a Solar Neutrino Puzzle (SNP) emerges wherein the fluxes measured in terrestrial detectors fall significantly short of SSM predictions.[1] The SSM is constrained by knowledge of the solar luminosity and is now independently tested using helioseismology. The data are inconsistent with a sun that "shines" based upon our basic notions of stellar evolution and the basic tenets of nuclear and particle physics—which hint of new physics not contained in the present Standard Model of elementary particles. In particular, electron neutrinos born in nuclear fusion reactions powering the sun are thought to somehow transform into different types of neutrinos that go undetected in experiments on the earth—a hypothesis known as *neutrino-flavor transformation.*[4] Because the sun is energetic enough to produce only electron neutrinos and because, until recently, terrestrial detectors are sensitive largely only to electron neutrinos, the SNP can be resolved if sun-born electron neutrinos are somehow transformed to muon and/or tau neutrinos before their arrival on the earth. Testing neutrino-flavor transformation requires a solar-neutrino detector that can detect the disappearance of electron neutrinos and the appearance of muon and/or tau neutrinos.

The SNO experiment may realize the possibility of neutrino-flavor transformations. At the heart of the SNO detector is 1,000 tonnes of ultra-pure heavy water (D_2O), which serves as a neutrino target. Neutrino interactions are identified through the production of Cerenkov light detected in an array of 10,000 PMTs (Figure 2). The SNO experiment exploits three unique interactions of ^{8}B solar neutrinos on deuterium (^{8}B is an element produced in the sun; it beta decays to produce electron neutrinos):

$$\text{(CC)} \quad \nu_e + d \rightarrow p + p + e^- - 1.44 \text{ MeV},$$

$$\text{(ES)} \quad \nu_x + e^- \rightarrow \nu_x + e^-, \text{ and}$$

$$\text{(NC)} \quad \nu_x + d \rightarrow p + n + \nu_x - 2.22 \text{ MeV}.$$

The charged-current (CC) interaction can proceed only with electron neutrinos incident on deuterium, whereas the neutral-current (NC) interaction can proceed with equal probability for all active neutrino flavors. The elastic-scattering (ES) interactions are also sensitive to all active neutrino flavors; however, the cross-section is about 6.5 times larger for electron neutrinos than for muon and/or tau neutrinos. The basic concept relies on a direct comparison of the CC flux to that measured in the ES and/or NC channels. A measurement of high ES and/or NC fluxes relative to the CC flux would provide a smoking gun for active neutrino-flavor transformation of electron neutrinos into muon and/or tau neutrinos.

SNO is a heavy-water Cerenkov detector that took over a decade in the making with some 100 collaborators in Canada, the U.S., and the United Kingdom (Figure 2). Its results are best represented in terms of the *flavor content* of the ^{8}B solar-neutrino flux depicted in Figure 3. In the simplest sense, the 35-year-old SNP is resolved with data from the SNO experiment. The deficit of electron neutrinos born in the sun is a result of flavor transformation into muon and/or tau neutrinos that are now detected at earth through the unique NC interaction in SNO. Moreover, the total flux of ^{8}B neutrinos extracted from this measurement is in very good agreement with predictions of the SSM. Consequently, our basic concepts of how the sun shines appear intact, and we have witnessed the discovery of new physics in the guise of solar-neutrino flavor transformation. We now know that this flavor transformation definitely results because neutrinos have non-zero mass and that neutrino oscillations occur in nature.

Conclusion

Present and future plans for SNO. These milestone results from SNO were obtained while operating the detector during the "pure-D_2O" phase from November 2, 1999, through May 28, 2001.[5,6,7] The NC rate of solar neutrinos was deduced by counting the neutrons liberated when neutrinos disintegrate the deuteron. In D_2O, this signal ensues from the Cerenkov light produced when these neutrons recapture on deuterium and create 6.25-MeV gamma rays in the process. Significant improvements in precision can be made in the "dissolved-salt" phase in SNO whereby the detector is operated after dissolving 2 tonnes of NaCl into the 1,000-tonne D_2O volume. In addition, because of the multi-gamma cascade associated with neutron capture on chlorine, an additional degree of freedom, or "event isotropy," allows for better separation of the various solar-neutrino signals. The SNO detector has been operating in the dissolved-salt phase since mid May 2001. Results from the dissolved-salt phase have recently been released[8]; these results improve sensitivity to the NC by about a factor of three over the pure-D_2O phase with significant improvement in the constraints on fundamental neutrino parameters (Figure 4).

Ultimately, the CC and NC signals will be independently and simultaneously extracted in SNO by detecting neutrons in a discrete array of neutral current detectors (NCDs) comprised of some 400 m of ultra-low-background ^{3}He proportional counters. A research and development program was started over a decade ago at LANL to develop an NCD array with intrinsically low radioactivity and with the capability of operating effectively under water. In collaboration with colleagues at the University of Washington and Lawrence Berkeley Laboratory, we have completed a full-scale construction of the NCD array. Plans are under way to deploy the array into SNO now that the dissolved-salt phase is complete.

New-generation experiments. With data from the SNO experiment, the 35-year-old SNP is resolved, and we now know that neutrinos have mass and that neutrino oscillations occur. Improvements in precision measurements at SNO will better define the neutrino mass and mixing parameters and further test our models of stellar evolution. Nonetheless, fundamental questions remain for the neutrino sector that cannot be addressed in existing experiments.

The evidence for neutrino oscillations described above constrains the flavor-mixing parameters but only for the splitting of the mass between the different neutrino states. Determining the absolute mass scale for the neutrinos (which is now known to be very small relative to the other elementary particles in nature) is also interesting. One exciting possibility for determining the absolute scale of neutrino mass is zero-neutrino double-beta decay. Two-neutrino double-beta decay is a second-order weak process that has been observed

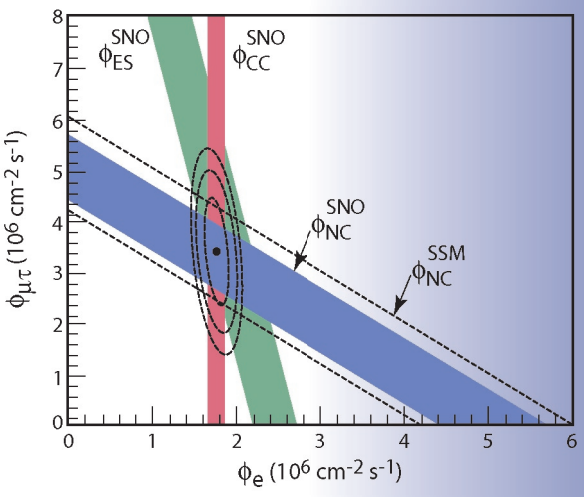

Figure 3. Flavor-content analysis of the ^{8}B solar-neutrino flux based upon data from the SNO experiment. Two-thirds of the electron neutrinos born in the sun disappear because of active neutrino-flavor transformation whereby they reappear as muon and/or tau neutrinos in the SNO detector. The total flux of ^{8}B neutrinos is in very good agreement with SSM calculations.

although it is very rare. A typical half-life is 10^{20} years, which is long compared to the age of the universe (~ 10^{10} years). A more interesting process, if it exists, is neutrinoless double-beta decay. This process, where no neutrinos are emitted, requires special characteristics of the neutrino and incorporates a two-step process. In both steps of this exchange, an electron would be emitted; however, no neutrino is released. For the exchange to take place, there must be no distinction between a neutrino and an anti-neutrino. If the neutrino has this property, we refer to it as a *Majorana* neutrino. Additionally, neutrinoless double-beta decay requires that neutrinos be the massive Majorana flavor. The Majorana Project at LANL will use 500 kg of enriched ^{76}Ge to search for this rare process with unprecedented precision.

In addition to the Majorana project, new research and development efforts are also under way at LANL to obtain a detector that can detect low-energy solar neutrinos in real time. About 90% of the solar-neutrino flux is contained below an energy threshold of 1 MeV, which is far below the achievable threshold of a Cerenkov detector such as SNO. A detector with such low-energy capability would serve as the best means for a precision measurement of neutrino parameters and would test models of stellar evolution at the 1% level. Interestingly enough, such detectors, including perhaps the Majorana detector, could serve a valuable dual role. If the intrinsic radioactivity of these detectors can be achieved with a very-low-energy threshold, then they can also be used to intensively search for the missing energy (or dark matter) of the universe.

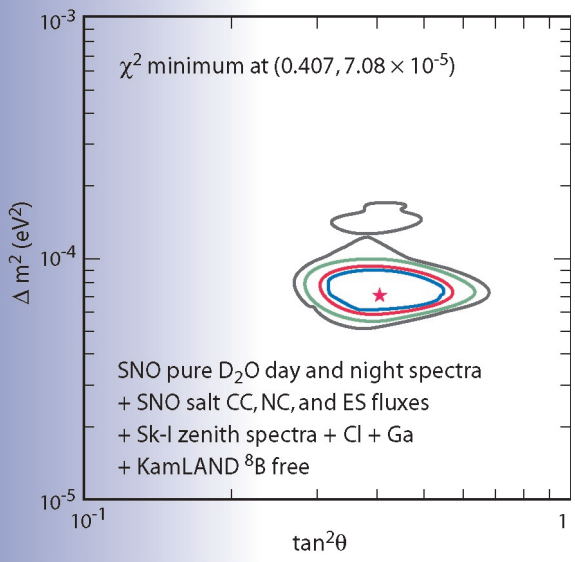

Figure 4. Constraints on the solar-neutrino mass and mixing parameters based on a global fit to all existing solar-neutrino and reactor-neutrino data. The central star indicates the best-fit value as indicated by the parameters found at minimum chi-square. Contours are shown at the 90%, 95%, 99%, and 99.73% confidence levels.

References

1. A. Hime, "Exorcising ghosts–In pursuit of the missing solar neutrinos," *Celebrating the Neutrino, Los Alamos Science* **25**, 137-151 (1997).
2. T.J. Bowles, "The Russian-American gallium experiment," *Celebrating the Neutrino, Los Alamos Science* **25**, 152-155 (1997).
3. J.N. Bahcall, *Neutrino Astrophysics* (Cambridge University Press, 1989).
4. R. Slansky, S. Raby, T. Goldman, and G. Garvey, "The oscillating neutrino–An introduction to neutrino masses and mixing," *Celebrating the Neutrino, Los Alamos Science* **25**, 28-77 (1997).
5. SNO Collaboration, "Measurement of the rate of electron neutrino interactions produced by ^{8}B solar neutrinos at the Sudbury Neutrino Observatory," *Physical Review Letters* **87**, 071301 (2001).
6. SNO Collaboration, "Direct evidence for neutrino flavor transformation from neutral-current interactions in the Sudbury Neutrino Observatory," *Physical Review Letters* **89**, 011301 (2002).
7. SNO Collaboration, "Measurement of day and night neutrino energy spectra at SNO and constraints on neutrino mixing parameters," *Physical Review Letters* **89**, 011302 (2002).
8. SNO Collaboration, "Measurement of the total ^{8}B solar neutrino flux at SNO with enhanced neutral-current sensitivity," to appear in *Physical Review Letters* (2003).

Acknowledgment

We gratefully acknowledge the support of the DOE Office of Nuclear Physics and the LANL LDRD Program.

For more information, contact Andrew Hime at 505- 667-0191, ahime@lanl.gov.

Accelerator Neutrino Experiments on the LSND and MiniBooNE

W.C. Louis III (P-25), representing the LSND and MiniBooNE Collaborations

The neutrino is one of the most elusive particles in the universe, yet it exists in great abundance and is a fundamental element in the universe's subatomic structure. Because these low-energy particles interact weakly with other particles, neutrinos had defied detection for years until 1953 when LANL scientists Fredrick Reines (Figure 1) and Clyde Cowan, Jr., detected these elusive particles in experiments that used liquid scintillator detectors at reactors in Washington and South Carolina. The neutrino, originally thought to be massless, exists in three distinct states (commonly called "flavors")—electron, muon, and tau forms.

LANL researchers used the LSND[1] from 1993–1998 to conduct experiments designed to collect data and obtain evidence that neutrinos oscillate from the muon neutrino form into the electron neutrino form. Neutrino oscillations are the transformation of one neutrino flavor into another neutrino flavor, and these transformations occur only if neutrinos have mass and if there is mixing among the neutrino flavors. The LSND results imply that neutrinos constitute at least 1% of the universe's total mass. MiniBooNE,[2] which is now operational at FNAL in Illinois, is the first phase of the larger BooNE that will definitively test the LSND evidence for neutrino oscillations and precisely measure the oscillation parameters. MiniBooNE is looking for oscillations of muon neutrinos (ν_μ) into electron neutrinos (ν_e). A large tank filled with mineral oil (CH_2) is used to look for particles produced when neutrinos hit the nuclei of the atoms that make up the oil. The signature of such an interaction is a cone of light, known as Cerenkov light, which hits light-sensitive devices (PMTs) mounted on the inside surface of the tank. If successful, MiniBooNE will provide a unique environment to observe physics beyond the Standard Model.

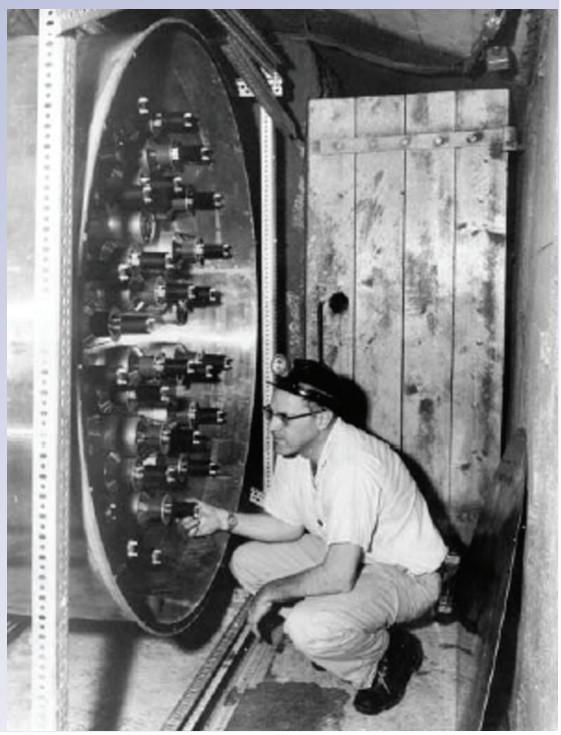

Figure 1. Fred Reines working on an underground neutrino experiment at a South African mine in 1966 (photo courtesy of the University of California, Irvine).

LSND—The Foundation for Future Neutrino Research

The LSND experiment was designed to search for oscillations of muon antineutrinos to electron antineutrinos ($\bar{\nu}_\mu \rightarrow \bar{\nu}_e$) from positively charged muon (μ^+) decay at rest (DAR) with high sensitivity. (The LSND collaboration consisted of groups from eleven organizations, including LANL). Over the six-year running period from 1993–1998, the LANSCE accelerator delivered 28,896 C (~ 0.3 g) of protons to the production target. The resulting DAR neutrino fluxes were well understood because almost all detectable neutrinos arose from positively charged pion (π^+) or μ^+ decay.

The LSND was an 8.3-m-long, 5.7-m-diam cylindrical tank that contained 167 tons of mineral

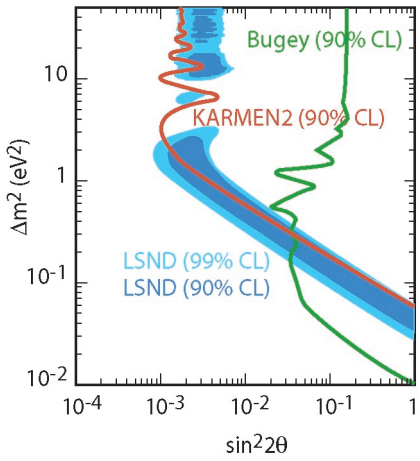

Figure 2. The ($sin^2 2\theta$, Δm^2) oscillation parameter fit for the entire LSND data sample. (CL is "confidence level.")

oil with a dab of scintillating compound to amplify light signals used to reconstruct neutrino events. The Cerenkov light (described later) from these events was detected by 1,220 PMTs (each 8 in.) located on the inside surface of the LSND tank. The PMTs convert the light into electrical signals, which are gathered and interpreted by data-acquisition computers. The center of the LSND was 30 m from the neutrino source. The main veto shield consisted of a 15-cm layer of liquid scintillator in an external tank and 15-cm layer of lead in an internal tank. Designed to search for the presence of electron antineutrinos with great sensitivity, the LSND witnessed over 80 neutrino events that were consistent with muon antineutrinos oscillating into electron antineutrinos.

The primary neutrino-oscillation search in LSND was for $\overline{\nu}_\mu \rightarrow \overline{\nu}_e$ (i.e., a muon antineutrino to an electron antineutrino), where the $\overline{\nu}_\mu$ arise from DAR μ^+ in the beam stop, and the ν_e are identified through the reaction $\overline{\nu}_e p \rightarrow e^+ n$. This reaction allowed a two-fold signature of a positron with a 52.8-MeV endpoint and a correlated 2.2-MeV gamma ray (γ) from neutron capture on a free proton. More events were observed than expected, and the excess was consistent with neutrino oscillations.

Figure 2 shows the ($sin^2 2\theta$, Δm^2) oscillation parameter fit for the entire data sample, $20 < E_e < 200$ MeV. The mixing angle between the two neutrinos is "$sin^2 2\theta$," and the difference in masses squared of the two neutrinos is "Δm^2." The fit includes both $\overline{\nu}_\mu \rightarrow \overline{\nu}_e$ and $\nu_\mu \rightarrow \nu_e$ oscillations and all known neutrino backgrounds. The inner and outer regions correspond to 90% and 99% confidence-level allowed regions, whereas the curves are 90% confidence-level limits from the Bugey reactor experiment and the KARMEN2 experiment at ISIS, the Rutherford-Appleton Laboratory Neutron Facility in the United Kingdom. The allowed region that is most favorable is the band from 0.2–2.0 eV^2, although a region around 7 eV^2 is also possible.

MiniBooNE—The First Phase for Confirmation of Neutrino Oscillations

The MiniBooNE detector consists of a 12-m-diam spherical tank contained within a cylindrical vault (Figure 3a and b). An inner tank supports 1,280 individual PMTs pointed inward and optically isolated from the tank's outer region, which contains an additional 240 PMTs (Figure 3c). The inner tank is filled with 800 tons of mineral oil, which is the equivalent of 44 tanker trucks filled with liquid. An outer tank serves as a veto shield for identifying particles both entering and exiting the detector. MiniBooNE is located ~ 500 m from FNAL's neutrino source, and it detects one neutrino collision every 20 s. For this first phase of the experiment, we expect to detect one million neutrino events per year.

In MiniBooNE, the 8-GeV protons from FNAL's Booster accelerator interact with the atoms in a beryllium target located inside a magnetic focusing horn (Figure 4). (The Booster accelerator can reliably deliver protons for most of a calendar year, which allows the experiment to receive up to ~ 5×10^{20} protons per year.) The positively charged

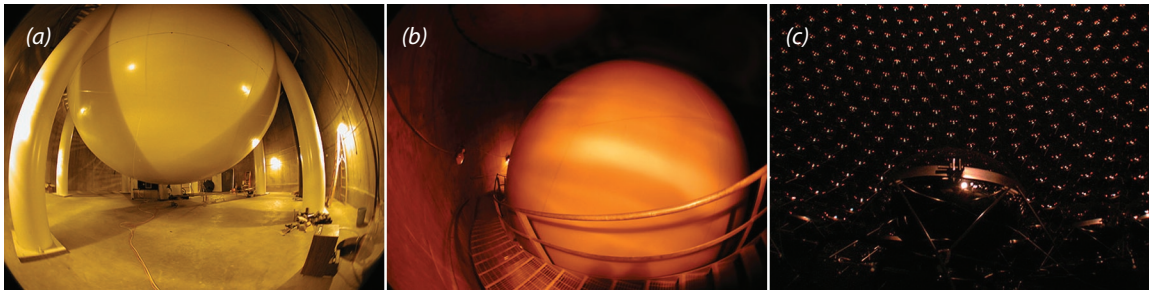

Figure 3. The MiniBooNE detector tank viewed from the floor (a) and from the stairway (b) in the underground vault. (c) A portion of the PMTs installed inside the detector.

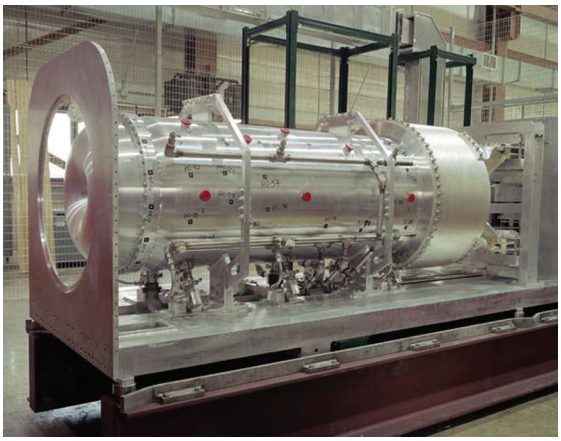

Figure 4. FNAL's magnetic focusing horn. The beryllium target that produces pions through proton interactions with the target material is located in the upstream position inside the horn.

pions (π) produced from these interactions are focused by the magnet horn into a 2-m-diam, 50-m-long steel pipe where they decay into muon neutrinos (ν_μ). At the end of the decay pipe, a concrete/steel absorber stops all particles except the muon neutrinos, which continue through ~ 450 m of earth to reach the detector tank. The muon neutrinos—delivered in bursts that last 1.6 millionths of second, 5 times per second—collide with carbon atoms in the mineral oil, producing muons (μ^+). These subatomic charged particles create cones of Cerenkov light—a key factor in these experiments—as they travel through the mineral oil. (Cerenkov light is essentially the electromagnetic equivalent of a sonic boom. It travels to the edges of the detector tank where the PMTs receive the light and convert it to electrical signals.)

Some of the muon neutrinos entering the detector tank can oscillate into electron neutrinos (ν_e) *before* they collide with carbon atoms. If this occurs, electrons (instead of energetic muons) will be produced when the electron neutrinos collide with the carbon atoms in the mineral oil. The electrons scatter and quickly come to rest after colliding with atoms in the mineral oil. The subsequent Cerenkov cone of light is distinct (i.e., the inner and outer edges of the cone are hazy) from that produced by other interactions within the detector tank. If MiniBooNE verifies the LSND experiment, then approximately 1,000 $\nu_e C \rightarrow e^- X$ events should be observed above background from $\nu_\mu \rightarrow \mu_e$ oscillations. There are three main backgrounds to the oscillation search: (1) intrinsic ν_e background in the beam from μ and K (kaon) decay in the decay pipe, (2) misidentified μ events ($\nu_\mu C \rightarrow \mu^- X$), and (3) misidentified π^0 (pion) events ($\nu_\mu C \rightarrow \nu_\mu \pi^0 X$). Figure 5 shows the expected oscillation sensitivity for the two-year ν_μ or $\overline{\nu}_\mu$ run cycle.

The MiniBooNE detector and beam are now fully operational and taking data. The detector was calibrated with laser-calibration events; the energy scale and resolution were determined from cosmic-muon and Michel-electron events, and approximately 160,000 clean neutrino events were recorded after the first year of data taking with about 1.5×10^{20} protons on target. At present, the experiment is clearly reconstructing both $\nu_\mu C \rightarrow \mu^- X$ charged-current events and $\nu_\mu C \rightarrow \nu_\mu \pi^0 X$ neutral-current events, which are the two main backgrounds to the $\nu_\mu \rightarrow \nu_e$ oscillation search. As shown in Figure 5, π^0 events are being reconstructed at approximately the correct mass with a mass resolution of about 21 MeV.

The current plan is to run the first two full years (1×10^{21} protons on target) with ν_μ and then switch to a $\overline{\nu}_\mu$ run cycle. First results are expected by 2005, and if the LSND oscillation signal is confirmed, a BooNE detector will then be built at a different distance than the MiniBooNE detector to obtain the highest precision measurement of the oscillation parameters.

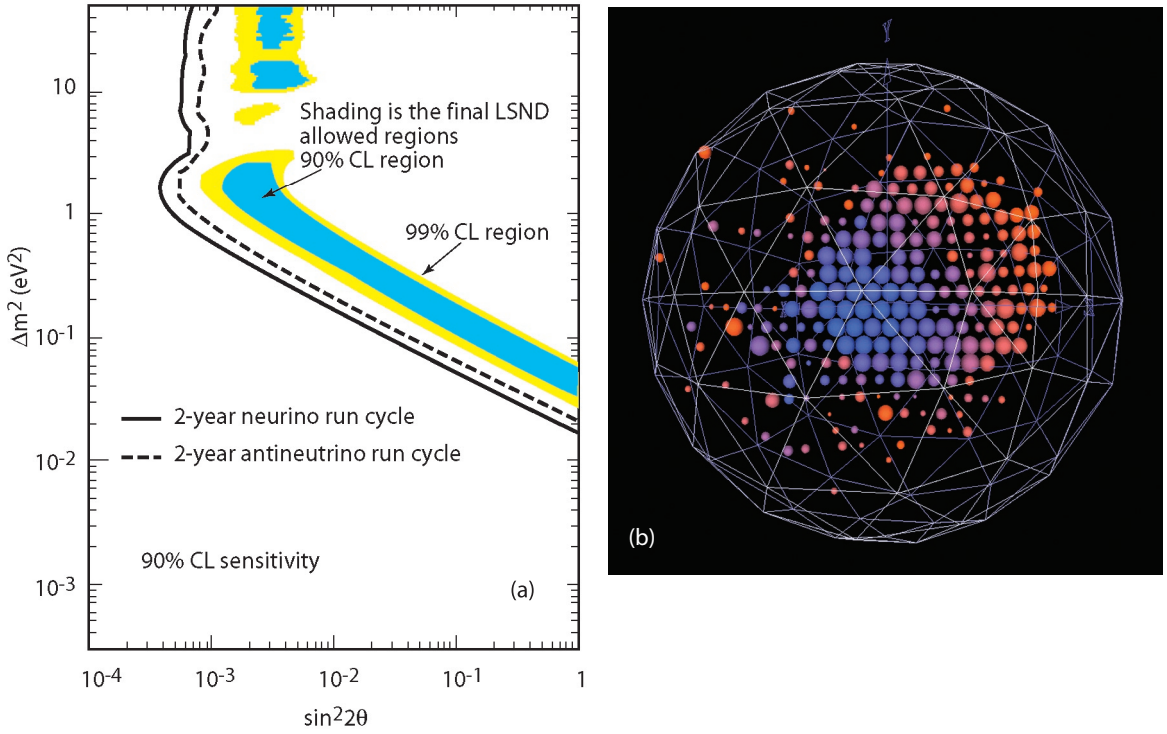

Figure 5. (a) The MiniBooNE expected oscillation sensitivity for a full two-year run cycle. (CL is "confidence level.") (b) A typical MiniBooNE neutrino-induced event. The colors relate to elapsed time; the blue represents early PMT hits and the orange reprsents later PMT hits. In this particular data event, there were less than 6 veto hits and over 200 tank hits.

Conclusion

The confirmation of neutrino oscillations at high Δm^2 would have a huge impact on astrophysics, as well as particle and nuclear physics. When combined with the evidence for neutrino oscillations from solar and atmospheric neutrino experiments, the present data seem to imply physics beyond the Standard Model, such as the existence of light, sterile neutrinos or the violation of CPT. (CPT is the combined operation of charge conjugation, parity inversion, and time reversal.) The MiniBooNE experiment at Fermilab will provide a definitive test of the LSND evidence for neutrino oscillations.

References

1. A. Aguilar *et al.*, *Physical Review D* **64**, 112007 (2001).
2. E. Church *et al.*, "A proposal for an experiment to measure $\nu_\mu \rightarrow \nu_e$ oscillations and ν_μ disappearance at the Fermilab booster: BooNE," LANL report LA-UR-98-352 (FNAL experiment 898); A. O. Bazarko, *Nuclear Physics B* **91**, 210 (2001).

Acknowledgment

This research was made possible by the dedicated accelerator operational support at both LANL and FNAL. Funding support for P-25 work from the DOE Office of Nuclear Physics and the LANL LDRD program is gratefully acknowledged.

For more information, contact Bill Louis at 505-667-6723, louis@lanl.gov.

The Electric Dipole Moment of the Neutron

S.K. Lamoreaux (P-23), representing the EDM collaboration

We have a general notion of the meaning of the term "symmetry" particularly in regard to art and biology. In biological systems, symmetry at the molecular level has been known since 1848 when Pasteur discovered that tartaric acid could exist in two forms (e.g., "left-handed" and "right-handed," referred to as stereoisomers) that are mirror images of each other. Both forms are produced in inorganic processes, whereas only one-handedness is produced by or is useful to natural organic processes. The very fact that molecules can exist with either handedness implies that the atomic constituents are themselves very highly symmetric. This is expected because the electrostatic interaction that binds electrons in atoms does not distinguish between left and right.

In 1949, Norman Ramsey and Ed Purcell questioned the character of the nuclear force, in particular, whether it "conserved parity symmetry," P, which is to ask whether the force is the same if viewed as a mirror image (e.g., if left and right are important). They concluded that lack of P conservation would imply the possible existence of an EDM of the neutron. Shortly after, P asymmetry was observed in radioactive decay and subsequent theoretical work showed that a neutron EDM (nEDM) would require the existence of time reversal (T) asymmetry in addition to P asymmetry. As in the case of the question of P symmetry, in our daily lives we know that just as there is a distinction between left and right, there is a distinction between time moving forward and backward. If we drop a glass object on the floor and see it shatter, we do not expect to see the pieces subsequently come back together and the

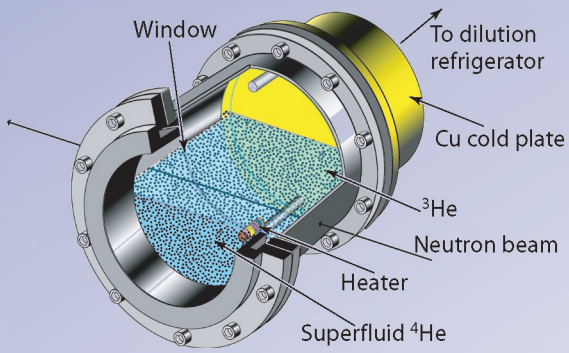

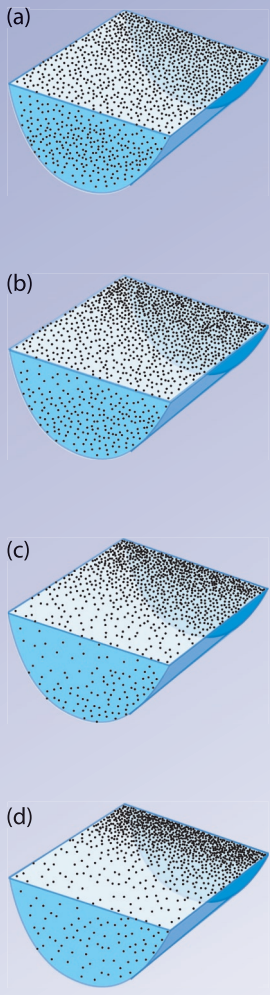

Figure 1. A three-dimensional rendering of the apparatus used to measure the diffusion and distribution of ^{3}He (dots) in superfluid ^{4}He (blue liquid in the bottom half of the cryostat cylinder). The window at the near end of the cylindrical cryostat is normally covered by a PMT, which is used to detect the scintillation light. The neutron beam enters from the right. The horizontal cryostat is mounted on a motion-controlled frame that allows it to be moved in two dimensions transverse to the beam. The effects of increasing heater power on the ^{3}He distribution in the cell are shown in the panels along the right side [Figure 1(a) through (d)]. In each case, the ^{3}He (dots) rapidly migrates away from the heater and towards the end of the cryostat connected to the dilution refrigerator. Figure 1(a) through (d) shows that the migration becomes more pronounced as the heater is set to 1, 2, 3, and 10 (arbitrary) heat units, respectively.

object jump back into our hand. However, nothing in the microscopic interactions that describe the object, its falling, and its subsequent shattering precludes this possibility. In this case, the direction of time we perceive is because such odd behavior is so improbable as to be impossible. As of 1964, it was assumed that the fundamental interactions governing the microscopic behavior of matter were time-reversal symmetric and that the flow of time in the universe was due to statistics as in the case of the shattering glass.

In 1964, T asymmetry, in addition to P asymmetry, in a fundamental interaction was (indirectly) observed in the decay of the "strange" K_0 meson. This again opened the possibility of an nEDM, and experimental limits on the possible size of the nEDM have been crucial in establishing the veracity of theories put forward to explain K_0 decay. The continuously improving nEDM experiments, with sensitivity increased by 9 orders of magnitude since 1950, have ruled out more theories than any other set of experiments in the history of physics. At the present level of EDM experiments, theoretical extensions to the so-called Standard Model, such as "supersymmetry," are being stringently tested.

The nEDM

A neutron has three quarks, a net charge of zero, and a magnetic moment. An nEDM would be evidence that the charge distribution of the internal quark constituents of the neutron is displaced relative to the center of mass. This displacement must lie along the neutron spin along with the magnetic moment.[1]

The usual technique employed for measuring the nEDM is magnetic resonance. When a polarized neutron is placed in parallel electric and magnetic fields, the spin precesses at the Larmor frequency (modified by the electric-field term)

$$f = \gamma B \pm 2dE, \qquad (1)$$

where γ = 3 Hz/mG (milli-Gauss) is the neutron gyromagnetic ratio, B is the applied magnetic field (typically, 10 mG or less), d is the nEDM usually expressed in "electron-centimeters" ($e$cm), and E is the applied electric field (typically 10 kV/cm)—the factor two in the second term results from the fundamental definition of the EDM. Under T reversal, the sign of B changes relative to E. We can produce this reversal in the laboratory by reversing E; a change in precession frequency with this reversal would be a direct detection of T asymmetry. The figure of merit, F, for an nEDM experiment is

$$F = E\sqrt{N\tau}, \qquad (2)$$

where E is the applied electric field, N is the number of neutrons measured per measurement cycle, and τ is the coherence time of the spin precession. The present best limit for the nEDM results from an experiment that employs spin-polarized UCNs stored for about 100 s in a 10 kV/cm electric field.[2]

UCNs are neutrons with kinetic energy so low they can be reflected from material surfaces for all angles of incidence. The energy of a UCN ($< 300 \times 10^{-9}$ eV) corresponds to a velocity of less than 7 m/s (just about the speed required for a four-minute mile!) and an effective temperature of 0.005 K.[3] UCNs can be stored in "bottles" for times approaching the β-decay lifetime of the neutron (~ 900 s).

Because the neutron precession frequency depends on the value of the magnetic field (see Equation 1), a spurious magnetic field associated with application of the electric field (caused by leakage currents, for example) can create a "false" or systematic EDM signal. To account for this possibility, the most recent experiment employs a "co-magnetometer" based on a dilute spin-polarized ^{199}Hg gas that fills the UCN storage vessel and is detected optically.

The results of this work limit the nEDM to $d < 5 \times 10^{-26}$ $e$cm. To understand the smallness of this limit, if the neutron were enlarged to the size of the earth, the displacement of the charge would correspond to about one wavelength of visible light.

An nEDM Experiment in Superfluid ^{4}He

For the experiment described in Reference 2, the UCN density was limited to 50/cm^3. More effective "superthermal processes" of producing UCNs are now under study at LANL.[4] In a superthermal source, relatively high-energy neutrons with an effective temperature of 10 K to 100 K (as a result of conventional moderation) inelastically scatter to lower energy in a material and become UCNs. If the scattering material is in a UCN storage bottle, the UCNs are trapped (the incoming high-energy neutrons easily penetrate the bottle). If the scattering material is at a very low temperature, the inverse process of inelastic scattering to high energy is impossible. Furthermore, if the material has low neutron absorption, the density of UCN builds

up until the rate of production equals the rate of loss due to β-decay and unavoidable losses on the storage-bottle surfaces. Two effective superthermal converters are superfluid ^{4}He and solidified deuterium gas. Superfluid ^{4}He is a nearly perfect superthermal converter because it has no nuclear absorption. We anticipate that we can obtain a UCN density of over 500/cm^3; we demonstrated the basic technology at the LANSCE in December 2001. We are proposing a new type of nEDM experiment based on this technology[1,5] and expect a possible factor of 100 improvement in the experimental limit, because we anticipate

- a factor of 5 increase in the electric field because of the good dielectric properties of superfluid helium,
- a factor of 100 increase in the number of stored UCNs, and
- a factor of 5 increase in the spin coherence time.

Using Equation 2 above, this implies a factor of about a 100 increase in the figure of merit.

^{3}He Magnetometry

The only substance that can dissolve and remain in solution in superfluid ^{4}He at low temperatures is the rare isotope ^{3}He. ^{3}He has an intrinsic nuclear spin of one-half and a magnetic moment. Furthermore, it is expected to have an extremely small EDM because of shielding by the atomic electrons. ^{3}He can be polarized and dissolved in superfluid ^{4}He, and we are presently studying the possibility of using it for a co-magnetometer in a superfluid ^{4}He nEDM experiment.

It is well-known that ^{3}He absorbs neutrons readily, with the reaction yielding a proton, a triton, and 764 keV of kinetic energy. The energy released by this reaction creates scintillation light in superfluid helium, and the fact that such a reaction occurred can be readily detected. Furthermore, the reaction is spin-dependent; when the ^{3}He and UCN spins are parallel, there is no reaction, but if the spins are oppositely directed, the reaction rate is twice the unpolarized rate.

If the UCN and ^{3}He spin polarization are perpendicular to the applied magnetic field, they will precess at their respective Larmor frequencies, which are the same to within 10% because the gyromagnetic ratios are equal to within 10%. The spin polarizations will oscillate between being parallel and antiparallel, and the scintillation light will be modulated at 10% of the Larmor precession frequency. A change in this frequency with a change in the electric field orientation would be evidence for an nEDM.

Because the ^{3}He-UCN relative precession rate is sensitive to the static magnetic field, our experiment still needs a co-magnetometer. In practice, monitoring the field external to the UCN storage volume does not provide an adequate measure of systematic magnetic fields (e.g., due to leakage currents) seen by the UCN.[1,2] Our current plan is to use SQUID sensors to directly monitor the ^{3}He precession to provide a measurement of the time- and volume-average magnetic field seen by both the ^{3}He atoms and the UCN while they are being stored together. SQUID sensors being studied by P-21 have enough sensitivity to measure the magnetic fields from a functioning brain and therefore will have sufficient sensitivity to detect the magnetic field from the population of precessing ^{3}He atoms as proposed in the EDM experiment. Experiments at LANL have focused on proving that SQUID sensors will perform in the environment of the proposed EDM experiment.[5,6]

The Diffusion of ^{3}He Atoms in Superfluid Helium

For ^{3}He atoms to be effective as a co-magnetometer, they must uniformly sample the UCN storage bottle. We predicted that the diffusion rate should be proportional to the temperature to the inverse-seventh power. Using the scintillation light from the ^{3}He neutron-capture reaction, we were able to perform tomography on a cylindrical cell 50 mm in diameter and 50 mm long. We used the cold neutron beam on flight path 11A (located at the Lujan Center at LANSCE), collimated to a

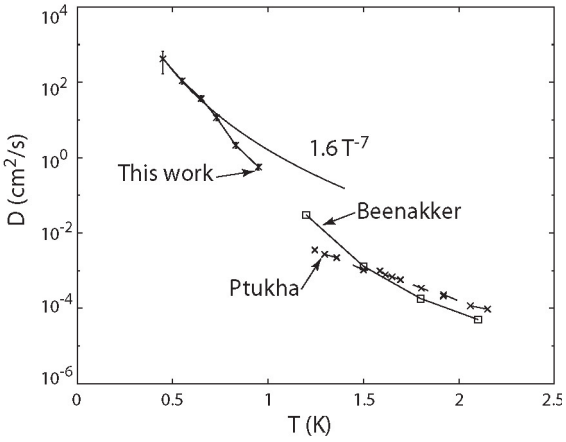

Figure 2. Our experimental results for the diffusion coefficient compared to previous measurements.

diameter of about 2 mm. The cell was mounted on a horizontal dilution refrigerator that could be cooled to 0.3 K. The entire refrigerator/cell cryostat assembly was mounted on a translation apparatus so that it could be moved relative to the fixed cold neutron beam. A three-dimensional rendering of the apparatus is shown in Figure 1. The integrated ^{3}He concentration along a path through the cell was determined by the scintillation rate. The subpanels in Figure 1(a) through (d) show the effects when a heater located near the side of the cell is turned on; the ^{3}He becomes more concentrated at the refrigerated end of the cell.

The results of our experimental measurements of the diffusion coefficient are shown in Figure 2. Our technique allowed extending the measurements from the previous lower limit of 1.2 K to a new lower limit of 0.4 K. Most importantly, we verified that the ^{3}He distribution is uniform (in the absence of a heat flux) and that the diffusion coefficient follows the T^{-7} prediction at temperatures below 0.7 K. These results were published along with an accompanying paper that provides a theoretical analysis of our results.[7]

Conclusion

We are developing a new experiment at LANL to improve the limit of the nEDM by over two orders of magnitude, and we expect to be producing data by 2008. Such an improved limit is crucial to our understanding of T asymmetry in fundamental interactions and has broad applications from elementary particle physics to our understanding of the matter-antimatter asymmetry in the universe.

References

1. I.B. Khriplovich and S.K. Lamoreaux, *CP Violation Without Strangeness* (Springer-Verlag, Heidelberg, 1997).
2. P.G. Harris, C.A. Baker, K. Green *et al.*, "New experimental limit on the electric dipole moment of the neutron," *Physical Review Letters* **82**(5), 904–907 (1999).
3. R. Golub, D.J. Richardson, and S.K. Lamoreaux, *Ultracold Neutrons* (Adam-Hilger, Bristol, 1991).
4. C.L. Morris, J.M. Anaya, T.J. Bowles *et al.*, "Measurements of ultracold-neutron lifetimes in solid deuterium," *Physical Review Letters* **89**(27), 272501 (2002).
5. M.A. Espy, A.N. Matlachov, R.H. Kraus, Jr. *et al.*, "SQUIDs as detectors in a new experiment to measure the neutron electric dipole moment," *IEEE Transactions on Applied Superconductivity* **9**(2), 3696–3699 (1999).
6. M.A. Espy, A.N. Matlashov, R.H. Kraus, Jr., *et al.*, "The temperature dependence of SQUID noise at temperatures below 4 K," *Physica C* **368**, 185–190 (2002).
7. S.K. Lamoreaux, G. Archibald, P.D. Barnes *et al.*, "Measurement of the ^{3}He mass diffusion coeffiecient in superfluid ^{4}He over the 0.45–0.95 K temperature range," *Europhysics Letters* **58**, 718–724 (2002).

Acknowledgment

This work is supported by the LANL LDRD program.

For more information, contact Steve Lamoreaux at 505-665-1768, lamore@lanl.gov, or visit the EDM web page at http://p25ext.lanl.gov/edm/edm.html (which includes a complete list of the experiment's collaborators).

The NPDGamma Experiment

J.D. Bowman, M. Gericke, G.S. Mitchell, S.I. Penttilä, G. Peralta, P-N. Seo, W.S. Wilburn (P-23), representing the NPDGamma collaboration

The nature of weak interactions between strongly interacting hadrons is not well understood. The NPDGamma ($\vec{n} + p \rightarrow d + \gamma$) experiment,[1] currently under construction at the LANSCE, will study the parity-violating weak interaction between the most common hadrons, protons, and neutrons. The hadronic weak interaction is observed in nuclei and nuclear processes,[2] but interpretation of these experiments is difficult because of the complicated many-body dynamics of a nucleus. The goal of the NPDGamma experiment is to measure the parity-violating directional gamma-ray asymmetry in the reaction $\vec{n} + p \rightarrow d + \gamma$ to an accuracy of 5×10^{-9}, which is approximately 10% of its predicted value.[3,4] Such a result, in a simple system, will provide a theoretically clean measurement of the weak pion-nucleon coupling, thus resolving the long-standing nuclear-physics controversy over its value.

Theory Background

The flavor-conserving weak interaction between hadrons is the most poorly tested aspect of electroweak theory.[4] While much is known about quark-quark weak interactions at high energies, the low-energy weak interactions of hadrons (particles made of quarks, such as the nucleons—the proton and the neutron) are not well measured. At low energies, the effects of the weak interaction are typically obscured by other processes, making their experimental study challenging. In terms of the meson-exchange picture of the weak nucleon-nucleon interaction,[4] the weak-pion exchange is particularly interesting because it is the longest-range component of the interaction and is therefore presumably the most reliably calculable. The hadronic exchange of neutral currents, which is expected to dominate the weak-pion exchange between nucleons, has not been isolated experimentally in an unambiguous way. For both of these reasons, the coupling constant, H_π^1, for pion exchange in the weak nucleon-nucleon interaction is of special interest.

An accurate measurement of H_π^1 in a simple nucleon-nucleon system is needed to resolve previous experimental inconsistencies. A two-nucleon system, such as in the $\vec{n} + p \rightarrow d + \gamma$ process, is sufficiently simple that the measured asymmetry of the emitted gamma rays can be related to the weak meson-nucleon-nucleon coupling with negligible uncertainty to nuclear structure. The relationship between the parity-violating asymmetry A_γ and H_π^1 (where A_γ is the correlation between the direction of emission of the gamma ray and the neutron polarization) is calculated to be $A_\gamma \approx -0.045\ H_\pi^1$. The goal of NPDGamma is to measure A_γ to a precision of $\pm 5 \times 10^{-9}$, which will determine H_π^1 to $\pm 1 \times 10^{-7}$. Such a result will clearly distinguish between the values for H_π^1 extracted from experiments in nuclear systems and between predictions by various theories of the weak interaction of hadrons in the nonperturbative QCD regime.

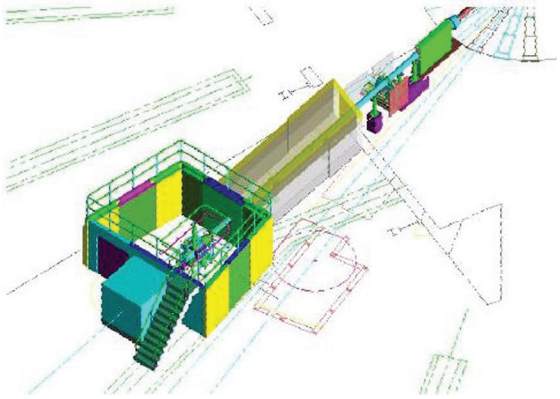

Figure 1. Depiction of FP12 at the Lujan Center at LANSCE. Construction of the flight path and the experimental cave is essentially complete. Commissioning of the flight path and the experimental apparatus will begin in January 2004.

NPDGamma Experiment

To determine H_{π}^{1} with an uncertainty of 1×10^{-7}, we must achieve a statistical uncertainty of 0.5×10^{-8} on A_{γ}. This means that the experiment must detect a few $\times 10^{17}$ of the 2.2-MeV gamma-rays from the $\vec{n} + p \rightarrow d + \gamma$ reaction. In addition, possible systematic errors in the experiment require careful attention. The tiny parity-violating signal in the reaction will be isolated by flipping the neutron spin. The real asymmetry will change sign under spin reversal, while spin-independent false asymmetries will not. The weak interaction is the only fundamental-particle interaction that can produce a parity-violating signal; parity violation is simply described as a difference between a physical process and its mirror image. For example, in the $\vec{n} + p \rightarrow d + \gamma$ reaction, if more gamma rays are emitted in the same direction as the neutron spin, rather than in the opposite direction, then that is a parity-violating signal and must be caused by the weak interaction. The experiment then consists of observing the direction of emission of the gamma rays from many $\vec{n} + p \rightarrow d + \gamma$ captures, and if there is an asymmetry in their distribution with respect to the neutron-polarization direction, the effect of H_{π}^{1} has been observed.

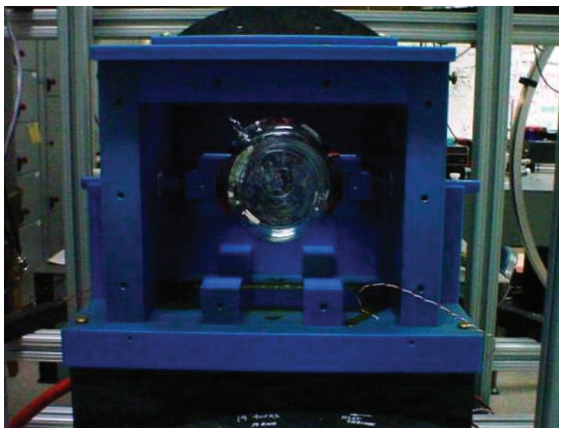

Figure 2. The ^{3}He spin filter used to polarize the neutron beam. The glass cell is 11 cm in diameter and contains ^{3}He and rubidium. A laser is used to polarize the rubidium atoms, which then transfer their polarization to the ^{3}He nuclei. The blue structure is used to support the glass cell and to provide an environment where it can be kept at a warm temperature (150°C) to produce rubidium vapor.

The requirements for the experiment are a large number of polarized, cold neutrons; a method of flipping the neutron polarization; a proton target; and a detector system for the 2.2-MeV gamma rays. The experiment consists of a pulsed, cold neutron beam, transversely polarized by transmission through polarized ^{3}He, with polarization reversal achieved on a pulse-by-pulse basis by an rf spin flipper. The neutrons are incident on a liquid parahydrogen target. The 2.2-MeV gamma rays from the capture reaction will be detected by an array of cesium-iodide scintillators coupled to vacuum photodiodes and operated in current mode.

Cold Neutron Beam and Polarizer

The experiment requires a high flux of cold neutrons with energies below 15 meV. Although such neutrons are available from cold moderators at both reactors and spallation neutron sources, the nature of the neutron flux from a pulsed spallation source provides a very powerful diagnostic tool for a number of possible systematic effects for this experiment. At LANSCE, the cold neutron source consists of a liquid-hydrogen moderator coupled to the 20-Hz pulsed neutron source. At cold-neutron energies, it is possible to use neutron guides to transport neutrons. Just as a difference in the indices of refraction will cause total internal reflection of light incident at shallow angles on the interface between two media, magnetic properties of the surface of a neutron guide can be used to reflect neutrons incident at glancing angles (below a well-known critical angle) on the guide surface. The function of the neutron guide is to conserve the high cold-neutron flux available near the moderator.

For the experiment, a new beam line and neutron guide, flight path 12 (FP12), have been built at the Lujan Center.[5] A drawing of the FP12 layout with the experimental cave at its end is shown in Figure 1. To observe parity violation (in the distribution of gamma rays with respect to the neutron-polarization direction), the experiment requires polarized neutrons. Cold neutron beams can be polarized in several ways, but the best technology for NPDGamma is a ^{3}He spin filter.[6] ^{3}He spin filters (Figure 2) are compact, possess a

large phase-space acceptance, produce a negligible fraction of capture gamma-ray background, and do not require strong magnetic fields or produce field gradients. This is important for the control of systematic errors in the experiment. The thickness of the spin filter can be optimized for polarization versus transmission.

Neutron Spin Flipper

For NPDGamma, the neutron spins are flipped on a 20-Hz pulse-by-pulse basis with an rf spin rotator, or spin flipper (RFSF). The RFSF is a shielded solenoid that operates according to the well-known principles of nuclear magnetic resonance. In the presence of a homogeneous constant magnetic field and an oscillating magnetic field in a perpendicular direction, the neutron spin will precess, and the amplitude of the oscillating field can be selected to precess the spin by 180° as the neutron travels through the spin-flipper volume. The spin flip is introduced on a pulse-by-pulse basis by simply turning the rf field on and off. The solenoid produces only negligible external magnetic fields and field gradients—an important property given the possible sensitivity of the detector apparatus to magnetic-field-induced gain shifts.

Proton Target

In the liquid-hydrogen (proton) target, it is essential that the polarized neutrons retain their polarization until they are captured. Many of the neutrons will scatter in the target before they are captured, and the spin dependence of the scattering is therefore important. The ground state of the hydrogen molecule (known as parahydrogen) has spin of zero (J=L=S=0), and the first excited state, the lowest orthohydrogen state, is at 15 meV above the parastate. A large fraction of the cold neutrons possess energies lower than 15 meV. Because these neutrons cannot excite the parahydrogen molecule into its first excited state, only elastic scattering and capture are allowed, and spin-flip scattering is forbidden. The neutron polarization therefore survives the scattering events that occur before the capture. Higher-energy neutrons will undergo spin-flip scattering and therefore lose their polarization. The liquid-hydrogen target must be in the parastate. For liquid hydrogen held at 20 K and atmospheric pressure, the equilibrium concentration of parahydrogen is 99.8%, which is low enough to ensure a negligible population of orthohydrogen.

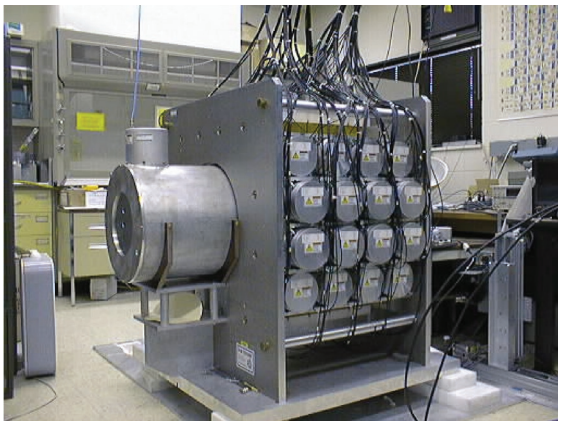

Figure 3. The gamma-ray detector array includes 48 cesium-iodide crystals. The housings of 16 of the crystals are visible in the photo. The effect of the hadronic weak interaction is measured as an asymmetry in the event rate between the upper and lower detector hemispheres. The RFSF is mounted on the left side of the array.

Cesium-Iodide Gamma-Ray Detector Array

Finally, the experiment must detect the 2.2-MeV gamma rays from the neutron capture. Given the small size of the expected asymmetry and the goal precision of the experiment, the number of events required to achieve sufficient statistical accuracy in a reasonable time immediately leads to the conclusion that the 2.2-MeV gamma rays must be counted in current mode. This means that instead of observing individual events in the detector, many are seen at once, and the sum of their presence is detected as a total voltage or current from the detector electronics rather than as individual pulses. It is important to demonstrate in a current-mode measurement that the electronic noise is negligible compared to the shot noise because of

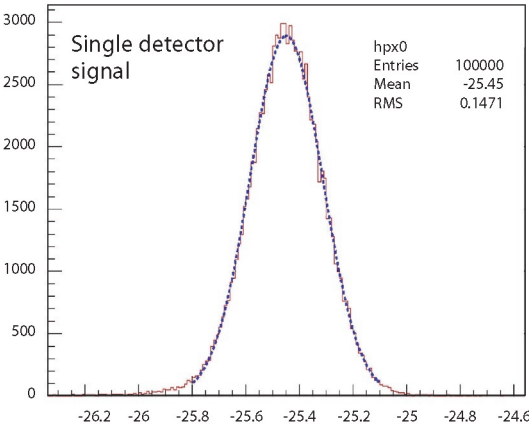

Figure 4. A histogram of a detector signal, measuring the electronic noise. The width of the distribution is of order 0.1 mV, which corresponds to the theoretical limit due to preamplifier Johnson noise of 20 fA/√Hz . This will allow the current-mode detectors to take data at the counting-statistics limit and to quickly demonstrate that no false asymmetry effects are observed in the electronics and data-acquisition system.

the discrete nature of the energy deposited by each gamma ray and the number of photoelectrons produced by each event. In addition, the detector must cover a large solid angle with a large, time-independent efficiency that is unaffected by neutron spin reversal and radiation damage. Segmentation of the detector is required to resolve the angular dependence of the expected parity-violating signal and to discriminate false effects. A photo of the fully constructed detector array of 48 cesium-iodide scintillator crystals is shown in Figure 3. The noise performance of the detectors and their preamplifier electronics has been measured in the laboratory, and it corresponds well to predictions based on the fundamental limit of Johnson noise. (A histogram of a single detector signal is shown in Figure 4, and the width of the distribution is a measure of the noise in the electronics.) This will allow the detectors to accumulate data at the counting statistics limit and to quickly demonstrate that no false experimental effects exist in the electronics.

Conclusion

A sensitive measurement of the parity-violating gamma asymmetry in the reaction $\vec{n} + p \rightarrow d + \gamma$ can give definitive information on one of the most important and interesting components of the weak nucleon-nucleon interaction. Engineering runs have demonstrated the performance of the essential components of the experiment; this includes published results for the FP12 moderator performance and measurements of parity-violating asymmetries in neutron capture on nuclear targets (chlorine, cadmium, and lanthanum) to a precision of 6×10^{-6}—limited only by counting statistics. Construction of the detector array is complete and laboratory tests indicate that noise levels of the electronics are close to the theoretical limits and thus allow the measurement of asymmetries at the level of a few parts per billion. The experimental design incorporates a number of powerful diagnostics to isolate systematic effects. Commissioning of the final construction of the experiment will begin in early 2004, and data taking will commence in late 2004. The NPDGamma experiment to search for the parity-violating gamma asymmetry in the reaction $\vec{n} + p \rightarrow d + \gamma$ will achieve a sensitivity that is likely to obtain a nonzero result, providing an experimental and unambiguous measure of the hadronic weak interaction in a simple and calculable system.

References

1. W.M. Snow, A. Bazhenov, C.S. Blessinger *et al.*, "Measurement of the parity violating asymmetry A_γ in $\vec{n} + p \rightarrow d + \gamma$," *Nuclear Instruments and Methods A* **440**(3), 729–735 (2000).
2. G.E. Mitchell, J.D. Bowman, S.I. Penttila *et al.*, "Parity violation in compound nuclei: Experimental methods and recent results," *Physics Reports* **354**(3), 157–241 (2001).
3. B. Desplanques, J.F. Donoghue, and B.R. Holstein, "Unified treatment of the parity-violating nuclear force," *Annals of Physics* **124**, 449–495 (1980).
4. E.G. Adelberger and W.C. Haxton, "Parity violation in the nucleon-nucleon interaction," *Annual Review of Nuclear and Particle Science* **35**, 501–558 (1985).
5. The brightness of the FP12 moderator has been measured by the NPDGamma collaboration. The peak brightness is 1.25×10^8 neutrons/cm^2/s/sr/meV/μA at 3.3 meV. (P.-N. Seo *et al.*, submitted in 2003 to *Nuclear Instruments and Methods A*).
6. G.L. Jones, T.R. Gentile, A.K. Thompson *et al.*, "Test of ^{3}He-based neutron polarizers at NIST," *Nuclear Instruments and Methods A* **440**(3), 772–776 (2000); D.R. Rich, J.D. Bowman, B.E. Crawford *et al.*, "A measurement of the absolute neutron beam polarization produced by an optically pumped ^{3}He neutron spin filter," *Nuclear Instruments and Methods A* **481**, 431–453 (2002).

Acknowledgment

Assistance in the construction and design of this experiment has been provided by LANSCE-12 and LANSCE-3. This work was supported in part by the DOE Office of Energy Research (Contract W-7405-ENG-36), the National Science Foundation (Grant No. PHY-0100348), and the Natural Sciences and Engineering Research Council of Canada.

For further information, contact Gregory Mitchell at 505-665-8484, gmitchell@lanl.gov.

Extreme Astrophysics—The High-Resolution Fly's Eye Experiment

C. Sinnis, C.M. Hoffman, M.H. Holzscheiter, C.A. Painter (P-23), J.F. Amann, M.D. Cooper, L.J. Marek, T.N. Thompson, D. Tupa (P-25), J.S. Sarracino (X-5), R.U. Abbasi, T. Abu-Zayyad, G. Archbold, K. Belov, Z. Cao, H. Dai, A.A. Everett, J.H.V. Girard, R.C. Gray, W.F. Hanlon, P. Huntemeyer, B.F. Jones, C.C.H. Jui, D.B. Keida, K. Kim, E.C. Loh, K. Martens, J.N. Matthews, J.R. Meyer, S.A. Moore, P. Morrison, A.N. Moosman, J.R. Mumford, K. Reil, R. Riehle, P. Shen, J.D. Smith, P. Sokolsky, R.W. Springer, B.T. Stokes, S.B. Thomas, L.R. Wiencke, T.D. VanderVeen (University of Utah), J.A. Bellido, R.W. Clay, B.R. Dawson, K.M. Simpson (University of Adelaide, Australia), J.W. Blez, M.A. Kirn, M.W. Munro (University of Montana), D.R. Bergman, L. Perera, S.R. Schnetzer, G.B. Thomson, A. Zech (Rutgers University), J. Boyer, B. Knapp, E. Mannel, M. Seman, C. Song, S. Westerhoff, X. Zhang (Columbia University), N. Mango, M. Sasaki (University of Tokyo, Japan), G. Martin, J.A.J. Matthews, M. Roberts (University of New Mexico)

The earth is constantly bombarded by high-energy particles of unknown origin. These particles, known as cosmic rays, have energies up to and beyond 10^{20} eV (10^{20} eV = 16 J, which is nearly the energy packed into a major league fastball). These are the highest energy particles in the universe. Their origin is unknown, and they represent one of the mysteries of modern science. What are they? How do they attain their enormous energies? How do they propagate to earth? Compounding the inherent difficulty of studying extraterrestrial particles is the rarity of these ultra-high-energy cosmic rays. Above 10^{20} eV, only one of these particles will pass through a square kilometer of the earth in a century. Figure 1 shows the cosmic-ray spectrum from 1 GeV (i.e., a billion electron-volts to above 10^{20} eV). The HiRes experiment located in Dugway, Utah, seeks to gain an understanding of the properties of these particles: how many there are, where they come from, and what they are.

The HiRes Experiment

When a UHECR enters the atmosphere, it interacts with the molecules in the air, creating an EAS. The EAS is composed of billions of particles (electron, positrons, gamma rays, and muons) traveling at the speed of light towards the earth. The passage of the charged particles excites nitrogen molecules in the air. These excited molecules emit fluorescence light. Because this light is emitted isotropically, a detector does not need to be "in the beam" to be detected—therefore, a relatively small detector with an enormous aperture will do the job. The HiRes detector consists of two independent sites separated by 12.6 km so that each event may be viewed stereoscopically. This stereoscopic view gives the detector depth perception and allows us to measure the distance to each event. At each site, there is a set of 5-m^2 mirrors, each equipped with a 256-PMT camera placed in the focal plane. Each PMT has a 1° field of view. The HiRes I site has 21 mirrors covering an elevation range from 3° to 17°, and the HiRes II site has 44 mirrors covering an elevation range from 3° to 31°. Both sites provide a 2-π azimuthal coverage of the sky. The aperture of the full HiRes detector is 10,000 km^2 sr at 10^{20} eV. In HiRes I, the shower images are stored in sample-and-hold electronics with a 5.6-μs window; in HiRes II, the information is digitized with a 10-MHz flash (analog-to-digital converter) system. The air-fluorescence technique (Figure 2) used in our experiments allows us to detect the passage of an air shower with the HiRes instrument. The entire longitudinal development of the air shower is obtained by recording the amount of light detected in each PMT.

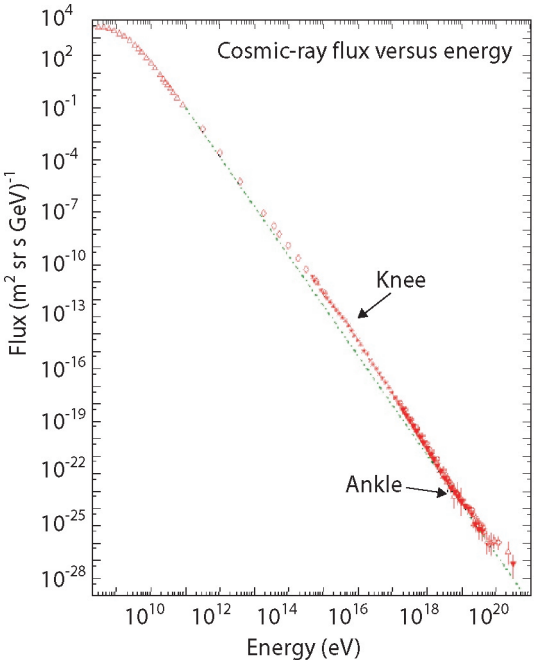

Figure 1. The cosmic-ray spectrum from 1 GeV to 10^{20} eV. The spectrum is well represented by a power law but with two features. At an energy of roughly 10^{15} eV, the spectrum begins to fall faster with energy (which is the knee of the cosmic-ray spectrum), and at an energy of roughly $10^{18.5}$ eV, the spectrum hardens slightly (which is the ankle of the cosmic-ray spectrum). Above 10^{20} eV, the flux is about one particle per square kilometer per century.

UHECR Science

A UHECR flux above an energy of 6 x 10^{19} eV is of fundamental importance in astrophysics studies. Protons with energies in excess of this will interact with microwave background radiation and lose energy through pion production—this process is known as the GZK effect (for Greisen, Zatsepin, and Kuzmin, the co-discoverers of the effect).[1,2] The mean-free path for this interaction is roughly 20 million light years; therefore, the flux of particles above this energy is expected to fall rapidly—unless the "point" sources of these particles are relatively close to the earth. If the point sources *are* close to the earth, the particles should point back to them because at these energies the particles bend via intergalactic magnetic fields at relatively small (< 2°) angles. However, the particles that we detected to date do not appear to point back to any objects capable of accelerating particles to these energies.[3]

At present, there is disagreement between the only two experiments that have measured the flux at these energies—the HiRes and the Akeno Giant Air Shower Array (AGASA). The AGASA is a traditional scintillator array composed of 111 particle detectors spread over 100 km^2. Figure 3 shows the present status of the world's dataset.[4] The curve on the figure is what one would expect if the sources of UHECRs were uniformly distributed throughout the universe and if the GZK effect were included. (The data from HiRes and AGASA are indicated in the legend.) Although the HiRes data are consistent with this curve, the AGASA data are not. The overall offset of the two datasets is due to systematic uncertainties in the absolute energy scale of the two experiments. The HiRes data were taken in "monocular" mode—determining the distance to the air shower (and therefore the energy of the primary cosmic ray) is not made directly but relies instead on a fit to the shower profile. At present, neither experiment has the statistical power or an understanding of systematic effects to make a definitive statement on the existence of the GZK effect.

If the GZK effect is not present, then there are many possible explanations, most of which involve exciting new physics. The solutions can be grouped into either a "top-down" or a "bottom-up" scenario. In the top-down scenario, the particles are the decay products of very massive particles, possibly relics left from the Big Bang.[5,6] In the bottom-up scenario, the particles are accelerated to high energies by astrophysical sources such as gamma-ray bursts or active galactic nuclei. In these scenarios, super-GZK events can be caused by a suppression of the proton-photon interaction at high energies, which would clearly violate Lorentz invariance and may be a signal of quantum gravity.[7,8] The super-GZK events may also be caused by the existence of a new strongly interacting particle (for example, a massive, stable hadron) that does not suffer from the energy loss in the 3-K radiation field.[9,10] Moreover, there may be unseen "local" astrophysical sources of UHECRs or ultra-high-energy neutrinos that may propagate over cosmological distances and interact with (massive) relic neutrinos within 160 million light years of the earth. If the latter were the case, a cascade of gamma rays and hadronic particles (known as the "Z-burst" model) would be detected.[11]

Each of the scenarios described above make different predictions as to the nature of UHECRs—are they protons, gamma rays, heavy nuclei, neutrinos, or some as yet undiscovered particle? Each of these particles is expected to have a different cross section; therefore, they will interact at different depths in the atmosphere, and the resulting air shower will have a different altitude of maximum development. Because the HiRes experiments observe the entire longitudinal development of the air shower, we can measure the altitude of the maximum shower with a resolution of roughly 30 g/cm^2. Although shower-to-shower

fluctuations preclude us from measuring the particle type on an event-by-event basis, we can determine the average composition of the UHECRs using the air-fluorescence technique. Finally, we want to know where these UHECRs are coming from. Do they come from point sources (if so, which objects are accelerating particles to such high energies) or are they isotropic? There is preliminary evidence from AGASA that the UHECRs come in clusters. If this claim is correct, it would imply that there are numerous stable sources of UHECRs. With an angular resolution of 0.4°, HiRes can verify or repudiate this claim.

Conclusion

Because the GZK effect is predicted to occur at a well-defined energy, knowing the true energy of each event is critical. Systematic errors must therefore be of the same order or smaller than statistical errors. The systematic errors in the current HiRes analysis are caused by a 10% uncertainty in the absolute fluorescence yield and by the attenuation of particles as they are absorbed in the atmosphere. To reduce the errors from atmospheric absorption, we have installed a set of lasers that allow us to continuously monitor the atmosphere over the entire aperture of the detectors. With these lasers, we can make atmospheric corrections on an event-by-event basis and calculate the aperture of the experiment on an hourly timescale. Most importantly, because HiRes was built to view all events stereoscopically, we can determine the shower distance and inclination angle from purely geometrical considerations. Figure 4 shows the stereo reconstruction of a typical event. Once the geometry of the shower is known, crosschecks can be performed on the atmospheric attenuation (because the two detector sites are, in general, a different distance from the shower). Such a crosscheck will allow us to better measure and control systematic uncertainties. A complete stereo analysis is now under way. Within five years of taking data, HiRes will detect 50 events with energies in excess of 6 x 10^{19} eV and 20 events above 10^{20} eV if there is no GZK effect. With these results, we will be able to make a statistically significant measurement of the GZK effect. Within the next several years, HiRes will have solved a major riddle of modern physics—the nature of the highest-energy particles in the universe.

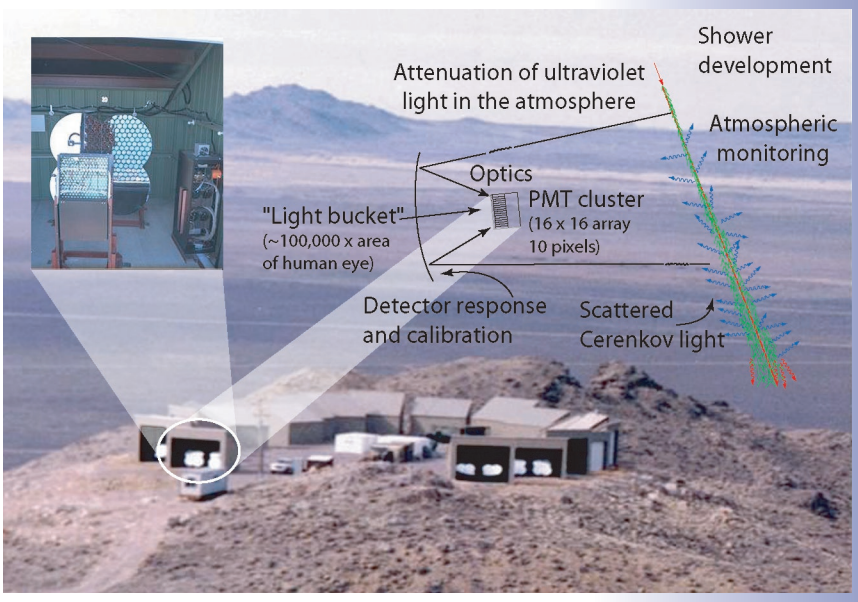

Figure 2. Schematic view of the detection of an EAS using the air-fluorescence technique. The electromagnetic particles in the air shower excite nitrogen molecules in the atmosphere, which radiate ultraviolet light. This light passes through the atmosphere (as much as 40 km) where it is absorbed and scattered. The surviving light is reflected from the mirrors and focused onto a fast camera composed of PMTs.

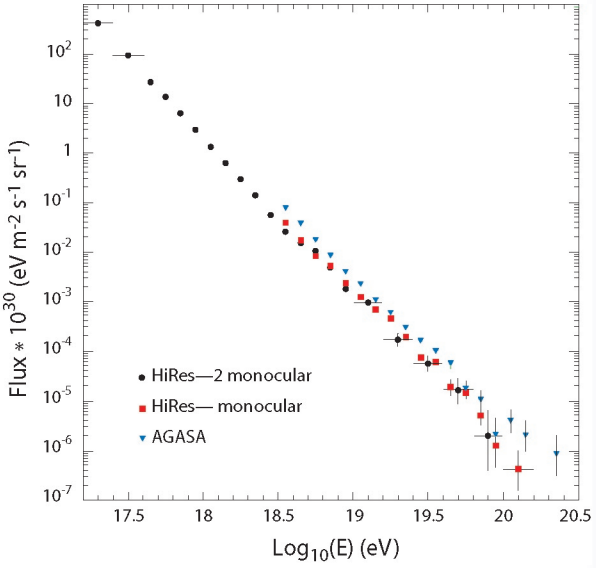

Figure 3. The UHECR as measured by HiRes in monocular mode and the AGASA experiment. The flux has been multiplied by E^3 to show the structure. The offset between the two experiments arises from systematic uncertainties in the absolute energy calibration of the two detectors. Although the HiRes data are consistent with the existence of the GZK effect, the AGASA data indicate that the spectrum hardens above 10^{20} eV.

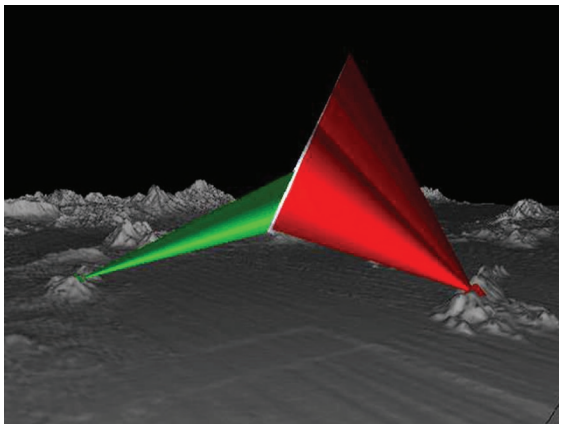

Figure 4. A typical event as seen by HiRes in stereo mode. Each detector determines a plane in which the shower lies. The intersection of the two planes determines the full three-dimensional geometry of the event.

References

1. K. Greisen, "End to the cosmic-ray spectrum," *Physical Review Letters* **16**(17), 748 (1966).
2. G.T. Zatsepin and V.A. Kuzmin, "Upper limit of spectrum of cosmic rays," *Journal of Experimental and Theoretical Physics* **4**(3), 78 (1966).
3. J.E. Elbert and P. Sommers, "In search of a source for the 320-EeV fly's eye cosmic ray," *Astrophysical Journal* **441,** 151 (1995).
4. T. Abu-Zayyad *et al.,* "Measurement of the flux of ultra-high-energy cosmic rays from monocular observations by the high resolution fly's eye experiment," submitted to *Physical Review Letters.*
5. P. Bhattacharjee, C.T. Hill, and D.N. Schramm, "Grand unified theories, topological defects, and ultrahigh-energy cosmic rays," *Physical Review Letters* **69,** 567 (1992).
6. C.T. Hill, D.N. Schramm, and T.P. Walker, "Ultrahigh-energy cosmic rays from superconducting cosmic strings," *Physical Review D* **36,** 1007 (1987).
7. S. Coleman and S.L. Glashow, "High-energy tests of Lorentz invariance," *Physical Review D* **59,** 151 (1999).
8. G. Amelino-Camelia and T. Piran, "Planck-scale deformation of Lorentz symmetry as a solution to the ultra-high-energy cosmic rays and the TeV-photon paradoxes," *Physical Review D* **64,** 036005 (2001).
9. G.R. Farrar, "Detecting light-gluino-containing hadrons," *Physical Review Letters* **76,** 4111 (1996).
10. I.F.M. Albuquerque, G.R. Farrar, and E.W. Kolb, "Exotic massive hadrons and ultra-high-energy cosmic rays," *Physical Review D* **59,** 015021 (1999).
11. T.J. Weiler, "Cosmic-ray neutrino annihilation on relic neutrinos revisited: A mechanism for generating air showers above the Greisen-Zatsepin-Kuzmin cutoff," *Astroparticle Physics* **11,** 303 (1999).

Acknowledgment

We gratefully acknowledge the contributions from the technical staffs of our home institutions and the Utah Center for High Performance Computing. The cooperation of Colonel E. Fischer and Colonel G. Harter of the U.S. Army Dugway Proving Grounds staff is greatly appreciated. This work is supported by grants from the National Science Foundation, including PHY-9321949, PHY-9974537, PHY-9904048, PHY-0071069, and PHY-0140688; by DOE grant FG03-92ER40732; and by the Australian Research Council.

For more information, contact Gus Sinnis at 505-665-6943, gus@lanl.gov.

Teravolt Astrophysics—The Milagro Gamma-Ray Observatory

C. Sinnis, B.L. Dingus, T.J. Haines, C.M. Hoffman, F.W. Samuelson (P-23), G.R. Gisler (X-2), R. Atkins, M.M. Gonzalez, J.E. McEnery, M.E. Wilson (University of Wisconsin), W. Benbow, D.G. Coyne, D.E. Dorfan, L.A. Kelley, M.F. Morales, D.A. Williams, S. Westerhoff (University of California, Santa Cruz), D. Berley, E. Blaufuss, J. Bussons, J.A. Goodman, E. Hays, C.P. Lansdell, D. Noyes, A.J. Smith, G.W. Sullivan (University of Maryland), T. DeYoung (University of California, Santa Cruz, and University of Maryland), R.W. Ellsworth (George Mason University), L. Fleysher, R. Fleysher, A.I. Mincer, P. Nemethy (New York University), J. Linnemann, X. Xu (Michigan State University), R.S. Miller, J.M. Ryan (University of New Hampshire), A. Shoup, G.B. Yodh (University of California, Irvine)

Milagro is a new type of astronomical telescope. Like conventional telescopes, Milagro is sensitive to light, but the similarities end there. Whereas "normal" astronomical telescopes view the universe in visible light, Milagro "sees" the universe at very high energies. The "light" that Milagro sees is about one trillion times more energetic than visible light. Although these particles of light, known as photons, are the same as the photons that make up visible light, they behave quite differently simply because they are much more energetic. Viewing the heavens in high-energy photons creates quite a different picture from what we see when we look up at the night sky. There are fewer objects, and they are much more extreme—in the visible, we detect mostly thermal processes and blackbody radiation.

When we view the universe in TeV gamma rays (1 TeV is one trillion electron volts; normal light has a few electron volts of energy), we detect non-thermal radiation and particle acceleration. The light sources that we detect contain super-massive black holes and neutron stars. Some of these sources are highly variable, flaring on a timescale of minutes to days. Until the advent of the Milagro Observatory, located at the LANL Fenton Hill site, there was no instrument capable of continuously monitoring the entire overhead sky in the TeV-energy regime. The existing instruments, known as air Cerenkov telescopes (ACTs), had to be pointed at small regions of the sky (usually at known sources) and could only look at a light source during the time of year that it is overhead at night. Even then, they could only look at the source if the weather was good and the moon was set. But Milagro is ideally suited to monitor the variable TeV universe and discover new sources of TeV gamma rays. With this instrument, we hope to discover new sources of TeV photons, to observe TeV emission from gamma-ray bursts, and to discover primordial black holes or some completely new phenomena.

Physics with Milagro

High-energy gamma-ray astronomy seeks to understand the most extreme environments in the universe and to use the beams of gamma rays from these distant sources to further our understanding of the fundamental laws of physics at energies not attainable in earth-bound experiments. The known sources of gamma rays include supernova remnants, super-massive black holes (known as active galactic nuclei, or AGN), and gamma-ray bursts (the most energetic phenomena in the universe). Gamma rays are also produced when high-energy cosmic rays interact with matter in our galaxy. Other potential sources include more exotic objects (which may or may not be detectable) such as "evaporating" primordial black holes, topological defects, and dark-matter particle annihilation and decay. The gamma rays from distant sources interact with the ambient fields in the universe as they travel to earth. By measuring the effects of these interactions, we can understand the nature of the fields that pervade the universe. Two particle-interaction effects are of concern to us—particle interactions with the intergalactic-infrared-radiation fields and those with the quantum fields that define the universe. The infrared-radiation field results from the formation of, and the nuclear-burning process in, stars and from the subsequent absorption and re-radiation of the energy produced in this process

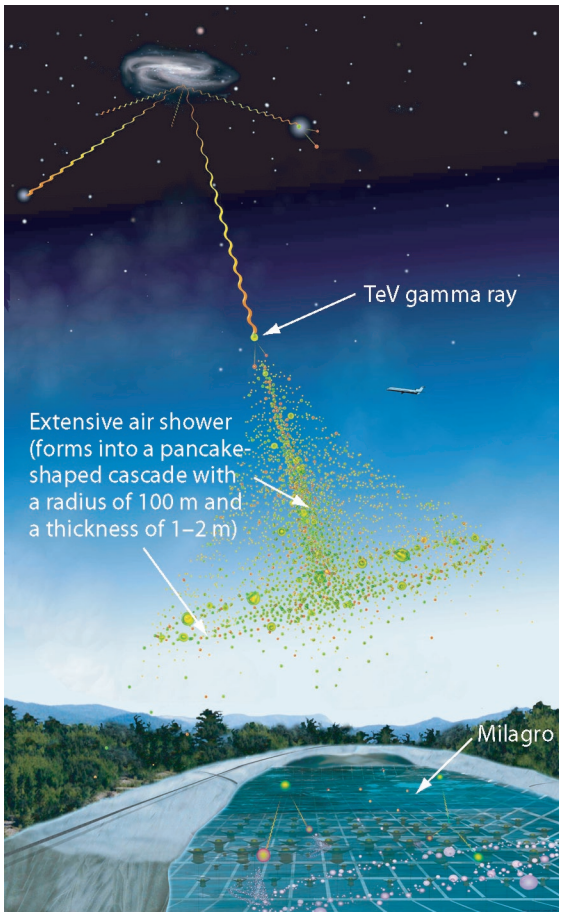

Figure 1. Rendering of Milagro. An astrophysical source emits TeV gamma rays, which propagate to earth. The gamma ray interacts in the atmosphere to generate an EAS. The EAS is composed mostly of electrons, positrons, and gamma rays. The electrons and the positrons emit Cerenkov light as they traverse the water in Milagro. (Cerenkov light is emitted by a charged particle traveling faster than the speed of light in a medium and is similar to a sonic boom.) The gamma rays in the EAS convert to electrons and positrons, which then emit Cerenkov light. The resultant Cerenkov light is detected by the PMTs in the pool of water (see Figure 2). The green particles represent gamma rays; the red particles represent electrons and positrons. (Rendering courtesy of Aurore Simonnet, Scientific Illustrator, Sonoma State University, aurore@universe.sonoma.edu.)

by dust. The field can be determined by measuring the energy- and redshift-dependent absorption of TeV radiation from AGN. Direct measurements are difficult (and so far unsuccessful) because of the large and uncertain foreground fields within our galaxy. The effect of the quantum fields of the universe may be manifest as a violation of Lorentz invariance—an energy dependence of the velocity of light.[1] This effect can be observed (or limited) by measuring the time delay between photons of different energies arriving from across the universe. Bursts of gamma rays provide an excellent source for observing this effect.[2]

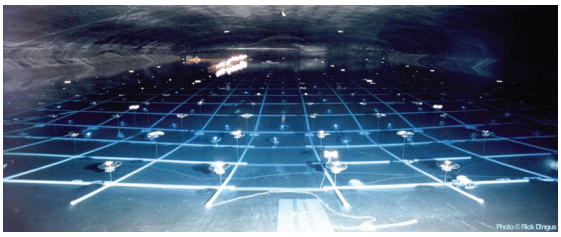

Figure 2. A view inside Milagro. The top layer of PMTs is located at the crossing of the grid, and the bottom layer of PMTs is halfway between the grid crossing points. In the photograph, the cover is inflated for installation.

The Milagro Observatory

A cosmic ray or gamma ray entering the earth's atmosphere interacts with atoms and nuclei and loses energy in the process. At high energies, the dominant energy-loss mechanisms are the creation of particles through nuclear interactions in the case of cosmic rays and electromagnetic interactions in the case of gamma rays. The result is a cascade of particles, or EAS. As the cascade propagates through the atmosphere, particles continue to be created until the energy per particle drops below the critical energy of 80 MeV. At this point, the energy loss of the particles becomes dominated by non-particle-creating mechanisms and the EAS begins to die. When the cascade reaches the ground, it has the shape of a rough pancake with a radius of 100 m and a thickness of 1–2 m (Figure 1). A particle cascade initiated by a gamma ray comprises electrons, positrons, and lower-energy gamma rays. A particle cascade initiated by a cosmic ray will also contain muons and some hadrons in addition to the electrons, positrons, and gamma rays.

The Milagro Observatory has 723 PMTs submerged in a six-million-gallon water reservoir. The detector is located at an altitude of 2,630 m above sea level (750 g/cm^2 atmospheric overburden). The reservoir measures 80 m × 60 m × 8 m (depth) and is covered by a light-tight barrier. Each PMT is secured by a Kevlar string to a grid of sand-filled PVC (polyvinyl chloride) pipes sitting on the bottom of the reservoir. The PMTs are arranged in two layers, each on a 2.8-m × 2.8-m grid (Figure 2). The top layer of 450 PMTs (which is under 1.4 m of water) is used primarily to reconstruct the direction of the air shower. By measuring the relative arrival time of the air shower across the array, we can reconstruct the direction of the primary cosmic ray with an accuracy of roughly 0.75°. The bottom layer of 273 PMTs (which is under 6 m of water) is used primarily to discriminate between gamma-ray-initiated air showers and hadronic air showers.

Milagro Results

Background rejection. Because hadronic cosmic rays (mainly protons) are charged, they are deflected by the magnetic fields that pervade our galaxy. Outnumbering the gamma rays by ~ 10,000 to one, they form an isotropic background over which any signal must be detected. The bottom layer of PMTs in Milagro is under a sufficient amount of water such that only the penetrating component of an EAS (muons and showering hadrons) can reach it. Because a gamma-ray-induced EAS is almost completely electromagnetic and a cosmic-ray-induced EAS contains a penetrating component of muons and showering hadrons, Miagro's ability to detect the penetrating component allows us to

reject the cosmic-ray background and therefore increases our sensitivity to gamma rays. Figure 3 shows the pattern of light in the bottom layer from three gamma-ray-induced events and three proton-induced events (from Monte Carlo simulations). The proton-induced events contain small bright clumps of light, whereas the gamma-ray-induced events have a relatively uniform, low level of illumination. We have developed a *compactness* parameter that is sensitive to this difference. Using the compactness of the events, we can reject roughly 90% of the cosmic-ray background while retaining 50% of the gamma-ray-induced events.

Observation of the Crab Nebula. The Crab Nebula was the famous supernova observed by Chinese astronomers in 1066. Since that time, it has been detected in every wavelength of astronomy, from the radio to TeV gamma rays. It was the first source to be detected in TeV gamma rays,[3] and it serves as a standard candle for the field of TeV astrophysics. It was critical for Milagro to detect the Crab Nebula and to prove the efficacy of the water Cerenkov technique and our ability to reject the cosmic-ray background. This is the first detection of any source of TeV gamma rays with an EAS array.[4] The flux that we measured from the Crab Nebula is in agreement with the previous measurements by ACTs.

TeV map of the northern hemisphere. Using the same compactness parameter that we used in the Crab Nebula study, we searched for sources of TeV gamma rays from the entire northern hemisphere. Figure 4 shows the most sensitive map to date of the entire northern hemisphere in TeV gamma rays (previous maps have only been made by Milagro and its prototype Milagrito). Notice that in addition to the Crab Nebula there is another bright region in the sky, which corresponds to the active galaxy Markarian 421. Markarian 421 consists of a super-massive black hole with a jet of relativistic particles directed at earth. This black hole has experienced several flaring episodes (in the x-ray band) during our period of observation, and the TeV emission associated with these episodes is correlated with the x-ray emission. This correlation is consistent with leptonic models of gamma-ray production. In these models, electrons are accelerated at shocks that propagate down the jet of relativistic particles that is emitted along the rotation axis; these electrons radiate synchrotron radiation as they bend in the magnetic fields present in the jet. This synchrotron radiation is responsible for the observed x-ray emission. The TeV gamma rays arise from inverse Compton reactions between the primary electrons and the synchrotron photons. Aside from the Crab Nebula and the Markarian 421 black hole, no other object in the northern hemisphere appears as bright as the Crab Nebula (or the Markarian 421) in TeV gamma rays.

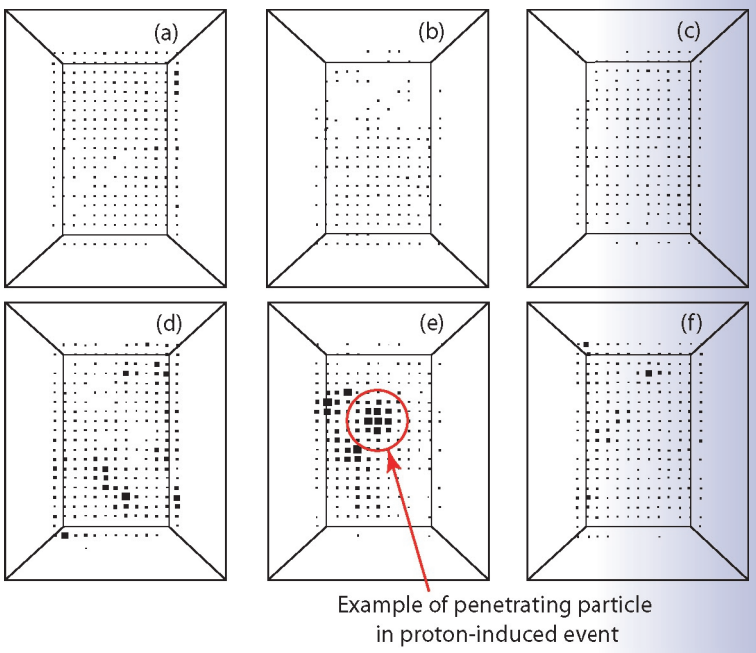

Figure 3. Monte Carlo simulations of the response of the bottom layer of detectors to EASs. The area of each square is proportional to the light level detected in a PMT. The top three events (a, b, and c) are gamma-ray induced events, and the bottom three events (d, e, and f) are proton-induced events. Clear clumps of light are observed in the proton-induced events.

Galactic-diffuse gamma rays. The origin of cosmic rays is still a matter of debate—nearly a century after their discovery! One of the clues to their origin is the energy spectrum of the gamma rays produced by the interactions of the cosmic rays with the matter in our galaxy. The highest-energy measurement of these *galactic-diffuse* gamma rays obtained to date was made by the EGRET instrument onboard the Compton Gamma Ray Observatory.[5] These measurements extend up to ~ 30 GeV and indicate an excess over predictions above several hundred MeV. The measurement of the TeV flux of the galactic-diffuse gamma rays has proven impossible to date. However, this past year Milagro has, for the first time, presented evidence of the existence of a TeV flux of gamma rays arising from interactions of cosmic rays and matter within our galaxy. Milagro has detected a signal based on the analysis of a two-year data run with a significance of 2.8 standard deviations. With another two-year run cycle on Milagro, we will be able to make a conclusive measurement of the TeV flux of galactic-diffuse gamma rays in the galaxy.

Large-scale cosmic-ray anisotropy. We generally assume that the arrival directions of cosmic rays on earth are isotropic. Milagro is the first detector that can make a high-statistics two-dimensional map of the comic-ray arrival directions. With our current data set, we can detect anisotropies as small as one part in 100,000. Figure 5 shows a two-dimensional map of the northern hemisphere in cosmic rays. This figure is similar to Figure 4, except that we have not applied our background rejection cut to the data (which increases our statistics by an order of magnitude). Moreover, we have binned the sky

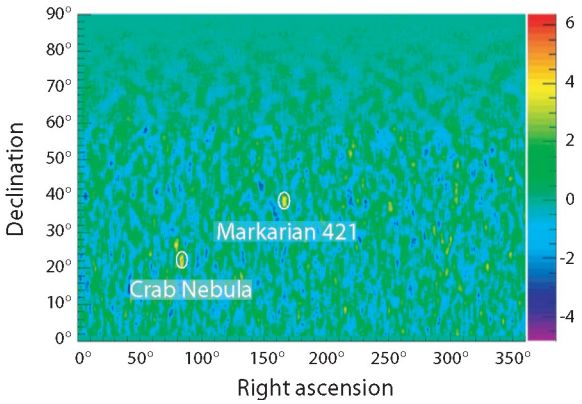

Figure 4. The northern hemisphere as seen in TeV gamma rays. Milagro is the only experiment capable of making such a plot. The two bright regions (circled and marked) are the Crab Nebula and the active galaxy, Markarian 421. The color coding corresponds to the significance of the observed excesses or deficits expressed as standard deviations.

in coarser bins to more clearly show the large-scale structure. A large-scale anisotropy is evident in this data. The red and black regions are areas with an excess of cosmic rays, and the blue regions are areas with a deficit of cosmic rays. The size of the effect is quite small (~ one part in 10,000). The origin of this anisotropy—which is currently under study—may be caused by effects of the solar magnetic field, or it may be imprinted by cosmic-ray production and propagation effects within our galaxy.

Conclusion

Milagro is the first detector of its kind—a large, water Cerenkov EAS detector. Our observations discussed above proved that the technique is sensitive to astrophysical sources of TeV gamma rays and can make measurements that no other current instrument can. Milagro will continue to operate over the next three to five years while we investigate methods to improve the instrument's sensitivity and to explore possible future detectors of a similar design. With the launch of the SWIFT satellite[6] (i.e., a detector that is sensitive to the gamma-ray, x-ray, and optical emissions from gamma-ray bursts) in 2004, Milagro's *all-sky* and *all-time* capabilities will be more important than ever before. As the only instrument capable of measuring the prompt TeV component of gamma-ray bursts, Milagro is poised to make enormous contributions to our understanding of gamma-ray bursts and perhaps of quantum gravity.

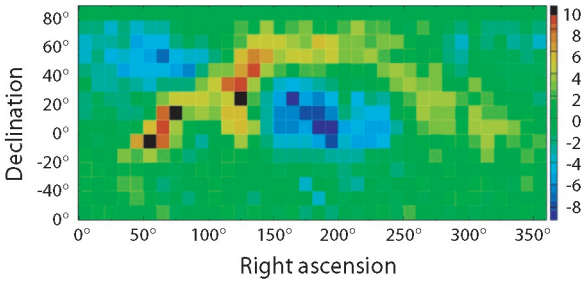

Figure 5. The northern sky as seen in TeV cosmic rays. The red to black areas represent directions from which there is an excess (over uniform) of cosmic rays, and blue regions are directions from which there is a deficit of cosmic rays.

References

1. G. Amelino-Camelia *et al.*, "Tests of quantum gravity from observations of gamma-ray bursts," *Nature* **393**, 763 (1998).
2. J. Ellis, N.E. Mavromatos, and D.V. Nanopoulos, "Search for quantum gravity," *General Relativity and Gravitation* **31**(9), 1257 (1999).
3. T.C. Weeks *et al.*, "Observation of TeV gamma rays from the Crab Nebula using the atmospheric Cerenkov imaging technique," *Astrophysical Journal* **342**, 379 (1989).
4. R. Atkins *et al.*, "Observation of TeV gamma rays from the Crab Nebula with Milagro using a new background rejection technique," *Astrophysical Journal* **595** (2003).
5. S.D. Hunter *et al.*, "EGRET observations of the diffuse gamma-ray emission from the galactic plane," *Astrophysical Journal* **481**, 205 (1997).
6. See http://swift.gsfc.nasa.gov/.

Acknowledgment

We acknowledge Scott Delay and Michael Schneider for their dedicated efforts in the construction and maintenance of the Milagro experiment. This work has been supported by grants from the National Science Foundation, including PHY-0070927, PHY-0070933, PHY-0075326, PHY-0096256, PHY-0097315, PHY-0206656, PHY-0302000, and ATM-0002744; the DOE Office of High-Energy Physics and Office of Nuclear Physics; LANL; the University of California; and the Institute of Geophysics and Planetary Physics.

For more information, contact Gus Sinnis at 505-665-6943, gus@lanl.gov.

The PHENIX Silicon Vertex Tracker Project

H.M. van Hecke, G.J. Kunde, D.M. Lee, M. Leitch, P. McGaughey (P-25), V. Ciancolo, K. Read (Oak Ridge National Laboratory), A. Drees, J. Heuser (Stony Brook University), H. En'yo, N. Saito, K. Tanida, J. Tojo [RIKEN (The Institute of Physical and Chemical Research), Japan], Y. Goto (RIKEN Brookhaven National Laboratory Research Center), N. Grau, J. Hill, J. Lajoie, C.A. Ogilvie, H. Ohnishi, H. Pei, J. Rak, G. Tuttle (Iowa State University, Ames), J. Haggerty, V. Rykov, S. White, C. Woody (Brookhaven National Laboratory), M. Togawa (Kyoto University)

A state of matter not seen in the universe since the first few microseconds after the Big Bang is the object of study of an international community of physicists at RHIC, the Relativistic Heavy-Ion Collider at BNL. When the universe was too hot for even protons and neutrons to form, it consisted almost entirely of a soup of truly elementary particles: quarks and gluons that mediate the force between the quarks. Under the conditions that prevailed for this brief span of time, quarks and gluons were free to roam. As this quark-gluon plasma (QGP) expanded and cooled, the quarks and gluons joined up to form the protons and neutrons that are part of ordinary matter today. Ever since this transition from quark matter to so-called hadronic matter, quarks have been confined to the interior of particles that we can observe.

Relativistic Heavy-Ion Collider

The RHIC complex is an accelerator/collider that can produce two counter-rotating beams of gold ions, with each beam accelerated to an energy of 100 GeV (billion electron volts) per nucleon. Thus in a head-on collision between two ions, almost 40,000 GeV of energy is available. For a fleeting instant, conditions in the collision region are thought to be sufficient to form the QGP. These collisions occur at four locations around the 2.4-mile RHIC ring; at each location, experimental apparatus observe/detect the end products of these events. The largest of these experiments is PHENIX (Figure 1).

Besides gold ions, the RHIC complex can also accelerate lighter ions, as well as deuterons (the nuclei of deuterium atoms) and protons. Studies of deuteron-gold and proton-proton collisions are necessary for the proper interpretation of the larger gold-gold events. Finally, RHIC can collide polarized, or spin-oriented, protons—enabling the study of fundamental issues related to proton spin.

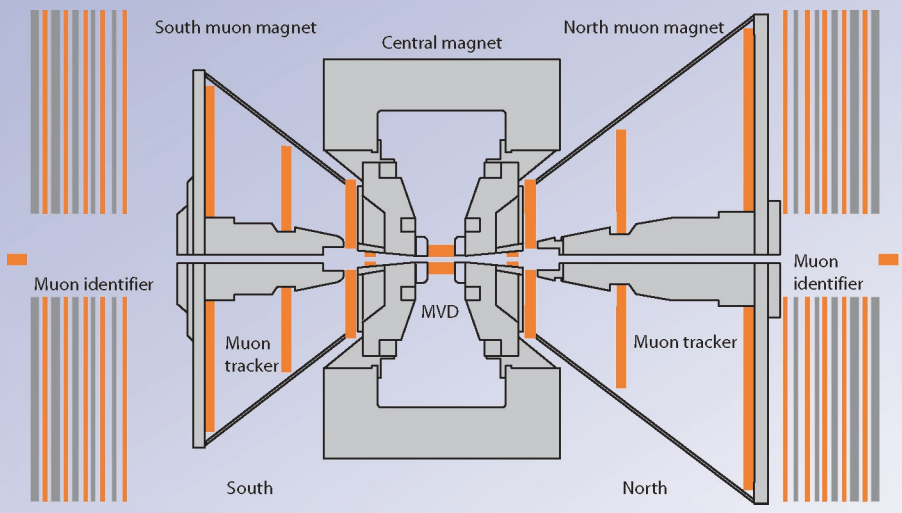

Figure 1. Side view of the PHENIX detector. Beams enter from the left and right and collide in the center. The new silicon vertex tracker will replace the multiplicity/vertex detector (MVD) in the center. Note the north and south muon magnets with three layers of tracking each. The horizontal size is 15 m. (Not shown are detectors wrapping around the collision point on the east and west side of the central magnet.)

PHENIX

The PHENIX experiment is a multipurpose detector of high-energy nuclear interactions, consisting of many different detector types. PHENIX can measure the global distribution of the thousands of particles that are produced in a gold-gold collision. These global measures can be used to determine the "centrality" of the collision—whether the ions barely grazed each other or if it was a head-on collision. The global observables also tell us, for the most central collisions, that the densities reached are many times the normal nuclear density and that these particles come blasting out at two-thirds the speed of light [at a temperature of 140 to 170 MeV, (equivalent to 10^{12}K)]. These observations indicate that the conditions for the formation of the QGP indeed exist in these events, but because the bulk of these particles are formed late in the collision, these global measures cannot give us a direct look at the earlier, hotter stages.

Hard Probes

To get a closer glimpse of the QGP, if it is indeed formed early on, the study of so-called hard probes is necessary. These can be particles that formed very early in the event and then escaped relatively unaffected by the subsequent evolution of the collision. One class of hard probes is the heavy quarks, charm and beauty (the light ones being up, down, and strange). One way to observe these heavy-quark states is to look for one of their characteristic decay modes into muons. PHENIX has a major muon-detection system, largely designed and built by LANL. Data taken in 2003 will yield results on the production of the J/ψ particle, a charm-anticharm bound state. One problem that arises in the study of muons from heavy quarks is that many other processes can produce muons. A property of the heavy-quark mesons (D mesons that contain one charm quark and B mesons that contain one beauty quark) can be exploited in this context: these particles live long enough—before decaying into muons—to travel a significant distance away from the collision point, of an order of tens or hundreds of microns. Thus the decay-muon track will appear to originate from a "secondary vertex." Our strategy, therefore, is to build a tracking detector with sufficient resolution to be sensitive to this decay distance, so that the muons from charm- and beauty-flavored mesons can be separated from the background muon sources.

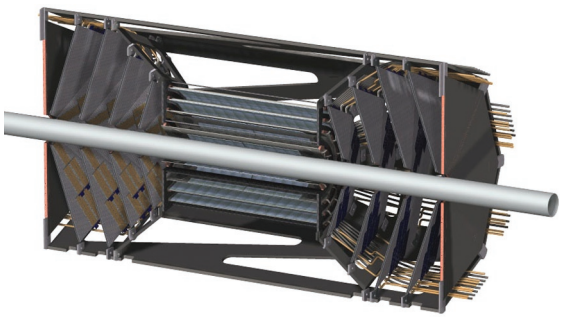

Figure 2. View of one-half of the silicon vertex tracker, surrounding the beam pipe. Visible in the center are the four concentric half cylinders of the central barrel. At either end are the endcap sections, containing four conical disks each. The diameter is 40 cm, and the length is 80 cm.

The Silicon Vertex Tracker

We have embarked on a project to build a silicon vertex tracker that will be installed in the PHENIX detector in the next five years. Figure 2 shows a cutaway drawing of this detector, which wraps around the beam pipe. Beam particles circulate through the pipe in both directions, and collisions occur near the center of the silicon vertex tracker.

The silicon vertex tracker consists of a central section and two endcaps. In the central section, four concentric silicon barrels will locate the event vertex and pick up secondary vertices of tracks roughly transverse to the beam direction. The particles headed towards the muon arms are more parallel to the beam direction and are tracked by silicon detectors in two sets of disks or lampshades that cover the muon arm acceptance.

LANL has taken on the design and hopes to lead the construction of these silicon endcaps, as well as the responsibility for the overall mechanical structure of the silicon vertex tracker. This structure will be designed and built in collaboration with HYTEC, Inc., a local company that has extensive experience in similar projects. The design requirements are stringent because the detector must be built to close mechanical tolerances but must also be as light as possible. The structure shown in Figure 2 is made of fiber-reinforced polymer and carbon-carbon composite materials, and it meets the design requirements.

To achieve the required track resolution, the silicon in the endcaps will be segmented radially into 50-μm-wide strips and azimuthally into 96 segments. Strip sizes will range from 50 × 2000 μm nearest the beam pipe to 50 × 11,000 μm at the outside perimeter. We plan on using existing

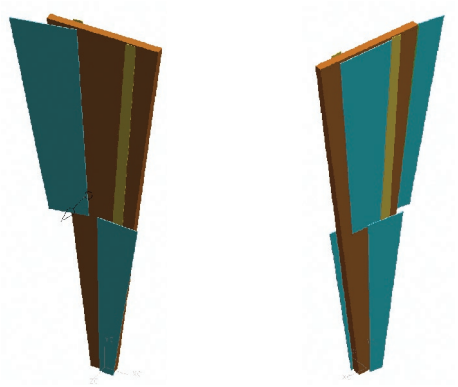

Figure 3. Front (left) and back (right) view of a carbon-composite panel (brown) with four mounted silicon detectors (blue).

technology for the silicon sensors. Silicon pixel designs from the ALICE, ATLAS, or CMS experiments at CERN, the European Laboratory for Particle Physics, can be modified to match the strip sizes that we need. Developing the masks for this effort will be done in concert with the vendors of the CERN sensors, and lengthy and costly research and development in this area is not necessary.

A conceptual design for the layout of the silicon disks, or lampshades, is shown in Figures 3 and 4. Carbon-composite panels (brown) carry four silicon detectors each (blue)—two on the front and two on the back. The silicon detectors on the front and back have small overlaps, so that the final assembly will have no gaps in the coverage. A complete lampshade consists of 24 panels.

The silicon detectors are segmented along the long dimension into 50-μm-high strips, which, in turn, are split along the center line. The readout chips (not shown) are placed directly over the centerline and bonded to the strips on both sides. Signals from the smallest silicon strips at the narrow end of these assemblies are carried to the outer perimeter on kapton cables (yellow strips in Figure 3).

For the readout electronics, we similarly plan to rely heavily on existing research and development projects. We can adapt chip designs developed at FNAL for the proposed BTeV experiment to match our silicon detectors on the input end and the requirements of the PHENIX data-acquisition system on the output end. Figure 5 shows a chip layout developed from existing components. The left side of the figure shows the logical layout of the chip: two parallel arrays of electronics with signals processed from the outside in. Green is the area where the chip is bonded to the silicon strips. Red is the area reserved for preamplification and discrimination of the signals, orange is pipeline circuitry, and yellow is for digital-signal processing.

The bonding locations are staggered, as shown in Figure 5 on the right. This allows us to use a connection technology called bump-bonding, with widely spaced bumps, thereby avoiding technological hurdles associated with dense bump-bonding patterns.

These chips are 13 mm tall. So, three, five, or six of them need to be chained together lengthwise to service the different silicon detectors. One special feature of the readout-chip design is that the chip itself has power and signal bus lines running from the (green) bonding areas on the top and bottom of each chip, allowing them to be chained together. In this manner, no additional cable is needed to carry communication signals and power from each readout chip to the perimeter of the lampshades. This design simplifies construction and keeps the total mass of the device down.

Figure 4. Four lampshades, spaced 6 cm apart, each consisting of 24 panel assemblies, make up one silicon endcap.

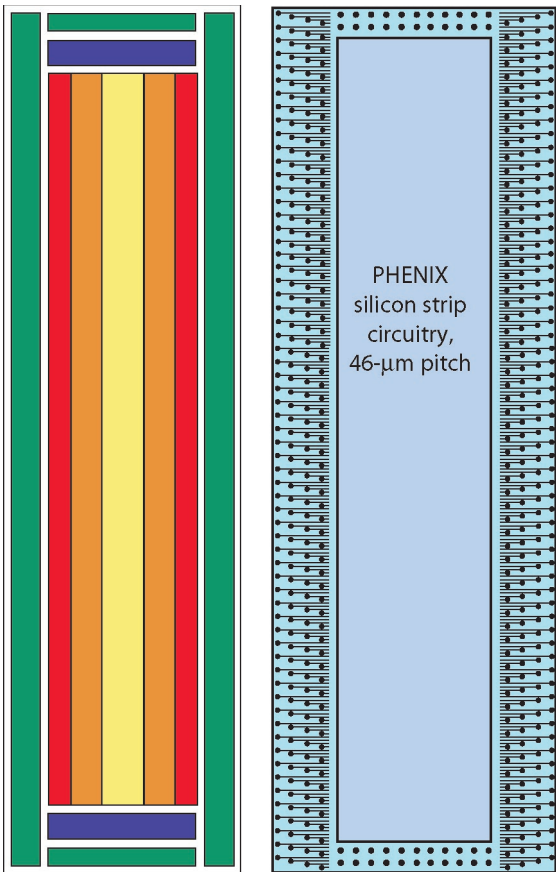

Figure 5. The logical layout of the readout chip is displayed on the left. Green is the bonding area, blue is the programming interface, red is the preamp/discriminator, orange is the pipeline, and yellow is the digital processing and signal bus. The bump-bond pattern of the chip is displayed on the right. The chip measures 3.8 mm × 13 mm and services 2 × 256 strips.

Conclusion

We have embarked on a project to extend the physics reach of the PHENIX experiment through the study of charm and beauty signals. Plans call for research and development on the silicon-vertex-tracker endcaps to continue through 2006 and for construction to proceed for the two years following. The first data taken with the new device are expected in late 2008.

Acknowledgment

I would like to thank Dave Lee and Pat McGaughey for help in the preparation of this article. The LANL silicon-vertex-tracker effort was supported by LDRD funding.

For further information, contact Hubert van Hecke at 505-667-5384, hubert@lanl.gov. For more detailed information on the silicon-vertex-tracker project, visit the project website at http://p25ext.lanl.gov/~hubert/phenix/silicon/.

Theoretical Research on Strong, Electromagnetic, and Weak Interactions

M.B. Johnson (P-25), J. Raufeisen (P-25)

In addition to the fundamental experiments conducted in P-25, we have a strong theory component consisting of a staff member, a postdoctoral fellow, and a number of short- and medium-term visitors from universities and laboratories throughout the world. Theoretical research focuses on basic issues of strong, electromagnetic-, and weak-interaction topics; these topics complement our current experimental activity and impact possible future scientific directions in the group. As such, our theoretical team is involved in both experimental and theoretical activities in the nuclear- and particle-physics community and contributes to a balanced scientific atmosphere within P-25. Recent theoretical activity has focused on parity violation in chaotic nuclei, deep inelastic and Drell-Yan reactions on nucleons and nuclei, QCD at finite temperatures, and phase transitions in the early universe.

Our analyses of Drell-Yan data from FNAL have been used to quantify how quarks propagating in nuclei lose energy and gain transverse momentum. They are based on a light-cone, target-rest-frame approach. This approach has the advantage over previous analyses in that the contribution of the shadowing of quarks is calculated rather than fit to data. Results show that both energy loss and momentum broadening of quarks occur at a rate greater than previously expected. For example, Figure 1 shows a preliminary, parameter-free, theoretical prediction of the transverse momentum distribution of the dileptons in the Drell-Yan reaction, which is based on a color-dipole representation of the quark-nucleon interaction. The result is consistent with a rate of momentum broadening about twice the currently accepted value.

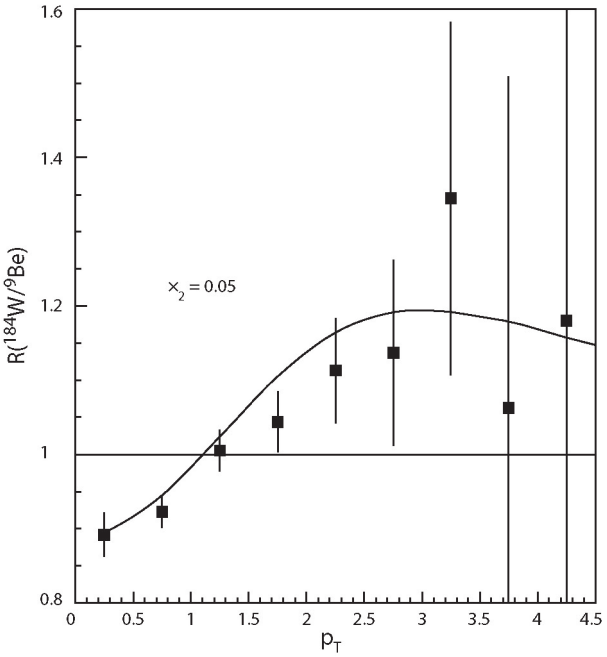

Figure 1. Comparison of theoretical prediction of $R^{W/Be}(p_T)$ versus p_T (in GeV/c) to experiment for $x_2 = 0.05$. Data are from the FNAL E772/E866 collaboration.

Radio-Frequency Emission from a Pulsed Reactor

R.E. Kelly (P-22), K.V. Lindsay (NIS-10)

In anticipating the possible move of the TA-18 nuclear reactor, an experimental and theoretical effort is under way to investigate the initiation, propagation, and detection of electromagnetic radiation in the rf portion of the spectrum resulting from a pulsed reactor. Several source mechanisms are under theoretical investigation, including bremsstrahlung, transition radiation, neutron interactions, and fission-fragment time-dependent charge exchange. The experimental method consists mainly of using various antennas, such as triaxial dipoles, monopoles, and loops. In addition, surface B-dots and D-dots and current transformers have been installed to detect possible surface waves that are guided by any conductor from the reactor environment. All measurements are in the near field due to the emitted long wavelengths. Although the project is in its initial stage, theory predicts, and experiments verify (via Fourier transforms), a continuous low-frequency emission. In addition, the instrumentation output duplicates those of the nuclear detectors in displaying the fission pulse shape. Several new experiments are planned in parallel with theoretical predictions to support potential applications.

Solid Oxygen as an Ultra-Cold Neutron Source

C.-Y. Liu (P-23), A. Saunders, C. Morris, G.E. Hogan (P-25), J.C. Long (LANSCE-3)

Following our previous success with a solid-deuterium-based UCN source at LANSCE, our team is pursuing an experimental study on another promising material, solid oxygen, for intense UCN production. The physics of UCN production in solid oxygen, involving magnon (spin wave) exchanges, is fundamentally different from the well-known phonon mechanism in solid deuterium and has the potential to produce a UCN-flux output several orders of magnitude greater than that for solid deuterium. In the solid-oxygen mechanism, the neutrons are down-scattered through coupling to the magnons in the antiferromagnetic phase of the solid—the strength of which is comparable to the nuclear scattering (phonon) in solid deuterium. This mechanism has several advantages. For one, the smaller nuclear-absorption cross section of oxygen leads to a much longer UCN lifetime in this material. Also, the UCN loss due to the absorption of the excess energy from paramolecules (a major source of loss in solid deuterium) is absent in oxygen. The UCN density achievable should be about an order of magnitude greater than that for solid deuterium. Furthermore, a factor-of-ten gain in source volume should be possible by taking advantage of the much smaller neutron-absorption probability and the infinite elastic-scattering mean-free path of a UCN in solid oxygen.

The optimal solid-oxygen operational temperature is 2 K, somewhat lower than that of solid deuterium (5 K). Nevertheless, the experiment requires minimal modification of the existing prototype solid-deuterium UCN source, mainly the extension of the cryostat capability to 2 K. Currently, we are designing such a cryostat with variable-temperature and -cooling-surface-area capabilities. Using this cryostat, we plan to carry out a comprehensive study of UCN production in solid oxygen using the LANSCE proton beam next year.

Education and Outreach

J.F. Amann (P-25)

P-25 group members continue to be active in education and outreach activities, both as participants in programs sponsored by LANL and as individual citizens who volunteer their time for various activities. Recent group-member activities include visiting classrooms for a weekly science hour and maintaining a website for this activity at http://users.hubwest.com/hubert/mrscience/science1.html. We also coordinated, organized, and participated in the "Teacher's Day" event at the annual meeting of the American Physical Society's Division of Nuclear Physics. Members of our group are technical recruiters for LANL; our recruiters visit college campuses and organize targeted recruiting activities at scientific meetings. In addition to these outreach activities, P-25 sponsors several high school, undergraduate, and graduate students to work on projects within the group (Figure 2). Through their individual schools, these students study physics, computing, engineering, and electromechanical technical support. They also supplement their learning through interactions with LANL mentors and through real on-site experience. Several students are writing theses based on the work they do at P-25.

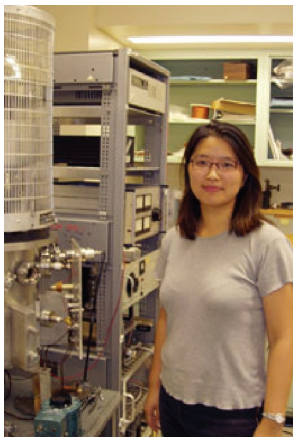

Figure 2. On September 4, 2003, the Rosen Prize Committee of the LANSCE User Group announced the selection of Chen-Yu Liu, Princeton University (now a post-doctoral appointee in P-23) as the 19th Louis Rosen Prize recipient for her outstanding Ph.D. thesis, "A Superthermal Ultra-Cold Neutron Source." Chen-Yu Liu is a member of the UCN team, a collaborative effort between P-23, P-25, Princeton University, North Carolina State University, California Institute of Technology, the Institut Laue-Langevin, Virginia Polytechnic Institute and State University, the University of Kyoto, and the Petersburg Institute for Nuclear Physics. The Rosen Prize is awarded to the student with the best thesis based on work done in whole or in large part at LANSCE.

Alpha-Dot Experiment

J.R. Torgerson, S.K. Lamoreaux, F.G. Omenetto, M.M. Schauer, and W.T. Buttler (P-23)

It has long been understood that our physical theories are incomplete descriptions of nature. An idea that is seeing renewed interest within the physics community is that this incompleteness may be manifest in space-time variation of the fine structure constant (alpha, α). One experimental effort, which compared quasar spectra to theoretical analyses of atomic structure, has suggested that a time variation of $\dot{\alpha}/\alpha = 6 \times 10^{-16}$/year may exist. This is in contrast to an analysis of the natural nuclear reactor which existed in the Oklo natural reactor in Gabon, Africa, two billion years ago and suggests that $\dot{\alpha}/\alpha < 10^{-17}$/year.

This last year, we developed two experimental plans to pursue a search for the time variation of α. The first involves the comparison of three atomic optical-frequency standards based upon trapped ions. The particular ions, In^+, Tl^+, and Yb^{2+}, are insensitive to field shifts and also have very different sensitivities to changes in α. This comparison has the potential to achieve a sensitivity to changes in α of $\delta(\dot{\alpha}/\alpha) \approx 10^{-18}$/year for a series of short measurements spanning a year. We developed a collaboration with the research group of Dmity Budker at the University of California, Berkeley; the theory group of Victor Flambaum at the University of New South Wales (Sydney); and Scott Diddams and coworkers at NIST in Boulder, Colorado. We also successfully pursued LDRD funding to support this effort for the next three years.

We are pursuing the second experimental effort in collaboration with the University of California, Berkeley; it involves a dysprosium atomic-beam apparatus. Atomic dysprosium possesses two nearly degenerate energy levels with opposite parity that exhibit a sensitivity similar to Tl^+ and Yb^{2+}. However, the levels of interest are nearly degenerate, which allows us to use rf spectroscopy rather than optical-frequency metrology—significantly easing our experimental requirements. Our experiment should achieve a sensitivity better than $\delta(\dot{\alpha}/\alpha) \approx 10^{-16}$/year within the next two years and has the potential to achieve a sensitivity of nearly $\delta(\dot{\alpha}/\alpha) \approx 10^{-18}$/year for measurements during a single year. This experiment

has recently received additional funding through a NIST Precision Measurements Grant. Finally, we reanalyzed the Oklo natural reactor data with a more realistic model for the neutron spectrum within a functioning reactor; this new analysis suggests statistically significant deviation from $\dot{\alpha} = 0$ at $\dot{\alpha}/\alpha = 2 \times 10^{-17}$/year and has inspired others to reinvestigate their own work regarding the Oklo natural reactor.

Plasma Astrophysics on the Flowing Magnetized Plasma Experiment

Z. Wang, C.W. Barnes, P.D. Beinke, S.C. Hsu, E.R. Mignardot, C. Munson, G.A. Wurden (P-24), D.C. Barnes, H. Li (X-1), K. Noguchi, X. Tang (T-15), R. Santillo (College of New Jersey), M. Martin (Texas A&M)

It is well recognized that magnetic fields can change motion of plasmas in the universe and cause structure formation on galactic (and smaller) scales. We have been building the first dedicated plasma experimental facility [the Flowing Magnetized Plasma (FMP) facility] that takes advantage of existing LANL resources and expertise to study how magnetic fields can affect plasma flow and how plasma flow, such as rotation, can be modified by magnetic field (one example is the magneto-rotational instability). The expected results will lead to a better understanding of astrophysical phenomena and their underlying physics. Such understanding can also be useful to fusion-energy research, whereby the role of plasma flows has attracted more and more attention. The experimental design and construction are guided by close interaction with theoretical and computational study.

The initial phase of construction is finished. We have constructed of a capacitor-bank system that can deliver up to 300 kJ of energy for 10 ms. The main FMP vacuum tank has achieved the base vacuum in the target regime of a few × 10^{-6} torr with 1,000 l/s turbomolecular pumps. FMP solenoids have delivered an axial, dc magnetic field up to 500 G. Theoretical studies on magneto-rotational instability caused by couette flow point out the regime of interests for our experiments. In addition to the capacitor-bank-energy-sustained plasma flow (couette flow), we also successfully created a helicon plasma that will be used to benchmark and test diagnostics for plasma flow and magnetic field.

Through a unique design of a Penning-trap-like magnetic-field structure inside the coaxial gun, we have achieved consistent plasma breakdown with as low as a 400-V capacitor-bank voltage. This is much smaller than previously reported numbers of 1 to 5 kV. The low-voltage breakdown allowed us to create a 4-ms-long pulse plasma with modest capacitor-bank energy of 60 to 100 kJ. The FMP plasma has been diagnosed with Rogowski coils, Pearson transformers, a Mach probe, a Phantom fast-framing camera, and several channels of B-dot probes. The gun-plasma peak power ranges from 10 to 40 MW depending on the capacitor-bank voltage. Thirty to fifty percent of the capacitor-bank energy is observed to convert into plasma energy (coaxial-gun current and voltage product integrated for the duration of the plasma lifetime). Initial Mach data analysis showed plasma flow on the order of 0.1–0.5 times the ion sonic speed. Both plasma imaging and B-dot measurements indicate interesting plasma self-organization and structure-formation processes, which give rise to magnetic fields in both the axial and azimuthal directions in the cylindrical geometry of the FMP.

Search for a Permanent Electric Dipole Moment of the Electron Using a Paramagnetic Crystal

C.-Y. Liu, S.K. Lamoreaux (P-23), M.A. Espy, A. Matlachov (P-21)

As it is free from hadronic uncertainties, the EDM of the electron can be used to make direct measurements of (or set limits on) the interaction strength of new particles postulated by popular extensions to the Standard Model. The sensitivity of current EDM measurements is approaching that of several predictions for new physics. We are carrying out one such high-sensitivity search for the electron EDM. This search uses a solid-state system, and hence it promises orders-of-magnitude improvement over atomic beams solely from the available electron density. An electrically insulating paramagnetic material will become spin-polarized in the presence of an electric field, if an electron EDM exists. For an electron EDM even many times smaller than the current limit, the polarized sample develops a net magnetization that can be detected with high sensitivity using state-of-the-art SQUID

magnetometers. This electric-field-induced spin-order increases as the sample temperature decreases. We are studying gadolinium gallium garnet (GGG) that has a low conductivity and a high concentration of heavy ions, Gd^{3+}, as a candidate material for this experiment. The gadolinium ion, in the garnet crystal field, is predicted to have an EDM 2.2 times that of the bare electron. Using a practical sample size of 100 cm^3 and a typical high electric field of 10 kV/cm, we expect, after 10 days of data averaging, to place an experimental limit on the electron EDM on the level of 10^{-29} *e*cm (electron-centimeters). This is 100 times more sensitive than the current limit set by the thallium atomic-beam experiment at the University of California, Berkeley.

Over the past year, we have synthesized large polycrystalline GGG samples (using the solid-state reaction method) in our laboratory. We have performed a series of sample characterizations using x-ray scattering and magnetic susceptibility measurements below 4 K. We have designed and constructed the experimental apparatus, which includes high-voltage electrodes, a magnetic-shielding package, a SQUID gradiometer, and a liquid-helium cryostat. Currently, we are testing a large-capacity dilution refrigerator, an essential component of this experiment, which will be used to cool the whole assembly to below 100 mK. We expect to perform systematic studies this winter and produce preliminary results on the electron EDM next year.

High-Energy Nuclear Physics

D.M. Lee (P-25), representing the PHENIX collaboration

An important area of study in P-25 is the distribution of partons in nucleons and nuclei. This includes the nuclear modification of QCD processes such as the production of J/ψ particles (made up of a charm/anticharm quark pair). We are continuing to publish research on this topic from a program centered at FNAL, where we have performed measurements of Drell-Yan and heavy-quark production in fixed-target proton-nucleus collisions since 1987. Our most recent measurement from the NuSea Experiment (E866) is an analysis of the absolute Drell-Yan cross sections in p-p and p-d collisions at 800 GeV/c. This is the first measurement of the Drell-Yan cross section in p-p collisions over a broad kinematic range and the most extensive study of p-d collisions. A detailed comparison with recent global parton distribution fits is in good agreement for the light antiquark sea, but the parton fits overestimate the valence quark distributions as Bjorken-x approaches 1.

Our new proposal (E906), titled "Drell-Yan Measurements of Nucleon and Nuclear Structure with the FNAL Main Injector," aims to improve on the E866 measurement of the ratio of anti-d/anti-u quarks, with coverage to much larger values of Bjorken-x. E906 has been approved by the FNAL program-advisory committee and a formal funding proposal has been submitted to DOE. Approximately $3 million was requested for the construction of a new large-dipole magnet and additional detector construction funds. E906 is currently scheduled to begin taking data in 2008. The recently installed and commissioned muon arms at PHENIX are well poised to continue these studies. Measurements of J/ψ production in p-p and d-Au collisions at $\sqrt{S} = 200$ GeV are currently under way.

The Majorana Experiment

S.R. Elliott (P-23), representing the Majorana collaboration

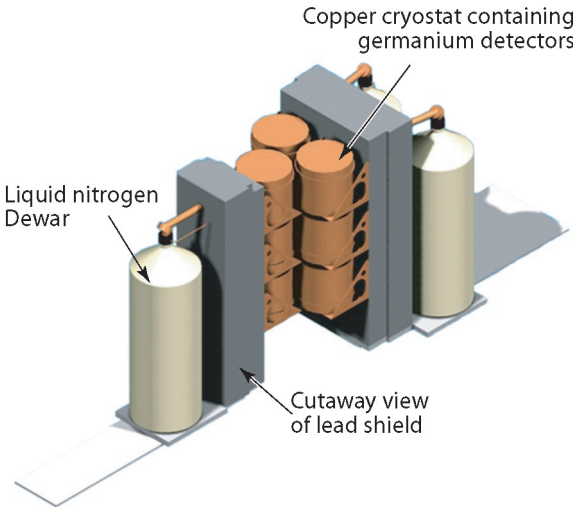

Figure 3. A cut-away concept drawing for the proposed Majorana apparatus.

The objective of the Majorana experiment (Figure 3) is to study neutrinoless double beta decay ($0\nu\beta\beta$) with an effective Majorana-neutrino mass sensitivity below 50 meV to characterize the Majorana nature of the neutrino, the neutrino mass spectrum, and the absolute mass scale. An experimental study of the neutrino mass scale implied by neutrino oscillation results is now technically within our grasp. This exciting physics goal is best pursued using the well-established technique of searching for $0\nu\beta\beta$ of ^{76}Ge, augmented with recent advances in signal processing and detector design. The Majorana experiment will consist of a large mass of ^{76}Ge in the form of high-resolution intrinsic germanium detectors located deep underground within a low-background shielding environment. Observation of a sharp peak at the $\beta\beta$ endpoint will quantify the $0\nu\beta\beta$ half-life and thus the effective Majorana mass of the electron neutrino. The collaboration has recently finished a draft proposal to build and operate this experiment.

The Majorana proposal is based on well-established technology that does not require proof-of-principle research and development. However, there are two research and development projects that are currently under way to optimize the engineering design of the Majorana experiment. These projects are called SEGA (segmented enriched germanium assembly) and MEGA (multiple element germanium array). Not only do these efforts help to optimize the Majorana design, but they will also achieve physics goals in and of themselves. The goal of SEGA is to optimize the previously successful, signal-processing techniques for crystals whose charge collection is segmented. The goal of MEGA is to optimize the arrangement and packaging for multiple crystals sharing a single cooling system. For the Majorana experiment, we will implement the optimum configuration determined by the SEGA and MEGA activities and operate with a large quantity of enriched germanium material to reach a significant sensitivity for the $0\nu\beta\beta$ half-life.

Wide-Angle Cerenkov Telescope

G. Sinnis, B.L. Dingus, F. Samuelson, X. Xu (P-23), R. Atkins (University of Wisconsin), J. A. Goodman (University of Maryland), L.A. Kelley, D.A. Williams (University of California, Santa Cruz), G. Mohanty (University of California, Riverside), T. Stephens, S. Stochaj (New Mexico State University), G.B. Yodh (University of California, Irvine)

The origin of cosmic rays is still a mystery 100 years after their discovery. An important clue to their origin lies in their nuclear composition. Beyond an energy of ~ 100 TeV, the composition cannot be directly measured from space but must be inferred from indirect, ground-based measurements. To date, no ground-based technique has been able to measure the composition of the cosmic rays in an energy regime (< 100 TeV) where direct measurements have been performed. This has left the veracity of conflicting ground-based measurements in question.

The WACT is an array of six atmospheric Cerenkov telescopes, each equipped with a fast camera (composed of 25 PMTs) that measures the lateral distribution of the Cerenkov light generated by EASs. The lateral distribution of the shower light is sensitive to the altitude at which the air shower reaches its greatest development (shower maximum). Shower maximum is, in turn, dependent upon the nuclear species of the primary cosmic ray—lighter nuclei such as protons have a smaller cross section and therefore penetrate deeper into the atmosphere. During the past year, WACT has acquired over 10,000 high-quality events that are currently undergoing analysis.

Qweak: A Precision Measurement of the Proton's Weak Charge

G.S. Mitchell, J.D. Bowman, S.I. Penttilä, W.S. Wilburn (P-23), and the Qweak collaboration

The Qweak experiment (Figure 4) at the Thomas Jefferson National Accelerator Facility (JLab) aims to make a 4% measurement of the parity-violating asymmetry in elastic scattering at very low Q^2 of a longitudinally polarized electron beam on a proton target. The experiment will measure the weak charge of the proton (and thus the weak mixing angle at low-energy scale), providing a precision test of the Standard Model. Because the value of the weak mixing angle ($\sin^2\theta_w$) is approximately one-quarter, the weak charge of the proton ($Q_w^p = 1 - 4\sin^2\theta_w$) is suppressed in the Standard Model, making it especially sensitive to the value of the mixing angle and also to possible new physics. The experiment is approved to run at JLab, and the construction plan calls for the hardware to be ready to install in Hall C in 2007. The experiment will be a 2,200-hour measurement, employing an 80% polarized, 180-μA, 1.2-GeV electron beam; a 35-cm liquid-hydrogen target; and a toroidal magnet to focus electrons scattered at 9°, which is a small forward angle corresponding to $Q^2 = 0.03$ $(GeV/c)^2$. With these kinematics, the systematic uncertainties from hadronic processes are strongly suppressed. To obtain the necessary statistics, the experiment must run at an event rate of over 6 GHz. This requires current mode detection of the scattered electrons, which will be achieved with synthetic-quartz Cerenkov detectors. We will use a tracking system in a low-rate counting mode to determine average Q^2 and the dilution factor of background events.

LANL members of the Qweak collaboration are responsible for the design and construction of the quartz detector system. The expected event rate for scattered electrons of 760 MHz per detector octant precludes counting the individual events. Instead, the experiment will use current-mode detection and low-noise, front-end electronics, which are areas of technical expertise of the LANL collaborators. Preliminary design work and prototype testing has begun at LANL. Simulations indicate that the detector design will be sufficient to produce 50 photoelectrons per event in the photomultiplier at each end of each quartz bar, a level which will allow the collection of data to be limited only by counting statistics.

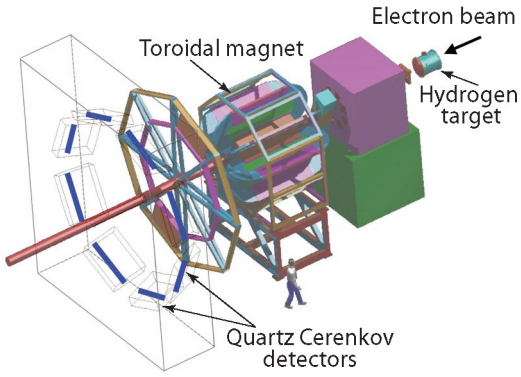

Figure 4. Conceptual design for the Qweak experimental setup in Hall C at JLab. The electron beam (1.2 GeV, 180 μA, P = 80%, 30 Hz reversal) enters the experimental apparatus at the upper right (at the 35-cm-long liquid hydrogen target and scattering chamber). The eight current-mode, synthetic-quartz Cerenkov detectors (~ 6-GHz total rate) are each 2 m × 12 cm × 2.5 cm. The spectrometer provides clean separation of elastic and inelastic electrons at its focal plane.

Pulsed-Cold Neutron Beta Decay

W.S. Wilburn, J.D. Bowman, G.S. Mitchell, S.I. Penttilä, P.-N. Seo (P-23), J.M. O'Donnell (LANSCE-3)

The beta (β) decay of the neutron provides one of the most sensitive tests of the Standard Model of electroweak interactions. The neutron, which consists of two down quarks and one up quark, is converted into a proton, which consists of one down quark and two up quarks. During the decay process, an electron and an electron-type anti-neutrino are created. Precise measurements of various decay parameters (including correlations between the momenta of the decay particles and the initial neutron spin) and of the shape of the electron energy spectrum are sensitive to the physics of the electroweak interaction. Previous measurements have been consistent with present theory; however, the most precise measurements obtained from the most recent β-decay experiment differ from theory by three standard deviations. Previous measurements have been limited by systematic errors.

We are developing a new experimental approach that uses a pulsed-cold neutron beam like the current one at LANSCE and the one planned for the Spallation Neutron Source at Oak Ridge National Laboratory (ORNL). Our approach incorporates two key technologies: an existing ^{3}He spin-filter neutron polarizer and a new spectrometer with two large-area silicon detectors having thin dead layers on either end (Figure 5). (Our team has been developing the new spectrometer.) Combining a pulsed-cold neutron beam and a ^{3}He spin-filter neutron polarizer allows us to determine neutron polarization with unprecedented accuracy. The new spectrometer will allow us to detect both the proton and electron events from each neutron β decay in coincidence—thus greatly reducing background noise. All sources of systematic errors that have limited the sensitivity of previous experiments to approximately 1% are expected to be less than 0.1% with our approach; these effects are monitored by *in situ* checks. If successful, this spectrometer-development work will lead to an important experimental program at LANL.

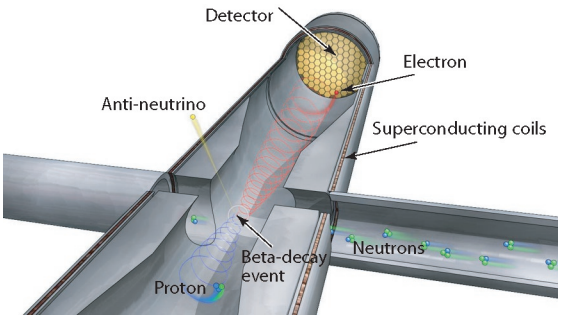

Figure 5. A cut-away drawing of the neutron-beta-decay spectrometer. A neutron-beta-decay event is shown with the newly created proton and electron spiraling toward opposite detectors under the influence of the spectrometer's magnetic field. One of the two silicon detectors is visible.

In the past year, we have made progress on several fronts. The preliminary design of the spectrometer is at a point where an engineering design can begin. The design achieves the required magnetic field and homogeneity and allows for adiabatic transport of the polarized neutrons into the decay region. We have worked closely with silicon-detector manufacturers and now have a quote for producing a suitable prototype spectrometer. The silicon detectors will be 4 in. in diameter and 2 mm thick with thin dead layers. In addition, the detectors will be capable of withstanding high-bias voltages to achieve high charge-carrier drift velocities. An apparatus has been constructed at LANL to measure the timing resolution of the two silicon detectors. It consists of an ^{90}Sr β source; a thin, fast, plastic scintillator that will provide a timing fiducial signal; and a vacuum chamber with a cold finger (i.e., a cooled cooper rod that conducts heat away from the silicon detectors) for mounting and cooling the silicon detectors to 80 K. Working with our collaborators at ORNL and a company with expertise in designing analog-to-digital converters (ADCs), we now have a working concept of how to digitize the detector signals while preserving energy and timing information. The ADC modules sample at 100 MHz and include a sophisticated field-programmable gate array and a digital-signal processor to handle the high data rates on board.

The PHENIX Program at RHIC

D.M. Lee, P.D. Barnes, J.G. Boissevain, M.L. Brooks, J. Burward-Hoy, G.J. Kunde, M.J. Leitch, M.X. Liu, P.L. McGaughey, J.M. Moss, D.O. Silvermyr, W.E. Sondheim, J.P. Sullivan, H.W. van Hecke (P-25)

Members of Group P-25 are developing innovative technology for a large international program at BNL's RHIC aimed at helping researchers better understand the subatomic physics that defined the early universe. "Big Bang" cosmology pictures a time very early in the evolution of the universe when the density of quarks and gluons was so large that they existed as a plasma; they were not confined in the hadrons we know today (neutrons, protons, pions, and related particles). A large international research team—known as the PHENIX collaboration—is attempting to produce a small sample of this primordial QGP in the laboratory and to study its exotic properties. (The PHENIX collaboration includes about 500 physicists and engineers from universities and laboratories in the U.S. and in 14 foreign countries.) The challenge facing this team is to identify the fleeting transition from two colliding gold beams to this de-confined phase of matter, QGP, using the PHENIX collider detector (Figure 6) at the RHIC. Los Alamos plays a major role in defining both the search for the QGP and the related physics program at RHIC. To help realize this goal, researchers and engineers from P-25 are constructing major subsystems for PHENIX—an MVD and two muon spectrometers.

The MVD is the smallest and among the most technically complex of the PHENIX subsystems. It surrounds the interaction region where two beams of 200-GeV/nucleon ions collide. The functions of the MVD are to determine the precise location of the interaction vertex where the transition to the QGP should occur and to measure the global distribution and total number of secondary charged particles; these properties are crucial parameters used to determine the energy density achieved in the collision fireball. A fully instrumented MVD has been installed and is now taking data during the physics runs of PHENIX. The muon spectrometers, the largest subsystem on PHENIX, consist of two conically shaped radial field magnets on opposite ends of the PHENIX detector, with three stations of position-sensitive tracking chambers inside the magnets. These chambers are the largest of their kind in the world. The muon subsystem plays a central role in P-25's physics agenda because it is optimized for examining hard-scattering observables at very high temperatures and densities, where the strong force is smaller and easier to calculate using a method known as "perturbative quantum chromodynamics." Both spectrometers are completely installed and are presently taking data. Analysis of the recorded data shows clear mass peaks for the J/Psi resonance, which will help researchers determine if the QGP exists—a keystone of the PHENIX physics program and a clear demonstration of the successful operation of the muon-spectrometer systems.

Figure 6. Rendering of the PHENIX collider detector.

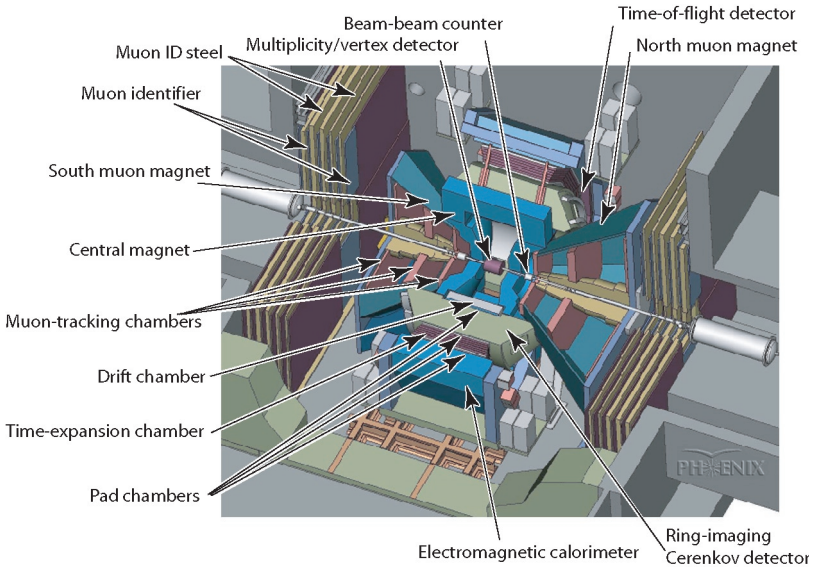

Neutron-Beta-Decay-Asymmetry Measurement Using the New Ultra-Cold Neutron Source at LANL

A. Saunders (P-25), representing the UCN-A collaboration

An experiment is under construction at LANL that will measure the angular correlation between the neutron spin and the direction of emission of the electron in polarized neutron beta (β) decay, which is characterized by the coefficient *A* and is usually called the β asymmetry of neutron decay. A measurement of the β asymmetry involves a determination of the forward-backward asymmetry of the β with respect to the direction of the neutron polarization. A measurement of *A*, when combined with knowledge of the neutron lifetime, provides a determination of the fundamental-vector and axial-vector weak coupling constants. Previous measurements of *A* have disagreed both among themselves and with other measurements of the vector weak coupling constant and with the requirement of the Standard Model that the Cabibbo-Kobayashi-Maskawi (CKM) matrix be unitary. In short, a β-asymmetry measurement provides a sensitive means to search for physics beyond the Standard Model (such as right-handed currents)—phenomena that are predicted to occur in a number of Grand Unified Field Theories (GUTs).

The new experiment at LANL will measure the β asymmetry of the decay of ultracold neutrons (UCNs). UCNs provide a uniquely sensitive tool for this kind of measurement, because they can be held for long periods of time in storage bottles and guide systems and also because they can be polarized to close to 100% polarization using the $\vec{\mu} \cdot \vec{B}$ potential. The first property allows them to be created in a high-radiation environment then piped to a very-low-background environment for the measurement, and the second property allows UCN measurements on polarized neutrons to achieve lower systematic uncertainties caused by the neutron polarization than other techniques. Because UCNs have temperatures of only about a milli-Kelvin, UCN experiments in the past have typically been limited by the available density of neutrons. Therefore, an important part of the LANL work has been to design and construct a new UCN source capable of supplying much higher densities of neutrons to an experiment.

The UCN source and experiment are being built at the Los Alamos Neutron Science Center (LANSCE). An overhead view of the layout of the new facility is shown in Figure 7. The source is designed to produce the neutrons using a 4-μA beam of 800-MeV protons from the LANSCE accelerator; it therefore lies behind a shield package consisting of about 5000 tons of steel behind a 6-ft layer of concrete. The UCNs are piped out through the wall of the shield package using special quartz guides coated with a diamond-like carbon coating—chosen for the high velocity of neutrons that they can guide and for the low probability of losing a neutron when it collides with the wall of the guide. The experiment consists of a 7-T superconducting solenoid magnet to polarize the UCNs, another 1-T magnet to maintain the UCN polarization and guide the β-decay particles to detector stacks, and other associated guide and calibration hardware.

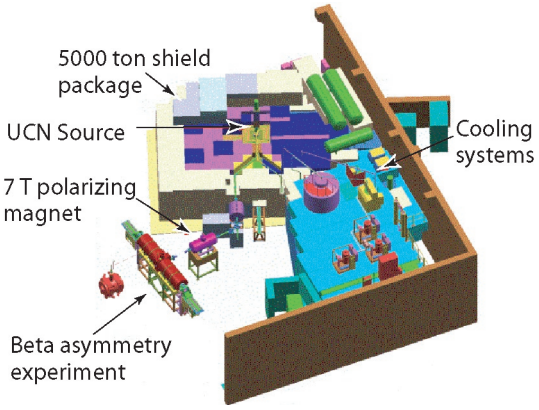

Figure 7. Experimental Area B at LANSCE showing the installation of the new UCN source, associated cooling systems, and the experiment that will use the UCNs to measure the neutron-β-decay asymmetry. Installation of the systems shown is nearing completion.

The UCN source uses a solid-deuterium converter to produce the UCNs through a nonequilibrium superthermal process in which more UCNs are produced than would be expected from the Maxwell-Boltzman distribution at the temperature of the moderator. This technology has been developed over the last few years at LANL by this team and has resulted in a new understanding of the physics of UCN interactions with solid deuterium, a prototype UCN source that produced a greater density of UCNs than any other existing UCN source, and also a design for a full-scale source that is predicted to produce even more UCNs. Construction of the new source and experiment are nearly complete; all the major components are on site and are now being installed in the experimental area at LANSCE. First beam on target is expected in early 2004, with first measurements of neutron-β-decay asymmetry expected shortly thereafter.

Gamma-Ray Burst Science

M.M. Gonzalez, B.L. Dingus (P-23), Y. Kaneko, R.D. Preece, M.S. Briggs (University of Alabama, Huntsville), C.D. Dermer (Naval Research Laboratory)

Using archival data taken by EGRET and BATSE (both of which are instruments on board the Compton Gamma Ray Observatory satellite), team members have searched for a new high-energy component to gamma-ray burst emission. Of 24 bursts examined, they found one burst with just such a component. This work was published in *Nature,* and the lead author, Maria Gonzalez (a graduate student in P-23), received an award from the Los Alamos Awards Program for her work.

Existing models of high-energy particle production in gamma-ray bursts cannot explain the existence of this spectral component; it appears that the acceleration of protons in gamma-ray bursts is needed to explain this result. This gives credence to the idea that gamma-ray bursts may be the source of UHECRs.

Spin Physics at RHIC

D.M. Lee (P-25), representing the PHENIX collaboration

The muon detectors at PHENIX are also designed to study which subatomic components of the proton carry its spin. When both beams at the RHIC are composed of polarized protons, the p-p interactions are directly sensitive to the fraction of spin carried by the gluons. The measurements of heavy-quark and quarkonium production through muon channels are one of the most promising tools to directly probe the polarized-gluon structure function inside the proton. During 2001 and 2002, we successfully measured J/ψ production with the newly installed south muon detector from the first polarized p-p collisions at RHIC.

Previous deep-inelastic-scattering measurements were only sensitive to the sum of the quark and antiquark contributions to the proton spin. However, by using polarized proton beams to induce the Drell-Yan process, it will be possible for the first time to separately determine the spin of the antiquarks. Additionally, by measuring the asymmetry of the charge states of the intermediate-vector boson (W), the flavor dependence (i.e., the difference between up- and down-quark contributions to the spin) can be extracted. There is no doubt that the RHIC spin program will produce exciting physics results as the polarization and luminosity improve in the coming years.

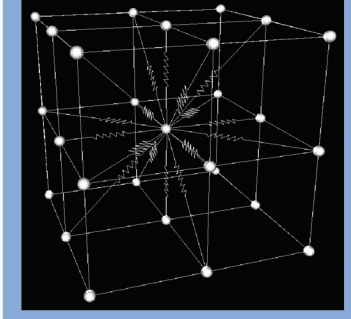

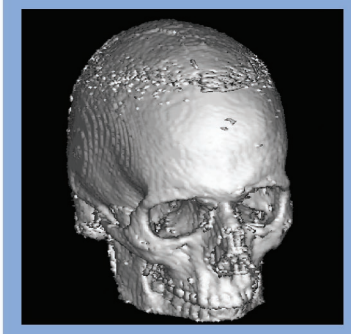

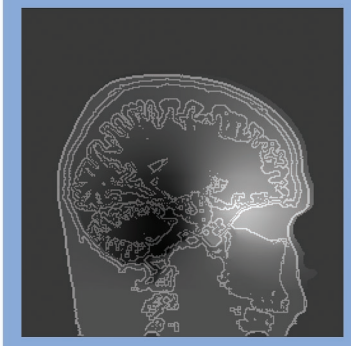

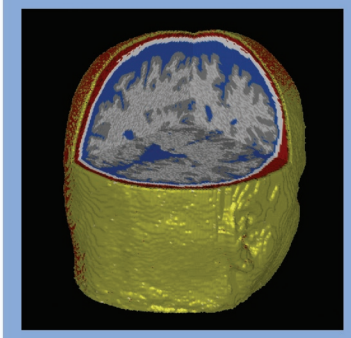

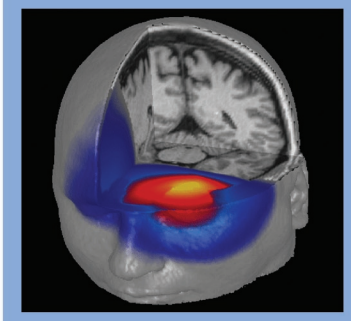

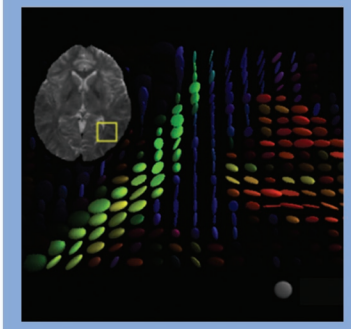

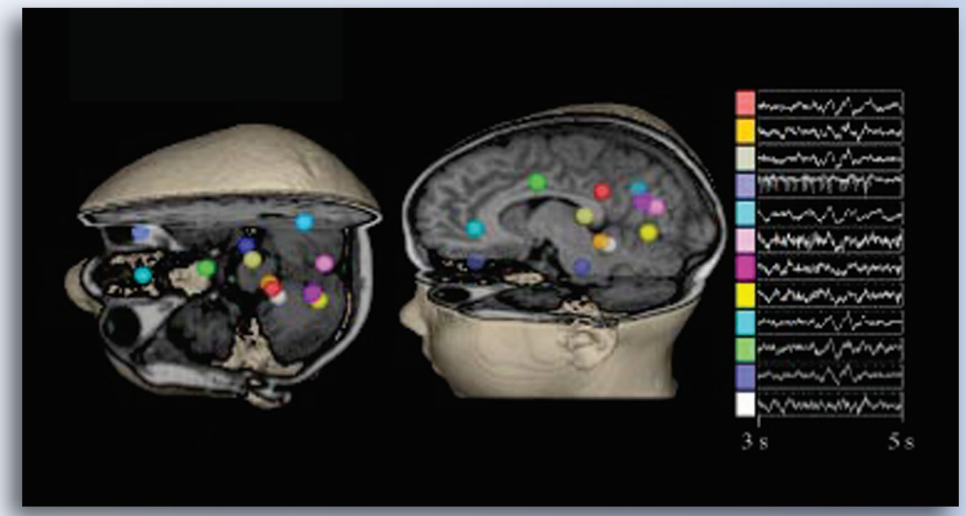
3 s
5 s

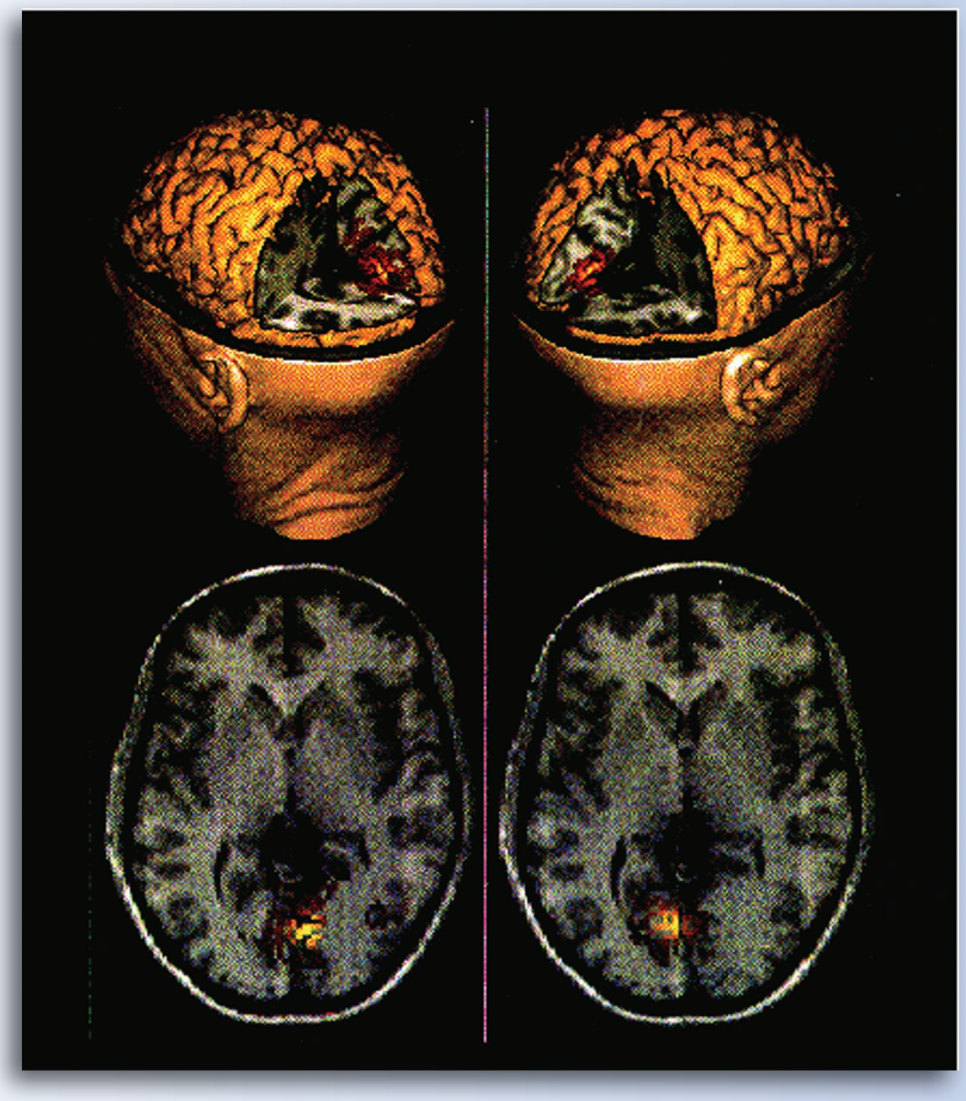

Biophysics

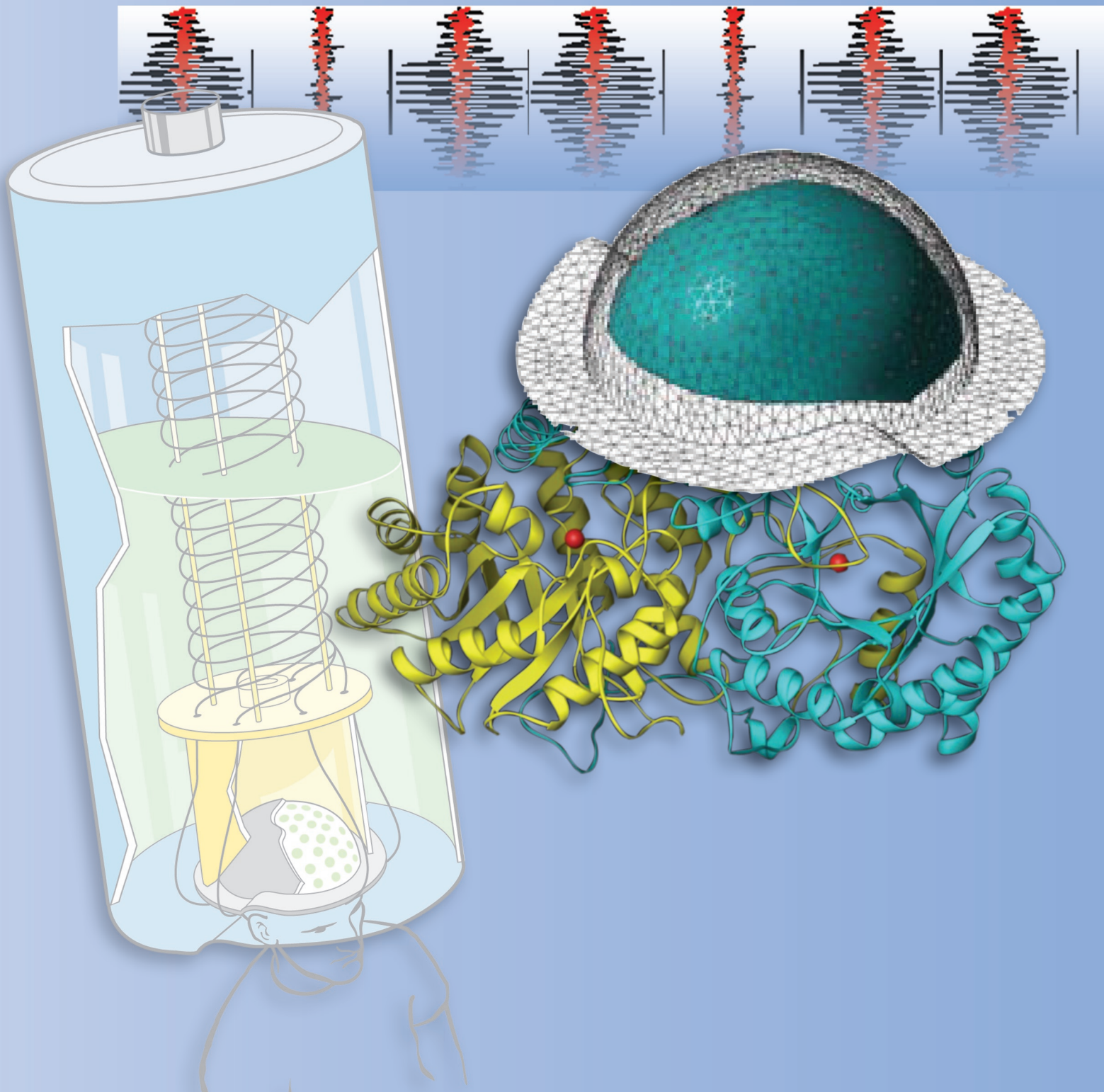

Biophysics Contents

Research Highlights

Multi-Modality Imaging and Modeling of Dynamic Brain Function 167
Computer Models of Neural Circuits 171
SQUID Magnetometry—Harnessing the Power of Tiny Magnetic Fields 175

Project Descriptions

Single-Molecule Detection and Characterization 179
Protein Structure, Dynamics, and Function 180

Multi-Modality Imaging and Modeling of Dynamic Brain Function

J.S. George, D.M. Schmidt, C.C. Wood, G. Kenyon (P-21), B.J. Travis (EES-2)

The past few decades have witnessed extraordinary progress in the development of techniques for structural and functional imaging of the human brain. MRI is the premier technique for imaging the soft tissue anatomy of the human brain, but it has significant limitations for defining the geometry of the skull, which computerized tomography does very well. Functional MRI provides detailed pictures of spatial patterns of neural activation based on associated hemodynamic changes but does not capture the characteristic temporal dynamics of neurophysiological activation. MEG and EEG provide excellent temporal resolution of neural population dynamics but are limited in spatial resolution by the ambiguity and ill-posed nature of the source reconstruction problem. Electrophysiology, microanatomy, optical imaging, and other methods each provide important though limited insight into neural function and functional organization. Although the mix and relative importance of imaging technologies will evolve, the need to integrate information from multiple methods will remain.

Dynamic neuroimaging techniques allow measurement of neural population responses that reflect integrated activity of the underlying networks. Evolving analytical strategies allow increasingly reliable source localization and time-course estimation based on MEG and EEG, incorporating anatomy from MRI.[1,2] These tools allow us to observe the dynamic responses of neural populations; but to understand the nature and basis of network function, it is necessary to build models. Computational models of the physical systems and of the physiological processes that give rise to observable responses are essential to connect experimental measures with models of the distribution and dynamics of neural activation. *Forward models* of field or potential distributions at the head surface associated with primary currents within the brain are the basis for *inverse procedures* for MEG and EEG that attempt to estimate the

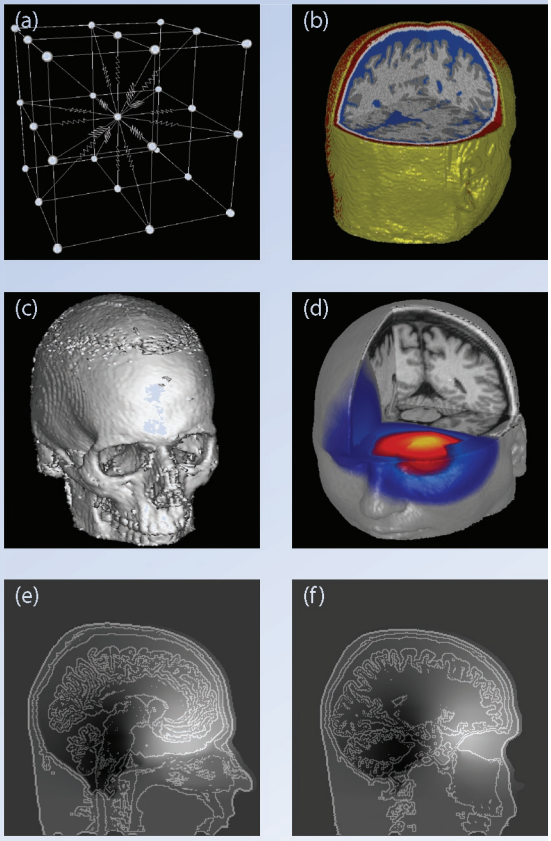

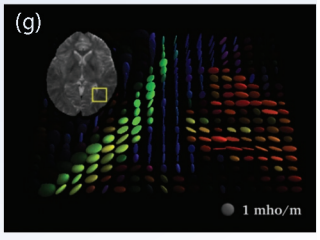

Figure 1. Forward calculations by the FDM. (a) Influence scheme showing resistive links between neighboring nodes. (b) Segmented MRI used to set conductivities for simulation. (c) Skull segmented from MRI before post processing. (d) Surface/cut plane rendering of potentials from Figure 1(c). (e and f) Two slices through computed potential volume, showing current leakage along the optic nerve penetration. (g) Computed conductivity tensors based on DT-MRI. Note the anisotropy of conductivity corresponding to white matter tracts.

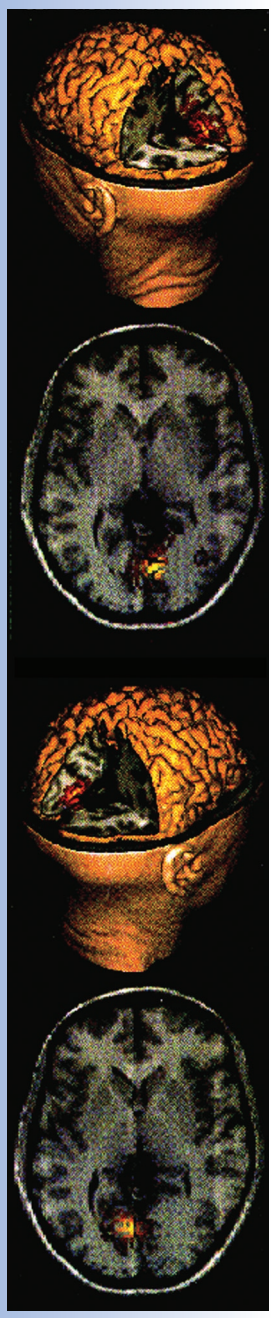

Figure 2. Bayesian Inference probability maps of source locations derived from MEG studies of visual responses.

number, location, extent, and time courses of regions of cortical activation. Simulation tools that capture the three-dimensional architecture and functional dynamics of neurons and of extended networks allow us to predict interesting dynamic responses and to optimize network models that account for experimental observations.

Advanced Forward Models

Source localization based on MEG and EEG has traditionally employed analytical or semi-analytical forward calculations based on simple geometries such as spherical shells, assuming that errors introduced by the forward calculation are small relative to the uncertainty associated with the inverse estimation procedure. For some applications, boundary element methods have been used, incorporating the gross geometry of the major conductivity boundaries of the head and employing a small number of tissue classes of simplified geometry.[1] However, as inverse methods get better, the simplifying assumptions inherent in these methods are less tenable.

Finite difference calculation. We have adopted an alternative strategy based on a finite difference method (FDM) that can incorporate more detailed geometry based on MRI and estimates of volume conductivity provided by emerging imaging methods, including diffusion tensor (DT) MRI, current density MRI, and electrical impedance tomography. FDM does not require construction of a specialized computational mesh or explicit identification and topological checking of boundaries; the calculation is performed on a rectangular grid that is the most natural representation of the MRI data used to define the geometry. Various techniques improve the performance of the FDM on a rectangular grid, e.g., adaptive mesh refinement to control error in regions with high field variation and formulations that reduce errors caused by the staircase approximation of a curved boundary.

Because the FDM allows easy manipulation of geometrical details of the volume conductor, we have examined the effects of skull penetrations on observed field distributions. These studies demonstrated significant effects of the optic nerve and ear canal on both the magnitude and distribution of the potential field compared to a model that did not incorporate these shunts (Figure 1). These effects might significantly influence localization of sources in frontal or temporal lobes. We anticipate that it will be important to account for surgical penetrations of the cranium for neurosurgical patients in whom source localization studies are undertaken.

Conductivity estimation. Although our computational formalism handles anisotropic conductivity, in the past such capability was of little consequence because there were no methods for the noninvasive estimation of tissue conductivity or anisotropy. However, our recent work has demonstrated the feasibility of estimating anisotropic conductivity based on DT-MRI [Figure 1(g)]. Tuch[3] has shown that DT-MRI has a well-defined relationship to tissue conductivity. Diffusion and conductivity tensors share the same eigenvectors as a result of the common microgeometry. The relationship between the eigenvalues for diffusion and conductivity can be derived using an "effective medium" theory; we conclude that conductivity and diffusion are strongly and linearly related. Advances in measurement technology and analytical procedures may allow estimation of head conductivity using electrical impedance tomography coupled with models of tissue geometry from MRI.

The Neural Electromagnetic Inverse Problem

To estimate the dynamics of neural systems, an adequate model of the spatial distribution of the underlying sources is needed. Building this source model is the principal business of inverse procedures. Over the past decade, we and others have made significant advances in the development and implementation of inverse procedures for MEG and EEG. Increasingly, these methods employ information derived from other imaging modalities such as MRI to inform or constrain source localization procedures.

Bayesian Inference. We have previously described a technique for Bayesian Inference that addresses the fundamental ambiguity of the inverse problem and the complex error surface associated with the model parameter space by explicitly sampling the posterior probability distribution.[4] A Markov Chain Monte Carlo (MCMC) technique is used to conduct a series of numerical experiments and to see which stochastic solutions best account for the data (Figure 2). Source models accommodate an extended region of activation within a bounding volume defined by a few parameters. Because Bayesian methods explicitly employ prior

knowledge to help solve the inverse problem, they provide a natural and formal method to integrate multiple forms of image data.

Parametric distributed source model. In the 1999 paper describing Bayesian Inference,[4] we employed a parametric source model consisting of a set of elemental currents, each aligned orthogonal to the local cortical surface and all contained with a bounding sphere centered on some cortical voxel. We recently have implemented a new technique to define the bounding volume for our activation model that produces regular two-dimensional patches across the cortex sheet. The patch is defined by a series of dilation operations (i.e., stepwise labeling of successive layers of contiguous voxels) about some seed voxel. This method produces source models based on patches of cortical activation, more consistent with our expectations, and allows useful constraints on the polarity of cortical currents.

Spatio-Temporal Bayesian Inference. Our initial formulation of Bayesian Inference was applied to single instantaneous field maps. However, our experience has underscored the value of spatio-temporal modeling procedures that attempt to fit an extended sequence of field maps across time with a consistent ensemble of sources. This strategy produces a more parsimonious model and exploits the strong, local correlation within the time domain of integrated neural population activity. We have developed a scheme for Spatio-Temporal Bayesian Inference (STBI) in which each parametric model source has an associated time course. The MCMC algorithm is used to sample the posterior probability distribution of the time courses structured as vectors with an element corresponding to each time point of the sampled field distributions. By this strategy, we are able to estimate the form and variance of the time course associated with each probabilistic source.

Studies with simulated data. Figure 3 outlines the results of a numerical study applying STBI to a simulated data set. In this example, we defined three small, distributed sources. Two of the sources have time courses that are highly correlated—a condition that creates difficulties for some spatio-temporal methods. STBI recovered all three of the sources and time courses with surprising fidelity and with very tight confidence intervals. In another study, we were able to resolve two sources separated by less than a centimeter near the posterior pole of occipital cortex on the basis of differences in orientation and time course. Our experience with simulated data suggests that much of the ambiguity of the MEG inverse problem is eliminated by STBI.

Coupling Experiments and Network Models

In spite of the advances in analytical methodology, noninvasive methods are unlikely to ever provide the spatial and temporal resolution required to monitor the activity of the entire ensemble of individual neurons in a local circuit within the brain. Network-modeling techniques offer the only viable strategy to truly understand dynamic measures of brain function in terms of the underlying synaptic and cellular dynamics and network connectivity. To do this properly, we must model at least some of the physiological and geometrical complexity of real neurons while accommodating very-large-scale networks.

Visual system model. The mammalian visual system represents an ideal structure for employing cellular-level network models to relate dynamic measures of neural activity to underlying neural architecture and population dynamics. In the retina, cellular-network simulations can be related to measures of activity provided by individual microelectrodes or electrode arrays or by dynamic-optical-imaging techniques, thus providing a method to validate and optimize the first steps of the system simulation. We have already used such models to predict and account for experimentally observed dynamic responses.[5]

Large-scale, biologically realistic networks are modeled with the Sensory Enhanced Neural Simulation Engine (SENSE)—a general-purpose neural simulator originally developed by LANL investigators.[6] SENSE can model systems containing as few as one neuron up to millions of geometrically and physiologically realistic neurons. SENSE has recently been implemented as a parallel code to increase the size and complexity of tractable models. With high-performance computers, extended systems such as the early visual pathways can be simulated. SENSE has been coupled to conjugate

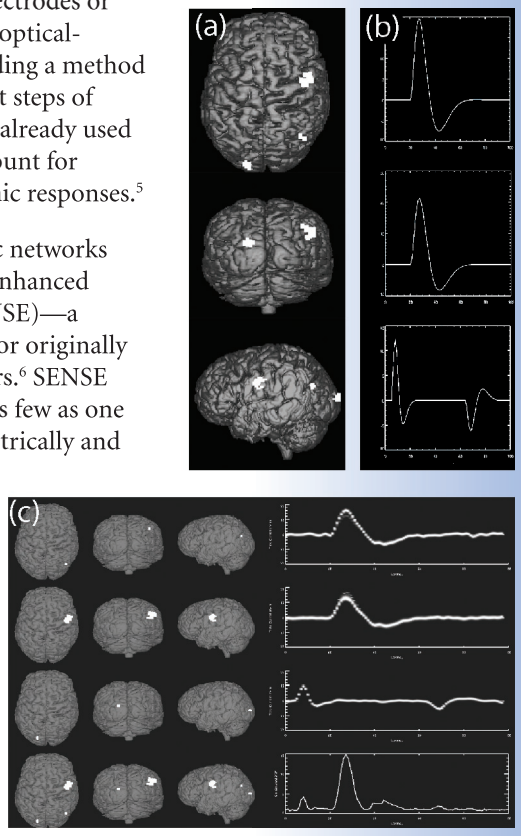

Figure 3. Source location and dynamics estimated by STBI. (a) Locations and (b) timecourses of simulated sources. (c) Locations and timecourses estimated by STBI.

gradient-based inverse and optimization algorithms, allowing data fitting or optimization as a function of any SENSE variable or combination of variables.

Extensions for physical modeling. SENSE captures the realistic three-dimensional spatial arrangements and connectivity patterns of neurons seen in neural tissue and the geometric, electrochemical, and synaptic properties of individual neuronal types. Evolution of the voltage of each neuron's compartments is computed through a series of time steps. We have exploited this capability to compute the net current vector associated with activation of an individual neuron or population of neurons. Such a model can be coupled with the forward models previously described to predict patterns of response observable with MEG or EEG.

Optimization and applications of network models. We have begun to compare model network responses to functional imaging data at the cellular-network level in order to disclose dynamic spatial and temporal patterns of activation that underlie interesting functional properties of neuronal networks. We continue to develop a network model of the retina that can be fit to experimental ensemble data produced with electrode arrays and optical imaging techniques in an effort to optimize neuronal and network properties. We have prototype models of much of the early visual system, and we will calibrate coupled-system model parameters against MEG and EEG data using efficient optimization algorithms to produce quantitative models of neural electromagnetic responses. This work is motivated by our role in a DOE-sponsored project to develop an electroneural prosthetic retinal implant.

Conclusion

Computational integration of multiple techniques for structural and functional neuroimaging provides a much more powerful strategy for dynamic measurement of brain function than the use of any individual method in isolation. Network models allow us to generate experimentally testable predictions of network behavior, such as modulation of dynamic activity and phase-locked oscillations within a population that should set up large signals detectable by MEG or EEG. Such responses are of increasing theoretical interest for understanding the computation by the brain.

References

1. J.S. George, C.J. Aine, J.C. Mosher, D.M. Ranken, H.A. Schlitt, C.C. Wood, J.D. Lewine, J.A. Sanders, and J.W. Belliveau, "Mapping function in the human brain with MEG, anatomical MRI, and functional MRI," *Journal of Clinical Neurophysiology* **12**(5), 406-431 (1995).
2. J.S. George, D.M. Schmidt, D.M. Rector, and C.C. Wood, "Dynamic functional neuroimaging integrating multiple modalities," in *Functional MRI: An Introduction to Methods* (Oxford University Press, United Kingdom, 2001)**,** pp. 353-382**.**
3. D.S. Tuch, V.J. Wedeen, A.M. Dale, J.S. George, and J.W. Belliveau, "Conductivity tensor mapping of the human brain using diffusion MRI," in *Proceedings of the National Academy of Science* **98**,11697-11701 (2001).
4. D.M. Schmidt, J.S. George, and C.C. Wood, "Bayesian Inference applied to the electromagnetic inverse problem," *Human Brain Mapping* **7**, 195-212 (1999).
5. G.T. Kenyon, B. Moore, J. Jeffs, G.S. Stephens, B.J. Travis, J.S. George, J. Theiler, and D.W. Marshak, "A model of high frequency oscillatory potentials in retinal ganglion cells," *Visual Neuroscience* (in press).
6. S. Coghlan, M.V. Gremillion, and B.J. Travis, "NeuroBuilder: A user interface and network simulator for building neurobiological networks," in *Analysis and Modeling of Neural Systems I*, F.H. Eeckman, Ed. (Kluwer Academic Publishers, Massachusetts, 1992), pp. 115-122.

Acknowledgment

This work was supported, in part, by the LANL LDRD program, the MIND Institute, and NIH.

For more information, contact John George at 505-665-2550, jsg@lanl.gov.

Computer Models of Neural Circuits

G.T. Kenyon, G.J. Stephens, M.C. Flynn, J.S. George, J.M Galbraith (P-21), B.J. Travis (EES-2), J. Theiler (ISR-2)

We are using computer simulations to study the dynamics of neural circuits. Although much is known about the inner workings of individual nerve cells, called neurons, the operational principles governing the dynamics of complex interconnected networks of neurons remain poorly understood. By simulating large, heterogeneous neural systems on modern digital computers, we hope to discover some of the operational principles that underlie the extraordinary processing power of biological computers. A better understanding of biological computation will likely contribute to the development of new technologies for treating neurological disease and may well lead to revolutionary advances in machine intelligence.

Understanding Information Processing in the Vertebrate Retina

Many of our studies to date have been directed toward understanding information processing in the vertebrate retina. The retina has many advantages as a target system for developing realistic computer models. The anatomy and physiology of the retina have been extensively studied, especially in comparison with many other parts of the central nervous system; the inputs and outputs of the retina can be well characterized; and the retina receives no major feedback projections from the brain, allowing it to be treated as a stand-alone circuit. Furthermore, we may reasonably expect that by understanding how the retina talks to the brain, we will gain fundamental insight into how the different parts of the brain talk to each other. The following results were obtained using a computer model of the cat retina that has allowed us to investigate the function of retinal circuitry at a level that would be very difficult with currently available experimental techniques.[1]

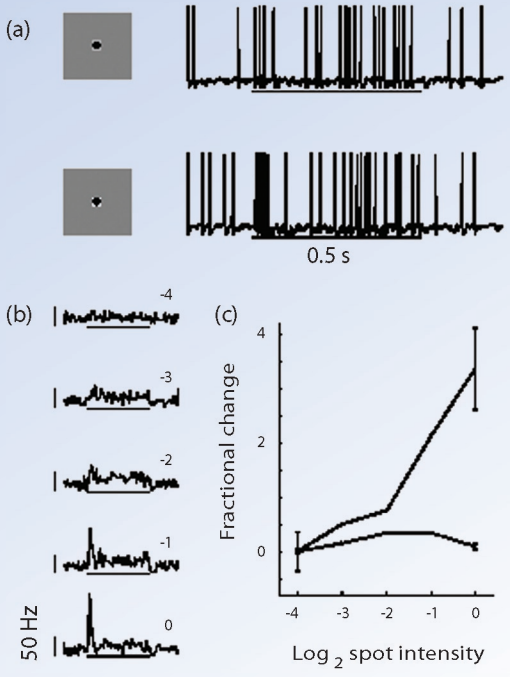

Figure 1. Responses of model ganglion cells to small spots. (a) Ganglion-cell output consists of discrete, uniform pulses. A relatively dim spot (top) produces a small increase in the firing rate, whereas a relatively bright spot (bottom) produces a large transient peak in the firing rate. (b) Peri-stimulus time histograms, giving the change in firing rate versus time, are plotted for various spot intensities (log_2 units). (c) Plot of peak (solid line) and plateau (long-short dashed line) firing rate as a function of spot intensity. Local inhibition prevents the plateau-firing rate from increasing significantly with stimulus intensity.

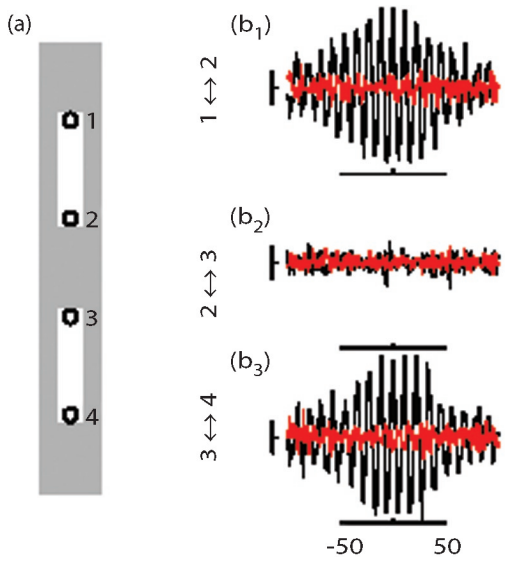

Figure 2. Stimulus-selective synchronization of ganglion cells. (a) Stimulus dimensions relative to the receptive field centers of individual ganglion cells. (b) Cross-correlation histograms computed during the plateau portion of the response between spike trains from pairs of ganglion cells at opposite ends of the same bar or at opposing tips of separate bars. All ganglion-cell pairs were separated by 7 diameters (bin size: 1 ms; scale: 100 ms, 0.5). Also, b_1 is the pair from the upper bar; b_2 is the pair from separate bars; and b_3 is the pair from the lower bar. Correlations were only significant for pairs from the same bar.

Our most intriguing finding is that retinal neurons can encode visual information in rather surprising ways. The output of a neuron cannot be classified in conventional electrical engineering terms as either analog or digital, but rather it consists of something altogether different—a temporal sequence of impulses, or spikes. Because each spike is (to a first approximation) identical to every other spike, information can only be conveyed by the temporal pattern of impulses. Neuroscientists continue to debate how information is encoded within the temporal structure of neural spike trains, but there is widespread agreement that one very important variable is the firing rate. Figure 1 shows an example of how a typical neuron in our retinal model encodes the local intensity, or contrast, of a small stimulus as a transient increase in firing rate.

About 10 years ago, Wolf Singer's laboratory in Germany reported that retinal neurons use the relative timing of spikes to encode global information about visual stimuli that is not conveyed by their local firing rates.[2,3,4] Using our retinal model, we were able to demonstrate a very similar phenomenon by examining the relative timing of spikes produced by neurons responding to either the same or to different objects (Figure 2). For retinal neurons activated by the same large object, their spike trains were strongly correlated, or phase locked, by a common underlying oscillation at a frequency of approximately 100 Hz. Pairs of retinal neurons activated by different objects, however, were not correlated because the phases of their underlying oscillations varied randomly with respect to each other. Thus, our retinal model captures the interesting property of biological neurons—their evoked oscillations in responses to appropriate large visual features are stimulus-specific and are only phase-locked between cells responding to the same contiguous object.

We used the retinal model to ask what information-stimulus-specific oscillations between retinal neurons might convey to the brain. To investigate this question, we were guided by two principles. (1) Because it only takes us a fraction of a second to form a visual impression, the information conveyed by stimulus-specific oscillations must be available on short, physiologically meaningful time scales—roughly a few hundred milliseconds. (2) Because the spatial convergence of retinal neurons onto target cells in the brain is rather low, with each target cell receiving input from only a few retinal neurons, the information conveyed by stimulus-specific oscillations must be available locally in the firing activity of a similarly small number of neighboring cells. We thus used the retinal model to quantify the information conveyed about the global properties of a stimulus—in this case, the total size of the object—by a 2 × 2 neighborhood of retinal output neurons in a few hundred milliseconds. At the same time, we were fortunate to receive data from Wolf Singer's laboratory recorded from output neurons in the cat retina under similar experimental circumstances. These data allowed us to directly test the predictions of our retinal model.

The oscillations evoked by stimuli of various sizes in our retinal model were very similar to those measured from the cat retina (Figure 3). In both sets of data, small stimuli evoked little or no oscillatory response, whereas large stimuli evoked very large oscillations. Because our model is consistent with the known anatomy and physiology of the cat retina, it can provide a useful tool for investigating how information may be encoded by spike trains in the optic nerve.

Why Stimulus Size Matters

To determine the information content of both artificial and biological spike trains, we asked whether it was possible to determine if a group of neighboring cells was responding to a small or large object using their local firing activity alone (Figure 4). Our results are plotted as a percent correct, which was proportional to the fraction of trials on which the total size of the stimulus could be correctly inferred from the local firing activity. Random events were added to the model spike trains to ensure that the average number of spikes, or firing rate, did not change as a function of stimulus size. The only cue available from the local firing activity regarding the total size of the stimulus was therefore the amplitude of the synchronous oscillations. Our results showed that in 300 ms (using as few as 4 spike trains from a small 2 x 2 neighborhood), it was possible to achieve performance levels approaching 90% correct.

In related experiments, we showed that there was a tradeoff between the number of cells included in the analysis and the total time allowed for accomplishing the size discrimination task. Specifically, as more cells were included in the analysis, shorter time windows were required to achieve the same performance levels.

Why, one might ask, is it important for retinal neurons to convey information about stimulus size in their local firing activity? For a possible answer to this question, consider the frog retina, where Tachibanna's laboratory in Japan has shown that there are specialized neurons, called dimming detectors, that exhibit strong synchronous oscillations when activated by a large dimming object but not when activated by a small dimming object.[5] Considering that from a frog's perspective, a small dimming spot might be a fly or other food source, whereas a large dimming spot is more likely to be a bird or other dangerous predator, one can quickly appreciate why size matters.

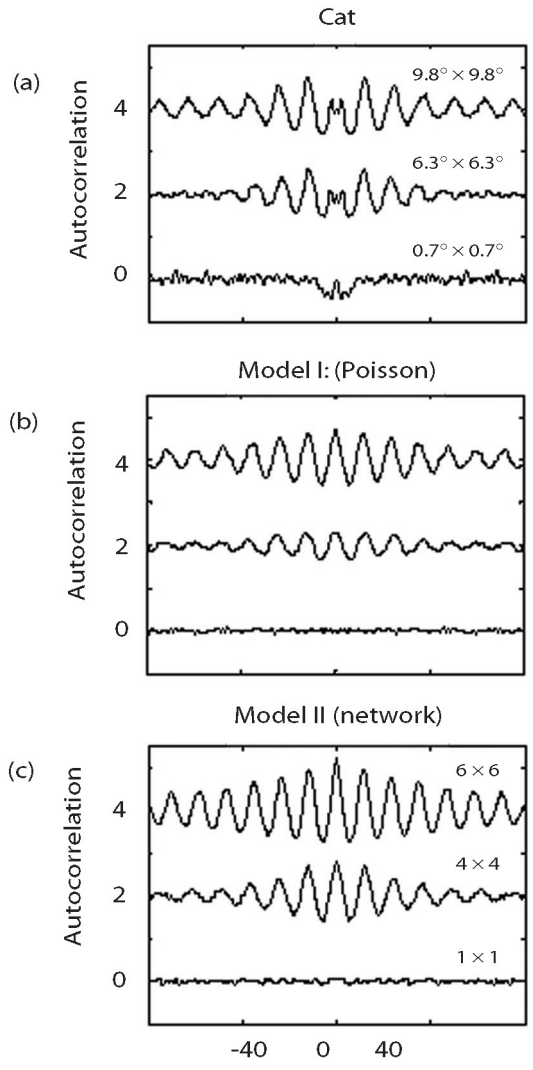

Figure 3. Multi-unit auto-correlograms and cross-correlograms reveal size-dependent high-frequency oscillations. (a) Auto-correlograms computed from multi-unit spike trains recorded from cat retina at the center-of-square spots of increasing size (data were re-plotted from Reference 3). Correlations are expressed as a fraction of the expected level due to chance. (b) Multi-unit cross-correlograms of artificial spike trains, generated by a Poisson process, containing four identically modulated units, each with a mean firing rate of 50 Hz. (c) Multi-unit cross-correlograms produced by an integrate-and-fire feedback circuit consistent with retinal anatomy. Multi-unit spike trains were recorded from a fixed 2 x 2 array of ganglion cells located at the center of each spot (intensity = -2). Poisson-distributed spikes were added to each train to maintain a constant mean firing rate of 50 Hz regardless of spot size.

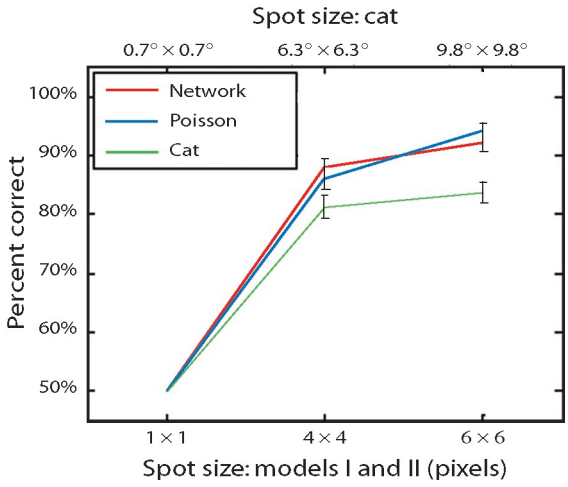

Figure 4. Theoretically optimal performance on a size-discrimination task. Individual 200-ms segments of multi-unit spike-train data were obtained in response to spots of one of two sizes: (1) either an intermediate or small spot (top abscissa = 6.3° x 6.3°, bottom abscissa = 4 x 4) or (2) either a large or small spot (top abscissa = 9.8° x 9.8°, bottom abscissa = 6 x 6). The ordinate gives the maximum percentage of trials that could be classified correctly, assuming each binary possibility was equally likely a priori, based on the total energy in the single-trial power spectra between 75 and 95 Hz. All three data sets indicate that high-frequency oscillations within a small group of ganglion cells yield good single trial discrimination of stimulus size.

References

1. G.T. Kenyon, B. Moore, J. Jeffs, K.S. Denning, G.S. Stephens, B.J. Travis, J.S. George, J. Theiler, and D.W. Marshak, "A model of high frequency oscillatory potentials in retinal ganglion cells," *Visual Neuroscience* (in press, 2003).
2. C.M. Gray, P. Konig, A.K. Engel, and W. Singer, "Oscillatory responses in cat visual cortex exhibit inter-columnar synchronization which reflects global stimulus properties," *Nature* **338**(6213), 334-337 (1989).
3. S. Neuenschwander, M. Castelo-Branco, and W. Singer, "Synchronous oscillations in the cat retina," *Vision Research* **39**(15), 2485-2497 (1999).
4. S. Neuenschwander and W. Singer, "Long-range synchronization of oscillatory light responses in the cat retina and lateral geniculate nucleus," *Nature* **379**(6567), 728-32 (1996).
5. H. Ishikane, A. Kawana, and M. Tachibana, "Short- and long-range synchronous activities in dimming detectors of the frog retina," *Visual Neuroscience* **16**(6), 1001-1014 (1999).

Acknowledgment

This work is supported by the LDRD program at LANL, by the Deployable Adaptive Processing Systems program funded by the DOE Office of Nuclear Nonproliferation, and by the DOE Office of Biomedical and Environmental Research.

For more information, contact Garrett Kenyon at 505-667-1900, gkenyon@lanl.gov.

SQUID Magnetometry—Harnessing the Power of Tiny Magnetic Fields

R.H. Kraus, Jr., M.A. Espy, A.N. Matlachov, P.L. Volegov, J.C. Kumaradas, C. Carr, V. Armijo, S.G. Newman, J. Mattson (P-21), W.P. Roybal (ESA-WMM)

Measurements associated with the neural currents in the brain can be used to diagnose epilepsy, stroke, and mental illness and to study brain function. One way to observe these tiny electrical currents is to measure the magnetic fields they produce outside the skull—a technique called magnetoencephalography (MEG).

The traditional way to monitor the brain's electrical activity is with EEG, which requires gluing as many as 150 electrodes to the scalp. MEG is a noninvasive technique that measures the direct consequence of neuronal activity in the living brain. MEG, together with EEG, are the only noninvasive techniques of measuring brain function at millisecond time resolution or better. MEG measures brain currents as precisely as EEG does but without physical contact, making it possible to screen large numbers of patients quickly and easily. MEG is also insensitive to the conductivities of the scalp, skull, and brain—which can affect EEG measurements.

Enter the SQUID

Measuring the brain's magnetic fields is not easy, however, because they are so weak. Just above the skull, they have strengths of 0.1 to 1 pT, less than a hundred millionth of the earth's magnetic field. In fact, brain fields can be measured only with the most sensitive magnetic-field sensor known—the superconducting quantum interference device (SQUID).

A SQUID is a loop of superconducting material interrupted by one rf or two dc resistive regions known as Josephson junctions. When cooled to very low temperatures, superconductors conduct electricity without resistance. This lack of resistance allows a SQUID to measure the interference of quantum-mechanical electron waves as the magnetic flux enclosed by the loop changes. A SQUID can measure magnetic fields as small as 1 fT.

Cohen first reported detecting a magnetic signal originating from the human brain in 1968 using a nonsuperconducting sensor.[1] Shortly thereafter, an rf SQUID sensor was used for the first time to measure a biomagnetic signal originating from the human heart,[2] and after only two more years, the same instrument was successfully used to record a human magnetic alpha rhythm with a satisfactory signal-to-noise ratio.[3] The first evoked-response magnetic signals associated with brain activity evoked by peripheral sensory stimulation measured with a SQUID sensor was reported in 1975.[4]

The LANL Superconducting Image Surface Whole-Head MEG System

The LANL SQUID team has designed and built a whole-head MEG system that uses 155 dc SQUIDs to provide simultaneous recordings of MEG activity over the entire head. The SQUIDs become superconducting when immersed in

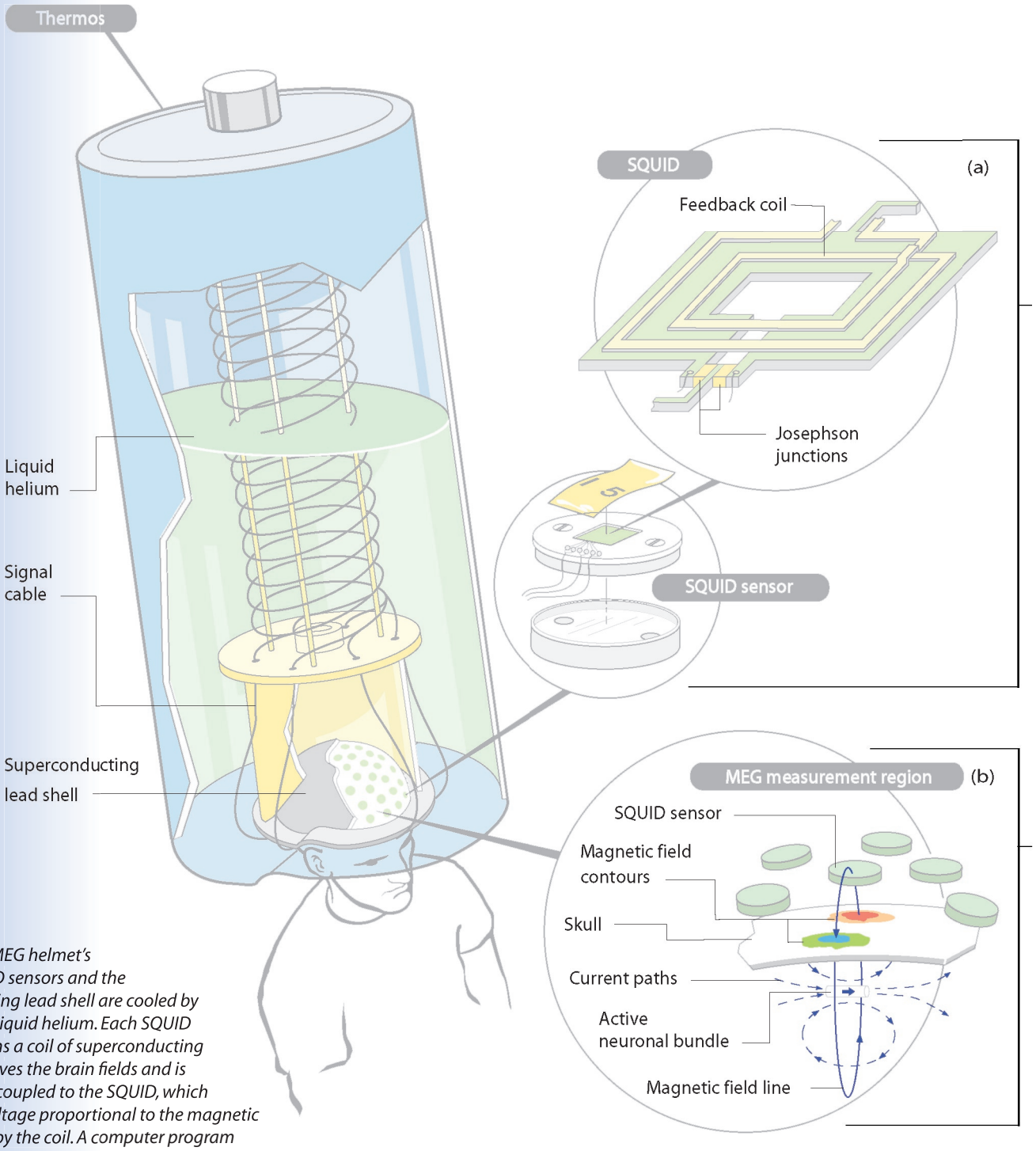

Figure 1. The MEG helmet's array of SQUID sensors and the superconducting lead shell are cooled by immersion in liquid helium. Each SQUID sensor contains a coil of superconducting wire that receives the brain fields and is magnetically coupled to the SQUID, which produces a voltage proportional to the magnetic field received by the coil. A computer program converts the SQUID data into maps of the currents flowing throughout the brain as a function of time. (a) The magnetic field lines that pass through the square hole at the SQUID's center determine the phases of electron waves circulating in the SQUID's superconducting region (green): the waves' interference is proportional to the magnetic flux over the hole. Because superconductors have no electrical resistance, the interference can be measured only by interrupting the superconductor with small regions that have electrical resistance—the two Josephson junctions—so that voltage drops will develop across them. The voltage measured across the junctions is proportional to the magnetic flux over the SQUID's square hole. The feedback coil magnetically couples the SQUID to the pick-up coil in the SQUID sensor. A SQUID is typically 10 to 100 μm on a side. (b) The colored contours show how the magnetic field produced by neural brain currents (dashed arrows) changes in intensity and polarity over the skull's surface. In the red region, the field is most intense in a direction pointing out of the skull. In the blue region, the field is most intense in a direction pointing into the skull.

liquid helium (4 K) contained in a large thermos. The helmet is positioned over a patient's head as he or she sits in a chair (Figure 1).

With sophisticated computer algorithms, MEG data are converted into current maps that give researchers a real-time image of where activity is occurring in the brain. The LANL system responds to brain-current changes in less than a thousandth of a second, adequate for most brain-current studies. The SQUIDs themselves respond in about a millionth of a second. Using specially designed current coils, the LANL MEG system has achieved a spatial resolution of better than 0.25 mm, better than presently reported by any other MEG system (Figure 2).

Eliminating "Noise"

During a MEG measurement, the SQUIDs must be shielded from ambient magnetic fields, whose "noise" tends to swamp the brain signals. Ambient fields are produced mainly by the power lines in a building, although the earth's magnetic field and even the steel in a passing car contribute. (Ferromagnetic materials like steel locally distort the earth's field.) At the frequencies of interest in brain studies—a few to several hundred hertz—the ambient fields must typically be reduced by a factor of 10,000 to 100,000. The helmet's SQUIDs are partially shielded from ambient fields by a thick, hemispherical shell of lead, which becomes superconducting at liquid-helium temperatures. Because superconductors perfectly reflect magnetic fields, the shell reduces ambient fields to as little as one thousandth of their initial strengths. The shielding is not perfect because the shell does not completely enclose the head. The SQUIDs near the shell's crown are better shielded than those near its brim. The shell also reflects the brain's magnetic fields back to the SQUID array, increasing the helmet's sensitivity.

Usually, ambient fields are reduced by taking MEG data in a specially shielded room built with very expensive materials. The superconducting shell effectively blocks magnetic fields from zero to several thousand hertz. Thus, measurements made with the shell require only a "low-end" shielded room, which costs about $100,000—one-fifth that of conventional shielded rooms.

The team has recently added external SQUIDs to the helmet that further reduce the effects of ambient fields. The external SQUIDs measure these fields at several points just outside the superconducting shell, and a computer program then subtracts the fields from the brain-field data to reduce the ambient fields' effects by another factor of 1,000—at all frequencies.

Applications of the MEG/SQUID Technologies

Diagnosing epileptic seizures. For 20% of epilepsy patients, drugs cannot adequately control seizures, and surgically removing the brain tissue where the seizures originate—the epileptigenic tissue—is the only option. But the surgeon must know precisely where the aberrant tissue is to avoid removing nearby tissue required for motor control, sense perception, language, and memory. In addition, by pinpointing how the brain responds to visual, auditory, tactile, or other stimuli, MEG can help

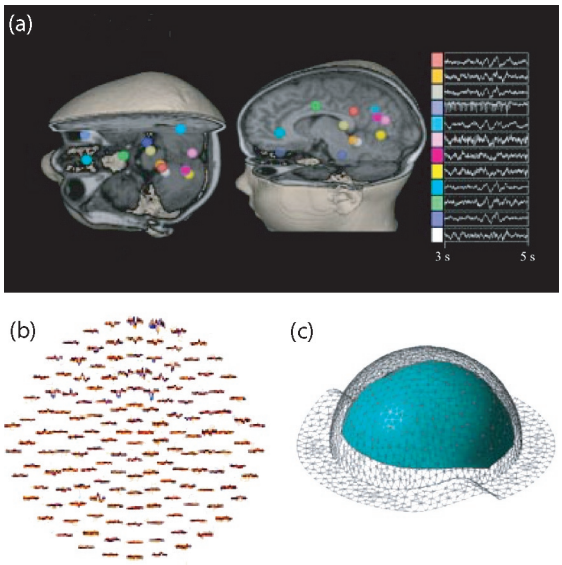

Figure 2. (a) A computer program converts the raw MEG data into maps of the brain's electrical activity as a function of time. These maps can be used to diagnose epilepsy, stroke, and mental disease and to study brain function. (b) The raw data obtained from the 155 SQUID sensors in the MEG helmet. The red waveforms were obtained with the patient's eyes closed. The blue waveforms were obtained as the patient observed a flashing light. (c) The superconducting lead shell. The gray mesh defines the shell's contour. SQUID sensors are attached to the blue surface. At liquid-helium temperatures, the lead shell becomes superconducting and is therefore an excellent magnetic shield. Because a superconductor perfectly reflects magnetic fields at all frequencies, the shell helps shield the underlying SQUID array from ambient magnetic fields. The shell also shields SQUIDs placed outside the shell from the brain's magnetic fields. These external SQUIDs provide data used to help cancel the effects of ambient fields. The superconducting shell and external-field-cancellation method greatly reduce the cost of the magnetically shielded room required for MEG measurements, making them more affordable.

assess the effects of possible collateral damage during surgery.

A brain scan can precisely locate the epileptigenic tissue if the imaging method has high spatial resolution and is fast enough to detect the seizure discharge or the electrical activity that precedes a seizure, which also originates in the epileptigenic tissue. Although seizures occur sporadically, the electrical activity associated with them occurs continually.

Peering into the brain columns. The SQUID team has also developed MicroMEG—using a centimeter-long linear array of SQUIDs with a potential spatial resolution of tens of micrometers. Made of "high-temperature" superconductors, the array's twelve SQUIDs are cooled by liquid nitrogen (77 K) instead of liquid helium (4 K). The MicroMEG array requires less thermal insulation than arrays cooled with liquid helium. Thus, the MicroMEG SQUIDs can be brought within half a millimeter of the tissue under study, allowing extremely high-resolution measurements.

MicroMEG will be used to probe the electrical activity of as few as a few thousand to tens of thousands neurons in one of the brain's cortical columns. The columns are believed to operate in parallel, like the hundreds of microprocessors in a supercomputer that work in parallel to achieve high overall speed. Such studies will improve our understanding of brain function.

Measuring a baby's heartbeat. A variant of MEG called fetal magnetocardiography (FMCG) can be used to diagnose and treat fetal heart conditions. In fact, FMCG is the only way to measure the electrical signals produced by the heartbeat of a baby in the womb. And only the heart's electrical signals contain the detailed timing information required to diagnose and treat fetal arrhythmias. Stethoscopes and ultrasound cannot provide this information because they use sound. Nor is electrocardiography (ECG) useful, because it directly measures the electricity produced by the heart through electrodes taped to the body. However, the baby is electrically insulated from the mother.

Around the twentieth week, the baby's sebaceous glands secrete a waxy, white substance called *vernix caseosa*, which covers the baby's skin to protect it from amniotic fluid in the womb. Because the *vernix* is electrically insulating, electrical signals from the baby's heartbeat cannot pass into the mother's body for measurement on her skin. However, the magnetic fields produced by the baby's heartbeat pass easily through the *vernix* and can be measured with FMCG. Although in principle ECG could be used before the *vernix* forms, the fetal heart is then too small to produce a detectable electrical signal. Unlike other medical diagnostic techniques, FMCG poses no risk to the unborn baby or the mother because it merely receives the magnetic signals sent out by the baby's heart.

References

1. D. Cohen, "Magnetoencephalography: Evidence of magnetic fields produced by alpha-rhythm currents," *Science* **161** 784–786 (1968).
2. D. Cohen, "Magnetoencephalography: Detection of the brain's electrical activity with a superconducting magnetometer," *Science* **175** 664–666 (1970).
3. D. Cohen, E.A. Edelsack, and J.E. Zimmerman, "Magnetocardiograms taken inside a shielded room with a superconducting point contact magnetometer," *Applied Physics Letters* **16** 278–280 (1972).
4. D. Brenner, S.J. Williamson, and L. Kaufman, "Visually evoked magnetic fields of the human brain," *Science* **190** 480–482 (1975).

Acknowledgment

Our work was funded by NIH and the DOE Office of Biological and Environmental Research.

For further information, contact Robert Kraus at 505-665-1938, rkraus@lanl.gov.

Single-Molecule Detection and Characterization

A. Castro, O.C. Marina, F. Martinez (P-21)

Group P-21 efforts in single-molecule detection and spectroscopy focus on the development of novel methods for the ultra-sensitive detection and analysis of biological molecules and their applications to molecular biology and medical diagnosis. Recent developments include the implementation of a technique for the rapid, direct detection of specific nucleic acid sequences in biological samples without the need for enzymatic amplification. Our approach in these experiments is based on detecting the presence of a specific nucleic acid sequence of bacterial, human, plant, or other origin. The nucleic acid sequence may be a DNA or RNA sequence and may be characteristic of a specific taxonomic group, a specific physiological function, or a specific genetic trait. The method we use consists of synthesizing a highly fluorescent nucleic acid reporter molecule using a sequence of the target as a template. A short oligonucleotide primer that is complementary to the target is added to the sample along with a suitable polymerase and free nucleotides. One of these oligonucleotides is partially labeled with a fluorophore. If the target is present in the sample, the primer binds to it, and the polymerase will incorporate the labeled and unlabeled nucleotides, thus reconstructing the target's complementary sequence (Figure 1). The sample is then pumped through the capillary cell of a single-molecule detector. Detection of the reporter signifies the presence of the target being sought. We have applied this method to the detection of specific sequences of DNA from a variety of sources. Most notably, we have demonstrated the detection of DNA from *B. anthracis* at trace concentrations, and in the presence of large amounts of unrelated DNA. *B. anthracis*, the causing agent of anthrax disease, is the weapon of choice in biological warfare. Our recent experiments provide vital research and insight into the intricate workings of specific biological pathogens and supports LANL's defense mission.

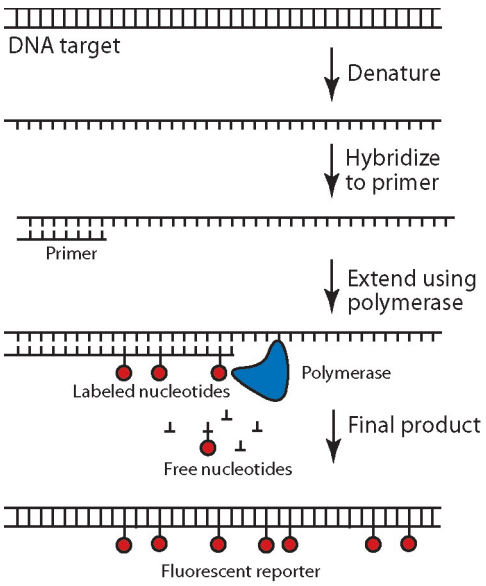

Figure 1. Schematic representation of the polymerase extension reaction for fluorescently labeled reporter molecule synthesis.

Protein Structure, Dynamics, and Function

L.-W. Hung, J. Berendzen, L. Flaks (P-21), T.C. Terwilliger, G.S. Waldo, C.-Y. Kim (B-2), E. Bursey, M. Yu, G. Rajagopalan (Lawrence Berkeley National Laboratory), B. Rupp, B. Segelke (Lawrence Livermore National Laboratory), D. Eisenberg (University of California, Los Angeles), T. Alber (University of California, Berkeley), J. Sacchettini (Texas A&M)

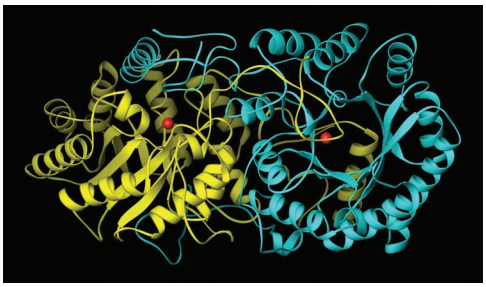

Figure 2. LeuA protein of Mycobacterium tuberculosis (TB), a protein central to Leucine biosynthesis in TB and a potential drug target for TB anti-TB treatment. The structure was determined by Li-Wei Hung (P-21) in collaboration of one of the TBSGC consortium members, Professor Ted Baker of the University of Auckland, New Zealand.

Proteins are the smallest functional unit in living cells. Knowing the structures of proteins is the key to understanding the mechanistic and kinetic modes of these molecular nanomachines. We are pursuing high-throughput x-ray-crystallography technology using high-brilliance synchrotron x-ray beam lines at the Advanced Light Source at Lawrence Berkeley National Laboratory to determine the three-dimensional atomic structures of proteins on a genomic scale. We are one of the integral components of the LANL Tuberculosis Structural Genomics Consortium (TBSGC), one of the ten centers funded by the NIH Protein Structure Initiative to determine a large quantity of novel protein structures in a relatively short amount of time. With the researchers in B Division and LLNL, we established an integrated research resource encompassing the full spectrum of modern structural biology. This includes gene cloning, protein overexpression (B Division), crystallization (LLNL), and x-ray data collection and structure determination (P-21, see Figure 2). Working as a team, we are developing scalable technologies to increase the efficiency and reduce the cost to map each protein structure.

Along with the structural-genomics efforts, we are also developing methods in computational biology to combine protein structure with sequence information to infer their molecular functions. One of the big findings from the completion of genome projects are that over 30%–60% of the genes discovered in most of the organisms have no known functions in humans based on sequence homology alone. These genes and their functions may largely represent the part of biology yet to be discovered. The three-dimensional structures (the shapes) of proteins, have been shown to provide unique information in predicting protein functions. We are working on computational methods to extract structural information to predict protein functions at a much deeper level. From protein sequence and structure to protein function, we are laying out the groundwork to uncover the secret of life.

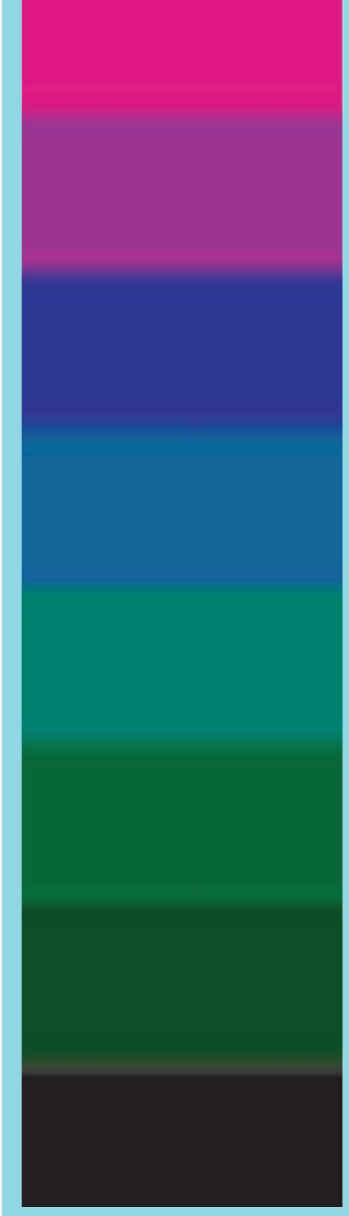

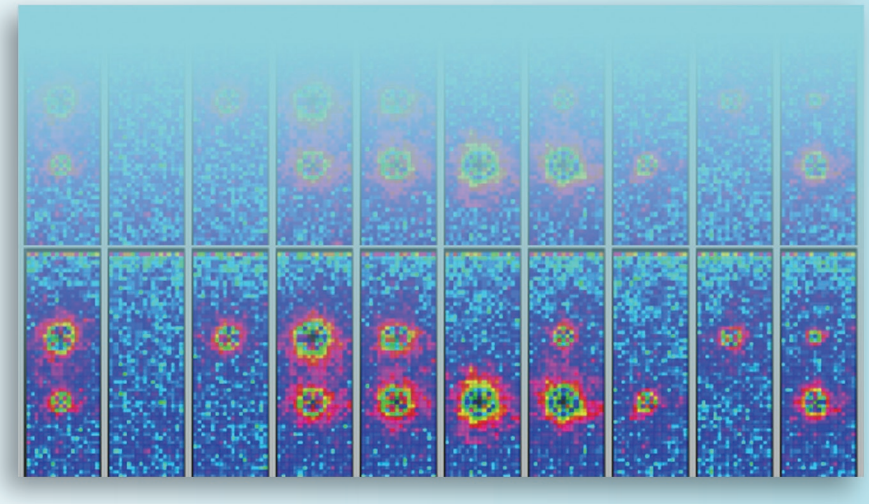

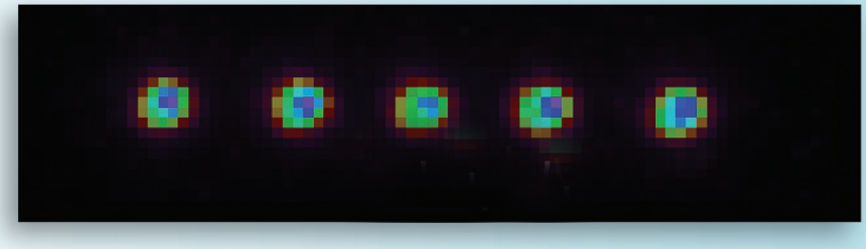

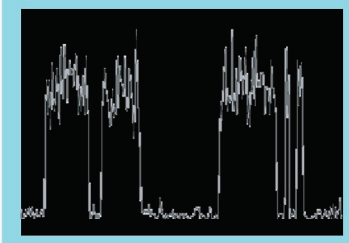

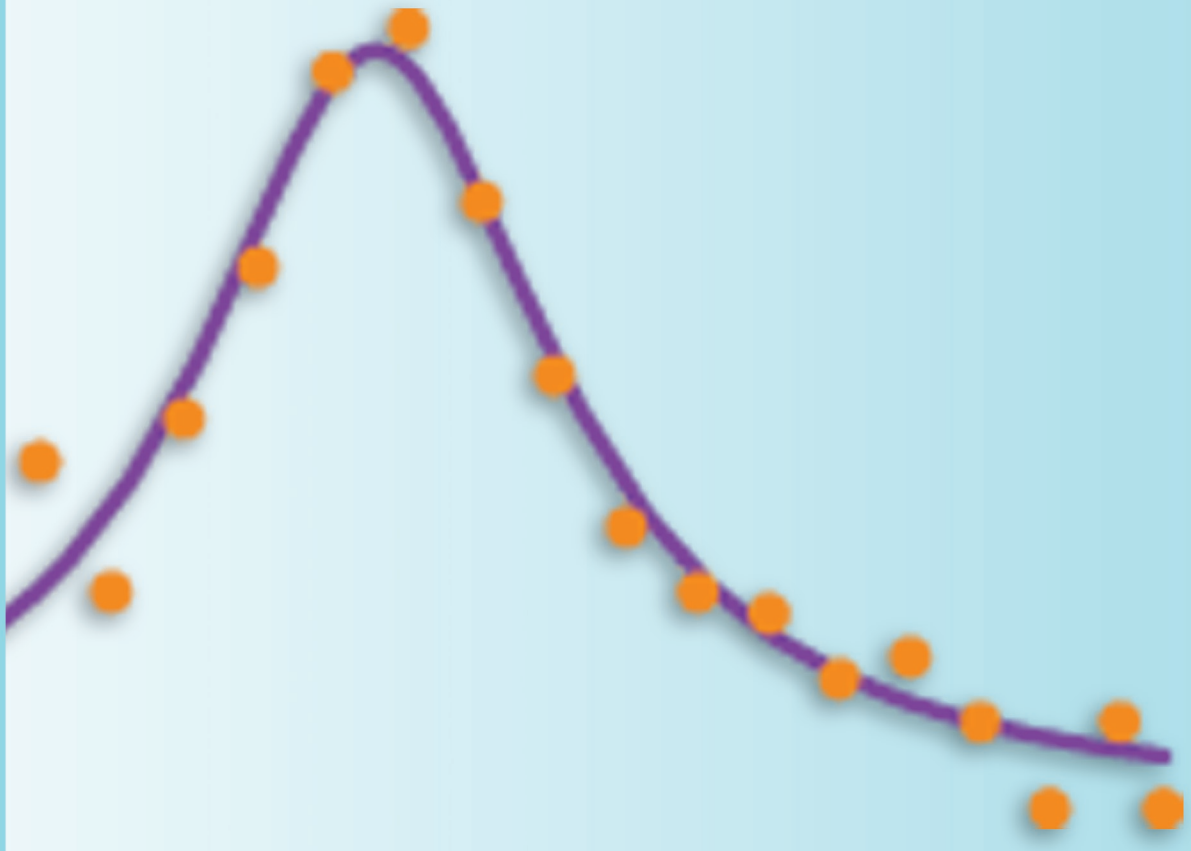

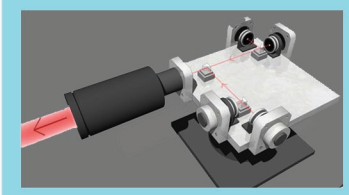

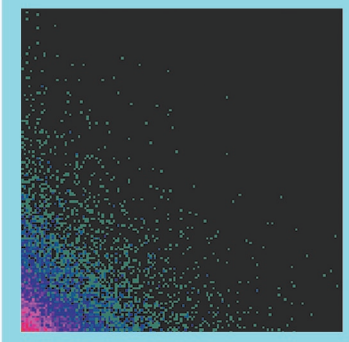

Atomic Physics

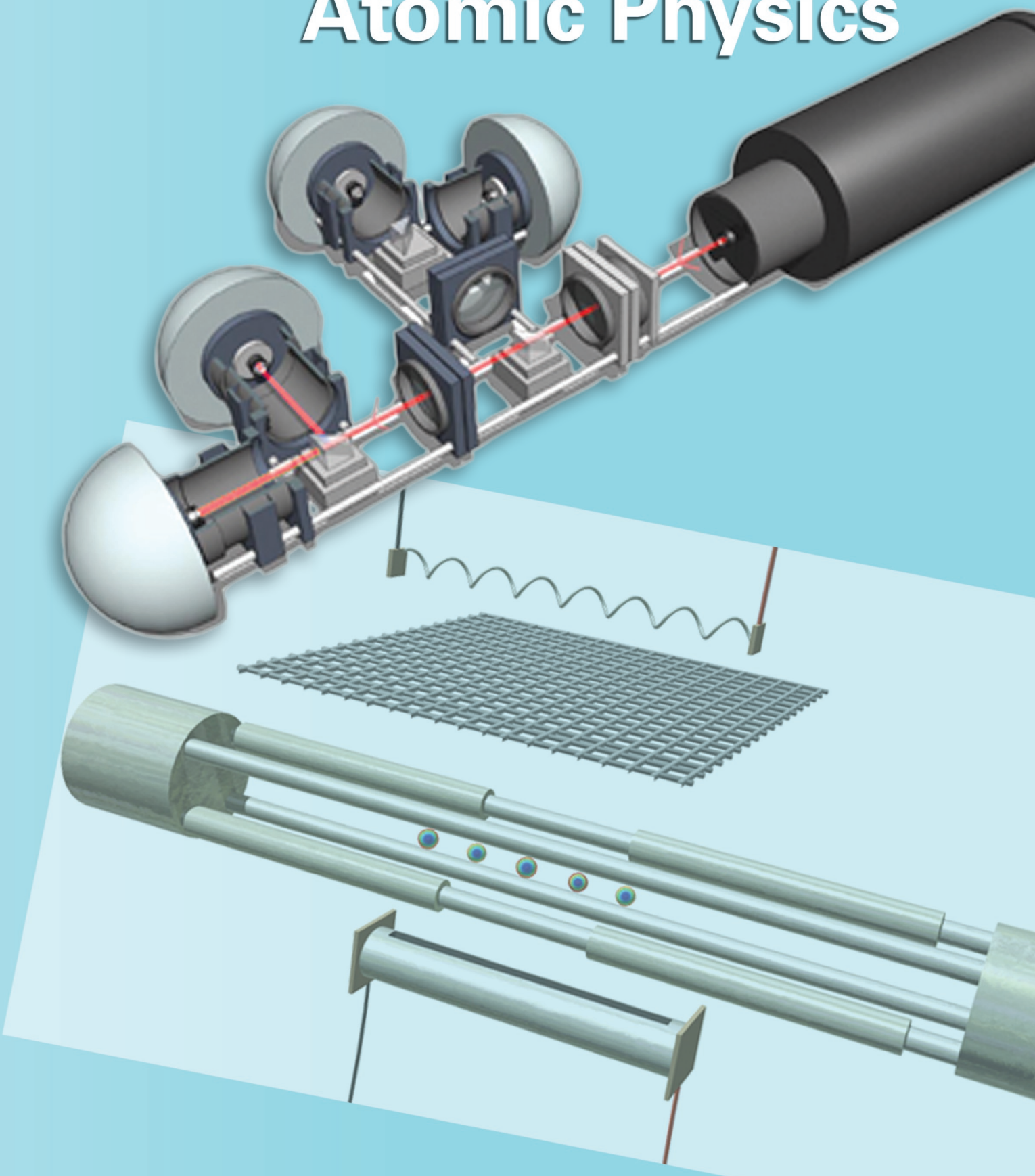

Atomic Physics Contents

Research Highlights

Testing the Randomness of Quantum Mechanics 185
Atom Interferometry with Bose-Einstein Condensates 189
Quantum Key Distribution 193

Testing the Randomness of Quantum Mechanics

D.J. Berkeland (P-21)

Possibly the most nonintuitive aspect of quantum mechanics is that a single particle can be put into a superposition of two distinct states. Moreover, when one makes a measurement, the particle is found in only one state, and that result is unpredictable, or random. Since its inception, quantum theory has been rigorously tested under many diverse conditions and often with extremely high precision. Surprisingly, there are very few statistically significant tests of the *randomness* of a quantum-mechanical process, including the transitions between quantum states. Some experiments have monitored the decays of a large sample of nuclear particles, whereas others have measured whether a photon is transmitted or reflected from a beamsplitter. However, these methods have limitations such as accounting for interactions between their nuclei or the inability to detect every decay particle or photon—only a small level of paranoia is required to imagine that the detectors are missing patterns in the directions of decaying particles or in the timing of photon transmissions.

It is important to improve these tests of the statistics of quantum-mechanical processes for several reasons. First, quantum mechanics is such a fundamental part of our view of the physical world that we must test it as carefully as possible. History is full of scientific theories that were widely accepted until precise and accurate measurements illuminated their subtle deficiencies. Second, applications such as quantum cryptography rely on the generation of strings of numbers that are as random as possible. Devices based on quantum-mechanical processes are ideal candidates for quantum cryptography. We must therefore demonstrate that the underlying processes behind these devices are indeed free of cyclic behavior and correlations between number sequences. Finally, the trapped strontium ions that we use to perform our experiments could also be used to implement a quantum computer. It is imperative that the quantum-mechanical processes that make quantum computation so powerful are not compromised by systematic effects. For all these reasons, we have developed an experimental system based on trapped strontium ions that permits us to observe spontaneous and laser-induced transitions between internal states in single ions and pairs of ions. We then statistically analyze them, searching for signs of memory in these physical systems and patterns in their behavior.

Trapping Ions to Study Quantum Effects

Our tests of quantum mechanics are, in principle, cleaner than those of previous experiments because we monitor the transitions of a single ion between two sets of its internal states. Because we use only a single ion that is suspended in space and localized to less then 100 nm by electric fields, our experiments are not susceptible to multiparticle effects. Also, because we can tell with near-unity efficiency the state of the ion, our experiments are immune to detector-efficiency loopholes. Previous researchers have used a similar trapped-ion system to analyze approximately 1,000 such transitions; we analyze

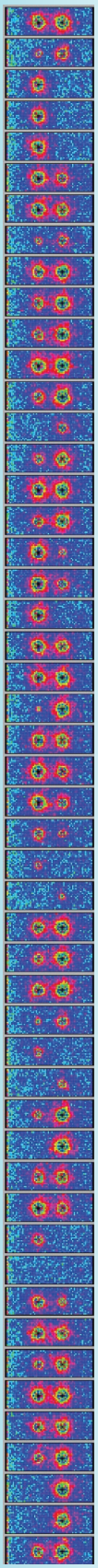

Figure 1. A time series of two ions simultaneously undergoing quantum jumps.

240,000 transitions in single ions and 230,000 transitions and 8,600 spontaneous decays in two simultaneously trapped ions.

To do this, we first confine ions in a trap such as that shown in Figure 2(a).[1] An rf voltage is applied to two diagonally opposite rods, while dc potentials are applied to the remaining electrodes. This creates a time-averaged potential that forces ions towards the trap's long axis. We apply several hundred volts to the "sleeve" electrodes to keep the ions from leaking from the ends of the trap. Ions are formed inside the trap when neutral strontium vapor from a small oven intersects with an electron beam from a tungsten filament. The whole apparatus is inside a small chamber at ultra-high-vacuum conditions.

Typically, tens of ions are created inside the trap. They make a relatively hot cloud that is hundreds of microns long and about a hundred microns in diameter. The motion of the ions is forced by the trap's rf electric field and by the Coulomb interactions between the charged ions, and individual ions cannot be distinguished. In this state, they are not useful for our experiments, so we reduce their motion by Doppler cooling them with laser light. In this process, 422-nm laser light is tuned slightly below the ions' $S_{1/2} \leftrightarrow P_{1/2}$ resonance (Figure 3). When ions travel towards the light source, they absorb a 422-nm photon, which reduces their speed due to conservation of momentum. On the other hand, if the ion is moving away from the light source and absorbs a photon, its speed increases. But the frequency of the laser light is such that an ion moving away from the light source is Doppler shifted far out of resonance with the light. So, on average, the laser light cools the ions.

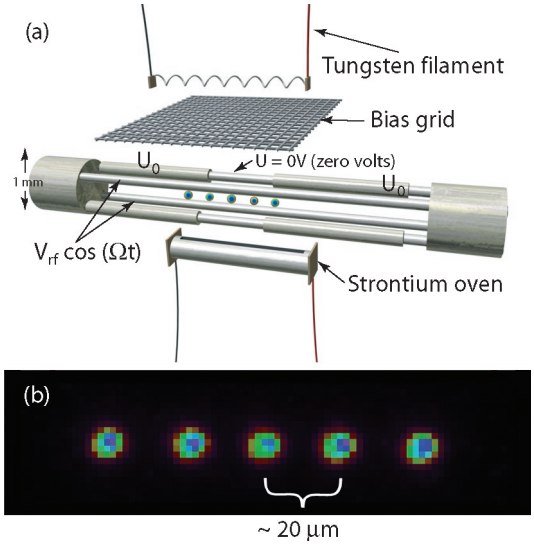

When the ions are cold enough, they undergo a sudden phase change, freezing into ion crystals such as that shown in Figure 2(b). This shows a crystal of five strontium ions that scattered 422-nm light into an imaging camera. The ions are forced together by the trap potential that we have applied to the sleeve electrodes, and they are forced apart because they are all positively charged. Typically, the ions are spaced tens of microns apart. We have formed linear chains of approximately 40 ions but typically experiment with only a single ion in the trap. Once an ion is trapped and laser cooled, it stays in the trap indefinitely so that we can perform experiments that were considered impossible when quantum mechanics was first conceived.

Observing Quantum Jumps in Trapped Ions

For example, we can observe quantum jumps. To begin, we can briefly drive the $S_{1/2} \leftrightarrow D_{5/2}$ transition with a 674-nm laser while the 422-nm light is blocked. After the laser pulse, we can ask whether or not the ion is in the long-lived ($\tau = 0.4$ s) $D_{5/2}$ state. To do this, we shine 422-nm and 1,092-nm light on the ion. If the ion is in the $D_{5/2}$ state, then neither of these lasers can drive a resonance in the ion; the detector that would observe 422-nm light from the atom *does not register any signal*. But if the 674-nm laser failed to drive the ion to the $D_{5/2}$ state, 422-nm and 1,092-nm light continually excites the atom, and the detector *registers tens of thousands of blue photons in a single second*. As we scan the 674-nm laser frequency, we observe a resonance such as that in Figure 4.

Instead of pulsing the red 674-nm laser light while the blue 422-nm laser light is blocked, we can leave all of the lasers on at the same time. Then it is as though the 422-nm light were continuously measuring whether or not the 674-nm laser has

Figure 2. (a) A rendering of the linear rf trap. Current traveling through the tungsten filament heats it to produce electrons, which are directed towards the trap by the bias grid. The strontium oven is heated so that the neutral atoms flow through the trapping region and collide with the electrons, making ions. To trap the ions, we apply potentials to the trap electrodes, $V_{rf} \sim 100$ to 200 V, $\Omega/2\pi \sim 7.1$ MHz and $U_0 \sim 50$ to 500 V. The trapped ions are immediately cooled to several mK by lasers propagating through the trap openings. In addition, the trap is placed in a vacuum chamber with pressure < 10^{-10} torr. The crystallized ions are depicted lying along the trap axis and (b) as imaged by our intensified CCD camera.

driven the atom into or out of the $D_{5/2}$ state. As quantum mechanics predicts, the results of such a measurement (i.e., is the atom in the $D_{5/2}$ state or not) should be unpredictable. Indeed, the 422-nm signal from the ion under these conditions is shown in Figure 5, and it randomly and suddenly switches between a large and small value. We collect such data in continuous blocks of approximately 30 minutes each, during which we monitor on the order of 10,000 quantum jumps. In total, we analyze 230,000 quantum jumps in a search for patterns or correlations in the times between jumps.[2]

Analyzing the Trapped-Ion Data

Although there are very many different statistical tests that have been performed on our data, we will illustrate only one in this article. We ask the following question: "If we are told the interval time between one set of quantum jumps, do we then have more information about subsequent interval times than we would otherwise?" The most direct way to answer this question is to measure the joint entropy between pairs of intervals. The entropy of a set of data tells us how many bits of data are required to describe the full data set; the more random the data, the higher the entropy. The joint entropy for two data sets tells us how many fewer bits are required to describe one data set if the other data set is known. We normalize this value so that if the data sets are completely correlated we obtain a value $U = 1$, and if they are completely unrelated, we obtain $U = 0$.

For example, if we have a stack of playing cards ordered by the face value of the cards (so the four 3s are together, the four 8s are together, etc.), if a 6 is drawn from the top of the deck then we immediately know that a 6 will be drawn from the top of the deck next. The normalized joint entropy, U, of pairs of cards drawn from this deck would be 1. If the deck of cards is shuffled well and we play this game long enough, we would find that the normalized joint entropy approaches zero.

Instead of using the values of playing cards, we use the interval times generated by the ion. Figure 6 represents a typical data set that we analyze this way. Here we have made a scatter plot of the lengths of adjacent intervals (T_i, T_{i+1}) during which the ion is scattering many blue photons (i.e., when it is not in the $D_{5/2}$ state). One feature we search for in such plots is asymmetry about the diagonal axis. For example, one possible result of potential memory in the ion (that is, nonrandomness) would be that a short interval, T_i, is more likely to be followed by a long interval, T_{i+1}, than a short interval. This would manifest itself by showing many more events in the upper left quadrant of the plot than in the lower right quadrant. We make such plots not only for consecutive intervals but also for intervals that are separated by up to 20 other intervals (i.e., we plot the frequencies of pairs $\{T_i, T_{i+k}\}$, where k ranges from 1 to 20). We also analyze intervals for which the ion is in the $D_{5/2}$ state and intervals between times of emitting a 674-nm photon and between times of absorbing a 674-nm photon. Qualitatively, we see no features in any of these graphs. Quantitatively, we calculate the normalized U between the two data sets comprising the first and second intervals for all the pairs of data. We find that $U < 7 \times 10^{-4}$ for all of our data and does not depend on the interval spacing for any of the different types of intervals. This analysis is an order of magnitude more sensitive than those previously performed on quantum jump data, and we expect to reduce our limit on U as we collect even more statistics.

Conclusion

Our experimental work has increased the sensitivity of our power to observe quantum effects and reduced the uncertainty in the randomness of those effects by over an order of magnitude. In addition to collecting more data with a recently improved laser system, we are developing the

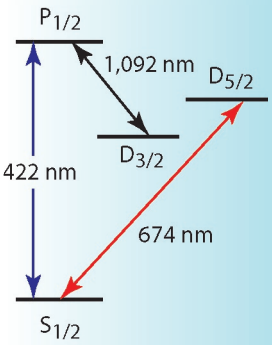

Figure 3. A partial energy level diagram of Sr^+. A frequency-doubled Ti:S laser drives the 422-nm transition to Doppler cool the ions, and we detect this scattered light to monitor the ions. A fiber laser drives the 1,092-nm transition to optically pump the ions out of the $D_{3/2}$ state. A diode laser with a bandwidth of < 2 kHz drives the 674-nm transition to induce quantum jumps and to coherently manipulate the ions.

Figure 4. Resonance curve of the $S_{1/2} \leftrightarrow D_{5/2}$ transition. At each frequency step, the 422-nm light is blocked and a 3-ms pulse of 674-nm laser light interacts with the ion. After each pulse, the state of the ion is measured by returning the 422-nm light to the ion. By repeating this process 100 times, we determine the average probability of exciting the ion from the $S_{1/2}$ to $D_{5/2}$ state. After accounting for broadening caused by laser intensity, we conclude that the laser linewidth is 1.3 kHz. This corresponds to jitter in the length of the 674-nm laser cavity of only 0.4 pm (the radius of a hydrogen atom in its ground state is 53 pm).

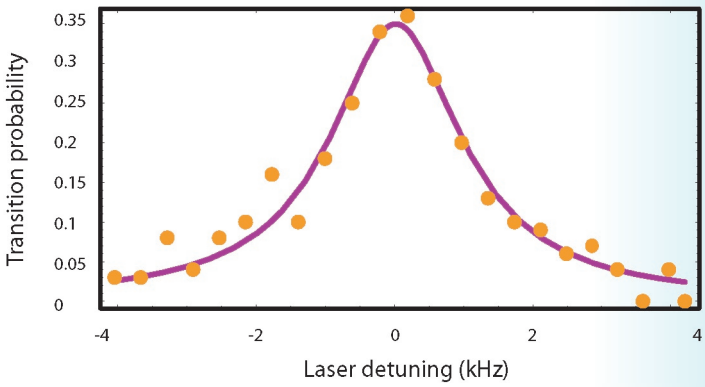

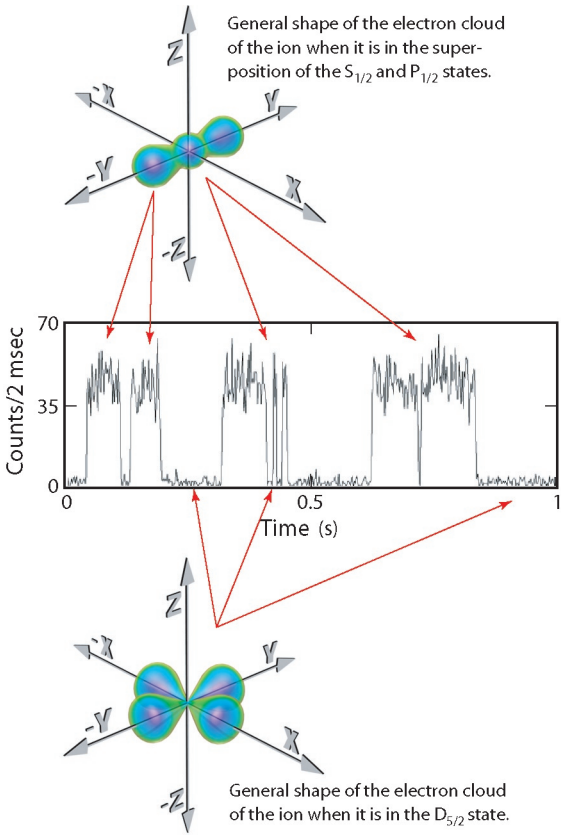

Figure 5. Quantum jumps in a single ion. Times at which the count rate is relatively high correspond to the atom being in a superposition of the $S_{1/2}$ and $P_{1/2}$ states. Times at which the count rate is very low are when the atom is in the $D_{5/2}$ state. Transitions between these two conditions indicate either the absorption or emission of a 674-nm photon.

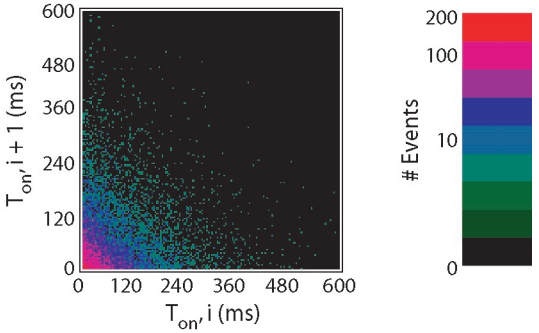

Figure 6. Scatter plot of the lengths of adjacent intervals during which the ion continually scattered 422-nm light.

capability to coherently control the external and internal states of the ion. We do this by driving the $S_{1/2} \leftrightarrow D_{5/2}$ transition with our narrow-bandwidth 674-nm laser, which can also cleanly couple specific quantized motional states of the trapped ion.

This work opens up the possibility of performing many other experiments. The ion can be laser-cooled to the ground state of its external motion where its temperature is nearly absolute zero. From this point, we can manipulate every physical aspect of the ion, tailoring its quantum-mechanical wavefunction as we see fit. We can control the interactions of the ion with the laser light to put it into quantum mechanical superpositions of states and observe their behavior and interactions with the environment. Or we can build a quantum logic gate for a quantum computer. And this, of course, is one of the motivations for testing the randomness of quantum mechanics as we have done.

References

1. D.J. Berkeland, "Linear Paul trap for strontium ions," *Review of Scientific Instruments* **73**(8), 2856–2860 (2002).
2. D.J. Berkeland, D.A. Raymondson, and V.M. Tassin, "Tests for non-randomness in quantum jumps," Los Alamos National Laboratory report (submitted 2003).

Acknowledgment

I am grateful for the efforts of Véronique Tassin and Daisy Raymondson (currently in the graduate program at the University of Colorado, Boulder) in the analysis and collection of statistics of transitions with multiple ions. This work was funded through the LANL LDRD program as part of 20020052DR, "Applied Quantum Technologies."

For further information, contact Dana Berkeland at 505-665-9148, djb@lanl.gov.

Atom Interferometry with Bose-Einstein Condensates

M.G. Boshier, C. MacCormick (P-21)

The demonstration in 1995 of gaseous Bose-Einstein condensation (BEC) took atomic physics into an exciting new regime in which the motion of large clouds of atoms is clearly governed by quantum, rather than classical, mechanics. All of the atoms in a condensate occupy the ground state of the potential well confining the system, so BEC represents the tightest control possible over matter. This control is at the heart of the field of coherent atom optics, in which the lenses, mirrors, and gratings of light optics are replaced by magnetic or optical potentials, which manipulate the atomic de Broglie wave. Figures 1 and 2 show two examples from our own laboratory of BEC atom optics.

As our next step in this area, we are developing techniques to divide a condensate into two (or more) coherent parts through appropriate manipulation of the confining potential. A division of the matter wave like this is analogous to a beamsplitter in optics. The analogy with optics can be carried further—the process of splitting the condensate (exposing one-half to a perturbation) and then recombining the two parts so that their wave functions can interfere forms an atom interferometer. These devices can respond with extreme sensitivity to any interaction that affects atomic energies. In addition, just as with light optics, the atom optical technology can also be miniaturized ultimately down to the level of an integrated "atom chip" with dimensions of just a few millimeters. Interferometry with BECs might therefore lead to a new generation of miniature sensors having unprecedented sensitivity to electromagnetic fields, to gravity and gravity gradients, and to accelerations. Focusing on just one of these interactions, sensitive instruments for measuring gravity have many important applications, such as underground structure detection; passive navigation and obstacle avoidance for submarines; and location of subterranean deposits of oil, minerals, and water.

Waveguide Interferometry

A simple calculation illustrates the power of atom interferometry—the earth's gravitational field causes the phase between two rubidium-atom wave packets separated vertically by 1 mm to evolve relative to each other at a rate of 2×10^6 cycles/s. It follows that an interferometer using a condensate of 10^6 atoms would have a statistical sensitivity to $\delta g/g$ of order 10^{-9} if the condensate was split for 1 s. This sensitivity is otherwise reached only by start-of-the-art laboratory instruments that are expensive, complicated, and most definitely not as portable.

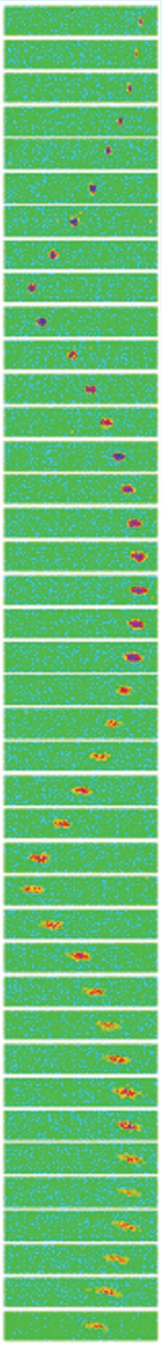

Figure 1. A BEC bouncing on a pulsed magnetic mirror.[1] The anisotropic expansion (fast in the vertical direction, slow in the horizontal direction) is a characteristic of the quantum evolution of the BEC. Images are 1.5 mm high and separated in time by 2 ms.

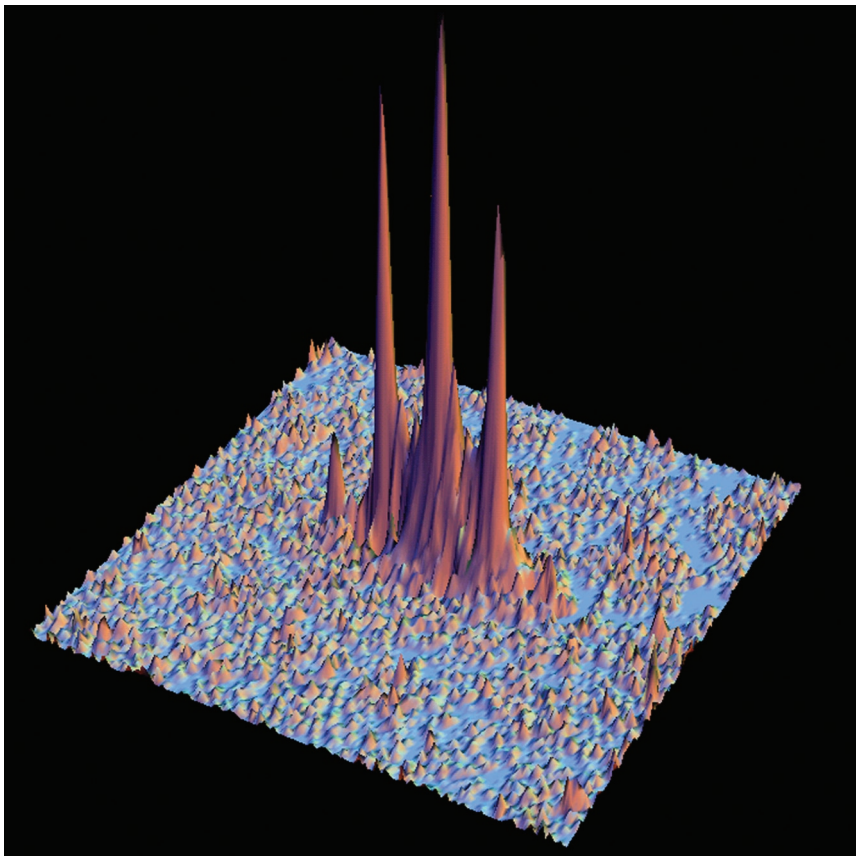

Figure 2. Diffraction of a BEC by a pulsed standing wave. The image shows the condensate density distribution after a free expansion that allows the momentum components created in the diffraction process to separate spatially.

The standing wave grating shown in Figure 2 can be used as the beamsplitter in a simple Mach-Zehnder-type interferometer (Figure 3), but the splitting time in this geometry is limited to much less than one second because the falling condensate soon hits the bottom of the apparatus. One can do considerably better by making use of the important fact that atoms, unlike photons, can be brought to rest, thereby allowing for very long measurement times. Because our stationary condensate interferometer design[1] has some similarities to light interferometers based on optical fibers, it is natural to refer to it as a condensate waveguide interferometer.

Implementation

Figure 4 illustrates the general principle of waveguide interferometry. The initial state is the condensate confined in the ground state of a thin, cylindrically symmetric harmonic waveguide potential. The potential is then deformed adiabatically into two separated waveguides (Step 1) forming a two-dimensional, double-well potential. In this process, the condensate wavefunction evolves into the symmetric ground state of this potential. Next (Step 2), the perturbation, V(t), under study is applied to one arm of the interferometer for time, τ, introducing a phase shift, ϕ, between the two arms. The resulting wavefunction can then be written in terms of the double-well eigenstates as a superposition of the degenerate symmetric and anti-symmetric ground states. The two arms of the interferometer are now overlapped by adiabatically transforming the potential back to the original single well. In this process (Step 3), the symmetric ground state of the double-well potential returns to the ground state of the single-well potential, and the anti-symmetric double-well state becomes the lowest-energy state of the single well with odd parity, i.e., the first excited state. The output ports of this interferometer in time are therefore the ground state and a first excited state of the waveguide. We present a full quantum-mechanical analysis of this interferometer in Reference 2. The process described above could also be realized as an interferometer in space using waveguides, which physically divide and recombine—in which case the device would resemble an optical fiber interferometer.

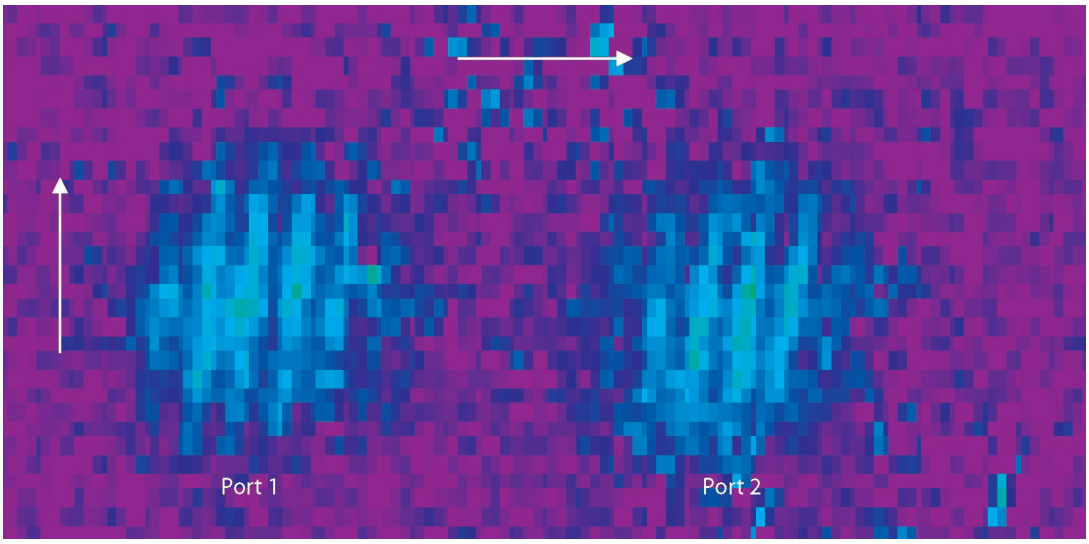

Figure 3. Interferometer fringes formed at the output ports of a freefall Mach-Zehnder condensate interferometer using standing-wave light pulses as beamsplitters.

We are exploring two complementary implementations of the waveguide interferometer—one based on magnetic forces and the other using the optical dipole force exerted by a far-detuned laser beam. The magnetic waveguide configuration consists of two long wires carrying currents in the same direction with a superimposed constant bias magnetic field applied parallel to the plane of the wires.[2] A waveguide for weak-field-seeking atoms (such as the F = 2, m = 2 ground-state atoms in our condensate) exists where the field is zero. We have shown that there are in general two such regions and that at a critical value of the bias field these two regions merge into a single waveguide. Increasing the bias field then splits the potential symmetrically into two, forming a beamsplitter. A full quantum mechanical analysis of this system can be found in our paper[2] along with a discussion of readout techniques—simple direct imaging of the condensate wavefunction is adequate, but there are better alternatives based on further manipulation of the potential.

The optical waveguide interferometer will make use of the optical dipole force, which pushes an atom towards a region of high intensity in a focused laser beam detuned below the atomic resonance. A low-power beam from an infrared diode laser can form a waveguide trap that confines a condensate for several seconds with negligible spontaneous emission. Radial trapping frequencies in such a trap are typically several kilohertz. This simple potential can be manipulated by scanning the laser beam through space at a much higher frequency (e.g., megahertz) than the trap frequency so that the condensate sees only the time-averaged potential. This promises to be a simple, yet powerful and flexible, approach to modifying the potential. A beamsplitter can be realized by passing the laser beam through an acousto-optic modulator used as a deflector to switch the beam back and forth between two positions whose separation increases

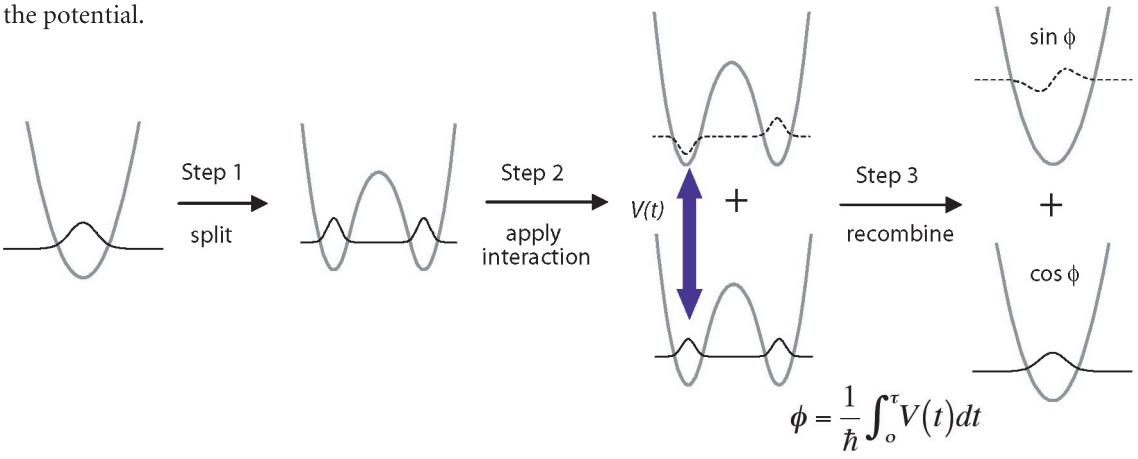

Figure 4. The waveguide interferometer.

slowly. The resulting time-averaged potential evolves into a double well. The scheme extends easily to more complicated geometries, such as dual interferometers for measuring gravity gradients, or to a potential that alternates between horizontal and vertical splitting to suppress systematic effects in a measurement of ***g***.

Conclusion

The sensitivity computed above is based on treating the condensate as a simple coherent matter wave in which each atom occupies the same single-particle state and interactions between atoms are negligible. Although this is the simplest regime in which to work initially, it should be possible to enhance the sensitivity by several orders of magnitude by harnessing the many-body nature of the condensate. The interactions between atoms in the condensate can be used to engineer exotic entangled states in which the measurement uncertainty scales with atom number N as 1/N, instead of the classical scaling factor $1/\sqrt{N}$. Not surprisingly, this enhanced sensitivity comes with a price, which in this case is a decrease in robustness to perturbations from the environment. The open problem of finding the optimal exotic states and devising techniques to create them in the laboratory is currently the subject of research by our T Division colleagues Diego Dalvit, Eddy Timmermans, and Daniel Steck.

References

1. A.S. Arnold, C. MacCormick, and M.G. Boshier, "An adaptive inelastic magnetic mirror for Bose-Einstein condensates," *Physical Review A* **65**, 031601(R), (2002).
2. E.A. Hinds, C.J. Vale, and M.G. Boshier, "Two-wire waveguide and interferometer for cold atoms," *Physical Review Letters* **86**, 1462, (2001).

Acknowledgment

Our work in this area is supported by funding from the LANL LDRD program.

For more information, contact Malcolm Boshier at 505-665-8892, boshier@lanl.gov.

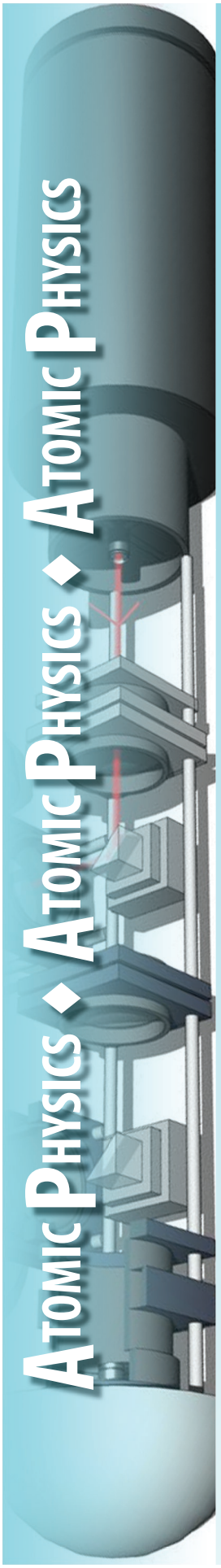

Quantum Key Distribution

R.J. Hughes, J.E. Nordholt, C.G. Peterson, W.R. Scarlett, J. Anaya, D. Derkacs, J. Franken, P. Hiskett, W.J. Marshall, R. Sedillo, C. Wipf (P-21), K.P. McCabe, I. Bernstein, N. Dallman, I. Medina, P. Montano, N. Olivas, S. Storms, J. Thrasher, K. Tyagi, R.M. Whitaker (ISR-4), J. Wren (ISR-2), P. Milonni (T-DO), J.M. Ettinger, M. Neergaard (N-3), D. Ranken, R. Gurule (CCN-12)

On April 27, 1986, a satellite television broadcast to the east coast of the U.S. was briefly taken over by a hacker calling himself "Captain Midnight." With the growing reliance on satellites for communications, this notorious incident highlights the importance of assured command and control of orbital assets, as well as protection of downlinked data. In 1994, two LANL researchers, Richard Hughes and Jane Nordholt, set out a methodology whereby QKD using single-photon transmissions could be used to provide greater long-term security, based on fundamental principles of quantum physics, for secure satellite communications. Since then, our QKD team has been conducting research toward that goal, and we have developed another secure communications concept that would become possible with a satellite QKD capability—secure data dissemination between dynamically reconfigurable networks of users.[1] This research is leading to QKD becoming a higher-security alternative to present-day public-key-cryptography-based methods of establishing secure communication—today's public-key broadcasts, which we must assume are being recorded by adversaries, will become retroactively vulnerable if a large-scale quantum computer becomes feasible in the future, potentially allowing an adversary access to still-valuable information.

The Basics of Cryptography

The science of cryptography provides two parties ("Alice" and "Bob") with the ability to communicate with long-term *confidentiality*—they have the assurance that any third party (an eavesdropper, "Eve") will not be able to read their messages. Alice can encrypt a message ("plaintext"), P, before transmitting it to Bob, using a cryptographic algorithm, E, to produce a "ciphertext," C, which depends on K, a secret parameter known as a cryptographic key. [K is a random binary number sequence, typically a few hundred bits in length. For example, in the Advanced Encryption Standard the keys are up to 256 bits in length.] Bob is able to invert the encryption process to recover the original message, P, provided he too knows the secret key, K. Although the encryption algorithm E may be publicly known, Eve passively monitoring transmission C would be unable to discern the underlying message, P, because of the randomization introduced by the encryption process—provided the cryptographic key, K, remains secret. (The algorithm E is designed so that without knowledge of K, Eve's best strategy is no better than an exhaustive search over all possible keys—a computationally infeasible task.) In this so-called *symmetric key* cryptography, *secret* key material is therefore a very valuable resource, but there is an underlying problem; before Alice and Bob can communicate securely it is of paramount importance that they have a method of securely distributing their keys. It is this problem of key distribution that QKD solves, providing the ultimate security assurance of the laws of physics (Figure 1).

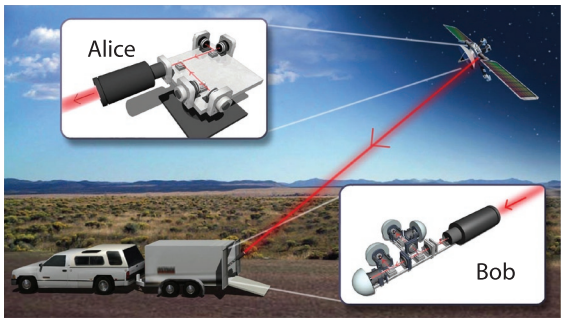

Figure 1. In our conceptual satellite QKD system, the transmitter of the quantum key material (Alice) is on the orbiting satellite and the receiver (Bob) is on the ground. Alice's four attenuated lasers (top left) will transmit polarized photons to Bob's receiving telescope (lower right), which collects them and directs them to one of four detectors. The registered signal from these detectors forms the raw key material for a cryptographic system whose secrecy is guaranteed by the laws of quantum physics.

The QKD Concept

QKD was first proposed in 1984 by Charles Bennett (IBM) and Gilles Brassard (University of Montreal). Alice and Bob, equipped with the ability to perform conventional, nonsecret ("public") but authenticated communications with each other, could produce copious quantities of shared, secret random key bits, for use as cryptographic keys, by using quantum communications. In their "BB84" QKD protocol, Alice (the transmitter) sends a sequence of random bits over a "quantum channel" to Bob (the receiver) that are randomly encoded as linearly polarized single photons in either of two conjugate polarization bases with (0, 1) = (H, V), where "H" ("V") denotes horizontal (vertical) polarization (respectively), in the "rectilinear" basis, or (0, 1) = (+45°, -45°), where "+45°" and "-45°" denote the polarization directions in the "diagonal" basis. Bob randomly analyzes the polarization of arriving photons in either the rectilinear or diagonal basis, assigning the corresponding bit value to detected photons. Then using the public channel, which is assumed to be susceptible to passive monitoring by Eve, he informs Alice in which time slots he detected photons but without revealing the bit value he assigned to each one.

Next, Alice reveals her basis choice for each bit but not the bit value. Bob communicates back the time slots of his detected bits for which he used the same basis as Alice. In an ideal system, Alice's transmitted bits and the results of Bob's measurements on this random, matching-basis portion, known as the "sifted" key, are perfectly correlated; they discard the bits for which Bob used the wrong basis (e.g., his receiver "looked" in the diagonal basis when she transmitted the bits in the rectilinear basis and *vice versa*) (Figure 2).

In practice, Bob's sifted key contains errors. Fundamental quantum principles ensure that Eve is both limited in how much information she may obtain by eavesdropping on the quantum communications and that she cannot do so without introducing errors in Bob's sifted key from which Alice and Bob can deduce a rigorous upper bound on leaked information. Alice and Bob determine this bound after reconciling their sifted keys using *post facto* error correction over their public channel. From their partially secret reconciled keys, Alice and Bob extract the shorter, final *secret* key after a final stage known as "privacy amplification." For example, if Alice and Bob form the parities of suitable random subsets of their reconciled bits, they can be sure that Eve will be ignorant of at least one of the bits in each subset and hence ignorant of the final secret bits.

Free-Space QKD

A satellite-to-ground free-space QKD capability has particularly appealing security features. Typically, satellites are launched with all the keys they will ever have but they may exceed their design lifetime or they may need to encrypt more data than expected. Then one must face the challenge of providing new keys to a possibly very high-value satellite asset on-orbit. Clearly it is infeasible to use a human courier for this task, and although public-key cryptography allows keys to be transferred conveniently, its use already presents a latent vulnerability to unanticipated computation advances, including quantum computers. In contrast, QKD provides much greater long-term security guarantees—it can only be attacked by technology in existence at the time of transmission and cannot be attacked by a quantum computer. A second advantage of QKD is in the context of *key generation*; it allows a fresh key to be produced at transmission time using the intrinsic randomness of quantum mechanics. This could be very useful to support the demands for large amounts of key material within a transformational communications scenario, as well as reducing the risks associated with conventional keys—that they might be (accidentally or maliciously) compromised by insiders. Finally, QKD narrows an adversary's window of opportunity; Eve's best strategy is to attempt a "man-in-the-middle" attack, but to do so she would have to break the initial authentication

in time to insert herself into the channel between Alice and Bob. Breaking the authentication *after* the quantum communications have taken place is of no use to Eve.

For satellite-to-ground (or any other line-of-sight application) QKD, one must reliably transmit and detect single photons through the atmosphere in the presence of background radiance, which is a strong error source even at night. We effectively deal with this challenging problem using a combination of spectral, spatial, and temporal filtering. The synchronization requirements are especially important; we must only accept photons that reach the receiver within specific 1-ns time windows. Our solution to this difficult problem makes QKD possible even in full daylight, which is one of the unique features of our research that sets us apart from our competitors.

In 2001, using a readily transportable system, we carried out a QKD experiment over a 10-km line-of-sight range between Pajarito Mountain and TA-53, LANL, which had optics (extinction of one air mass, background, and turbulence) representative of a satellite-to-ground path.[2] We were able to reliably produce shared, secret keys at rates of several hundred bits per second throughout the day and night (i.e., 1–2 keys per second). On each clock cycle (1 MHz at the time), the transmitter (Alice) generates two secret random bits, which determine which one of four attenuated "data" diode lasers emits about a 1-ns optical pulse with one of the BB84 polarizations (see the Alice inset in Figure 1) and an average photon number less than one (with Poissonian photon-number statistics) that is launched towards the receiver (Bob). At Bob, a telescope collects the data pulse and directs it into an optical system where its polarization is randomly analyzed in one of the BB84 bases. Single-photon detectors, one for each of the four BB84 polarizations, register the result (see the Bob inset in Figure 1). This process is repeated for one second, following which the session is completed with the various public-channel processes (sifting, reconciliation, and privacy amplification) using a wireless Ethernet connection before starting up the next 1-s session. (In subsequent work using the data from this experiment, we implemented for the first time in QKD research the all-important authentication aspect and demonstrated that self-sustaining, authenticated, secret-key production is possible with minimal overhead in secret bits.) The background rejection in our system was sufficiently high that we were even able to transfer secret key bits under worst-case conditions with the sun directly illuminating the receiver.

Implications and Developments for Satellite QKD

With input from the results of this experiment, we have developed a model that allows free-space QKD performance to be predicted in other regimes. In particular, we have modeled a QKD link between a satellite and a ground location.[3] We have determined that it is optimal to locate the transmitter (Alice) on the satellite and the receiver (Bob) on the ground so that the optical effects of atmospheric turbulence are in the transmitter's far-field zone. For low-earth-orbit (LEO) satellites, we find that useful QKD contacts can be established over wide areas of the earth's surface, day or night, using only modest-scale (~ 50-cm in diameter) optical ground facilities, whereas with larger aperture (> 1-m in diameter) optical ground facilities, QKD from higher altitude orbits (such as geosynchronous ones) would be feasible at night.

We have also developed a preflight QKD transmitter (a so-called "brassboard"). This device is sufficiently small and lightweight that it could be accommodated on a satellite, yet sufficiently rugged that it could survive the rigors of launch. So far, we have tested this in a laboratory environment and produced large quantities of high-quality, secret key

Figure 2. The raw QKD key material must be "sifted" to produce useful, matching bit strings. In this example, Bob is receiving a single photon that Alice transmitted in the "diagonal" basis (see text for details). The first beamsplitter randomly directs the photon either to the right (a) or straight ahead (b). If the photon goes to the right, a second polarizing beamsplitter will direct it to the correct "diagonal basis" detector, and it becomes a useful bit of key material (a "1" or a "0"). If the photon goes straight ahead, another polarizing beamsplitter will randomly send it to a "horizontal/vertical basis" detector—this randomness eliminates its usefulness as key material. Bob communicates with Alice over a public channel how he detected each photon—but not the result. Alice tells Bob which photons were tested correctly, and those bits form the "sifted" cryptographic key.

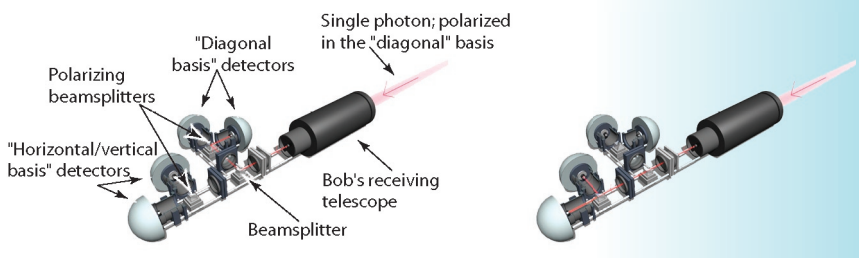

(a) Bob correctly detects a single photon from Alice. (b) Bob incorrectly detects a single photon from Alice.

bits. The performance of this device, together with our modeling results give us great confidence that satellite-to-ground QKD would be possible at useful rates with existing technology.

It is likely that on-orbit re-keying would be performed with a QKD ground unit located at a satellite's operations center or mission-control center, but the modest parameters required of a ground-receive unit (for LEO satellites) suggests another use—the transfer of keys between ground users via a QKD-capable satellite. For example, a QKD capable satellite could generate keys with each of two QKD ground units in different parts of the world (which could be transportable systems). The satellite could then communicate to the second user which bits to flip so that his key matches the first user's; this information could be sent in the clear without compromising security. These ground users could now establish secure communications over any convenient channel using this shared key. Several cross-linked QKD-capable satellites could support worldwide on-demand secure communications to the coalitions of land-, sea-, air-, and space-based users envisioned in emerging "transformational-communications" concepts. This concept can be further extended with optical-fiber QKD links to the satellite QKD ground units. Building on previous work in which we have demonstrated QKD over a 48-km optical-fiber path in LANL's network,[4] we have recently shown the feasibility of the much harder problem of performing QKD over a fiber that is also carrying network traffic.[5] Optical-fiber QKD would therefore not require a dedicated fiber connection.

Conclusion

While considerable basic and applied research remains to be done, QKD is the first aspect of quantum information science to enter the technology-development era; it is possible with existing technology and is capable of providing solutions to the pressing secure-communications requirements of the next decade. The LANL QKD team is in the forefront of this "first wave" of QKD research and development, but we are also engaged in the basic research of the "second wave" of QKD that will be based on the uniquely quantum-mechanical properties of "entangled" two-photon states.

References

1. R.J. Hughes and J.E. Nordholt, "A new face for cryptography," *Los Alamos Science* **27**, 68–85 (2002).
2. R.J. Hughes, J.E. Nordholt, D. Derkacs *et al.*, "Practical free-space quantum key distribution over 10 km in daylight and at night," *New Journal of Physics* **4**, 43.1–43.14 (2002).
3. J.E. Nordholt, R.J. Hughes, G.L. Morgan *et al.*, "Present and future free-space quantum key distribution," in *Free-Space Laser Communication Technologies XIV*, G.S. Mecherle, Ed. (SPIE, Bellingham, Washington, 2002), Proceedings of SPIE Vol. 4635, pp. 116–126.
4. R.J. Hughes, G.L. Morgan, and C.G. Peterson, "Quantum key distribution over a 48-km optical fiber network," *Journal of Modern Optics* **47**, 533–547 (2000).
5. P. Tolliver, R.J. Runser, T.E. Chapuran *et al.*, "Experimental investigation of quantum key distribution through transparent optical switch elements," *IEEE Photonics Technology Letters* **15**(11), 1669–1671 (2003).

Acknowledgment

It is a pleasure to acknowledge collaborations with P. Kwiat of the University of Illinois; S. Nam, A. Miller, and D. Rosenberg of the NIST; A. Ellsasser, M. Dulski, R. Baker, and R. Trevino of the DoD; R. Blake, S. McNown, P. Hendrickson, R. Shea, and T. Persons of the U.S. government; M. Goodman, R. Runser, T. Chapuran, P. Tolliver, and J. Jackel of Telcordia; and N.C. Donnangelo of The MITRE Corporation. This research was funded by the Advanced Research and Development Activity and the Secretary of the Air Force.

For further information, contact Richard Hughes at 505-667-3876, hughes@lanl.gov, or Jane Nordholt at 505-667-3897, jnordholt@lanl.gov.

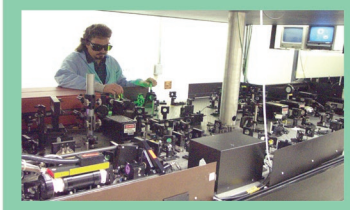

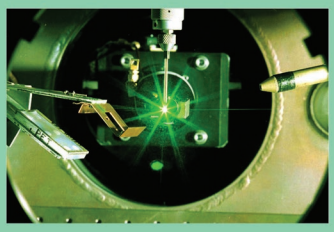

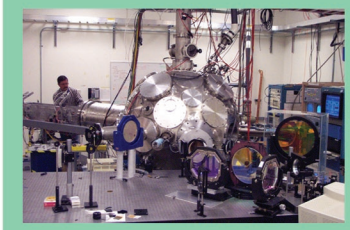

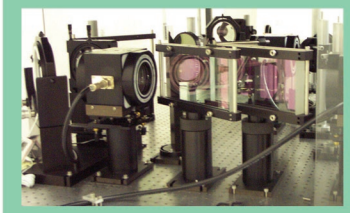

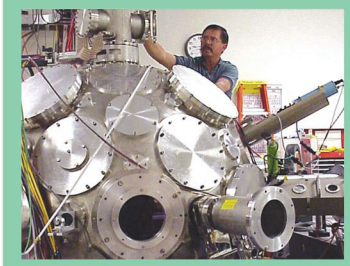

$$t_{ms} = \int_0^{\theta_c} \frac{1}{\theta_0^2} e^{-\frac{\theta^2}{2\theta_0^2}} \sin(\theta) d\theta$$

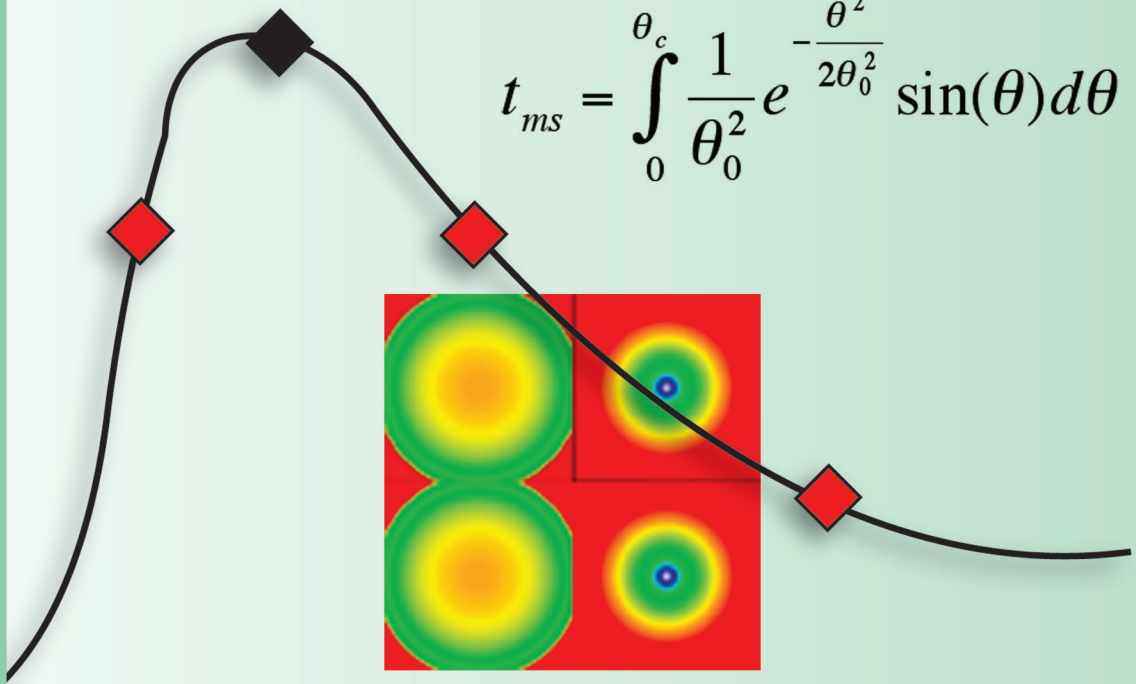

Facilities

$$\frac{\Delta L}{L} = \sqrt{\frac{2}{N}}$$

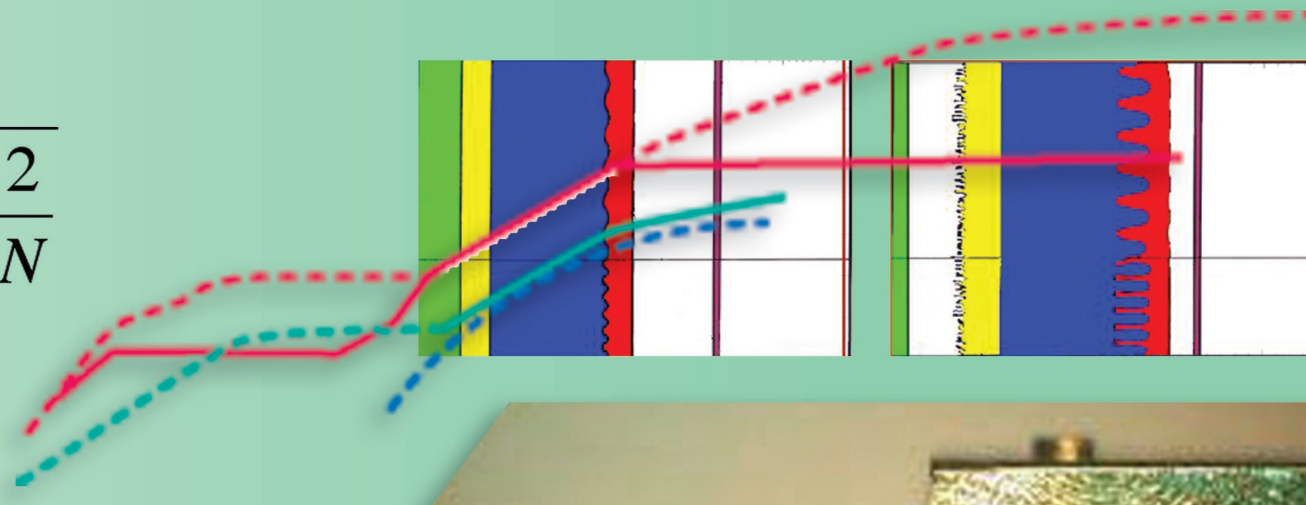

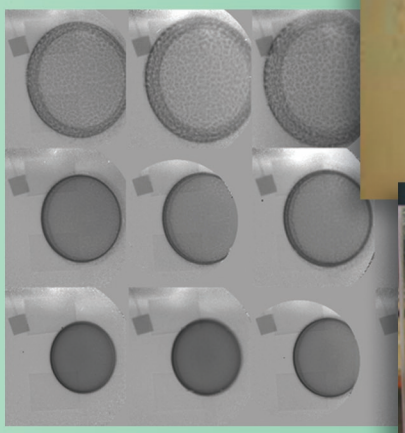

$$t_c = (1 - e^{-\frac{\kappa}{l}})$$

Facilities Contents

Research Highlights

Trident Laser Laboratory 201
Charged-Particle Radiography—Providing New Methods of Imaging 205
Shock-Wave and Material-Properties Experiments Using the Atlas Pulsed-Power Machine 209

Project Descriptions

Relocation of Atlas to the Nevada Test Site 213
High-Energy Ultra-Short Laser Pulses at Trident 214
Trident Laboratory Operations 215

Trident Laser Laboratory

F.L. Archuleta, R.B. Gibson, R.P. Gonzales, T.R. Hurry, R.P. Johnson, N.K. Okamoto, T.A. Ortiz, T. Shimada (P-24)

Lasers—light amplification by stimulated emission of radiation—are among the most varied and versatile tools of modern science and technology. LANL has been a leader in laser technology since the early 1970s, particularly in the arena of high-energy pulsed lasers. The latest of these is Trident, a multipurpose laboratory that principally supports ICF, HED physics, and basic research. Since becoming operational in 1993, Trident has fired over 800 high-energy target shots (Figure 1) each year for experiments requiring high-energy pulsed laser light.

The Trident laser laboratory provides varied and flexible experimental configurations for a wide variety of experiments. It features a powerful Nd:glass laser driver with flexible characteristics in pulse shape, duration, intensity, and focus; two well-instrumented vacuum target chambers with a suite of resident optical and x-ray diagnostics; and ancillary equipment and facilities for optical fabrication and diagnostic checkout. A dedicated staff maintains and operates the Trident laboratory and assists users. The Target Fabrication Facility in the MST Division at LANL designs, fabricates, and characterizes targets for experiments conducted on Trident. Users from more than a dozen major research institutions have executed ~ 200 experimental campaigns in the past decade, including studies of x-ray generation and diffraction, plasma waves and instabilities, shock waves in solids and gases, energetic proton and ion generation, and EOS and other material properties. In addition, high-speed plasma and x-ray diagnostic techniques and instruments are routinely developed and tested at the laboratory for use on Trident and at other major laser laboratories.

Trident Laser Driver

Trident's laser driver produces several hundred joules of energy over a pulse-length duration that spans more than 6 orders of magnitude from less than a picosecond to several microseconds. It uses an Nd:YLF master oscillator and three chains of Nd:glass rod and disk amplifiers in a conventional master-oscillator power-amplifier (MOPA) configuration (Figure 2) operating at 1,054-nm wavelength. Trident's main A and B beam lines, which use 14-cm-aperture amplifiers, produce the highest energy after frequency doubling and conversion into the 527-nm green light shown in Figure 1. The third C beam line, which uses 10-cm-aperture final amplifiers, produces lower energy but is more flexible with better beam quality, focus, and ability to be converted to other wavelengths. (Three beams—hence the name "Trident"!) The high-energy stages of the amplifier chain are shown in Figure 3. The laser-driver system operates in three different modes, depending on the pulse-

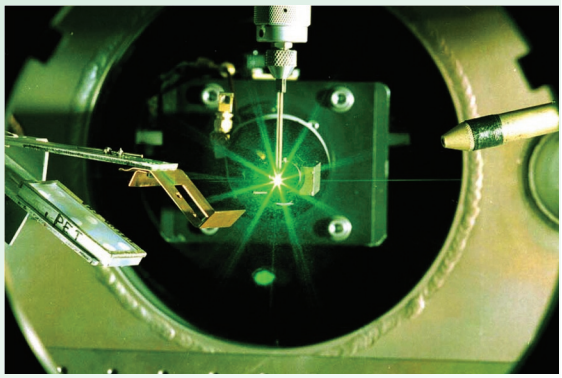

Figure 1. View inside Trident's target chamber. Targets may be illuminated with up to several hundred joules of energy in pulses ranging from picoseconds to microseconds in length.

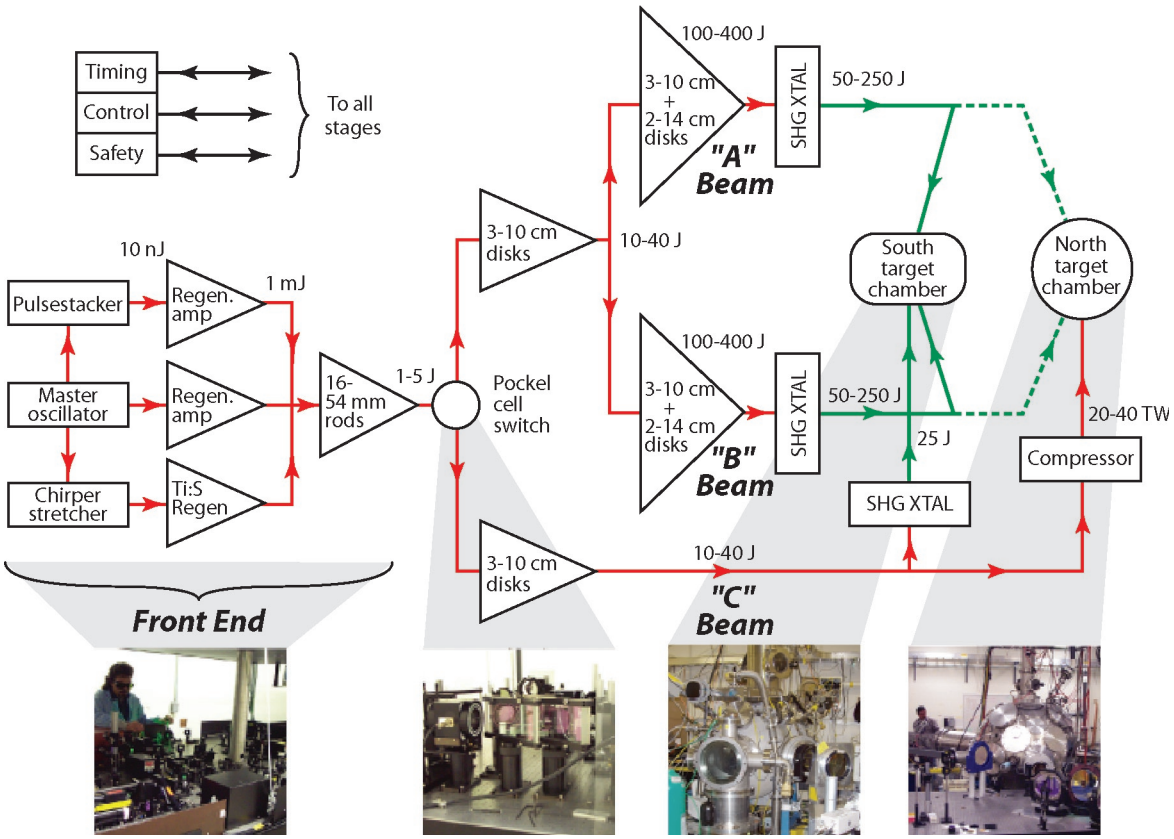

Figure 2. Trident's laser driver uses a conventional MOPA architecture. Main laser pulses (A and B beam lines) and auxiliary laser pulses (C beam line) are amplified sequentially through the front end of the laser system before they are routed to separate disk amplifier chains for further amplification. Shaping and timing can be controlled separately.

length range. For microsecond-length pulses, one regenerative amplifier is used as an oscillator and the frequency-doubling crystals are bypassed. For nanosecond-length pulses, output from the master oscillator is temporally shaped (Figure 4) before amplification. The C beam line pulse can be independently shaped and timed. It is also normally frequency-doubled to 527 nm but can also run at a fundamental output of 1,054 nm, at a third harmonic output of 351 nm, or at a fourth harmonic output of 263 nm. It can also be operated at reduced energy in a *single-hot-spot* (SHS) mode in which the spot on target is nearly diffraction-limited. For pulses in the picosecond range, the output of the master oscillator is frequency-broadened and "chirped" before amplification in the C beam line. The 1,054-nm output is then compressed with a pair of large diffraction gratings before being focused on target. Energies available on target are summarized in Table 1 and Figure 5.

Target Chambers

Experiments are regularly conducted in two high-vacuum target chambers, each in its own room. The south target chamber is a cylinder approximately 150 cm long and 75 cm in diameter (Figure 2). Single- or double-sided target illumination is possible through several 20-cm-diam ports on each end of the chamber. More than 40 smaller ports are available for diagnostic instrumentation. Individual targets are inserted through an airlock. The target insertion and positioning mechanism provides x-y-z and rotation adjustment under computer control with 1-μm linear resolution and 350-μrad angular resolution. The three-axis, target-viewing system has 20-μm resolution. The chamber is fitted with a Nova-standard six-inch instrument manipulator (SIM) to accept all SIM-based instruments for checkout, characterization, or use.

Trident's north target chamber is a sphere with an inside diameter of 145 cm (Figure 2). This target chamber is capable of very flexible target illumination and diagnostic placement geometry because of the 92 ports, ranging in diameter from 2 in. to 14 in., distributed around the chamber surface. The target insertion and positioning mechanism is similar to that in the south chamber. The chamber is fitted with a standard ten-inch instrument manipulator (TIM) that accepts all TIM- and SIM-based instruments.

Trident Target Diagnostics

Optical diagnostics routinely used on Trident include illumination and backscattered-light calorimeters, backscattered-light spectrometers, and high-bandwidth (5 GHz) and streak-camera-based power monitors. Both point and line VISARs are also available. Filtered, photoconductive diamond detectors and x-ray streak cameras with < 10-ps resolution monitor the emission of x-rays from the target. A gated, filtered, x-ray imager provides 16 frames with 80-ps resolution. Various filtered x-ray power and spectral diagnostics covering 0 to 35 keV can be installed as needed. Static x-ray pinhole cameras are also available.

Table 2 summarizes the diagnostic instrumentation available on Trident. Most can be installed on either the north or south target chamber. Users are also welcome to provide their own unique instruments; interfacing information is provided upon request.

Administration

The Plasma Physics Group (P-24) operates Trident as a multipurpose facility for LANL and outside users (national laboratories, universities, and industry). Trident is funded largely through the Laboratory's Thermonuclear Experiments program element. The quality of proposed research and its relevance to Laboratory missions are major criteria in determining what experiments are fielded on Trident. Proposals are normally solicited annually each winter for the following federal fiscal year.

Trident is located at LANL's Technical Area 35—an area open to visitors without security clearances. However, security plans are in place to permit appropriately cleared personnel to conduct classified experiments, if necessary.

Acknowledgment

Many individuals beyond those presently operating Trident have contributed to its construction and operational success over the years, including Hank Alvestad, Tom Archuleta, Bentley Boggs, Max Byers, Paula Diepolder, Scott Evans, Jim Faulkner, George Faulkner, Jody Godard, Sam Letzring, Kent Moncur, Danielle Pacheco, Sam Reading, Tom Sedillo, Bob Watt, and scores of others. Trident is funded by the DOE Secondaries and Inertial Fusion Division.

Figure 3. Trident's two power amplifier chains feature 10- and 14-cm-aperture Nd: glass disk amplifiers (gray boxes) and a fully enclosed beam transport system (blue vacuum spatial filters and transport tubes).

Figure 4. Pulse-stacker output. These figures are examples of the diverse pulse shapes made possible by the coherent pulse stacker, which follows the master oscillator.

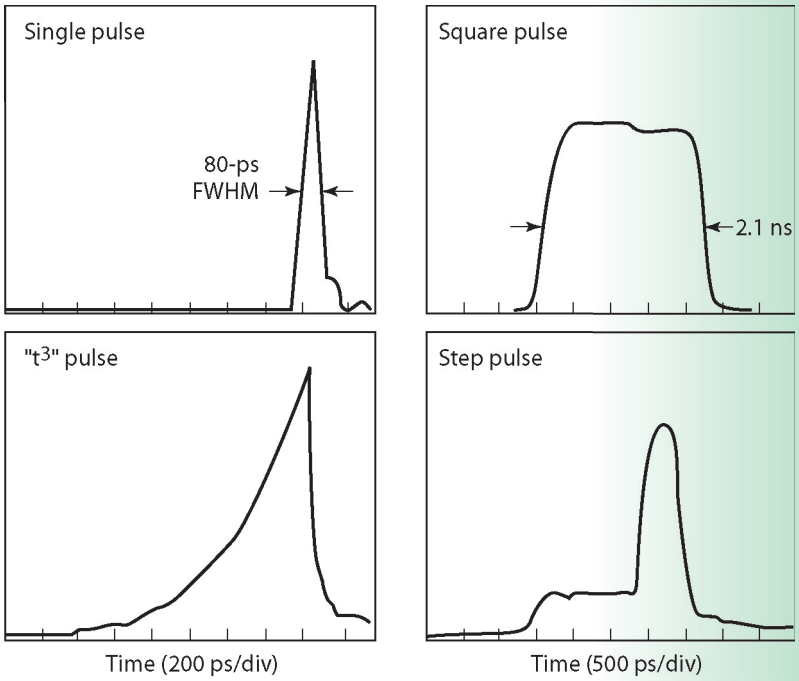

Table 1. Trident target environment.

	A and B Beams		C Beam		
Parameters (units)	ns mode	μs mode	ns mode	SHS	ps mode
Wavelength (nm)	527	1053	1053/527 351	1053/527 351/263	1053
Pulse length (ns)	0.08–5.0	100–2000	0.1–2.0	0.1–2.0	0.7
Energy/beam (J) 100 ps 1–2 ns 100–2000 ns	 50 250	 300	 50/30/20 100/60/40	 5/3/1.5/0.5	 30
Spot diameter (μm)	100	100	50	5	20
Irradiance (W cm^{-2})	10^{16}		10^{16}	10^{16}	$> 10^{19}$
Number of beams	2	1	1	1	1

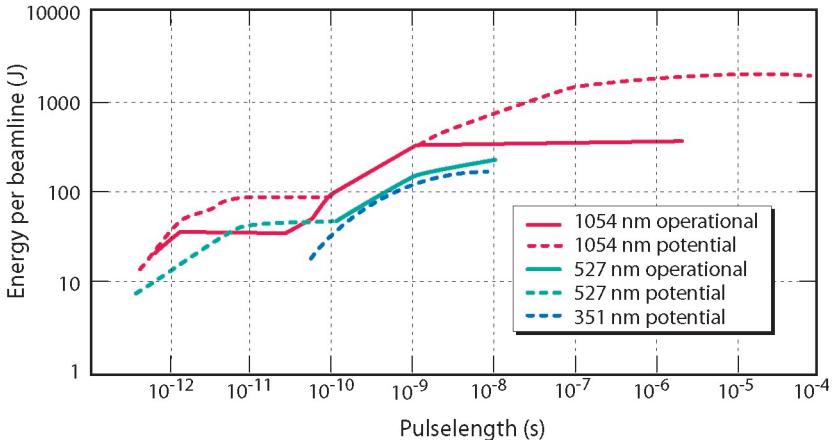

Figure 5. The laser driver operates over more than 6 orders of magnitude in pulse length. The solid lines show the energy that can presently be produced in one beam line. The dashed lines indicate energies that would be possible with modest enhancements. Red indicates 1,054 nm (infrared), green is 527 nm (green light), and blue is 351 nm (ultraviolet).

Table 2. Trident target diagnostics.

X-ray Diagnostics	Optical Diagnostics
Streak cameras	Streak cameras
CCD cameras	Spectrometers
Gated imagers	Backscatter diagnostics
Crystal spectrometers	Point and line-imaging interferometers (VISARs)
Grating spectrometers	CCD cameras
X-ray (and optical) photodiodes coupled to high-speed digitizers	
Microscope	

For more information about Trident, visit http://plasmasys.lanl.gov/~knc/TRIDENT/tritecbl.htm or contact Robert Gibson (505-667-5040, rbg@lanl.gov), Cris Barnes (505-665-5687, cbarnes@lanl.gov), or Allan Hauer (505-667-5167, hauer@lanl.gov).

Charged-Particle Radiography—Providing New Methods of Imaging

C. Morris (P-25), representing the Radiography Team

When energetic charged particles travel through matter, the Coulomb force between the particles and the atomic nuclei in the medium leads to a large number of small deflections of the particle trajectories. The nature of the Coulomb interaction leads to a cross section for scattering that is not integrable, but, in aggregate, the multiple scattering of a particle can be treated analytically.[1] To a good approximation, the angular distribution that results when a particle of momentum p traverses from a length of material l is given by

$$\frac{dN}{d\Omega} = \frac{1}{2\pi\theta_0^2} e^{-\frac{\theta^2}{2\theta_0^2}}, \quad (1)$$

where θ_0, the multiple scattering angle, is given by

$$\theta_0 = \frac{14.1}{p\beta}\sqrt{\frac{l}{X_0}}. \quad (2)$$

Here β is the velocity of the particle in units of the speed of light, and X_0 is a material-dependent constant that characterizes the length scale for Coulomb effects such as multiple scattering and pair production:

$$X_0 = \frac{716}{Z(Z+1)\ln(287/\sqrt{Z})}. \quad (3)$$

Here, Z is the atomic charge, and the units are in gm/cm^2. Equation 2 can be used to determine the thickness of the object if the angular deflection of a particle or the angular dispersion of a beam of particles that traverses an object can be measured. This observation has formed the basis for new kinds of radiography that are finding rather broad application at LANL, including pRad at LANSCE, electron radiography, and, most recently, muon radiography.

Charged particles also scatter from electrons in the medium. Because the electrons are light, charged-particle scattering generally leads to continuous energy loss rather than to angular deflections. This energy-loss mechanism provides a method for detecting the particles. In proton and electron radiography, images can be formed on scintillator screens with high efficiency. For cosmic-ray muon radiography, the energy deposited in a multiwire drift detector is used to measure the trajectory of individual cosmic rays. Multiple scattering leads to a stochastic trajectory through the medium. This is one of the limitations of charged-particle radiography. Position resolution is ultimately limited by the scale established by the product, multiple-scattering angle, and object thickness, $\Delta x = k\theta_0 l$, where k is a case dependent constant of order unity.

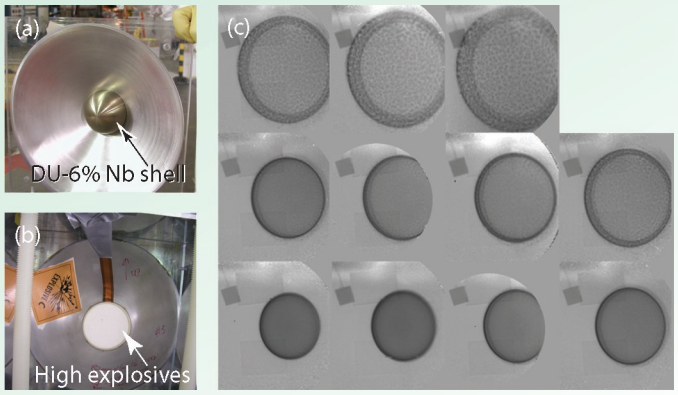

Figure 1. Photos of the (a) front and (b) back of the U-6% Nb fragmentation experiment. (c) Time sequence of the experiment. The frames start in the lower left and progress to the upper right. The spacing between frames is about 1 μs.

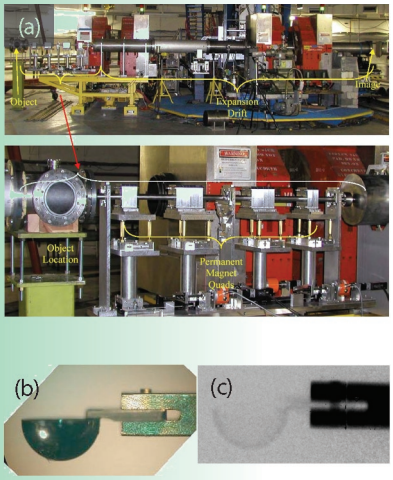

Figure 2. Photo of (a) the newly commissioned magnifier with images of one-half of a beryllium capsule (b) and its radiograph (c).

Radiography 2003

Proton radiography. Charged particles are bent by the Lorenz force in a magnetic field. Lenses that focus charged particle beams can be constructed from quadrupole magnets. Highly symmetric lens systems have been developed for pRad that sort the scattering angles in a beam transmitted by an object in one plane (the Fourier plane); these lenses then form an image of the transmitted beam in another plane (the image plane) further downstream.

Proton radiography was originally developed to take advantage of the enormous gain in statistical precision that can be obtained by using the long, hadronic mean-free path of protons, λ_p = 200 gm/cm^3, when compared to the relatively short mean-free path of high-energy photons, λ = 25 gm/cm^3, for thick-object hydrotest radiography. This has been studied at the AGS at BNL using higher-energy proton beams (24 GeV/c) than those available at LANL (1.4 GeV/c), and indeed the expected advantage of about a factor of 100 over the first axis of DARHT has been demonstrated.[2]

The 800-MeV proton beam provided by the LANSCE accelerator has proven to be very useful for smaller-scale experiments, even though this energy is too low for hydrotest radiography, by using the principles laid out above. A collimator placed in the Fourier plane controls the contrast in the image plane by adjusting its size to provide the optimum contrast for a given experiment. The transmission through an object using a collimator that passes the transmitted beam up to some maximum angle, θ_c, can be calculated by integrating Equation 1:

$$t_{ms} = \int_0^{\theta_c} \frac{1}{\theta_0^2} e^{-\frac{\theta^2}{2\theta_0^2}} \sin(\theta) d\theta, \tag{4}$$

which for small angles gives

$$t_c = (1 - e^{-\frac{\kappa}{l}}), \tag{5}$$

where

$$\kappa = \frac{\theta^2 p^2 \beta^2 X_0}{14.1^2}. \tag{6}$$

Here, κ is the thickness scale set at the collimator angle cut. The collimator angle can be chosen to optimize the measurement of l for the most interesting part of an experiment for a given incident number of particles, N_0:

$$\frac{\Delta l}{l} = \frac{l}{\kappa} \frac{\sqrt{t_{ms}}}{1 - t_{ms}} \frac{1}{\sqrt{N_0}} \tag{7}$$

Equation 7 can be solved for a minimum as a function of κ. The result is $\kappa = 0.64\, l$ (i.e., a transmission of 47%). From the discussion above, one sees that within the limits imposed by beam luminosity, pRad can be used for dynamic radiography on thin and thick systems. This is the observation that has made the pRad facility at LANSCE so useful to the weapons program.

Deuterium-uranium experiment. The fragmentation of shocked pieces of metal has been experimentally studied since the Civil War[3] to obtain information needed for designing ordnance. Recently, models have been developed and incorporated into computer codes that may for the first time allow this phenomenon to be predicted.[4] X-ray radiography can provide detailed snapshots of fragments in material at high strain rates in explosively driven experiments. The single images obtained cannot follow the time development of the material damage, and they are not quantitative. Although the x-ray experiments have been of great importance in the model development, pRad has been pursued because it can follow the time development of a single experiment (which is important because of the stochastic nature of these phenomena) and because it can provide quantitative data.

A recent series of experiments were performed on a strategically interesting material—uranium alloyed with 6% niobium. Small shells of this material were put under biaxial strain using a point-detonated hemispherical charge. A photo of one of these experiments along with a series of pRad images is shown in Figure 1. As can be seen, the fragmentation of the metal can be clearly followed.

Magnifier. Much the same as with an optical microscope, charged-particle images can be magnified using magnetic lenses. We have recently commissioned a proton magnifier (Figure 2) that uses permanent magnets to provide an enlarged image. Magnification also reduces the contribution of aberrations to the position resolution of the final image. As a consequence, the magnifier produced images with position resolution that is better than 15 µm over a 2-cm field of view, which is much better than the 200 µm that we have obtained with our larger lenses. This smaller field of view can be illuminated to a relatively high particle density with very short pulses from the LANSCE proton beam. We hope to perform studies of explosives and explosively driven phenomena on a much shorter length scale using this magnifier.

Electron radiography. The NIF being built at LLNL has a goal of reaching thermonuclear ignition by driving the spherical implosion of a DT ice layer frozen to the inside of a capsule that is imploded using x-rays generated by very high-power laser beams. The time scale of the implosion is about 20 ns. The spatial and time scales and the dynamic range provide a challenge for existing diagnostics. The required position resolution of better than 10 μm can be obtained with charged-particle radiography using a magnifier. However, it would be difficult, as well as expensive, to obtain enough luminosity with a proton beam for this task.

We have performed studies of electron radiography to determine if it can cover the dynamic range of a NIF implosion. Because electron sources are very bright, we have shown that the intensity needed can be obtained from existing sources. Simulated radiographs at t = 0 and at t = 17 ns, nuclear time, for a NIF capsule are shown in Figure 3 for a simple permanent-magnet magnifier and a 400-MeV electron beam. These results indicate that the electrons may provide a unique diagnostic. Further theoretical studies are needed to ensure that the coupling between the electrons and the plasma do not perturb the image. Meanwhile, an electron accelerator and lens are being built at LANL to further study the experimental issues in electron radiography. The goal of this work is to provide a diagnostic tool for static radiography aimed at studying the uniformity of the ice layer inside of NIF capsules.

Muon radiography. An explosion, or even a fizzle, of a nuclear device in a major city would be catastrophic. The likelihood of such an attack from terrorist activities has been placed at 0.1–0.01 per year.[5] The direct consequences in deaths and economic damage would dwarf the destruction of the World Trade Centers. The aftermath would be likely to shut down international trade. The impact on world economies would be enormous. Strategies to prevent nuclear weapons or the components needed to build them from becoming available to terrorists are currently being formulated. Components include tightly controlling the world's supply of fissile materials, reducing or diluting the material that is suitable for building nuclear weapons, and providing surveillance at transportation choke points to interdict the illicit transport of fissionable materials.

The essential component of any nuclear explosive device is the fissile core. This material is radioactive, emitting gamma rays, alpha particles, and neutrons. Both gamma radiation and neutron emission allow detection at a distance of meters. Detection schemes deployed to date have measured the gamma radiation or have used horizontal x-ray radiography to try to image the material. The gamma radiation, however, is easily shielded with a few centimeters of lead, tungsten, or other heavy metal, and the radiography has been shown to be ineffective. X-ray radiography with currently deployed test systems has failed to detect shipments of depleted uranium.

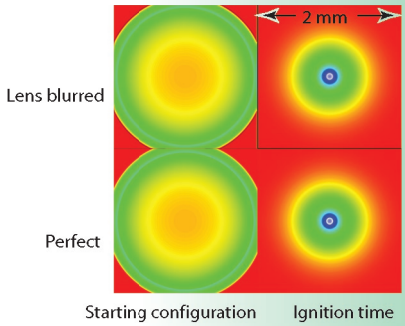

Figure 3. Simulated radiographs at t = 0 and t = 17 ns for a NIF capsule.

We have investigated the feasibility of using cosmic-ray muon radiography for homeland defense and compared the process to other active radiography approaches. In muon radiography, the charged particles are cosmic-ray muons. Because of their low rates, the muons can be individually detected.

Conventional radiography takes advantage of the absorption of penetrating radiation. For x-ray radiography,[6] the brightness of a pixel in the image is determined by the absorption or scattering of the incident beam:

$$N = N_0 e^{-\frac{L}{L_0}}, \tag{8}$$

where L is the path length (areal density) through an object, and L_0 is the mean-free path for scattering or absorption. The precision of radiographic measurements is limited by Poisson counting statistics of the transmitted flux,

$$\frac{\Delta L}{L_0} = \frac{1}{\sqrt{N}}. \tag{9}$$

The maximum mean-free path for photons in high-Z elements occurs at a few MeV. The mean-free path is approximately 25 gm/cm^2 for all materials at this energy. This corresponds to less than 2 cm of lead. To penetrate objects of tens of L_0 requires a large incident dose. An alternative is provided by charged-particle[2] radiography using cosmic-ray muons. In a 10-cm-thick layer, a 3-GeV muon (the average cosmic-ray energy) will scatter with a mean angle of 2.3 mrad in water (X = 36 cm), 11 mrad in iron (X = 1.76 cm), and 20 mrad in tungsten (X = 0.56 cm). If the muon-scattering angle in an object can be measured and if its momentum is known, then the path length, L, can be determined to a precision of

$$\frac{\Delta L}{L} = \sqrt{\frac{2}{N}}. \tag{10}$$

where N, the number of transmitted muons, is very nearly equal to the number of incident muons. Thus, each transmitted muon provides information about the thickness of the object.

We have constructed models of realistic shipping containers and vehicles for use in the Monte Carlo radiation codes known as MCNPX[7] and GEANT.[8] These have been used to compare existing x-ray and gamma-ray techniques with muon radiography. Muon radiography has been shown to discriminate all of the scenarios considered in less than four minutes scanning time. In Figure 4, a container has been filled with two layers of half-density iron balls, 20 cm in radius on 50-cm centers. A 20-kg sphere of high-enriched uranium has been hidden in the container. The muon radiograph in Figure 4 clearly shows the ease with which nuclear materials can be distinguished from background scatter. An x-ray radiography of a portion of the container, also shown in Figure 4, is plagued with problems from background scatter. Also, x-ray radiography does not provide three-dimensional views of a scene. Two-view x-ray radiography may be able to address some of these problems. The results of this study show that within the boundaries of weight limits, shielded containers of fissionable material can be easily obscured in ways that make it impossible to discriminate the material from legitimate cargo with x-rays. However, these are easily detected using muon radiography.

Conclusion

Charged-particle radiography is providing a versatile new probe that has advantages over conventional x-ray radiography for some unique applications. In pRad, charged-particle radiography has been used to make quantitative motion pictures of dynamic events. By taking advantage of magnetic lenses to magnify images and by using the very bright beams that can be made with electrons, we have suggested that charged-particle radiography might even be useful for studying the fine spatial detail and very fast motion in a NIF implosion. Finally, we have demonstrated that radiographs can be made using cosmic-ray muons for homeland-defense applications.

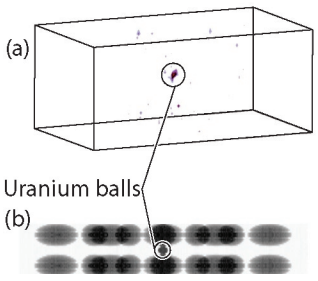

Figure 4. (a) Muon-radiography result. The uranium is visible and easily detectable above a threshold automatically. (b) X-ray result. The contrast has been reduced by scatter background. The uranium is not easily detectable automatically and cannot be distinguished from the iron cargo automatically. It could be moved so that it is shielded by the iron.

References

1. B. Rossi, *High-Energy Particles* (Prentice-Hall, NJ, 1952), p. 66.
2. C.L. Morris *et al.*, "A comparison of proton and x-ray thick object radiography," *Defense Review,* to be published (2003).
3. G.T. Gray, private communication, 2003.
4. P.J. Maudlin, Weapons Working Group, Los Alamos National Laboratory, December 2003.
5. S.E. Koonin, "Concealed nuclear devices," Jason Fall Meeting, McClean, Virginia, 2003.
6. N.B. Konstantin, G.E. Hogan, C. Morris, W.C. Priedhorsky, A. Saunders, L.J. Schultz, and M.E. Teasdale, "Radiographic imaging with cosmic ray muons," *Nature* **422** , 277 (2003); W.C. Priedhorsky *et al.*, "Detection of high-Z objects using multiple scattering of cosmic ray muons," *Review of Scientific Instruments* **74**, 4294-4297 (2003); and L.J. Schultz, K.N. Borozdin, J.J. Gomez, G.E. Hogan, J.A. McGill, C. Morris, W.C. Priedhorsky, A. Saunders, and M.E. Teasdale, "Image reconstruction and material Z discrimination via cosmic ray muon radiography," *Nuclear Instruments and Methods in Physics Research*, in press (2003).
7. J.S. Hendricks *et al.*, "MCNPX, Version 2.5.c," Los Alamos National Laboratory report LA-UR-03-2202, (2002).
8. Application Software Group Computing and Networks Division, "GEANT detector description and simulation tool," CERN Program Library (W5013), http://wwwasdoc.web.cern.ch/wwwasdoc/pdfdir/geant.pdf.

For more information, contact Chris Morris at 505-667-5652, cmorris@lanl.gov.

Shock-Wave and Material-Properties Experiments Using the Atlas Pulsed-Power Machine

R.E. Reinovsky (P-DO), C. Thompson (P-22), W.L. Atchison, R.J. Faehl, and I.R. Lindemuth (X-1), R.K. Keinigs (X-4), W. Anderson (MST-7), and T. Taylor (MST-10)

The Atlas facility built by LANL is the worlds first, and only, laboratory system designed specifically to provide pulsed-power-driven hydrodynamics capability for shock-wave physics, materials properties, instability, and hydrodynamics experiments in converging geometry. Constructed in 2000 and commissioned in August 2001, Atlas is a 24-MJ, high-performance capacitor bank capable of delivering up to 30 MA with a current rise time of 5–6 μs. Atlas completed its first year of physics experiments in October 2002, using ultra-high-precision magnetically imploded, cylindrical liners to reliably and reproducibly convert electrical energy to hydrodynamic energy in targets whose volume is many cubic centimeters. Multiview (transverse and axial) radiography, laser-illuminated shadowgraphy, and VISAR measurements of liner and target surface motion, in addition to electrical diagnostics, provide a detailed description of the behavior of the experimental package. In the first year, material-damage and -failure experiments, dynamic-friction experiments, and a family of converging-shock experiments were conducted in addition to a detailed series of liner-implosion-characterization experiments. These experiments will continue, and an additional experimental series will be added in the future to evaluate material strength at very high rates of strain, ejecta formation from surfaces, and instability growth at interfaces.

Ultra-high-precision cylindrical liners imploded with pulsed-power techniques have been applied to a variety of interesting questions broadly addressing the properties and behavior of condensed matter and plasmas. Generally, these topics fall into three categories:

(1) the properties of condensed matter at the extremes of pressure, temperature, and energy density;

(2) the hydrodynamic behavior of imploding systems; and

(3) the properties and behavior of dense plasmas.

In the first category, pulsed-power-driven liner experiments can explore the EOS of materials and phase transitions under single-shock (Hugoniot) conditions at higher shock pressures than those attainable by two-stage gas-gun/flyer-plate techniques. Magnetic drive offers shockless compression [1,2,3] that can drive materials to states not accessible through single-shock processes and to strains and strain rates far exceeding those available from other shockless techniques.

In the category of implosion hydrodynamics, liner-driven techniques are excellent for exploring

- instability growth in materials displaying full strength and in strengthless materials;
- the behavior of materials at interfaces (friction); and
- hydrodynamic flows in complex geometries.

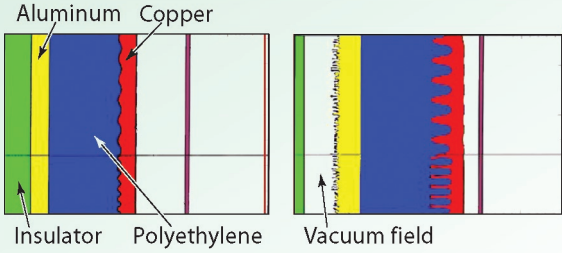

Figure 1. Multilayer liner with perturbations.

In the third category, Atlas can produce plasmas in which the ion and electron physics are strongly coupled—where little experimental data are available. For the initial Atlas experiments, material strength and failure (spall), interfacial dynamics (friction), and complex hydrodynamic flow experiments were selected.

Material Properties

Pulsed-power-driven liners permit the study of strength of (and ultimately the failure of) materials under extremes of strain and the rate of strain. Because of cylindrical convergence, the inner surface of an imploding Atlas liner reaches strains exceeding 200% at strain rates of 10^4 to 10^6 per second. By proper choice of liner designs (e.g., a high-conductivity aluminum armature surrounding a thin cylinder of the material of interest), the test sample can be isolated from the effects of the drive (including magnetic fields and ohmic heating), and the acceleration can be applied in a way that ensures that the sample material is not shocked. A third layer, intermediate between liner and sample, can further isolate the sample from processes happening in the liner. This also allows additional control of the pressure history applied to the target. (Barns *et al.* pioneered such techniques with high explosives in 1974.[4]) For Atlas-based studies of material strength, a "three-layer liner" (Figure 1) has been designed by a joint LANL/VNIIEF team, including the All-Russia Scientific Research Institute of Experimental Physics (at Arzamas-16). The system employs an aluminum, current-carrying liner; a polyethylene intermediate layer; and a copper sample. Perturbations up to a hundred microns in amplitude and a few millimeters in wavelength are preformed (machined) into the outer surface of the copper sample. The perturbations can be detected by radiography before and during acceleration and are predicted to grow in amplitude by a factor of 2 to 8 during approximately 8 μs of drive (Figure 2).

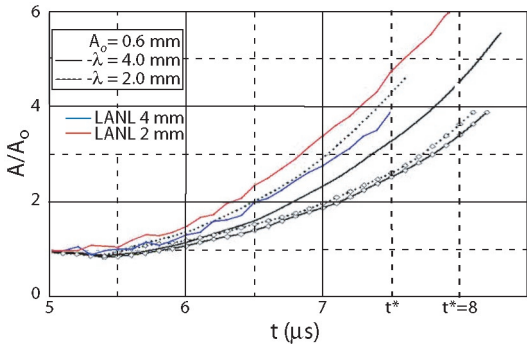

Figure 2. Perturbation growth for three-layer liners. A/A_O is the amplitude ratio.

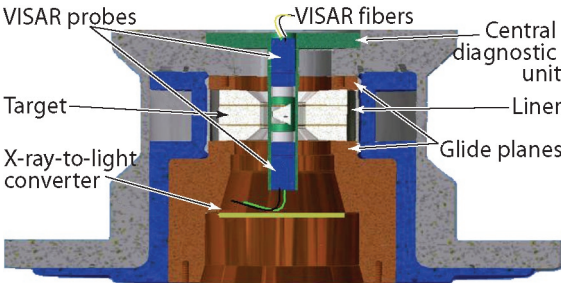

Figure 3. Atlas spall experiment.

While material-strength parameters can be deduced directly from the perturbation growth, the growth rates alone are sufficient to distinguish between several material models and among different computational techniques.

Liner implosions also offer unique opportunities for studying material failure (ultimate strength) at very high strain rates (in shocks) and at pressures that range from below the failure threshold to pressures many times that threshold. One convenient and familiar geometry for studying failure is the interacting shock geometry leading to "spall." Implemented in cylindrical geometry, the experiment is described in Figure 3. A series of four Atlas experiments have been conducted using a specially characterized, grain-oriented aluminum target material (driven by an identical aluminum liner) at shock pressures of 40–110 kbar. With these parameters, the tension in the sample ranges from that producing incipient spall to parameters where the sample clearly fails. Material behavior is diagnosed by monitoring the (inner) free surface velocity using VISAR. Figure 4 shows VISAR measurements of inner-surface velocity at two points, including shock breakout; the "pull back" as material is placed in tension; and the ringing after material failure. From peak velocity and velocity at failure, a spall strength can be found using established analysis techniques. In addition to VISAR, both transverse and longitudinal radiography is used to image the formation of the spall layer. Postfailure metallurgy provides important information about the behavior of the material during a spallation event. The controllability of pulsed-power-driven liners allows recovery of both native material and, in some cases, even the spalled material for post-event analysis—this is a significant advantage.

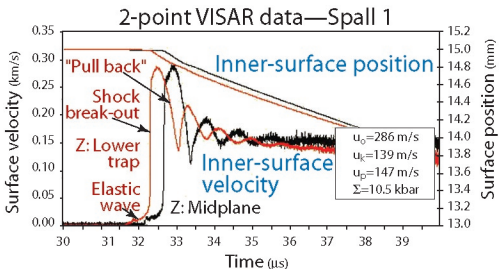

Figure 4. VISAR measurement of a spall experiment.

Implosion Hydrodynamics

Cartesian geometry is traditionally used to explore material properties; these studies of converging, liner-driven geometry represent an extension of those traditional methods. Symmetrical, radially imploding geometries can be readily studied by numerical simulation. Experimental data from configurations that are readily definable and calculable, but for which analytic solutions are not available, are important in benchmarking (both old and new) hydrodynamic (hydro) codes. The five-shot Atlas Hydro-Features (HF) series [preceded by the four-shot Near-Term Liner Experiments[5] (NTLX) series] began the process of gathering such data and demonstrated a sophisticated suite of experimental diagnostics for liner-driven experiments. Both HF and NTLX series employed a high-precision, shocklessly accelerated aluminum liner that drove a symmetrical cylindrically converging shock in a tin shock receiver. Tin melts at relatively low shock pressure; in the HF and NTLX experiment series, the shocked tin is a strength-free liquid. The converging shock emerges from the tin into a lower-density, optically transparent medium (acrylic or water) where its motion is characterized by two diagnostics simultaneously (Figure 5). A two-pass, axially directed, laser-illuminated shadowgraph records the change in refractive index and opacity of the material during passage of the shock, and a multiframe axially directed x-ray radiograph (Figure 6) records the change in material density as the shock moves through the material. Because of radial convergence, the shock speed should increase slightly as the shock approaches the axis, and the shock should reflect from the axis and expand uniformly through the once-shocked medium. Simulating the reflected shock is nontrivial, and the Atlas data constitutes nearly the only experimental data with high enough fidelity and precision to challenge the computational codes.

The next most challenging configuration for the simulation tools is where the symmetrical shock in the receiver emerges asymmetrically into the inner medium. This is accomplished in the experiment by introducing an offset between the axis of the inner medium and the axis of the shock receiver. The shadowgraph and radiographic diagnostics show that the convergence of the shock in the inner medium arrives off-axis as predicted. Taken together, these data constitute a significant test of both old and new simulation tools.

The imploding liner also presents opportunities for exploring the differential motion of material at an interface. Typically, experimental data on the behavior of material at "sliding" interfaces are limited to modest relative velocities and modest normal pressures. As relative velocities between the materials increase, one model predicts (supported by molecular-dynamic simulation) that the material at the interface melts and the presence of liquid at the interface reduces the effective frictional force. An experiment (Figure 7) has been designed to explore parameter space where the interfacial velocity varies from just below that for which the frictional force peaks and extends to values three to five times that value. The first of these experiments was conducted on Pegasus in 1998 and the second on Atlas during this first year of operation. For these experiments, a very thick, slow-moving liner impacts a cylindrical target—providing a supported shock of several microseconds duration. The target was configured as a sandwich of circular disks with a low-density (aluminum) disk between two high-density (tantalum) disks. The converging shocks generated when the liner impacts the target produce different particle velocities in the aluminum and tantalum disks—resulting in relative motion at the interfaces while simultaneously

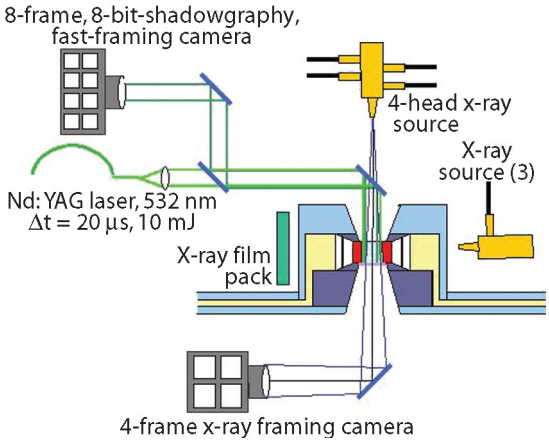

Figure 5. Diagnostics for HF experiments.

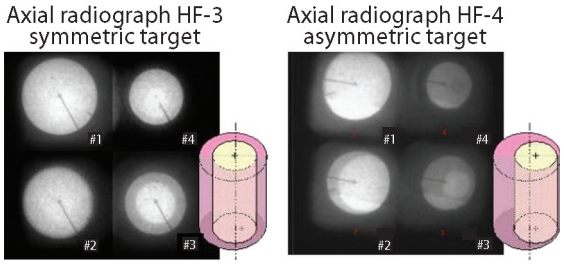

Figure 6. Radiographic data from symmetric and asymmetric targets. These are the third and fourth shots in the HF series.

pressurizing the target. Lead marker wires, 200 to 300 μm in diameter, are imbedded in the aluminum and radiographed in the transverse direction. Development of the boundary-layer motion is diagnosed by radiographying curvature and distortion of the wires. The experiment is performed as a function of shock strength (relative interfacial velocity), materials, and surface condition.

Conclusion

The development of economical, highly reliable, low-impedance capacitor banks coupled to high-precision, near-solid-density liners imploding at 5 to 20 km/s have made possible a wide variety of hydrodynamic experiments. The uniformity, controllability, and high liner velocities enable experiments not otherwise possible and represent a complement to lasers and nanosecond pulsed power used for radiation-driven experiments.

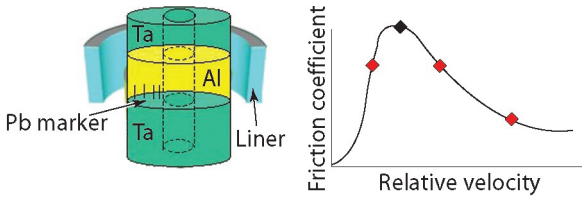

Figure 7. Atlas friction experiment.

References

1. J.R. Asay, C.A. Hall, K.G. Holland *et al.*, "Isentropic compression experiments on the Z accelerator," in *Proceedings of the Conference of the American Physical Society Topical Group on Shock Compression of Condensed Matter*, M.D. Furnish, L.C, Chhabildas, R.S. Hixson (Eds.), (American Institute of Physics, 2000), Vol. 505 pp. 1151–1154.
2. D.G. Tasker, C.M. Fowler, J.H. Goforth *et al.*, "Isentropic compression experiments using high explosive pulsed power," in *Proceedings of the Ninth International Conference on Megagauss Magnetic Fields Generation and Related Topics,* V.D. Selemir and L.N. Plyashkevich (Eds.), (VNIIEF, Sarov, Russia, to be published 2004).
3. A.M. Buyko, G.G. Ivanova, I.V. Morozova *et al.*, "Computation of electrically exploded opening switch for capacitor bank Atlas," in *Proceedings of the Ninth International Conference on Megagauss Magnetic Fields Generation and Related Topics,* V.D. Selemir and L.N. Plyashkevich (Eds.), (VNIIEF, Sarov, Russia, to be published 2004).
4. J.F. Barnes, P.J. Blewett, R.G. McQueen *et al.*, "Taylor instability in solids," *Journal of Applied Physics* **45**(2), 727 (1974).
5. P.J. Turchi, K. Alvey, C. Adams *et al.*, "Design, fabrication, and operation of a high energy liner implosion experiment at 16 megamperes," *IEEE Transactions on Plasma Science* **30**(5), 1777–1788 (2002).

Acknowledgment

This work was supported by the NNSA Office of Defense Programs. The Atlas experimental team includes operational functions provided by P-22 and Bechtel Nevada; diagnostic functions provided by P-22 and MST-10; precision-fabrication functions provided by MST-7; and design, simulation, and analysis functions provided by X-1, X-2, and X-4.

For further information, contact Robert Reinovsky at 505-667-8214, bobr@lanl.gov.

Relocation of Atlas to the Nevada Test Site

R.E. Reinovsky (P-DO), J.M. Neff-Shampine, W.B. Hinckley, J.E. Martinez, M.C. Thompson (P-22)

Atlas is a Marx-based capacitor-bank driver designed to deliver currents up to 30 MA to cylindrical target assemblies for the purpose of conducting high energy-density, hydrodynamic experiments in convergent geometry. The experiments planned for the Atlas machine are predominantly metallurgical in nature and include, but are not limited to, studies in accelerated-membrane stability, spall, interfacial friction, and high-strain/high-strain-rate forms. The Atlas power-flow/experimental-fixture design allows highly uniform magnetic drive for this experiment type. Funding for the machine's construction at LANL was provided by a line-item congressional decision in 1999.

The bulk of the experimental-effort funding is seated in the stockpile stewardship program (from the Associate Director for Weapons Physics) with the inclusion of (by direction from the NNSA) basic science expected from academia and similar proposals. P, DX, MST, and X Divisions collaborated in Atlas experiments. The operations and diagnostics teams from Bechtel Nevada have also been involved in the design of experiment diagnostics and operations training to a very significant degree.

Atlas has proven to be a precise tool in the arena of hydrodynamics and can produce delivered energy within 1% repeatability. It was one of the first such capacitor-bank systems to be totally controlled and managed via fiber-linked (ethernet) programmable logic controllers. The Atlas machine was designed in semi-autonomous bank divisions called "maintenance units" that allow all of the safety (interlocks and readiness), charge, and fire sequences to be conducted and managed by computer control, thus allowing the machine's controllers to interface with and maintain awareness of many nodes of information and control.

Atlas construction was completed and the machine was commissioned in December 2000. A series of 16 program experiments were conducted through October 2002 at LANL before shutting down Atlas to move it to NTS. The disassembly and move to NTS began in fall 2002, wherein the machine was turned over to Bechtel Nevada. Atlas is presently being reassembled at a new facility in Area 6 at NTS by the Bechtel Nevada crew. This crew was trained on the machine at LANL while the first series of experiments was performed—both for proof of principle of the Atlas machine and to finalize the experience of operations for the Bechtel Nevada operations crew and experiment designers. Final reconstruction and recommissioning of Atlas at the NTS facility is planned for March 2004. Presently, 23 program experiments are planned for the first full year of machine operations at NTS. An April 2004 start date will mean that the first funded series (FY 2004) will cover about the first half of the 23 experiments.

High-Energy Ultra-Short Laser Pulses at Trident

F.L. Archuleta, R.B. Gibson, R.P. Gonzales, T.R. Hurry, R.P. Johnson, N.K. Okamoto, T.A. Ortiz, T. Shimada (P-24)

Extremely high peak power (10^{13}–10^{15} W) lasers focused to spot sizes ~ 10 μm in diameter produce electric fields comparable to those found in intra-atomic regions, relativistic electron motion, and multimegagauss magnetic fields. These optical power levels open exciting opportunities for research in numerous areas such as intense x-ray sources, energetic-particle production, and the "fast-ignition" approach to ICF. Trident's modest capability to produce high-peak-power, ultra-short (≤ 1 ps) pulses was replaced by a new system that produces 30 TW focused to an irradiance of ~ 10^{19} W cm^{-2} in Trident's north target chamber. The new capability makes use of most of the original pulse chirper and stretcher, the existing C-beam amplifier chain, and an entirely new large-aperture pulse compressor constructed next to the north target chamber where the amplified, chirped 0.5-ns pulse is temporally compressed about 1,000 times (with > 75% energy efficiency), which greatly increases its power (Figure 1). This compressor is built on a standard optical table rather than in the large vacuum vessel normally used. While the nonlinear susceptibility of air and the target-chamber vacuum window ultimately limit peak optical power, cost and time to implement the capability were an order of magnitude less than what a vacuum compressor of similar performance would have required. Because all Trident beams are derived from the same master oscillator, either of the main beam lines can be used simultaneously to preheat or compress a target with a nanosecond-duration pulse synchronized to the ultra-short pulse with negligible jitter.

The ultra-short-pulse capability at Trident has now been used for approximately 100 target shots producing multi-MeV protons and ions and for the study of metal removal for the DoD. Other potential applications include pRad, intense x-ray generation, and the study of the fast-igniter approach to ICF.

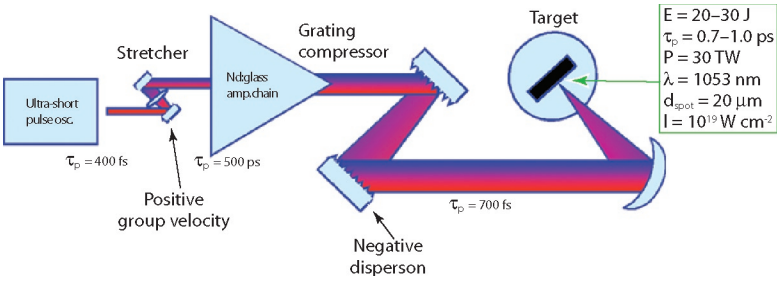

Figure 1. High-energy, subpicosecond pulses are produced by chirping and stretching a low-level ultra-short pulse, amplifying it to a high level, and then compressing it. Large diffraction gratings are configured to be the temporally dispersive elements.

Trident Laboratory Operations

F.L. Archuleta, R.B. Gibson, R.P. Gonzales, T.R. Hurry, R.P. Johnson, N.K. Okamoto, T.A. Ortiz, T. Shimada (P-24)

Trident is LANL's multipurpose laboratory for conducting experiments requiring high-energy laser-light pulses. It supports laser-driven HED physics experiments and associated diagnostic development in ICF, weapons physics, and basic science. Trident has a three-beam frequency-doubled Nd: glass laser driver and two vacuum target chambers. It has operated reliably for a decade, principally at its design pulse-length range of 0.1–2.5 ns, producing up to 250 J in each of its two main beam lines and up to 60 J in the third, smaller beam line. In FY 2002 and FY 2003, a high-energy ultrashort-pulse capability was added, producing 20–30 TW in a subpicosecond pulse. Production of multi-microsecond infrared pulses also became more routine. This flexible facility now conducts experiments over more than 6 orders of magnitude in pulse length.

More than 800 high-energy target shots are fired in approximately 20 experimental campaigns each year. In FY 2002 and FY 2003, Trident

- hosted laser-plasma-interaction experiments that verified nonlinear dispersion relations;
- developed 1.5-keV large scale-length plasmas;
- developed and characterized moderately collisional, moderately coupled plasmas;
- studied the transition from fluid to kinetic nonlinearity for Langmuir waves; and
- studied stimulated-Brillouin-scattering detuning by a velocity gradient.

Laser-induced MeV proton beams were produced, characterized, and used for radiography. Laser-launched flyer plates were launched into several different materials to study EOS and other properties. In addition, high-speed imaging cameras are routinely checked out, debugged, and calibrated at Trident before being used at other laboratories.

Appendices

Appendices Contents

Appendix A: Acronyms 219

Appendix B: Publications

2001 Journal Articles 222

2001 Conference Papers 229

2002 Journal Articles 241

2002 Conference Papers 246

2003 Journal Articles 259

2003 Conference Papers 266

Appendix A: Acronyms

A

ACT	Air Cerenkov Telescope
ADDS	Asymmetric Direct Drive Spheres
ADC	Analog-to-Digital Converter
AFRL	Air Force Research Laboratory
AGASA	Akeno Giant Air Shower Array
AGEX	Aboveground Experiment
AGN	Active Galactic Nuclei
AGS	Alternating Gradient Synchrotron
APD	Atmospheric Pressure Decontamination
APPJ	Atmospheric-Pressure Plasma Jet
ASIP	Applied-Science Internship Program
ASRT	Advanced, Single-Rotor Turbine
AWE	Atomic Weapons Establishment (United Kingdom)

B

BATSE	Burst and Transient Source Experiment
BCM	Binary Collision Model
BEC	Bose-Einstein Condensation
BG	Bacillus Globigii
BGO	Bismuth Germanium Oxide
BNL	Brookhaven National Laboratory
BooNE	Booster Neutrino Experiment

C

CAS	Canberra Alpha Spectrometer
CBW	Chemical and Biological Warfare
CC	Charged Current
CCD	Charged-Coupled Device
CERN	European Organization for Nuclear Research
CJ	Chapman-Jouguet
CMOS	Complementary Metal Oxide Semiconductor
CMU	Central Measuring Unit
CP	Charge Conjugation/Parity Transformation
CPT	Charge Conjugation/Parity Transformation/Time Reversal
CRADA	Cooperative Research and Development Agreement
CZT	Cadmium Zinc Telluride

D

DAR	Decay at Rest
DARHT	Dual-Axis Radiographic Hydrodynamic Test (facility)
DCA	Distance of Closest Approach
DEMG	Disk Explosive Magnetic Generator
DIM	Diagnostic Insertion Manipulator
DoD	Department of Defense
DOE	Department of Energy
DT	Deuterium-Tritium
DT	Diffusion Tensor
DU	Depleted Uranium
DynEx	Dynamic Experiment

E

EAS	Extensive Air Shower
ECG	Electrocardiography
*e*CM	Electron-Centimeters
EDM	Electric Dipole Moment
EEG	Electroencephalography
EGRET	Energetic Gamma Ray Experiment Telescope
EM600D	Eberline Radiation Monitor
EMSP	Environmental Management Science Program
EOS	Equation of State
EPW	Electron Plasma Waves
ES	Elastic Scattering
ETR	Enhanced Test Readiness (program)

F

FDM	Finite Difference Method
FMCG	Fetal Magnetocardiography
FMP	Flowing Magnetized Plasma (facility)
FNAL	Fermi National Accelerator Laboratory
FP	Flight Path
FRC	Field-Reversed Configuration
FRX-L	Field-Reversed Experiment-Liner
FWHM	Full-Width at Half Maximum
FY	Fiscal Year

Appendix A: Acronyms

G

GCD	Gas Cerenkov Detector
GGG	Gadolinium Gallium Garnet
GZK	Greisen, Zatsepin, Kuzmin (effect)

H

HDTV	High-Definition TV
HE	High Explosive
HED	High Energy Density
HEDH	High-Energy-Density Hdyrodynamics
HEMG	Helical Explosive Magnetic Generator
HEU	Highly Enriched Uranium
HEX	Hexagonal
HiRes	High Resolution Fly's Eye (experiment)
HPGe	High-Purity Germanium
HF	Hydro-Features (experiments)

I

ICA	Idaho Accelerator Center
ICE	Isentropic Compression Experiments
ICF	Inertial Confinement Fusion
ICF/RP	Inertial Confinement Fusion/Radiation Physics (program)
IEC	Inertial Electrostatic Confinement
IFE	Inertial Fusion Energy

J

JLab	Thomas Jefferson National Accelerator Facility

K

L

LAMPF	Los Alamos Meson Physics Facility
LANL	Los Alamos National Laboratory
LANSCE	Los Alamos Neutron Science Center
LDRD	Laboratory-Directed Research and Development
LDRD-DR	Laboratory-Directed Research and Development-Director's Reserve
LDRD-DR	Laboratory-Directed Research and Development-Directed Research
LDRD-ER	Laboratory-Directed Research and Development-Exploratory Research
LEO	Low Earth Orbit
LFC	Large Format Camera
LHS	Left-Hand Side
LICE	Laser-induced Isentropic Compression Experiment
LLE	Laboratory for Laser Energetics (University of Rochester)
LLNL	Lawrence Livermore National Laboratory
LOS	Line of Sight
LPI	Laser-Plasma Instabilities
LSND	Liquid Scintillator Neutrino Detector
LSO	Lutetium Oxyorthosilicate
Lujan Center	Lujan Neutron Scattering Center

M

MCMC	Markov Chain Monte Carlo
MCP	Microchannel Plate
MD	Molecular Dynamics
MDA	Missile Defense Agency
MEG	Magnetoencephalography
MEGA	Multiple Element Germanium Array
MFE	Magnetic Fusion Energy
MHD	Magnetohydrodynamics
MIT	Massachusetts Institute of Technology
MITL	Magnetically Insulated Transmission Line
MOPA	Master-Oscillator Power Amplifier
MRC	Mission Research Corporation
MRI	Magnetic Resonance Imaging
MTF	Magnetized Target Fusion
MVD	Multiplicity/Vertex Detector

N

NC	Neutral Current
NCD	Neutral Current Detector
nEDM	Neutron Electric Dipole Moment
NIF	National Ignition Facility
NIH	National Institutes of Health
NIR	Near Infrared
NIS	Nonproliferation and International Security
NIST	National Institute of Standards and Technology
NNMCC	Northern New Mexico Community College
NNSA	National Nuclear Security Administration
NRL	Naval Research Laboratory
NRS	Neutron Resonance Spectroscopy
NSLS	National Synchrotron Light Source
NSTX	National Spherical Torus Experiment

NTS	Nevada Test Site
NTSC	National Television System Committee
NTXL	Near-Term Liner Experiments
NUEX	Neutron Experiment

O

ORNL	Oak Ridge National Laboratory

P

P Division	Physics Division
PFL	Pulse-Forming Line
PFN	Pulse-Forming Network
PHELIX	Precision High Energy Liner Implosion Experiment
PHENIX	Pioneering High Energy Nuclear Interaction Experiment
PHERMEX	Pulsed High Energy Radiographic Machine Emitting X-rays (facility)
PINEX	Pinhole Neutron Experiment
PMT	Photomultiplier Tube
POPS	Periodically Oscillating Plasma Sphere
pRad	Proton Radiography
PSR	Proton Storage Ring
PZT	Lead Zirconate Titanate

Q

QCD	Quantum Chromodynamics
QGP	Quark-Gluon Plasma
QKD	Quantum Key Distribution

R

REH	Radiation Exit Hole
rf	Radio Frequency
RFSF	Radio Frequency Spin Flipper
RHIC	Relativistic Heavy-Ion Collider
RHS	Right-Hand Side
RHSR	Russian High Strain Rate (experiment)
RMI	Richtmyer-Meshkov Instabilities
RSX	Reconnection Scaling Experiment

S

SAGE	Soviet-American Gallium Experiment
SCE	Subcritical Experiment
SDP	Silent Discharge Plasma
SEGA	Segmented Enriched Germanium Assembly
SENSE	Sensory Enhanced Neural Simulation Engine
SHS	Single Hot Spot
SIM	Six-inch Instrument Manipulator
SIS	Superconducting Image Surface
SNL	Sandia National Laboratories
SNM	Special Nuclear Material
SNO	Sudbury Neutrino Observatory
SNP	Solar Neutrino Puzzle
SNS	Spallation Neutron Source
SOR	Successive Over-Relaxation
SQUID	Superconducting Quantum Interference Device
SRS	Stimulated Raman Scattering
SSC	Superconducting Supercollider
SSM	Standard Solar Model
STBI	Spatio-Temporal Bayesian Inference
STP	Standard Temperature and Pressure

T

T	Time Reversal
THREX	Threshold Experiment
TIM	Ten-inch Instrument Manipulator
TIM	Time Interval Meter
TWH	Thin-Wall Hohlraum
TXD	Transient X-ray Diffraction

U

UCN	Ultra-Cold Neutron
UGT	Underground Nuclear Test
UHECR	Ultra-High-Energy Cosmic Ray
UHV	Ultra-High Vacuum
UPOP	Undergraduate Practice Opportunity Program
U.S.	United States

V

VISAR	Velocity Interferometer System for Any Reflector
VLAND	Very Large Area Neutron Detector
VNIIEF	All-Russian Scientific Research Institute of Experimental Physics (Arzamas-16)

W

WACT	Wide-Angle Cerenkov Telescope

X, Y, Z

ZBL	Z Beamlet Laser

Appendix B: Publications

2001 Journal Articles

W.P. Abfalterer, F.B. Bateman, F.S. Dietrich, R.W. Finlay, R.C. Haight, and G.L. Morgan, "Measurement of neutron total cross sections up to 560 MeV," *Physical Review C* **63**, 044608 (2001).

K. Adcox, S.S. Adler, N.N. Ajitanand *et al.* (including Los Alamos scientists: P.D. Barnes, M.J. Bennett, M.L. Brooks, T.A. Carey, A.G. Hansen, W.W. Kinnison, D.M. Lee, M.J. Leitch, M.-X. Liu, P.L. McGaughey, R.E. Mischke, J.M. Moss, A.P.T. Palounek, B.R. Schlei, T. Shiina, J. Simon-Gillo, J.P. Sullivan, R.S. Towell, and H.W. van Hecke), "Centrality dependence of charged particle multiplicity in Au-Au collisions at $\sqrt{S_{NN}}$ = 130 GeV," *Physical Review Letters* **86**, 3500–3505 (2001).

K. Adcox, S.S. Adler, N.N. Ajitanand *et al.* (including Los Alamos scientists: P.D. Barnes, M.J. Bennett, M.L. Brooks, T.A. Carey, A.G. Hansen, W.W. Kinnison, D.M. Lee, M.J. Leitch, M.-X. Liu, P.L. McGaughey, R.E. Mischke, J.M. Moss, A.P.T. Palounek, B.R. Schlei, T. Shiina, J. Simon-Gillo, J.P. Sullivan, R.S. Towell, and H.W. van Hecke), "Measurement of the midrapidity transverse energy distribution from = 130 GeV Au + Au collisions at RHIC," *Physical Review Letters* **87**, 052301 (2001).

A. Aguilar, L.B. Auerbach, R.L. Burman, D.O. Caldwell, E.D. Church, A.K. Cochran, J.B. Donahue, A. Fazely, G.T. Garvey, R.M. Gunasingha, R. Imlay, W.C. Louis, R. Majkie, A. Malik, W. Metcalf, G.B. Mills, V. Sandberg, D. Smith, I. Stancu, M. Sung, R. Tayloe, G.J. VanDalen, W. Vernon, N. Wadia, D.H. White, and S. Yellin, "Evidence for neutrino oscillations from the observation of $\overline{\nu}_e$ appearance in a $\overline{\nu}_\mu$ beam," *Physical Review D* **64**, 112007 (2001).

M.W. Ahmed, D. Androic, I. Bertovic, J. Bjoraker, R.E. Chrien, X. Cui, D. Dehnhard, A. Empl, M. Furic, J. Gerald, R. Gill, E.V. Hungerford, H. Juengst, K.J. Lan, J.H. Liu, C.L. Morris, J.M. O'Donnell, J.-C. Peng, T. Petkovic, P. Pile, M. Planinic, C.M. Riedel, A. Rusek, R. Sutter, L. Tang, H.A. Thiessen, M. Youn, and V. Zeps, "The construction and operating characteristics of a cathode strip chamber system designed to measure the reaction vertices of a stopping kaon beam," *Nuclear Instruments and Methods in Physics Research Section A-Accelerators Spectrometers Detectors and Associated Equipment* **469**, 95–105 (2001).

Q.R. Ahmad, R.C. Allen, T.C. Andersen *et al.* (including Los Alamos scientists: A. Hamer, A. Hime, K. Kirch, G.G. Miller, R.G.H. Robertson, H. Seifert, P. Thornewell, R.G. Van de Water, D.L. Wark, J.B. Wilhelmy, J.F. Wilkerson, and J.M. Wouters), "Measurement of the rate of $\nu_e + d \rightarrow p + p + e^-$ interactions produced by ^8B Solar neutrinos at the Sudbury Neutrino Observatory," Physical Review Letters 87, 071301 (2001).

P. Allport, E. Atwood, W. Atwood, G. Beck, B. Bhatnager, E. Bloom, J. Broeder, V. Chen, J. Clark, N. Cotton, E.D.E. Silva, B. Feerick, G. Giebels, G. Godfrey, T. Handa, J.A. Hernando, M. Hirayama, R.P. Johnson, T. Kamae, S. Kashiguine, W. Kroeger, C. Milbury, W. Miller, O. Millican, M. Nikolaou, M. Nordby, T. Ohsugi, G. Paliaga, E. Ponslet, W. Rowe, H.F.W. Sadrozinski, E. Spencer, S. Stromberg, E. Swensen, M. Takayuki, D. Tournear, A. Webster, G. Winkler, K. Yamamoto, K. Yamamura, and S. Yoshida, "The assembly of the silicon tracker for the GLAST beam test engineering model," *Nuclear Instruments and Methods in Physics Research Section A-Accelerators Spectrometers Detectors and Associated Equipment* **466**, 376–382 (2001).

E. Atwood, W. Atwood, B. Bhatnager, E. Bloom, J. Broeder, V. Chen, J. Clark, N. Cotton, E.D.E. Silva, B. Feerick, B. Giebels, G. Godfrey, T. Handa, J.A. Hernando, M. Hirayama, R.P. Johnson, T. Kamae, S. Kashiguine, W. Kroeger, C. Milbury, W. Miller, O. Millican, M. Nikolaou, M. Nordby, T. Ohsugi, G. Paliaga, E. Ponslet, W. Rowe, H.F.W. Sadrozinski, E. Spencer, S. Stromberg, E. Swensen, M. Takayuki, D. Tournear, A. Webster, G. Winkler, K. Yamamoto, K. Yamamura, and S. Yoshida, "The silicon tracker of the beam test engineering model of the GLAST large-area telescope," *Nuclear Instruments and Methods in Physics Research Section A-Accelerators Spectrometers Detectors and Associated Equipment* **457**, 126–136 (2001).

L.B. Auerbach, R.L. Burman, D.O. Caldwell, E.D. Church, J.B. Donahue, A. Fazely, G.T. Garvey, R.M. Gunasingha, R. Imlay, W.C. Louis, R. Majkic, A. Malik, W. Metcalf, G.B. Mills, V. Sandberg, D. Smith, I. Stancu, M. Sung, R. Tayloe, G.J. VanDalen, W. Vernon, N. Wadia, D.H. White, and S. Yellin, "Measurements of charged current reactions of ν_e on ^{12}C," *Physical Review C* **64**, 065501 (2001).

L.B. Auerbach, R.L. Burman, D.O. Caldwell, E.D. Church, J.B. Donahue, A. Fazely, G.T. Garvey, R.M. Gunasingha, R. Imlay, W.C. Louis, R. Majkic, A. Malik, W. Metcalf, G.B. Mills, V. Sandberg, D. Smith, I. Stancu, M. Sung, R. Tayloe, G.J. VanDalen, W. Vernon, N. Wadia, D.H. White, and S. Yellin, "Measurement of ν_e electron elastic scattering," *Physical Review D* **63**, 112001 (2001).

S.E. Babayan, J.Y. Jeong, A. Schutze, V.J. Tu, M. Moravej, G.S. Selwyn, and R.F. Hicks, "Deposition of silicon dioxide films with a non-equilibrium atmospheric-pressure plasma jet," *Plasma Sources Science and Technology* **10**, 573–578 (2001).

I.G. Bearden, H. Boggild, J. Boissevain, P. Christiansen, L. Conin, J. Dodd, B. Erazmus, S. Esumi, C.W. Fabjan, D. Ferenc, D.E. Fields, A. Franz, J. Gaardhoje, A.G. Hansen, O. Hansen, D. Hardtke, H. van Hecke, E.B. Holzer, T.J. Humanic, P. Hummel, B.V. Jacak, R. Jayanti, K. Kaimi, M. Kaneta, T. Kohama, M. Kopytine, M. Leltchouk, A. Ljubicic, B. Lorstad, N. Maeda, L. Martin, A. Medvedev, M. Murray, H. Ohnishi, G. Paic, S.U. Pandey, F. Piuz, J. Pluta, V. Polychronakos, M. Potekhin, G. Poulard, D. Reichold, A. Sakaguchi, J. Schmidt-Sorensen, J. Simon-Gillo, W. Sondheim, T. Sugitate, J.P. Sullivan, Y. Sumi, W.J. Willis, K.L. Wolf, N. Xu, and D.S. Zachary, "One- and two-dimensional analysis of 3π correlations measured in Pb + Pb interactions," *Physics Letters B* **517**, 25–31 (2001).

I.G. Bearden, H. Boggild, J. Boissevain, P. Christiansen, L. Conin, J. Dodd, B. Erazmus, S. Esumi, C.W. Fabjan, D. Ferenc, D.E. Fields, A. Franz, J. Gaardhoje, A.G. Hansen, O. Hansen, D. Hardtke, H. van Hecke, E.B. Holzer, T.J. Humanic, P. Hummel, B.V. Jacak, R. Jayanti, K. Kaimi, M. Kaneta, T. Kohama, M. Kopytine, M. Leltchouk, A. Ljubicic, B. Lorstad, N. Maeda, L. Martin, A. Medvedev, M. Murray, H. Ohnishi, G. Paic, S.U. Pandey, F. Piuz, J. Pluta, V. Polychronakos, M. Potekhin, G. Poulard, D. Reichold, A. Sakaguchi, J. Schmidt-Sorensen, J. Simon-Gillo, W. Sondheim, T. Sugitate, J.P. Sullivan, Y. Sumi, W.J. Willis, K.L. Wolf, N. Xu, and D.S. Zachary, "Two-kaon correlations in central Pb + Pb collisions at 158 A GeV/c," *Physical Review Letters* **87**, 112301 (2001).

C.W. Barnes, T.J. Murphy, and J.A. Oertel, "High-yield neutron activation system for the National Ignition Facility," *Review of Scientific Instruments* **72**, 818–821 (2001).

A.R. Berdoz, J. Birchall, J.B. Bland, J.D. Bowman, J.R. Campbell, G.H. Coombes, C.A. Davis, P.W. Green, A.A. Hamian, Y. Kuznetsov, L. Lee, C.D.P. Levy, R.E. Mischke, S.A. Page, W.D. Ramsay, S.D. Reitzner, T. Ries, G. Roy, A.M. Sekulovich, J. Soukup, T. Stocki, V. Sum, N.A. Titov, W.T.H. van Oers, R.J. Woo, and A.N. Zelenski, "A monitor of beam polarization profiles for the TRIUMF parity experiment," *Nuclear Instruments and Methods in Physics Research Section A-Accelerators Spectrometers Detectors and Associated Equipment* **457**, 288–298 (2001).

A.R. Berdoz, J. Birchall, J.B. Bland, J.D. Bowman, J.R. Campbell, G.H. Coombes, C.A. Davis, A.A. Green, P.W. Green, A.A. Hamian, R. Helmer, S. Kadantsev, Y. Kuznetsov, L. Lee, C.D.P. Levy, R.E. Mischke, S.A. Page, W.D. Ramsay, S.D. Reitzner, T. Ries, G. Roy, A.M. Sekulovich, J. Soukup, G.M. Stinson, T.J. Stocki, V. Sum, N.A. Titov, W.T.H. van Oers, R.J. Woo, S. Zadorozny, and A.N. Zelenski, "Parity violation in proton-proton scattering at 221 MeV," *Physical Review Letters* **87**, 272301 (2001).

A.R. Berdoz, J. Birchall, J.B. Bland, J.D. Bowman, J.R. Campbell, G.H. Coombes, C.A. Davis, P.W. Green, A.A. Hamian, Y. Kuznetsov, L. Lee, C.D.P. Levy, R.E. Mischke, S.A. Page, W.D. Ramsay, S.D. Reitzner, T. Ries, G. Roy, A.M. Sekulovich, J. Soukup, T. Stocki, V. Sum, N.A. Titov, W.T.H. van Oers, R.J. Woo, and A.N. Zelenski, "A monitor of beam polarization profiles for the TRIUMF parity experiment," *Nuclear Instruments and Methods in Physics Research Section A-Accelerators Spectrometers Detectors and Associated Equipment* **457**, 288–298 (2001).

R.R. Berggren, S.E. Caldwell, J.R. Faulkner, R.A. Lerche, J.M. Mack, K.J. Moy, J.A. Oertel, and C.S. Young, "Gamma-ray-based fusion burn measurements," *Review of Scientific Instruments* **72**, 873–876 (2001).

G.P. Berman, A.R. Bishop, D.F.V. James, R.J. Hughes, and D.I. Kamenev, "Dynamical stability of an ion in a linear trap as a solid-state problem of electron localization," *Physical Review A* **64**, 053406 (2001).

E. Blaufuss, G. Guillian, Y. Fukuda *et al.* (including Los Alamos scientist: T.J. Haines), "^{16}N as a calibration source for Super-Kamiokande," *Nuclear Instruments and Methods in Physics Research Section A-Accelerators Spectrometers Detectors and Associated Equipment* **458**, 638–649 (2001).

C.N. Brown, T.C. Awes, M.E. Beddo, M.L. Brooks, J.D. Bush, T.A. Carey, T.H. Chang, W.E. Cooper, C.A. Gagliardi, G.T. Garvey, D.F. Geesaman, E.A. Hawker, X.C. He, L.D. Isenhower, D.M. Kaplan, S.B. Kaufman, P.N. Kirk, D.D. Koetke, G. Kyle, D.M. Lee, W.M. Lee, M.J. Leitch, N. Makins, P.L. McGaughey, J.M. Moss, B.A. Mueller, P.M. Nord, V. Papavassiliou, B.K. Park, J.-C. Peng, G. Petitt, P.E. Reimer, M.E. Sadler, W.E. Sondheim, P.W. Stankus, T.N. Thompson, R.S. Towell, R.E. Tribble, M.A. Vasiliev, J.C. Webb, J.L. Willis, D.K. Wise, and G.R. Young, "Observation of polarization in bottomonium production at $\sqrt{S}$ = 38.8 GeV," *Physical Review Letters* **86**, 2529–2532 (2001).

C.R. Brome, J.S. Butterworth, S.N. Dzhosyuk, C.E.H. Mattoni, D.N. McKinsey, J.M. Doyle, P.R. Huffman, M.S. Dewey, F.E. Wietfeldt, R. Golub, K. Habicht, G.L. Greene, S.K. Lamoreaux, and K.J. Coakley, "Magnetic trapping of ultracold neutrons," *Physical Review C* **63**, 055502 (2001).

W.T. Buttler, C. Soriano, J.M. Baldasano, and G.H. Nickel, "Remote sensing of three dimensional winds with elastic Lidar: Explanation of maximum cross correlation method," *Boundary Layer Meteorology* **101**, 305–327 (2001).

I.H. Campbell, D.L. Smith, C.J. Neef, and J.P. Ferraris, "Charge-carrier effects on the optical properties of poly(p-phenylene vinylene)," *Physical Review B* **64**, 035203 (2001).

Appendix B: Publications—2001 Journal Articles

I.H. Campbell, D.L. Smith, C.J. Neef, and J.P. Ferraris, "Optical properties of single-carrier polymer diodes under high electrical injection," *Applied Physics Letters* **78**, 270–272 (2001).

S.G. Crane, S.J. Brice, A. Goldschmidt, R. Guckert, A. Hime, J.J. Kitten, D.J. Vieira, and X. Zhao, "Parity violation observed in the β decay of magnetically trapped ^{82}Rb atoms," *Physical Review Letters* **86**, 2967–2970 (2001).

B.E. Crawford, J.D. Bowman, S.I. Penttilä, and N.R. Roberson, "A spin-transport system for a longitudinally polarized epithermal neutron beam," *Nuclear Instruments and Methods in Physics Research Section A-Accelerators Spectrometers Detectors and Associated Equipment* **474**, 159–171 (2001).

H.A. Davis, R.K. Keinigs, W.E. Anderson, W.L. Atchison, R.R. Bartsch, J.F. Benage, E.O. Ballard, D.W. Bowman, J.C. Cochrane, C.A. Ekdahl, J.M. Elizondo, R.J. Faehl, R.D. Fulton, R.F. Gribble, J.A. Guzik, G.A. Kyrala, R.B. Miller, K.E. Nielsen, J.V. Parker, W.M. Parsons, C.P. Munson, D.M. Oro, G.E. Rodriguez, H.H. Rogers, D.W. Scudder, J.S. Shlachter, J.L. Stokes, A.J. Taylor, R.J. Trainor, P.J. Turchi, and B.P. Wood, "The Atlas high energy-density physics project," *Japanese Journal of Applied Physics Part 1 Regular Papers Short Notes and Review Papers* **40**, 930–934 (2001).

J.H. Degnan, J.M. Taccetti, T. Cavazos, D. Clark, S.K. Coffey, R.J. Faehl, M.H. Frese, D. Fulton, J.C. Gueits, D. Gale, T.W. Hussey, T.P. Intrator, R.C. Kirpatrick, G.H. Kiuttu, F.M. Lehr, J.D. Letterio, I. Lindemuth, W.F. McCullough, R. Moses, R.E. Peterkin, R.E. Reinovsky, N.F. Roderick, E.L. Ruden, J.S. Shlachter, K.F. Schoenberg, R.E. Siemon, W. Sommars, P.J. Turchi, G.A. Wurden, and F. Wysocki, "Implosion of solid liner for compression of field-reversed configuration," *IEEE Transactions on Plasma Science* **29**, 93–98 (2001).

M.A. Espy, A.N. Matlashov, J.C. Mosher, and R.H. Kraus, Jr., "Non-destructive evaluation with a linear array of 11 HTS SQUIDs," *IEEE Transactions on Applied Superconductivity* **11**, 1303–1306 (2001).

A.C. Forsman and G.A. Kyrala, "Non-doppler shift related experimental shock wave measurements using velocity interferometer systems for any reflector," *Physical Review E* **63**, 056402 (2001).

M.C. Fujiwara, M. Amoretti, C. Amsler, G. Bendiscioli, G. Bonomi, A. Bouchta, P. Bowe, C. Carraro, M. Charlton, M. Collier, M. Doser, V. Filippini, K. Fine, A. Fontana, R. Funakoshi, P. Genova, D. Grogler, J.S. Hangst, R.S. Hayano, H. Higaki, M.H. Holzscheiter, W. Joffrain, L. Jorgensen, V. Lagomarsino, R. Landua, C.L. Cesar, D. Lindelof, E. Lodi-Rizzini, M. Macri, N. Madsen, G. Manuzio, M. Marchesotti, P. Montagna, H. Pruys, C. Regenfus, P. Riedler, A. Rotondi, G. Rouleau, P. Salvini, G. Testera, D.P. Van der Werf, A. Variola, L. Venturelli, T. Watson, T. Yamazaki, and Y. Yamazaki, "Producing slow antihydrogen for a test of CPT symmetry with ATHENA," *Hyperfine Interactions* **138**, 153–158 (2001).

S. Fukuda, Y. Fukuda, M. Ishitsuka *et al.* (including Los Alamos scientist: T.J. Haines), "Constraints on neutrino oscillations using 1258 days of Super Kamiokande Solar neutrino data," *Physical Review Letters* **86**, 5656–5660 (2001).

S. Fukuda, Y. Fukuda, M. Ishitsuka *et al.* (including Los Alamos scientist: T.J. Haines), "Solar ^{8}B and HEP neutrino measurements from 1258 days of Super Kamiokande data," *Physical Review Letters* **86**, 5651–5655 (2001).

G.T. Garvey and J.-C. Peng, "Flavor asymmetry of light quarks in the nucleon sea," *Progress in Particle and Nuclear Physics* **47**, 203–243 (2001).

V.N. Gavrin, Y.P. Kozlova, E.P. Veretenkin, T.J. Bowles, V.K. Eremin, E.M. Verbitskaya, A.V. Markov, A.Y. Polyakov, O.G. Koshelev, and V.F. Morozova, "Bulk GaAs as a Solar neutrino detector," *Nuclear Instruments and Methods in Physics Research Section A-Accelerators Spectrometers Detectors and Associated Equipment* **466**, 119–125 (2001).

W.J. Hogan, E.I. Moses, B.E. Warner, M.S. Sorem, and J.M. Soures, "The National Ignition Facility," *Nuclear Fusion* **41**, 567–573 (2001).

P.R. Huffman, C.R. Brome, J.S. Butterworth, S.N. Dzhosyuk, R. Golub, S.K. Lamoreaux, C.E.H. Mattoni, D.N. McKinsey, and J.M. Doyle, "Magnetically stabilized luminescent excitations in hexagonal boron nitride," *Journal of Luminescence* **92**, 291–296 (2001).

I.H. Hutchinson, R. Boivin, P.T. Bonoli, C. Boswell, R. Bravenec, N.L. Bretz, R. Chatterjee, T. Chung, E. Eisner, C. Fiore, S. Gangadhara, K. Gentle, J.A. Goetz, R.S. Granetz, M.J. Greenwald, J.C. Hosea, A.E. Hubbard, J. Hughes, Y. In, J. Irby, B. LaBombard, Y. Lin, B. Lipschultz, R.J. Maqueda, E.S. Marmar, A. Mazurenko, D. Mikkelsen, D. Mossessian, R. Nachtrieb, R. Nazikian, E. Nelson-Melby, D. Pappas, R.R. Parker, T.S. Pedersen, P. Phillips, C.S. Pitcher, M. Porkolab, J.E. Rice, W. Rowan, G. Schilling, J.A. Snipes, G. Taylor, J.L. Terry, J.R. Wilson, S.M. Wolfe, S.J. Wukitch, H. Yuh, S.J. Zweben, P. Acedo, M. Brambilla, B.A. Carreras, R. Gandy, G.A. Hallock, W. Dorland, D. Johnson, N. Krashennikova, C. Phillips, T. Tutt, C. Watts, and M. Umansky, "Overview of recent Alcator C-Mod results," *Nuclear Fusion* **41**, 1391–1400 (2001).

M.B. Johnson, B.Z. Kopeliovich, and A.V. Tarasov, "Broadening of transverse momentum of partons propagating through a medium," *Physical Review C* **63**, 035203 (2001).

M.B. Johnson, B.Z. Kopeliovich, I.K. Potashnikova, P.L. McGaughey, J.M. Moss, J.-C. Peng, G.T. Garvey, M.J. Leitch, M.R. Adams, D.M. Alde, H.W. Baer, M.L. Barlett, C.N. Brown, W.E. Cooper, T.A. Carey, G. Danner, G.W. Hoffmann, Y.B. Hsiung, D.M. Kaplan, A. Klein, C. Lee, J.W. Lillberg, R.L. McCarthy, C.S. Mishra, and M.J. Wang, "Energy loss of fast quarks in nuclei," *Physical Review Letters* **86**, 4483–4487 (2001).

S.M. Kaye, M.G. Bell, R.E. Bell, J. Bialek, T. Bigelow, M. Bitter, P. Bonoli, D. Darrow, P. Efthimion, J. Ferron, E. Fredrickson, D. Gates, L. Grisham, J. Hosea, D. Johnson, R. Kaita, S. Kubota, H. Kugel, B. LeBlanc, R. Maingi, J. Manickam, T.K. Mau, R.J. Maqueda, E. Mazzucato, J. Menard, D. Mueller, B. Nelson, N. Nishino, M. Ono, F. Paoletti, S. Paul, Y.K.M. Peng, C.K. Phillips, R. Raman, P. Ryan, S.A. Sabbagh, M. Schaffer, C.H. Skinner, D. Stutman, D. Swain, E. Synakowski, Y. Takase, J. Wilgen, J.R. Wilson, W. Zhu, S. Zweben, A. Bers, M. Carter, B. Deng, C. Domier, E. Doyle, M. Finkenthal, K. Hill, T. Jarboe, S. Jardin, H. Ji, L. Lao, K.C. Lee, N. Luhmann, R. Majeski, S. Medley, H. Park, T. Peebles, R.I. Pinsker, G. Porter, A. Ram, M. Rensink, T. Rognlien, D. Stotler, B. Stratton, G. Taylor, W. Wampler, G.A. Wurden, X.Q. Xu, and L. Zeng, "Initial physics results from the National Spherical Torus Experiment," *Physics of Plasmas* **8**, 1977–1987 (2001).

L.S. Kisslinger, M.B. Johnson, "Scalar mesons, glueballs, instantons and the glueball/sigma," *Physics Letters B* **523**, 127–134 (2001).

B. Kopeliovich, J. Raufeisen, and A.V. Tarasov, "The color dipole picture of the Drell-Yan process," *Physics Letters B* **503**, 91–98 (2001).

G.A. Kyrala and J.B. Workman, "Fluorescence concerns in high energy x-ray yield scaling and imaging studies," *Review of Scientific Instruments* **72**, 682–685 (2001).

G.A. Kyrala, G.T. Schappert, and S.C. Evans, "Effect of film development on uniformity and modulation transfer function of the gated/fast x-ray imagers data," *Review of Scientific Instruments* **72**, 521–524 (2001).

S.K. Lamoreaux, "Impressions of physics education," *American Journal of Physics* **69**, 633–633 (2001).

A. Loveridge-Smith, A. Allen, J. Belak, T. Boehly, A.A. Hauer, B. Holian, D. Kalantar, G.A. Kyrala, R.W. Lee, P. Lomdahl, M.A. Meyers, D. Paisley, S. Pollaine, B. Remington, D.C. Swift, S. Weber, and J.S. Wark, "Anomalous elastic response of silicon to uniaxial shock compression on nanosecond time scales," *Physical Review Letters* **86**, 2349–2352 (2001).

D.K. Mansfield, D.W. Johnson, B. Grek, H.W. Kugel, M.G. Bell, R.E. Bell, R.V. Budny, C.E. Bush, E.D. Fredrickson, K.W. Hill, D.L. Jassby, R.J. Maqueda, H.K. Park, A.T. Ramsey, E.J. Synakowski, G. Taylor, and G.A. Wurden, "Observations concerning the injection of a lithium aerosol into the edge of TFTR discharges," *Nuclear Fusion* **41**, 1823–1834 (2001).

R.J. Maqueda, G.A. Wurden, J.L. Terry, and J. Gaffke, "Digital-image capture system for the IR camera used in Alcator C-Mod," *Review of Scientific Instruments* **72**, 927–930 (2001).

R.J. Maqueda, G.A. Wurden, S. Zweben, L. Roquemore, H. Kugel, D. Johnson, S. Kaye, S. Sabbagh, and R. Maingi, "Edge turbulence measurements in NSTX by gas puff imaging," *Review of Scientific Instruments* **72**, 931–934 (2001).

A.V. Markov, M.V. Mezhennyi, A.Y. Polyakov, N.B. Smirnov, A.V. Govorkov, V.K. Eremin, E.M. Verbitskaya, V.N. Gavrin, Y.P. Kozlova, Y.P. Veretenkin, and T.J. Bowles, "Semi insulating LEC GaAs as a material for radiation detectors: Materials science issues," *Nuclear Instruments and Methods in Physics Research Section A-Accelerators Spectrometers Detectors and Associated Equipment* **466**, 14–24 (2001).

R.J. Mason, D.E. Hollowell, G.T. Schappert, and S.H. Batha, "Long term instability growth of radiatively driven thin planar shells," *Physics of Plasmas* **8**, 2338–2343 (2001).

A.N. Matlashov, M.A. Espy, R.H. Kraus, Jr., K.R. Ganther, Jr., and L.D. Snapp, "Electronic gradiometer using HT_c SQUIDs with fast feedback electronics," *IEEE Transactions on Applied Superconductivity* **11**, 876–879 (2001).

Y. Matsuda, J.D. Bowman, B.E. Crawford, P.P.J. Delheij, T. Haseyama, J.N. Knudsen, L.Y. Lowie, A. Masaike, Y. Masuda, G.E. Mitchell, S.I. Penttilä, H. Postma, N.R. Roberson, S.J. Seestrom, E.I. Sharapov, S.L. Stephenson, Y.F. Yen, and V.W. Yuan, "Parity violation in neutron resonances of antimony and iodine," *Physical Review C* **64**, 015501 (2001).

H.S. McLean, A. Ahmed, D. Buchenauer, D. Den Hartog, C.W. Domier, D.N. Hill, C. Holcomb, E.B. Hooper, E.C. Morse, M. Nagata, Y. Roh, B. Stallard, R.D. Wood, S. Woodruff, G.A. Wurden, and Z. Wang, "Plasma diagnostics for the Sustained Spheromak Physics Experiment," *Review of Scientific Instruments* **72**, 556–561 (2001).

J.E. Menard, B.P. LeBlanc, S.A. Sabbagh, M.G. Bell, R.E. Bell, E.D. Fredrickson, D.A. Gates, S.C. Jardin, D.W. Johnson, S.M. Kaye, H.W. Kugel, R. Maingi, R.J. Maqueda, D. Mueller, M. Ono, F. Paoletti, S.F. Paul, C.H. Skinner, and D. Stutman, "Ohmic flux consumption during initial operation of the NSTX spherical torus," *Nuclear Fusion* **41**, 1197–1206 (2001).

Appendix B: Publications—2001 Journal Articles

F.E. Merrill, T. Iijima, P. Koran, P.D. Barnes, B. Bassalleck, A.R. Berdoz, T. Burger, M. Burger, R.E. Chrien, C.A. Davis, G.E. Diebold, H. En'yo, H. Fischer, G.B. Franklin, J. Franz, L. Gan, D.R. Gill, K. Imai, Y. Kondo, M. Landry, L. Lee, J. Lowe, R. Magahiz, A. Masaike, R. McCrady, C.A. Meyer, J.M. Nelson, K. Okada, S.A. Page, K. Paschke, P.H. Pile, B.P. Quinn, W.D. Ramsay, E. Rossle, A. Rusek, R. Sawafta, H. Schmitt, R.A. Schumacher, R.L. Stearns, R.W. Stotzer, I.R. Sukaton, V. Sum, R. Sutter, J.J. Szymanski, F. Takeutchi, W.T.H. van Oers, K. Yamamoto, V.J. Zeps, and R. Zybert, "H-dibaryon search via Ξ^- capture on the deuteron," *Physical Review C* **63**, 035206 (2001).

M.C. Miller, J.R. Celeste, M.A. Stoyer, L.J. Suter, M.T. Tobin, J. Grun, J.F. Davis, C.W. Barnes, and D.C. Wilson, "Debris-characterization diagnostic for the NIF," *Review of Scientific Instruments* **72**, 537–539 (2001).

G.B. Mills, "Neutrino oscillation results from LSND," *Nuclear Physics B-Proceedings Supplements* **91**, 198–202 (2001).

D.S. Montgomery, R.J. Focia, H.A. Rose, D.A. Russell, J.A. Cobble, J.C. Fernández, and R.P. Johnson, "Observation of stimulated electron-acoustic-wave scattering," *Physical Review Letters* **87**, 155001 (2001).

D.S. Montgomery and R.P. Johnson, "Design considerations for fiber-coupled streaked optical spectroscopy," *Review of Scientific Instruments* **72**, 979–982 (2001).

D.S. Montgomery, "Comment on 'First observation of ion acoustic waves produced by the Langmuir decay instability,'" *Physical Review Letters* **86**, 3686 (2001).

G.L. Morgan, L. Disdier, R.R. Berggren, P.A. Bradley, F.H. Cverna, J.R. Faulkner, P.L. Gobby, J.A. Oertel, F.J. Swenson, J.A. Tegtmeier, R.B. Walton, M.D. Wilke, and D.C. Wilson, "Development of a neutron imaging diagnostic for inertial confinement fusion experiments," *Review of Scientific Instruments* **72**, 865–868 (2001).

J.D. Moses, D.B. Holtkamp, J.D. King, P.W. Lisowski, and J.E. Simmons, "Angular distribution of neutral hydrogen following collisional electron detachment from H^- at 2, 4, and 6 MeV," *Physical Review A* **63**, 042716(12) (2001).

R.W. Moses, R.A. Gerwin, and K.F. Schoenberg, "Transport implications of current drive by magnetic helicity injection," *Physics of Plasmas* **8**, 4839–4848 (2001).

T.J. Murphy, C.W. Barnes, R.R. Berggren, P. Bradley, S.E. Caldwell, R.E. Chrien, J.R. Faulkner, P.L. Gobby, N. Hoffman, J.L. Jimerson, K.A. Klare, C.L. Lee, J.M. Mack, G.L. Morgan, J.A. Oertel, F.J. Swenson, P.J. Walsh, R.B. Walton, R.G. Watt, M.D. Wilke, D.C. Wilson, C.S. Young, S.W. Haan, R.A. Lerche, M.J. Moran, T.W. Phillips, T.C. Sangster, R.J. Leeper, C.L. Ruiz, G.W. Cooper, L. Disdier, A. Rouyer, A. Fedotoff, V.Y. Glebov, D. D. Meyerhofer, J. M. Soures, C. Stockl, J. A. Frenje, D. G. Hicks, C. K. Li, R. D. Petrasso, F. H. Seguin, K. Fletcher, S. Padalino, and R.K. Fisher, "Nuclear diagnostics for the National Ignition Facility (invited)," *Review of Scientific Instruments* **72**, 773–779 (2001).

T.J. Murphy, J.L. Jimerson, R.R. Berggren, J.R. Faulkner, J.A. Oertel, and P.J. Walsh, "Neutron time-of-flight and emission time diagnostics for the National Ignition Facility," *Review of Scientific Instruments* **72**, 850–853 (2001).

T.J. Nash, M.S. Derzon, G.A. Chandler, D.L. Fehl, R.J. Leeper, J.L. Porter, R.B. Spielman, C. Ruiz, G. Cooper, J. McGurn, M. Hurst, D. Jobe, J. Torres, J. Seaman, K. Struve, S. Lazier, T. Gilliland, L. A. Ruggles, W.A. Simpson, R. Adams, J.A. Seaman, D. Wenger, D. Nielsen, P. Riley, R. French, B. Stygar, T. Wagoner, T.W.L. Sanford, R. Mock, J. Asay, C. Hall, M. Knudson, J. Armijo, J. McKenney, R. Hawn, D. Schroen-Carey, D. Hebron, T. Cutler, S. Dropinski, C. Deeney, P.D. LePell, C.A. Coverdale, M. Douglas, M. Cuneo, D. Hanson, J.E. Bailey, P. Lake, A. Carlson, C. Wakefield, J. Mills, J. Slopek, T. Dinwoodie, and G. Idzorek, "Diagnostics on Z (invited)," *Review of Scientific Instruments* **72**, 1167–1172 (2001).

J.A. Oertel, T.N. Archuleta, and L.S. Schrank, "The large format x-ray imager," *Review of Scientific Instruments* **72**, 701–704 (2001).

M. Ono, M.G. Bell, R.E. Bell *et al.* (including Los Alamos scientists: R. Maqueda, and G.A. Wurden), "Overview of the initial NSTX experimental results," *Nuclear Fusion* **41**, 1435–1447 (2001).

J. Park, I. Henins, H.W. Herrmann, and G.S. Selwyn, "Gas breakdown in an atmospheric pressure radio-frequency capacitive plasma source," *Journal of Applied Physics* **89**, 15–19 (2001).

J. Park, I. Henins, H.W. Herrmann, G.S. Selwyn, and R.F. Hicks, "Discharge phenomena of an atmospheric pressure radio-frequency capacitive plasma source," *Journal of Applied Physics* **89**, 20–28 (2001).

E.A. Pasyuk, R.L. Boudrie, P.A.M. Gram, C.L. Morris, J.D. Zumbro, J.L. Matthews, Y. Tan, V.V. Zelevinsky, G. Glass, and B.J. Kriss, "A study of the Δ^--component of the wave function in light nuclei," *Physics Letters B* **523**, 1–5 (2001).

J.-C. Peng, "Flavor asymmetry of the nucleon sea," *Nuclear Physics A* **684**, 80C–88C (2001).

H. Postma, J.D. Bowman, F. Corvi, B.E. Crawford, P.P.J. Delheij, C.M. Frankle, C.A. Grossmann, F. Gunsing, T. Haseyama, J.N. Knudson, L.Y. Lowie, A. Masaike, Y. Matsuda, G.E. Mitchell, S.I. Penttilä, N.R. Roberson, S.J. Seestrom, E.I. Sharapov, D.A. Smith, S.L. Stephenson, Y.F. Yen, V.W. Yuan, and L. Zanini, "Parity violation at neutron resonances and related neutron spectroscopy experiments," *Czechoslovak Journal of Physics* **51**, A289–A298 (2001).

D.M. Rector and J.S. George, "Continuous image and electrophysiological recording with real-time processing and control," *Methods* **25**, 151–163 (2001).

D.M. Rector, R.F. Rogers, J.S. Schwaber, R.M. Harper, and J.S. George, "Scattered-light imaging *in vivo* tracks fast and slow processes of neurophysiological activation," *Neuroimage* **14**, 977–994 (2001).

S.A. Sabbagh, S.M. Kaye, J. Menard, F. Paoletti, M. Bell, R.E. Bell, J.M. Bialek, M. Bitter, E.D. Fredrickson, D.A. Gates, A.H. Glasser, H. Kugel, L.L. Lao, B.P. LeBlanc, R. Maingi, R.J. Maqueda, E. Mazzucato, D. Mueller, M. Ono, S.F. Paul, M. Peng, C.H. Skinner, D. Stutman, G.A. Wurden, and W. Zhu, "Equilibrium properties of spherical torus plasmas in NSTX," *Nuclear Fusion* **41**, 1601–1611 (2001).

G.T. Schappert, S.H. Batha, K.A. Klare, D.E. Hollowell, and R.J. Mason, "Rayleigh-Taylor spike evaporation," *Physics of Plasmas* **8**, 4156–4162 (2001).

J.M. Scott, J.B. Beck, S.H. Batha, C.W. Barnes, and D.L. Tubbs, "Radiographic image analysis of cylindrical implosion experiments (invited)," *Review of Scientific Instruments* **72**, 643–650 (2001).

G.S. Selwyn, H.W. Herrmann, J. Park, and I. Henins, "Materials processing using an atmospheric pressure, rf-generated plasma source," *Contributions to Plasma Physics* **41**, 610–619 (2001).

E.I. Sharapov, J.D. Bowman, S.I. Penttilä, and G.E. Mitchell, "Parity violation in *p*-wave neutron resonances," *Physics of Particles and Nuclei* **32**, S129–S131 (2001).

D.A. Smith, J.D. Bowman, B.E. Crawford, C.A. Grossmann, T. Haseyama, M.B. Johnson, A. Masaike, Y. Matsuda, G.E. Mitchell, V.A. Nazarenko, S.I. Penttilä, N.R. Roberson, S.J. Seestrom, E.I. Sharapov, L.M. Smotritsky, S.L. Stephenson, S. Tomsovic, and V.W. Yuan, "Parity violation in neutron resonances of ^{117}Sn," *Physical Review C* **64**, 015502 (2001).

C. Soriano, J.M. Baldasano, W.T. Buttler, and K.R. Moore, "Circulatory patterns of air pollutants within the Barcelona air basin in a summertime situation: Lidar and numerical approaches," *Boundary Layer Meteorology* **98**, 33–55 (2001).

S. Sudo, Y. Nagayama, M. Emoto, M. Goto, Y. Hamada, K. Ida, T. Ido, H. Iguchi, S. Inagaki, M. Isobe, K. Kawahata, K. Khlopenkov, S. Masuzaki, T. Minami, S. Morita, S. Muto, H. Nakanishi, K. Narihara, A. Nishizawa, S. Ohdachi, M. Osakabe, T. Ozaki, B. J. Peterson, S. Sakakibara, M. Sasao, K. Sato, M. Shoji, K. Tanaka, K. Toi, T. Tokuzawa, K. Watanabe, T. Watanabe, I. Yamada, N. Ashikawa, T. Kobuchi, Y. Liang, N. Tamura, H. Sasao, A. Ejiri, S. Okajima, A. Mase, S. Tsuji-Iio, T. Akiyama, V. Zanza, G. Bracco, A. Sibio, B. Tilia, A.V. Krasilnikov, J.F. Lyon, L.N. Vyacheslavov, and G.A. Wurden, "Overview of large helical device diagnostics (invited)," *Review of Scientific Instruments* **72**, 483–491 (2001).

D.C. Swift, G.J. Ackland, A.A. Hauer, and G.A. Kyrala, "First-principles equations of state for simulations of shock waves in silicon," *Physical Review B* **64**, 214107 (2001).

Y.C.F. Thio, C.E. Knapp, R.C. Kirkpatrick, R.E. Siemon, and P.J. Turchi, "A physics exploratory experiment on plasma liner formation," *Journal of Fusion Energy* **20**, 1–11 (2001).

W.B. Tippens, V. Abaev, M. Batinic, V. Bekrenev, W.J. Briscoe, R.E. Chrien, M. Clajus, D. Isenhower, N. Kozlenko, S. Kruglov, M.J. Leitch, A. Marusic, T. Moriwaki, T. Morrison, B.M.K. Nefkens, J.-C. Peng, P.H. Pile, J.W. Price, D. Rigsby, M.E. Sadler, R. Sawafta, I. Slaus, H. Seyfarth, A. Starostin, I. Supek, R.J. Sutter, A. Svarc, and D.B. White, "Measurement of charge symmetry breaking by the comparison of $\pi^+ d \rightarrow pp\eta$ with $\pi^- d \rightarrow nn\eta$," *Physical Review D* **63**, 052001 (2001).

S.J. Tobin, W.A. Reass, L.S. Schrank, G.A. Wurden, H.Y. Guo, A.L. Hoffman, and D. Lotz, "Rotating magnetic field oscillator system for current drive in the translation, confinement, and sustainment experiment," *Review of Scientific Instruments* **72**, 3528–3533 (2001).

R.S. Towell, P.L. McGaughey, T.C. Awes, M.E. Beddo, M.L. Brooks, C.N. Brown, J.D. Bush, T.A. Carey, T.H. Chang, W.E. Cooper, C.A. Gagliardi, G.T. Garvey, D.F. Geesaman, E.A. Hawker, X.C. He, L.D. Isenhower, D.M. Kaplan, S.B. Kaufman, P.N. Kirk, D.D. Koetke, G. Kyle, D.M. Lee, W.M. Lee, M.J. Leitch, N. Makins, J.M. Moss, B.A. Mueller, P.M. Nord, V. Papavassiliou, B.K. Park, J.-C. Peng, G. Petitt, P.E. Reimer, M.E. Sadler, W.E. Sondheim, P.W. Stankus, T.N. Thompson, R.E. Tribble, M.A. Vasiliev, Y.C. Wang, Z.F. Wang, J.C. Webb, J.L. Willis, D.K. Wise, and G.R. Young, "Improved measurement of the $\bar{d}/\bar{u}$ asymmetry in the nucleon sea," *Physical Review D* **64**, 052002 (2001).

J.R. Walston, C.R. Gould, D.G. Haase, B.W. Raichle, M.L. Seely, W. Tornow, W.S. Wilburn, S.I. Penttilä, and G.W. Hoffmann, "Low energy *NN* tensor force from $\vec{n}$–$\vec{P}$ scattering: Results of an accurate experimental approach," *Physical Review C* **63**, 014004 (2001).

K. Wang, R. Atkins, W. Benbow, D. Berley, M.L. Chen, D.G. Coyne, B.L. Dingus, D.E. Dorfan, R.W. Ellsworth, A. Falcone, L. Fleysher, R. Fleysher, G. Gisler, J.A. Goodman, T.J. Haines, C.M. Hoffman, S. Hugenberger, L.A. Kelley, I. Leonor, M. McConnell, J.F. McCullough, J.E. McEnery, R.S. Miller, A.I. Mincer, M.F. Morales, P. Nemethy, J.M. Ryan, F.W. Samuelson, B. Shen, A. Shoup, C. Sinnis, A.J. Smith, G.W. Sullivan, O.T. Tumer, O. Wascko, S. Westerhoff, D.A. Williams, T. Yang, and G.B. Yodh, "A survey of the northern sky for TeV point sources," *Astrophysical Journal* **558**, 477–481 (2001).

Appendix B: Publications—2001 Journal Articles

Z.H. Wang and C.W. Barnes, "On electrostatic acceleration of plasmas with the Hall effect using electrode shaping," *Physics of Plasmas* **8**, 4218–4226 (2001).

Z.H. Wang and C.W. Barnes, "Exact solutions to magnetized plasma flow," *Physics of Plasmas* **8**, 957–963 (2001).

Z.H. Wang, G.A. Wurden, C.W. Barnes, C.J. Buchenauer, H.S. McLean, D.N. Hill, E.B. Hooper, R.D. Wood, and S. Woodruff, "Density and H_a diagnostics and results for the Sustained Spheromak Physics Experiment," *Review of Scientific Instruments* **72**, 1059–1062 (2001).

R.G. Watt, R.E. Chrien, K.A. Klare, T.J. Murphy, D C. Wilson, and S. Haan, "A sensitive neutron spectrometer for the National Ignition Facility," *Review of Scientific Instruments* **72**, 846–849 (2001).

R.D. Wood, D.N. Hill, E.B. Hooper, D. Buchenauer, H. McLean, Z. Wang, S. Woodruff, and G.A. Wurden, "Particle control in the Sustained Spheromak Physics Experiment," *Journal of Nuclear Materials* **290**, 513–517 (2001).

J. Workman and G.A. Kyrala, "X-ray yield scaling studies performed on the Omega laser," *Review of Scientific Instruments* **72**, 678–681 (2001).

J. Workman, S. Evans, and G.A. Kyrala, "One-dimensional x-ray imaging using a spherically bent mica crystal at 4.75 keV," *Review of Scientific Instruments* **72**, 674–677 (2001).

G.A. Wurden, T.P. Intrator, D.A. Clark, R.J. Maqueda, J.M. Taccetti, F.J. Wysocki, S.K. Coffey, J.H. Degnan, and E.L. Ruden, "Diagnostics for a magnetized target fusion experiment," *Review of Scientific Instruments* **72**, 552–555 (2001).

W. Younes, J.A. Becker, L.A. Bernstein, P.E. Garrett, C.A. McGrath, D.P. McNabb, R.O. Nelson, G.D. Johns, W.S. Wilburn, and D.M. Drake, "Transition from asymmetric to symmetric fission in the $^{235}U_{n,f}$ reaction," *Physical Review C* **64**, 054613 (2001).

2001 Conference Papers

J.D. Anderson, R.W. Bauer, F.S. Dietrich, S.M. Grimes, R.W. Finlay, W.P. Abfalterer, F.B. Bateman, R.C. Haight, G.L. Morgan, E. Bauge, J.-P. Delaroche, and P. Romain, "Failure of standard optical models to reproduce neutron total cross section differences in the W isotopes," the International Conference on Nuclear Data for Science and Technology (ND2001), Tsukuba, Japan, October 7–12, 2001, Los Alamos National Laboratory report LA-UR-01-0028 (January 2001).

G. Archibald, P.D. Barnes, J.G. Boissevain, D. Budker, D.J. Clark, M.D. Cooper, J.M. Doyle, M.A. Espy, T.R. Gentile, D.M. Gilliam, R. Golub, G.L. Greene, M.E. Hayden, PR. Huffman, M.B. Johnson, S.K. Lamoreaux, C. Lei, L.J. Marek, A. Matlachov, R.E. Mischke, J.C. Peng, S. Penttilä, A.B. Sushkov, F.E. Wietfeldt, and V. Yashchuk, "Measurement of the electric dipole moment of the neutron," Fundamental Neutron Physics at the Spallation Neutron Source (FNPSNS 2001), Oak Ridge, Tennessee, USA, September 20–21, 2001, Los Alamos National Laboratory report LA-UR-01-6216 (November 2001).

W.L. Atchison, W.E. Anderson, R.K. Keinigs, D.M. Oro, M.A. Salazar, M.G. Sheppard, and J.L. Stokes, "Summary of the Rayleigh-Taylor instability studies at the Pegasus facility," Pulsed Power/Plasma Sciences (PPPS-2001), Las Vegas, Nevada, USA, June 17–22, 2001, Los Alamos National Laboratory report LA-UR-01-0237 (January 2001).

P. Ausmus, T.P. Intrator, M. Taccetti, W.J. Fienup, W.J. Waganaar, D. Begay, M.C. Langner, G.A. Wurden, P. Sanchez, Z. Wang, K. Barela, and E. Mignardot, "Inductive magnetic diagnostic techniques for magnetic target fusion," Student Symposium, Santa Fe, New Mexico, USA, August 5–6, 2001, Los Alamos National Laboratory report LA-UR-01-3982 (July 2001).

E.O. Ballard, J.C. Cochrane, H.A. Davis, K.E. Nielsen, J.V. Parker, and W.M. Parsons, "Atlas facility fabrication and assembly," Pulsed Power and Plasma Sciences (PPPS-2001), Las Vegas, Nevada, USA, June 17–22, 2001, Los Alamos National Laboratory report LA-UR-01-2369 (May 2001).

C.W. Barnes, "New project leader's perspectives on high energy density science at Los Alamos (and particularly on mix)," Meeting of the Joint Working Group (USA-UK) (JOWOG-32P), Aldermaston, UK, July 2001, Los Alamos National Laboratory report LA-UR-01-2275 (April 2001).

C.W. Barnes, R.D. Day, S.H. Batha, N.E. Elliott, N.E. Lanier, G.R. Magelssen, J.M. Scott, D.L. Tubbs, S. Rothman, C. Horsfield, and A.M. Dunne, "Characterization of surface roughness and initial conditions for mix experiments (U)," Meeting of the Joint Working Group (USA-UK) (JOWOG 32M), Los Alamos, New Mexico, USA, January 2001, Los Alamos National Laboratory controlled publication LA-CP-01-0036 (January 2001).

C.W. Barnes, S.H. Batha, A.M. Dunne, N.E. Lanier, G.R. Magelssen, T.J. Murphy, K. Parker, S. Rothman, J.M. Scott, and D. Youngs, "Improvements to convergent cylindrical plasma mix experiments using laser direct drive," 8th International Workshop on the Physics of Compressible Turbulent Mixing, Pasadena, California, USA, December 9–14, 2001, Los Alamos National Laboratory report LA-UR-01-2544 (May 2001).

C.W. Barnes, S.H. Batha, N.E. Lanier, G.R. Magelssen, J.M. Scott, R.L. Holmes, T.J. Murphy, S. Rothman, and A.M. Dunne, "Further adventures in convergent mix," 31st Anomalous Absorption Conference, Sedona, Arizona, USA, June 3–8, 2001, Los Alamos National Laboratory report LA-UR-01-2332 (April 2001).

C.W. Barnes, S.H. Batha, N.E. Lanier, T.J. Murphy, G.R. Magelssen, K. Parker, A.M. Dunne, S. Rothman, and D. Youngs, "Computational modeling of 2-shell cylindrical implosions with mix," 8th International Workshop on the Physics of Compressible Turbulent Mixing, Pasadena, California, USA, December 9–14, 2001, Los Alamos National Laboratory report LA-UR-01-4690 (August 2001).

C.W. Barnes, S.H. Batha, N.E. Lanier, T.J. Murphy, G.R. Magelssen, J.M. Scott, A.M. Dunne, K. Parker, S. Rothman, and D. Youngs, "Improvements to convergent cylindrical plasma mix experiments using laser drive," 42nd Annual Meeting of the American Physical Society Division of Plasma Physics, Long Beach, California, USA, October 29–November 2, 2001, Los Alamos National Laboratory report LA-UR-01-5816 (October 2001).

P.D. Barnes, J.G. Boissevain, D.J. Clark, M.D. Cooper, M.A. Espy, G.L. Greene, L J. Marek, S.K. Lamoreaux, A. Matlachov, J.-C. Peng, S.I. Penttilä, R. Golub, J.M. Doyle, P.R. Huffman, F. E. Wietfeldt, G. Archiband, M.E. Hayden, and C. Lei, "New search for the neutron electric dipole moment," 9th International Conference on the Structure of Baryons (Baryons 2001), Newport News, Virginia, USA, September 16–21, 2001, Los Alamos National Laboratory report LA-UR-01-3771 (July 2001).

R.R. Bartsch, C. Ekdahl, E.A. Rose, D.M. Custer, R.N. Ridlon, and S. Eylon, "Beam emittance diagnostic for the DARHT second axis injector," Pulsed Power and Plasma Sciences (PPPS-2001), Las Vegas, Nevada, USA, June 17–22, 2001, Los Alamos National Laboratory report LA-UR-01-3179 (June 2001).

S.H. Batha, C.W. Barnes, N.E. Lanier, G.R. Magelssen, R.L. Holmes, J.M. Scott, A.M. Dunne, S. Rothman, and K. Parker, "Observation of compressible plasma mix in cylindrically convergent implosions (U)," Meeting of the Joint Working Group (USA-UK) (JOWOG 32M), Los Alamos, New Mexico, USA, January 2001, Los Alamos National Laboratory controlled publication LA-CP-01-0037 (January 2001).

Appendix B: Publications—2001 Conference Papers

S.H. Batha, J.A. Guzik, and B.J.Warthen, "Underground test data relevant to the W76 (U)," Nuclear Explosives Design and Physics Conference (NEDPC 2001), Livermore, California, USA, October 15–19, 2001, Los Alamos National Laboratory controlled publication LA-CP-01-0264 (July 2001).

S.H. Batha, K. Parker, C.W. Barnes, A.M. Dunne, N.E. Lanier, G.R. Magelssen, T.J. Murphy, S. Rothman, J.M. Scott, and D. Youngs, "Mixing between two compressing cylinders," 8th International Workshop on the Physics of Compressible Turbulent Mixing, Pasadena, California, USA, December 9–14, 2001, Los Alamos National Laboratory report LA-UR-01-2575 (May 2001).

R.R. Berggren, J.R. Faulkner, R. Lerche, J.M. Mack, Jr., K. Moy, J.A. Oertel, S.E. Caldwell, and C.S. Young, "Recent progress on high-bandwidth DT reaction history measurements with gas Cerenkov detectors," Inertial Fusion Sciences and Applications Conference (IFSA 2001), Kyoto, Japan, September 10–14, 2001, Los Alamos National Laboratory report LA-UR-01-1803 (March 2001).

D. Berkeland and M. Boshier, "Destabilization of dark states, optical spectroscopy and laser cooling in Zeeman degenerate atomic systems," American Physical Society Meeting of the Division of Atomic and Molecular Physics (DAMOP2001), London, Ontario, Canada, May 16–19, 2001, Los Alamos National Laboratory report LA-UR-01-1286 (March 2001).

D. Berkeland, "Optical spectroscopy of trapped and cooled Sr^+," 15th International Conference on Laser Spectroscopy (ICOLS-XV), Snowbird, Utah, USA, June 10–15, 2001, Los Alamos National Laboratory report LA-UR-01-1697 (March 2001).

D. Berkeland, D. Enzer, M. Gulley, M.H. Holzscheiter, D.F. James, P.G. Kwiat, S.K. Lamoreaux, V.D. Sandberg, M.M. Schauer, J.R. Torgerson, D. Tupa, R.J. Hughes, "Progress toward sideband-cooling trapped calcium ions," the International Conference on Experimental Implementation of Quantum Computation, Sydney, Australia, January 16–19, 2001, Los Alamos National Laboratory report LA-UR-00-5612 (November 2000).

T.J. Bowles, "Low energy neutrino spectroscopy," 1st Joint Meeting of the Nuclear Physicists of the American and Japanese Physical Societies, Maui, Hawaii, USA, October 17–20, 2001, Los Alamos National Laboratory report LA-UR-01-5837 (October 2001).

J.D. Bowman, G.L. Greene, J.K. Knudson, S.K. Lamoreaux, G.S. Mitchell, G.L. Morgan, S.I. Penttilä, W.S. Wilburn, V.W. Yuan, C.S. Blessinger, M. Gericke, G. Hansen, H. Nann, T.B. Smith, W.M. Snow, T.E. Chupp, K.P. Coulter, T.R. Gentile, D.R. Rich, F.E. Wietfeldt, T. Case, S.J. Freedman, B.K. Fujikawa, S. Ishimoto, Y. Masuda, K. Morimoto, G.L. Jones, B. Hersmann, M.B. Leuschner, S. Page, W.D. Ramsay, and E.I. Sharapov, "$n + p \rightarrow d + \gamma$: A measurement of weak force between protons and neutrons," Fundamental Neutron Physics at the Spallation Neutron Source (FNPSNS 2001), Oak Ridge, Tennessee, USA, September 20–21, 2001, Los Alamos National Laboratory report LA-UR-01-6126 (November 2001).

P.A. Bradley, D.C. Wilson, J.A. Cobble, T.J. Murphy, J.C. Cooley, M.A. Salazar, G. Rivera, and A. Nobile, "Direct drive beryllium ablator capsules for the Omega laser," 43rd Annual Meeting of the American Physical Society Division of Plasma Physics (APS-DPP), Long Beach, California, USA, October 29–November 2, 2001, Los Alamos National Laboratory report LA-UR-01-4003 (July 2001).

P.A. Bradley, S.A. Becker, B.J. Warthen, A.B. Kaye, M.L. Stelts, and C.F. Lebeda, "Sheepshead NUEX (U)," Nuclear Explosives Design and Physics Conference (NEDPC 2001), Livermore, California, USA, October 15–19, 2001, Los Alamos National Laboratory controlled publication LA-CP-01-0528 (December 2001).

M.J. Burns, B.E. Carlsten, H.A. Davis, C.A. Ekdahl, Jr., B.T. McCuistian, F.E. Merrill, K.E. Nielsen, C.A. Wilkinson, K.P. Chow, H.L. Rutkowski, W.L. Waldron, S.S. Yu, G. Caporaso, Y. Chen, S. Sampayan, and J.A. Watson, "Status of the DARHT Phase 2 long-pulse accelerator," 2001 Particle Accelerator Conference (PAC2001), Chicago, Illinois, USA, June 18–22, 2001, Los Alamos National Laboratory report LA-UR-01-0329 (January 2001).

G.H. Canavan, "Transition from adversarial to cooperative strategic interaction," International Seminars on Planetary Emergencies, 26th Session, Erice, Sicily, Italy, August 19–24, 2001, Los Alamos National Laboratory report LA-UR-01-4562 (August 2001).

K.M. Carter, A.T. Martinez, D.M. Rector, and J.S. George, "Spatial and temporal dynamics of optical changes in crustacean nerve," Student Symposium, Santa Fe, New Mexico, USA, August 2001, Los Alamos National Laboratory report LA-UR-01-3698 (July 2001).

R.E. Chrien, R.L. Bowers, D.L. Peterson, R.G. Watt, G.C. Idzorek, M. Dunn, J. Foster, and P. Rosen, "Radiation hydrodynamic code validation experiments on Z (U)," Nuclear Explosives Design and Physics Conference (NEDPC 2001), Livermore, California, USA, October 15–19, 2001, Los Alamos National Laboratory controlled publication LA-CP-01-0231 (July 2001).

C.R. Christensen and T.J. Murphy, "Direct numerical calculation of x-ray and neutron imaging using apertures," 31st Anomalous Absorption Conference, Sedona, Arizona, USA, June 3–8, 2001, Los Alamos National Laboratory report LA-UR-01-2448 (May 2001).

C.R. Christensen, C.W. Barnes, G.L. Morgan, T.J. Murphy, M. Wilke, and D.C.Wilson, "Direct numerical calculation of neutron and x-ray imaging using apertures," 42nd Annual Meeting of the American Physical Society Division of Plasma Physics, Long Beach, California, USA, October 29–November 2, 2001, Los Alamos National Laboratory report LA-UR-01-5900 (October 2001).

D.A. Clark, B.G. Anderson, G. Rodriguez, J.L. Stokes, and L.J. Tabaka, "Liner velocity, current, and symmetry measurements on the 32 MEGAMP flux compression generator experiment ALT-1," Pulsed Power and Plasma Sciences (PPPS-2001), Las Vegas, Nevada, USA, June 17–22, 2001, Los Alamos National Laboratory report LA-UR-01-4468 (August 2001).

J.A. Cobble, R.P. Johnson, N.A. Kurnit, and D.S. Montgomery, "Cyclic plasma shearing interferometry for temporal characterization of a laser-produced plasma," 31st Anomalous Absorption Conference, Sedona, Arizona, USA, June 3–8, 2001, Los Alamos National Laboratory report LA-UR-01-2226 (April 2001).

J.A. Cobble, R.P. Johnson, T. Cowan, N. LeGalloudec, and M. Allen, "Proton beam generation with a TW laser," 43rd Annual Meeting of the American Physical Society Division of Plasma Physics (APS-DPP), Long Beach, California, USA, October 29–November 2, 2001, Los Alamos National Laboratory report LA-UR-01-3977 (July 2001).

J.C. Cochrane, J.V. Parker, W.B. Hinckley, K.W. Hosack, D. Mills, W.M. Parsons, D.W. Scudder, J.L. Stokes, L.J. Tabaka, M.C. Thompson, F.J. Wysocki, T.N. Campbell, D.L. Lancaster, and C.Y. Tom, "Atlas acceptance test," Pulsed Power and Plasma Sciences (PPPS-2001), Las Vegas, Nevada, USA, June 17–22, 2001, Los Alamos National Laboratory report LA-UR-01-3259 (June 2001).

D.G. Crabb, S. Bultmann, D. Day, Y. Prok, G.R. Court, M.A. Houlden, S. Penttilä, and C. Keith, "Improved NMR system with non-resonant cable arrangement for target polarization measurements," in *Proceedings of 14th International Spin Physics Symposium*, Osaka, Japan, 2000, K. Hatanaka, T. Nakano, K. Imai, and H. Ejiri, Eds., (AIP, Melville, New York, 2001), Vol. 570, p. 819.

N.D. Delamater, R.G. Watt, W.S. Varnum, D.C. Wilson, R.D. Day, A. Nobile, G. Pollak, J. Elliott, N.E. Elliott, S.C. Evans, V.M. Gomez, T.H. Pierce, P.J. Walsh, P. Amendt, J. Colvin, R. Turner, V. Glebov, and C. Stoeckl, "Progress toward ignition with non-cryogenic double-shell capsules," Inertial Fusion Sciences and Applications Conference (IFSA 2001), Kyoto, Japan, September 10–14, 2001, Los Alamos National Laboratory report LA-UR-01-4130 (July 2001).

C.A. Ekdahl, Jr., R.R. Bartsch, D.M. Custer, E.A. Rose, S. Eylon, W. Broste, and J. Johnson, "Measuring the emittance of the DARHT-II electron beam," 43rd Annual Meeting of the American Physical Society Division of Plasma Physics, Long Beach, California, USA, October 29–November 2, 2001 Los Alamos National Laboratory report LA-UR-01-3769 (July 2001).

N.E. Elliott, C.W. Barnes, R.D. Day, T.H. Pierce, J.E. Moore, V.M. Gomez, and R. Manzanzres, "Fabrication of direct drive cylindrical targets," 14th Target Fabrication Specialist's Meeting, West Point, New York, USA, July 15–19, 2001, Los Alamos National Laboratory report LA-UR-01-1974 (April 2001).

N.E. Elliott, C.W. Barnes, S.H. Batha, R.D. Day, P.L. Gobby, V.M. Gomez, D.J. Hatch, N.E. Lanier, G.R. Magelssen, R. Manzanzres, R.A. Perea, T.H. Pierce, G. Rivera, D. Sandoval, J.M. Scott, W.P. Steckle, and D.L. Tubbs, "Best practice procedures for making direct drive cylindrical targets for studies of convergent hydrodynamics," 14th Target Fabrication Specialist's Meeting, West Point, New York, USA, July 15–19, 2001, Los Alamos National Laboratory report LA-UR-01-3893 (July 2001).

E.-I. Esch, A. Hime, and T.J. Bowles, "Background underground at WIPP," April Meeting of the American Physical Society (2001), Washington D.C., USA, April 28–May 1, 2001, Los Alamos National Laboratory report LA-UR-01-2191 (April 2001).

M.A. Espy, A. Matlachov, R.H. Kraus, Jr., F.F. Balakirev, and J. Betts, "Temperature dependence of SQUID noise at temperatures below 4 K," SQUID 2001: Physics and Applications of Superconducting Quantum Interference, Gothenburg, Sweden, August 31–September 3, 2001, Los Alamos National Laboratory report LA-UR-01-3831 (July 2001).

M.V. Fazio, B.E. Carlsten, J.E. Farnham, K.W. Habiger, W.B. Haynes, E.M. Nelson, J.R. Smith, and J.L. Myers, "Progress toward a gigawatt-class annular beam Klystron with a thermionic electron gun," rf 2001 Workshop, Snowbird, Utah, USA, October 1–5, 2001, Los Alamos National Laboratory report LA-UR-01-5512 (September 2001).

E.N. Ferm, C.L. Morris, J.P. Quintana, P. Pazuchanic, H.L. Stacy, J.D. Zumbro, G.E. Hogan, and N.S.P. King, "Proton radiography examination of unburned regions in PBX 9502 corner turning experiments," 12th American Physical Society Topical Conference on Shock Compression of Condensed Matter (SCCM Shock 01), Atlanta, Georgia, USA, June 24–29, 2001, Los Alamos National Laboratory report LA-UR-01-3555 (June 2001).

J.C. Fernández, D.S. Montgomery, H.A. Rose, and R.P. Johnson, "Scaling of the SRS reflective of a single hot spot laser beam with laser intensity," 31st Anomalous Absorption Conference, Sedona, Arizona, USA, June 3–8, 2001, Los Alamos National Laboratory report LA-UR-01-2906 (May 2001).

Appendix B: Publications—2001 Conference Papers

J.C. Fernández, D.S. Montgomery, R. Focia, B. Bezzerides, J.A. Cobble, D.F. DuBois, H.A. Rose, and H. Vu, "Recent results on the role of kinetic effects and wave-wave interactions in simulated Raman backscattering in long-scale plasma," Inertial Fusion Sciences and Applications Conference (IFSA 2001), Kyoto, Japan, September 10–14, 2001, Los Alamos National Laboratory report LA-UR-01-1784 (March 2001).

J.C. Fernández, D.S. Montgomery, R. Focia, H.A. Rose, B. Bezzerides, J.A. Cobble, D.F. DuBois, and H.X. Vu, "Role of kinetic and wave-wave interactions in stimulated Raman backscattering," Inertial Fusion Sciences and Applications Conference (IFSA 2001), Kyoto, Japan, September 10–14, 2001, Los Alamos National Laboratory report LA-UR-01-5094 (September 2001).

J.C. Fernández, J.A. Cobble, D.S. Montgomery, R. Focia, H.A. Rose, B. Bezzerides, D.F. DuBois, and H.X. Vu, "Observed scaling of the SRS reflectivity of a single hot spot with laser intensity," 43rd Annual Meeting of the American Physical Society Division of Plasma Physics (APS-DPP), Long Beach, California, USA, October 29–November 2, 2001, Los Alamos National Laboratory report LA-UR-01-6031 (October 2001).

W.J. Fienup, T.P. Intrator, J.M. Taccetti, P. Ausmus, W.J. Waganaar, D. Begay, M.C. Langner, G.A. Wurden, P. Sanchez, Z. Wang, K. Barela, and E. Mignardot, "Magnetic diagnostic instrument for the magnetized target fusion experiment," Student Symposium, Santa Fe, New Mexico, USA, August 5–6, 2001, Los Alamos National Laboratory report LA-UR-01-3979 (July 2001).

M. Fisher, K.A. Werley, T.P. Intrator, K. Barela, and K. Vermare, "Prelininary investigation into kink stability of plasma current channels," Student Symposium, Santa Fe, New Mexico, USA, August 5–6, 2001, Los Alamos National Laboratory report LA-UR-01-3981 (July 2001).

N. Fotiadis, R.O. Nelson, M. Devlin, P.G. Young Jr., J.A. Becker, C.A. McGrath, D.P. McNabb, G.D. Johns, M.B. Chadwick, W.S. Wilburn, D.E. Archer, L.A. Bernstein, P.E. Garrett, and W. Younes, "Absolute partial gamma-ray cross sections in $^{238}U_{n,xn\gamma}$ reactions," the International Conference on Nuclear Data for Science and Technology (ND2001), Tsukuba, Japan, October 7–12, 2001, Los Alamos National Laboratory report LA-UR-01-4513 (August 2001).

J.S. George and D.M. Rector, "Novel confocal microscope for dynamic imaging of neural function," Society for Neuroscience 31st Annual Meeting, San Diego, California, USA, November 10–15, 2001, Los Alamos National Laboratory report LA-UR-01-4641 (August 2001).

G.R. Gisler, T.J. Haines, C.M. Hoffman, F. Samuelson, and C. Sinnis, "Contributions from the Milagro collaboration to the XXVII international cosmic ray conference, Hamburg, Germany," August 7–15, 2001, Los Alamos National Laboratory report LA-UR-01-3009 (June 2001).

A. Glocer, T. Tierney, and J.F. Benage, Jr., "Four-color temperature measurements of a strongly coupled plasma jet," Student Symposium, Santa Fe, New Mexico, USA, August 5–6, 2001, Los Alamos National Laboratory report LA-UR-01-4010 (July 2001).

J.A. Guzik, S.B. Kemic, S.H. Batha, K.H. Despain, R. Baltrusaitis, and D.E. Hollowell, "Lowball reinvestigation," Nuclear Explosives Design and Physics Conference (NEDPC 2001), Livermore, California, USA, October 15–19, 2001, Los Alamos National Laboratory controlled publication LA-CP-01-0256 (July 2001).

A.S. Hamer, "^{8}Li calibration source for the Sudbury Neutrino Observatory," April Meeting of the American Physical Society (2001), Washington D.C., USA, April 28–May 1, 2001, Los Alamos National Laboratory report LA-UR-01-2229 (April 2001).

A.S. Hamer, "SNO energy response in the pure D_2O phase," 1st Joint Meeting of the Nuclear Physicists of the American and Japanese Physical Societies, Maui, Hawaii, USA, October 17–20, 2001, Los Alamos National Laboratory report LA-UR-01-5769 (October 2001).

A.C. Hayes, D. Barr, S.A. Becker, G.D. Doolen, S.C. Frankle, J.A. Guzik, S.K. Lamoreaux, R. Little, and M.R. MacInnes, "Discrepancy in the $^{87}Y/^{88}Y$ radiochemical diagnostic for fusion neutrons (U)," Nuclear Explosives Design and Physics Conference (NEDPC 2001), Livermore, California, USA, October 15–19, 2001, Los Alamos National Laboratory controlled publication LA-CP-01-0340 (August 2001).

M.Y. Hockaday and R. Papazian, "DynEx: A roadmap to advanced dynamic experiments with Pu (U)," Presentation to the Mitre Corporation, La Jolla, California, USA, July 2001, Los Alamos National Laboratory controlled publication LA-CP-01-0244 (July 2001).

M.Y. Hockaday, "Overview of the stockpile stewardship program from a LANL perspective," NNSA Underground Nuclear Weapons Testing, Las Vegas, Nevada, USA, December 2001, Los Alamos National Laboratory report LA-UR-01-6548 (November 2001).

D.E. Hollowell, G.T. Schappert, S.H. Batha, K.A. Klare, and R.J. Mason, "Rayleigh-Taylor spike evolution (U)," Nuclear Explosives Design and Physics Conference (NEDPC 2001), Livermore, California, USA, October 15–19, 2001, Los Alamos National Laboratory controlled publication LA-CP-01-0241 (July 2001).

M.H. Holzscheiter, "Physics with ultra-low energy antiprotons," Workshop on a Low-Energy pbar Storage Ring (PBAR 2000), Chicago, Illinois, USA, August 3–5, 2000, Los Alamos National Laboratory report LA-UR-01-0799 (February 2001).

R.J. Hughes, J.E. Nordholt, G.L. Morgan, W.T. Buttler, and C.G. Peterson, "Quantum key distribution in daylight," 15th International Conference on Laser Spectroscopy (ICOLS-XV), Snowbird, Utah, USA, June 10–15, 2001, Los Alamos National Laboratory report LA-UR-01-1535 (March 2001).

T.P. Hughes, H.A. Davis, D.C. Moir, R.T. Olson, C. Vermare, and W.M. Wood, "Electron beam distruction due to ion release from targets: Comparison between computer calculations and observations," 43rd Annual Meeting of the American Physical Society Division of Plasma Physics (APS-DPP), Long Beach, California, USA, October 29–November 2, 2001, Los Alamos National Laboratory report LA-UR-01-3855 (July 2001).

G.C. Idzorek, R.E. Chrien, D.L. Peterson, R.G. Watt, B.H. Wilde, J. Armijo, D. Ortega, and J.S. Sandoval, "Rad-flow Experiments on the Z-machine (U)," Nuclear Explosives Computional Design Conference (NECDC 2002), Livermore, California, USA, October 15–19, 2001, Los Alamos National Laboratory report LA-UR-01-5722 (October 2001).

G.C. Idzorek, R.E. Chrien, D.L. Peterson, R.G. Watt, G.A. Chandler, D.L. Fehl, and T.W. Sanford, "Spectral output of Z-machine implosions," Pulsed Power and Plasma Sciences (PPPS-2001), Las Vegas, Nevada, USA, June 17–22, 2001, Los Alamos National Laboratory report LA-UR-01-3135 (June 2001).

T.P. Intrator, I. Furno, L. Vermare, D. Begay, C.R. Sovinec, K. Werley, M. Fisher, and W. Fienup, "Reconnection scaling experiment (RSX): First data from the magnetic reconnection at LANL," 43rd Annual Meeting of the American Physical Society Division of Plasma Physics (APS-DPP), Long Beach, California, USA, October 29–November 2, 2001, Los Alamos National Laboratory report LA-UR-01-6030 (October 2001).

J.H. Jett, K.L. Albright, S.W. Graves, R.C. Habbersett, J.C. Martin, M.A. Naivar, J.D. Parson, M.E. Wilder, and T.M. Yoshida, "Spectral analysis flow cytometry," Analytical Cytology XXI International Congress, San Diego, California, USA, May 4–9 2002, Los Alamos National Laboratory report LA-UR-01-5924 (October 2001).

R.J. Kanzleiter, W.L. Atchison, R.L. Bowers, M.L. Gittings, J.A. Guzik, D.M. Oro, J.P. Roberts, G. Rodriguez, J.L. Stokes, P.J. Turchi, S. Coffey, J. Degnan, and G. Kiuttu, "Using pulsed power for hydrodynamic code verification and validation," Pulsed Power and Plasma Sciences (PPPS-2001), Las Vegas, Nevada, USA, June 17–22, 2001, Los Alamos National Laboratory report LA-UR-01-3085 (June 2001).

R.E. Kelly, "Underground structure detection by surface magnetic gradient measurements," 46th Annual Meeting of SPIE: The International Society for Optical Engineering (SPIE 2001), San Diego, California, USA, July 29–August 3, 2001, Los Alamos National Laboratory report LA-UR-01-3357 (June 2001).

B.Z. Kopeliovich, J. Raufeisen, and A.V. Tarasov, "Color dipole approach to the Drell-Yan process in p-A collisions," the 36th Rencontres de Moriond on QCD and High Energy Hadronic Interactions, Les Arcs, Savoie, France, March 17–24, 2001, Los Alamos National Laboratory report LA-UR-01-1457 (March 2001).

R.H. Kraus, Jr., A. Matlachov, M.A. Espy, K. Maharajh, and P. Volegov, "Forward model for the superconducting imaging-surface MEG system," 3rd International Symposium on Noninvasive Functional Source Imaging (NFSI 2001), Innsbruck, Austria, September 6–9, 2001, Los Alamos National Laboratory report LA-UR-01-1915 (April 2001).

R.H. Kraus, Jr., A. Matlachov, M.A. Espy, P. Volegov, E.R. Flynn, and K. Maharahj, "Source localization precision of the superconducting imaging-surface MEG system," 3rd International Symposium on Noninvasive Functional Source Imaging (NFSI 2001), Innsbruck, Austria, September 6–9, 2001, Los Alamos National Laboratory report LA-UR-01-4539 (August 2001).

R.H. Kraus, Jr., A. Matlachov, M.A. Espy, P. Volegov, K. Maharajh, and E.R. Flynn, "Imaging magnetic sources in the presence of superconducting surfaces: Model and experiment," 3rd International Symposium on Noninvasive Functional Source Imaging (NFSI 2001), Innsbruck, Austria, September 6–9, 2001, Los Alamos National Laboratory report LA-UR-01-4893 (August 2001).

R.H. Kraus, Jr., A. Matlachov, M.A. Espy, P. Volegov, K. Maharajh, and E.R. Flynn, "Performance of a novel SQUID-based superconducting imaging-surface magnetoencephalography system," SQUID 2001: Physics and Applications of Superconducting Quantum Interference, Gothenburg, Sweden, August 31–September 3, 2001, Los Alamos National Laboratory report LA-UR-01-4892 (August 2001).

T.J.T. Kwan, F.L. Cochran, C.M. Snell, J.F. Benage, Jr., and D.C. Wolkerstorfer, "Magnetically driven targets for DARHT-II multiple pulse radiography," 43rd Annual Meeting of the American Physical Society Division of Plasma Physics (APS-DPP), Long Beach, California, USA, October 29–November 2, 2001, Los Alamos National Laboratory report LA-UR-01-1522 (March 2001).

T.J.T. Kwan, F.L. Cochran, C.M. Snell, J.F. Benage, Jr., and D.C. Wolkerstorfer, "Magnetically driven Bremsstrahlung targets for multiple-pulse x-ray radiography," 43rd Annual Meeting of the American Physical Society Division of Plasma Physics, Long Beach, California, USA, October 29–30, 2001, Los Alamos National Laboratory report LA-UR-01-6012 (October 2001).

Appendix B: Publications—2001 Conference Papers

S.K. Lamoreaux, "Solid state systems for electron electric dipole moment and other fundamental measurements," Institute for Theoretical Atomic and Moleculat Physics (ITAMP) Workshop, Boston, Massachusetts, USA, November 29–December 1, 2001, Los Alamos National Laboratory report LA-UR-01-5299 (September 2001).

J. Langenbrunner, C.H. Aldrich, K.L. Buescher, J.W. Howse, R.N. Collinsworth, K.M. Hanson, A.R. Mathews, C.S. Reese, M.L. Rogers, B.C. Trent, B.J. Warten, and T.W. Tunnel, "Parameter estimation in event simulation of an UGT (U)," Nuclear Explosives Design and Physics Conference (NEDPC 2001), Livermore, California, USA, October 15–19, 2001, Los Alamos National Laboratory controlled publication LA-CP-01-0427 (October 2001).

M.C. Langner, G.A. Wurden, D. Begay, T.P. Intrator, R.J. Maqueda, M. Taccetti, W.J. Waganaar, J. Wang, K. Barela, E. Mignardot, P. Sanchez, and P. Ausmus, "Use of stark broadening to determine density in field reverse plasma experiment," Student Symposium, Santa Fe, New Mexico, USA, August 5–6, 2001, Los Alamos National Laboratory report LA-UR-01-3978 (July 2001).

M.C. Langner, G.A. Wurden, D. Begay, T.P. Intrator, R.J. Maqueda, M. Taccetti, W.J. Waganaar, J. Wang, K. Barela, E. Mignardot, P. Sanchez, and P. Ausmus, "Optical plasma diagnostics," Student Symposium, Santa Fe, New Mexico, USA, August 5–6, 2001, Los Alamos National Laboratory report LA-UR-01-4469 (August 2001).

N.E. Lanier and C.W. Barnes, "Feasibility of fluorescence-based imaging for turbulence and mix studies in compressible, convergent implosions," 31st Anomalous Absorption Conference, Sedona, Arizona, USA, June 3–8, 2001, Los Alamos National Laboratory report LA-UR-01-2872 (May 2001).

N.E. Lanier, C.W. Barnes, W.P. Steckle, and R.A. Perea, "Feasibility of fluorescence-based imaging for laser driven turbulence and mix studies," 43rd Annual Meeting of the American Physical Society Division of Plasma Physics (DPP01), Long Beach, California, USA, October 29–November 2, 2001, Los Alamos National Laboratory report LA-UR-01-4043 (July 2001).

M.J. Leitch, "Charmonium production in p-A collisions," International Workshop on the Physics of the Quark-Gluon Plasma, Palaiseau Cedex, France, September 4–7, 2001, Los Alamos National Laboratory report LA-UR-01-6499 (November 2001).

E.C. Liong, J.-D. Pedelacq, B.-S. Rho, C.Y. Kim, K.C. Menes, T. Zyla, H.L. Cornelius, M.S. Park, G.S. Waldo, S. Fitz-Gibbon, J.H. Miller, J.R. Berendzen, and T.C. Terwilliger, "High-throughput structure determination and analysis in the post genome era," Los Alamos National Laboratory Science Day, Los Alamos, New Mexico, USA, February 13, 2002, Los Alamos National Laboratory report LA-UR-01-0731 (February 2002).

W.C. Louis, "Final LSND neutrino oscillation results," International Europhysics Conference on High Energy Physics, Budapest, Hungary, July 12–18, 2001, Los Alamos National Laboratory report LA-UR-01-2789 (May 2001).

G.R. Magelssen, J.M. Scott, S.H. Batha, C.W. Barnes, R.L. Holmes, N.E. Lanier, D.L. Tubbs, R.L. Holmes, A.M. Dunne, S. Rothman, K. Parker, and D. Youngs, "Recent results of radiation hydrodynamics and turbulence experiments in cylindrical geometry," Inertial Fusion Sciences and Applications Conference (IFSA 2001), Kyoto, Japan, September 10–14, 2001, Los Alamos National Laboratory report LA-UR-01-4983 (August 2001).

G.R. Magelssen, R.E. Chrien, S.E. Caldwell, D.C. Wilson, B.H. Wilde, D. Hoarty, C. Smith, J.M. Foster, M. Dunne, R.E. Turner, C.A. Back, and T. Perry, "Integrated radiation flow and capsule imposion experiments on Nova (U)," Nuclear Explosives Design Physics/NEDPC, Los Alamos, New Mexico, USA, October 1999, Los Alamos National Laboratory controlled publication LA-CP-01-0196 (June 2001).

G.R. Magelssen, S.E. Caldwell, R.E. Chrien, B.H. Wilde, J. Abdallah, Jr., D. Hoarty, C. Smith, and M. Dunne, "Calculations of the English concept experiments done on Omega (U)," Meeting of the Joint Working Group (USA-UK) (JOWOG-32S), Aldermaston, UK, October 16–20, 2000, Los Alamos National Laboratory controlled publication LA-CP-01-0069 (February 2001).

G.R. Magelssen, S.H. Batha, C.W. Barnes, R.D. Day, A.M. Dunne, S. Rothman, J.M. Scott, D.L. Tubbs, D. Youngs, T.R. Boehly, and P. Jaanimagi, "Compressible turbulence experiments in cylindrical geometry," 43rd Annual Meeting of the American Physical Society Division of Plasma Physics (DPP01), Long Beach, California, USA, October 29–November 2, 2001, Los Alamos National Laboratory report LA-UR-01-2627 (May 2001).

G.R. Magelssen, S.H. Batha, C.W. Barnes, R.D. Day, A.M. Dunne, N.E. Elliott, R.L. Holmes, J.M. Scott, D.L. Tubbs, D. Youngs, S. Rothman, T.R. Boehly, and P. Jaanimagi, "Recent results at Los Alamos National Laboratory of radiation hydrodynamics and turbulence experiments in cylindrical geometry," Inertial Fusion Sciences and Applications Conference (IFSA 2001), Kyoto, Japan, September 10–14, 2001, Los Alamos National Laboratory report LA-UR-01-1757 (March 2001).

G.R. Magelssen, S.H. Batha, C.W. Barnes, R.D. Day, A.M. Dunne, N.E. Elliott, R.L. Holmes, S. Rothman, J.M. Scott, D.L. Tubbs, D. Youngs, T.R. Boehly, and P. Jaanimagi, "Calculational results of 'end effects' in Los Alamos cylindrical experiments," 42nd Annual Meeting of the American Physical Society Division of Plasma Physics, Long Beach, California, USA, October 29–November 2, 2001, Los Alamos National Laboratory report LA-UR-01-5996 (October 2001).

G.R. Magelssen, S.H. Batha, C.W. Barnes, R.L. Holmes, A.M. Dunne, K. Oades, S. Rothman, and P. Graham, "Calculations of the cylinder mix experiment done on Omega (U)," Meeting of the Joint Working Group (USA-UK) (JOWOG-32S), Aldermaston, UK, October 16–20, 2000, Los Alamos National Laboratory controlled publication LA-CP-01-0068 (February 2001).

G.R. Magelssen, S.H. Batha, C.W. Barnes, R.L. Holmes, A.M. Dunne, K. Oades, S. Rothman, P. Graham, and D. Youngs, "Calculations of the Clymix experiment (U)," Meeting of the Joint Working Group (USA-UK) (JOWOG 32M), Los Alamos, New Mexico, USA, January 2001, Los Alamos National Laboratory controlled publication LA-CP-01-0070 (February 2001).

J.B. McClelland, "Workshop on fundamental neutron physics at the Spallation Neutron Source (FNPSN 2001)," Fundamental Neutron Physics at the Spallation Neutron Source (FNPSNS 2001), Oak Ridge, Tennessee, USA, September 20–21, 2001, Los Alamos National Laboratory report LA-UR-01-5324 (September 2001).

B.H.J. McKellar, M. Garbutt, G.J. Stephenson, Jr., and T.J. Goldman, "Neutrino clustering and the Z-burst model," European Physical Society International Europhysics Conference on High Energy Physics, Budapest, Hungary, July 12–18, 2001, Los Alamos National Laboratory report LA-UR-01-3234 (June 2001).

B.H.J. McKellar, M. Garbutt, G.J. Stephenson, Jr., and T.J. Goldman, "Neutrino masses for new interactions," European Physical Society International Europhysics Conference on High Energy Physics, Budapest, Hungary, July 12–18, 2001, Los Alamos National Laboratory report LA-UR-01-3522 (June 2001).

G.E. Mitchell, C.A. Grossmann, L.Y. Lowie, S.L. Stephenson, J.D. Bowman, J.N. Knudson, S.I. Penttilä, S.J. Seestrom, D.A. Smith, Y.-F. Yen, V.W. Yuan, B.E. Crawford, N.R. Roberson, P.P.J. Delheij, T. Haseyama, A. Masaike, Y. Matsuda, H.Postma, and E.I. Sharapov, "PNC experiments with heavy nuclei," in *Fundamental Physics with Pulsed Neutron Beams*, C.R. Gould, G.L. Greene, F. Plasil, and W.M. Snow, Eds., (World Scientific, Singapore, 2001), p. 108.

D.S. Montgomery, J.A. Cobble, J.C. Fernández, R. Focia, R.P. Johnson, and N. LeGalloudec, "Recent Trident single hot spot experiments: Evidence for kinetic effects, and observation of Langmuir decay instability cascade," 43rd Annual Meeting of the American Physical Society Division of Plasma Physics (APS-DPP), Long Beach, California, USA, October 29–November 2, 2001, Los Alamos National Laboratory report LA-UR-01-6086 (October 2001).

D.S. Montgomery, R. Focia, H.A. Rose, J.A. Cobble, J.C. Fernández, and R.P. Johnson, "Strong SRS at high K*lambda-debye in Trident experiments, and the observation of stimulated scattering from an electron-acoustic wave," 4th International Workshop on Laser-Plasma Interaction Physics, Banff, Alberta, Canada, February 21–24, 2001, Los Alamos National Laboratory report LA-UR-01-0973 (February 2001).

D.S. Montgomery, R. Focia, J.A. Cobble, J.C. Fernández, H.A. Rose, and D.A. Russell, "Observation of stimulated electron acoustic wave scattering: The case for nonlinear kinetic effects," 31st Anomalous Absorption Conference, Sedona, Arizona, USA, June 3–8, 2001, Los Alamos National Laboratory report LA-UR-01-2413 (May 2001).

D.S. Montgomery, R. Focia, J.A. Cobble, J.C. Fernández, H.A. Rose, and D.A. Russell, "Observation of stimulated electron acoustic wave scattering: The case for nonlinear kinetic effects," 43rd Annual Meeting of the American Physical Society Division of Plasma Physics (APS-DPP), Long Beach, California, USA, October 29–November 2, 2001, Los Alamos National Laboratory report LA-UR-01-4065 (July 2001).

D.S. Montgomery, R. Focia, J.A. Cobble, N. LeGalloudec, J.C. Fernández, H.A. Rose, D.A. Russell, and B.B. Afeyan, "Recent Trident single hot spot experiments: Evidence for kinetic effects, and observation of LDI cascade," 31st Anomalous Absorption Conference, Sedona, Arizona, USA, June 3–8, 2001, Los Alamos National Laboratory report LA-UR-01-2414 (May 2001).

K.B. Morley, "Analysis of test objects using proton and x-ray radiographic data," Nuclear Explosives Design and Physics Conference (NEDPC 2001), Livermore, California, USA, October 15–19, 2001, Los Alamos National Laboratory report LA-UR-01-4119 (July 2001).

C.L. Morris, "Proton radiography," Los Alamos National Laboratory Science Day, Los Alamos, New Mexico, USA, February 13, 2001, Los Alamos National Laboratory report LA-UR-01-0818 (February 2001).

J.M. Moss, G.T. Garvey, M.B. Johnson, M.J. Leitch, P.L. McGaughey, B.Z. Kopeliovich, and I.K. Potashnikova, "Energy loss of fast quarks in nuclei," International Nuclear Physics Conference (INPC2001), Berkeley, California, USA, July 30–August 3, 2001, Los Alamos National Laboratory report LA-UR-01-4960 (August 2001).

R.N. Mulford and D.C. Swift, "Mesoscale modeling of shock initiation in HMX-based explosives," in *Proceedings of the American Physical Society Topical Conference on Shock Compression of Condensed Matter*, Atlanta, Georgia, USA, June 25–29, 2001, (Springer-Verlag, Heidelberg, 2002), Vol. 620, pp. 415–418.

R.N. Mulford and D.C. Swift, "Temperature-based reactive flow model for ANFO," The International Workshop on Non-Ideal Explosives, Socorro, New Mexico, USA, May 19–22, 2001, Los Alamos National Laboratory report LA-UR-01-4072 (July 2001).

Appendix B: Publications—2001 Conference Papers

J.E. Nordholt and S.P. Gary, "Results of the mass analysis performed by PEPE aboard DS1," 41st Aerospace Science Meeting and Exhibit, Reno, Nevada, USA, January 6–9, 2001, Los Alamos National Laboratory report LA-UR-01-0001 (January 2001).

A.W. Obst, G.L. Morgan, and M.L. Stelts, "NUEX measurements on secondaries," Nuclear Explosives Design and Physics Conference (NEDPC 2001), Livermore, California, USA, October 15–19, 2001, Los Alamos National Laboratory report LA-UR-01-3948 (July 2001).

A.W. Obst, G.L. Morgan, M.L. Stelts, and R.A. Hilko, "Secondary NUEX measurements (U)," Nuclear Explosives Design and Physics Conference (NEDPC 2001), Livermore, California, USA, October 15–19, 2001, Los Alamos National Laboratory controlled publication LA-CP-01-0423 (October 2001).

A.W. Obst, K.R. Alrick, K. Boboridis, W.T. Buttler, S.K. Lamoreaux, S.L. Montgomery, J. Payton, M.D. Wilke, W.W. Anderson, and B.R. Marshall, "Ellipsometry in the study of dynamic material properties," American Physical Society Shock Compression of Condensed Matter Meeting 2001, Atlanta, Georgia, USA, June 24–29, 2001, Los Alamos National Laboratory report LA-UR-01-3483 (June 2001).

R.T. Olson, D.M. Oro, B.G. Anderson, J.K. Studebaker, K. Alvey, K. Peterson, and B.C. Frogget, "Radiographic results from the NTLX series of hydrodynamic experiments," Pulsed Power/ Plasma Sciences (PPPS-2001), Las Vegas, Nevada, USA, June 17–22, 2001, Los Alamos National Laboratory report LA-UR-01-3134 (June 2001).

D.L. Paisley and D.C. Swift, "Laser-launched flyer plates and direct laser shocks for dynamic material property measurements," in *Proceedings of the American Physical Society Topical Conference on Shock Compression of Condensed Matter*, Atlanta, Georgia, USA, June 25–29, 2001, (Springer-Verlag, Heidelberg, 2002), Vol. 620, pp. 1343–1346.

R. Papazian, T.T. Fife, and F.H. Cverna, "Unicorn status update to AWE (U)," Meeting of the Joint Working Group (USA-UK) (JOWOG-32/9), Aldermaston, UK, July 2001, Los Alamos National Laboratory controlled publication LA-CP-01-0302 (July 2001).

W.M. Parsons, P.L. Walstrom, M. Murray, W. Zhang, J. Sandberg, E. Cook, and E. Hartouni, "Design considerations of fast kicker systems for high intensity proton accelerators," Pulsed Power and Plasma Sciences (PPPS-2001), Las Vegas, Nevada, USA, June 17–22, 2001, Los Alamos National Laboratory report LA-UR-01-3252 (June 2001).

R.A. Pelak, L.M. Hull, H.H. Watanabe, D.M. Oro, M.D. Ulibarri, W.F. Hemsing, M.A. Shinas, J. Binstock, and P.T. Sheehey, "Recent experiments in case behavior (U)," Nuclear Explosives Design and Physics Conference (NEDPC 2001), Livermore, California, USA, October 15–19, 2001, Los Alamos National Laboratory controlled publication LA-CP-01-0283 (July 2001).

D.L. Peterson, R.E. Chrien, R.G. Watt, G.C. Idzorek, T.W. Sanford, and R.W. Lemki, "Weapons physics Z-pinch sources on Z and ZR (U)," Nuclear Explosives Design and Physics Conference (NEDPC 2001), Livermore, California, USA, October 15–19, 2001, Los Alamos National Laboratory controlled publication LA-CP-01-0265 (July 2001).

E.J. Pitcher, R.T. Klann, G.L. Morgan, J.M. Oostens, M.A. Paciotti, and M.R. James, "Assessment of neutron yield and spectra from a thick Pb-Bi target for irradiation by 800 MeV protons," 11th International Symposium on Reactor Dosimetry, Brussels, Belgium, August 18–23, 2002, Los Alamos National Laboratory report LA-UR-01-6109 (November 2001).

K.P. Prestridge, C.A. Zoldi, C.D. Tomkins, P.M. Rightley, P. Vorobieff, and R.F. Benjamin, "Velocity-field measurements of shock-accelerated fluid instabilities," 23rd International Symposium on Shock Waves, Fort Worth, Texas, USA, July 22–27, 2001, Los Alamos National Laboratory report LA-UR-01-4086 (July 2001).

M. Rawool-Sullivan, J.P. Sullivan, J. E. Koster, and B. Rooney, "Validity and limitations of the three plane Compton imaging technique via simulations," IEEE Nuclear Science Symposium and Medical Imaging Conference, San Diego, California, USA, November 4–10, 2001, Los Alamos National Laboratory report LA-UR-01-2021 (April 2001).

D.M. Rector, K.M. Carter, A.T. Martinez, F.M. Guerra, and J.S. George, "Spatial and temporal dynamics of optical changes in crustacean nerve," Society for Neuroscience 31st Annual Meeting, San Diego, California, USA, November 10–15, 2001, Los Alamos National Laboratory report LA-UR-01-4642 (August 2001).

R.E. Reinovsky, W.E. Anderson, W.L. Atchison, C.A. Ekdahl, JR., R.J. Faehl, I.R. Lindemuth, G.D. Morgan, M.S. Murillo, J.L. Stokes, and J.S. Shlachter, "Instability growth in magnetically imploded high conductivity cylindrical liners with material strength," Pulsed Power and Plasma Sciences (PPPS-2001), Las Vegas, Nevada, USA, June 17–22, 2001, Los Alamos National Laboratory report LA-UR-01-5490 (September 2001).

P.M. Rightley, C.D. Tomkins, K.P. Prestridge, C.A. Zoldi, R.F. Benjamin, and P. Vorobieff, "Comparison between experiment, calculation and a simple model for interacting shock-accelerated cylinders," 54th Meeting of the Division of Fluid Dynamics of the American Physical Society, San Diego California, November 18–20, 2001, Los Alamos National Laboratory report LA-UR-01-4345 (August 2001).

P.M. Rightley, K.P. Prestridge, C.D. Tomkins, P. Vorobieff, C.A. Zoldi, and R.F. Benjamin, "Studies of shock-wave/cylinder interactions and vorticity transport, using velocity-field data,"

Nuclear Explosives Design and Physics Conference (NEDPC 2001), Livermore, California, USA, October 15–19, 2001, Los Alamos National Laboratory report LA-UR-01-3936 (July 2001).

M.A. Salazar, W.E. Anderson, E.V. Armijo, J.J. Bartos, F. Garcia, B. Randolph, W.L. Atchison, M.G. Sheppard, and J.L. Stokes, "Liquid butane filled load for liner driven Pegasus experiment," Pulsed Power and Plasma Sciences (PPPS-2001), Las Vegas, Nevada, USA, June 17–22, 2001, Los Alamos National Laboratory report LA-UR-01-3226 (June 2001).

J.S. Sandoval, G.C. Idzorek, and D. Ortega, "Fiber optic diagnostics for Z-experiments," Pulsed Power and Plasma Sciences (PPPS-2001), Las Vegas, Nevada, USA, June 17–22, 2001, Los Alamos National Laboratory report LA-UR-01-3251 (June 2001).

A. Saunders, T.J. Bowles, R.E. Hill, G.E. Hogan, K.S. Kirch, S.K. Lamoreaux, C.L. Morris, A. Pichlmaier, S.J. Seestrom, C.Y. Liu, S. Hoedl, D.A. Smith, A.N. Young, B. Filippone, T.M. Ito, J.W. Martin, B. Tipton, J. Yuan, P. Geltenbort, and A.P. Serebrov, "Dedicated UCN source at LANSCE," 3rd UCN Workshop, St. Petersburg, Russia, June 18–22, 2001, Los Alamos National Laboratory report LA-UR-01-2497 (May 2001).

M.M. Schauer, D.C. Barnes, and K.R. Umstadter, "Ion trapping in the virtual cathode of the Penning fusion experiment ions," 2001 Workshop on Non-Neutral Plasmas at the University of California-San Diego, San Diego, California, USA, July 30–August 2, 2001, Los Alamos National Laboratory report LA-UR-01-2042 (April 2001).

J.M. Scott, C.W. Barnes, S.H. Batha, G.R. Magelssen, and N.E. Lanier, "RAGE simulations of mix in a compressible plasma in a convergent geometry," 8th International Workshop on the Physics of Compressible Turbulent Mixing, Pasadena, California, USA, December 9–14, 2001, Los Alamos National Laboratory report LA-UR-01-6575 (November 2001).

J.M. Scott, G.R. Magelssen, C.W. Barnes, and S.H. Batha, "RAGE direct numerical simulations of mix in a compressible plasma in convergent geometry," 8th International Workshop on the Physics of Compressible Turbulent Mixing, Pasadena, California, USA, December 9–14, 2001, Los Alamos National Laboratory report LA-UR-01-2576 (May 2001).

D.W. Scudder, S. Archuleta, E.O. Ballard, G. Barr, J.C. Cochrane, H.A. Davis, J.R. Griego, E.S. Hadden, W.B. Hinckley, K.W. Hosack, J.E. Martinez, D. Mills, J.N. Padilla, J.V. Parker, W.M. Parsons, R.E. Reinovsky, J.L. Stokes, M.C. Thompson, C.Y. Tom, F.J. Wysocki, B.N. Vigil, J. Elizondo, R.B. Miller, H.D. Anderson, and T.N. Campbell, "Atlas—A new pulsed power tool at Los Alamos National Laboratory," Pulsed Power and Plasma Sciences (PPPS-2001), Las Vegas, Nevada, USA, June 17–22, 2001, Los Alamos National Laboratory report LA-UR-01-3136 (June 2001).

S.J. Seestrom, T.J. Bowles, R.E. Hill, G.E. Hogan, K.S. Kirch, S.K. Lamoreaux, C.L. Morris, A. Pichelmaier, A. Saunders, C.Y. Liu, S. Hoedl, D.A. Smith, A.N. Young, B. Filippone, T.M. Ito, B. Titpton, J. Yuan, P. Geltenbort, and A.P. Serebrov, "Development of an intense spallation UCN source at Los Alamos," 9th International Seminar on Interaction of Neutrons with Nuclei: Neutron Spectroscopy, Nuclear Structure, Related Topics, Dubna, Russia, May 23–26, 2001, Los Alamos National Laboratory report LA-UR-01-1324 (March 2001).

M. Shappirio, R.C. Wiens, J.E. Nordholt, D.A. Cremers, and M.J. Ferris, "Development of an instrument for isotopic and elemental composition analyses at stand-off distances on airless planetary surfaces," 33rd Lunar and Planetary Science Conference, Houston, Texas, USA, March 11–15, 2002, Los Alamos National Laboratory report LA-UR-01-6934 (December 2001).

M. Shappirio, R.C. Wiens, J.E. Nordholt, D.A. Cremers, and M.J. Ferris, "Elemental compositions at stand-off distances from a rover: Development and testing of a laser-induced breakdown spectroscopy (LIBS) field prototype instrument," 32nd Lunar and Planetary Science Conference, Houston, Texas, USA, March 12–16, 2001, Los Alamos National Laboratory report LA-UR-01-0113 (January 2001).

D.P. Smitherman, W.T. Buttler, W.W. Anderson, N.T. Gray, K.R. Alrick, and D.L. Shampine, "Richtmyer-Meshkov instability in liquid tin," Nuclear Explosives Design and Physics Conference (NEDPC 2001), Livermore, California, USA, October 15–19, 2001, Los Alamos National Laboratory report LA-UR-01-3591 (June 2001).

R.L. Smitherman, W.J. Buttler, W.W. Anderson, K.R. Alrick, S.A. Jaramillo, and D.L. Shampine, "Richtmyer-Meshkov instability modeling and experiments (U)," Meeting of the Joint Working Group (USA-UK) (JOWOG 32M), Los Alamos, New Mexico, USA, January 2001, Los Alamos National Laboratory controlled publication LA-CP-01-0040 (January 2001).

W.M. Snow, C.S. Blessinger, G. Hansen, H. Nann, D.R. Rich, E.I. Sharapov, S. Ishimoto, Y. Masuda, K. Morimoto, J.D. Bowman, G.L. Greene, G.E. Hogan, J.K. Knudson, S.K. Lamoreaux, G.L. Morgan, S.I. Penttilä, T.B. Smith, W.S. Wilburn, V.W. Yuan, T.R. Gentile, G.L. Jones, F.E. Wietfeldt, S.J. Freedman, B.K. Fujikawa, S. Page, T.E. Chupp, K.P. Coulter, and M.B. Leuschner, "Measurement of the parity violating asymmetry A_γ in $n + p \rightarrow d + \gamma$," in Fundamental Physics with Pulsed Neutron Beams, C.R. Gould, G.L. Greene, F. Plasil, and W.M. Snow, Eds., (World Scientific, Singapore, 2001), p. 203.

D.S. Sorenson, R. Minich, J.L. Romero, T.W. Tunnell, and R. Malone, "Ejecta particle size distributions for shock loaded Sn and Al metals," 12th American Physical Society Topical Conference on Shock Compression of Condensed Matter (SCCM Shock 01), Atlanta, Georgia, USA, June 24–29, 2001 Los Alamos National Laboratory report LA-UR-01-0332 (January 2001).

Appendix B: Publications—2001 Conference Papers

D.S. Sorenson, R. Minich, J.L. Romero, T.W. Tunnell, and R. Malone, "Measured ejecta particle size distributions for the Thoroughbred and Cimarron subcritical Pu experiments," Nuclear Explosives Design and Physics Conference (NEDPC 2001), Livermore, California, USA, October 15–19, 2001, Los Alamos National Laboratory report LA-UR-01-3895 (July 2001).

D.S. Sorenson, R. Minich, T.W. Tunnell, and R. Malone, "Ejecta particle size distributions from the Cimarron and Thoroughbred subcritical experiments (U)," Nuclear Explosives Design and Physics Conference (NEDPC 2001), Livermore, California, USA, October 15–19, 2001, Los Alamos National Laboratory controlled publication LA-CP-01-0539 (December 2001).

J.L. Stokes, J.V. Parker, L.J. Tabaka, S. Coffey, J. Degnan, D. Anderson, R. Pritchett, and R. Corrow, "Measurement of the current and symmetry of the impact liner on the NTLX," Pulsed Power and Plasma Sciences (PPPS-2001), Las Vegas, Nevada, USA, June 17–22, 2001, Los Alamos National Laboratory report LA-UR-01-3309 (June 2001).

D.C. Swift, D.L. Paisley, A.C. Forsman, G.A. Kyrala, R.A. Kopp, and A.A. Hauer, "Measuring dynamic behavior of shocked materials with the Trident laser," 23rd International Symposium on Shock Waves, Fort Worth, Texas, USA, July 22–27, 2001, Los Alamos National Laboratory report LA-UR-01-0339 (January 2001).

D.C. Swift, D.L. Paisley, G.A. Kyrala, and A. Hauer, "Simultaneous VISAR and TXD measurements on shocks in beryllium crystals," in *Proceedings of the American Physical Society Topical Conference on Shock Compression of Condensed Matter*, Atlanta, Georgia, USA, June 25–29, 2001, (Springer-Verlag, Heidelberg, 2002), Vol. 620, pp. 1192–1195.

J.M. Taccetti, T.P. Intrator, G.A. Wurden, W.J. Waaganar, P. Sanchez, D. Begay, E. Mignardot, R.J. Maqueda, Z. Wang, K. Barela, M. Tuszewski, R.E. Siemon, C. Grabowski, E. Ruden, J.H. Degnan, W. Sommars, D. Gale, and T. Cavazos, "FRXL: A high-density field reversed configuration suitable for magnetized target fusion," 42nd Annual Meeting of the American Physical Society Division of Plasma Physics, Long Beach, California, USA, October 29–November 2, 2001, Los Alamos National Laboratory report LA-UR-01-5901 (October 2001).

J.M. Taccetti, T.P. Intrator, G.A. Wurden, H.R. Snyder, M. Tuszewski, R.E. Siemon, D. Begay, E. Mignardot, and R.R. Newton, "Pre-ionization experiments on a high-density field reversed configuration suitable for magnetized target fusion," Pulsed Power and Plasma Sciences (PPPS-2001), Las Vegas, Nevada, USA, June 17–22, 2001, Los Alamos National Laboratory report LA-UR-01-0340 (January 2001).

J.M. Taccetti, T.P. Intrator, G.A. Wurden, R.J. Maqueda, D. Begay, E. Mignardot, R.R. Newton, P. Sanchez, G. Sandoval, W.J. Waganaar, M. Tuszewski, R.E. Siemon, J.H. Degnan, W. Sommars, C. Grabowski, D. Gale, T. Cavazos, and B. Pearson, "FRX-L: A high-density field reversed configuration suitable for magnetized target fusion," 2nd International Magnetized Target Fusion Workshop, Reno, Nevada, USA, August 7–9, 2001, Los Alamos National Laboratory report LA-UR-01-3888 (July 2001).

T.C. Terwilliger, G.S. Waldo, J.-D. Pedelacq, J.R. Berendzen, M.S. Park, E.C. Liong, and C.Y. Kim, "Make structural genomics practical: Engineering proteins and automating structure determination," American Crystallographic Association, Los Angeles, California, USA, July 21–26, 2001, Los Alamos National Laboratory report LA-UR-01-1433 (March 2001).

T. Tierney, J.F. Benage, Jr., S.C. Evans, A. Glocer, G.A. Kyrala, R.R. Montoya, C.P. Munson, J.P. Roberts, B. Skidmore, A.J. Taylor, B.P. Wood, J. Workman, and F.J. Wysocki, "Laser-induced shocks in strongly-coupled aluminum plasmas," 43rd Annual Meeting of the American Physical Society Division of Plasma Physics, Long Beach, California, USA, October 29–30, 2001, Los Alamos National Laboratory report LA-UR-01-4129 (July 2001).

T. Tierney, J.F. Benage, Jr., S.C. Evans, A. Glocer, G.A. Kyrala, R.R. Montoya, C.P. Munson, J.P. Roberts, B. Skidmore, A.J. Taylor, and J. Workman, "Novel strongly-coupled plasma target for shock physics experiments," Student Symposium, Santa Fe, New Mexico, USA, August 5–6, 2001, Los Alamos National Laboratory report LA-UR-01-4011 (July 2001).

T. Tierney, J.F., Benage, Jr., S.C. Evans, G.A. Kyrala, R. R. Montoya, C.P. Munson, J.P. Roberts, A.J. Taylor, and J. Workman, "Using tamped exploding wires to generate strongly coupled plasmas," Pulsed Power/Plasma Sciences (PPPS-2001), Las Vegas, Nevada, USA, June 17–22, 2001, Los Alamos National Laboratory report LA-UR-01-0292 (January 2001).

C.D. Tomkins, K.P. Prestridge, C.A. Zoldi, P.M. Rightley, P. Vorobieff, and R.F. Benjamin, "Investigation of shock-accelerated, unstable gas cylinders using simultaneous desity-field visualization and PIV," 4th International Symposium on Particle Image Velocimetry (PIV01), Gottingen, Germany, September 17–19, 2001, Los Alamos National Laboratory report LA-UR-01-3802 (July 2001).

C.D. Tomkins, K.P. Prestridge, C.A. Zoldi, P. Vorobieff, P.M. Rightley, and R.F. Benjamin, "Validation of computed instabilities in a shock-accelerated gas cylinder using PIV," 4th International Symposium on Particle Image Velocimetry (PIV01), Gottingen, Germany, September 17–19, 2001, Los Alamos National Laboratory report LA-UR-01-1076 (February 2001).

C.D. Tomkins, K.P. Prestridge, P.M. Rightley, C.A. Zoldi, and R.F. Benjamin, "Evolution and interaction of two unstable gas cylinders," 8th International Workshop on the Physics of Compressible Turbulent Mixing, Pasadena, California, USA, December 9–14, 2001, Los Alamos National Laboratory report LA-UR-01-2479 (May 2001).

J.R. Torgerson, W.T. Buttler, M.H. Holzscheiter, and S.K. Lamoreaux, "Precision test for variation of fine structure constant," 43rd Annual Meeting of the American Physical Society Division of Plasma Physics, Long Beach, California, USA, October 29–November 2, 2001 Los Alamos National Laboratory report LA-UR-01-5746 (October 2001).

D.S. Tuch, V.J. Wedeen, A.M. Dale, J.S. George, and J.W. Belliveau, "Conductivity tensor mapping of the human brain using diffusion-tensor MRI," *Proceedings of the National Academy of Sciences of the United States of America* **98**, 11697–11701 (2001).

P.J. Turchi, B. Anderson, D. Anderson, W.E. Anderson, W.L. Atchison, J.J. Bartos, R.L. Bowers, J.A. Guzik, R. Kanzleiter, C.F. Lebeda, R.T. Olson, D.M. Oro, R.B. Randolph, R.E. Reinovsky, J.P. Roberts, G. Rodriguez, G.M. Sandoval, M.A. Salazar, J.L. Stokes, J.K. Studebaker, A.J. Taylor, T. Cavazos, S. Coffey, J.H. Degnan, and D. Gale, "Design and operation of high energy liner implosions at 16 MA for studies of converging shocks," Pulsed Power and Plasma Sciences (PPPS-2001), Las Vegas, Nevada, USA, June 17–22, 2001, Los Alamos National Laboratory report LA-UR-01-0200 (January 2001).

G.L. ver Steeg and J. Raufeisen, "Coherence effects in deep inelastic scattering from nuclei," Student Symposium, Santa Fe, New Mexico, USA, August 5–6, 2001, Los Alamos National Laboratory report LA-UR-01-4398 (July 2001).

C. Vermare, H.A. Davis, T.P. Hughes, D.C. Moir, R.T. Olson, and W.M. Wood, "Electron beam distruption due to ion realse from targets: Experimental observations," 43rd Annual Meeting of the American Physical Society Division of Plasma Physics (APS-DPP), Long Beach, California, USA, October 29–November 2, 2001, Los Alamos National Laboratory report LA-UR-01-3863 (July 2001).

C. Vermare, H.A. Davis, T.P. Hughes, D.C. Moir, R.T. Olson, and W.M. Wood, "Intense electron beam distruption due to ion release from surface," Pulsed Power/Plasma Sciences (PPPS-2001), Las Vegas, Nevada, USA, June 17–22, 2001, Los Alamos National Laboratory report LA-UR-01-3220 (June 2001).

L. Vermare, T.P. Intrator, K. Barela, M. Fisher, and K.A. Werley, "Theoretical and experimental investigations of kink stability of a plasma current channel," Student Symposium, Santa Fe, New Mexico, USA, August 5–6, 2001, Los Alamos National Laboratory report LA-UR-01-4132 (July 2001).

W.T. Vestrand, K.L. Albright, D.E. Casperson, E.E. Fenimore, C. Ho, W.C. Priedhorsky, and J. Wren, "Detector for photon-counting spectrophotometry of prompt optical emissions from gamma ray bursts," Gamma Ray Burst and Afterglow Astronomy 2001, Wood's Hole, Massachusetts, USA, November 2001, Los Alamos National Laboratory report LA-UR-01-5295 (September 2001).

D.J. Vieira, E. Burt, S.G. Crane, M. DiRosa, A.S. Hamer, A. Hime, J.J. Kitten, W.A. Taylor, and X.-X. Zhao, "Trapping radioactive atoms for basic and applied research," Los Alamos Science Day, Los Alamos, New Mexico, February 13, 2001, USA, Los Alamos National Laboratory report LA-UR-01-0719 (February 2001).

P. Vorobieff, C.D. Tomkins, K.P. Prestridge, P.M. Rightley, J. Doyle, M.D. Schneider, and R.F. Benjamin, "Dynamics of shock-accelerated vortex columns," 54th Meeting of the Division of Fluid Dynamics of the American Physical Society, San Diego California, November 18–20, 2001, Los Alamos National Laboratory report LA-UR-01-4346 (August 2001).

Z. Wang, G.A. Wurden, C.W. Barnes, D.N. Hill, E.B. Hooper, H. McLean, B.W. Stallard, R.D. Wood, and S. Woodruff, "Optimization of coaxial plasma source for spheromak magnetic helicity," 43rd Annual Meeting of the American Physical Society Division of Plasma Physics (DPP01), Long Beach, California, USA, October 29–November 2, 2001, Los Alamos National Laboratory report LA-UR-01-3980 (July 2001).

R.G. Watt, N.D. Delamater, W.S. Varnum, D.C. Wilson, G. Pollak, A. Nobile, P.J. Walsh, S.C. Evans, P. Amendt, J. Colvin, R.E. Turner, V. Glebov, J. Soures, and C. Stoeckl, "Experimental studies of inertial confinement fusion (ICF) double shell implosions with nearly 1D behavior in cylindrical and tetrahedral hohlraums," 31st Anomalous Absorption Conference, Sedona, Arizona, USA, June 3–8, 2001, Los Alamos National Laboratory report LA-UR-01-2091 (April 2001).

R.C. Wiens, D.A. Cremers, J.E. Nordholt, and J.D. Blacic, "Elemental composition measurements using laser-induced breakdown spectroscopy (LIBS)," 23rd Forum on Innovative Approaches to Outer Planetary Exploration, Houston, Texas, USA, February 21–23, 2001, Los Alamos National Laboratory report LA-UR-01-0489 (January 2001).

W.S. Wilburn, J.D. Bowman, G.L. Greene, J. Kapustinsky, S.I. Penttilä, and T.B. Smith, "A new approach to measure the neutron decay correlations with cold neutrons at LANSCE," in *Fundamental Physics with Pulsed Neutron Beams*, C.R. Gould, G.L. Greene, F. Plasil, and W.M. Snow, Eds., (World Scientific, Singapore, 2001), p. 214.

B.H. Wilde, J.A. Cobble, M.L. Gittings, P.A. Rosen, J.M. Foster, M.J. Edwards, B. Remington, and T.S. Perry, "Simulations of 2D and 3D jet experiments at Omega," 43rd Annual Meeting of the American Physical Society Division of Plasma Physics (APS-DPP), Long Beach, California, USA, October 29–November 2, 2001, Los Alamos National Laboratory report LA-UR-01-5902 (October 2001).

M.D. Wilke, F.H. Cverna, W.W. Anderson, and R.S. Hixson, "Single-stage gas gun ejecta experiments on tin," American Physical Society Shock Compression of Condensed Matter Meeting 2001, Atlanta, Georgia, USA, June 24–29, 2001, Los Alamos National Laboratory report LA-UR-01-0399 (January 2001).

W.M. Wood, G.R. Magelssen, J. Abdallah, Jr., S.E. Caldwell, D.J. Hoarty, C. Smith, and A.M. Dunne, "Time-resolved temperature measurements of driven hohlraums using spectroscopic techniques developed at AWE," Meeting of the Joint Working Group (USA-UK) (JOWOG 37), Livermore, California, USA, January 2002, Los Alamos National Laboratory report LA-UR-01-5966 (October 2001).

W.M. Wood, G.R. Magelssen, J. Abdallah, Jr., S.E. Caldwell, D.J. Hoarty, C. Smith, and A.M. Dunne, "Point backlighter radiography of driven hohlraums on the Omega laser: Data and methods," Meeting of the Joint Working Group (USA-UK) (JOWOG 37), Livermore, California, USA, January 2002, Los Alamos National Laboratory report LA-UR-01-5967 (October 2001).

G.A. Wurden, P.N. Assmus, W.J. Feinup, T.P. Intrator, M.C. Langner, R.J. Maqueda, K.J. Scott, R.E. Siemon, E.M. Tejero, J.M. Taccetti, M.G. Tuszewski, Z. Wang, C. Grabowski, S.K. Coffey, J.H. Degnan, D. Gale, E. Ruden, and W. Sommars, "Progress on the FRX-L KRC plasma injector at LANL for magnetized target fusion," USA-Japan Workshop on the Physics of Compact Toroids Plasmas, Friday Harbor, Washington, USA, September 2001, Los Alamos National Laboratory report LA-UR-01-5301 (September 2001).

F.J. Wysocki, J.F. Benage, Jr., R.R. Newton, and B.P. Wood, "Analysis of experimental production of dense titanium plasma," 43rd Annual Meeting of the American Physical Society Division of Plasma Physics (APS-DPP), Long Beach, California, USA, October 29–November 2, 2001, Los Alamos National Laboratory report LA-UR-01-4040 (July 2001).

G.J. Yates, T.E. McDonald, Jr., D.E. Bliss, S.M. Cameron, K. Greives, and F.J. Zutavern, "Near infrared (NIR) imaging techniques using lasers and nonlinear crystal optical parametric oscillator/amplifier (OPO/OPA) imaging and transferred electron (TE) photocathode image intensifiers," IS&T/SPIE, Photonics West 2001 Electronic Imaging Symposium: High Speed Imaging and Sequence Analysis III Conference, January 21–26, 2001, San Jose, California, USA, Los Alamos National Laboratory report LA-UR-00-5957 (December 2000).

G.J. Yates and T.E. McDonald, "Advanced technology imaging sensor development," TCG XIII/DoD/DOE Munitions Technology Development, Albuquerque, New Mexico, USA, July 2001, Los Alamos National Laboratory report LA-UR-01-3548 (June 2001).

2002 Journal Articles

J.N. Abdurashitov, E.P. Veretenkin, V.M. Vermul, V.N. Gavrin, S.V. Girin, V.V. Gorbachev, P.P. Gurkina, G.T. Zatsepin, T.V. Ibragimova, A.V. Kalikhov, T.V. Knodel, I.N. Mirmov, N.G. Khairnasov, A.A. Shikhin, V.E. Yants, T.J. Bowles, W.A. Teasdale, J.S. Nico, J.F. Wilkerson, B.T. Cleveland, and S.R. Elliott, "Solar neutrino flux measurements by the Soviet-American Gallium Experiment (SAGE) for half the 22-year Solar cycle," *Journal of Experimental and Theoretical Physics* **95**, 181–193 (2002).

J.N. Abdurashitov, V.N. Gavrin, I.N. Mirmov, E.P. Veretenkin, V.E. Yants, N.N. Oshkanov, A.I. Karpenko, V.V. Maltsev, V.I. Barsanov, K.S. Trubin, S.B. Zlokazov, Y.S. Khomyakov, V.M. Poplavsky, T.O. Saraeva, B.A. Vasiliev, O.V. Mishin, T.J. Bowles, W.A. Teasdale, K. Lande, P. Wildenhain, B.T. Cleveland, S.R. Elliott, W. Haxton, J.F. Wilkerson, A. Suzuki, Y. Suzuki, and M. Nakahata, "The new status of ^{37}Ar artificial neutrino source project," *Nuclear Physics B-Proceedings Supplements* **110**, 326–328 (2002).

P.D. Adams, R.W. Grosse-Kunstleve, L.W. Hung, T.R. Ioerger, A.J. McCoy, N.W. Moriarty, R.J. Read, J.C. Sacchettini, N.K. Sauter, and T.C. Terwilliger, "PHENIX: Building new software for automated crystallographic structure determination," *Acta Crystallographica Section D-Biological Crystallography* **58**, 1948–1954 (2002).

K. Adcox, S.S. Adler, N.N. Ajitanand *et al.* (including Los Alamos scientists: P.D. Barnes, M.J. Bennett, M.L. Brooks, T.A. Carey, M.S. Chung, A.G. Hansen, W.W. Kinnison, D.M. Lee, M.J. Leitch, M.X. Liu, P.L. McGaughey, R.E. Mischke, J.M. Moss, A.P.T. Palounek, B.R. Schlei, T. Shiina, J. Simon-Gillo, J.P. Sullivan, R.S. Towell, and H.W. van Hecke), "Transverse-mass dependence of two-pion correlations in Au + Au collisions at $\sqrt{S_{NN}}$ = 130 GeV," *Physical Review Letters* **88**, 192302 (2002).

K. Adcox, S.S. Adler, N.N. Ajitanand *et al.* (including Los Alamos scientists: P.D. Barnes, M.J. Bennett, M.L. Brooks, T.A. Carey, M.S. Chung, A.G. Hansen, W.W. Kinnison, D.M. Lee, M.J. Leitch, M.X. Liu, P.L. McGaughey, R.E. Mischke, J.M. Moss, A.P.T. Palounek, B.R. Schlei, T. Shiina, J. Simon-Gillo, J.P. Sullivan, R.S. Towell, and H.W. van Hecke), "Suppression of hadrons with large transverse momentum in central Au + Au collisions at $\sqrt{S_{NN}}$ = 130 GeV," *Physical Review Letters* **88**, 022301 (2002).

K. Adcox, S.S. Adler, N.N. Ajitanand *et al.* (including Los Alamos scientists: P.D. Barnes, M.J. Bennett, M.L. Brooks, T.A. Carey, M.S. Chung, A.G. Hansen, W.W. Kinnison, D.M. Lee, M.J. Leitch, M.X. Liu, P.L. McGaughey, R.E. Mischke, J.M. Moss, A.P.T. Palounek, B.R. Schlei, T. Shiina, J. Simon-Gillo, J.P. Sullivan, R.S. Towell, and H.W. van Hecke), "Centrality dependence of $\pi^{+/-}$, $K^{+/-}$, p, and $\bar{p}$ production from $\sqrt{S_{NN}}$ = 130 GeV Au + Au collisions at RHIC," *Physical Review Letters* **88**, 242301 (2002).

K. Adcox, S.S. Adler, N.N. Ajitanand *et al.* (including Los Alamos scientists: P.D. Barnes, M.J. Bennett, M.L. Brooks, T.A. Carey, M.S. Chung, A.G. Hansen, W.W. Kinnison, D.M. Lee, M.J. Leitch, M.X. Liu, P.L. McGaughey, R.E. Mischke, J.M. Moss, A.P.T. Palounek, B.R. Schlei, T. Shiina, J. Simon-Gillo, J.P. Sullivan, R.S. Towell, and H.W. van Hecke), "Flow measurements via two-particle azimuthal correlations in Au + Au collisions at $\sqrt{S_{NN}}$ = 130 GeV," *Physical Review Letters* **89**, 212301 (2002).

K. Adcox, S.S. Adler, N.N. Ajitanand *et al.* (including Los Alamos scientists: P.D. Barnes, M.J. Bennett, M.L. Brooks, T.A. Carey, M.S. Chung, A.G. Hansen, W.W. Kinnison, D.M. Lee, M.J. Leitch, M.X. Liu, P.L. McGaughey, R.E. Mischke, J.M. Moss, A.P.T. Palounek, B.R. Schlei, T. Shiina, J. Simon-Gillo, J.P. Sullivan, R.S. Towell, and H.W. van Hecke), "Net charge fluctuations in Au + Au interactions at $\sqrt{S_{NN}}$ = 130 GeV," *Physical Review Letters* **89**, 082301 (2002).

K. Adcox, S.S. Adler, N.N. Ajitanand *et al.* (including Los Alamos scientists: P.D. Barnes, M.J. Bennett, M.L. Brooks, T.A. Carey, M.S. Chung, A.G. Hansen, W.W. Kinnison, D.M. Lee, M.J. Leitch, M.X. Liu, P.L. McGaughey, R.E. Mischke, J.M. Moss, A.P.T. Palounek, B.R. Schlei, T. Shiina, J. Simon-Gillo, J.P. Sullivan, R.S. Towell, and H.W. van Hecke), "Event-by-event fluctuations in mean p_T and mean e_T in $\sqrt{S_{NN}}$ = 130 GeV Au + Au collisions," *Physical Review C* **66**, 024901 (2002).

K. Adcox *et al.*, "Measurement of Single Electrons and Implications for Charm Production in Au + Au Collisions at $\sqrt{S_{NN}}$ = 130 GeV," *Physical Review Letters* **88**, 192303 (2002).

K. Adcox *et al.*, "Measurement of the Λ and $\bar{\Lambda}$ particles in Au + Au Collisions at $\sqrt{S_{NN}}$ = 130 GeV," *Physical Review Letters* **89**, 092302 (2002).

Q.R. Ahmad, R.C. Allen, T.C. Andersen *et al.* (including Los Alamos scientists: M.G. Boulay, T.J. Bowles, S.J. Brice, M.C. Browne, P.J. Doe, M.R. Dragowsky, S.R. Elliott, M.M. Fowler, N. Gagnon, A.S. Hamer, J. Heise, A. Hime, G.G. Miller, A.W.P. Poon, R.G.H. Robertson, H. Seifert, R.G. Van de Water, D.L. Wark, J.B. Wilhelmy, J.F. Wilkerson, and J.M. Wouters), "Direct evidence for neutrino flavor transformation from neutral-current interactions in the Sudbury Neutrino Observatory," *Physical Review Letters* **89**, 011301 (2002).

Q.R. Ahmad, R.C. Allen, T.C. Andersen *et al.* (including Los Alamos scientists: M.G. Boulay, T.J. Bowles, S.J. Brice, M.C. Browne, P.J. Doe, M.R. Dragowsky, S.R. Elliott, M.M. Fowler, N. Gagnon, A.S. Hamer, J. Heise, A. Hime, G.G. Miller, A.W.P. Poon, R.G.H. Robertson, H. Seifert, R.G. Van de Water, D.L. Wark, J.B. Wilhelmy, J.F. Wilkerson, and J.M. Wouters), "Measurement of day and night neutrino energy spectra at SNO and constraints on neutrino mixing parameters," *Physical Review Letters* **89**, 011302 (2002).

Appendix B: Publications—2002 Journal Articles

M. Ahmed, J.F. Amann, D. Barlow, K. Black, R.D. Bolton, M.L. Brooks, S. Carius, Y.K. Chen, A. Chernyshev, H.M. Concannon, M.D. Cooper, P.S. Cooper, J. Crocker, J.R. Dittmann, M. Dzemidzic, A. Empl, R.J. Fisk, E. Fleet, W. Foreman, C.A. Gagliardi, D. Haim, A. Hallin, C.M. Hoffman, G.E. Hogan, E.B. Hughes, E.V. Hungerford, C.C.H. Jui, G.J. Kim, J.E. Knott, D.D. Koetke, T. Kozlowski, M.A. Kroupa, A.R. Kunselman, K.A. Lan, V. Laptev, D. Lee, F. Liu, R.W. Manweiler, R. Marshall, B.W. Mayes, R.E. Mischke, B.M.K. Nefkens, L.M. Nickerson, P.M. Nord, M.A. Oothoudt, J.N. Otis, R. Phelps, L.E. Piilonen, C. Pillai, L. Pinsky, M.W. Ritter, C. Smith, T.D.S. Stanislaus, K.M. Stantz, J.J. Szymanski, L. Tang, W.B. Tippens, R.E. Tribble, X.L. Tu, L.A. Van Ausdeln, W.H. von Witch, D. Whitehouse, C. Wilkinson, B. Wright, S.C. Wright, Y. Zhang, and K.O.H. Ziock, "Search for the lepton-family-number nonconserving decay $\mu^+ \rightarrow e^+\gamma$," *Physical Review D* **65**, 112002 (2002).

L.B. Auerbach, R.L. Burman, D.O. Caldwell, E.D. Church, J.B. Donahue, A. Fazely, G.T. Garvey, R.M. Gunasingha, R. Imlay, W.C. Louis, R. Majkic, A. Malik, W. Metcalf, G.B. Mills, V. Sandberg, D. Smith, I. Stancu, M. Sung, R. Tayloe, G.J. VanDalen, W. Vernon, N. Wadia, D.H. White, and S. Yellin, "Measurements of charged current reactions of ν_μ on ^{12}C," *Physical Review C* **66**, 015501 (2002).

R. Barber, M.W. Ahmed, M. Dzemidzic, A. Empl, E.V. Hungerford, K.J. Lan, J. Wilson, M.D. Cooper, C.A. Gagliardi, D. Haim, G.J. Kim, D.D. Koetke, R.E. Tribble, and L.A. Van Ausdeln, "Characteristics of a delay-line readout in a cylindrical drift chamber system," *Nuclear Instruments and Methods in Physics Research Section A-Accelerators Spectrometers Detectors and Associated Equipment* **479**, 591–598 (2002).

C.W. Barnes, R.D. Day, N.E. Elliott, S.H. Batha, N.E. Lanier, G.R. Magelssen, J.M. Scott, S. Rothman, C. Horsfield, A.M. Dunne, and K.W. Parker, "Characterization of surface roughness and initial conditions for cylindrical hydrodynamic and mix experiments," *Fusion Science and Technology* **41**, 203–208 (2002).

C.W. Barnes, S.H. Batha, A.M. Dunne, G.R. Magelssen, S. Rothman, R.D. Day, N.E. Elliott, D.A. Haynes, R.L. Holmes, J.M. Scott, D.L. Tubbs, D.L. Youngs, T.R. Boehly, and P. Jaanimagi, "Observation of mix in a compressible plasma in a convergent cylindrical geometry," *Physics of Plasmas* **9**, 4431–4434 (2002).

I.G. Bearden, H. Boggild, J.G. Boissevain, P.H.L. Christiansen, L. Conin, J. Dodd, B. Erazmus, S. Esumi, C.W. Fabjan, D. Ferenc, D.E. Fields, A. Franz, J.J. Gaardhoje, M. Hamelin, A.G. Hansen, O. Hansen, D. Hardtke, H.W. van Hecke, E.B. Holzer, T.J. Humanic, P. Hummel, B.V. Jacak, K. Kaimi, M. Kaneta, T. Kohama, M. Kopytine, M. Leltchouk, A. Ljubicic, B. Lorstad, N. Maeda, R. Malina, L. Martin, A. Medvedev, M. Murray, H. Ohnishi, G. Paic, S.U. Pandey, F. Piuz, J. Pluta, V. Polychronakos, M. Potekhin, G. Poulard, D. Reichhold, A. Sakaguchi, J. Schmidt-Sorensen, J. Simon-Gillo, W. Sondheim, M. Spegel, T. Sugitate, J.P. Sullivan, Y. Sumi, W.J. Willis, K.L. Wolf, N. Xu, and D.S. Zachary, "Particle production in central Pb + Pb collisions at 158*A* GeV/*c*," *Physical Review C* **66**, 044907 (2002).

I.G. Bearden, H. Boggild, J.G. Boissevain, P.H.L. Christiansen, L. Conin, J. Dodd, B. Erazmus, S. Esumi, C.W. Fabjan, D. Ferenc, A. Franz, J.J. Gaardhoje, A.G. Hansen, O. Hansen, D. Hardtke, H.W. van Hecke, E.B. Holzer, T.J. Humanic, P. Hummel, B.V. Jacak, K. Kaimi, M. Kaneta, T. Kohama, M. Kopytine, M. Leltchouk, A. Ljubicic, B. Lorstad, L. Martin, A. Medvedev, M. Murray, H. Ohnishi, G. Paic, S.U. Pandey, F. Piuz, J. Pluta, V. Polychronakos, M. Potekhin, G. Poulard, D. Reichhold, A. Sakaguchi, J. Schmidt-Sorensen, J. Simon-Gillo, W. Sondheim, T. Sugitate, J.P. Sullivan, Y. Sumi, W.J. Willis, K. Wolf, N. Xu, and D.S. Zachary, "Deuteron and triton production with high energy sulphur and lead beams," *European Physical Journal C* **23**, 237–247 (2002).

I.G. Bearden, H. Boggild, J.G. Boissevain, L. Conin, J. Dodd, B. Erazmus, S. Esumi, C.W. Fabjan, D. Ferenc, D.E. Fields, A. Franz, J.J. Gaardhoje, A.G. Hansen, O. Hansen, D. Hardtke, H.W. van Hecke, E.B. Holzer, T.J. Humanic, P. Hummel, B.V. Jacak, R. Jayanti, K. Kaimi, M. Kaneta, T. Kohama, M.L. Kopytine, M. Leltchouk, A. Ljubicic, B. Lorstad, N. Maeda, L. Martin, A. Medvedev, M. Murray, H. Ohnishi, G. Paic, S.U. Pandey, F. Piuz, J. Pluta, V. Polychronakos, M. Potekhin, G. Poulard, D. Reichhold, A. Sakaguchi, J. Schmidt-Sorensen, J. Simon-Gillo, W. Sondheim, T. Sugitate, J.P. Sullivan, Y. Sumi, W.J. Willis, K.L. Wolf, N. Xu, and D.S. Zachary, "Event texture search for phase transitions in Pb + Pb collisions," *Physical Review C* **65**, 044903 (2002).

D. Berkeland, "Linear Paul trap for strontium ions," *Review of Scientific Instruments* **73**, 2856–2860 (2002).

D. Berkeland and M.G. Boshier, "Destabilization of dark states and optical spectroscopy in Zeeman-degenerate atomic systems," *Physical Review A* **65**, 033413 (2002).

L.A. Bernstein, J.A. Becker, P.E. Garrett, W. Younes, D.P. McNabb, D.E. Archer, C.A. McGrath, H. Chen, W.E. Ormand, M.A. Stoyer, R.O. Nelson, M.B. Chadwick, G.D. Johns, W.S. Wilburn, M. Devlin, D.M. Drake, and P.G. Young, "^{239}Pu(n, 2n) ^{238}Pu cross section deduced using a combination of experiment and theory," *Physical Review C* **65**, 021601 (2002).

T.J. Bowles, "Quantum physics: Quantum effects of gravity," *Nature* **415**, 267–268 (2002).

W.J. Briscoe, B.L. Berman, R.W.C. Carter, K.S. Dhuga, S.K. Matthews, N.J. Nicholas, S.J. Greene, B.M.K. Nefkens, J.W. Price, L.D. Isenhower, M.E. Sadler, I. Slaus, and I. Supek, "Elastic scattering of charged pions from ^{3}H and ^{3}He," *Physical Review C* **66**, 054006 (2002).

W.T. Buttler, J.R. Torgerson, and S.K. Lamoreaux, "New, efficient and robust, fiber-based quantum key distribution schemes," *Physics Letters A* **299**, 38–42 (2002).

E.D. Church, K. Eitel, G.B. Mills, and M. Steidl, "Statistical analysis of different $\overline{\nu}_\mu \rightarrow \overline{\nu}_e$ searches," *Physical Review D* **66**, 013001 (2002).

J.A. Cobble, R.P. Johnson, N.A. Kurnit, D.S. Montgomery, and J.C. Fernández, "Cyclic plasma shearing interferometry for temporal characterization of a laser-produced plasma," *Review of Scientific Instruments* **73**, 3813–3817 (2002).

J.A. Cobble, R.P. Johnson, T.E. Cowan, N. Renard-Le Galloudec, and M. Allen, "High resolution laser-driven proton radiography," *Journal of Applied Physics* **92**, 1775–1779 (2002).

M.E. Cuneo, R.A. Vesey, J.L. Porter, Jr., G.R. Bennett, D.L. Hanson, L.E. Ruggles, W.W. Simpson, G.C. Idzorek, W.A. Stygar, J.H. Hammer, J.J. Seamen, J.A. Torres, J.S. McGurn, and R.M. Green, "Double Z-pinch hohlraum drive with excellent temperature balance for symmetric inertial confinement fusion capsule implosions," *Physical Review Letters* **88**, 215004 (2002).

N. Elliott, C.W. Barnes, S.H. Batha, R.D. Day, J. Elliott, P. Gobby, V. Gomez, D. Hatch, N.E. Lanier, G.R. Magelssen, R. Manzanares, R. Perea, T. Pierce, G. Rivera, D. Sandoval, J.M. Scott, W.P. Steckle, D.L. Tubbs, S. Rothman, C. Horsfield, A.M. Dunne, and K.W. Parker, "Best practice procedures for making direct drive cylindrical targets for studies of convergent hydrodynamics," *Fusion Science and Technology* **41**, 196–202 (2002).

D.G. Enzer, P.G. Hadley, R.J. Hughes, C.G. Peterson, and P.G. Kwiat, "Entangled-photon six-state quantum cryptography," *New Journal of Physics* **4**, 45 (2002).

M.A. Espy, A.N. Matlashov, R.H. Kraus, Jr., F. Balakirev, and J. Betts, "The temperature dependence of SQUID noise at temperatures below 4 K," *Physica C* **368**, 185–190 (2002).

M.A. Espy, A.N. Matlashov, R.H. Kraus, Jr., P. Volegov, and K. Maharajh, "Experimental investigation of high temperature superconducting imaging surface magnetometry," *Review of Scientific Instruments* **73**, 2360–2363 (2002).

D.H. Froula, L. Divol, H.A. Baldis, R.L. Berger, D.G. Braun, B.I. Cohen, R.P. Johnson, D.S. Montgomery, E.A. Williams, and S.H. Glenzer, "Observation of ion heating by stimulated-Brillouin-scattering-driven ion-acoustic waves using Thomson scattering," *Physics of Plasmas* **9**, 4709–4718 (2002).

S. Fukuda, Y. Fukuda, M. Ishitsuka *et al.* (including Los Alamos scientist: T.J. Haines), "Search for neutrinos from gamma-ray bursts using Super-Kamiokande," *Astrophysical Journal* **578**, 317–324 (2002).

S. Fukuda, Y. Fukuda, M. Ishitsuka *et al.* (including Los Alamos scientist: T.J. Haines), "Determination of Solar neutrino oscillation parameters using 1496 days of Super-Kamiokande-I data," *Physics Letters B* **539**, 179–187 (2002).

T. Haseyama, K. Asahi, J.D. Bowman, P.P.J. Delheij, H. Funahashi, S. Ishimoto, G. Jones, A. Masaike, Y. Masuda, Y. Matsuda, K. Morimoto, S. Muto, S.I. Penttilä, V.R. Pomeroy, K. Sakai, E.I. Sharapov, D.A. Smith, and V.W. Yuan, "Measurement of parity-nonconserving rotation of neutron spin in the 0.734-eV *p*-wave resonance of ^{139}La," *Physics Letters B* **534**, 39–44 (2002).

J. Haueisen, D.S. Tuch, C. Ramon, P.H. Schimpf, V.J. Wedeen, J.S. George, and J.W. Belliveau, "The influence of brain tissue anisotropy on human EEG and MEG," *Neuroimage* **15**, 159–166 (2002).

H.W. Herrmann, G.S. Selwyn, I. Henins, J. Park, M. Jeffery, and J.M. Williams, "Chemical warfare agent decontamination studies in the plasma decon chamber," *IEEE Transactions on Plasma Science* **30**, 1460–1470 (2002).

A.L. Hoffman, H.Y.Y. Guo, J.T. Slough, S.J. Tobin, L.S. Schrank, W.A. Reass, and G.A. Wurden, "The TCS rotating magnetic field FRC current-drive experiment," *Fusion Science and Technology* **41**, 92–106 (2002).

L. Huang, L.-W. Hung, M. Odell, H. Yokota, R. Kim, and S.H. Kim, "Structure-based experimental confirmation of biochemical function to a methyltransferase, MJ0882, from hyperthermophile Methanococcus jannaschii," *Journal of Structural and Functional Genomics* **2**, 121–127 (2002).

R.J. Hughes, J.E. Nordholt, D. Derkacs, and C.G. Peterson, "Practical free-space quantum key distribution over 10 km in daylight and at night," *New Journal of Physics* **4**, 43 (2002).

T.P. Intrator, J.M. Taccetti, D.A. Clark, J.H. Degnan, D. Gale, S. Coffey, J. Garcia, P. Rodriguez, W. Sommars, B. Marshall, F.J. Wysocki, R. Siemon, R. Faehl, K. Forman, R. Bartlett, T. Cavazos, R.J. Faehl, M.H. Frese, R.D. Fulton, J.C. Gueits, T.W. Hussey, R. Kirkpatrick, G.F. Kiuttu, F.M. Lehr, J.D. Letterio, I. Lindemuth, W. McCullough, R. Moses, R.E. Peterkin, R.E. Reinovsky, N.F. Roderick, E.L. Ruden, K.F. Schoenberg, D.W Scudder, J. Shlachter, and G.A. Wurden, "Experimental measurements of a converging flux conserver suitable for compressing a field reversed configuration for magnetized target fusion," *Nuclear Fusion* **42**, 211–222 (2002).

T.P. Intrator, B. Marshall, D. Clark, T. McCuistan, B. Anderson, B. Broste, K. Forman, and J.M. Taccetti, "High sensitivity Faraday rotation technique for measurements of magnetic fields with immunity to x-ray effects," *Review of Scientific Instruments* **73**, 141–146 (2002).

Appendix B: Publications—2002 Journal Articles

J. Jia, V.V. Lunin, V. Sauve, L.-W. Hung, A. Matte, and M. Cygler, "Crystal structure of the YciO protein from Escherichia coli," *Proteins: Structure, Function, and Genetics* **49**, 139–141 (2002).

M.B. Johnson, B.Z. Kopeliovich, I.K. Potashnikova, P.L. McGaughey, J.M. Moss, J.-C. Peng, G. Garvey, M.J. Leitch, C.N. Brown, and D.M. Kaplan, "Energy loss versus shadowing in the Drell-Yan reaction on nuclei," *Physical Review C* **65**, 025203 (2002).

R.H. Kraus, Jr., P. Volegov, K. Maharajh, M.A. Espy, A.N. Matlashov, and E.R. Flynn, "Performance of a novel SQUID-based superconducting imaging-surface magnetoencephalography system," *Physica C* **368**, 18–23 (2002).

K.K. Kwiatkowski, J.F. Beche, M.T. Burks, G. Hart, G.E. Hogan, P.F. Manfredi, J.E. Millaud, C.L. Morris, N.S.P. King, P.D. Pazuchanics, and B. Turko, "Development of multiframe detectors for ultrafast radiography with 800 MeV protons," *IEEE Transactions on Nuclear Science* **49**, 293–296 (2002).

S.K. Lamoreaux and R. Golub, "Calculation of the ultracold neutron upscattering loss probability in fluid walled storage bottles using experimental measurements of the liquid thermomechanical properties of fomblin," *Physical Review C* **66**, 044309 (2002).

S.K. Lamoreaux, "Solid-state systems for the electron electric dipole moment and other fundamental measurements," *Physical Review A* **66**, 022109 (2002).

S.K. Lamoreaux, G. Archibald, P.D. Barnes, W.T. Buttler, D.J. Clark, M.D. Cooper, M.A. Espy, G.L. Greene, R. Golub, M.E. Hayden, C. Lei, L.J. Marek, J.-C. Peng, and S.I. Penttilä, "Measurement of the ^{3}He mass diffusion coefficient in superfluid ^{4}He over the 0.45–0.95 K temperature range," *Europhysics Letters* **58**, 718–724 (2002).

T. Li, J.W. Balk, P.P. Ruden, I.H. Campbell, and D.L. Smith, "Channel formation in organic field-effect transistors," *Journal of Applied Physics* **91**, 4312–4318 (2002).

R. Maingi, M.G. Bell, R.E. Bell, C.E. Bush, E.D. Fredrickson, D.A. Gates, S.M. Kaye, H.W. Kugel, B.P. LeBlanc, J.E. Menard, D. Mueller, S.A. Sabbagh, D. Stutman, G. Taylor, D.W. Johnson, R. Kaita, R.J. Maqueda, M. Ono, F. Paoletti, S.F. Paul, Y.K.M. Peng, A.L. Roquemore, C.H. Skinner, V.A. Soukhanovskii, and E.J. Synakowski, "Characteristics of the first *H*-mode discharges in the national spherical torus experiment," *Physical Review Letters* **88**, 035003 (2002).

A.V. Markov, A.Y. Polyakov, N.B. Smirnov, A.V. Govorkov, V.I. Biberin, N.S. Korovin, V.N. Gavrin, G.D. Efimov, A.V. Kalikhov, Y.P. Kozlova, E.P. Veretenkin, V.K. Eremin, E.M. Verbitskaya, and T.J. Bowles, "Electrical properties and deep levels in bulk solution grown GaAs crystal," *Solid State Electronics* **46**, 2161–2168 (2002).

J.J. McDevitt, P.N. Breysse, J.D. Bowman, and D.M. Sassone, "Comparison of extremely low frequency (ELF) magnetic field personal exposure monitors," *Journal of Exposure Analysis and Environmental Epidemiology* **12**, 1–8 (2002).

H.S. McLean, S. Woodruff, E.B. Hooper, R.H. Bulmer, D.N. Hill, C. Holcomb, J. Moller, B.W. Stallard, R.D. Wood, and Z. Wang, "Suppression of MHD fluctuations leading to improved confinement in a gun-driven spheromak," *Physical Review Letters* **88**, 125004 (2002).

P.G. Mikellides, P.J. Turchi, and I.G. Mikellides, "Design of a fusion propulsion system—part 1: Gigawatt-level magnetoplasmadynamic source," *Journal of Propulsion and Power* **18**, 146–151 (2002).

J.T. Mitchell, Y. Akiba, L. Aphecetche, R. Averbeck, T.C. Awes, V. Baublis, A. Bazilevsky, M.J. Bennett, H. Buesching, J. Burward-Hoy, S. Butsyk, M. Chiu, T. Christ, T. Chujo, P. Constantin, G. David, A. Denisov, A. Drees, A.G. Hansen, T.K. Hemmick, J. Jia, S.C. Johnson, E. Kistenev, A. Kiyomichi, T. Kohama, J.G. Lajoie, J. Lauret, A. Lebedev, C.F. Maguire, F. Messer, P. Nilsson, H. Ohnishi, J. Park, M. Rosati, A.A. Rose, S.S. Ryu, A. Sakaguchi, S. Sato, K. Shigaki, D. Silvermyr, T. Sugitate, J.P. Sullivan, M. Suzuki, H. Tydesjo, H.W. Van Hecke, J. Velkovska, M.A. Volkov, S. White, and W. Xie, "Event reconstruction in the PHENIX central arm spectrometers," *Nuclear Instruments and Methods in Physics Research Section A-Accelerators Spectrometers Detectors and Associated Equipment* **482**, 491–512 (2002).

D.S. Montgomery, J.A. Cobble, J.C. Fernández, R.J. Focia, R.P. Johnson, N. Renard-LeGalloudec, H.A. Rose, and D.A. Russell, "Recent Trident single hot spot experiments: Evidence for kinetic effects, and observation of Langmuir decay instability cascade," *Physics of Plasmas* **9**, 2311–2320 (2002).

C.L. Morris, J.M. Anaya, T.J. Bowles, B.W. Filippone, P. Geltenbort, R.E. Hill, M. Hino, S. Hoedl, G.E. Hogan, T.M. Ito, T. Kawai, K. Kirch, S.K. Lamoreaux, C.-Y. Liu, M. Makela, L.J. Marek, J.W. Martin, R.N. Mortensen, A. Pichlmaier, A. Saunders, S.J. Seestrom, D. Smith, W. Teasdale, B. Tipton, M. Utsuro, A.R. Young, and J. Yuan, "Measurements of ultracold-neutron lifetimes in solid deuterium," *Physical Review Letters* **89**, 272501 (2002).

C.E. Moss and C.M. Frankle, "Gamma-ray measurements of a 6-kg neptunium sphere," *Transactions of the American Nuclear Society* **87**, 391 (2002).

M.G. Nickelsen, W.J. Cooper, D.A. Secker, L.A. Rosocha, C.N. Kurucz, and T.D. Waite, "Kinetic modeling and simulation of PCE and TCE removal in aqueous solutions by electron-beam irradiation," *Radiation Physics and Chemistry* **65**, 579–587 (2002).

A.W. Obst, K.R. Alrick, K. Boboridis, W.T. Buttler, B.R. Marshall, J.R. Payton, and M.D. Wilke, "Ellipsometry in the study of dynamic material properties," *International Journal of Thermophysics* **23**, 1259–1266 (2002).

J.L. Raaf, A.O. Bazarko, G.T. Garvey, E.A. Hawker, R.A. Johnson, G.B. Mills, A. Pla-Dalmau, and R. Tayloe, "Mineral oil tests for the MiniBooNE detector," *IEEE Transactions on Nuclear Science* **49**, 957–962 (2002).

J. Raufeisen, J.-C. Peng, and G.C. Nayak, "Parton model versus color dipole formulation of the Drell-Yan process," *Physical Review D* **66**, 034024 (2002).

M.W. Rawool-Sullivan, J.P. Sullivan, J.E. Koster, and B.D. Rooney, "Validity and limitations of the three-plane Compton-imaging technique via simulations," *IEEE Transactions on Nuclear Science* **49**, 3290–3294 (2002).

D.R. Rich, J.D. Bowman, B.E. Crawford, P.P.J. Delheij, M.A. Espy, T. Haseyama, G. Jones, C.D. Keith, J. Knudson, M.B. Leuschner, A. Masaike, Y. Masuda, Y. Matsuda, S.I. Penttilä, V.R. Pomeroy, D.A. Smith, W.M. Snow, J.J. Szymanski, S.L. Stephenson, A.K. Thompson, and V.W. Yuan, "A measurement of the absolute neutron beam polarization produced by an optically pumped ^{3}He neutron spin filter," *Nuclear Instruments and Methods in Physics Research Section A-Accelerators Spectrometers Detectors and Associated Equipment* **481**, 431–453 (2002).

F.B. Rosmej, H.R. Griem, R.C. Elton, V.L. Jacobs, J.A. Cobble, A.Y. Faenov, T.A. Pikuz, M. Geissel, D.H.H. Hoffmann, W. Suss, D.B. Uskov, V.P. Shevelko, and R.C. Mancini, "Charge-exchange-induced two-electron satellite transitions from autoionizing levels in dense plasmas," *Physical Review E* **66**, 056402 (2002).

T.W.L. Sanford, R.W. Lemke, R.C. Mock, G.A. Chandler, R.J. Leeper, C.L. Ruiz, D.L. Peterson, R.E. Chrien, G.C. Idzorek, R.G. Watt, and J.P. Chittenden, "Dynamics and characteristics of a 215-eV dynamic-hohlraum x-ray source on Z," *Physics of Plasmas* **9**, 3573–3594 (2002).

D.A. Smith, J.D. Bowman, B.E. Crawford, C.A. Grossmann, T. Haseyama, A. Masaike, Y. Matsuda, G.E. Mitchell, S.I. Penttilä, N.R. Roberson, S.J. Seestrom, E.I. Sharapov, S.L. Stephenson, A.M. Sukhovoj, and V.W. Yuan, "Neutron resonance spectroscopy of ^{104}Pd, ^{105}Pd, and ^{110}Pd," *Physical Review C* **65**, 024607 (2002).

D.A. Smith, J.D. Bowman, B.E. Crawford, C.A. Grossmann, T. Haseyama, A. Masaike, Y. Matsuda, G.W. Mitchell, S.I. Penttilä, N.R. Roberson, S.J. Seestrom, E.I. Sharapov, S.L. Stephenson, and V.W. Yuan, "Parity violation in neutron resonances of palladium," *Physical Review C* **65**, 035503(9) (2002).

D.S. Sorenson, R.W. Minich, J.L. Romero, T. W. Tunnell, and R.M. Malone, "Ejecta particle size distributions for shock loaded Sn and Al metals," *Journal of Applied Physics* **92**, 5830–5836 (2002).

J.M. Taccetti, T.P. Intrator, F.J. Wysocki, K.C. Forman, D.G. Gale, S.K. Coffey, and J.H. Degnan, "Magnetic field measurements inside a converging flux conserver for magnetized target fusion applications," *Fusion Science and Technology* **41**, 13–23 (2002).

S. Vogel, E. Ustundag, J.C. Hanan, V.W. Yuan, and M.A.M. Bourke, "*In situ* investigation of the reduction of NiO by a neutron transmission method," *Materials Science and Engineering A-Structural Materials Properties: Microstructure and Processing* **333**, 1–9 (2002).

Z.H. Wang, C.W. Barnes, G.A. Wurden, D.N. Hill, E.B. Hooper, H.S. McLean, R.D. Wood, and S. Woodruff, "Large-amplitude electron density and H^{α} fluctuations in the Sustained Spheromak Physics Experiment," *Nuclear Fusion* **42**, 643–652 (2002).

Z.H. Wang, V.I. Pariev, C.W. Barnes, and D.C. Barnes, "Laminar plasma dynamos," *Physics of Plasmas* **9**, 1491–1494 (2002).

Z.H. Wang, "Discrete rocket effect and its implication for micron grain acceleration," *Applied Physics Letters* **80**, 1094–1096 (2002).

R.L. Williamson, J.R. Fincke, and C.H. Chang, "Numerical study of the relative importance of turbulence, particle size and density, and injection parameters on particle behavior during thermal plasma spraying," *Journal of Thermal Spray Technology* **11**, 107–118 (2002).

S.J. Zweben, D.P. Stotler, J.L. Terry, B. LaBombard, M. Greenwald, M. Muterspaugh, C.S. Pitcher, K. Hallatschek, R.J. Maqueda, B. Rogers, J.L. Lowrance, V.J. Mastrocola, and G.F. Renda, "Edge turbulence imaging in the Alcator C-Mod tokamak," *Physics of Plasmas* **9**, 1981–1989 (2002).

2002 Conference Papers

T.J. Abrams, F.M. Guerra, K.L. Albright, J.S. George, B.D. Wienberg, N. Dabbish, D.M. Rector, C. Ho, and M.S. Schweiger, "Time-resolved photon-counting imager for photon migration tomography," Optical Society of America (OSA) Biomedical Topical Meetings and Exhibit, Miami Beach, Florida, USA, April 7–10, 2002, Los Alamos National Laboratory report LA-UR-02-1801 (March 2002).

B.G. Anderson, D.M. Oro, R.T. Olson, J.K. Studebaker, and D. Platts, "Flash x-ray system for diagnostic liner implosion experiments," Megagauss-IX: International Conference on High Magnetic Fields and Applications, Moscow/St. Petersburg, Russia, July 7–14, 2002, Los Alamos National Laboratory report LA-UR-02-1112 (February 2002).

R.J. Aragonez, "Vacuum control system for operating the field reversed configuration experiment (FRX-L) for magnetized target fusion," Los Alamos National Laboratory Symposium 2002, Los Alamos, New Mexico, USA, July 29–30, 2002, Los Alamos National Laboratory report LA-UR-02-4293 (July 2002).

R.J. Aragonez, "Vacuum control system for operating the field reversed configuratin experiment (FRX-L) for magnetized target fusion," 44th Annual Meeting of the American Physical Society Division of Plasma Physics, Orlando, Florida, USA, November 11–15, 2002, Los Alamos National Laboratory report LA-UR-02-4706 (July 2002).

M.M. Balkey, J.M. Scott, C.W. Barnes, S.H. Batha, and N.D. Delamater, "Single-mode Richtmyer-Meshkov growth in a compressible, miscible, convergent system," 44th Annual Meeting of the American Physical Society Division of Plasma Physics, Orlando, Florida, USA, November 11–15, 2002, Los Alamos National Laboratory report LA-UR-02-4329 (July 2002).

C.W. Barnes, "Asymmetric direct drive spherical implosions and neutron imaging and direct drive," Omega Experimental Effectiveness Workshop, Rochester, New York, USA, July 2002, Los Alamos National Laboratory report LA-UR-02-4608 (July 2002).

C.W. Barnes, "Hydrodynamic instability and mix in ICF and cylindrical implosions," University of Nevada, Reno, Nevada, USA, September 2002, Los Alamos National Laboratory report LA-UR-02-5992 (September 2002).

D.C. Barnes, E. Belova, R.C. Davidson, A. Ishida, H. Ji, R. Milroy, P. Parks, D. Ryutov, M. Schaffer, L. Steinhauer, and M. Yamadab, "Field-reversed configuration (FRC) equilibrium and stability," 19th IAEA Fusion Energy Conference, Lyon, France, October 14–19, 2002, Los Alamos National Laboratory report LA-UR-02-6289 (October 2002).

P.D. Barnes, "New search for the neutron electric dipole moment," 9th International Conference on the Structure of Baryons—Baryons 2002, Newport News, Virginia, USA, March 3–8, 2002, Los Alamos National Laboratory report LA-UR-02-7090 (November 2002).

C.M. Bass, "Optical tomography provides a method for determining time dependent density shifts in field reversed plasma," Los Alamos National Laboratory Symposium 2002, Los Alamos, New Mexico, USA, July 29–30, 2002, Los Alamos National Laboratory report LA-UR-02-4328 (July 2002).

S.H. Batha, "Los Alamos perspective on experimental effectiveness at Omega," Omega Experimental Effectiveness Workshop, Rochester, New York, USA, July 17, 2002, Los Alamos National Laboratory report LA-UR-02-4172 (July 2002).

S.H. Batha, C.W. Barnes, and C.R. Christensen, "Backlighter predictive capability," 14th Topical Conference on High Temperature Plasma Diagnostics, Madison, Wisconsin, USA, July 8–11, 2002, Los Alamos National Laboratory report LA-UR-02-4158 (July 2002).

S.H. Batha, C.W. Barnes, N.E. Lanier, G.R. Magelssen, J.M. Scott, N.D. Delamater, S. Rothman, A.M. Dunne, and K.W. Parker, "Compressible, convergent Richtmyer-Meshkov studies: Experiments and simulations," Science Day, Los Alamos, New Mexico, USA, April 17, 2002, Los Alamos National Laboratory report LA-UR-02-1322 (March 2002).

S.H. Batha, C.W. Barnes, N.E. Lanier, G.R. Magelssen, J.M. Scott, S. Rothman, A.M. Dunne, K.W. Parker, and D. Youngs, "Compressible, convergent Rightmyer-Meshkov studies: Experiments and simulations," Meeting of the Joint Working Group (USA-UK) (JOWOG 37), Livermore, California, USA, January 28–February 1, 2002, Los Alamos National Laboratory report LA-UR-02-0361 (January 2002).

S.H. Batha, C.W. Barnes, N.E. Lanier, M.M Balkey, G.R. Magelssen, N.D. Delamater, and J.M. Scott, "Overview of the LANL program in cylindrical mix," Meeting of the Joint Working Group (USA-UK) (JOWOG 37), Aldermaston, UK, September 30–October 4, 2002, Los Alamos National Laboratory report LA-UR-02-6153 (September 2002).

S.H. Batha, C.W. Barnes, N.E. Lanier, M.M Balkey, G.R. Magelssen, N.D. Delamater, and J.M. Scott, "Convergent, compressible Richtmyer-Meshkov instability," Meeting of the Joint Working Group (USA-UK) (JOWOG 37), Aldermaston, UK, September 30–October 4, 2002, Los Alamos National Laboratory report LA-UR-02-6154 (September 2002).

S.H. Batha, C.W. Barnes, N.E. Lanier, M.M Balkey, N.D. Delamater, G.R. Magelssen, J.M. Scott, S. Rothman, and A.M. Dunne, "Convergent, compressible Richtmyer-Meshkov experiment," 55th Annual Meeting of the Division of Fluid Dynamics of the American Physical Society Dallas, Texas, USA, November 24–26, 2002, Los Alamos National Laboratory report LA-UR-02-4061 (July 2002).

S.H. Batha, C.W. Barnes, N.E. Lanier, M.M Balkey, N.D. Delamater, G.R. Magelssen, J.M. Scott, S. Rothman, and A.M. Dunne, "Mixing between two compressing cylinders," 44th Annual Meeting of the APS Division of Plasma Physics, Orlando, Florida, USA, November 11–15, 2002, Los Alamos National Laboratory report LA-UR-02-4449 (July 2002).

P.D. Beinke, "Measuring thermal dispostion of rotating magnetic nano-particles," Los Alamos National Laboratory Symposium 2002, Los Alamos, New Mexico, USA, July 29–30, 2002, Los Alamos National Laboratory report LA-UR-02-4303 (July 2002).

J.F. Benage, Jr., "Physics topics in high energy density plasmas," NNSA/DAM Meeting on Atomic and Plasma Physics, Paris, France, April 8–11, 2002, Los Alamos National Laboratory report LA-UR-02-1893 (April 2002).

J.F. Benage, Jr., "Application of x-ray Thomson scattering to strongly coupled, electron-ion plasmas," International Conference on Warm Dense Matter (ICWDM), Hamburg, Germany, June 3–5, 2002, Los Alamos National Laboratory report LA-UR-02-2862 (May 2002).

D. Berkeland and D. Raymondson, "Precise tests of the randomness of quantum jumps," in *Proceedings of the 18th International Conference on Atomic Physics (ICAP2002),* H.R. Sadeghpour, D.E. Pritchard, and E.J. Heller, Eds., (World Scientific, London, 2002), Vol. 18.

D. Berkeland and D. Raymondson, "Quantum information and spectroscopy with trapped strontium ions," 33rd APS Meeting of the Division of Atomic and Molecular Physics (DAMOP2002), Williamsburg, Virginia, USA, May 24–28, 2002, Los Alamos National Laboratory report LA-UR-02-2766 (May 2002).

D. Berkeland and M. Boshier, "Destabilization of dark states, optical spectroscopy and laser cooling in Zeeman degenerate atomic systems," in *Proceedings of the 18th International Conference on Atomic Physics (ICAP2002),* H.R. Sadeghpour, D.E. Pritchard, and E.J. Heller, Eds., (World Scientific, London, 2002), Vol. 18.

D. Berkeland, "Randomness of quantum mechanical processes," 4th Annual Meeting of Southwest Quantum Information Technology (SQuInT) Network, Boulder, Colorado, USA, March 2–4, 2002, Los Alamos National Laboratory report LA-UR-02-1225 (March 2002).

K. Boboridis and A.W. Obst, "A high-speed four-channel infrared prytometer," 8th International Temperature Symposium, Chicago, Illinois, USA, October 21–24, 2002, Los Alamos National Laboratory report LA-UR-02-5359 (August 2002).

M.G. Boulay, "Recent results from the Sudbury Neutrino Observatory," SNO Results at DESY Synchrotron Lab, Zeuthen, Germany, June 4–5, 2002, Los Alamos National Laboratory report LA-UR-02-2782 (May 2002).

J.K. Campbell, "Magnetic probe construction and use in magnetic reconnection plasma experiments," Los Alamos National Laboratory Symposium 2002, Los Alamos, New Mexico, USA, July 29–30, 2002, Los Alamos National Laboratory report LA-UR-02-4330 (July 2002).

C.S. Carey, "Study of the stark broadening of Balmer lines in a high density FRC plasma," Los Alamos National Laboratory Symposium 2002, Los Alamos, New Mexico, USA, July 29–30, 2002, Los Alamos National Laboratory report LA-UR-02-4292 (July 2002).

K.M. Carter, D.M. Rector, A.T. Martinez, F.M. Guerra, and J.S. George, "Advances in recording scattered light changes in crustacean nerve with electrical activation," Optical Society of America (OSA) Biomedical Topical Meetings and Exhibit, Miami Beach, Florida, USA, April 7–10, 2002, Los Alamos National Laboratory report LA-UR-02-1800 (March 2002).

A.M. Chamberlin, "Head localization in a MEG system," Los Alamos National Laboratory Symposium 2002, Los Alamos, New Mexico, USA, July 29–30, 2002, Los Alamos National Laboratory report LA-UR-02-4305 (July 2002).

R.E. Chrien, R.L. Bowers, D.L. Peterson, R.G. Watt, G.C. Idzorek, and T.W. Sanford, "Radiation flow driven by a dynamic hohlraum radiation source (U)," Nuclear Explosives Design and Physics Conference (NEDPC 2001), Livermore, California, USA, October 15–19, 2001, Los Alamos National Laboratory controlled publication LA-CP-02-0001 (January 2002).

C.R. Christensen and C.W. Barnes, "Reconstruction of pinhole neutron images," CEA/NNSA Technical Collaboration Meeting, Livermore, California, USA, February 11–15, 2002, Los Alamos National Laboratory report LA-UR-02-0764 (February 2002).

C.R. Christensen, C.W. Barnes, D.C. Wilson, G.L. Morgan, and M.D. Wilke, "Pinhole neutron imaging," WBS-4 Video Teleconference, Livermore California, USA, May 16, 2002, Los Alamos National Laboratory report LA-UR-02-2982 (May 2002).

Appendix B: Publications—2002 Conference Papers

C.R. Christensen, G.L. Morgan, M.D. Wilke, C.W. Barnes, and D.C. Wilson, "First results of pinhole neutron imaging for inertial confinement fusion," 14th Topical Conference on High Temperature Plasma Diagnostics, Madison, Wisconsin, USA, July 8–11, 2002, Los Alamos National Laboratory report LA-UR-02-4169 (July 2002).

C.R. Christensen, G.L. Morgan, M.D. Wilke, C.W. Barnes, and D.C. Wilson, "Neutrons versus x-rays: A comparison of reconstructions of neutron images to x-ray images of asymmetric direct-drive implosions," 44th Annual Meeting of the APS Division of Plasma Physics, Orlando, Florida, USA, November 11–15, 2002, Los Alamos National Laboratory report LA-UR-02-6816 (July 2002).

D.D. Clark, M.A. Espy, R.H. Kraus, Jr., and P.D. Beinke, "Preliminary results from using a SQUID array microscope for evaluating weld quality," Noncontact Gauging Workshop, Kansas City, Misouri, USA, March 26, 2002, Los Alamos National Laboratory report LA-UR-02-1664 (March 2002).

D.D. Clark, M.A. Espy, R.H., Kraus, Jr., A.N. Matlachov, and J.S. Lamb, "Weld quality evaluation using a high temperature SQUID array," ASC-2002: Applied Superconductivity Conference, Houston, Texas, USA, August 4–9, 2002, Los Alamos National Laboratory report LA-UR-02-5647 (September 2002).

J.A. Cobble, J.C. Fernández, S. Letzring, T. Shimada, N.R. LeGalloudec, T. Cowan, J. Fuchs, and M. Geissel, "Initial 30-TW Trident and target physics," Short Pulse Working Group Meeting, Petersburg, Russia, November 2002, Los Alamos National Laboratory report LA-UR-02-6762 (October 2002).

J.A. Cobble, R.B. Gibson, R.P. Johnson, J.C. Fernández, M. Allen, T. Cowan, and N.R. LeGalloudec, "Short-pulse capabilities and applications at the Trident laser," Meeting of the Joint Working Group (USA-UK) (JOWOG 37), Livermore, California, USA, January 2002, Los Alamos National Laboratory report LA-UR-02-0362 (January 2002).

J.A. Cobble, R.P. Johnson, G.A. Cowan, and N.R. LeGalloudec, "MeV proton production with the LANL Trident laser (and its use in radiography)," General Atomics/Ritsumeikan University, Kyoto, Japan, March 25–28, 2002, Los Alamos National Laboratory report LA-UR-02-0965 (February 2002).

J.A. Cobble, J.L. Kline, and D.S. Montgomery, "Forward SRS from a diffraction limited laser beam," 44th Annual Meeting of the American Physical Society Division of Plasma Physics, Orlando, Florida, USA, November 11–15, 2002, Los Alamos National Laboratory report LA-UR-02-4423 (July 2002).

J.A. Cobble, J.C. Fernández, R.B. Gibson, R.P. Johnson, N.R. LeGalloudec, G.A. Cowan, and M. Allen, "Laser-produced MeV protons on Trident," 32nd Anomalous Absorption Conference Oahu, Hawaii, USA, July 21–26, 2002, Los Alamos National Laboratory report LA-UR-02-4424 (July 2002).

J.C. Cochran, "Summary of Atlas experimental performance," Megagauss-IX: International Conference on High Magnetic Fields and Applications, Moscow–St. Petersburg, Russia, July 7–14, 2002, Los Alamos National Laboratory report LA-UR-02-1227 (March 2002).

J.C. Cochran and P.J. Turchi, "Design and performance of a current transformer for efficient liner implosions," 29th IEEE International Conference on Plasma Science (ICOPS 2002), Banff, Alberta, Canada, May 26–30, 2002, Los Alamos National Laboratory report LA-UR-02-0192 (January 2002).

J.C. Cochran, R.E. Reinovsky, and J.S. Ladish, "Atlas: Experimental update," Meeting of the Joint Working Group (USA-UK) (JOWOG 37), Livermore, California, USA, January 2002, Los Alamos National Laboratory report LA-UR-02-0398 (January 2002).

F.C. Collman, "Dynamic object recognition in neutral network model," Los Alamos National Laboratory Symposium 2002, Los Alamos, New Mexico, USA, July 29–30, 2002, Los Alamos National Laboratory report LA-UR-02-4304 (July 2002).

K.R. Costigan, C.D. Tomkins, E.P. Springer, C.L. Winter, D.L. Langley, and J.R. Stalker, "Evaluation of down scaling predicted precipitation in a coupled modeling system," 16th Conference on Hydrology (at the 82nd Annual Meeting of the American Meteorological Society), Orlando, Florida, USA, January 13–17, 2002, Los Alamos National Laboratory report LA-UR-02-0164 (January 2002).

H.A. Davis, "Status of the Dual-Axis Radiographic Hydrodynamics Test (DARHT) Facility," 14th International Conference on High-Power Particle Beams (BEAMS-2002) and 5th International Conference on Dense Z-Pinches (DZP-2002), Albuquerque, New Mexico, USA, July 23–28, 2002, Los Alamos National Laboratory report LA-UR-02-3811 (June 2002).

H.A. Davis, C. Vermare, T.P. Hughes, D.C. Moir, and R.T. Olson, "Electron beam disruption due to ion release from targets: Comparison between computer calculations and observations," 29th IEEE International Conference on Plasma Science (ICOPS 2002), Banff, Alberta, Canada, May 26–30, 2002, Los Alamos National Laboratory report LA-UR-02-3027 (May 2002).

H.A. Davis, C. Vermare, T.P. Hughes, D.C. Moir, and R.T. Olson, "Electron beam distuption due to ion release from targets," 21st International Linear Accelerator Conference (Linac 2002), Gyeongju, Korea, August 19–23, 2002, Los Alamos National Laboratory report LA-UR-02-1890 (April 2002).

H.A. Davis, C. Vermare, T.P. Hughes, D.C. Moir, and R.T. Olson, "Electron beam disruption due to ion release from targets: Comparison between computer calculations and observations," 29th IEEE International Conference on Plasma Science (ICOPS 2002), Banff, Alberta, Canada, May 26–30, 2002, Los Alamos National Laboratory report LA-UR-02-0230 (January 2002).

H.A. Davis, C. Vermare, T.P. Hughes, D.C. Moir, and R.T. Olson, "Electron beam disruption due to ion release from targets: Experimental observations," 14th International Conference on High-Power Particle Beams (BEAMS-2002) and 5th International Conference on Dense Z-Pinches (DZP-2002), Albuquerque, New Mexico, USA, July 23–28, 2002, Los Alamos National Laboratory report LA-UR-02-3839 (June 2002).

N.D. Delamater, J.A. Guzik, W.S. Varnum, G.D. Pollak, D.A. Haynes, R.G. Watt, W.M. Wood, and G.A. Kyrala, "Double shell target implosions on Omega," Meeting of the Joint Working Group (USA-UK) (JOWOG-32S), Aldermaston, UK, October 2002, Los Alamos National Laboratory report LA-UR-02-4896 (August 2002).

N.D. Delamater, R.G. Watt, and W.S. Varnum, "Review of high convergence implosion experiments with single and double shell targets," Seminar at the Fusion Technology Institute, University of Wisconsin, Madison, Wisconsin, USA, May 2002, Los Alamos National Laboratory report LA-UR-02-2917 (May 2002).

N.D. Delamater, G.R. Magelssen, J.M. Scott, S.H. Batha, and N.E. Lanier, "Calcualtions of double cylinder implosions at Omega," Meeting of the Joint Working Group (USA-UK) (JOWOG 37), Aldermaston, UK, September 30–October 4, 2002, Los Alamos National Laboratory report LA-UR-02-6115 (September 2002).

N.D. Delamater, S.H. Batha, M.M Balkey, C.W. Barnes, and G.R. Magelssen, "Calculations of double cylinder implosions at Omega," 44th Annual Meeting of the American Physical Society Division of Plasma Physics, Orlando, Florida, USA, November 11–15, 2002, Los Alamos National Laboratory report LA-UR-02-4281 (July 2002).

M.R. Douglas, R.L. Bowers, R.E. Chrien, G.C. Idzorek, D.L. Peterson, R.G. Watt, and B.H. Wilde, "A study of the interior region and exit hole of a dynamic hohlraum radiation source on Z," 44th Annual Meeting of the American Physical Society Division of Plasma Physics, Orlando, Florida, USA, November 11–15, 2002, Los Alamos National Laboratory report LA-UR-02-4494 (July 2002).

C.A. Ekdahl, Jr., B. Carlsten, H.A. Davis, B.T. McCuistian, D.C. Moir, T.L. Houck, W. Fawley, S. Yu, W.B. Broste, H.A. Bender, K.C. Jones, K. Moy, C.Y. Tom, and T.P. Hughes, "First beam at DARHT-II," 14th International Conference on High-Power Particle Beams (BEAMS-2002) and 5th International Conference on Dense Z-Pinches (DZP-2002), Albuquerque, New Mexico, USA, July 23–28, 2002, Los Alamos National Laboratory report LA-UR-02-3826 (June 2002).

C.A. Ekdahl, Jr., M.A. Brubaker, M.H. Holtzscheiter, J.B. Johnson, D.M. Oro, P.J. Rodriguez, and M.D. Wilke, "DARHT-II Beam Diagnostics," 14th International Conference on High-Power Particle Beams (BEAMS-2002) and 5th International Conference on Dense Z-Pinches (DZP-2002), Albuquerque, New Mexico, USA, July 23–28, 2002, Los Alamos National Laboratory report LA-UR-02-3825 (June 2002).

E.-I. Esch, J.M. O'Donnell, S.A. Wender, J.D. Bowman, G.L. Morgan, and J.L. Matthews, "Measurements of the $n + p \rightarrow d + \gamma$ cross section for big bang nucleosynthesis with the Spallation Neutron Source at the Los Alamos Neutron Science Center," Gamma-Ray Techniques in Astrophysics, Prague, Czech Republic, September 2002, Los Alamos National Laboratory report LA-UR-02-5639 (September 2002).

E.-I. Esch, J.M. O'Donnell, S.A. Wender, S. Olmstead, J.D. Bowman, G.L. Morgan, and J.L. Matthews, "Test of big bang nucleosynthessis model predictions by precision measurement of the N+1H-2D+Y cross section at the WNR facility at LANL," 2002 April Meeting of the American Physical Society (with the High Energy Astrophysics Division of the Americal Astronomical Society), Albuquerque, New Mexico, USA, April 20–23, 2002, Los Alamos National Laboratory report LA-UR-02-0142 (January 2002).

M.A. Espy, R.H. Kraus, Jr., and A.H. Cogbill, "SQUIDs for detection of underground activities," Workshop on the Role of the Nuclear Physics Comminity in Combating Terrorism, Washington, D.C., USA, July 11–12, 2002, Los Alamos National Laboratory report LA-UR-02-4302 (July 2002).

J.C. Fernández and J.A. Cobble, "Using laser-driven MeV/nucleon ion beams to study dense plasmas," 32nd Anomalous Absorption Conference Oahu, Hawaii, USA, July 21–26, 2002, Los Alamos National Laboratory report LA-UR-02-3229 (May 2002).

S.W. Forrest, "Measurements of the magnetic field of propagating action potentials in a frog sciatic nerve," Los Alamos National Laboratory Symposium 2002, Los Alamos, New Mexico, USA, July 29–30, 2002, Los Alamos National Laboratory report LA-UR-02-4308 (July 2002).

Appendix B: Publications—2002 Conference Papers

I. Furno, T.P. Intrator, E. Torbert, J.K. Campbell, C.S. Carey, and C.A. Werley, "Overview of reconnection scaling experiment at LANL and first experimental results," 44th Annual Meeting of the American Physical Society Division of Plasma Physics, Orlando, Florida, USA, November 11–15, 2002, Los Alamos National Laboratory report LA-UR-02-4606 (July 2002).

R.B. Gibson and J.M. Mack, Jr., "Trident: A versatile laser lethality laboratory," High-Energy Pulsed Laser Lethality Effects and Beam Propagation Workshop, Huntsville, Alabama, USA, August 27–28, 2002, Los Alamos National Laboratory report LA-UR-02-4564 (July 2002).

R.B. Gibson, J.A. Cobble, and J.C. Fernández, "Ultrashort pulse upgrade of the Trident laser," Fast Ignition, Biwako-Kusatsu, Japan, March 25–28, 2002, Los Alamos National Laboratory report LA-UR-02-1420 (March 2002).

J.A. Guzik, D.E. Hollowell, S.H. Batha, J.B. Beck, R.E. Chrien, and A.L. Peratt, "Omega experiment for radiation hydrodynamics code validation (U)," Nuclear Explosives Computional Design Conference (NECDC 2002) Monterey, California, USA, October 22–25, 2002, Los Alamos National Laboratory controlled publication LA-CP-02-0276 (June 2002).

R.E. Hackenberg, D.C. Swift, K. Chen, J. Cooley, D.L. Paisley, D.J. Thoma, and A.A. Hauer, "Phase changes in No-Ti under shock loading," International Workshop on New Models and Hydrocodes for Shock Wave Processes in Condensed Matter (NMHSWPCM), Edinburgh, Scotland, May 19–24, 2002, Los Alamos National Laboratory report LA-UR-02-1754 (March 2002).

R.E. Hackenberg, D.C. Swift, J.C. Cooley, K.C. Chen, D.J. Thoma, D.L. Paisley and A. Hauer, "Phase changes in Ni-Ti under laser shock loading," the International Workshop on New Models and Hydrocodes for Shock Wave Processes in Condensed Matter, Edinburgh, Scotland, UK, May 19–24, 2002, Los Alamos National Laboratory report LA-UR-02-3112 (May 2002).

A.C. Hayes, D. Barr, S.A. Becker, S.C. Frankle, G. Jungman, R. Little, M.A. MacInnes, R.S. Rundberg, J.C. Solem, S.M. Sterbenz, W.B. Wilson, and W.S. Wilburn, "Discrepancy in the radiochemical diagnostic for fusion neutrons (U)," Nuclear Explosives Design and Physics Conference (NEDPC 2001), Livermore, California, USA, October 15–19, 2001, Los Alamos National Laboratory controlled publication LA-CP-02-0034 (January 2002).

M.H. Holzscheiter, "Forming of cold antihydrogen for tests of CPT and WEP," 2002 April Meeting of the American Physical Society (with the High Energy Astrophysics Division of the Americal Astronomical Society), Albuquerque, New Mexico, USA, April 20–23, 2002, Los Alamos National Laboratory report LA-UR-02-2249 (April 2002).

R.J. Hughes, "Quantum cryptography," Science Day, Los Alamos, New Mexico, USA, April 17, 2002, Los Alamos National Laboratory report LA-UR-02-3587 (June 2002).

R.J. Hughes, "Quantum key distribution," Science Day, Los Alamos, New Mexico, USA, April 17, 2002, Los Alamos National Laboratory report LA-UR-02-2118 (April 2002).

R.J. Hughes, J.E. Nordholt, G.L. Morgan, and C.G. Peterson, "Free-space quantum key distribution over 10 km in daylight and at night," 6th International Conference on Quantum Communication, Measurement, and Computing (QCMC'02), MIT, Cambridge, Massachusetts, USA, July 22–26, 2002, Los Alamos National Laboratory report LA-UR-02-2115 (April 2002).

R.J. Hughes, J.E. Nordholt, G.L. Morgan, and C.G. Peterson, "Free-space quantum key distribution in daylight," 10th Quantum Electronics and Laser Science Conference (QELS 2002), Long Beach, California, USA, May 19–24, 2002, Los Alamos National Laboratory report LA-UR-02-2116 (April 2002).

A.J. Hurd, J.D. Bowman, M.R. Fitzsimmons, and R. Pynn, "Overview of polarized neutrons at LANSCE," Workshop on Polarized Neutrons in Condensed Matter Investigations, Julich, Germany, September 15–19, 2002, Los Alamos National Laboratory report LA-UR-02-4256 (July 2002).

T.P. Intrator, J.M. Taccetti, G.A. Wurden, R. Siemon, P. Sanchez, W.J. Waganaar, S. Zhang, R.J. Maqueda, D. Begay, C.M. Bass, J.K. Campbell, C. Carey, M.P. Kozar, J.Y. Liang, R. Renneke, M.G. Tuszewski, T.C. Grabowski, E.L. Ruden, D.G. Gale, and T. Cavasos, "Overview of reversed field configuration plasma target research at LANL for magnetized target fusion," 44th Annual Meeting of the American Physical Society Division of Plasma Physics, Orlando, Florida, USA, November 11–15, 2002, Los Alamos National Laboratory report LA-UR-02-4705 (July 2002).

J.R. Kamm, W.J. Rider, C.D. Tomkins, C.A. Zoldi, K.P. Prestridge, M. Marr-Lyon, P.M. Rightley, P. Vorobieff, and R. F. Benjamin, "Statistical comparison between experiments and numerical simulations of two shock-accelerated gas cylinders," Nuclear Explosives Computional Design Conference (NECDC 2002), Monterey, California, USA, October 22–25, 2002, Los Alamos National Laboratory report LA-UR-02-3211 (May 2002).

R.J. Kanzleiter, J.L. Stokes, R.L. Bowers, M.A. Salazar, J.A. Guzik, G. Rodriguez, J.S. Ladish, and D.M. Oro, "Hydrodynamic features experiments using pulsed power sources for code/data comparisons," Meeting of the Joint Working Group (USA-UK) (JOWOG 32P), Livermore, California, USA, April 22–25, 2002, Los Alamos National Laboratory report LA-UR-02-2145 (April 2002).

R.E. Kelley, "Shaded relief topographic map using 2000 R-foot lidar data," 22nd Annual ESRI (Environmental Systems Research Institute) International Users Conference, San Diego, California, USA, July 8–12, 2002, Los Alamos National Laboratory report LA-UR-02-3979 (June 2002).

R.E. Kelley, "EMP characteristics from explosives deep in tunnels," American Electro-magnetics 2002 Symposium (AMEREM 2002), U.S. Naval Academy, Annapolis, Maryland, USA, June 2–7, 2002, Los Alamos National Laboratory report LA-UR-02-0188 (January 2002).

D.E. Kharzeev and J. Raufeisen, "High energy nuclear interactions and QCD: An introduction," in *American Institute of Physics Proceedings of Pan American Advanced Study Institute* (New States of Matter in Hadronic Interactions), Campos do Jordão, Brazil, January 7–18, 2002, Los Alamos National Laboratory report LA-UR-02-3956 (June 2002).

N.S.P. King, S. Baker, K.K. Kwiatkowski, S. Lutz, G.E. Hogan, V.H. Holmes, Jr., C.L. Morris, P. Nedrow, P. Pazuchanics, J.S. Rohrer, D.S. Sorenson, and R.T. Thompson, "Imaging detector systems for soft x-ray and proton radiography," 25th International Congress on High Speed Photography and Photonics, Beaune, France, September 29–October 3, 2002, Los Alamos National Laboratory report LA-UR-02-5037 (August 2002).

J.L. Kline, D.S. Montgomery, J.A. Cobble, R.P. Johnson, H.A. Rose, and H. Vu, "Observation of a transition from fluid to kinetic: Nonlinearities for Langmuir waves driven by stimulated Raman scattering," 44th Annual Meeting of the American Physical Society Division of Plasma Physics, Orlando, Florida, USA, November 11–15, 2002, Los Alamos National Laboratory report LA-UR-02-4296 (July 2002).

M.P. Kozar, G.A. Wurden, T.P. Intrator, J.M. Taccetti, and D. Begay, "Constructing a bolometer array diagnostic for the FRX-L plasma," 44th Annual Meeting of the American Physical Society Division of Plasma Physics, Orlando, Florida, USA, November 11–15, 2002, Los Alamos National Laboratory report LA-UR-02-4834 (July 2002).

R.H. Kraus, Jr., M.A. Espy, A. Matlachov, V. Armijo, S.G. Newman, D.A. Clark, P.D. Beinke, and M.V. Peters, "SQUIDs for biological measurements," Science Day, Los Alamos, New Mexico, USA, April 17, 2002, Los Alamos National Laboratory report LA-UR-02-1884 (April 2002).

K.K. Kwiatkowski, "Development of 3-D packaging for high-bandwidth massively paralleled imager," 4th International Workshop on Radiation Imaging Detectors, Amsterdam, The Netherlands, September 8–12, 2002, Los Alamos National Laboratory report LA-UR-02-5593 (September 2002).

K.K. Kwiatkowski, J. Lyke, R.J. Wojnarowski, R. Fillion, C. Kapusta, N.S.P. King, R. Saia, and M.D. Wilke, "Development of vertically stacked readout substrate packaging for high-band width massively paralleled imager," 4th International Workshop on Radiation Imaging Detectors, Amsterdam, The Netherlands, September 8–12, 2002, Los Alamos National Laboratory report LA-UR-02-3690 (June 2002).

K.K. Kwiatkowski, N.S.P. King, J. Lyke, J.F. Beche, and J.E. Mullaud, "Development of a multi-frame optical imaging detector for proton radiography at LANL," 25th International Congress on High-Speed Photography and Photonics, Beaune, France, September 29–October 3, 2002, Los Alamos National Laboratory report LA-UR-02-6162 (September 2002).

J.S. Lamb, "Using superconducting quantum interference devices in non-destructive evaluation problems," Los Alamos National Laboratory Symposium 2002, Los Alamos, New Mexico, USA, July 29–30, 2002, Los Alamos National Laboratory report LA-UR-02-4307 (July 2002).

N.E. Lanier, C.W. Barnes, S.H. Batha, R.D. Day, A.M. Dunne, N.D. Delamater, N.E. Elliott, R.L. Holmes, G.R. Magelssen, K.W. Parker, S. Rothman, and J.M. Scott, "Effect of multi-mode initial surface perturbations on Richtmyer-Meshkov mixing in compressible convergent, plasma systems," 44th Annual Meeting of the American Physical Society Division of Plasma Physics, Orlando, Florida, USA, November 11–15, 2002, Los Alamos National Laboratory report LA-UR-02-3034 (May 2002).

H. Li, K. Nisimura, S.P. Gary, D.C. Barnes, and S.A. Colgate, "PIC simulations of force-free magnetic reconnection," 44th Annual Meeting of the American Physical Society Division of Plasma Physics, Orlando, Florida, USA, November 11–15, 2002, Los Alamos National Laboratory report LA-UR-02-4538 (July 2002).

W.C. Louis and R.C. Schirato, "Very Large Area Neutron Detector (VLAND)," Workshop on the Role of the Nuclear Physics Research Community in Combating Terrorism, Washington, D.C., USA, July 11–12, 2002, Los Alamos National Laboratory report LA-UR-02-4120 (July 2002).

G.R. Magelssen, J.M. Scott, N.E. Lanier, S.H. Batha, M.M. Balkey, C.W. Barnes, N.D. Delamater, A.M. Dunne, K.W. Parker, S. Rothman, and D. Youngs, "Convergent, compresible Richtmyer-Meshkov experiment-zero order," 44th Annual Meeting of the American Physical Society Division of Plasma Physics, Orlando, Florida, USA, November 11–15, 2002, Los Alamos National Laboratory report LA-UR-02-4167 (July 2002).

Appendix B: Publications—2002 Conference Papers

G.R. Magelssen, W.M. Wood, J. Abdallah, D.J. Hoarty, E. Clark, C. Smith, and A.M. Dunne, "Integrated radiography and fluorescent experiments (U)," Meeting of the Joint Working Group (USA-UK) (JOWOG 37), Livermore, California, USA, January 2002, Los Alamos National Laboratory controlled publication LA-CP-02-0036 (January 2002).

M. Marr-Lyon, C.D. Tomkins, J.M. Sicilian, K.P. Prestridge, P.M. Rightley, R.F. Benjamin, and P. Vorobieff, "Initial condition measurements of one and two shock-accelerated gas cylinders," 55th Annual Meeting of the Division of Fluid Dynamics of the American Physical Society Dallas, Texas, USA, November 24–26, 2002, Los Alamos National Laboratory report LA-UR-02-4879 (July 2002).

A.N. Matlachov, R.H. Kraus, Jr., M.A. Espy, E.D. Best, M.C. Briles, E.Y. Raby, and E.R. Flynn, "Design and performance of the LANL 158-channel magnetoence phalography system," 13th International Conference on Biomagnetism, Jena, Germany August 10–14, 2002, Los Alamos National Laboratory report LA-UR-02-3147 (May 2002).

T.J. Matsson, "Measuring moments of micromagnetic particles for bioassay," Los Alamos National Laboratory Symposium 2002, Los Alamos, New Mexico, USA, July 29–30, 2002, Los Alamos National Laboratory report LA-UR-02-4306 (July 2002).

B.H.T. McKellar, M. Garbutt, G.J. Stephenson, Jr., and J.T. Goldman, "Some implications of the NUTEV anomaly," Joint CSSM/JHF/NITP Workshop on Physics at the Japan Hadron Facility, Adelaide, Australia, March 14–21, 2002, Los Alamos National Laboratory report LA-UR-02-3842 (June 2002).

F.E. Merrill, C.L. Morris, and R.E. Chrien, "Electron radiography," Simulation and Analysis Workshop, Part 1: Tools, Los Alamos, New Mexico, USA, August 5–9, 2002, Los Alamos National Laboratory report LA-UR-02-4899 (August 2002).

R.E. Mischke, "Neutron electric dipole moment," 15th International Spin Physics Symposium (SPIN 2002), Brookhaven National Laboratory, Brookhaven, New York, USA, September 9–14, 2002, Los Alamos National Laboratory report LA-UR-02-6264 (October 2002).

G.E. Mitchell, J.D. Bowman, S.I. Penttilä, and E.I. Sharapov, "Parity violation in epithermal neutron resonances," Workshop on Astrophysics, Symmetries, and Applied Physics at Spallation Neutron Sources, Oak Ridge, Tennessee, USA, March 11–13, 2002, P.E. Kohler, C.R. Gould, R.C. Haight, and T.E. Valentine, Eds., (World Scientific, Singapore, 2002) p. 155.

D.S. Montgomery, J.L. Kline, T.E. Tierney, J.A. Cobble, J.C. Fernández, R.P. Johnson, and R.J. Focia, "Verification of trapped electron acoutsic wave dispersion relation," 44th Annual Meeting of the American Physical Society Division of Plasma Physics, Orlando, Florida, USA, November 11–15, 2002, Los Alamos National Laboratory report LA-UR-02-4501 (July 2002).

D.S. Montgomery, J.L. Kline, T.E. Tierney, R.J. Focia, J.A. Cobble, J.C. Fernández, and R.P. Johnson, "Trident single hot spot experiments at high KLD: Verification of seas dispersion relation," 32nd Anomalous Absorption Conference Oahu, Hawaii, USA, July 21–26, 2002, Los Alamos National Laboratory report LA-UR-02-4502 (July 2002).

D.S. Montgomery, J.L. Kline, T.E. Tierney, R.J. Focia, J.A. Cobble, J.C. Fernández, and R.P. Johnson, "Trident single hot spot experiments at high k*lambda Debye," 32nd Anomalous Absorption Conference Oahu, Hawaii, USA, July 21–26, 2002, Los Alamos National Laboratory report LA-UR-02-3177 (May 2002).

C.L. Morris, "Recent proton radiographic experiements at the AGS (U)," Simulation and Analysis Workshop, Part 1: Tools, Los Alamos, New Mexico, USA, August 5–9, 2002, Los Alamos National Laboratory controlled publication LA-CP-02-0189 (April 2002).

R. Moses, R.A. Gerwin, and K.F. Schoenberg, "Transport implications of Taylor relaxation," 44th Annual Meeting of the American Physical Society Division of Plasma Physics, Orlando, Florida, USA, November 11–15, 2002, Los Alamos National Laboratory report LA-UR-02-5106 (August 2002).

C.E. Moss, C.M. Frankle, V. Litvinenko, and H.R. Weller, "Recent results using the high intensity gamma-ray source facility," 10th Symposium on Radiation Measurements and Applications, Ann Arbor, Michigan, USA, May 21–23, 2002, Los Alamos National Laboratory report LA-UR-02-2491 (April 2002).

R.N. Mulford and D.C. Swift, "Reactive flow models for nitromethane," the International Workshop on New Models and Hydrocodes for Shock Wave Processes in Condensed Matter, Edinburgh, Scotland, UK, May 19–24, 2002, Los Alamos National Laboratory report LA-UR-02-4004 (June 2002).

R.N. Mulford, D.C. Swift, and M. Braithwaite, "Temperature-based reactive flow model for ANFO," 12th International Detonation Symposium, San Diego, California, USA, August 11–16, 2002, Los Alamos National Laboratory report LA-UR-02-3676, (June 2002).

D.M. Oro, "Atlas radiographic system," Meeting of the Joint Working Group (USA-UK) (JOWOG 37), Livermore, California, USA, January 2002, Los Alamos National Laboratory report LA-UR-02-0572 (January 2002).

R. Papazian and F.H. Cverna, "LANL SCE project update and issues (U)," LANL/AWE Subcritical Experiment Planning Meeting, Aldermaston, UK, March 19–21, 2002, Los Alamos National Laboratory controlled publication LA-CP-02-0114 (March 2002).

R.A. Pelak, L.M. Hull, H.H. Watanabe, D.M. Oro, M.D. Ulibarri, W.F. Hemsing, M.A. Shinas, J. Binstock, P.T. Sheehey, F.N. Mortensen, and J.A. Echave, "Recent experiments in case behavior (U)," Nuclear Explosives Design and Physics Conference (NEDPC 2001), Livermore, California, USA, October 15–19, 2001, Los Alamos National Laboratory controlled publication LA-CP-02-0003 (January 2002).

S.I. Penttilä, "Development on dynamic nuclear polarized targets," 9th International Workshop on Polarized Sources and Targets (PST 2001), Nashville, Indiana, USA, September 30–October 4, 2001, Los Alamos National Laboratory report LA-UR-02-0307 (January 2002).

S.I. Penttilä, "New experimental capabilities for parity non-conservation and time reversal invariance violation in neutron transmission," Workshop on Astrophysics, Symmetries, and Applied Physics, Oak Ridge, Tennessee, USA, March 11–13, 2002, Los Alamos National Laboratory report LA-UR-02-4034 (June 2002).

S.I. Penttilä, J.D. Bowman, R.D. Carlini, T. Case, T.E. Chupp, K.P. Coulter, S.J. Freedman, T.R. Gentile, M. Gericke, G.L. Greene, B. Hersmann, S. Ishimoto, G.L. Jones, M.B. Leuschner, Y. Masuda, G.S. Mitchell, K. Morimoto, H. Nann, S. Page, W.D. Ramsay, E.I. Sharapov, T.B. Smith, W.M. Snow, W.S. Wilburn, and V.W. Yuan, "A measurement of the parity-violating gamma-ray asymmetry in the neutron-proton capture," 11th International Symposium on Capture Gamma-Ray Spectroscopy and Related Topics, Pruhonice, Prague, Czech Republic, September 2–6, 2002, Los Alamos National Laboratory report LA-UR-02-6560 (October 2002).

D.L. Peterson, R.E. Chrien, F.L. Cochran, G.C. Idzorek, R.G. Watt, T.W.L. Sanford, and R.W. Lemke, "Simulating dynamic hohlraum Z-pinches," 44th Annual Meeting of the American Physical Society Division of Plasma Physics, Orlando, Florida, USA, November 11–15, 2002, Los Alamos National Laboratory report LA-UR-02-4613 (July 2002).

D.L. Peterson, R.E. Chrien, R.G. Watt, T.W. Sanford, and R.W. Lemke, "Simulations and dymamics of the Z dynamic hohlraum," 14th International Conference on High-Power Particle Beams (BEAMS-2002) and 5th International Conference on Dense Z-Pinches (DZP-2002), Albuquerque, New Mexico, USA, July 23–28, 2002, Los Alamos National Laboratory report LA-UR-02-0195 (January 2002).

R. Peterson, B. Wood, G. Kyrala, P. Keiter, J. Kindel, G. Idzorek, D. Peterson, R. Watt, R. Chrien, and J. Aubrey, "Legacy and ASCI computer code simulations of Z radiation transport experiments," Nuclear Explosives Computional Design Conference (NECDC 2002), Monterey, California, USA, October 22–25, 2002, Los Alamos National Laboratory report LA-UR-02-5264 (August 2002).

G.D. Pollak, R.G. Watt, D.C. Wilson, and N.D. Delamater, "Comparison of calculated and measured gated images for recent implosion experiments," 32nd Anomalous Absorption Conference Oahu, Hawaii, USA, July 21–26, 2002, Los Alamos National Laboratory report LA-UR-02-4401 (July 2002).

P.W. Randles, A.G. Petschek, L.D. Libersky, and C.T. Dyka, "Stability of DPD and SPH," in *Meshfree Methods for Partial Differential Equations (*Bonn, 2001), M. Griebel and M.A. Schweitzer, Eds., (Springer-Verlag, Heidelberg, 2002), *Lecture Notes in Computational Science and Engineering,* Vol. 26, pp. 330–350.

J. Raufeisen, "Heavy quark production at RHIC and LHC," Workshop on Current and Future Directions at RHIC, Upton, New York, USA, August 5–23, 2002, Los Alamos National Laboratory report LA-UR-02-6142 (September 2002).

J. Raufeisen, "Nuclear effects in the Drell-Yan process," Pan American Advanced Studies Institute on New States of Matter in Hadronic Interactions (PASI 2002), Sao Paulo, Brazil, January 7–18, 2002, in *American Institute of Physics Proceedings of New States of Matter in Hadronic Interactions,* Vol. 631, pp. 525–532.

J. Raufeisen, "Relation between the BDMPS transport coefficient and the dipole cross section," Workshop on Hard Probes in Heavy Ion Collisions at the Large Hadron Collider, Geneva, Switzerland, March 11–15, 2002, Los Alamos National Laboratory report LA-UR-02-2275 (April 2002).

J. Raufeisen, "QCD coherence effects in high energy reactions with nuclei," 6th World Multiconference on Systemics, Cybernetics and Informatics (SCI 2002), Orlando, Florida, USA, July 14–18, 2002, Los Alamos National Laboratory report LA-UR-02-0070 (January 2002).

M.W. Rawool-Sullivan, J.P. Sullivan, and R.M. Kippen, "Compton gamma-ray imaging for countering nuclear or radiological threats," Workshop on Countering Nuclear and Radiological Threats, Los Alamos, New Mexico, USA, August 27–29, 2002, Los Alamos National Laboratory report LA-UR-02-5396 (August 2002).

W.A. Reass, D.L. Borovina, V.W. Brown, J.D. Doss, R.F. Gribble, T.W. Hardek, M.T. Lynch, D.E. Rees, P.J. Tallerico, and D.E. Anderson, "The polyphase resonant converter modulator system for the Spallation Neutron Source linear accelerator," 2002 International Power Modulator Conference and High Voltage Workshop, Hollywood, California, USA, June 30–July 3, 2002, Los Alamos National Laboratory report LA-UR-02-3986 (June 2002).

Appendix B: Publications—2002 Conference Papers

W.A. Reass, D.M. Baca, J.D. Doss, and R.F. Gribble, "The polyphase resonant converter modulator for pulse power and plasma applications," Japan-USA Symposium on Pulsed Power and Plasma Applications, Kailua-Kona, Hawaii, USA, August 4–8, 2002, Los Alamos National Laboratory report LA-UR-02-4452 (July 2002).

W.A. Reass, T.W. Hardek, P.J. Tallerico, J.D. Doss, D.L. Borovina, M.T. Lynch, D.E. Rees, and R.F. Gribble, "Design and status of the ployphase resonant converter modulator system for the Spallation Neutron Source linear accelerator," 21st International Linear Accelerator Conference (LINAC 2002), Gyeongju, Korea, August 19–23, 2002, Los Alamos National Laboratory report LA-UR-02-1912 (April 2002).

D.M. Rector, K.M. Carter, X. Yao, and J.S. George, "Optical imaging of fast, dynamic neurophysiological function," Optical Society of America Biomedical Topical Meetings and Exhibit, Miami Beach, Florida, USA, April 7–10, 2002, Los Alamos National Laboratory report LA-UR-02-0606 (February 2002).

D.B. Reisenfeld, J.E. Nordholt, R.C. Wiens, S.P. Gary, and J.T. Steinberg, "Deep Space 1 encounter with comet Borrelly: Composition measurements by the PEPE ion mass spectrometer," 27th General Assembly of the European Geophysical Society, Nice, France, April 21–26, 2002, Los Alamos National Laboratory report LA-UR-02-0213 (January 2002).

W.J. Rider, J.R. Kamm, C.A. Zoldi, and C.D. Tomkins, "Statistical comparison between experiments and numerical simulations of shock-accelerated gas cylinders," 5th World Congress on Computational Mechanics, Vienna, Austria, July 7–12, 2002, Los Alamos National Laboratory report LA-UR-02-2212 (April 2002).

W.J. Rider, J.R. Kamm, C.D. Tomkins, C.A. Zoldi, M. Marr-Lyon, K.P. Prestridge, P.M. Rightley, and R.F. Benjamin, "Effects of numerical methods on comparison between experiments and simulations of shock-accelerated mixing," 3rd International Symposium on Finite Volumes for Complex Applications: Problems and Perspectives, Porquerolles, France, June 24–28, 2002, Los Alamos National Laboratory report LA-UR-02-1514 (March 2002).

E.A. Rose, R.R. Bartsch, D.M. Custer, C.A. Ekdahl, Jr., R.R. Montoya, and J.R. Smith, "Fast solenoid magnet at DARHT incorporated into a beam emittance diagnostic," 14th International Conference on High-Power Particle Beams (BEAMS-2002) and 5th International Conference on Dense Z-Pinches (DZP 2002), Albuquerque, New Mexico, USA, July 23–28, 2002, Los Alamos National Laboratory report LA-UR-02-3838 (June 2002).

E.A. Rose, R.R. Bartsch, D.M. Custer, C.A. Ekdahl, Jr., R.R. Montoya, and J.R. Smith, "Low inductance pulser system drives a fast magnet at DARHT," 2002 International Power Modulator Conference and High Voltage Workshop, Hollywood, California, USA, June 30–July 3, 2002, Los Alamos National Laboratory report LA-UR-02-3945 (June 2002).

C. Rousculp and D.C. Barnes, "Computational MHD on Lagrangian, staggered grids," 14th International Conference on High-Power Particle Beams (BEAMS 2002) and 5th International Conference on Dense Z-Pinches (DZP 2002), Albuquerque, New Mexico, USA, July 23–28, 2002, Los Alamos National Laboratory report LA-UR-02-0281 (January 2002).

W.P. Roybal, "Magnetic particle recognition using magnetic resonance imaging," Los Alamos National Laboratory Symposium 2002, Los Alamos, New Mexico, USA, July 29–30, 2002, Los Alamos National Laboratory report LA-UR-02-4309 (July 2002).

T.W.L. Sanford, D.L. Peterson, R.W. Lemke, R.C. Mock, G.A. Chandler, J.P. Chittenden, R.E. Chrien, G.C. Idzorek, R.G. Watt, R.J. Leeper, T.A. Mehlhorn, T.J. Nash, and C.L. Ruiz, "Characteristics and dynamics of a 215-eV dynamic-hohlraum x-ray source on Z," Beams DZP Conference, Albuquerque, New Mexico, USA, June 23–28, 2002 (paper originated at Sandia National Laboratories).

T.W.L. Sanford, R.W. Lemke, R.C. Mock, B.V. Oliver, G.A. Chandler, R.J. Leeper, T.A. Mehlhorn, T.J. Nash, C.L. Ruiz, E.M. Waisman, D.L. Peterson, R.E. Chrien, G.C. Idzorek, R.G. Watt, N.F. Roderick, and M.G. Haines, "Unexpected Up/Down asymmetry measured in axial radiation exiting high-temperature dynamic-hohlraum x-ray source" 44th Annual Meeting of the American Physical Society Division of Plasma Physics, Orlando, Florida, USA, November 11–15, 2002 (paper originated at Sandia National Laboratories).

T.W.L. Sanford, R.C. Mock, G.A. Chandler, R.J. Leeper, R.W. Lemke, T.A. Mehlhorn, T.J. Nash, G.S. Sarkisov, E. Waisman, R.E. Chrien, G.C. Idzorek, D.L. Peterson, R.G. Watt, M.G. Haines, and D. Mosher, "Top/Bottom asymmetry measured in axial radiation exiting Z-pinch driven dynamic hohlraum x-ray source on Z," International Conference on Plasma Science, May 26–30, 2002 Banff, Alberta, Canada (paper originated at Sandia National Laboratories).

M.M. Schauer and D.C. Barnes, "Ion trapping in the virtual cathode of PFX-1," 44th Annual Meeting of the American Physical Society Division of Plasma Physics, Orlando, Florida, USA, November 11–15, 2002, Los Alamos National Laboratory report LA-UR-02-4406 (July 2002).

D.M. Schmidt, D.M. Ranken, J.S. George, and C.C. Wood, "Magnetic resonance imaging and magnetoencepholography data," 13th International Conference on Biomagnetism, Jena, Germany August 10–14, 2002, Los Alamos National Laboratory report LA-UR-02-5094 (August 2002).

L. Schultz, K.K. Kwiatkowski, C.L. Morris, A. Saunders, G.W. Hart, G.E. Hogan, F.E. Merrill, and K.B. Morley, "A narrow-gap ion chamber for beam motion correction in proton radiography experiments," 2002 Simulation and Analysis Workshop, Los Alamos, New Mexico, USA, August 5–9, 2002, Los Alamos National Laboratory report LA-UR-02-4822 (July 2002).

J.M. Scott, M.M Balkey, C.W. Barnes, S.H. Batha, N.D. Delamater, G.R. Magelssen, and N.E. Lanier, "RAGE simulations of single-mode nonlinear Richtmyer-Meshkov growth in convergent geometry," 44th Annual Meeting of the American Physical Society Division of Plasma Physics, Orlando, Florida, USA, November 11–15, 2002, Los Alamos National Laboratory report LA-UR-02-4541 (July 2002).

D.B. Sinars, M.E. Cuneo, E. Waisman, D.F. Wenger, J.L. Porter, R.A. Vesey, R.G. Adams, G.C. Idzorek, P.K. Rambo, L.E. Ruggles, W.W. Simpson, and I.C. Smith, "Radiation pulse-shaping techniques for Z-pinch driven hohlraums on the Z accelerator," 44th Annual Meeting of the American Physical Society Division of Plasma Physics, Orlando, Florida, USA, November 11–15, 2002 (paper originated at Sandia National Laboratories).

G. Sinnis, "Results form the Milagro All-Sky TeV Gamma Ray Observatory," *Proceedings of the Universe Viewed in Gamma Rays* (Universal Academy Press, Tokyo, Japan, 2002), S13, pp. 1–7.

G. Sinnis, "The Milagro all-sky TeV gamma ray observatory," Society for Optical Engineering Astronomical Telescopes and Instrumentation Meeting, Waikoloa, Hawaii, USA, August 22–28, 2002, Los Alamos National Laboratory report LA-UR-02-4898 (August 2002).

J.R. Smith, R.L. Carlson, R.D. Fulton, J.R. Chavez, W.L. Coulter, W.A. Gibson, T.B. Helvin, D.J. Henderson, C.V. Mitton, E.C. Ormond, P.A. Ortega, R.N. Ridlon, and A.R. Valerio, "Performance of the Cygnus x-ray source," 14th International Conference on High-Power Particle Beams (BEAMS 2002) and 5th International Conference on Dense Z-Pinches (DZP 2002), Albuquerque, New Mexico, USA, July 23–28, 2002, Los Alamos National Laboratory report LA-UR-02-0429 (January 2002).

J.R. Smith, R.L. Carlson, R.D. Fulton, J.R. Chavez, W.L. Coulter, W.A. Gibson, T.B. Helvin, D.J. Henderson, C.V. Mitton, I. Molina, E.C. Ormond, P.A. Ortega, R.N. Ridlon, and A.R. Valerio, "Performance of the Cygnus x-ray source," 29th IEEE International Conference on Plasma Science (ICOPS 2002), Banff, Alberta, Canada, May 26–30, 2002, Los Alamos National Laboratory report LA-UR-02-2969 (May 2002).

G.J. Stephenson, Jr., J.T. Goldman, B.H.T. McKellar, and M. Garbutt, "NUTEV constraints on effects in tritium beta decay," 2002 April Meeting of the American Physical Society (with the High-Energy Astrophysics Division of the American Astronomical Society), Albuquerque, New Mexico, USA, April 20–23, 2002, Los Alamos National Laboratory report LA-UR-02-3694 (June 2002).

G.J. Stephenson, Jr., J.T. Goldman, B.H.T. McKellar, and M. Garbutt, "Neutrino oscillations and the Pascho-Wolfenstein ratio," 2002 April Meeting of the American Physical Society (with the High-Energy Astrophysics Division of the American Astronomical Society), Albuquerque, New Mexico, USA, April 20–23, 2002, Los Alamos National Laboratory report LA-UR-02-3695 (June 2002).

D.C. Swift, D.L. Paisley, G.A. Kyrala, A.A. Hauer, and G.J. Ackland, "Multiscale modeling of beryllium: Quantum mechanics and laser-driven shock experiments using novel diagnostics," International Workshop on New Models and Hydrocodes for Shock Wave Processes in Condensed Matter (NMHSWPCM), Edinburgh, Scotland, May 19–24, 2002, Los Alamos National Laboratory report LA-UR-02-2700 (May 2002).

D.C. Swift and S.J. White, "Links between detonation wave propagation and reactive flow models," 12th International Detonation Symposium, San Diego, California, USA, August 11–16, 2002, Los Alamos National Laboratory report LA-UR-02-4998 (August 2002).

D.C. Swift, R.N. Mulford, R.E. Winter, P. Taylor, D. Salisbury, and E.J. Harris, "Mesoscale modeling of reaction in HMX-based explosives," 12th International Detonation Symposium, San Diego, California, USA, August 11–16, 2002, Los Alamos National Laboratory report LA-UR-02-4603 (July 2002).

J.M. Taccetti, T.P. Intrator, S. Zhang, G.A. Wurden, R.J. Maqueda, D. Begay, E.R. Midnardot, W.J. Waganaar, R. Siemon, M.G. Tuszewski, P.G. Sanchez, J.H. Degnan, W.R. Sommars, C. Grabowski, and E. Ruden, "High-density FRC formation studies of FRX-L," 44th Annual Meeting of the American Physical Society Division of Plasma Physics, Orlando, Florida, USA, November 11–15, 2002, Los Alamos National Laboratory report LA-UR-02-4604 (July 2002).

J.M. Taccetti, T.P. Intrator, S. Zhang, G.A. Wurden, R.J. Maqueda, D. Begay, E.R. Midnardot, W.J. Waganaar, R. Siemon, M.G. Tuszewski, P.G. Sanchez, J.H. Degnan, W.R. Sommars, C. Grabowski, and E. Ruden, "Overview of high-density FRC research on FRX-L at Los Alamos," 2002 USA-Japan Workshop on New Directions in Controlling and Sustainning Compact Toroids, Osaka, Japan, September 9–12, 2002, Los Alamos National Laboratory report LA-UR-02-5224 (August 2002).

H.L. Teslow, H.W. Herrmann, J. Park, and I. Henins, "Atmospheric-pressure plasma jet for actinide decontamination," Los Alamos National Laboratory Symposium 2002, Los Alamos, New Mexico, USA, July 29–30, 2002, Los Alamos National Laboratory report LA-UR-02-4327 (July 2002).

M.C. Thompson, R.E. Reinovsky, P.G. Sanchez, and J.C. Cochrane, "Atlas: A new high performance system and the optical-transponder DC probe as applied to bank controls instrumentation," International Power Modulator Conference and High Voltage Workshop 2002, Hollywood California, USA, June 30–July 3, 2002, Los Alamos National Laboratory report LA-UR-02-1258 (March 2002).

T.E. Tierney, J.F. Benage, D.S. Montgomery, M.S. Murillo, F.J. Wysocki, and R.P. Johnson, "Observation of anomalous broadening in moderately coupled, moderately collisional plasmas," International Conference on Strongly Coupled Coulomb Systems, Santa Fe, New Mexico, USA, September 3–7, 2002, Los Alamos National Laboratory report LA-UR-02-5281 (July 2002).

T.E. Tierney, J.F. Benage, Jr., D.S. Montgomery, M.S. Murillo, and F.J. Wysocki, "Anomalous broadening of IAW collective Thomson scattering signals," International Conference on Warm Dense Matter (ICWDM), Hamburg, Germany, June 3–5, 2002, Los Alamos National Laboratory report LA-UR-02-1522 (March 2002).

T.E. Tierney, J.F. Benage, Jr., D.S. Montgomery, M.S. Murillo, and F.J. Wysocki, "Technique for temperature and density measurements using collective Thomson scattering from Langmuir waves," 14th Topical Conference on High Temperature Plasma Diagnostics, Madison, Wisconsin, USA, July 8–11, 2002, Los Alamos National Laboratory report LA-UR-02-2861 (May 2002).

T.E. Tierney, J.F. Benage, Jr., D.S. Montgomery, M.S. Murillo, and F.J. Wysocki, "Collective Thomson scattering measurements of moderately coupled plasmas," American Physical Society Four Corners Section Meeting, Salt Lake City, Utah, USA, October 3–4, 2002, Los Alamos National Laboratory report LA-UR-02-3103 (May 2002).

T.E. Tierney, D.S. Montgomery, J.F. Benage, F.J. Wysocki, and M.S. Murillo, "Ion acoustic wave broadening observations in moderately coupled, moderately collisional plasmas," International Conference on Strongly Coupled Coulomb Systems, Santa Fe, New Mexico, USA, September 2–6, 2002, Los Alamos National Laboratory report LA-UR-02-6766 (October 2002).

C.D. Tomkins, M. Marr-Lyon, K.P. Prestridge, P.M. Rightley, R.F. Benjamin, and P. Vorobieff, "Planar concentration and velocity measurements of two interacting shock-accelerated gas cylinders," 55th Annual Meeting of the Division of Fluid Dynamics of the American Physical Society, Dallas, Texas, USA, November 24–26, 2002, Los Alamos National Laboratory report LA-UR-02-4865 (July 2002).

E. Torbert, T.P. Intrator, I. Furno, and C.S. Carey, "RSX experimental data," Los Alamos National Laboratory Symposium 2002, Los Alamos, New Mexico, USA, July 29–30, 2002, Los Alamos National Laboratory report LA-UR-02-4326 (July 2002).

E. Torbert, T.P. Intrator, I. Furno, J.K. Campbell, C.S. Carey, W.J. Fienup, and C.A. Werley, "Overview of diagnostic system on the reconnection scaling experiment at LANL," 44th Annual Meeting of the American Physical Society Division of Plasma Physics, Orlando, Florida, USA, November 11–15, 2002, Los Alamos National Laboratory report LA-UR-02-4605 (July 2002).

S. Vogel, M.A. Bourke, V. Yuan, J. Huang, W. Poole, P.J. Jacques, and H.G. Priesmeyer, "*In situ* real-time neutron transmission study of bainite formation," 14th Annual Rio Grande Regional Symposium on Advanced Materials Albuquerque, New Mexico, USA, October 21, 2002, Los Alamos National Laboratory report LA-UR-02-5817 (September 2002).

W.J. Waganaar, T.P. Intrator, J.M. Taccetti, P. Sanchez, J.C. Cochrane, M.C. Thompson, and C. Grabowski, "Design and performance of the prefire detection system for the FRX-L main capacitor bank," 44th Annual Meeting of the American Physical Society Division of Plasma Physics, Orlando, Florida, USA, November 11–15, 2002, Los Alamos National Laboratory report LA-UR-02-4704 (July 2002).

R.G. Watt, N.D. Delamater, W.S. Varnum, P.A. Amendt, G. Dimonte, and H.F. Robey, "Further investigations of indirectly drived double shell caps," 32nd Anomalous Absorption Conference Oahu, Hawaii, USA, July 21–26, 2002, Los Alamos National Laboratory report LA-UR-02-2556 (May 2002).

K. Werley and W.J. Fienup, "A computer controlled three dimentional probe drive system for the magnetic reconnection scaling experiment," Los Alamos National Laboratory Symposium 2002, Los Alamos, New Mexico, USA, July 29–30, 2002, Los Alamos National Laboratory report LA-UR-02-4295 (July 2002).

R.C. Wiens, J.E. Nordholt, D.B. Reisenfeld, and S.P. Gary, "Ion composition of comet 19P/Borrelly as measured by the PEPE ion mass spectrometer," American Geophysical Union 2002 Fall Meeting, San Francisco, California, USA, December 6–10, 2002, Los Alamos National Laboratory report LA-UR-02-5702 (September 2002).

W.S. Wilburn, "Neutron beta decay studies with a pulsed cold neutron beam," Workshop on Low-Energy Precision Electroweak Measurements, Vancouver, British Columbia, Canada, April 4–6, 2002, Los Alamos National Laboratory report LA-UR-02-2455 (April 2002).

B.H. Wilde, J.A. Cobble, M.L. Gittings, J.M. Foster, P.A. Rosen, T.S. Perry, M.J. Edwards, and B. Remington, "Supersonic jet experiments at past/present/future laser and pulsed-power facilities (U)," Meeting of the Joint Working Group (USA-UK) (JOWOG 37), Livermore, California, USA, January 2002, Los Alamos National Laboratory controlled publication LA-CP-02-0029 (January 2002).

B.H. Wilde, J.M. Foster, P.A. Rosen, T.S. Perry, M.J. Edwards, M.L. Gittings, B. Remington, J.A. Cobble, and M. Fell, "Simulations of laser and pulsed-power supersonic jet experiments for radiation-hydrodynamic code validation (U)," 4th International Conference on High-Energy-Density Laboratory Astrophysics, Ann Arbor, Michigan, USA, February 23–25, 2002, Los Alamos National Laboratory report LA-UR-02-0782 (February 2002).

D.C. Wilson, C.R. Christensen, T.J. Murphy, G.L. Morgan, M.D. Wilke, F.H. Cverna, J.M. Mack, Jr., C.S. Young, J. Langenbrunner, E.L. Vold, and P.S. Ebey, "Experiment to study the combined effects of mix and gas cavity asymmetry," CEA/NNSA Technology Collaboration Meeting, Livermore, California, USA, February 2002, Los Alamos National Laboratory report LA-UR-02-0746 (February 2002).

D.C. Wilson, C.R. Christensen, G.L. Morgan, M.D. Wilke, P.A. Bradley, and P.L. Gobby, "Goals and design of a neutron pinhole imaging system for the National Ignition Facility," 14th Topical Conference on High Temperature Plasma Diagnostics, Madison, Wisconsin, USA, July 8–11, 2002, Los Alamos National Laboratory report LA-UR-02-2506 (April 2002).

D.C. Wilson, C.R. Christensen, G.L. Morgan, M.D. Wilke, P.A. Bradley, and P.L. Gobby, "Goals for and design of a neutron pinhole imaging system for ignition capsules," 14th Topical Conference on High-Temperature Plasma Diagnostics, Madison, Wisconsin, USA, July 8–11, 2002, Los Alamos National Laboratory report LA-UR-02-4184 (July 2002).

D.C. Wilson, C.R. Christensen, P.A. Bradley, C.W. Barnes, P.E. Ebey, P.L. Gobby, P.E. Littleton, G.L. Morgan, T.A. Ortiz, M.D. Wilke, V.Y. Glebov, F.J. Marshall, and C. Stoeckl, "Modeling fuel/shell mixing in asymmetrically driven direct drive ICF implosions," 44th Annual Meeting of the American Physical Society Division of Plasma Physics, Orlando, Florida, USA, November 11–15, 2002, Los Alamos National Laboratory report LA-UR-02-4617 (July 2002).

W.M. Wood, G.R. Magelssen, J. Abdallah, S.E. Caldwell, D.J. Hoarty, C.C. Smith, A.M. Dunne, and E. Clark, "Point backlighter radiography of driven hahlraums on the Omega laser: Data and methods (U)," Meeting of the Joint Working Group (USA-UK) (JOWOG 37), Livermore, California, USA, January 2002, Los Alamos National Laboratory controlled publication LA-CP-02-0038 (January 2002).

W.M. Wood, G.R. Magelssen, J. Abdallah, S.E. Caldwell, D.J. Hoarty, C.C. Smith, A.M. Dunne, and E. Clark, "Time-resolved temperature measurements of driven hahlraums using spectroscopic techniques developed at AWE (U)," Meeting of the Joint Working Group (USA-UK) (JOWOG 37), Livermore, California, USA, January 2002, Los Alamos National Laboratory controlled publication LA-CP-02-0037 (January 2002).

G.A. Wurden, C. Bass, S.A. Devries, J.R. Faulkner, and F.J. Wysocki, "Thomson scattering implementation on the FRX-L field configuration," 44th Annual Meeting of the American Physical Society Division of Plasma Physics, Orlando, Florida, USA, November 11–15, 2002, Los Alamos National Laboratory report LA-UR-02-4607 (July 2002).

F.J. Wysocki, J.F. Benage, Jr., N.D. Delamater, D.S. Montgomery, M.S. Murillo, J.P. Roberts, and A.J. Taylor, "An experiment to measure the electron-ion thermal equilibration rate in a strongly coupled plasma," 29th IEEE International Conference on Plasma Science (ICOPS 2002), Banff, Alberta, Canada, May 26–30, 2002, Los Alamos National Laboratory report LA-UR-02-3052 (May 2002).

F.J. Wysocki, J.F. Benage, Jr., N.D. Delamater, D.S. Montgomery, M.S. Murillo, J.P. Roberts, and A.J. Taylor, "An experiment to measure the electron-ion thermal equillibration rate in a strongly coupled plasma," 2002 International Conference on Strongly Coupled Coulomb Systems, Santa Fe, New Mexico, USA, September 2–6, 2002, Los Alamos National Laboratory report LA-UR-02-4493 (July 2002).

X. Yao and A. Castro, "Microfabrication inside capillaries with electrophoretically delivered particles using optical tweezers," 2002 Optical Society of America Annual Meeting and Exhibit, Orlando, Florida, USA, September 29–October 3, 2002, Los Alamos National Laboratory report LA-UR-02-5833 (September 2002).

X. Yao, D.M. Rector, and J.S. George, "Optical lever displacement from nerve bundles," Optical Society of America Biomedical Topical Meetings and Exhibit, Miami Beach, Florida, USA, April 7–10, 2002, Los Alamos National Laboratory report LA-UR-02-1802 (March 2002).

Appendix B: Publications—2002 Conference Papers

G.J. Yates and T.E. McDonald, "Advanced technology imaging sensor development (fast CCD sensors)," Meeting of the Joint Working Group (USA-UK) (JOWOG 32P), Livermore, California, USA, April 22–25, 2002, Los Alamos National Laboratory report LA-UR-02-1975 (April 2002).

G.J. Yates, M.D. Wilke, and N.S.P. King, "Fast readout shuttered cameras for imaging diagnostics," Meeting of the Joint Working Group (USA-UK) (JOWOG 32P), Livermore, California, USA, April 22–25, 2002, Los Alamos National Laboratory report LA-UR-02-2370 (April 2002).

S. Zhang, G.A. Wurden, J.M. Taccetti, T.P. Intrator, P. Sanchez, C.M. Bass, C. Carey, R.M. Renneke, M.S. Harris, and S.A. Devries, "Diagnosing the field reversed configuration plasmas on FRX-L," 44th Annual Meeting of the American Physical Society Division of Plasma Physics, Orlando, Florida, USA, November 11–15, 2002, Los Alamos National Laboratory report LA-UR-02-4672 (July 2002).

C.A. Zoldi, K.P. Prestridge, C.D. Tomkins, M. Marr-Lyon, P.M. Rightley, P. Vorobieff, and R.F. Benjamin, "An experimental and computational investigation of a shock-accelerated heavy gas cylinder," Nuclear Explosives Computional Design Conference (NECDC 2002), Monterey, California, USA, October 22–25, 2002, Los Alamos National Laboratory report LA-UR-02-3196 (May 2002).

C.A. Zoldi, K.P. Prestridge, C.D. Tomkins, M. Marr-Lyon, P.M. Rightley, and R.F. Benjamin, "An experimental and computational study of a shock-accelerated heavy gas cylinder," 55th Annual Meeting of the Division of Fluid Dynamics of the American Physical Society Dallas, Texas, USA, November 24–26, 2002, Los Alamos National Laboratory report LA-UR-02-4855 (July 2002).

2003 Journal Articles

K. Adcox, S.S. Adler, M. Aizama *et al.* (including Los Alamos scientists: J.B. Archuleta, J.R. Archuleta, V. Armijo, P.D. Barnes, M.J. Bennett, J.G. Boissevain, M.L. Brooks, M.M. Cafferty, T.A. Carey, M.S. Chung, D.J. Clark, R. Conway, R. Cunningham, M.A. Echave, S. Hahn, A.G. Hansen, G.W. Hart, J. Kapustinsky, D.M. Lee, M.J. Leitch, M.X. Liu, J.D. Lopez, X.B. Martinez, P.L. McGaughey, R.E. Mischke, B.C. Montoya, J.M. Moss, F.M.M. Murray, A.P.T. Palounek, S.H. Robinson, R. Roth, B.R. Schlei, T. Shiina, J. Simon-Gillo, G.D. Smith, W.E. Sondheim, J.P. Sullivan, G.W. Thornton, R.S. Towell, H.W. van Hecke, and B.G. Wong-Swanson), "PHENIX detector overview," *Nuclear Instruments and Methods in Physics Research Section A-Accelerators Spectrometers Detectors and Associated Equipment* **499**, 469–479 (2003).

K. Adcox, S.S. Adler, N.N. Ajitanand *et al.* (including Los Alamos scientists: P.D. Barnes, M.J. Bennett, M.L. Brooks, T.A. Carey, M.S. Chung, A.G. Hansen, W.W. Kinnison, D.M. Lee, M.J. Leitch, M.X. Liu, P.L. McGaughey, R.E. Mischke, J.M. Moss, A.P.T. Palounek, B.R. Schlei, T. Shiina, J. Simon-Gillo, J.P. Sullivan, R.S. Towell, and H.W. van Hecke), "Centrality dependence of the high p_T charged hadron suppression in Au + Au collisions at $\sqrt{S_{NN}}$ = 130 GeV," *Physics Letters B* **561**, 82–92 (2003).

S.S. Adler, S. Afanasiev, C. Aidala *et al.* (including Los Alamos scientists: P.D. Barnes, J.G. Boissevain, M.L. Brooks, J.M. Burward-Hoy, A.G. Hansen, G.J. Kunde, D.M. Lee, M.J. Leitch, M.X. Liu, P.L. McGaughey, J.M. Moss, A.P.T. Palounek, D. Silvermyr, W.E. Sondheim, J.P. Sullivan, and H.W. van Hecke), "Absence of suppression in particle production at large transverse momentum in $\sqrt{S_{NN}}$ = 200 GeV d + Au collisions," *Physical Review Letters* **91**, 072303 (2003).

S.S. Adler, S. Afanasiev, C. Aidala *et al.* (including Los Alamos scientists: P.D. Barnes, J.G. Boissevain, M.L. Brooks, A.G. Hansen, C.H. Kuberg, D.M. Lee, M.J. Leitch, M.X. Liu, P.L. McGaughey, R.E. Mischke, J.M. Moss, A.P.T. Palounek, J.-C. Peng, M.R. Shaw, T. Shiina, D. Silvermyr, W.E. Sondheim, J.P. Sullivan, J.D. Tepe, and H.W. van Hecke), "Midrapidity neutral-pion production in proton-proton collisions at $\sqrt{S}$ = 200 GeV," *Physical Review Letters* **91**, 241803 (2003).

S.S. Adler, S. Afanasiev, C. Aidala *et al.* (including Los Alamos scientists: P.D. Barnes, J.G. Boissevain, M.L. Brooks, A.G. Hansen, C.H. Kuberg, D.M. Lee, M.J. Leitch, M.X. Liu, P.L. McGaughey, R.E. Mischke, J.M. Moss, A.P.T. Palounek, J.-C. Peng, M.R. Shaw, T. Shiina, D. Silvermyr, W.E. Sondheim, J.P. Sullivan, J.D. Tepe, and H.W. van Hecke), "Suppressed π^0 production at large transverse momentum in central Au + Au collisions at $\sqrt{S_{NN}}$ = 200 GeV," *Physical Review Letters* **91**, 072301 (2003).

S.S. Adler, S. Afanasiev, C. Aidala *et al.* (including the Los Alamos scientists P.D. Barnes, J.G. Boissevain, M.L. Brooks, A.G. Hansen, C.H. Kuberg, D.M. Lee, M.J. Leitch, M.X. Liu, P.L. McGaughey, R.E. Mischke, J.M. Moss, A.P.T. Palounek, J.-C. Peng, M.R. Shaw, T. Shiina, D. Silvermyr, W.E. Sondheim, J.P. Sullivan, J.D. Tepe, and H.W. van Hecke), "Scaling properties of proton and antiproton production in $\sqrt{S_{NN}}$ = 200 GeV Au + Au collisions," *Physical Review Letters* **91**, 172301 (2003).

S.S. Adler, S. Afanasiev, C. Aidala *et al.* (including Los Alamos scientists: P.D. Barnes, J.G. Boissevain, M.L. Brooks, A.G. Hansen, C.H. Kuberg, D.M. Lee, M.J. Leitch, M.X. Liu, P.L. McGaughey, R.E. Mischke, J.M. Moss, A.P.T. Palounek, J.-C. Peng, M.R. Shaw, T. Shiina, D. Silvermyr, W.E. Sondheim, J.P. Sullivan, J.D. Tepe, and H.W. van Hecke), "Elliptic flow of identified hadrons in Au + Au collisions at $\sqrt{S_{NN}}$ = 200 GeV," *Physical Review Letters* **91**, 182301 (2003).

S.S. Adler, M. Allen, G. Alley *et al.* (including Los Alamos scientists: M.J. Bennett, J.G. Boissevain, T.A. Carey, S. Hahn, A.G. Hansen, B.V. Jacak, J. Kapustinsky, M.X. Liu, R.E. Mischke, T. Shiina, J. Simon-Gillo, G.D. Smith, J.P. Sullivan, and H.W. van Hecke), "PHENIX on-line systems," *Nuclear Instruments and Methods in Physics Research Section A-Accelerators Spectrometers Detectors and Associated Equipment* **499**, 560–592 (2003).

H. Akikawa, A. Al-Jamel, J.B. Archuleta *et al.* (including Los Alamos scientists: J.B. Archuleta, J.R. Archuleta, V. Armijo, P.D. Barnes, J.G. Boissevain, M.L. Brooks, M.M. Cafferty, T.A. Carey, D.J. Clark, M.A. Echave, G.W. Hart, W.W. Kinnison, D.M. Lee, M.J. Leitch, M.X. Liu, J.D. Lopez, X.B. Martinez, P.L. McGaughey, R.E. Mischke, B.C. Montoya, J.M. Moss, M.M. Murray, A.P.T. Palounek, S.H. Robinson, R. Roth, G.D. Smith, W.E. Sondheim, G.W. Thornton, R.S. Towell, and B.G. Wong-Swanson), "PHENIX muon arms," *Nuclear Instruments and Methods in Physics Research Section A-Accelerators Spectrometers Detectors and Associated Equipment* **499**, 537–548 (2003).

M. Allen, M.J. Bennett, M. Bobrek, J.B. Boissevain, S. Boose, E. Bosze, C. Britton, J. Chang, C.Y. Chi, M. Chiu, R. Conway, R. Cunningham, A. Denisov, A. Deshpande, M.S. Emery, A. Enokizono, N. Ericson, B. Fox, S.Y. Fung, P. Giannotti, T. Hachiya, A.G. Hansen, K. Homma, B.V. Jacak, D. Jaffe, J.H. Kang, J. Kapustinsky, S.Y. Kim, Y.G. Kim, T. Kohama, P.J. Kroon, W. Lenz, N. Longbotham, M. Musrock, T. Nakamura, H. Ohnishi, S.S. Ryu, A. Sakaguchi, R. Seto, T. Shiina, M. Simpson, J. Simon-Gillo, W.E. Sondheim, T. Sugitate, J.P. Sullivan, H.W. van Hecke, J.W. Walker, S.N. White, P. Willis, and N. Xu, "PHENIX inner detectors," *Nuclear Instruments and Methods in Physics Research Section A-Accelerators Spectrometers Detectors and Associated Equipment* **499**, 549–559 (2003).

Appendix B: Publications—2003 Journal Articles

P.L. Anthony, R.G. Arnold, T. Averett, H.R. Band, N. Benmouna, W. Boeglin, H. Borel, P.E. Bosted, S.L. Bultmann, G.R. Court, D. Crabb, D. Day, P. Decowski, P. DePietro, H. Egiyan, R. Erbacher, R. Erickson, R. Fatemi, E. Frlez, K.A. Griffioen, C. Harris, E.W. Hughes, C. Hyde-Wright, G. Igo, J. Johnson, P. King, K. Kramer, S.E. Kuhn, D. Lawrence, Y. Liang, R. Lindgren, R.M. Lombard-Nielsen, P. McKee, D.E. McNulty, W. Meyer, G.S. Mitchell, J. Mitchell, M. Olson, S. Penttilä, G.A. Peterson, R. Pitthan, D. Pocanic, R. Prepost, C. Prescott, B.A. Raue, D. Reyna, P. Ryan, L.S. Rochester, S. Rock, O. Rondon-Aramayo, F. Sabatie, T. Smith, L. Sorrell, S. St Lorant, Z. Szalata, Y. Terrien, A. Tobias, T. Toole, S. Trentalange, F.R. Wesselmann, T.R. Wright, M. Zeier, H. Zhu, B. Zihlmann, and E. Collaboration, "Precision measurement of the proton and deuteron spin structure functions g_2 and asymmetries A_2," *Physics Letters B* **553**, 18–24 (2003).

S.H. Aronson, J. Bowers, J. Chiba, G. Danby, A. Drees, O. Fackler, A. Franz, J.P. Freidberg, W. Guryn, A. Harvey, T. Ichihara, J. Jackson, R. Jayakumar, S. Kahn, V. Kashikhin, P.J. Kroon, M. Libkind, M.D. Marx, W.Z. Meng, F. Messer, S. Migluolio, I.D. Ojha, R. Prigl, G. Riabov, R. Ruggiero, N. Saito, R. Schleuter, Y. Severgin, A. Shajii, V. Shangin, T.K. Shea, W.E. Sondheim, K.H. Tanaka, R. Thern, J.H. Thomas, V. Vasiliev, C. Velissaris, and R. Yamamoto, "PHENIX magnet system," *Nuclear Instruments and Methods in Physics Research Section A-Accelerators Spectrometers Detectors and Associated Equipment* **499**, 480–488 (2003).

R. Atkins, W. Benbow, D. Berley, E. Blaufuss, J. Bussons, D.G. Coyne, R.S. Delay, T. DeYoung, B.L. Dingus, D.E. Dorfan, R.W. Ellsworth, A. Falcone, L. Fleysher, R. Fleysher, G. Gisler, M.M. Gonzalez, J.A. Goodman, T.J. Haines, E. Hays, C.M. Hoffman, L.A. Kelley, R.W. Laird, J. McCullough, J.E. McEnery, R.S. Miller, A.I. Mincer, M.F. Morales, P. Nemethy, D. Noyes, J.M. Ryan, F.W. Samuelson, M. Schneider, B. Shen, A. Shoup, G. Sinnis, A.J. Smith, G.W. Sullivan, O.T. Tumer, K. Wang, M. Wascko, D.A. Williams, S. Westerhoff, M.E. Wilson, X. Xu, and G.B. Yodh, "Observation of TeV gamma rays from the Crab Nebula with Milagro using a new background rejection technique," *Astrophysical Journal* **595**, 803–811 (2003).

R. Atkins, W. Benbow, D. Berley, M.L. Chen, D.G. Coyne, B.L. Dingus, D.E. Dorfan, R.W. Ellsworth, D. Evans, A. Falcone, L. Fleysher, R. Fleysher, G. Gisler, M.M. Gonzalez, J.A. Goodman, T.J. Haines, C.M. Hoffman, S. Hugenberger, L.A. Kelley, S. Klein, I. Leonor, J.F. McCullough, J.E. McEnery, R.S. Miller, A.I. Mincer, M.F. Morales, P. Nemethy, J.M. Ryan, F.W. Samuelson, B. Shen, A. Shoup, C. Sinnis, A.J. Smith, G.W. Sullivan, T. Tumer, K. Wang, M.O. Wascko, S. Westerhoff, D.A. Williams, T. Yang, and G.B. Yodh, "The high-energy gamma-ray fluence and energy spectrum of GRB 970417A from observations with Milagrito," *Astrophysical Journal* **583**, 824–832 (2003).

S.H. Batha, C.K. Barnes, and C.R. Christensen, "Backlighter predictive capability," *Review of Scientific Instruments* **74**, 2174–2177 (2003).

A.R. Berdoz, J. Birchall, J.B. Bland, J.D. Bowman, J.R. Campbell, G.H. Coombes, C.A. Davis, A.A. Green, P.W. Green, A.A. Hamian, R. Helmer, S. Kadantsev, Y. Kuznetsov, L. Lee, C.D.P. Levy, R.E. Mischke, N.T. Okumusoglu, S.A. Page, W.D. Ramsay, S.D. Reitzner, T. Ries, G. Roy, A.M. Sekulovich, J. Soukup, G.M. Stinson, T.J. Stocki, V. Sum, N.A. Titov, W.T.H. van Oers, R.J. Woo, S. Zadorozny, A.N. Zelenski, and T.E. Collaboration, "Parity violation in proton-proton scattering at 221 MeV," *Physical Review C* **68**, 034004 (2003).

M.A. Betemps, M.B.G. Ducati, M.V.T. Machado, and J. Raufeisen, "Investigating the Drell-Yan transverse momentum distribution in the color dipole approach," *Physical Review D* **67**, 114008 (2003).

L.M.A. Bettencourt and G.J. Stephens, "Vortex description of the first-order phase transition in the two-dimensional Abelian-Higgs model," *Physical Review E* **67**, 066105 (2003).

T.C. Black, P.R. Huffman, D.L. Jacobson, W.M. Snow, K. Schoen, M. Arif, H. Kaiser, S.K. Lamoreaux, and S.A. Werner, "Precision neutron interferometric measurement of the Nd coherent neutron scattering length and consequences for models of three-nucleon forces," *Physical Review Letters* **90**, 192502 (2003).

K.N. Borozdin, G.E. Hogan, C. Morris, W.C. Priedhorsky, A. Saunders, L.J. Schultz, and M.E. Teasdale, "Surveillance: Radiographic imaging with cosmic-ray muons," *Nature* **422**, 277–277 (2003).

M.G. Boulay, "Event reconstruction in the Sudbury Neutrino Observatory," *Nuclear Physics B-Proceedings Supplements* **118**, 443–443 (2003).

T.J. Bowles, "A national underground science and engineering laboratory," *International Journal of Modern Physics A* **18**, 4129–4133 (2003).

P.A. Bradley, D.C. Wilson, F.J. Swenson, and G.L. Morgan, "ICF ignition capsule neutron, gamma ray, and high energy x-ray images," *Review of Scientific Instruments* **74**, 1824–1827 (2003).

A.C. Bruno, M.A. Espy, D.D. Clark, A.N. Matlashov, and R.H. Kraus, "Digital spatial filter made from a SQUID array," *IEEE Transactions on Applied Superconductivity* **13**, 779–782 (2003).

R.L. Burman and W.C. Louis, "Neutrino physics at meson factories and spallation neutron sources," *Journal of Physics G-Nuclear and Particle Physics* **29**, 2499–2512 (2003).

C.E. Bush, M.G. Bell, R.E. Bell, J. Boedo, E.D. Fredrickson, S.M. Kaye, S. Kubota, B.P. LeBlanc, R. Maingi, R.J. Maqueda, S.A. Sabbagh, V.A. Soukhanovskii, D. Stutman, D.W. Swain, J.B. Wilgen, S.J. Zweben, W.M. Davis, D.A. Gates, D.W. Johnson, R. Kaita, H.W. Kugel, K.C. Lee, D. Mastrovito, S. Medley, J.E. Menard, D. Mueller, M. Ono, F. Paoletti, H. Park, S.J. Paul, Y.K.M. Peng, R. Raman, P.G. Roney, A.L. Roquemore, C.H. Skinner, E.J. Synakowski, G. Taylor, and N. Team, "H-mode threshold and dynamics in the National Spherical Torus Experiment," *Physics of Plasmas* **10**, 1755–1764 (2003).

W.T. Buttler, S.K. Lamoreaux, J.R. Torgerson, G.H. Nickel, C.H. Donahue, and C.G. Peterson, "Fast, efficient error reconciliation for quantum cryptography," *Physical Review A* **67**, 052303 (2003).

S.E. Caldwell, R.R. Berggren, B.A. Davis, S.C. Evans, J.R. Faulkner, J.A. Garcia, R.L. Griffith, D.K. Lash, R.A. Lerche, J.M. Mack, G.L. Morgan, K.J. Moy, J.A. Ortel, R.E. Sturges, and C.S. Young, "Observation of D-T fusion gamma rays (invited)," *Review of Scientific Instruments* **74**, 1837–1841 (2003).

C. Carr, D. Graham, J.C. Macfarlane, and G.B. Donaldson, "HTS SQUIDS for the nondestructive evaluation of composite structures," *Superconductor Science and Technology* **16**, 1387-1390 (2003).

T.H. Chang, M.E. Beddo, C.N. Brown, T.A. Carey, W.E. Cooper, C.A. Gagliardi, G.T. Garvey, D.F. Geesaman, E.A. Hawker, X.C. He, L.D. Isenhower, D.M. Kaplan, S.B. Kaufman, D.D. Koetke, P.L. McGaughey, W.M. Lee, M.J. Leitch, J.M. Moss, B.A. Mueller, V. Papavassiliou, J.C. Peng, P.E. Reimer, M.E. Sadler, W.E. Sondheim, P.W. Stankus, R.S. Towell, R.E. Tribble, M.A. Vasiliev, J.C. Webb, J.L. Willis, and G.R. Young, "J/ψ polarization in 800-GeV P-Cu interactions," *Physical Review Letters* **91**, 211801 (2003).

C.R. Christensen, C.W. Barnes, G.L. Morgan, M. Wilke, and D.C. Wilson, "First results of pinhole neutron imaging for inertial confinement fusion," *Review of Scientific Instruments* **74**, 2690–2694 (2003).

D.D. Clark, M.A. Espy, R.H. Kraus, A. Matlachov, and J.S. Lamb, "Weld quality evaluation using a high-temperature SQUID array," *IEEE Transactions on Applied Superconductivity* **13**, 235–238 (2003).

H.A. Davis, R.T. Olson, and D.C. Moir, "Neutral desorption from intense electron beam impact on solid surfaces," *Physics of Plasmas* **10**, 3351–3357 (2003).

F.S. Dietrich, J.D. Anderson, R.W. Bauer, S.M. Grimes, R.W. Finlay, W.P. Abfalterer, F.B. Bateman, R.C. Haight, G.L. Morgan, E. Bauge, J.P. Delaroche, and P. Romain, "Importance of isovector effects in reproducing neutron total cross section differences in the W isotopes," *Physical Review C* **67**, 044606 (2003).

P. Doe, H. Ejiri, S.R. Elliott, J. Engel, M. Finger, K. Fushimi, V. Gehman, A. Gorine, M. Greenfield, R. Hazama, K. Ichihara, T. Itahashi, P. Kavitov, V. Kekelidze, K. Kuroda, V. Kutsalo, K. Matsuoka, I. Manouilov, M. Nomachi, A. Para, A. RjazansTeV, R.G.H. Robertson, Y. Shichijo, L.C. Stonehill, T. Shima, G. Shirkov, A. Sissakian, Y. Sugaya, A. Titov, V. Vatulin, V. Voronov, O.E. Vilches, J.F. Wilkerson, D.I. Will, and S. Yoshida, "Neutrino studies in ^{100}Mo and MOON—Mo observatory of neutrinos," *Nuclear Physics A* **721**, 517C–520C (2003).

M.R. Dragowsky, A. Hime, J.J. Simpson, and S.N.O. Collaboration, "Neutron calibration for the Sudbury Neutrino Observatory," *Nuclear Physics B-Proceedings Supplements* **118**, 442–442 (2003).

A. Efimov, A.J. Taylor, F.G. Omenetto, J.C. Knight, W.J. Wadsworth, and P.S. Russell, "Phase-matched third harmonic generation in microstructured fibers," *Optics Express* **11**, 2567–2576 (2003).

S.R. Elliott, "Experiments for neutrinoless double-β decay," *International Journal of Modern Physics A* **18**, 4097–4111 (2003).

M.A. Espy, A.N. Matlachov, R.H. Kraus, and J.B. Betts, "SQUID noise as a function of temperature: A survey of three SQUIDs," *IEEE Transactions on Applied Superconductivity* **13**, 731–734 (2003).

A.Y. Faenov, T.A. Pikuz, V. Avrutin, N. Izyumskaya, L. Shabelnikov, E. Shulakov, and G.A. Kyrala, "Hard x-ray imaging using free-standing spherically bent crystals," *Review of Scientific Instruments* **74**, 2224–2227 (2003).

A. Falcone, R. Atkins, W. Benbow, D. Berley, M.L. Chen, D.G. Coyne, B.L. Dingus, D.E. Dorfan, R.W. Ellsworth, L. Fleysher, R. Fleysher, G. Gisler, J.A. Goodman, T.J. Haines, C.M. Hoffman, S. Hugenberger, L.A. Kelley, I. Leonor, J.F. McCullough, J.E. McEnery, R.S. Miller, A.I. Mincer, M.F. Morales, P. Nemethy, J.M. Ryan, B. Shen, A. Shoup, G. Sinnis, A.J. Smith, G.W. Sullivan, T. Tumer, K. Wang, M.O. Wascko, S. Westerhoff, D.A. Williams, T. Yang, and G.B. Yodh, "Observation of GeV Solar energetic particles from the 1997 November 6 event using Milagrito," *Astrophysical Journal* **588**, 557–565 (2003).

D.H. Froula, L. Divol, D.G. Braun, B.I. Cohen, G. Gregori, A. Mackinnon, E.A. Williams, S.H. Glenzer, H.A. Baldis, D.S. Montgomery, and R.P. Johnson, "Stimulated Brillouin scattering in the saturated regime," *Physics of Plasmas* **10**, 1846–1853 (2003).

S. Fukuda, Y. Fukuda, T. Hayakawa *et al.* (including Los Alamos scientist: T.J. Haines), "The Super-Kamiokande detector," *Nuclear Instruments and Methods in Physics Research Section A-Accelerators Spectrometers Detectors and Associated Equipment* **501**, 418–462 (2003).

Appendix B: Publications—2003 Journal Articles

I.G. Furno, T.P. Intrator, E. Torbert, C. Carey, M.D. Cash, J.K. Campbell, W.J. Fienup, C.A. Werely, G.A. Wurden, and G. Fiksel, "Reconnection scaling experiment: A new device for three-dimensional magnetic reconnection studies," *Review of Scientific Instruments* **74**(4), 2324 (2003).

I.G Furno, H. Weisen *et al.,* "Observation of inward and outward particle convection in the core of electron cyclotron heated and current driven plasmas in the Tokamak: A configuration variable," *Physics of Plasmas* **10**(6), 2422-2428 (2003).

C.A. Gagliardi, T.C. Awes, M.E. Beddo, M.L. Brooks, C.N. Brown, J.D. Bush, T.A. Carey, T.H. Chang, W.E. Cooper, G.T. Garvey, D.F. Geesaman, E.A. Hawker, X.C. He, L.D. Isenhower, D.M. Kaplan, S.B. Kaufman, P.N. Kirk, D.D. Koetke, G. Kyle, D.M. Lee, W.M. Lee, M.J. Leitch, N. Makins, P.L. McGaughey, J.M. Moss, B.A. Mueller, P.M. Nord, V. Papavassiliou, B.K. Park, J.C. Peng, G. Petitt, P.E. Reimer, M.E. Sadler, W.E. Sondheim, P.W. Stankus, T.N. Thompson, R.S. Towell, R.E. Tribble, M.A. Vasiliev, Y.C. Wang, Z.F. Wang, J.C. Webb, J.L. Willis, D.K. Wise, G.R. Young, and F.E.N. Collaboration, "Measurement of the absolute Drell-Yan dimuon cross sections in 800 GeV/*c pp* and *pd* collisions," *Nuclear Physics A* **721**, 344C–347C (2003).

Y. Gando, S. Fukuda, Y. Fukuda *et al.* (including Los Alamos scientist: T.J. Haines), "Search for $\overline{\nu}_e$ from the sun at Super-Kamiokande-I," *Physical Review Letters* **90**, 171302 (2003).

G.T. Garvey, and J.C. Peng, "Partonic energy loss and the Drell-Yan process," *Physical Review Letters* **90**, 092302 (2003).

V.N. Gavrin, J.N. Abdurashitov, T.J. Bowles, B.T. Cleveland, S.R. Elliott, S.V. Girin, V.V. Gorbachev, P.P. Gurkina, T.V. Ibragimova, A.V. Kalikhov, N.G. Khairnasov, T.V. Knodel, I.N. Mirmov, J.S. Nico, A.A. Shikhin, W.A. Teasdale, E.P. Veretenkin, V.M. Vermul, J.F. Wilkerson, V.E. Yants, G.T. Zatsepin, and S. Collaboration, "Measurement of the Solar neutrino capture rate in SAGE," *Nuclear Physics B-Proceedings Supplements* **118**, 39–46 (2003).

M.M. Gonzalez, B.L. Dingus, Y. Kaneko, R.D. Preece, C.D. Dermer, and M.S. Briggs, "A gamma-ray burst with a high-energy spectral component inconsistent with the synchrotron shock model," *Nature* **424**, 749–751 (2003).

M.E. Hayden, G. Archibald, P.D. Barnes, W.T. Buttler, D.J. Clark, M.D. Cooper, M. Espy, G.L. Greene, R. Golub, S.K. Lamoreaux, C. Lei, L.J. Marek, J.C. Peng, and S. Penttilä, "Neutron radiography of helium II," *Physica B-Condensed Matter* **329**, 236–237 (2003).

L. Heller, "Classical limit of demagnetization in a field gradient," *Physical Review B* **67**, 094417 (2003).

S.C. Hsu, and P.M. Bellan, "Experimental identification of the kink instability as a poloidal flux amplification mechanism for coaxial gun spheromak formation," *Physical Review Letters* **90**, 215002 (2003).

J. Huang, N. Hotta, K. Kasahara, I. Ohta, S. Ozawa, T. Saito, M. Shibata, X.W. Xu, and T. Yuda, "Primary proton spectrum around the knee deduced from the emulsion-chamber data obtained at Mts. Fuji and Kanbala," *Astroparticle Physics* **18**, 637–648 (2003).

T.P. Intrator, J.R. Myra *et al.,* "Three-dimensional finite-element model of the ion Bernstein wave antenna and excitation of coaxial electrostatic edge modes in the tokamak fusion test reactor," *Nuclear Fusion* **43**(7), 531 (2003).

T.P. Intrator, J.R. Myra, and D.A. D'Ippolito, "Three-dimensional finite-element model of the ion Bernstein wave antenna and excitation of coaxial electrostatic edge modes in the Tokamak fusion test reactor," *Nuclear Fusion* **43**, 531 (2003).

M.B. Johnson, H.M. Choi, and L.S. Kisslinger, "Bubble collisions in a SU_2 model of QCD," *Nuclear Physics A* **729**, 729–742 (2003).

S.C. Jun, B.A. Pearlmutter, and G. Nolte, "MEG source localization using an MLP with a distributed output representation," *IEEE Transactions on Biomedical Engineering* **50**, 786–789 (2003).

J.L. Kline, M.M. Balkey, P.A. Keiter, E.E. Scime, A.M. Keesee, X. Sun, R. Hardin, C. Compton, R.F. Boivin, and M.W. Zintl, "Ion dynamics in helicon sources," *Physics of Plasmas* **10**, 2127–2135 (2003).

J.L. Kline, and E.E. Scime, "Parametric decay instabilities in the helix helicon plasma source," *Physics of Plasmas* **10**, 135–144 (2003).

B.Z. Kopeliovich, J. Raufeisen, A.V. Tarasov, and M.B. Johnson, "Nuclear effects in the Drell-Yan process at very high energies," *Physical Review C* **67**, 014903 (2003).

J.P. Kozlova, T.J. Bowles, V.K. Eremin, V.N. Gavrin, O.G. Koshelev, A.V. Markov, V.A. Morozova, A.J. Polyakov, E.M. Verbitskaya, and E.P. Veretenkin, "A comparative study of EL2 and other deep centers in undoped SI GaAs using optical absorption spectra and photoconductivity measurements," *Nuclear Instruments and Methods in Physics Research Section A-Accelerators Spectrometers Detectors and Associated Equipment* **512**, 1–7 (2003).

K. Kwiatkowski, J.C. Lyke, R.J. Wojnarowski, J.F. Beche, R. Fillion, C. Kapusta, J. Millaud, R. Saia, and M.D. Wilke, "3D interconnect architecture for high-bandwidth massively paralleled imager," *Nuclear Instruments and Methods in Physics Research Section A-Accelerators Spectrometers Detectors and Associated Equipment* **509**, 200–205 (2003).

G.A. Kyrala, K. Klare, and J. Workman, "Optimizing area-backlighter performance in a difficult geometry," *Review of Scientific Instruments* **74**, 2182–2185 (2003).

N.E. Lanier, C.W. Barnes, S.H. Batha, R.D. Day, G.R. Magelssen, J.M. Scott, A.M. Dunne, K.W. Parker, and S.D. Rothman, "Multimode seeded Richtmyer-Meshkov mixing in a convergent, compressible, miscible plasma system," *Physics of Plasmas* **10**, 1816–1821 (2003).

N.E. Lanier, C.W. Barnes, R. Perea, and W.P. Steckle, "Feasibility of fluorescence-based imaging of high-energy-density hydrodynamics experiments," *Review of Scientific Instruments* **74**, 2169–2173 (2003).

T. Li, P.P. Ruden, I.H. Campbell, and D.L. Smith, "Investigation of bottom-contact organic field effect transistors by two-dimensional device modeling," *Journal of Applied Physics* **93**, 4017–4022 (2003).

C.Y. Liu, S.K. Lamoreaux, A. Saunders, D. Smith, and A.R. Young, "An apparatus to control and monitor the para-D_2 concentration in a solid deuterium, superthermal source of ultra-cold neutrons," *Nuclear Instruments and Methods in Physics Research Section A-Accelerators Spectrometers Detectors and Associated Equipment* **508**, 257–267 (2003).

S.N. Luo, T.J. Ahrens, T. Cagin, A. Strachan, W.A. Goddard, and D.C. Swift, "Maximum superheating and undercooling: Systematics, molecular dynamics simulations, and dynamic experiments," *Physical Review B* **68**, 134206 (2003).

J.M. Mack, R.R. Berggren, S.E. Caldwell, S.C. Evans, J.R. Faulkner, R.A. Lerche, J.A. Oertel, and C.S. Young, "Observation of high-energy deuterium-tritium fusion gamma rays using gas Cerenkov detectors," *Nuclear Instruments and Methods in Physics Research Section A-Accelerators Spectrometers Detectors and Associated Equipment* **513**, 566–572 (2003).

R. Maingi, M.G. Bell, R.E. Bell, J. Bialek, C. Bourdelle, C.E. Bush, D.S. Darrow, E.D. Fredrickson, D.A. Gates, M. Gilmore, T. Gray, T.R. Jarboe, D.W. Johnson, R. Kaita, S.M. Kaye, S. Kubota, H.W. Kugel, B.P. LeBlanc, R.J. Maqueda, D. Mastrovito, S.S. Medley, J.E. Menard, D. Mueller, B.A. Nelson, M. Ono, F. Paoletti, H.K. Park, S.F. Paul, T. Peebles, Y.K.M. Peng, C.K. Phillips, R. Raman, A.L. Rosenberg, A.L. Roquemore, P.M. Ryan, S.A. Sabbagh, C.H. Skinner, V.A. Soukhanovskii, D. Stutman, D.W. Swain, E.J. Synakowski, G. Taylor, J. Wilgen, J.R. Wilson, G.A. Wurden, S.J. Zweben, and N. Team, "Recent results from the National Spherical Torus Experiment," *Plasma Physics and Controlled Fusion* **45**, 657–669 (2003).

R. Maingi, M.G. Bell, R.E. Bell, C.E. Bush, E.D. Fredrickson, D.A. Gates, T. Gray, D.W. Johnson, R. Kaita, S.M. Kaye, S. Kubota, H.W. Kugel, C.J. Lasnier, B.P. LeBlanc, R.J. Maqueda, D. Mastrovito, J.E. Menard, D. Mueller, M. Ono, F. Paoletti, S.J. Pau, Y.K.M. Peng, A.L. Roquemore, S.A. Sabbagh, C.H. Skinner, V.A. Soukhanovskii, D. Stutman, D.W. Swain, E.J. Synakowski, T. Tan, J.B. Wilgen, and S.J. Zweben, "H-mode research in NSTX," *Nuclear Fusion* **43**, 969–974 (2003).

M. Malek, M. Morii, S. Fukuda *et al.* (including Los Alamos scientist: T.J. Haines), "Search for supernova relic neutrinos at Super-Kamiokande," *Physical Review Letters* **90**, 061101 (2003).

R.J. Maqueda, G.A. Wurden, D.P. Stotler, S.J. Zweben, B. LaBombard, J.L. Terry, J.L. Lowrance, V.J. Mastrocola, G.F. Renda, D.A. D'Ippolito, J.R. Myra, and N. Nishino, "Gas puff imaging of edge turbulence (invited)," *Review of Scientific Instruments* **74**, 2020–2026 (2003).

Y. Masuda, J.D. Bowman, R.D. Carlini, T. Case, T.E. Chupp, K.P. Coulter, S.J. Freedman, T.R. Gentile, M. Gericke, G.L. Greene, F.W. Hersmann, T. Ino, S. Ishimoto, G.L. Jones, M.B. Leuschner, G.S. Mitchell, K. Morimoto, S. Muto, H. Nann, S.A. Page, S.I. Perittila, W.D. Ramsay, E.I. Sharapov, T.B. Smith, W.M. Snow, S.W. Wilburn, and Y.W. Yuan, "Parity-violating gamma-ray asymmetry in the neutron-proton capture," *Nuclear Physics A* **721**, 485C–488C (2003).

C. McCann, J.C. Kumaradas, M.R. Gertner, S.R.H. Davidson, A.M. Dolan, and M.D. Sherar, "Feasibility of salvage interstitial microwave thermal therapy for prostate carcinoma following failed brachytherapy: Studies in a tissue equivalent phantom," *Physics in Medicine and Biology* **48**, 1041–1052 (2003).

D.N. McKinsey, C.R. Brome, S.N. Dzhosyuk, R. Golub, K. Habicht, P.R. Huffman, E. Korobkina, S.K. Lamoreaux, C.E.H. Mattoni, A.K. Thompson, L. Yang, and J.M. Doyle, "Time dependence of liquid-helium fluorescence," *Physical Review A* **67**, 062716 (2003).

J.E. Menard, M.G. Bell, R.E. Bell, E.D. Fredrickson, D.A. Gates, S.M. Kaye, B.P. LeBlanc, R. Maingi, D. Mueller, S.A. Sabbagh, D. Stutman, C.E. Bush, D.W. Johnson, R. Kaita, H.W. Kugel, R.J. Maqueda, F. Paoletti, S.F. Paul, M. Ono, Y.K.M. Peng, C.H. Skinner, E.J. Synakowski, and N.R. Team, "β-limiting MHD instabilities in improved-performance NSTX spherical torus plasmas," *Nuclear Fusion* **43**, 330–340 (2003).

G.L. Morgan, K.R. Alrick, A. Saunders, F.C. Cverna, N.S.P. King, F.E. Merrill, L.S. Waters, A.L. Hanson, G.A. Greene, R.P. Liljestrand, R.T. Thompson, and E.A. Henry, "Total cross sections for the production of ^{22}Na and ^{24}Na in proton-induced reactions on ^{27}Al from 0.40 to 22.4 GeV," *Nuclear Instruments and Methods in Physics Research Section B-Beam Interactions with Materials and Atoms* **211**, 297–304 (2003).

Appendix B: Publications—2003 Journal Articles

C.E. Moss, C.M. Frankle, V.N. Litvinenko, and H.R. Weller, "Recent results using the high intensity gamma-ray source facility," *Nuclear Instruments and Methods in Physics Research Section A-Accelerators Spectrometers Detectors and Associated Equipment* **505**, 374–376 (2003).

D. Mueller, M. Ono, M.G. Bell, R.E. Bell, M. Bitter, C. Bourdelle, D.S. Darrow, P.C. Efthimion, E.D. Fredrickson, D.A. Gates, R.J. Goldston, L.R. Grisham, R.J. Hawryluk, K.W. Hill, J.C. Hosea, S.C. Jardin, H. Ji, S.M. Kaye, R. Kaita, H.W. Kugel, D.W. Johnson, B.P. LeBlanc, R. Majeski, E. Mazzucato, S.S. Medley, J.E. Menard, H.K. Park, S.F. Paul, C.K. Phillips, M.H. Redi, A.L. Rosenberg, C.H. Skinner, V.A. Soukhanovskii, B. Stratton, E.J. Synakowski, G. Taylor, J.R. Wilson, S.J. Zweben, W.D. Dorland, Y.K.M. Peng, R. Barry, T. Bigelow, C.E. Bush, M. Carter, R. Maingi, M. Menon, P.M. Ryan, D.W. Swain, J. Wilgen, S.A. Sabbagh, F. Paoletti, J. Bialek, W. Zhu, R. Raman, T.R. Jarboe, B.A. Nelson, R.J. Maqueda, G.A. Wurden, R.I. Pinsker, M. Schaffer, J. Ferron, L. Lao, D. Stutman, M. Finkenthal, W. Wampler, S. Kubota, W.A. Peebles, M. Gilmore, T.K. Mau, K.C. Lee, C.W. Domier, B.H. Deng, M. Johnson, N.C. Luhmann, P. Bonoli, A. Bers, A. Ram, R. Akers, Y. Takase, A. Ejiri, Y. Ono, S. Shiraiwa, N. Nishino, O. Mitarai, M. Nagata, J.G. Yang, H. Na, and D. Pacella, "Results of NSTX heating experiments," *IEEE Transactions on Plasma Science* **31**, 60–67 (2003).

J. Murata, A. Al-Jamel, R.L. Armendariz, M.L. Brooks, T. Horaguchi, N. Kamihara, H. Kobayashi, D.M. Lee, T.A. Shibata, and W.E. Sondheim, "Optical alignment system for the PHENIX muon tracking chambers," *Nuclear Instruments and Methods in Physics Research Section A-Accelerators Spectrometers Detectors and Associated Equipment* **500**, 309–317 (2003).

G.C. Nayak, M.X. Liu, and F. Cooper, "Color octet contribution to high p(t) J/ψ production in *pp* collisions at $\sqrt{S}$ = 500 and 200 GeV at BNL RHIC," *Physical Review D* **68**, 034003 (2003).

J.E. Nordholt, D.B. Reisenfeld, R.C. Wiens, S.P. Gary, F. Crary, D.M. Delapp, R.C. Elphic, H.O. Funsten, J.J. Hanley, D.J. Lawrence, D.J. McComas, M. Shappirio, J.T. Steinberg, J. Wang, and D.T. Young, "Deep Space 1 encounter with comet 19p/Borrelly: Ion composition measurements by the PEPE mass spectrometer," *Geophysical Research Letters* **30**, 1465 (2003).

N. O'Toole, J. Barbosa, Y.G. Li, L.W. Hung, A. Matte, and M. Cygler, "Crystal structure of a trimeric form of dephosphocoenzyme a kinase from escherichia coli," *Protein Science* **12**, 327–336 (2003).

R.E. Olson, R.J. Leeper, A. Nobile, and J.A. Oertel, "Preheat effects on shock propagation in indirect-drive inertial confinement fusion ablator materials," *Physical Review Letters* **91**, 235002 (2003).

F.G. Omenetto, A. Efimov, A.J. Taylor, J.C. Knight, W. Wadsworth, P.S.J. Russe, and J. Arriaga, "Nonlinear effects in microstructured fibers," *Springer Series in Chemical Physics* **71**, 229–231 (2003).

F.G. Omenetto, A. Efimov, A.J. Taylor, J.C. Knight, W.J. Wadsworth, and P.S.J. Russell, "Polarization dependent harmonic generation in microstructured fibers," *Optics Express* **11**, 61–67 (2003).

J. Park, R.A. Nebel, W.G. Rellergert, and M.D. Sekora, "Experimental studies of electrostatic confinement on the intense neutron source-electron device," *Physics of Plasmas* **10**, 3841–3849 (2003).

J.C. Peng, "Status of spin physics: Experimental summary," *International Journal of Modern Physics A* **18**, 1513–1530 (2003).

G.R. Poe, D.M. Rector, and R.M. Harper, "State-dependent columnar organization of dorsal hippocampal activity in the freely-behaving cat," *Behavioural Brain Research* **138**, 107–112 (2003).

W.C. Priedhorsky, K.N. Borozdin, G.E. Hogan, C. Morris, A. Saunders, L.J. Schultz, and M.E. Teasdale, "Detection of high-Z objects using multiple scattering of cosmic ray muons," *Review of Scientific Instruments* **74**, 4294–4297 (2003).

J. Raufeisen, "Relating different approaches to nuclear broadening," *Physics Letters B* **557**, 184–191 (2003).

J. Raufeisen and J.C. Peng, "Relating the parton model and color dipole formulation of heavy quark hadron production," *Physical Review D* **67**, 054008 (2003).

D.M. Rector, D.M. Ranken, and J.S. George, "High-performance confocal system for microscopic or endoscopic applications," *Methods* **30**, 16–27 (2003).

W.H. Reeves, D.V. Skryabin, F. Biancalana, J.C. Knight, P.S. Russell, F.G. Omenetto, A. Efimov, and A.J. Taylor, "Transformation and control of ultra-short pulses in dispersion-engineered photonic crystal fibres," *Nature* **424**, 511–515 (2003).

L.J. Schultz, K.K. Kwiatkowski, C.L. Morris, A. Saunders, G.E. Hogan, F.E. Merrill, and K.B. Morley, "A narrow-gap ion chamber for beam motion correction in proton radiography experiments," *Nuclear Instruments and Methods in Physics Research Section A-Accelerators Spectrometers Detectors and Associated Equipment* **508**, 220–226 (2003).

A. Seifter, K. Boboridis, and A.W. Obst, "High-speed temperature and emissivity measurements for thermophysical property determination of conducting materials," *ESA Special Publications* **540**, 375–380 (2003).

W.M. Snow, W.S. Wilburn, J.D. Bowman, M.B. Leuschner, S.I. Penttilä, V.R. Pomeroy, D.R. Rich, E.I. Sharapov, and V.W. Yuan, "Progress toward a new measurement of the parity violating asymmetry in $\vec{n} + p \rightarrow d + \gamma$," *Nuclear Instruments and Methods in Physics Research Section A-Accelerators Spectrometers Detectors and Associated Equipment* **515**, 563–574 (2003).

J.P. Sullivan and P. Collaboration, "Global variables and identified hadrons in the PHENIX experiment," *Pramana Journal of Physics* **60**, 953–963 (2003).

D.C. Swift and G.J. Ackland, "Quantum mechanical predictions of nonscalar equations of state and nonmonotonic elastic stress-strain relations," *Applied Physics Letters* **83**, 1151–1153 (2003).

E.J. Synakowski, M.G. Bell, R.E. Bell, T. Bigelow, R. Maqueda, G.A. Wurden *et al.,* "The national spherical torus experiment (NSTX) research program and progress towards high-beta, long-pulse operating scenarios," *Nuclear Fusion* **43**, 1653 (2003).

J.M. Taccetti, T.P. Intrator, G.A. Wurden, S.Y. Zhang, R. Aragonez, P.N. Assmus, C.M. Bass, C. Carey, S.A. deVries, W.J. Fienup, I. Furno, S.C. Hsu, M.P. Kozar, M.C. Langner, J. Liang, R.J. Maqueda, R.A. Martinez, P.G. Sanchez, K.F. Schoenberg, K.J. Scott, R.E. Siemon, E.M. Tejero, E.H. Trask, M. Tuszewski, W.J. Waganaar, C. Grabowski, E.L. Ruden, J.H. Degnan, T. Cavazos, D.G. Gale, and W. Sommars, "FRX-L: A field-reversed configuration plasma injector for magnetized target fusion," *Review of Scientific Instruments* **74**, 4314–4323 (2003).

J.L. Terry, S.J. Zweben, K. Hallatschek, B. LaBombard, R.J. Maqueda, B. Bai, C.J. Boswell, M. Greenwald, D. Kopon, W.M. Nevins, C.S. Pitcher, B.N. Rogers, D.P. Stotler, and X.Q. Xu, "Observations of the turbulence in the scrape-off-layer of Alcator C-Mod and comparisons with simulation," *Physics of Plasmas* **10**, 1739–1747 (2003).

T.E. Tierney, D.S. Montgomery, J.F. Benage, Jr., M.S. Murillo, F.J. Wysocki, and N. Rostoker, "Modeling of collective Thomson scattering from collisional plasmas," *Journal of Physics A: Mathematical and General* **36**, 5981-5989 (2003).

P. Toliver, R.J. Runser, T.E. Chapuran, J.L. Jackel, T.C. Banwell, M.S. Goodman, R.J. Hughes, C.G. Peterson, D. Derkacs, J.E. Nordholt, L. Mercer, S. McNown, A. Goldman, and J. Blake, "Experimental investigation of quantum key distribution through transparent optical switch elements," *IEEE Photonics Technology Letters* **15**, 1669–1671 (2003).

E. Torbert, I. Furno *et al.,* "A plasma-shielded, miniature Rogowski probe," *Review of Scientific Instruments* **74**(12), 5097 (2003).

M. Tsang, D. Psaltis, and F.G. Omenetto, "Reverse propagation of femtosecond pulses in optical fibers," *Optics Letters* **28**, 1873–1875 (2003).

M. Tuszewski, R.R. White, and G.A. Wurden, "Relaxation oscillations of low-frequency Ar/SF_6 inductive plasma discharges," *Plasma Sources Science and Technology* **12**, 396-402 (2003).

J.L. Vincent, S. Luo, B.L. Scott, R. Butcher, C.J. Unkefer, C.J. Burns, G.J. Kubas, A. Lledos, F. Maseras, and J. Tomas, "Experimental and theoretical studies of bonding and oxidative addition of germanes and silanes, $EH_{4-n}Ph_n$ (E = Si, Ge; n = 0-3), to Mo(CO)(diphosphine)$_2$. The first structurally characterized germane σ complex," *Organometallics* **22**, 5307–5323 (2003).

Z.H. Wang and J.L. Kline, "Electrostatic method to accelerate nanoshells to extreme hypervelocity," *Applied Physics Letters* **83**, 1662–1664 (2003).

Z.H. Wang and G.A. Wurden, "Hypervelocity dust beam injection for internal magnetic field mapping," *Review of Scientific Instruments* **74**, 1887–1891 (2003).

D.C. Wilson, C.R. Christensen, G.L. Morgan, M.D. Wilke, P.A. Bradley, and P.L. Gobby, "Goals for and design of a neutron pinhole imaging system for ignition capsules," *Review of Scientific Instruments* **74**, 1705–1708 (2003).

J. Workman, N.E. Lanier, and G.A. Kyrala, "Analysis of TiK-shell emission produced from solid targets using nanosecond pulses on the Trident laser facility," *Review of Scientific Instruments* **74**, 2165–2168 (2003).

X.C. Yao and A. Castro, "Optical trapping microfabrication with electrophoretically delivered particles inside glass capillaries," *Optics Letters* **28**, 1335–1337 (2003).

X.C. Yao, D.M. Rector, and J.S. George, "Optical lever recording of displacements from activated lobster nerve bundles and nitella internodes," *Applied Optics* **42**, 2972–2978 (2003).

J. Yoo, Y. Ashie, S. Fukuda *et al.* (including Los Alamos scientist: T.J. Haines), "Search for periodic modulations of the Solar neutrino flux in Super-Kamiokande-I," *Physical Review D* **68**, 092002 (2003).

2003 Conference Papers

G.J. Ackland and D.C. Swift, "Accuracy of the scalar equation of state," 13th Biennial International Conference of the American Physical Society Topical Group on Shock Compression of Condensed Matter, Portland, Oregon, USA, July 20–25, 2003, Los Alamos National Laboratory report LA-UR-03-2132 (March 2003).

B.G. Anderson, D.M. Oro, R.T. Olson, J.K. Studebaker, and D. Platts, "A flash x-ray system for diagnosing liner implosions," 9th International Conference on Megagauss Magnetic Field Generation and Related Topics (Megagauss IX), Moscow, Russia, July 7–14, 2003, Los Alamos National Laboratory report LA-UR-03-1725 (March 2003).

W.W. Anderson, R.T. Olson, W.T. Buttler, R.S. Hixson, and M.D. Wilke, "Quantitative measurement of ejecta from shocked surfaces: A comparison of Asay foils, PZT pins, and radgiography," Meeting of the Joint Working Group (USA-UK) (JOWOG 32M), Livermore, California, USA, January 27-31, 2003, Los Alamos National Laboratory document LA-UR-03-0571 (January 2003).

R.J. Aragonez, P.G. Sanchez, and T.P. Intrator, "Operational amplifiers for low level signals," 2003 Los Alamos Student Symposium, Los Alamos, New Mexico, USA, August 6–7, 2003, Los Alamos National Laboratory report LA-UR-03-5314 (July 2003).

M.S. Bakeman, "Characterization of x-ray framing cameras for use in inertial confinement fusion and hydrodynamics experiments," 48th Annual Optical Science and Technology Symposium at the Annual Meeting of the International Society for Optical Engineering (SPIE), San Diego, California, USA, August 3–8, 2003, Los Alamos National Laboratory report LA-UR-03-5674 (July 2003).

M.S. Bakeman, S.C. Evans, J.A. Oertel, and P.J. Walsh, "Characterization of Los Alamos x-ray framing cameras," 48th Annual Meeting of the International Society for Optical Engineering (SPIE), San Diego, California, USA, August 3–8, 2003, Los Alamos National Laboratory report LA-UR-03-5319 (July 2003).

M.S. Bakeman, S.C. Evans, J.A. Oertel, and P.J. Walsh, "Characterization of the quantitative x-ray imager," 48th Annual Meeting of the International Society for Optical Engineering (SPIE), San Diego, California, USA, August 3–8, 2003, Los Alamos National Laboratory report LA-UR-03-0989 (February 2003).

M.M. Balkey, J.M. Scott, C.W. Barnes, S.H. Batha, N.D. Delamater, J.R. Fincke, R.M. Hueckstaedt, N.E. Lanier, and G.R. Magelssen, "Single-mode Richtmyer-Meshkov growth in a compressible, miscible, convergent system," 33rd Anomalous Absorption Conference, Lake Placid, New York, USA, June 22–27, 2003, Los Alamos National Laboratory report LA-UR-03-3170 (May 2003).

M.M. Balkey, J.M. Scott, C.W. Barnes, S.H. Batha, N.D. Delamater, and J.P. Fincke, "Single-mode Richtmyer-Meshkov growth in a compressible, miscible, convergent system," 45th Annual Meeting of the Division of Plasma Physics of the American Physical Society, Albuquerque, New Mexico, USA, October 27–31, 2003, Los Alamos National Laboratory report LA-UR-03-5061 (July 2003).

D.N. Barnes, J.S. George, O. Schwarz, and T.-N. Kwong, "Adaptive finite difference mesh refinement for neutral electromagnetic modeling," 2003 Biomedical Engineering Society Annual Fall Meeting (BMES 2003), Nashville, Tennessee, USA, October 1–4, 2003, Los Alamos National Laboratory report LA-UR-03-3392 (May 2003).

C.M. Bass and M.R. Leonard, "Optical tomography diagnostics on a FRC plasma," 2003 Los Alamos Student Symposium, Los Alamos, New Mexico, USA, August 6–7, 2003, Los Alamos National Laboratory report LA-UR-03-5215 (July 2003).

S.H. Batha, J.R. Fincke, J.A. Guzik, and A.L. Peratt, "Omega experimental results for radiation hydrodynamics code validation (U)," 14th Biennial Nuclear Explosives Design Physics Conference (NEDPC 2003), Los Alamos, New Mexico, USA, October 20–24, 2003, Los Alamos National Laboratory report LA-CP-03-0490 (June 2003).

S.H. Batha, N.E. Lanier, J.R. Fincke, N.D. Delamater, M.M. Balkey, G.R. Magelssen, R.M. Hueckstaedt, S.D. Rothman, K.W. Parker, A.M. Dunne, and C. Horsfield, "Second shock mixing in convergent geometry," 45th Annual Meeting of the Division of Plasma Physics of the American Physical Society, Albuquerque, New Mexico, USA, October 27–31, 2003, Los Alamos National Laboratory report LA-UR-03-7543 (October 2003).

P.D. Beinke, Z. Wang, E. Mignardot, and P. Sanchez, "Flow magnetized plasma experiment: Design overview and status," 2003 Los Alamos Student Symposium, Los Alamos, New Mexico, USA, August 6–7, 2003, Los Alamos National Laboratory report LA-UR-03-5211 (July 2003).

M.A. Betemps, M.B. Gay Ducati, M.V.T. Machado, and J. Raufeisen, "Dilepton transverse momentum in the color dipole approach," 11th International Workshop on Deep Inelastic Scattering (DIS 2003), St. Petersburg, Russia, April 23–27, 2003, Los Alamos National Laboratory report LA-UR-03-5879 (August 2003).

B. Bezzerides, D.C. Barnes, D.F. Dubois, E.S. Dodd, and H. Bu, "Modeling stimulated Raman scattering (SRS) in the trapping regime: Properties of a 3-wave, local space/time approach," 45th Annual Meeting of the Division of Plasma Physics of the American Physical Society, Albuquerque, New Mexico, USA, October 27–31, 2003, Los Alamos National Laboratory report LA-UR-03-5076 (July 2003).

J.J. Bloch, C. Ho, R. Shirey, and W.R. Scarlett, "RULLISAT: A novel idea for a space surveillance SMALLSAT demo (U)," 2003 AMOS Technical Conference: Space Situational Awareness, Wailea, Hawaii, USA, September 8–13, 2003, Los Alamos National Laboratory report LA-CP-03-0692 (September 2003).

J.J. Bloch, C. Ho, W.R. Scarlett, and R. Shirey, "Space situational awareness applications for the RULLI sensor," 2003 AMOS Technical Conference: Space Situational Awareness, Wailea, Hawaii, USA, September 8–13, 2003, Los Alamos National Laboratory report LA-UR-03-6549 (September 2003).

K. Boboridis, A. Seifter, A.W. Obst, and D. Basak, "Radiance temperatures and normal spectral emittances (in the wavelength range of 1,500 nm to 5,000 nm) of tin, zinc, uranium, and silver at their melting points by a pulse-heating," 15th Symposium on Thermophysical Properties, Boulder, Colorado, USA, June 22–27, 2003, Los Alamos National Laboratory report LA-UR-03-3395 (May 2003).

K. Boboridis, A. Seifter, A.W. Obst, and D. Basak, "Validation of a new high-speed fiber-coupled four-wavelength infrared pyrometer in the range of 505 K to 1,234 K by a pulsed-heating technique, using the melting points of tin, zinc," 15th Symposium on Thermophysical Properties, Boulder, Colorado, USA, June 22–27, 2003, Los Alamos National Laboratory report LA-UR-03-3394 (May 2003).

K. Boboridis, A. Seifter, and A.W. Obst, "A high-speed fiber-coupled four-wavelength infrared pyrometer for shock-temperature measurements," 2003 American Physical Society Topical Conference on Shock Compression of Condensed Matter, Portland, Oregon, USA, July 20–25, 2003, Los Alamos National Laboratory report LA-UR-03-2280 (April 2003).

K. Boboridis, A. Seifter, and A.W. Obst, "High-speed infrared pyrometry for surface temperature measurements on shocked solids," PTB-GMA Fachtagung TEMPERATUR 2003, Berlin, Germany, September 8-9, 2003, Los Alamos National Laboratory report LA-UR-03-3834 (June 2003).

K.N. Borozdin, G.E. Hogan, C.L. Morris, W.C. Priedhorsky, A. Saunders, R. Schirato, and L.J. Schultz, "Scattering muon radiography and its application to the detection of high-Z material," 2003 IEEE Nuclear Science Symposium and Medical Imaging Conference, Portland, Oregon, USA, October 19–25, 2003, Los Alamos National Laboratory report LA-UR-03-7999 (October 2003).

M.G. Boulay, "Neutral currents with SNO," 1st Yamada Symposium on Neutrinos and Dark Matter in Nuclear Physics (NDM03), Nara, Japan, June 9–14, 2003, Los Alamos National Laboratory report LA-UR-03-3342 (May 2003).

M.G. Boulay, "Present status and results from the SNO experiment," American Physical Society April Meeting, Philadelphia, Pennsylvania, USA, April 5–8, 2003, Los Alamos National Laboratory report LA-UR-03-3341 (May 2003).

J.D. Bowman, "Status of knowledge of hadronic weak couplings," Conference on the Intersection of Particle and Nuclear Physics (CIPANP), New York, New York, USA, May 19–24, 2003, Los Alamos National Laboratory report LA-UR-03-3163 (May 2003).

M.Q. Cannon, "A prototype resistive plate chambers for muon radiography," 2003 Los Alamos Student Symposium, Los Alamos, New Mexico, USA, August 6–7, 2003, Los Alamos National Laboratory report LA-UR-03-5059 (July 2003).

C.S. Carey and G.A. Wurden, "A singular value decomposition method for inverting line integrated electron density measurements in magnetically confined plasma," 2003 Los Alamos Student Symposium, Los Alamos, New Mexico, USA, August 6–7, 2003, Los Alamos National Laboratory report LA-UR-03-5182 (July 2003).

C.S. Carey and I.G. Furno, "A singular value decomposition method for inverting electron density measurement in magnetically," 45th Annual Meeting of the Division of Plasma Physics of the American Physical Society, Albuquerque, New Mexico, USA, October 27–31, 2003, Los Alamos National Laboratory report LA-UR-03-5764 (August 2003).

C. Carr, M.A. Espy, T.G. Abeln, and R.H. Kraus, Jr., "Characterization of inertial welds by SQUID NDE," 6th European Conference on Applied Superconductivity (EUCAS 2003), Sorrento, Napoli, Italy, September 14–18, 2003, Los Alamos National Laboratory report LA-UR-03-6495 (September 2003).

D.E. Casperson, G.R. Gisler, T.J. Haines, and J.M. O'Donnell, "Transient phenomena in astrophysics: A student challenge awards program expedition," Earthwatch Institute Annual Conference, Cambridge, Massachusetts, USA, November 7–8, 2003, Los Alamos National Laboratory report LA-UR-03-8219 (November 2003).

A. Castro, O.C. Marina, and D. Dalvit, "Direct detection of single-copy DNA sequences," 9th International Workshop on Single Molecule Detection and Ultra Sensitive Analysis in the Life Sciences, Berlin-Aldershof, Germany, September 24–26, 2003, Los Alamos National Laboratory report LA-UR-03-3960 (June 2003).

R.E. Chrien, C.W. Nakleh, R.P. Weaver, B.H. Wilde, G.L. Morgan, and B.J. Warthen, "Modern reanalysis of Topmast (U)," 14th Biennial Nuclear Explosives Design Physics Conference (NEDPC 2003), Los Alamos, New Mexico, USA, October 20–24, 2003, Los Alamos National Laboratory report LA-CP-03-0486 (June 2003).

Appendix B: Publications—2003 Conference Papers

C.R. Christensen, D.C. Wilson, C.W. Barnes, and S.H. Batha, "The influence of asymmetry on mix in direct-drive ICF experiments," 3rd International Conference on Inertial Fusion Sciences and Applications (IFSA 2003), Monterey, California, USA, September 7–12, 2003, Los Alamos National Laboratory report LA-UR-03-1772 (March 2003).

C.R. Christensen, D.C. Wilson, C.W. Barnes, G.P. Grim, G.L. Morgan, M.D. Wilke, and F.J. Marshall, "The influence of asymmetry on mix in direct-drive experiments," 3rd International Conference on Inertial Fusion Sciences and Applications (IFSA 2003), Monterey, California, USA, September 7–12, 2003, Los Alamos National Laboratory report LA-UR-03-6400 (September 2003).

J.A. Cobble, C.A. Werley, J.C. Weisheit, G.M. Lapenta, and T.P. Intrator, "Zeeman spectroscopy diagnosis of a magnetic field," 45th Annual Meeting of the Division of Plasma Physics of the American Physical Society, Albuquerque, New Mexico, USA, October 27–31, 2003, Los Alamos National Laboratory report LA-UR-03-5066 (July 2003).

H.A. Davis, D.C. Moir, and R.T. Olson, "Measurements of thermally desorbed ions from beam target interactions," 2003 Particle Accelerator Conference (PAC 2003), Portland, Oregon, USA, May 12–16, 2003, Los Alamos National Laboratory report LA-UR-03-3135 (May 2003).

N.D. Delamater, G.A. Kyrala, D.C. Wilson, R. Watt, and J. Guzik, "Progress with double shell target implosions at Omega," 45th Annual Meeting of the Division of Plasma Physics of the American Physical Society, Albuquerque, New Mexico, USA, October 27–31, 2003, Los Alamos National Laboratory report LA-UR-03-7721 (October 2003).

N.D. Delamater, J. Guzik, G.A. Kyrala, D.C. Wilson, R. Watt, W.M. Wood, W. Varnum, D. Haynes, G. Pollak, and M. Gunderson, "Progress with double shell target implosions on Omega," 3rd Inertial Fusion Sciences and Applications Conference (IFSA 2003), Monterey, California, USA, September, 7–12, 2003, Los Alamos National Laboratory report LA-UR-03-1170 (February 2003).

N.D. Delamater, G.A. Kyrala, J.A. Guzik, D.C. Wilson, D.A. Haynes, and W. Wood, "Double shell capsule implosions on Omega (U)," 14th Biennial Nuclear Explosives Design Physics Conference (NEDPC 2003), Los Alamos, New Mexico, USA, October 20–24, 2003, Los Alamos National Laboratory report LA-CP-03-0492 (June 2003).

B.G. Devolder, M.J. Berninger, L. Yin, T.J.T. Kwan, N.S.P. King, and S.M. Sterbenz, "Armando pre-shot calculations using the integrated x-ray radiographic chain model (U)," 14th Biennial Nuclear Explosives Design Physics Conference (NEDPC 2003), Los Alamos, New Mexico, USA, October 20–24, 2003, Los Alamos National Laboratory report LA-CP-03-0487 (June 2003).

B.L. Dingus, M.M. Gonzalez, R.D. Preece, M.S. Briggs, Y. Kaneko, and C. Dermer, "The highest energy gamma rays from gamma-ray bursts," 10th Marcel Grossman Meeting on General Relativity, Rio de Janeiro, Brazil, July 20–26, 2003, Los Alamos National Laboratory report LA-UR-03-4156 (June 2003).

N.D. Drummond, D.C. Swift, and G.J. Ackland, *"Ab initio* model of porous periclase," 13th Biennial International Conference of the American Physical Society Topical Group on Shock Compression of Condensed Matter, Portland, Oregon, USA, July 20–25, 2003, Los Alamos National Laboratory report LA-UR-03-2134 (March 2003).

S.R. Elliott, "Experimental prospects for direct measurements of neutrino mass (tritium experiments)," Summer Nuclear Institute at TRIUMF, Vancouver, British Columbia, Canada, July 5–16, 2003, Los Alamos National Laboratory report LA-UR-03-5838 (August 2003).

S.R. Elliott, "Neutrino mass patterns and future double-β decay experiment," 8th International Workshop on Topics in Astroparticle and Underground Physics (TAUP 2003), Seattle, Washington, USA, September 5–9, 2003, Los Alamos National Laboratory report LA-UR-03-6815 (September 2003).

S.R. Elliott, "Radiochemical experiments," Summer Nuclear Institute at TRIUMF, Vancouver, British Columbia, Canada, July 5–16, 2003, Los Alamos National Laboratory report LA-UR-03-5839 (August 2003).

S.R. Elliott, "New underground laboratories in North America," Neutrinos and Dark Matter Meeting, Nara, Japan, June 9-14, 2003, Los Alamos National Laboratory report LA-UR-03-4086 (June 2003).

S.R. Elliott, "Non-accelerator neutrino physics," High Energy Particle Physics Advisory Panel Meeting, Bethesda, Maryland, July 24, 2003, Los Alamos National Laboratory report LA-UR-03-5518 (July 2003).

S.R. Elliott, "Experiments for neutrinoless double-β decay," Summer Nuclear Institute at TRIUMF, Vancouver, British Columbia, Canada, July 5-16, 2003, Los Alamos National Laboratory report LA-UR-03-5838 (August 2003).

M.A. Espy, "HTS SQUID array magnetic field measurements of propagating action potentials in a frog sciatic nerve," 17th National Conference on Undergraduate Research, Salt Lake City, Utah, USA, March 13–15, 2003, Los Alamos National Laboratory report LA-UR-03-2564 (April 2003).

R.J. Faehl, J.E. Hammerberg, J.S. Ladish, and G. Rodriguez, "Validation tests of an Eulerian legacy code on Atlas (U)," 14th Biennial Nuclear Explosives Design Physics Conference (NEDPC 2003), Los Alamos, New Mexico, USA, October 20–24, 2003, Los Alamos National Laboratory report LA-CP-03-0537 (June 2003).

E.N. Ferm, S. Dennison, R. Lopez, K. Prestridge, J.P. Quintana, C. Espinoza, G.E. Hogan, N.S.P. King, F.E. Merrill, C.L. Morris, P. Pazuchanic, A. Saunders, S.A. Baker, and R. Liljestrand, "Proton radiography experiments on shocked high explosives products," 13th Biennial International Conference of the American Physical Society Topical Group on Shock Compression of Condensed Matter, Portland, Oregon, USA, July 20–25, 2003, Los Alamos National Laboratory report LA-UR-03-5256 (July 2003).

J.C. Fernández and S.R. Goldman, "Design and characterization of hohlraum targets for long-pulse radiation drive in early NIF operation," 45th Annual Meeting of the Division of Plasma Physics of the American Physical Society, Albuquerque, New Mexico, USA, October 27–31, 2003, Los Alamos National Laboratory report LA-UR-03-7572 (October 2003).

J.C. Fernández, "Interaction of high-energy lasers with underdense plasmas for inertial fusion: A perspective," American Physical Society April Meeting, Philadelphia, Pennsylvania, USA, April 5–8, 2003, Los Alamos National Laboratory report LA-UR-03-2482 (April 2003).

J.C. Fernández, J.L. Kline, D.S. Montgomery, and H.A. Rose, "Kinetic effects in the interaction of high-energy lasers with underdense plasmas for inertial fusion," 18th International Conference on Transport Theory (18 ICTT), Rio de Janeiro, Brazil, July 20–25, 2003, Los Alamos National Laboratory report LA-UR-03-4087 (June 2003).

J.R. Fincke, N.E. Lanier, S.H. Batha, R.L. Holmes, G.R. Magelssen, R.M. Hueckstaedt, M.M. Balkey, C. Horsfield, K.W. Parker, and S.D. Rothman, "Enhanced Richtmyer-Meshkov mixing from a Koninant wavelength in the presence of background multimode surface roughness (U)," 45th Annual Meeting of the Division of Plasma Physics of the American Physical Society, Albuquerque, New Mexico, USA, October 27–31, 2003, Los Alamos National Laboratory report LA-UR-03-7542 (October 2003).

J.R. Fincke, N.E. Lanier, S.H. Batha, R.L. Holmes, G.R. Magelssen, R.M. Hueckstaedt, N.D. Delamater, J.M. Scott, M.M. Balkey, C. Horsfield, K.W. Parker, and S.D. Rothman, "Compressible mixing in a shock-accelerated, convergent plasma system (U)," American Physical Society Division of Fluid Dynamics 56th Annual Meeting, East Rutherford, New Jersey, USA, November 23–25, 2003, Los Alamos National Laboratory report LA-UR-03-8666 (November 2003).

J.R. Fincke, N.E. Lanier, S.H. Batha, R.L. Holmes, G.R. Magelssen, A.M. Dunne, C. Horsfield, K.W. Parker, and S.D. Rothman, "Shell defect behavior in a shock-accelerated, convergent plasma system," 45th Annual Meeting of the Division of Plasma Physics of the American Physical Society, Albuquerque, New Mexico, USA, October 27–31, 2003, Los Alamos National Laboratory report LA-UR-03-4949 (July 2003).

S.W. Forrest, "Characterization of temperature effects on magnetoresistance and noise in $^{80}Ni^{20}Fe$/Cu multilayer spin values," 2003 Los Alamos Student Symposium, Los Alamos, New Mexico, USA, August 6–7, 2003, Los Alamos National Laboratory report LA-UR-03-5217 (July 2003).

I.G. Furno, T.P. Intrator, S.C. Hsu, G. Lapenta, and E.W. Hemsing, "Experimental investigation of the stability of a single and multiple magnetic flux ropes," American Geophysical Union Fall Meeting, San Francisco, California, USA, December 8–12, 2003, Los Alamos National Laboratory report LA-UR-03-9147 (December 2003).

J.T. Gammel, D.C. Swift, and T.E. Tierney, "Shock response of iron on sub-nanosecond time scales," 13th Biennial International Conference of the American Physical Society Topical Group on Shock Compression of Condensed Matter, Portland, Oregon, USA, July 20–25, 2003, Los Alamos National Laboratory report LA-UR-03-2067 (March 2003).

M.T. Gericke, "A low noise SSI detector array for the measurement of parity nonconservation in $n + p \rightarrow d + \gamma$," 2003 Fall Meeting of the Division of Nuclear Physics of the American Physical Society, Tucson, Arizona, USA, October 30–November 1, 2003, Los Alamos National Laboratory report LA-UR-03-8079 (October 2003).

M.T. Gericke, "Weak pion-nucleon coupling and parity violation in the radiative capture of polarized cold neutrons on hydrogen," TRIUMF Seminar (Invited), Vancouver, British Columbia, Canada, December 18, 2003, Los Alamos National Laboratory report LA-UR-03-9048 (December 2003).

J.D. Goetee, E.N. Ferm, and C.L. Morris, "Illuminating the dead zones in PBX9502 (U)," 14th Biennial Nuclear Explosives Design Physics Conference (NEDPC 2003), Los Alamos, New Mexico, USA, October 20–24, 2003, Los Alamos National Laboratory report LA-CP-03-0971 (December 2003).

S.R. Goldman, G.A. Kyrala, and J.B. Workman, "Code validation through hydrodynamics experiments at Omega (U)," 14th Biennial Nuclear Explosives Design Physics Conference (NEDPC 2003), Los Alamos, New Mexico, USA, October 20–24, 2003, Los Alamos National Laboratory report LA-CP-03-0117 (February 2003).

S.R. Goldman, J.C. Fernandez, N.M. Hoffman, D.L. Tubbs, and J.A. Cobble, "Exploring heterogeneous structuring of Cu-doped beryllium with early NIF drive," 45th Annual Meeting of the Division of Plasma Physics of the American Physical Society, Albuquerque, New Mexico, USA, October 27–31, 2003, Los Alamos National Laboratory report LA-UR-03-4982 (July 2003).

Appendix B: Publications—2003 Conference Papers

S.R. Greenfield, D.C. Swift, and, A.C. Koskelo, "Transient interferometric studies of shocked bicrystals," 13th Biennial International Conference of the American Physical Society Topical Group on Shock Compression of Condensed Matter, Portland, Oregon, USA, July 20–25, 2003, Los Alamos National Laboratory report LA-UR-03-5274 (July 2003).

J.A. Guzik, S.H. Batha, D.E. Hollowell, A.L. Peratt, and G.R. Magelssen, "Code validation experiments for W76 RadHydro simulations (U)," 14th Biennial Nuclear Explosives Design Physics Conference (NEDPC 2003), Los Alamos, New Mexico, USA, October 20–24, 2003, Los Alamos National Laboratory report LA-CP-03-0525 (June 2003).

B.R. Haberle and J.A. Fairfield, "Electron-ion thermal equilibration in strongly coupled plasmas," 2003 Los Alamos Student Symposium, Los Alamos, New Mexico, USA, August 6–7, 2003, Los Alamos National Laboratory report LA-UR-03-5192 (July 2003).

R. Hackenberg, D.C. Swift, N. Bourne, G.T. Gray, III, D.L. Paisley, D.J. Thoma, J. Cooley, and A. Hauer, "Dynamic properties of nickel-titanium alloys," 13th Biennial International Conference of the American Physical Society Topical Group on Shock Compression of Condensed Matter, Portland, Oregon, USA, July 20–25, 2003, Los Alamos National Laboratory report LA-UR-03-2135 (March 2003).

J.E. Hammerberg, R.J. Faehl, G.A. Kyrala, and P.M. Rightley, "Validation tests of a new friction model (U)," 14th Biennial Nuclear Explosives Design Physics Conference (NEDPC 2003), Los Alamos, New Mexico, USA, October 20–24, 2003, Los Alamos National Laboratory report LA-CP-03-0532 (June 2003).

M.L. Harris, V.M. Ferreri, A. Jensen, S.M. Stange, and L.A. Rosocha, "Plasma-assisted propane combustion," 2003 Los Alamos Student Symposium, Los Alamos, New Mexico, USA, August 6–7, 2003, Los Alamos National Laboratory report LA-UR-03-5318 (July 2003).

M. Hausmann, D.J. Vieira, J. Wu, X.-X. Zhao, M.G. Boulay, and A. Hime, "Experimental needs for fundamental symmetry studies with polarized trapped atoms," Workshop on Experimental Equipment for the Rare Isotope Accelerator, Oak Ridge, Tennessee, USA, March 18–22, 2003, Los Alamos National Laboratory report LA-UR-03-1993 (March 2003).

M. Hausmann, D.J. Vieira, J. Wu, X.-X. Zhao, M.G. Boulay, and A. Hime, "β-asymmetry studies on polarized ^{82}Rb atoms in a TOP trap," 6th International Conference on Radioactive Nuclear Beams (RNB6), Argonne, Illinois, USA, September 22–26, 2003, Los Alamos National Laboratory report LA-UR-03-7052 (September 2003).

M. Hausmann, D.J. Vieira, J. Wu, X.-X. Zhao, M.G. Boulay, and A. Hime, "Measurements of the β-asymmetry in the decay of polarized ^{82}Rb in a magnetic time-orbiting-potential trap," 2003 Fall Meeting of the Division of Nuclear Physics of the American Physical Society, Tucson, Arizona, USA, October 30–November 1, 2003, Los Alamos National Laboratory report LA-UR-03-8033 (October 2003).

B.M. Hegelich, J.A. Cobble, R.P. Johnson, S.A. Letzring, and J.C. Fernandez, "Laser acceleration of heavy ions: New experiments using the LANL Trident and LULI short-pulse lasers," 45th Annual Meeting of the Division of Plasma Physics of the American Physical Society, Albuquerque, New Mexico, USA, October 27–31, 2003, Los Alamos National Laboratory report LA-UR-03-8075 (October 2003).

M. Hegelich, J.C. Fernandez, J.A. Cobble, S.A. Letzring, J. Fuchs, T. Cowan, N. Renard, M. Geissel, E. Brambrink, and M. Roth, "Laser driven MeV-ion jets: Beam characteristics and possible applications," 3rd International Conference on Inertial Fusion Sciences and Applications (IFSA 2003), Monterey, California, USA, September 7–12, 2003, Los Alamos National Laboratory report LA-UR-03-1917 (March 2003).

J.C. Heise, "Future prospects for SNO," 4th International Workshop on Low Energy Solar Neutrinos, Paris, France, May 19–21, 2003, Los Alamos National Laboratory report LA-UR-03-3658 (May 2003).

L. Heller, D.M. Ranken, and E.D. Best, "The magnetic field inside special conducting geometries due to internal current," 4th International Symposium on Noninvasive Functional Source Imaging within the Human Brain and Heart (NFSI 2003), Chieti, Italy, September 20–24, 2003, Los Alamos National Laboratory report LA-UR-03-3648 (May 2003).

E.W. Hemsing, D. Wei, I.G. Furno, and T.P. Intrator, "Multi-dimensional magnetic probes for magnetic field mapping on the reconnection scaling experiment at Los Alamos National Laboratory," 2003 Los Alamos Student Symposium, Los Alamos, New Mexico, USA, August 6–7, 2003, Los Alamos National Laboratory report LA-UR-03-5214 (July 2003).

E.W. Hemsing, I.G. Furno, and T.P. Intrator, "Recent experimental results from the Reconnection Scaling eXperiment," 45th Annual Meeting of the Division of Plasma Physics of the American Physical Society, Albuquerque, New Mexico, USA, October 27–31, 2003, Los Alamos National Laboratory report LA-UR-03-7995 (October 2003).

N.M. Hoffman and D.C. Swift, "Predictions of the microstructural contribution to instability seeding in beryllium ICF capsules," 13th Biennial International Conference of the American Physical Society Topical Group on Shock Compression of Condensed Matter, Portland, Oregon, USA, July 20–25, 2003, Los Alamos National Laboratory report LA-UR-03-5676 (July 2003).

N.M. Hoffman, J.A. Cobble, D.L. Tubbs, D.C. Swift, and T.E. Tierney, "Microstructure, shock waves, and stability: The initial conditions leading to mix," 14th Biennial Nuclear Explosives Design Physics Conference (NEDPC 2003), Los Alamos, New Mexico, USA, October 20–24, 2003, Los Alamos National Laboratory report LA-UR-03-4256 (June 2003).

N.M. Hoffman, J.A. Cobble, D.L. Tubbs, D.C. Swift, and T.E. Tierney, "Microstructure, shock waves, and stability: Initiating mix," 14th Biennial Nuclear Explosives Design Physics Conference (NEDPC 2003), Los Alamos, New Mexico, USA, October 20–24, 2003, Los Alamos National Laboratory report LA-UR-03-7321 (October 2003).

N.M. Hoffman, J.A. Cobble, D.L. Tubbs, D.C. Swift, and T.E. Tierney, "Microstructure, shock waves, and stability: The initiator of mixing?" 45th Annual Meeting of the Division of Plasma Physics of the American Physical Society, Albuquerque, New Mexico, USA, October 27–31, 2003, Los Alamos National Laboratory report LA-UR-03-4980 (July 2003).

G.E. Hogan, C.L. Morris, L.J. Schultz, M.E. Teasdale, and A. Saunders, "Detection of high-Z objects using multiple scattering of cosmic ray muons," 7th LANSCE User Group Meeting, Los Alamos, New Mexico, USA, October 19–23, 2003, Los Alamos National Laboratory report LA-UR-03-7797 (October 2003).

G.E. Hogan, K.N. Borozdin, C.L. Morris, W.C. Priedhorsky, A. Saunders, L.J. Schultz, and M.E. Teasdale, "Detection of high-Z objects using multiple scattering of cosmic ray muons," Conference on the Intersection of Particle and Nuclear Physics (CIPANP), New York, New York, USA, May 19–24, 2003, Los Alamos National Laboratory report LA-UR-03-3442 (May 2003).

D.B. Holtkamp, "A survey of high-explosive-induced damage and spall in selected metals using proton," 13th Biennial International Conference of the American Physical Society Topical Group on Shock Compression of Condensed Matter, Portland, Oregon, USA, July 20–25, 2003, Los Alamos National Laboratory report LA-UR-03-4411 (June 2003).

D.B. Holtkamp, "Development of a non-radiographic spall and damage diagnostic," 13th Biennial International Conference of the American Physical Society Topical Group on Shock Compression of Condensed Matter, Portland, Oregon, USA, July 20–25, 2003, Los Alamos National Laboratory report LA-UR-03-4439 (July 2003).

S.C. Hsu, G.A. Wurden, T.P. Intrator, J.M. Taccetti, S. Zhang, and W.J. Waganaar, "Multi-point Thomson scattering system for the FRX-L high density field-reversed configuration," 2003 Innovative Confinement Concepts Workshop, Seattle, Washington, USA, May 28–30, 2003, Los Alamos National Laboratory report LA-UR-03-3262 (May 2003).

S.C. Hsu, I.G. Furno, T.P. Intrator, Z. Wang, Z. and C.W. Barnes, "Overview of laboratory plasma experiments on reconnection and MRI at Los Alamos," International Symposium on plasmas in the laboratory and in the universe: New insights and new challenges, Como, Italy, September 16–19, 2003, Los Alamos National Laboratory report LA-UR-03-6574 (September 2003).

S.C. Hsu, Z. Wang, K. Noguchi, D.C. Barnes, P.D. Beinke, and M.W. Martin, "A flowing plasma laboratory experiment for studying the magneto-rotational instability," 7th International Workshop on the Interrelationship Between Plasma Experiments in Laboratory and Space (IPELS 2003), Whitefish, Montana, USA, June 29–July 3, 2003, Los Alamos National Laboratory report LA-UR-03-4391 (June 2003).

S.C. Hsu, Z. Wang, K. Noguchi, P.D. Beinke, and M.W. Martin, "Status and plans of the flowing magnetized plasma (FMP) experiment at LANL," 45th Annual Meeting of the Division of Plasma Physics of the American Physical Society, Albuquerque, New Mexico, USA, October 27–31, 2003, Los Alamos National Laboratory report LA-UR-03-5523 (July 2003).

R.M. Hueckstaedt, R.L. Holmes, G.L. Magelssen, S.H. Batha, and N.E. Lanier, "RAGE validation efforts using cylindrical mix data," 45th Annual Meeting of the Division of Plasma Physics of the American Physical Society, Albuquerque, New Mexico, USA, October 27–31, 2003, Los Alamos National Laboratory report LA-UR-03-5081 (July 2003).

R.M. Hueckstaedt, S.H. Batha, M.M. Balkey, N.D. Delamater, J.R. Fincke, R.L. Holmes, N.E. Lanier, G.R. Magelssen, J.M. Scott, K.W. Parker, and S.D. Rothman, "Numerical simulations of cylindrical mix ICF experiments," 14th Biennial Nuclear Explosives Design Physics Conference (NEDPC 2003), Los Alamos, New Mexico, USA, October 20–24, 2003, Los Alamos National Laboratory report LA-UR-03-7579 (October 2003).

G.C. Idzorek, R.G. Watt, R.E. Chrien, D.L. Peterson, and B.H. Wilde, "The Z-machine as a driver for weapons-physics experiments," 14th Biennial Nuclear Explosives Design Physics Conference (NEDPC 2003), Los Alamos, New Mexico, USA, October 20–24, 2003, Los Alamos National Laboratory report LA-UR-03-4205 (June 2003).

T.P. Intrator, "A high density field reversed configuration plasma target for magnetized target fusion: First internal profile measurements," 45th Annual Meeting of the Division of Plasma Physics of the American Physical Society, Albuquerque, New Mexico, USA, October 27–31, 2003, Los Alamos National Laboratory report LA-UR-03-5526 (July 2003).

T.P. Intrator, "A high density field reversed configuration plasma target for magnetized target fusion: First profile measurements," New Mexico Environmental Health Conference, Albuquerque, New Mexico, USA, October 20–22, 2003, Los Alamos National Laboratory report LA-UR-03-7997 (October 2003).

Appendix B: Publications—2003 Conference Papers

T.P. Intrator, I.G. Furno, S.C. Hsu, and E.W. Hemsing, "Experimental investigation of the stability of a current carrying plasma column," 7th International Workshop on the Interrelationship Between Plasma Experiments in Laboratory and Space (IPELS 2003), Whitefish, Montana, USA, June 29–July 3, 2003, Los Alamos National Laboratory report LA-UR-03-4440 (July 2003).

T.P. Intrator, I.G. Furno, S.C. Hsu, and G. Lapenta, "Reconnection layer dynamics in the reconnection scaling experiment at LANL," 7th International Workshop on the Interrelationship Between Plasma Experiments in Laboratory and Space (IPELS 2003), Whitefish, Montana, USA, June 29–July 3, 2003, Los Alamos National Laboratory report LA-UR-03-1522 (March 2003).

T.P. Intrator, I.G. Furno, S.C. Hsu, G. Lapenta, and E.W. Hemsing, "Microphysics of magnetic reconnection: Experiments and simulation," American Geophysical Union Fall Meeting, San Francisco, California, USA, December 8–12, 2003, Los Alamos National Laboratory report LA-UR-03-8965 (December 2003).

T.P. Intrator, I.G. Furno, S.C. Hsu, G. Lapenta, E.W. Hemsing, and D. Wei, "Microphysics of magnetic reconnection: Experiments and simulation," 7th International Workshop on the Interrelationship Between Plasma Experiments in Laboratory and Space (IPELS 2003), Whitefish, Montana, USA, June 29–July 3, 2003, Los Alamos National Laboratory report LA-UR-03-4461 (July 2003).

T.P. Intrator, J.M. Tacetti, S. Zhang, G.A. Wurden, I.G. Furno, S.C. Hsu, S. R. Siemon, M. Tuzewski, W.J. Waganaar, C. Grabowski, J.H. Degnan, E.L. Ruden, W. Sommars, J. Slough, and M. Gilmore, "Overview of field reversed configuration research at Los Alamos National Laboratory and plans for a physics demonstration of magnetized target fusion," 2003 Innovative Confinement Concepts Workshop, Seattle, Washington, USA, May 28–30, 2003, Los Alamos National Laboratory report LA-UR-03-3260 (May 2003).

T.P. Intrator, I.G. Furno, S.C. Hsu, G. Lapenta, E.W. Hemsing, and D. Wei, "Microphysics of magnetic reconnection: Experiments and simulation," Plasma Astrophysics Workshop, Los Alamos, New Mexico, USA, July 11, 2003, Los Alamos National Laboratory report LA-UR-03-5521 (July 2003).

M.R. James, R.T. Klann, G.L. Morgan, E.J. Pitcher, M.A. Piciotti, J.M. Oostens, J.E. Platte, and D.R. Lowe, "Measurements from activation foils of a proton-irradiated lead-bismuth target," American Nuclear Society Annual Meeting, San Diego, California, USA, June 1–5, 2003, Los Alamos National Laboratory report LA-UR-03-3431 (May 2003).

M.B. Johnson, "Propagation of fast partons in the nuclear medium," 4th International Conference on Perspectives in Hadronic Physics, Trieste, Italy, May 12–16, 2003, Los Alamos National Laboratory report LA-UR-03-6871 (September 2003).

S.-C. Jun and B.A. Pearlmutter, "Application of an artificial neural network for MEG source localization," 4th International Symposium on Noninvasive Functional Source Imaging within the Human Brain and Heart (NFSI 2003), Chieti, Italy, September 20–24, 2003, Los Alamos National Laboratory report LA-UR-03-6441 (September 2003).

S.-C. Jun and B.A. Pearlmutter, "Subject-independent mangetoencephalographic source localization by a multilayer perception," Neural Information Processing Systems: Natural and Synthetic (NIPS 2003), Vancouver, British Columbia, Canada, December 8–13, 2003, Los Alamos National Laboratory report LA-UR-03-7986 (October 2003).

S.-C. Jun, J.S. George, J. Pare-Blagoev, S.M. Plis, D.M. Ranken, D.M. Schmidt, and C.C. Wood, "Dipole analysis on spatiotemporal MEG signals using Bayesian interface," 14th Conference of the International Society for Brain Electromagnetic Topography (ISBET 2003), Santa Fe, New Mexico, USA, November 19–23, 2003, Los Alamos National Laboratory report LA-UR-03-8575 (November 2003).

P.A. Keiter, G.A. Kyrala, R.G. Watt, G.C. Idzorek, R.R. Peterson, B.P. Wood, D.L. Peterson, R.E. Chrien, J.P. Adams, and M.M. Wood-Schultz, "A radiation transfer experiment on Z," 45th Annual Meeting of the Division of Plasma Physics of the American Physical Society, Albuquerque, New Mexico, USA, October 27–31, 2003, Los Alamos National Laboratory report LA-UR-03-5060 (July 2003).

G.F. Kessinger and M.C. Thompson, "Chop-leach dissolution of commercial reactor fuel," *American Institute of Physics Conference Proceedings* **673**, 288–290 (2003).

Y. Kim, L.A. Rosocha, and S.M. Stange, "Preliminary work on decomposition measurements of fuel and oxidant discharges for plasma-assisted combustion," International Workshop on Plasma-Assisted Combustion, Albuquerque, New Mexico, USA, November 3–5, 2003, Los Alamos National Laboratory report LA-UR-03-8132 (October 2003).

N.S.P. King, S. Baker, S. Jaramillo, K. Kwiatkowski, S. Lutz, G.E. Hogan, V. Homes, C.L. Morris, P. Nedrow, P.D. Pazuchanics, J. Rohrer, D. Sorenson, and R. Thompson, "Imaging detector systems for soft x-ray and proton radiography," *Proceedings of the Society of Photo Optical Instrumentation Engineers (SPIE)* **4948**, 610–615 (2003).

J.L. Kline, B. Afeyan, D.S. Montgomery, N.A. Kurnit, V. Savchenko, and K. Won, "Development of an experiment to detect kinetic eletrostatic electron nonlinear waves excited by optical mixing," 45th Annual Meeting of the Division of Plasma Physics of the American Physical Society, Albuquerque, New Mexico, USA, October 27–31, 2003, Los Alamos National Laboratory report LA-UR-03-7529 (October 2003).

J.L. Kline, D.S. Montgomery, B. Bezzerides, J.A. Cobble, D.F. DuBois, R.P. Johnson, H.A. Rose, and H.X. Vu, "Observation of a transition from fluid to kinetic nonlinearities for Langmuir waves driven by stimulated Raman scattering," 3rd International Conference on Inertial Fusion Sciences and Applications (IFSA 2003), Monterey, California, USA, September 7–12, 2003, Los Alamos National Laboratory report LA-UR-03-6368 (September 2003).

A.C. Koskelo, S.R. Greenfield, D.R. Greening, and D.C. Swift, "New windows into shocks at the mesoscale," 13th Biennial International Conference of the American Physical Society Topical Group on Shock Compression of Condensed Matter, Portland, Oregon, USA, July 20–25, 2003, Los Alamos National Laboratory report LA-UR-03-5272 (July 2003).

R.D. Kowalczyk, S.C. Hsu, G.A. Wurden, I.G. Furno, and T.P. Intrator, "High resolution optical spectroscopy on RSX to measure plasma flow and temperature," 2003 Los Alamos Student Symposium, Los Alamos, New Mexico, USA, August 6–7, 2003, Los Alamos National Laboratory report LA-UR-03-5317 (July 2003).

M.P. Kozar, I.G. Furno, T.P. Intrator, and C.A. Werley, "Design of an improved 3-D probe assembly and drive for the RSX plasma," 45th Annual Meeting of the Division of Plasma Physics of the American Physical Society, Albuquerque, New Mexico, USA, October 27–31, 2003, Los Alamos National Laboratory report LA-UR-03-5370 (July 2003).

M.P. Kozar, T.P. Intrator, I.G. Furno, and S.C. Hsu, "Design of an improved 3-D probe assembly and drive for the RSX plasma," 2003 Los Alamos Student Symposium, Los Alamos, New Mexico, USA, August 6–7, 2003, Los Alamos National Laboratory report LA-UR-03-5180 (July 2003).

R.H. Kraus, Jr., M.A. Espy, A.N. Matlachov, T.J. Matsson, C. Carr, J.C. Martin, J.P. Nolan, S. Graves, A.C. Bergstrom, M.D. Ward, and P. Grodzinski, "Bioassay with magnetic particles in flow: A method for highly parallel molecular separations of complex biological systems," 6th European Conference on Applied Superconductivity (EUCAS 2003), Sorento, Napoli, Italy, September 14–18, 2003, Los Alamos National Laboratory report LA-UR-03-6609 (September 2003).

J.C. Kumaradas and M.D. Sherar, "Simulations of microwave hyperthermia for breast cancer recurrences in the chest wall," Progress in Electromagnetics Research Symposium (PIERS 2003), Honolulu, Hawaii, USA, October 13–16, 2003, Los Alamos National Laboratory report LA-UR-03-1940 (March 2003).

K.K. Kwiatkowski, I.H. Cambell, and V. Douence, "Fast imagers for proton radiography: 2-D versus 3-D high-density interconnect approach," International Conference on Imaging Techniques in Subatomic Physics, Astrophysics, Medicine, Biology, and Industry (IMAGING 2003), Stockholm, Sweden, June 24–27, 2003, Los Alamos National Laboratory report LA-UR-03-4078 (June 2003).

K.K. Kwiatkowski, J. Lyke, C. Kapusta, R. Wojnarowski, and S. Kleinfelder, "3-D stacked electronics assembly for high-performance imaging detectors," 2003 IEEE Nuclear Science Symposium and Medical Imaging Conference, Portland, Oregon, USA, October 19–25, 2003, Los Alamos National Laboratory report LA-UR-03-7684 (October 2003).

K. Kwiatkowski, N.S.P. King, J. Lyke, J.F. Beche, G.E. Hogan, C. Kapusta, J.E. Millaud, C. Morris, and R. Wojnarowski, "Development of a multi-frame optical imaging detector for proton radiography at LANL," *Proceedings of the Society of Photo Optical Instrumentation Engineers (SPIE)* **4948**, 616–621 (2003).

G.A. Kyrala, K.A. Klare, N. Delamater, D.C. Wilson, and R.G. Watt, "Direct drive double shell target implosions on Omega," 45th Annual Meeting of the Division of Plasma Physics of the American Physical Society, Albuquerque, New Mexico, USA, October 27–31, 2003, Los Alamos National Laboratory report LA-UR-03-5068 (July 2003).

G.A. Kyrala, K.A. Klare, N.D. Delamater, D.C. Wilson, and R.G. Watt, "Direct drive double shell target implosion hydrodynamics on Omega," 56th Annual Meeting of the Division of Fluid Dynamics of the American Physical Society, East Rutherford, New Jersey, USA, November 23–25, 2003, Los Alamos National Laboratory report LA-UR-03-5762 (August 2003).

G.A. Kyrala, N. Delameter, K.A. Klare, J. Guzik, W.M. Wood, and R.G. Watt, "Double shell experimental validation (U)," 14th Biennial Nuclear Explosives Design Physics Conference (NEDPC 2003), Los Alamos, New Mexico, USA, October 20–24, 2003, Los Alamos National Laboratory report LA-CP-03-0497 (June 2003).

G.A. Kyrala, P.A. Keiter, G.C. Idzorek, R.G. Watt, B.P. Wood, D.L. Peterson, R.E. Chrien, P.J. Adams, M.M. Wood-Schults, and R.R. Peterson, "Radiation transfer experimental validation on Z (U)," 14th Biennial Nuclear Explosives Design Physics Conference (NEDPC 2003), Los Alamos, New Mexico, USA, October 20–24, 2003, Los Alamos National Laboratory report LA-UR-03-4297 (June 2003).

G.A. Kyrala, S. Luo, and D.C. Swift, "Time-dependence of shock-induced melting in beryllium," 13th Biennial International Conference of the American Physical Society Topical Group on Shock Compression of Condensed Matter, Portland, Oregon, USA, July 20–25, 2003, Los Alamos National Laboratory report LA-UR-03-2068 (March 2003).

Appendix B: Publications—2003 Conference Papers

N.E. Lanier, M.M. Balkey, C.W. Barnes, S.H. Batha, and R.D. Day, "Richtmyer-Meshkov mixing in directly driven cylindrically convergent systems: Overview," 3rd International Conference on Inertial Fusion Sciences and Applications (IFSA 2003), Monterey, California, USA, September 7–12, 2003, Los Alamos National Laboratory report LA-UR-03-6437 (September 2003).

N.E. Lanier, M.M. Balkey, C.W. Barnes, S.H. Batha, J.R. Fincke, N.D. Delamater, G.R. Magelssen, R.M. Hueckstaedt, J.M. Scott, A.M. Dunne, C. Horsfield, K.W. Parker, and S.D. Rothman, "Richtmyer-Meshkov mixing in directly driven cylindrically convergent systems," 3rd Inertial Fusion Sciences and Applications Conference (IFSA 2003), Monterey, California, USA, September, 7–12, 2003, Los Alamos National Laboratory report LA-UR-03-1441 (February 2003).

N.E. Lanier, S.H. Batha, J.R. Fincke, R.L. Holmes, and G.L. Magelssen, "Enhanced Richtmyer-Meshkov mixing from dominant wavelength in presence of background multimode surface roughness," 45th Annual Meeting of the Division of Plasma Physics of the American Physical Society, Albuquerque, New Mexico, USA, October 27–31, 2003, Los Alamos National Laboratory report LA-UR-03-5177 (July 2003).

D.M. Lee, "Design and performance of the PHENIX muon tracking systems," 2003 IEEE Nuclear Science Symposium and Medical Imaging Conference, Portland, Oregon, USA, October 19–25, 2003, Los Alamos National Laboratory report LA-UR-03-7796 (October 2003).

C.S. Leichter, "Issues when using independent component analysis and principal component analysis for noise reduction in analysis of single trial SIS magnetoencephalographic data," 2003 Los Alamos Student Symposium, Los Alamos, New Mexico, USA, August 6–7, 2003, Los Alamos National Laboratory report LA-UR-03-5216 (July 2003).

M.J. Leitch, "J/ψ and heavy-quark production in E866/FNAL and PHENIX," 4th International Conference on Perspectives in Hadronic Physics, Trieste, Italy, May 12–16, 2003, Los Alamos National Laboratory report LA-UR-03-6246 (August 2003).

C.-Y. Liu, "Electron electric dipole moment measurement using a paramagnetic crystal," 2003 Los Alamos Student Symposium, Los Alamos, New Mexico, USA, August 6–7, 2003, Los Alamos National Laboratory report LA-UR-03-5303 (July 2003).

M.X. Liu, "Study of heavy quark and quarkonium production in the polarized p-p collisions at RHIC," Conference on the Intersection of Particle and Nuclear Physics (CIPANP), New York, New York, USA, May 19–24, 2003, Los Alamos National Laboratory report LA-UR-03-4381 (June 2003).

W.C. Louis, "MiniBooNE," 10th International Workshop on Neutrino Telescopes, Venice, Italy, March 11–14, 2003, Los Alamos National Laboratory report LA-UR-03-2983 (May 2003).

S.-N. Luo, T.E. Tierney, D.C. Swift, D.L. Paisley, and R.P. Johnson, "Advances in direct laser drive experiments for dynamic materials testing," 45th Annual Meeting of the Division of Plasma Physics of the American Physical Society, Albuquerque, New Mexico, USA, October 27–31, 2003, Los Alamos National Laboratory report LA-UR-03-5064 (July 2003).

S.-N. Luo, D.C. Swift, and T.J. Ahrens, "Melting at the limit of superheating," 13th Biennial International Conference of the American Physical Society Topical Group on Shock Compression of Condensed Matter, Portland, Oregon, USA, July 20–25, 2003, Los Alamos National Laboratory report LA-UR-03-5353 (July 2003).

S.-N. Luo, D.C. Swift, T.E. Tierney, K. Xia, and O. Tschauner, "Time-resolved x-ray diffraction investigation of superheating-melting behavior of crystals under ultra-fast heating," 13th Biennial International Conference of the American Physical Society Topical Group on Shock Compression of Condensed Matter, Portland, Oregon, USA, July 20–25, 2003, Los Alamos National Laboratory report LA-UR-03-5360 (July 2003).

G.R. Magelssen, J.M. Scott, N.E. Lanier, S.H. Batha, M.M. Balkey, C.W. Barnes, N.D. Delamater, A.M. Dunne, K.W. Parker, and S.D. Rothman, "Defect-driven hydrodynamics and mix in convergent geometry," 45th Annual Meeting of the Division of Plasma Physics of the American Physical Society, Albuquerque, New Mexico, USA, October 27–31, 2003, Los Alamos National Laboratory report LA-UR-03-7758 (October 2003).

G.R. Magelssen, W.M. Wood, D. Hoarty, E. Clark, M. Taylor, and M. Dunne, "Supersonic and transonic radiation flow experiments on Omega (U)," 14th Biennial Nuclear Explosives Design Physics Conference (NEDPC 2003), Los Alamos, New Mexico, USA, October 20–24, 2003, Los Alamos National Laboratory report LA-CP-03-0769 (October 2003).

S. Mayor, S. Spuler, J. Fox, B. Morley, N. Kurnit, and R. Karl, "Design of an eye-safe elastic backscatter LIDAR at 1.54 microns," 48th Annual Meeting of the International Society for Optical Engineering (SPIE), San Diego, California, USA, August 3–8, 2003, Los Alamos National Laboratory report LA-UR-03-0607 (January 2003).

K.J. McClellan, D.C. Swift, D.L. Paisley, and A.C. Koskelo, "Dynamic properties of nickel-aluminum alloy," 13th Biennial International Conference of the American Physical Society Topical Group on Shock Compression of Condensed Matter, Portland, Oregon, USA, July 20–25, 2003, Los Alamos National Laboratory report LA-UR-03-6649 (September 2003).

C.W. McCluskey, W.W. Anderson, D.B. Holtkamp, M.D. Furnish, and V.R. Romero, "Discrete layer verification of the LIF window spall diagnostic," 13th Biennial International Conference of the American Physical Society Topical Group on Shock Compression of Condensed Matter, Portland, Oregon, USA, July 20–25, 2003, Los Alamos National Laboratory report LA-UR-03-5403 (July 2003).

F.E. Merrill, G.E. Hogan, C.L. Morris, and A. Saunders, "Capabilities of 800-MeV proton radiography at LANSCE," 14th Biennial Nuclear Explosives Design Physics Conference (NEDPC 2003), Los Alamos, New Mexico, USA, October 20–24, 2003, Los Alamos National Laboratory report LA-UR-03-4298 (June 2003).

F.E. Merrill, K.P. Prestridge, P.M. Rightley, and C.L. Morris, "Advanced imaging capabilities using proton radiography," 14th Biennial Nuclear Explosives Design Physics Conference (NEDPC 2003), Los Alamos, New Mexico, USA, October 20–24, 2003, Los Alamos National Laboratory report LA-UR-03-7708 (October 2003).

P.W. Milonni, J.H. Carter, C.G. Peterson, and R.J. Hughes, "Effects of propagation in air on photon statistics," *Proceedings of the Society of Photo Optical Instrumentation Engineers (SPIE)* **5111**, 7–11 (2003).

G.B. Mills, "The status of the Booster Neutrino Experiment at Fermilab (MiniBooNE)," 4th Topical Workshop on Particle Physics and Cosmology, Cairns, Queensland, Australia, June 9–13, 2003, Los Alamos National Laboratory report LA-UR-03-6247 (August 2003).

R.E. Mischke, "Neutron electric dipole moment," TRIUMF Seminar (Invited), Vancouver, British Columbia, Canada, October 16, 2003, Los Alamos National Laboratory report LA-UR-03-8716 (November 2003).

R.E. Mischke *et al.,* "Neutron electric dipole moment," *American Institute of Physics Conference Proceedings* **675**, 246–250 (2003).

G.S. Mitchell, "Q_{WEAK}: A precision measurement of the proton's weak charge," Conference on the Intersection of Particle and Nuclear Physics (CIPANP), New York, New York, USA, May 19–24, 2003, Los Alamos National Laboratory report LA-UR-03-6031 (August 2003).

D.S. Montgomery, J.L. Kline, and R.J. Focia, "Observation of multiple steps of Langmuir decay instability in Trident single hot spot experiments," 33rd Anomalous Absorption Conference, Lake Placid, New York, USA, June 22–27, 2003, Los Alamos National Laboratory report LA-UR-03-3166 (May 2003).

D.S. Montgomery, J.L. Kline, B. Bezzerides, J.A. Cobble, and D.F. DuBois, "Observation of fluid and kinetic nonlinearities for Langmuir waves driven by stimulated Raman scattering," 45th Annual Meeting of the Division of Plasma Physics of the American Physical Society, Albuquerque, New Mexico, USA, October 27–31, 2003, Los Alamos National Laboratory report LA-UR-03-5178 (July 2003).

D.S. Montgomery, J.L. Kline, R.J. Focia, J.A. Cobble, J.C. Fernandez, and R.P. Johnson, "Recent progress on Trident single hot spot interaction experiments," 5th International Workshop on Laser Plasma Interaction Physics, Banff, Alberta, Canada, February 19–22, 2003, Los Alamos National Laboratory report LA-UR-03-1021 (February 2003).

C.L. Morris, "Results from proton radiography experiment 963 (U)," 14th Biennial Nuclear Explosives Design Physics Conference (NEDPC 2003), Los Alamos, New Mexico, USA, October 20–24, 2003, Los Alamos National Laboratory report LA-CP-03-0702 (September 2003).

C.T. Mottershead, D.B. Barlow, B. Blind, G.E. Hogan, A.J. Jason, F.E. Merrill, K.B. Morley, C.L. Morris, R. Valdiviez, and A. Saunders, "Design and operation of a proton microscope for radiography at 800 MeV," 2003 Particle Accelerator Conference (PAC 2003), Portland, Oregon, USA, May 12–16, 2003, Los Alamos National Laboratory report LA-UR-03-3173 (May 2003).

R.N. Mulford and D.C. Swift, "Formation of plutonium dihydride: Reaction rate as a function of pressure and temperature," Plutonium Futures—The Science: 3rd Topical Conference on Plutonium and Actinides, Albuquerque, New Mexico, USA, July 6–10, 2003, Los Alamos National Laboratory report LA-UR-03-4535 (January 2003).

R.N. Mulford and D.C. Swift, "Laser-launched flyers with organic working fluids," 45th Annual Meeting of the Division of Plasma Physics of the American Physical Society, Albuquerque, New Mexico, USA, October 27–31, 2003, Los Alamos National Laboratory report LA-UR-03-7650 (October 2003).

R.N. Mulford and D.C. Swift, "Reactive flow in nitromethane using a quasi-harmonic equation of state," 13th Biennial International Conference of the American Physical Society Topical Group on Shock Compression of Condensed Matter, Portland, Oregon, USA, July 20–25, 2003, Los Alamos National Laboratory report LA-UR-03-6098 (August 2003).

R.N. Mulford, D.C. Swift, A.M. Collyer, and S.J. White, "On the interaction of shock and detonation waves in the TATB-based explosive EDC35," 5th International Symposium on Behavior of Dense Media Under High Dynamic Pressures, St. Malo, France, June 23–27, 2003, Los Alamos National Laboratory report LA-UR-03-4032 (June 2003).

Appendix B: Publications—2003 Conference Papers

R.N. Mulford and D.C. Swift, "Formation of plutonium hydride PuH_2: Description of the reaction rate surface as a function of pressure and temperature," *American Institute of Physics Conference Proceedings* **673**, 179–181 (2003).

E.L. Nelson and G.A. Wurden, "Improving the optics of the multi-point Thompson scattering system for the FRX-L high density field reverse configuration," 2003 Los Alamos Student Symposium, Los Alamos, New Mexico, USA, August 6–7, 2003, Los Alamos National Laboratory report LA-UR-03-5213 (July 2003).

J.G. Niemczura, D.L. Paisley, and D.C. Swift, "Accuracy of the laser-launched flyer technique for measuring equations of state," 13th Biennial International Conference of the American Physical Society Topical Group on Shock Compression of Condensed Matter, Portland, Oregon, USA, July 20–25, 2003, Los Alamos National Laboratory report LA-UR-03-5522 (July 2003).

J.E. Nordholt, R.J. Hughes, K.P. McCabe, and C.G. Peterson, "Single-photon detection needs for quantum key distribution," Workshop on Single-Photon: Detectors, Applications, and Measurement Methods (NIST), Gaithersburg, Maryland, USA, March 31–April 1, 2003, Los Alamos National Laboratory report LA-UR-03-2507 (April 2003).

J.A. Oertel, T.N. Archuleta, M. Bakeman, P. Sanchez, and G. Sandoval, "A large-format gated x-ray framing camera," 45th Annual Meeting of the Division of Plasma Physics of the American Physical Society, Albuquerque, New Mexico, USA, October 27–31, 2003, Los Alamos National Laboratory report LA-UR-03-7623 (October 2003).

R.T. Olson, "Russian high strain rate-1: X-radiographic results," Joint Russian/USA Meeting on RSHR-1 Results, Los Alamos, New Mexico, USA, November 12-19, 2003, Los Alamos National Laboratory report LA-UR-03-8393 (November 2003).

F.G. Omenetto, "Adaptive control in fibers," Conference on Laser and Electro-Optics/Quantum Electronics and Laser Science (CLEO/QELS), Baltimore, Maryland, USA, June 1–6, 2003, Los Alamos National Laboratory report LA-UR-03-3625 (May 2003).

F.G. Omenetto, "Ultrafast processes in conventional and photonic crystal fibers," Recent Trends in Nonlinear Optics and Ultrashort Pulse Generation, Pavia, Italy, June 15–16, 2003, Los Alamos National Laboratory report LA-UR-03-3624 (May 2003).

F.G. Omenetto, "Ultra-fast pulses in fibers: A nonlinear playground," Frontiers in Optics: The 87th Annual Meeting of the Optical Society of America/Laser Science XIX, Tucson, Arizona, USA, October 5–9, 2003, Los Alamos National Laboratory report LA-UR-03-2889 (April 2003).

D.L. Paisley, R.A. Kopp, D.C. Swift, and R.P. Johnson, "Optimization of laser and flyer parameters for laser-driven flyer plates for EOS and dynamic property measurements," 13th Biennial International Conference of the American Physical Society Topical Group on Shock Compression of Condensed Matter, Portland, Oregon, USA, July 20–25, 2003, Los Alamos National Laboratory report LA-UR-03-1798 (March 2003).

J. Park and G.A. Wurden, "Intense diagnostic neutral beam for ITER," U.S. ITER Forum, College Park, Maryland, USA, May 8–9, 2003, Los Alamos National Laboratory report LA-UR-03-3228 (May 2003).

J. Park, T.P. Intrator, G.A. Wurden, S.C. Hsu, J.M. Taccetti, S. Zhang, J.H. Degnan, C. Grabowski, and E.L. Ruden, "Overview of high density FRC research on FRX-L," IEEE International Conference on Plasma Science, Jeju, South Korea, June 2-5, 2003, Los Alamos National Laboratory report LA-UR-03-0801 (February 2003).

D.M. Partouche-Sebban, "High-speed multi-wavelength pytometry and emissivity measurement of shocked metals," 13th Biennial International Conference of the American Physical Society Topical Group on Shock Compression of Condensed Matter, Portland, Oregon, USA, July 20–25, 2003, Los Alamos National Laboratory report LA-UR-03-4224 (June 2003).

D.M. Partouche-Sebban, J.-L. Pelissier, W.W. Anderson, R.S. Hixson, and D.B. Holtkamp, "Characterization of sapphire for optical pyrometry to shock experiments," 13th Biennial International Conference of the American Physical Society Topical Group on Shock Compression of Condensed Matter, Portland, Oregon, USA, July 20–25, 2003, Los Alamos National Laboratory report LA-UR-03-4254 (June 2003).

P.D. Peralta, D.C. Swift, E.N. Loomis, C. Lim, and K.J. McClellan, "Characterization of laser-driven shocked NiA1 monocrystals and bicrystals," 13th Biennial International Conference of the American Physical Society Topical Group on Shock Compression of Condensed Matter, Portland, Oregon, USA, July 20–25, 2003, Los Alamos National Laboratory report LA-UR-03-5400 (July 2003).

A.L. Peratt, J.A. Guzik, and S.H. Batha, "Design and optimization of hohlraum geometries irradiated by multi-kilojoule, nanosecond laser light for the study of radiation hydrodynamic in foam media (U)," 14th Biennial Nuclear Explosives Design Physics Conference (NEDPC 2003), Los Alamos, New Mexico, USA, October 20–24, 2003, Los Alamos National Laboratory report LA-CP-03-0598 (July 2003).

R.J. Perkins and T.P. Intrator, "B-dot probes in FRX-L," 2003 Los Alamos Student Symposium, Los Alamos, New Mexico, USA, August 6–7, 2003, Los Alamos National Laboratory report LA-UR-03-5525 (July 2003).

D.L. Peterson, R.E. Chrien, R.G. Watt, G.C. Idzorek, and T.W.L. Sanford, "Weapons physics Z-pinch sources on Z And Zr (U)," 14th Biennial Nuclear Explosives Design Physics Conference (NEDPC 2003), Los Alamos, New Mexico, USA, October 20–24, 2003, Los Alamos National Laboratory report LA-CP-03-0813 (October 2003).

R.R. Peterson, G.A. Kyrala, P.A. Keiter, B.P. Wood, and G.C. Idzorek, "Diffusive radiation transport experiments in SiO_2 foams on Z (U)," 14th Biennial Nuclear Explosives Design Physics Conference (NEDPC 2003), Los Alamos, New Mexico, USA, October 20–24, 2003, Los Alamos National Laboratory report LA-CP-03-0924 (December 2003).

R.R. Peterson, G.A. Kyrala, P.A. Keiter, R.G. Watt, and D.L. Peterson, "Validating radiation transport calculations with Z-experiments on SiO_2 foams," 45th Annual Meeting of the Division of Plasma Physics of the American Physical Society, Albuquerque, New Mexico, USA, October 27–31, 2003, Los Alamos National Laboratory report LA-UR-03-7506 (October 2003).

R.R. Peterson, G.A. Kyrala, P.A. Keiter, R.G. Watt, and D.L. Peterson, "Validating radiation transport calculations with Z-experiments on SiO_2 foams," New Mexico Environmental Health Conference, Albuquerque, New Mexico, USA, October 20–22, 2003, Los Alamos National Laboratory report LA-UR-03-4941 (July 2003).

R.R. Peterson, B.P. Wood, G.A. Kyrala, P.A. Keiter, J.M. Kindel, G.C. Idzorek, D.L. Peterson, R.G. Watt, and R.E. Chrien, "Computer code simulations of Z radiation transport experiments in optically thick SiO_2 foams," Meeting of the Joint Working Group (USA-UK) (JOWOG 37), Livermore, California, USA, January 2002, Los Alamos National Laboratory report LA-UR-03-3687 (June 2003).

G.D. Pollak, A.J. Scannapieco, R.G. Watt, and D.C. Wilson, "Comparison of calculated and measured static and gated images," 3rd Inertial Fusion Sciences and Applications Conference (IFSA 2003), Monterey, California, USA, September, 7–12, 2003, Los Alamos National Laboratory report LA-UR-03-1393 (February 2003).

D. Post and R. Kendall, "Lessons learned from ASCI," in Proceedings of the Department of Energy Software Quality Forum, Washington D.C., March 25-26, 2003, Los Alamos National Laboratory report LA-UR-03-1290 (March 2003).

D. Post, "Lessons learned from ASCI applied to the fusion simulation project," American Physical Society Division of Plasma Physics Meeting, Albuquerque, New Mexico, October 27-31, 2003, Los Alamos National Laboratory report LA-UR-03-7540 (October 2003).

D. Post, R. Sheffield, J. Anderson, D. Cooke, D. Dombrowski, G. Lawrence, P. Lisowski, S. Maloy, J. Paisner, K. Schoenberg, D. Schrage, K. Sickafus, B. Stults, and S. Willms, "A proposal for an initial fusion materials testing facility," American Physical Society Division of Plasma Physics Meeting, Albuquerque, New Mexico, October 27-31, 2003, Los Alamos National Laboratory report LA-UR-03-7706 (October 2003).

D. Post, R. Sheffield, J. Anderson , D. Cooke, D. Dombrowski, G. Lawrence, P. Lisowski, S. Maloy, K. Schoenberg, D. Schrage, K. Sickafus, B. Stults, and S. Willms, "A proposal for an initial international fusion materials testing facility," International Conference on Fusion Reactor Materials, Kyoto, Japan, December 7-12, 2003, Los Alamos National Laboratory report LA-UR-03-8260 (December 2003).

K.P. Prestridge, P.M. Rightley, and F.E. Merrill, "Dynamic tests using the high spatial and temporal resolution of proton radiography," 14th Biennial Nuclear Explosives Design Physics Conference (NEDPC 2003), Los Alamos, New Mexico, USA, October 20–24, 2003, Los Alamos National Laboratory report LA-UR-03-4281 (June 2003).

K.P. Prestridge, P.M. Rightley, F.E. Merrill, L.M. Hull, and J.R. Faulkner, "U_6Nb fracture experiments using proton radiography," 14th Biennial Nuclear Explosives Design Physics Conference (NEDPC 2003), Los Alamos, New Mexico, USA, October 20–24, 2003, Los Alamos National Laboratory report LA-UR-03-7707 (October 2003)

M.A. Price, "Developing HE simulants for proton radiography experiments," 2003 Los Alamos Student Symposium, Los Alamos, New Mexico, USA, August 6–7, 2003, Los Alamos National Laboratory report LA-UR-03-4732 (July 2003).

J. Raufeisen, "Coherence length and nuclear shadowing for transverse and longitudinal photons," 2nd International Conference on Nuclear and Particle Physics, Dubrovnik, Croatia, May 26–31, 2003, Los Alamos National Laboratory report LA-UR-03-5382 (July 2003).

J. Raufeisen, "What can we learn about saturation from heavy quark hadron production?" 11th International Workshop on Deep Inelastic Scattering (DIS 2003), St. Petersburg, Russia, April 23–27, 2003, Los Alamos National Laboratory report LA-UR-03-1297 (February 2003).

J. Raufeisen, "What can we learn from d-Au collisions at RHIC?" Muon Collaboration Meeting, Santa Fe, New Mexico, USA, June 16–18, 2003, Los Alamos National Laboratory report LA-UR-03-3988 (June 2003).

Appendix B: Publications—2003 Conference Papers

W.A. Reass, S.E. Apgar, D.M. Baca, J.D. Doss, J.M. Gonzales, R.F. Gribble, and P.G. Trujillo, "Design technology of high-voltage multi-megawatt polyphase resonant converter mod," 29th Annual Conference of the IEEE Industrial Electronics Society (IECON 2003), Roanoke, Virginia, USA, November 2–6, 2003, Los Alamos National Laboratory report LA-UR-03-2205 (March 2003).

W.A. Reass, S. Apgar, D. Baca, J. Doss, J. Gonzales, R. Gribble, and P.G. Trujillo, "High power operation of the polyphase resonant converter modulator system for the Spallation Neutron Source linear accelerator," 14th International IEEE Pulsed-Power Conference, Dallas, Texas, USA, June 15–18, 2003, Los Alamos National Laboratory report LA-UR-03-3824 (June 2003).

R.E. Reinovsky, W.E. Anderson, W.L. Atchison, R.J. Faehl, R.K. Keinigs, I.R. Lindemuth, M.C. Thompson, and A.J. Taylor, "Shock-wave and material properties experiments on the Los Alamos Atlas system," 2003 American Physical Society Topical Conference on Shock Compression of Condensed Matter, Portland, Oregon, USA, July 20–25, 2003, Los Alamos National Laboratory report LA-UR-03-1944 (March 2003).

M. Rihaoui and J.C. Kumaradas, "Dipole-dipole interactions in magnetocarcinotherapy," 2003 Los Alamos Student Symposium, Los Alamos, New Mexico, USA, August 6–7, 2003, Los Alamos National Laboratory report LA-UR-03-4996 (July 2003).

E.A. Rose, R.L. Carlson, and J.R. Smith, "Radiographic performance of Cygnus 1 and the Febetron 705," 14th International IEEE Pulsed-Power Conference, Dallas, Texas, USA, June 15–18, 2003, Los Alamos National Laboratory report LA-UR-03-4011 (June 2003).

L.A. Rosocha, "Environmental applications of non-thermal plasmas," (Invited Talk) U.S. Air Force Academy, Colorado Springs, Colorado, USA, February 4-5, 2003, Los Alamos National Laboratory report LA-UR-03-0800 (February 2003).

L.A. Rosocha, "Proceedings of the first international workshop on plasma-assisted combustion," International Workshop on Plasma-Assisted Combustion, Albuquerque, New Mexico, USA, November 3-5, 2003, Los Alamos National Laboratory report LA-UR-03-8665 (November 2003).

L.A. Rosocha, "Non-thermal plasma (NTP) applications to the environment: Gaseous electronics," 14th International IEEE Pulsed-Power Conference, Dallas, Texas, USA, June 15–18, 2003, Los Alamos National Laboratory report LA-UR-03-3821 (June 2003).

L.A. Rosocha, D. Platts, D.M. Coates, and S.M. Stange, "Combustion enhancement with a silent discharge plasma," 45th Annual Meeting of the Division of Plasma Physics of the American Physical Society, Albuquerque, New Mexico, USA, October 27–31, 2003, Los Alamos National Laboratory report LA-UR-03-4957 (July 2003).

L.A. Rosocha, D. Platts, D.M. Coates, and S.M. Stange, "Combustion enhancement of propane by silent discharge plasma," International Workshop on Plasma-Assisted Combustion, Albuquerque, New Mexico, USA, November 3–5, 2003, Los Alamos National Laboratory report LA-UR-03-8129 (October 2003).

L.A. Rosocha, D. Platts, D.M. Coates, and S.M. Stange, "Combustion enhancement with a silent discharge plasma," 45th Annual Meeting of the Division of Plasma Physics of the American Physical Society, Albuquerque, New Mexico, USA, October 27–31, 2003, Los Alamos National Laboratory report LA-UR-03-7897 (October 2003).

L.A. Rosocha, D. Platts, D.M. Coates, and S.M. Stange, "Combustion enhancement using a silent discharge plasma reactor," 56th Annual Gaseous Electronics Conference, San Francisco, California, USA, October 21–24, 2003, Los Alamos National Laboratory report LA-UR-03-7862 (October 2003).

L.A. Rosocha and J.R. Fitzpatrick, "Actinide decontamination with an atmospheric pressure plasma jet," Radionuclide Decontamination Science and Technology Workshop, Los Alamos, New Mexico, USA, September 16-17, 2003, Los Alamos National Laboratory report LA-UR-03-7217 (September 2003).

T.W.L. Sanford, R.C. Mock, T.L. Gilliland, J.F. Seamen, R.J. Leeper, R.G. Watt, R.E. Chrien, G.C. Idzorek, D.L. Peterson, and P.U. Duselis, "Wire array holder critical in high-wire number Z-pinch implosions," 14th IEEE International Pulsed Power Conference, Dallas, Texas, USA, June 15–18, 2003 (paper originated at Sandia National Laboratories).

R.L. Santillo, Z. Wang, P.D. Beinke, and E. Mignardot, "Developing a Helivon plasma source for astrophysical simulations," 2003 Los Alamos Student Symposium, Los Alamos, New Mexico, USA, August 6–7, 2003, Los Alamos National Laboratory report LA-UR-03-5479 (July 2003).

A. Saunders, "Proton radiography analysis procedure," Accelerator Applications in a Nuclear Renaissance, San Diego, California, USA, June 1–5, 2003, Los Alamos National Laboratory report LA-UR-03-0902 (February 2003).

A. Saunders, C.L. Morris, L.J. Schultz, G.E. Hogan, M.E. Teasdale, K.N. Borozdin, W.C. Priedhorsky, and J. McGill, "Cosmic ray muon radiography," 2003 Spring IEEE Conference: Homeland Security Technologies, Cambridge, Massachusetts, USA, May 7–8, 2003, Los Alamos National Laboratory report LA-UR-03-3021 (May 2003).

L.J. Schultz, K.N. Borozdin, J.J. Gomez, G.E. Hogan, J.A. McGill, C.L. Morris, W.C. Priedhorsky, A. Saunders, and M.E. Teasdale, "Cosmic ray muon radiography for high-Z contraband detection," Accelerator Applications in a Nuclear Renaissance, San Diego, California, USA, June 1-5, 2003, Los Alamos National Laboratory report LA-UR-03-4804 (June 2003).

A. Seifter, "About the meaning of the Hagen-Rubens relation to radiation thermometry," 17th IMEKO World Congress, Metrology in the 3rd Millennium, Cavtat-Dubrovnik, Croatia, June 22–27, 2003, Los Alamos National Laboratory report LA-UR-03-3754 (June 2003).

A. Seifter, "High-speed temperature and emissivity measurements at Group P-23 at the Los Alamos National Laboratory," Technical Discussions on Polarimetry on Rough Surfaces, Graz, Austria, July 3-4, 2003, Los Alamos National Laboratory report LA-UR-03-3745 (June 2003).

A. Seifter, K. Boboridis, and A.W. Obst, "Comparison of emissivity measurements using an integrating sphere reflectometer and a laser polarimeter on surfaces with various degrees of roughness," 17th IMEKO World Congress, Metrology in the 3rd Millennium, Cavtat-Dubrovnik, Croatia, June 22–27, 2003, Los Alamos National Laboratory report LA-UR-03-3753 (June 2003).

A. Seifter, K. Boboridis, and A.W. Obst, "Emissivity measurements on metallic surfaces with various degrees of roughness: A comparison of laser polarimetry and integrating sphere reflectometry," 15th Symposium on Thermophysical Properties, Boulder, Colorado, USA, June 22–27, 2003, Los Alamos National Laboratory report LA-UR-03-3746 (June 2003).

A. Seifter, K. Boboridis, and A.W. Obst, "High-speed temperature and emissivity measurements for thermophysical property determination of conducting materials," 9th International Symposium on Materials in a Space Environment, Noordwijk, The Netherlands, June 16–20, 2003, Los Alamos National Laboratory report LA-UR-03-3755 (June 2003).

A. Seifter, A.W. Obst, and K. Boboridis, "A slow (millisecond-resolution) pulse-heating calorimeter for the validation of radiation thermometers and normal spectral emissivity measurement methods," PTB-GMA Fachtagung TEMPERATUR 2003, Berlin, Germany, September 8-9, 2003, Los Alamos National Laboratory report LA-UR-03-3834 (June 2003).

P.-N. Seo, J.D. Bowman, G.S. Mitchell, S.I. Penttilä, and W.S. Wilburn, "Silicon detector development for a pulsed cold neutron β decay correlation experiment," 2003 Fall Meeting of the Division of Nuclear Physics of the American Physical Society, Tucson, Arizona, USA, October 30–November 1, 2003, Los Alamos National Laboratory report LA-UR-03-7775 (October 2003).

G. Sinnis and C. Milagro, "The Milagro all-sky TeV gamma ray observatory," *Proceedings of the Society of Photo Optical Instrumentation Engineers (SPIE)* **4858**, 358–366 (2003).

J.R. Smith, D.W. Scholfield, and R.L. Carlson, "Magnetic field diffusion effects for recessed E-dot probes," 14th International IEEE Pulsed-Power Conference, Dallas, Texas, USA, June 15–18, 2003, Los Alamos National Laboratory report LA-UR-03-3973 (June 2003).

J.P. Sullivan, D.K. Hayes, R.M. Kippen, M.W. Rawool-Sullivan, and V.D. Sandberg, "Detector tests for a prototype Compton imager," 2003 IEEE Nuclear Science Symposium and Medical Imaging Conference, Portland, Oregon, USA, October 19–25, 2003, Los Alamos National Laboratory report LA-UR-03-3277 (May 2003).

D.C. Swift, D.L. Paisley, A. Forsman, T.E. Tierney, R.P. Johnson, G.A. Kyrala, and A. Hauer, "Dynamic flow stress and polymorphism in shocks induced by laser irradiation," 5th International Symposium on Behavior of Dense Media Under High Dynamic Pressures, St. Malo, France, June 23–27, 2003, Los Alamos National Laboratory report LA-UR-03-0799 (February 2003).

D.C. Swift, D.L. Paisley, and M.D. Knudson, "Equation of state measurements for beryllium in the ICF capsule regime," 13th Biennial International Conference of the American Physical Society Topical Group on Shock Compression of Condensed Matter, Portland, Oregon, USA, July 20–25, 2003, Los Alamos National Laboratory report LA-UR-03-5219 (July 2003).

D.C. Swift, T.E. Tierney, D.L. Paisley, G.A. Kyrala, R.P. Johnson, and A. Hauer, "Laser-driven materials experiments: New capabilities for probing dynamic behavior," Plutonium Futures—The Science: 3rd Topical Conference on Plutonium and Actinides, Albuquerque, New Mexico, USA, July 6–10, 2003, Los Alamos National Laboratory report LA-UR-03-4605 (July 2003).

D.C. Swift, T.E. Tierney, J. Cooley, R. Hackenberg, and K. McClellan, "Direct drive laser experiments on alloys and compounds," 45th Annual Meeting of the Division of Plasma Physics of the American Physical Society, Albuquerque, New Mexico, USA, October 27–31, 2003, Los Alamos National Laboratory report LA-UR-03-5067 (July 2003).

D.C. Swift, T.E. Tierney, D.L. Paisley, G.A. Kyrala, R.P. Johnson, and A. Hauer, "Laser-driven materials experiments: New capabilities for probing dynamic behavior," *American Institute of Physics Conference Proceedings* **673**, 209–210 (2003).

J.M. Taccetti, S. Zhang, T.P. Intrator, G.A. Wurden, W.J. Waganaar, I.G. Furno, S.C. Hsu, E.M. Tejero, C. Grabowski, and E.L. Ruden, "Flux retention and lifetime of FRX-L high-density field-reversed configurations," 2003 Innovative Confinement Concepts Workshop, Seattle, Washington, USA, May 28–30, 2003, Los Alamos National Laboratory report LA-UR-03-3254 (May 2003).

J.M. Taccetti, S. Zhang, T.P. Intrator, G.A. Wurden, W.J. Waganaar, I.G. Furno, S.C. Hsu, E.M. Tejero, C. Grabowski, and E.L. Ruden, "Magnetic flux retention of FRX-L high-density field-reversed configurations," 45th Annual Meeting of the Division of Plasma Physics of the American Physical Society, Albuquerque, New Mexico, USA, October 27–31, 2003, Los Alamos National Laboratory report LA-UR-03-5527 (July 2003).

Appendix B: Publications—2003 Conference Papers

E.M. Tejero, J.M. Tacceti, P.G. Sanchez, and R. Aragonez, "A Labview-based vacuum control system for FRX-L," 2003 Los Alamos Student Symposium, Los Alamos, New Mexico, USA, August 6–7, 2003, Los Alamos National Laboratory report LA-UR-03-5181 (July 2003).

W.R. Thissell, B. Henrie, E.K. Cerreta, W.E. Anderson, W.A. Atchison, J.C. Cochrane, R.K. Keinigs, and J.S. Ladish, "Metallurgical characterization of Atlas cylindrically convergent spallation experiments," 14th Biennial Nuclear Explosives Design Physics Conference (NEDPC 2003), Los Alamos, New Mexico, USA, October 20–24, 2003, Los Alamos National Laboratory report LA-UR-03-1422 (February 2003).

R.T. Thompson, C.L. Morris, A. Saunders, G.E. Hogan, and E.N. Ferm, "Proton radiography: A verification tool for dynamic models and simulations of HE," 34th International Conference of ICT (Fraunhofer Institute for Chemical Technology), Karlsruhe, Germany, June 24–27, 2003, Los Alamos National Laboratory report LA-UR-03-8907 (December 2003).

T.E. Tierney, D.S. Montgomery, J.F. Benage, Jr., M.S. Murillo, F.J. Wysocki, and N. Rostoker, "Modeling of collective Thomson scattering from collisional plasmas," International Conference on Strongly Coupled Coulomb Systems, Santa Fe, New Mexico, USA, September 2–6, 2002, Los Alamos National Laboratory report LA-UR-03-1988 (March 2003).

T.E. Tierney, D.C. Swift, and R.P. Johnson, "Novel techniques for laser-irradiation driven, dynamic materials experiments," 13th Biennial International Conference of the American Physical Society Topical Group on Shock Compression of Condensed Matter, Portland, Oregon, USA, July 20–25, 2003, Los Alamos National Laboratory report LA-UR-03-6756 (September 2003).

T.E. Tierney, D.C. Swift, D.L. Paisley, J.G. Niemczura, R.P. Johnson, G.A. Kyrala, A. Hauer, and A. Forsman, "Dynamic flow stress and polymorphism in samples shocked by direct laser irradiation," 5th International Symposium on Behavior of Dense Media Under High Dynamic Pressures, St. Malo, France, June 23–27, 2003, Los Alamos National Laboratory report LA-UR-03-4153 (June 2003).

T.E. Tierney, D.C. Swift, J.A. Cobble, N.M. Hoffman, D.L. Tubbs, D.E. Schmidt, A. Nobile, R.D. Day, and R.J. Sebring, "Experimental design for studies of beryllium ablator microstructure," 45th Annual Meeting of the Division of Plasma Physics of the American Physical Society, Albuquerque, New Mexico, USA, October 27–31, 2003, Los Alamos National Laboratory report LA-UR-03-8133 (October 2003).

T.E. Tierney, D.C. Swift, S.-N. Luo, J.T. Gammel, and R.P. Johnson, "Near Mbar-level dynamic loading of materials by direct laser-irradiation," American Geophysical Union Fall Meeting, San Francisco, California, USA, December 8–12, 2003, Los Alamos National Laboratory report LA-UR-03-6792 (September 2003).

T.E. Tierney, C.W. Barnes, S.H. Batha, J.F. Benage, Jr., N.M. Hoffman, M.S. Murillo, and R.R. Peterson, "The role of physics at high energy densities in basic and applied sciences," First Joint Graduate Student Conference of Canadian, American, and Mexican Physical Societies, Merida, Yucatan, Mexico, October 22-26, 2003, Los Alamos National Laboratory report LA-UR-03-5763 (August 2003).

J.R. Torgerson, "Method for measurement of DD/DT with optical frequency references based upon III-A and III-A-like ions," Astrophysics, Clocks, and Fundamental Constants, Physikzentrum Bad Honnef, Germany, July 16–18, 2003, Los Alamos National Laboratory report LA-UR-03-4069 (June 2003).

D. Tupa, "Atomic physics contributions to nuclear physics research at Los Alamos National Laboratory," Atomic Physics and Applications Symposium, Madison, Wisconsin, USA, November 8, 2003, Los Alamos National Laboratory publication LA-UR-03-8504 (November 2003).

M. Tuszewski, T.P. Intrator, J.M. Taccetti, W.J. Waganaar, and G.A. Wurden, "Field reversed configurations for magnetized target fusion," International Conference on Plasma Research and Applications (PLASMA 2003), Warsaw, Poland, September 9–12, 2003, Los Alamos National Laboratory report LA-UR-03-7183 (September 2003).

M. Tuszewski, S.P. Gary, R.A. White, and G.A. Wurden, "Downstream instabilities of AR/SF inductive plasma discharges," IEEE International Conference on Plasma Science, Jeju, South Korea, June 2-5, 2003, Los Alamos National Laboratory report LA-UR-03-0156 (January 2003).

RR. Valdiviez, F.E. Sigler, D.B. Barlow, B. Blind, A.J. Jason, C.T. Mottershead, J.J. Gomez, and C.J. Espinoza, "The mechanical design of a proton microscope for radiography at 800 MeV," 2003 Particle Accelerator Conference (PAC 2003), Portland, Oregon, USA, May 12–16, 2003, Los Alamos National Laboratory report LA-UR-03-3085 (May 2003).

D.T. Vo, P.-N. Seo, and T.K. Li, "Testing the Ortec's isotopic and Eberline's snap software for uranium waste measurements," 25th Annual Meeting of the European Safeguards Research and Development Association (ESARDA), Stockholm, Sweden, May 13–15, 2003, Los Alamos National Laboratory report LA-UR-03-2940 (May 2003).

Z. Wang, C.W. Barnes, D.C. Barnes, S.C. Hsu, T.P. Intrator, H. Li, K. Noguchi, X. Tang, and G.A. Wurden, "Astrophysical dynamo experiments in flowing magnetized plasmas (FMP)," 7th International Workshop on the Interrelationship between Plasma Experiments in Laboratory and Space (IPELS 2003), Whitefish, Montana, USA, June 29–July 3, 2003, Los Alamos National Laboratory report LA-UR-03-1437 (February 2003).

Z. Wang, S.C. Hsu, G.A. Wurden, C.W. Barnes, D.C. Barnes, P.D. Beinke, T.P. Intrator, H. Li, M. Martin, C.P. Munson, K. Noguchi, X. Tang, and V.I. Pariev, "Linearly stable magnetic structures with flow," 7th International Workshop on the Interrelationship between Plasma Experiments in Laboratory and Space (IPELS 2003), Whitefish, Montana, USA, June 29–July 3, 2003, Los Alamos National Laboratory report LA-UR-03-4387 (June 2003).

Z. Wang, S.C. Hsu, G.A. Wurden, C.W. Barnes, D.C. Barnes, P.D. Beinke, H. Li, M. Martin, C.P. Munson, K. Noguchi, and X. Tang, "Study of angular momentum transport in the Los Alamos flowing magnetized plasmas (FMP) experiment," 45th Annual Meeting of the Division of Plasma Physics of the American Physical Society, Albuquerque, New Mexico, USA, October 27–31, 2003, Los Alamos National Laboratory report LA-UR-03-7528 (October 2003).

R.G. Watt, G.C. Idzorek, and R.E. Chrien, "Investigation of radiation diffusion in a thin Au wall using x-ray backlift imaging," 45th Annual Meeting of the Division of Plasma Physics of the American Physical Society, Albuquerque, New Mexico, USA, October 27–31, 2003, Los Alamos National Laboratory report LA-UR-03-4850 (July 2003).

R.G. Watt, R.E. Chrien, and G.C. Idzorek, "Investigation of radiation diffusion through a hohlraum wall using radiography (U)," 14th Biennial Nuclear Explosives Design Physics Conference (NEDPC 2003), Los Alamos, New Mexico, USA, October 20–24, 2003, Los Alamos National Laboratory report LA-CP-03-0488 (June 2003).

M.D. Wilke, D.S. Sorenson, W.W. Anderson, F.H. Cverna, R.T. Olson, R.S. Hixson, J. Stevens, D. Turley, S. Lutz, and P.D. Smitherman, "Ejecta production and transport measurements (U)," 14th Biennial Nuclear Explosives Design Physics Conference (NEDPC 2003), Los Alamos, New Mexico, USA, October 20–24, 2003, Los Alamos National Laboratory report LA-CP-03-0828 (October 2003).

M.D. Wilke, W.W. Anderson, and F.H. Cverna, "Gas-gun ejecta production and transport measurements," 14th Biennial Nuclear Explosives Design Physics Conference (NEDPC 2003), Los Alamos, New Mexico, USA, October 20–24, 2003, Los Alamos National Laboratory report LA-UR-03-4731 (July 2003).

D.C. Wilson, C.W. Cranfill, S.A. Becker, P.A. Bradley, C.K. Choi, C.R. Christensen, K.C. New, and P.D. Pollak, "Mix modeling in weapons (U)," 14th Biennial Nuclear Explosives Design Physics Conference (NEDPC 2003), Los Alamos, New Mexico, USA, October 20–24, 2003, Los Alamos National Laboratory report LA-CP-03-0476 (June 2003).

D.C. Wilson, N.D. Delamater, G. Pollak, R.G. Watt, C.W. Cranfill, and W.S. Varnum, "Mixing in double shell capsules," 3rd Inertial Fusion Sciences and Applications Conference (IFSA 2003), Monterey, California, USA, September, 7–12, 2003, Los Alamos National Laboratory report LA-UR-03-6386 (September 2003).

J.B. Workman, G.A. Kyrala, J.P. Roberts, A.J. Taylor, and D.J. Funk, "Development of an ultra-fast x-ray source for measurements of shocked material structural dynamics," 45th Annual Meeting of the Division of Plasma Physics of the American Physical Society, Albuquerque, New Mexico, USA, October 27–31, 2003, Los Alamos National Laboratory report LA-UR-03-5065 (July 2003).

J.B. Workman, S.R. Goldman, G.A. Kyrala, J.R. Fincke, G.R. Magelssen, and K.A. Klare, "One aspect of ACE-B experiments on Omega (U)," 14th Biennial Nuclear Explosives Design Physics Conference (NEDPC 2003), Los Alamos, New Mexico, USA, October 20–24, 2003, Los Alamos National Laboratory report LA-CP-03-0955 (December 2003).

G.A. Wurden, "Magnetized target fusion 2003," 2003 Innovative Confinement Concepts Workshop, Seattle, Washington, USA, May 28–30, 2003, Los Alamos National Laboratory report LA-UR-03-3287 (May 2003).

G.A. Wurden, T.P. Intrator, J.M. Taccetti, I.G. Furno, S.C. Hsu, S. Zhang, J.H. Degnan, C. Grabowski, and E.L. Ruden, "FRX-L (Field Reversed Experiment-Liner) research status and plans," 45th Annual Meeting of the Division of Plasma Physics of the American Physical Society, Albuquerque, New Mexico, USA, October 27–31, 2003, Los Alamos National Laboratory report LA-UR-03-5221 (July 2003).

G.A. Wurden, T.P. Intrator, J.M. Tacetti, S.C. Hsu, S. Zhang, J.H. Degnan, C. Grabowski, and E.L. Ruden, "FRX-L research status and plans," 45th Annual Meeting of the Division of Plasma Physics of the American Physical Society, Albuquerque, New Mexico, USA, October 27–31, 2003, Los Alamos National Laboratory report LA-UR-03-7965 (October 2003).

L.Yin, T. Kwan, B. Devolder, M. Berninger, K.J. Bowers, and J.R. Smith, "Particle-in-cell simulations of the electron beam source for x-ray radiography generated by the rod-pinch diode in the Cygnus experiment," 45th Annual Meeting of the Division of Plasma Physics of the American Physical Society, Albuquerque, New Mexico, USA, October 27–31, 2003, Los Alamos National Laboratory report LA-UR-03-5185 (July 2003).

V.W. Yuan, C.E. Ragan, D.J. Funk, R.A. Pelak, and G.L. Morgan, "Temperature measurements in dynamic-loading experiments using neutron resonance spectroscopy (NRS)," 14th Biennial Nuclear Explosives Design Physics Conference (NEDPC 2003), Los Alamos, New Mexico, USA, October 20–24, 2003, Los Alamos National Laboratory report LA-UR-03-6604 (September 2003).

Appendix B: Publications—2003 Conference Papers

S. Zhang, G.A. Wurden, M.J. Taccetti, T.P. Intrator, W.J. Waganaar, and I.G. Furno, "Formation of the high density field-reversed configuration plasmas," New Mexico Environmental Health Conference, Albuquerque, New Mexico, USA, October 20–22, 2003, Los Alamos National Laboratory report LA-UR-03-5183 (July 2003).

S. Zhang, G.A. Wurden, M.J. Taccetti, T.P. Intrator, W.J. Waganaar, and I.G. Furno, "Formation of the high density field-reversed configuration plasmas," 45th Annual Meeting of the Division of Plasma Physics of the American Physical Society, Albuquerque, New Mexico, USA, October 27–31, 2003, Los Alamos National Laboratory report LA-UR-03-7992 (October 2003).

S. Zhang, G.A. Wurden, M.J. Taccetti, T.P. Intrator, W.J. Wagnaar, I.G. Furno, S.C. Hsu, E.M. Tejero, C. Grabowski, and E.L. Ruden, "Formation of the high density field-reversed configuration plasma in FRX-L," 2003 Innovative Confinement Concepts Workshop, Seattle, Washington, USA, May 28–30, 2003, Los Alamos National Laboratory report LA-UR-03-3261 (May 2003).

This report has been reproduced directly from the best available copy.

It is available to DOE and DOE contractors from the Office of Scientific and Technical Information, P.O. Box 62, Oak Ridge, TN 37831. Prices are available from 865-576-8401. http://www.doe.gov/bridge

It is available to the public from the National Technical Information Service, U.S. Department of Commerce, 5285 Port Royal Rd. Springfield, VA 22616 800-553-6847.

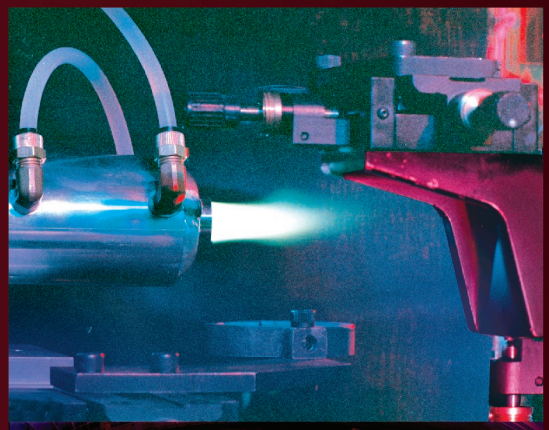

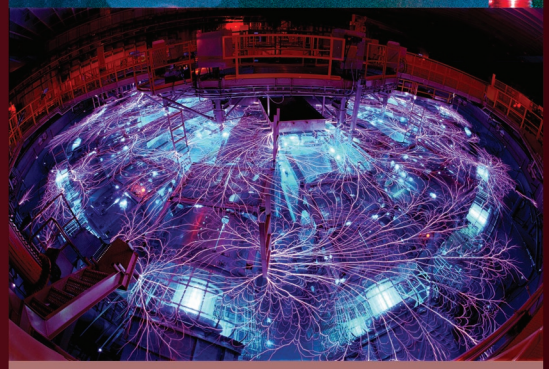

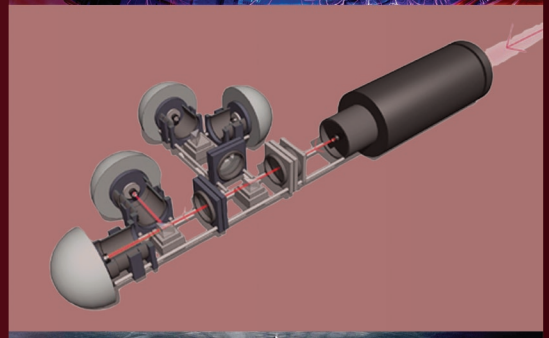

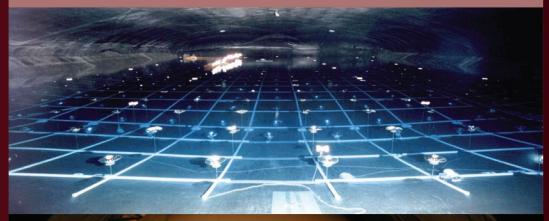

Los Alamos
NATIONAL LABORATORY